2015

Boron Functionalization of BODIPY Dyes, and Their Evaluation as Bioimaging Agents

Alex Long Nguyen
Louisiana State University and Agricultural and Mechanical College, lnguy62@lsu.edu

BORON FUNCTIONALIZATION OF BODIPY DYES, AND THEIR EVALUATION AS BIOIMAGING AGENTS

A Dissertation

Submitted to the Graduate Faculty of the
Louisiana State University and
Agricultural and Mechanical College
in partial fulfillment of the
requirements for the degree of
Doctor of Philosophy

in

The Department of Chemistry

by
Alex Long Nguyen
B.S., Louisiana State University, 2011
May 2016

As I close another important chapter of my life, I would like to dedicate this dissertation to my wonderful and supporting parents, Ngo V. Nguyen and Huynh M. Doan for their encouragement and motivation. My extraordinary sisters, Cynthia, Ashlee, Ally, and Oanh with their supports and advices. And of course, to my fiancee, Trang T. H. Nguyen for her undying love and patience through my long and challenging journey.

ACKNOWLEDGMENTS

First and foremost, I would like to express my most heartfelt thank you and sincere gratitude to my doctoral co-advisors, Dr. M. Graça H. Vicente and Dr. Kevin M. Smith, for their support and valuable guidance throughout my graduate school journey. Dr. Graça Vicente and Dr. Kevin Smith were always there to help me with my research and encouraged me to do my best to overcome my projects' challenges. I will never forget their acceptance into their group when I faced the toughest moment of my life.

I would also like to thank my doctoral committee members, Dr. Carol M. Taylor and Dr. Adam Melvin for taking time out of their demanding schedule and to serve on my advisory committee. In addition, I offer my appreciation to the faculty and staff of the LSU chemistry department. I am deeply grateful for the collaboration with Dr. Petia Bobadova-Parvanova, Associate Professor of Chemistry at Rockhurst University, Kansas City, MO, for sharing her computational knowledge and calculations discussed in Chapter 2. To Dr. Frank R. Fronczek and Dr. Svetlana Pakhomova for the crystal structure determinations, Dr. Thomas Weldeghiorghis for his expertise in NMR facility, and Ms. Connie David for the support in mass spectrometry.

My sincerest gratitude goes to the wonderful chemists in the Vicente and Smith groups. Thank you Dr. R. G. Waruna Jinadasa, Qianli Meng, Ning Zhao, Sunting Xuan, and Zehua Zhou for friendship, and sharing their prestigious suggestions and knowledge.

At the end, I would like to express my greatest thanks to my fiancee, Trang T. H. Nguyen, for her patience and encouragement to assist me in the completing of this dissertation. To my beloved parents and siblings who played an important role in every aspect of my life. This dissertation will not be completed without everyone's encouragement and guidance.

TABLE OF CONTENTS

GLOSSARY OF ABBREVIATIONS

δ	Chemical shift
ε	Extinction coefficient
λ_{max}	Maximum wavelength
^{11}B NMR	Boron 11 Nuclear Magnetic Resonance
BL	Bladder
BODIPY	Boron Dipyrromethene
Bz	Benzyl
^{13}C NMR	Carbon 13 Nuclear Magnetic Resonance
CuTc	Copper(I) thienyl-2-carboxylate
d	Doublet
DCM	Dichloromethane
DDQ	2,3-Dichloro-5,6-dicyano-1,4-benzoquinone
DFT	Density functional calculation
DNA	Deoxyribonucleic acid
EMA	European Medicines Agency
Et	Ethyl
EtOAc	Ethyl acetate
FDA	Food and Drug Administration
FRET	Förster Resonance Energy Transfer
GB	Gall bladder
^{1}H NMR	Proton Nuclear Magnetic Resonance
HRMS-ESI	High Resolution Mass Spectrometry Electrospray Ionization
h	Hours
HOMO	Highest Occupied Molecular Orbital
HPLC	High-Performance Liquid Chromatography
Hz	Hertz
ICT	Intramolecular Charge Transfer
IDG	Indocyanine Green
J	Coupling constant (Hz)
LUMO	Lowest Unoccupied Molecular Orbital

M	Molarity
m/z	Mass to charge ratio
Me	Methyl
mg	Milligram
MHz	Megahertz
min	Minutes
mL	Milliliter
NIR	Near-infrared
nm	Nanometer
PDT	Photodynamic therapy
PEG	Polyethylene glycol
PET	Positron Emission Tomography
Ph	Phenyl
ppm	Parts per million
rDA	Retro-Diels-Alder
RNA	Ribonucleic Acid
rt	Room temperature
s	Singlet
SI	Small intestine
S_NAr	Nucleophilic Aromatic Substitution
SNR	Signal to Noise Ratio
SPL	Sphingosine-1-phosphate
SPECT	Single-Photo Emission Computed Tomography
t	Triplet
THF	Tetrahydrofuran
TLC	Thin Layer Chromatography
UV-Vis	Ultra violet-visible

ABSTRACT

BODIPY, also known as "porphyrin's little sister," belongs to a class of fluorescent dyes. It contains a dipyrromethene π-system with a disubstituted boron atom. The basic 4,4-difluoro-4-bora-3a,4a-diaza-s-indacene (BODIPY) is known for its numerous useful applications in the fields of biology and materials. Modification of this well-known fluorophore has been shown to change its photophysical and chemical properties. There has been great interest in the modification at the boron center in recent years for synthesizing new dyads and cascade-type dyes. This work focuses on functionalization at the boron center with carbon and oxygen nucleophiles for further investigation as bioimaging agents.

Chapter 1 of this dissertation describes an overview of BODIPYs including synthetic development, post-synthetic functionalization strategies, and how BODIPYs can be involved in many biological applications.

Chapter 2 discusses the synthesis, characterization, and computational studies of 4,4-dialkoxy BODIPY and its derivatives. Preliminary studies with various Lewis acids and alcohols will be investigated and discussed. In collaboration with Dr. Petia Bobadova-Parvanova of Rockhurst University, the photophysical properties were studied using computational analysis. The structural, spectroscopic and fluorescence properties of all the synthesized BODIPYs will be studied and be compared.

Chapter 3 presents the synthesis and characterization of 4,4'-dicyano-BODIPYs. A novel route for preparation of 4,4'-difunctionalized BODIPYs bearing phenyl and various substituents at the boron center was developed. These compounds were synthesized in a three step one-pot reaction between dipyrromethenes and dichlorophenylborane, followed by replacement of chloride

with fluoride and various carbon- and oxygen-centered nucleophiles. These BODIPYs' structural, spectroscopic, and fluorescence properties are reported and discussed.

Chapter 4 represents the investigation of six 1,2,3-triazole-BODIPYs under the Cu(I)-catalyzed Huisgen cycloaddition reaction conditions. A novel BODIPY bearing a chiral moiety was synthesized using method C and X-ray crystallography confirmed its identity.

Chapter 5 reports the synthesis of chloroalcohol compounds via triphosgene-triethylamine activation. An asymmetric S_N1 reaction was investigated through the use of an oxazolidinone.

CHAPTER 1: INTRODUCTION

1.1 Structure of BODIPY® Dyes

In the last two decades, biomedical scientists have continued to search for new organic dyes for medicinal therapies in order to visualize intracellular processes.[1] New fluorophores that are capable of being excited and emitting within the "biological window" of 600-800 nm became an attractive and versatile tool as theranostic agents for various cancer treatments. Compounds in this red or near-infrared (NIR) region of the spectrum typically provided minimal interference from the endogenous chromophores, reduced light scattering, and prevented damage to cells and tissues.[2-5] The boron dipyrromethene (designated BODIPY) family of dyes have the desired framework for facile modification, making them tunable probes and sensors for many biological applications, in comparison to other alternative nonradioactive fluorophores, such as rhodamines, cyanines, and fluorescein (Figure 1.1).

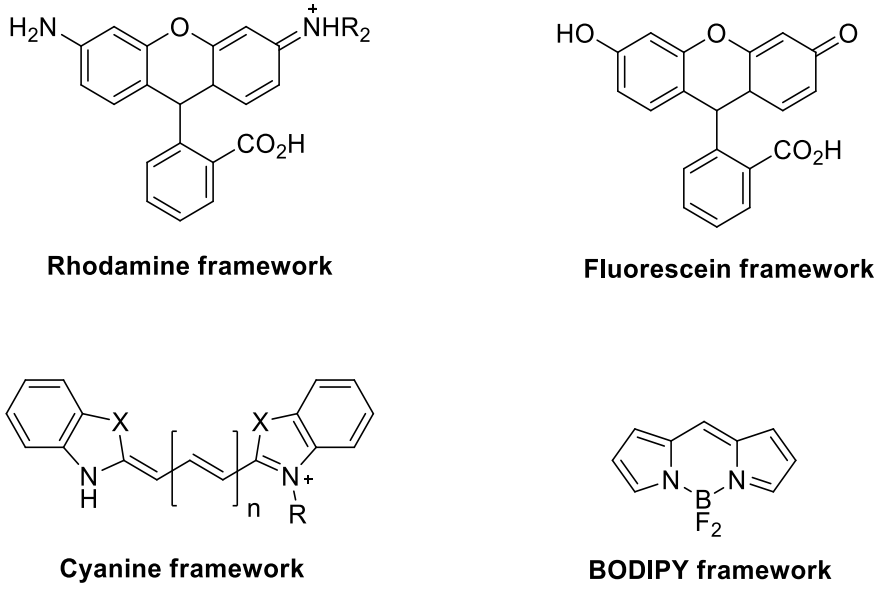

Figure 1.1: Structural framework of selected common fluorophores.

4,4-Difluoro-4-bora-3a,4a-diaza-s-indacene, or BODIPY, is often recognized as "porphyrin's little sister".[6] This family of fluorophores consists of a dipyrromethene framework complexed to a disubstituted boron unit. The dipyrromethene structure consists of two pyrrole units linked via an interpyrrolic methine bridge. The complexation system of dipyrromethene with a BF_2 unit provides a "constrained" conjugated system, giving planarity to the BODIPY conjugated π-system.[7] The advantage of complexation with the BF_2 moiety is to increase the rigidity of the tricyclic system and to prevent *cis*/*trans* isomerization of the dipyrromethene core. This restricted conformation allows for π-electron delocalization along the carbon-nitrogen backbone, which provides high fluorescence quantum yields.[8] The overall charge of BODIPY is neutral due to the zwitterionic species involving the boron and nitrogen atoms.

The systematic naming for the dipyrromethene and BODIPY cores are shown in Figure 1.2. In the BODIPY, positions 3 and 5 are denoted as *alpha* (*α*) while positions 1, 2, 6, and 7 are referred as *beta* (*β*) similar to the pyrrolic system.[9] The *meso*-position is located at the 8-carbon, while positions 4 and 4' are the two fluoride atoms connected to the boron center.

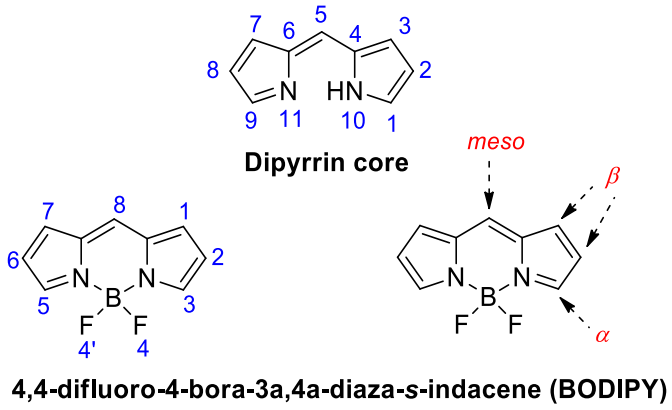

Figure 1.2: Numbering system for dipyrrin and BODIPY frameworks.

A single crystal structure analysis of the BODIPY core shows the three fused rings framework which consisting of a central six-membered ring and two five-membered pyrrolic rings

with a π-electron delocalization backbone (Figure 1.3).[10] The presence of B-N bonds interrupts the π-conjugation which shows that the BF_2 moiety does not play a significance role in extending the backbone delocalization. The approximate tetrahedral geometry of the boron atom (BF_2N_2) can be confirmed by the N_1-B_1-N_2 and F_1-B_1-F_2 bond angles.[11] The approximate bond length of N_1-C_4 shows a single bond, while N_1-C_3 indicates double bond characteristic. BODIPY was initially thought to resemble a monomethine cyanine dye by having 6π electrons equally delocalized over five atoms but found to be isoelectronic with heptamine cyanine having 12π distributed over eleven atoms.[12]

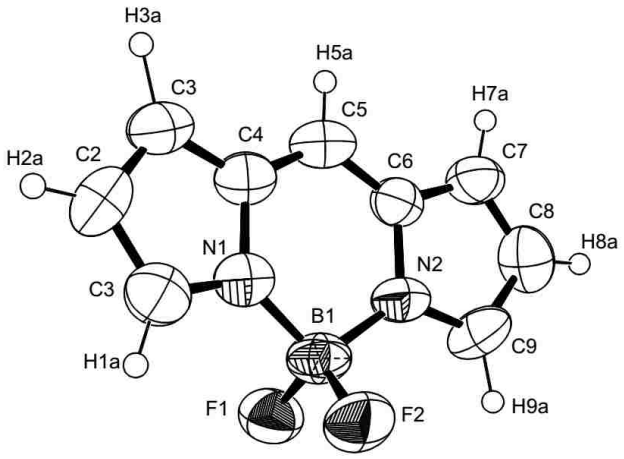

Figure 1.3: The X-ray crystal structure of unsubstituted BODIPY with atoms labeled and 50% probability displacement ellipsoids.[10]

The monoclinic unit cell of the BODIPY comprises of four molecules arranged head-to-tail geometry, which utilities the π-π interactions between adjacent hydrophobic fragments and avoids the variation from the fluorine dipole moments.[13] Little differences in heteroatoms dipole moment of BODIPY core provide modification at various positions via electrophilic and nucleophilic additions. The functionalization at the substituent-free positions unlocks new tunable routes to numerous novel BODIPY derivatives.[14]

BODIPY and its derivatives show remarkable photophysical characteristics. The characteristics are intense absorption and emission in the visible region ($\lambda_{max} \geq 450$ nm), high fluorescence quantum yields, high molar absorption coefficients (around 40,000 to 80,000 M^{-1} cm^{-1}), and relatively small Stokes shifts (~15 nm).[6,8] Various properties of BODIPYs include excellent photophysical stability, thermal- and photochemical stability in solution and solid states, high solubility in many organic solvents, and resistance to changes in pH and solvent polarity.[15-17]

The typically strong intense absorption band of the BODIPY fluorophore in the visible region comes from the S_0-S_1 (π-π^*) transition containing a shoulder of high energy around 480 nm from the 0-1 vibrational transition, while a broad weaker band around 350 nm is assigned to the S_0-S_2 (π-π^*) transition.[12,18] Excitation of an electron in either the S_1 or S_2 states, an equally narrow band from the absorption and emission spectra is perceived from the S_1 state. BODIPYs that have emission around 500-590 nm typically have a yellow to green color. Small Stokes shifts are often observed in many BODIPY compounds, which indicate that the S_0-S_1 transition and vibrational relaxation make no significant changes in the core structure.[19]

Addition of functional groups to the carbon atoms at the *α*-, *β*-, and *meso*-positions as well as the boron atom of BODIPY can alter its photophysical properties. The BODIPY absorption band can be shifted into the red or near-IR region by increasing the degree of π-electron delocalization. Having functional groups that are electron-withdrawing or -donating on the BODIPY core as well as intramolecular rotation can significantly affect the absorption and emission properties.[20]

Investigation of BODIPY's functionalization will further research development in the synthesis of new fluorophores for multi-purpose applications. By altering the spectroscopic properties and functionalities of BODIPY dyes, there are boundless possibilities for designing

novel, challenging and versatile fluorescent compounds. Throughout this Dissertation, various synthetic methodologies and investigation techniques will be described.

1.2 Synthetic Methodologies

In 1968, Treibs and Kreuzer were the first to synthesize a BODIPY by mixing 2,4-dimethylpyrrole, acetic anhydride, and $BF_3 \cdot OEt_2$, and found this robust class of compound could have potential application as tunable laser dyes.[21] This fluorophore was not fully explored until the late 1980s, where BODIPYs were found to be useful for biological applications, such as cellular imaging and probe sensors. For example, Wories and coworkers[22] reported the first water-soluble BODIPYs for cellular visualization. Since the mid-1990s, publications and patents reported on BODIPYs have increased tremendously. Extensive modifications to the BODIPY framework have led to many BODIPY derivatives with numerous applications: biomolecular imaging,[23-26] photosensitizers,[27-30] fluorescent switches,[31-34] chemosensors,[35-40] electroluminescence devices, laser dyes,[41-43] drug delivery agents,[28,44] and in photodynamic therapy.[45-46]

1.2.1 Synthesis of the BODIPY Core

There are many routes toward the synthesis of BODIPY using well-known pyrrole chemistry. First, a highly reactive electrophilic ketopyrrole and readily nucleophilic 2-unsubstituted-pyrrole afford the corresponding dipyrromethene compounds. Using a non-nucleophilic base, either a secondary or tertiary amine, followed by complexation using boron trifluoride etherate ($BF_3 \cdot OEt_2$) gives the desired BODIPY in moderate yields. Even though there are numerous reports of BODIPY syntheses in the literature, the fully unsubstituted BODIPY **1** remained a challenge due to the compound's reactivity. However, three independent research groups have reported successful routes to the fully unsubstituted BODIPY **1**. The first method was

reported by Bruce and coworkers (Scheme 1.1, Method A),[10] where dipyrromethane **3** was oxidized to the corresponding dipyrromethene by using DDQ or chloranil as the oxidizing agent. To avoid undesired side products, the oxidation step was carried out under inert conditions and at low temperature (-78 °C). The complexation step with $BF_3{\cdot}OEt_2$ was performed *in situ* using DBU as an additive to yield the desired compound in 5-10% yield. This unsubstituted compound **1** was characterized by ^{1}H-, ^{13}C-, ^{11}B-, and ^{19}F-NMR spectroscopy and its structure was confirmed by single crystal X-ray analysis.

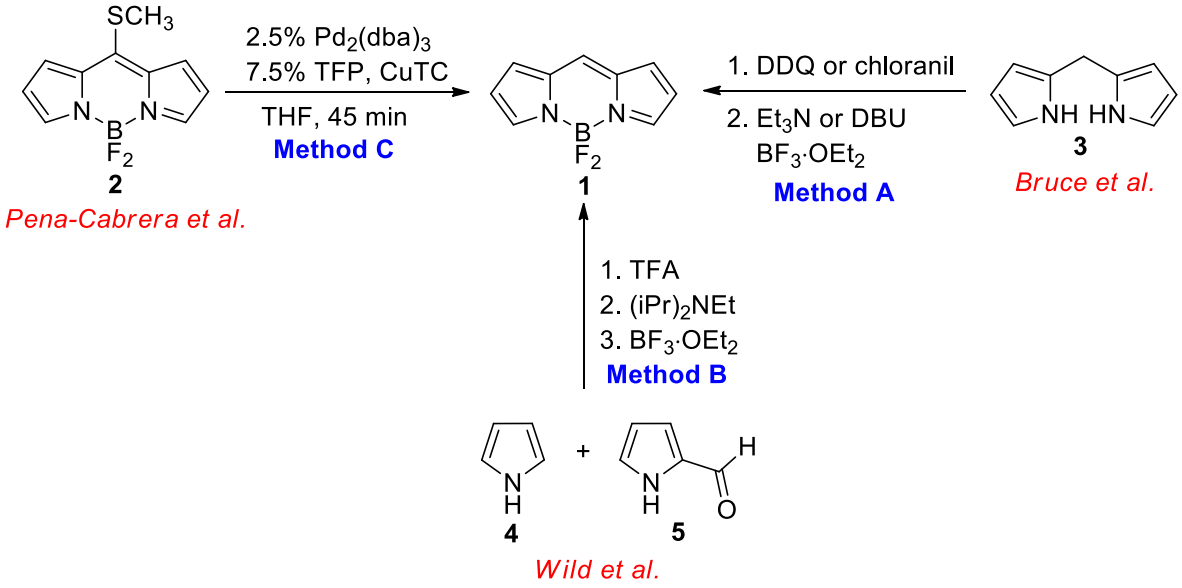

Scheme 1.1: Methods for syntheses of unsubstituted BODIPY **1**.

Another approach to the unsubstituted BODIPY **1** was through a classic acid-catalyzed condensation method between pyrrole-2-carbaldehyde **5** and unsubstituted pyrrole **4**, followed by complexation with $BF_3{\cdot}OEt_2$ in the presence of a base to afford the desired product **1** in 8% yield (Scheme 1.1, Method B).[14] However, the unsubstituted BODIPY can be synthesized in 98% yield from the most efficient method developed by Pena-Cabrera and coworkers,[13] where a *meso*-thiomethyl BODIPY **1** was treated with trimethylsilane under mild conditions using copper(I)

thienyl-2-carboxylate (CuTc) and palladium in THF for 45 min at reflux temperature (Scheme 1.1, Method C). No reaction was observed in the absence of CuTc or palladium. The impressive characteristic of BODIPY **1** is a high quantum yield (93%) in non-polar and polar solvents.

1.2.2 Synthesis of Symmetric BODIPY Dyes

8-Substituted symmetrical BODIPYs can by synthesized by acid-catalyzed condensation between acid chlorides, aldehydes, or anhydrides with α-free pyrroles to give the corresponding dipyrromethene (or dipyrromethane in the case of aldehyde). Polymerization of pyrrole typically occurs when both *α*-positions of the pyrroles are unsubstituted. To avoid this polymerization, only one *α*-position (C2) is usually unsubstituted. The most popular route consists of a "one-pot three step" reaction and has become the most efficient way to synthesize a wide range of *meso*-substituted BODIPYs with the desired appendages (Scheme 1.2).

Symmetrical BODIPY syntheses typically involve self-condensation between two equivalents of an *α*-free pyrrole with an aryl aldehyde to give a dipyrromethane (Scheme 1.2). A recent report shows that aldehydes and pyrroles can also react under neat conditions (no solvent required) to afford dipyrromethanes.[47] The dipyrromethanes are subsequently oxidized to give dipyrromethenes which then undergo complexation with $BF_3 \cdot OEt_2$. Alternatively, another method to synthesize BODIPYs requires treating the same two units of an *α*-free pyrrole with acyl chloride to directly give dipyrromethene. The advantage of this method is that no oxidation step is necessary, which usually increases the reaction yields and eases purification. Similar to acyl chlorides, anhydrides also react with an *α*-free pyrrole to give the corresponding dipyrromethene. Although introducing aromatic groups onto the BODIPY core is expected to extend the π-conjugation delocalization, the nearly perpendicular geometry of the groups at the *meso*-position prevent significant interaction of the two π-systems, but increases BODIPY stability.[6,11,16,48]

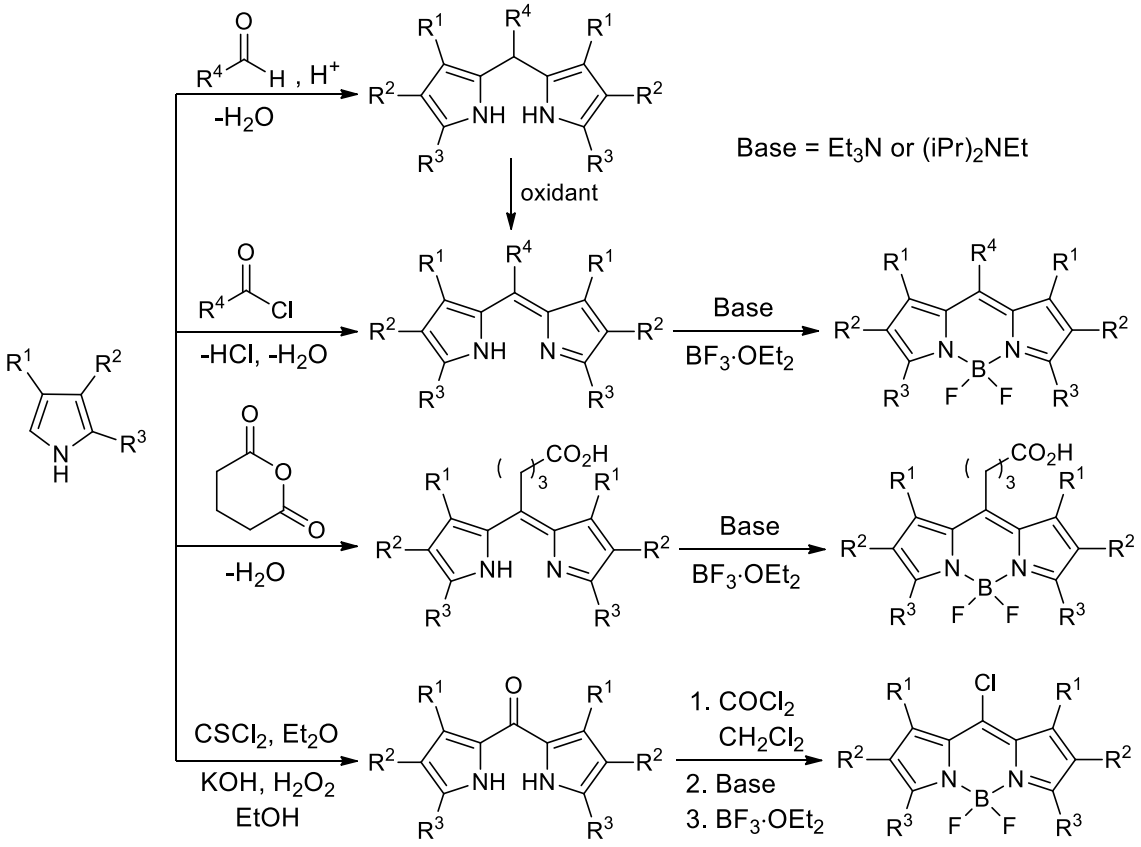

Scheme 1.2: General procedures for symmetrical BODIPY synthesis via condensation.

The approach using a cyclic anhydride provides the corresponding BODIPY bearing a terminal carboxylic acid, which are receptive to coupling to biological molecules such as proteins, DNA and lipids.[15,49] *meso*-Unsubstituted BODIPY can generally be prepared from pyrrole-2-carbaldehyde and an α-free pyrrole in an acid-catalyzed condensation reaction. An acid catalyst, such as *p*-toluenesulfonic acid or Montmorillonite clay, is often used in order to generate the pyrrole carbinyl cation which reacts with the α-free pyrrole to give dipyrromethane.[50-51] Symmetric and unsymmetric BODIPYs can also be synthesized from dipyrroketones.[52]

1.2.3 Synthesis of Unsymmetrical BODIPY Dyes

The approach to synthesize unsymmetrical BODIPYs relies on the use of two different pyrroles, for example by reacting the ketopyrrole (carbonyl-containing pyrrole) with a different α-

free pyrrole via Lewis acid mediated condensation (Scheme 1.3).[53-54] The ketopyrrole precursor fragment can be synthesized from an α-free pyrrole and Grignard reagents and an acid chloride.[53,55-56] The use of electron-rich and electron-deficient pyrroles determines the percent yields of the desired BODIPY product. Electron-rich pyrrole usually gives a high yield while electron-poor pyrrole usually gives a low yield due to self-condensation which results in the undesired symmetrical product. The dipyrromethene salt then reacts with $BF_3 \cdot OEt_2$ in the presence of a base to give a BODIPY scaffold with two different pyrrolic units for further functionalization. In addition, Zhao and coworkers[57] recently reported that unsymmetric BODIPYs can be synthesized from dipyrroketone precursors.

1.3 Derivatization of the BODIPY Core

Although BODIPYs have many advantages, some of their limitations are the typical absorption and emission wavelength maxima around 500 nm, relatively small Stokes shifts, poor solubility in an aqueous environment, and inability to directly conjugate to biomolecules. To overcome these drawbacks, functional groups can be attached directly to the BODIPY core via the use of a substituted pyrrolic precursor, substituted aldehyde, or by post-functionalization of the BODIPY dyes. The tunable properties of BODIPY allow the synthesis of derivatives that absorb and emit in the span over the desired wavelength in the visible and NIR ranges.

Many research groups (including Vicente,[48,58-59] Burgess,[60] Ziessel,[44] Boens,[1,61] Nagano,[30] Akkaya,[62] O'Shea,[63] Rurack and Daub,[64] and Carreira[65]) are currently exploring new methods to optimize the photophysical properties of these dyes while retaining their stabilities. BODIPY dyes can be derived from various approaches: i) nucleophilic substitutions or additions of styryl or alkynyl groups at the 3,5-positions, ii) electrophilic substitutions at the 2,6-positions, iii) cross-coupling reactions with palladium(0) on halogenated BODIPYs, iv) nucleophilic substitution at

the boron center. Metal-mediated cross-coupling reactions provide one of the most convenient methods to incorporate functionalities directly into the BODIPY core with halogens at the 2,3,5,6,8-positions. Typical palladium-mediated cross-coupling reactions can be accomplished through the Suzuki,[66-68] Sonagashira,[59,66,69] Heck,[70-71] and Stille[72] methods.

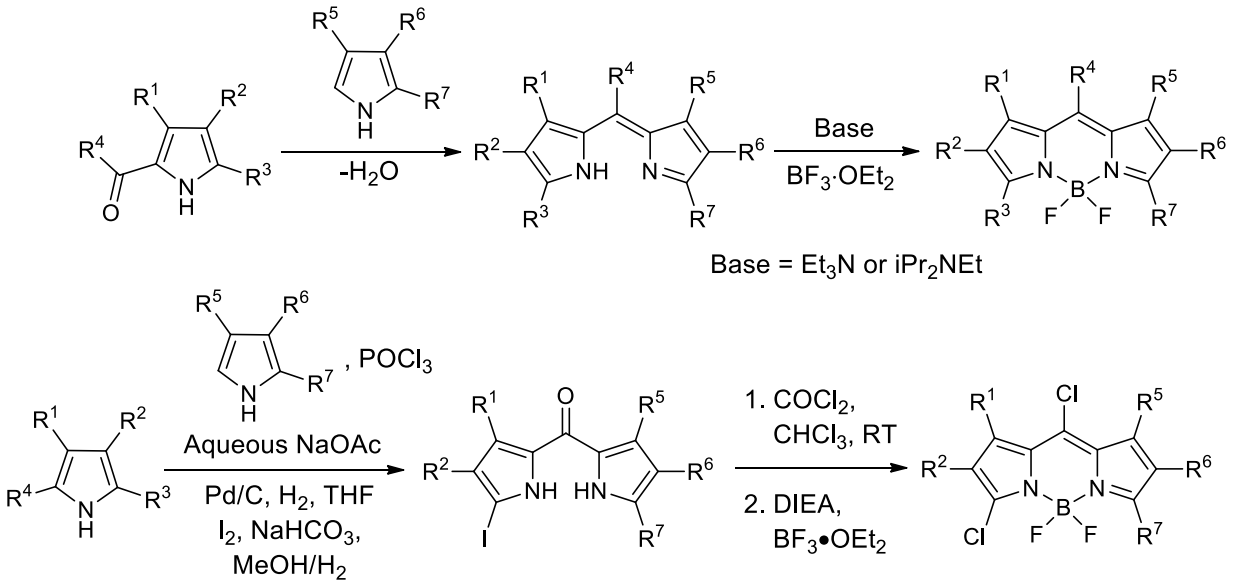

Scheme 1.3: General procedure for unsymmetrical BODIPY via ketopyrrole and dipyrroketone.

1.3.1 Functionalization at the 8-position

The *meso*-position (or 8-position) is the easiest position to introduce various "handles" on the BODIPY from the initial condensation step (examples are shown in Figure 1.4). This position can be functionalized with a variety of aromatic groups via acid-catalyzed condensation, using either an aldehyde or acyl chloride.[73] The introduction of useful groups on the 8-position for specialized purposes, such as incorporation of metal ion binding ligands,[1,6,74] functionality for donor-acceptor cassettes,[75-77] water-soluble groups,[5,17] and biomolecules[78] for biological applications, including as pH probes and chemical sensors. For example, probes with aliphatic ester 8-aryl BODIPYs are being used to investigate dynamic effects in membranes (Figure 1.4,

structure **9**).[79] Boens and coworkers[1,61,80] studied the effect of electron-donating and electron-withdrawing groups at the *meso*-position. BODIPYs with substituents at the 1,7-positions or bulky substituents on the 8-aryl group show restricted rotation of the *meso*-aryl group, which in turn increases the fluorescence quantum yields (Figure 1.4, structure **9**). In addition, replacing the *meso*-aryl group with a trifluoromethyl unit also increases quantum yields due to the reduction in the nonradiative decay through rotation.[1,15]

Substitution of the carbon atom at the 8-position with a nitrogen atom generates a new class of fluorophore called "aza-BODIPYs," which were not reported until 1994 (Figure 1.4, structure **11**). [81-84] The important characteristics of aza-BODIPYs are sharp absorption and emission wavelengths in the NIR (650-850 nm) range, high molar extinction coefficients, and moderate to good fluorescence quantum yields.[85] The *meso*-nitrogen with the lone pair can dramatically decrease the HOMO-LUMO energy gap through stabilization,[6] which induces a large red-shift in the absorption and fluorescence emission maxima (~100 nm). These aza-dipyrromethenes can be prepared by condensation between nitrosopyrrole and an α-free pyrrole or Michael addition product (reaction from chalcones and nitromethane) with formamide.[81-83] This class of fluorophore has found its usefulness in various applications: as photosensitizers for PDT,[72,86] NIR-emitting chemosensors, bioimaging probes,[32,65,87] and fluorescent biological labels.[88-89]

1.3.2 Modification at the 1,3,5,7-Positions

The photoelectronic properties of the BODIPY core can be fine-tuned by varying the subsitutents on the carbon framework. Analogous to other heteroaromatic systems, the methyl groups at the 1, 3, 5, and 7-positions are the most nucleophilic sites. The 3,5-methyl groups are considered relatively acidic due to being next to the pyrrolic nitrogen atom. In order to extend the π-conjugation, the methyl groups can be deprotonated and undergo condensation with electron-

rich aromatic aldehydes through Knoevenagel reactions to generate *trans*-stryryl groups (Figure 1.5).

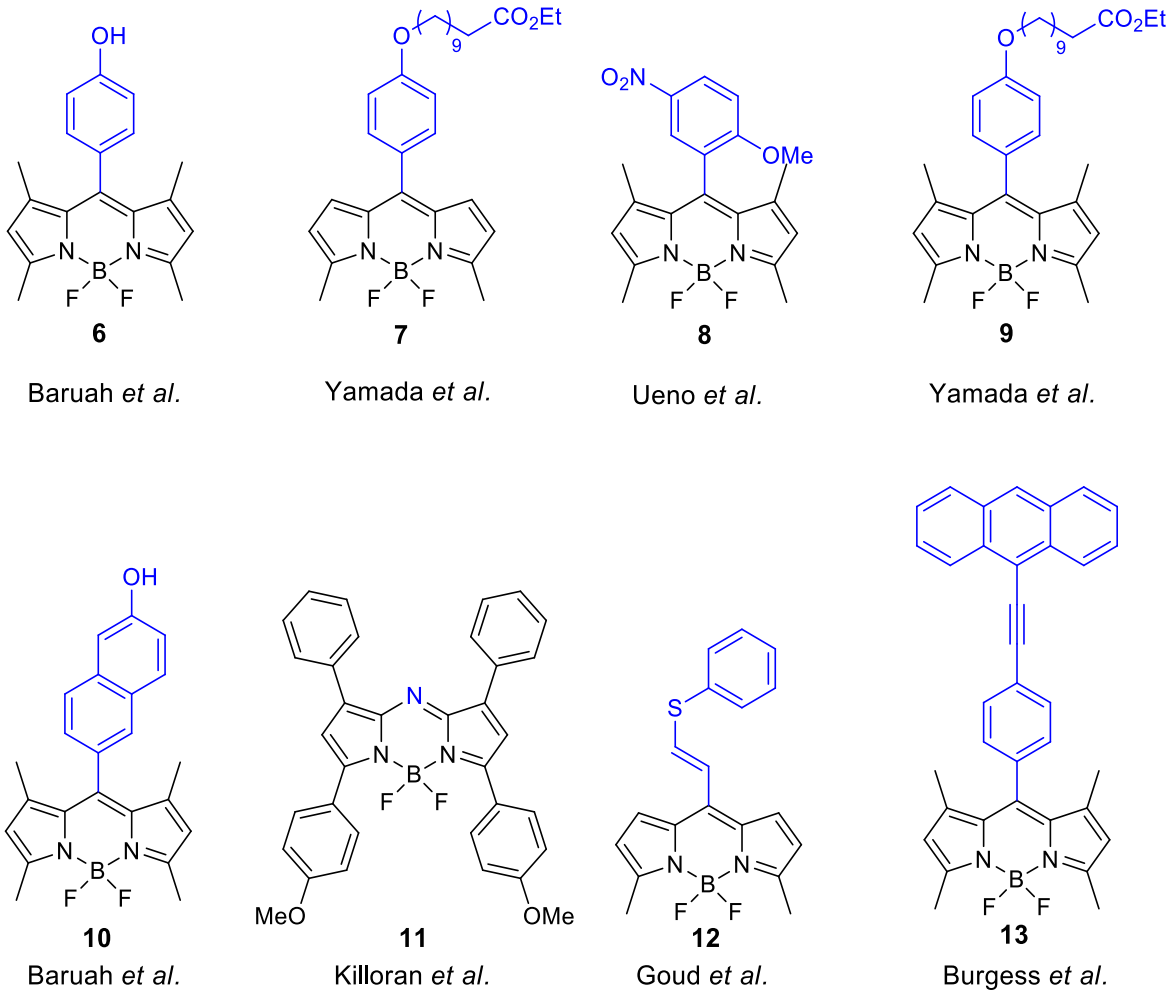

Figure 1.4: Selected examples of 8-substituted BODIPY structures: **6**,[80] **7**,[79] **8**,[90] **9**,[79] **10**,[80] **11**,[91] **12**,[92] and **13**.[93]

Some groups, such as dimethylamino on the 3,5-aryls induce high quantum yields only in the protonated form by disfavoring intramolecular charge transfer (ICT) in the excited state. Post-functionalization using various aryl-aldehyde groups provides a methodology for introducing "handle" through a simple modification, producing long-wavelength absorbing and emitting BODIPYs. Addition of halogens such as chloride or iodide at the 3,5-positions allows BODIPY to

become reactive toward nucleophilic aromatic substitutions (S_NAr) and palladium-catalyzed cross-coupling.

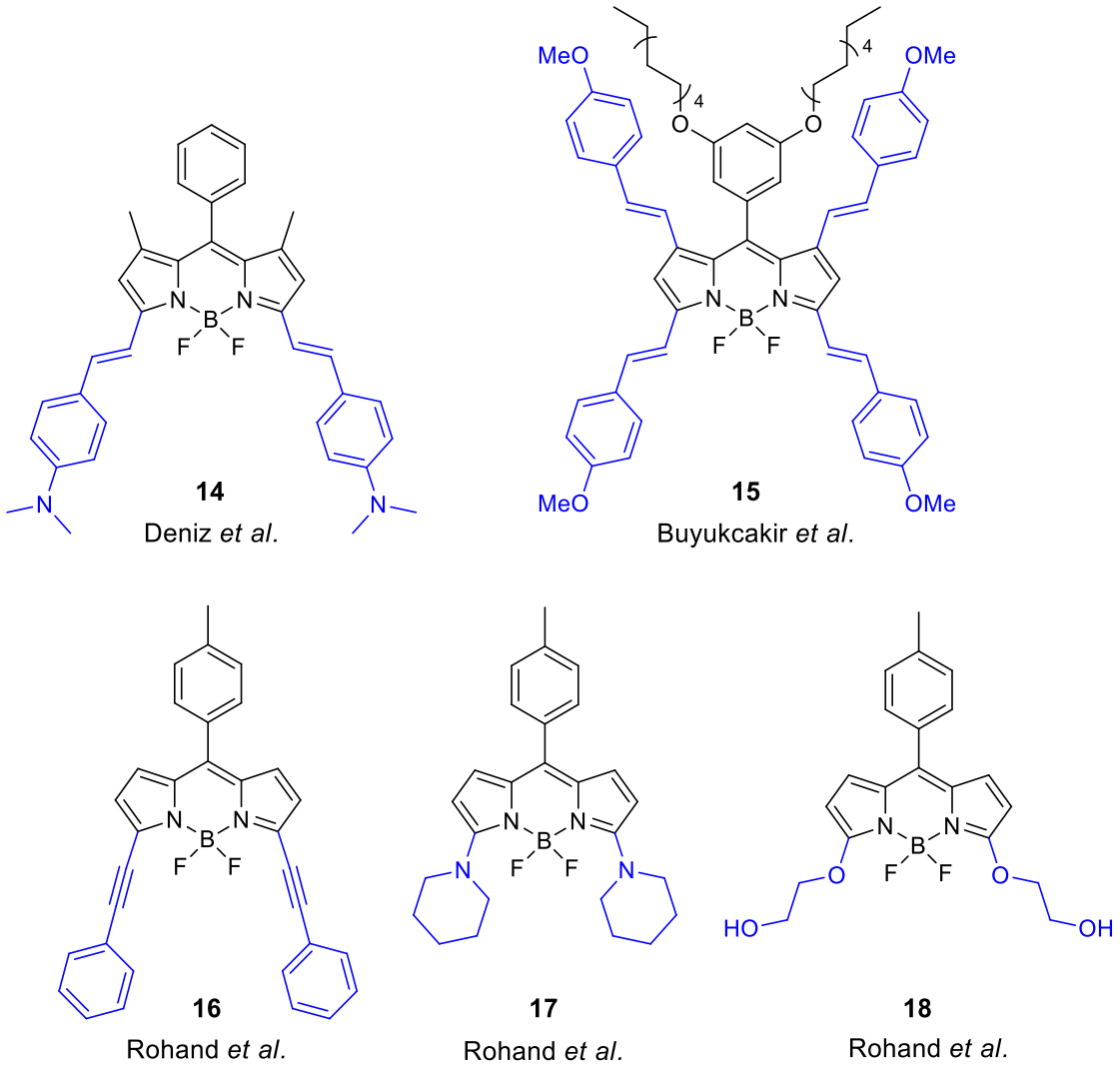

Figure 1.5: Selected examples of 3,5-substituted BODIPY structures: **14**,[94] **15**,[95] **16**,[96] **17**,[97] and **18**.[97]

While carbon- and oxygen-based nucleophiles produce BODIPYs with largely unchanged λ_{max} in the absorbance and emission spectral properties, nitrogen and sulfur with various substituents on the 3,5-positions have been demonstrated to red-shift the emission spectra. All these nucleophiles provided additional functionalities and extended conjugation.[15] Incorporation

of ethynyl, aryl, and styryl groups can be accomplished through palladium-mediated cross-coupling reactions, providing fluorescent probes for a variety of applications.

1.3.3 Functionalization at the 2,6-Positions

The reactivity of the BODIPY core can be predicted based on the resonance structure, as shown in Figure 1.6, where positions 2 and 6 contain the least positive charge. For this reason, they undergo electrophilic aromatic substitution. Different functional groups have been introduced at the 2- and 6-positions via halogenation,[30,98] nitration,[99-100] sulfonation,[15,49,101,22] and formylation.[73] Particularly, the introduction of sulfonate groups increase the BODIPY's water solubility properties for biological purposes (Figure 1.7, structure **19**). Even though sulfonate groups do not make a significance change in the absorption and emission spectra, BODIPYs containing these groups are strongly fluorescent in polar solvents and more stable than their precursors. On the other hand, addition of nitro groups at the 2,6-positions reduces the BODIPY fluorescence quantum yields (Figure 1.7, structure **21**).[99]

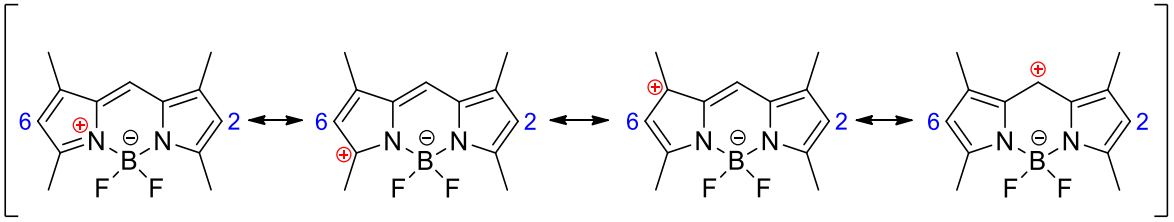

Figure 1.6: Resonance structures of positive charge delocalization through BODIPY core.

Addition of halogen groups (bromide or iodide) at the 2- and 6-positions can cause a significant red shift in the absorption and fluorescence emission maxima of BODIPYs but quench the quantum yield due to the heavy atom effect[16] (Figure 1.7, structure **20**). Furthermore, post-modification on these 2,6-halogenated BODIPYs typically involves through palladium-mediated cross-couplings, such as Suzuki,[102] Stille,[71] Sonagashira,[103] and Heck reactions.[104]

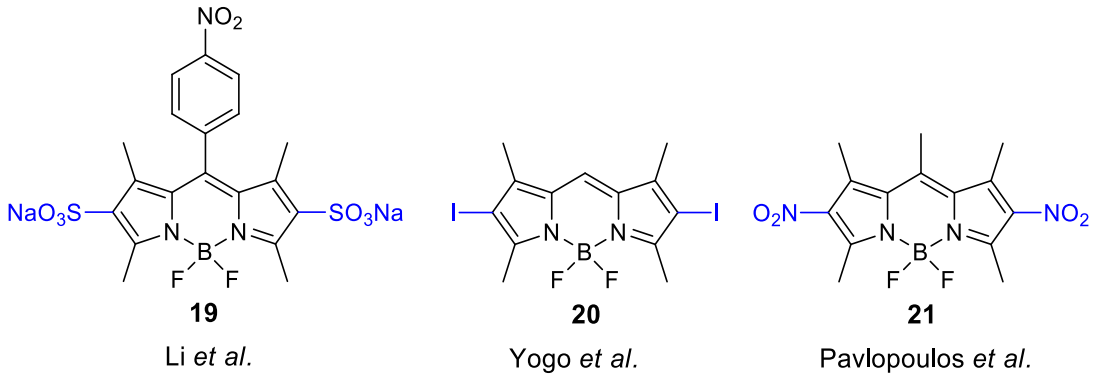

Figure 1.7: Selected examples of 2,6-functionalized BODIPY structures: **19**,[49] **20**,[30] and **21**.[99]

1.3.4 Modifications at the Boron Center

Boron-substituted BODIPYs have been of increased interest in the past few years. Many researches have investigated the increase in stability of BODIPYs, their redox properties, Stokes shifts, and development of donor-acceptor systems. There are many demonstrations using carbon nucleophiles to replace the fluoride atoms (Figure 1.8). The first example of 4,4-dialkyl-BODIPYs were synthesized via the reaction of dipyrromethenes with boron-alkyl compounds.[105] Alternatively, Ziessel and coworkers[34,101,106-111] investigated the synthesis of 4,4-dialkyl-, 4,4-diaryl-, and 4,4-diethynyl-BODIPYs by Grignard and organolithium methods. These modifications at the boron center can be used for synthesizing new BODIPY-based dyads and cascade-type dyes. These *B*-aryl BODIPYs have larger Stokes shifts compared to their BF_2 parents. Cyano groups can replace the fluoride atoms using trimethylsilyl cyanide in high yields in the presence of a Lewis acid.[15] Cyano substituents on the boron center enhance the fluorescence quantum yields and stability of BODIPYs. Recently, Ankush and coworkers[112] reported a new method to introduce ethyl groups directly onto the boron center in high yields via treating BODIPY with Et_2AlCl (Figure 1.8, structure **26**). They also compared their method to the Grignard method and reported that their method is more efficient.

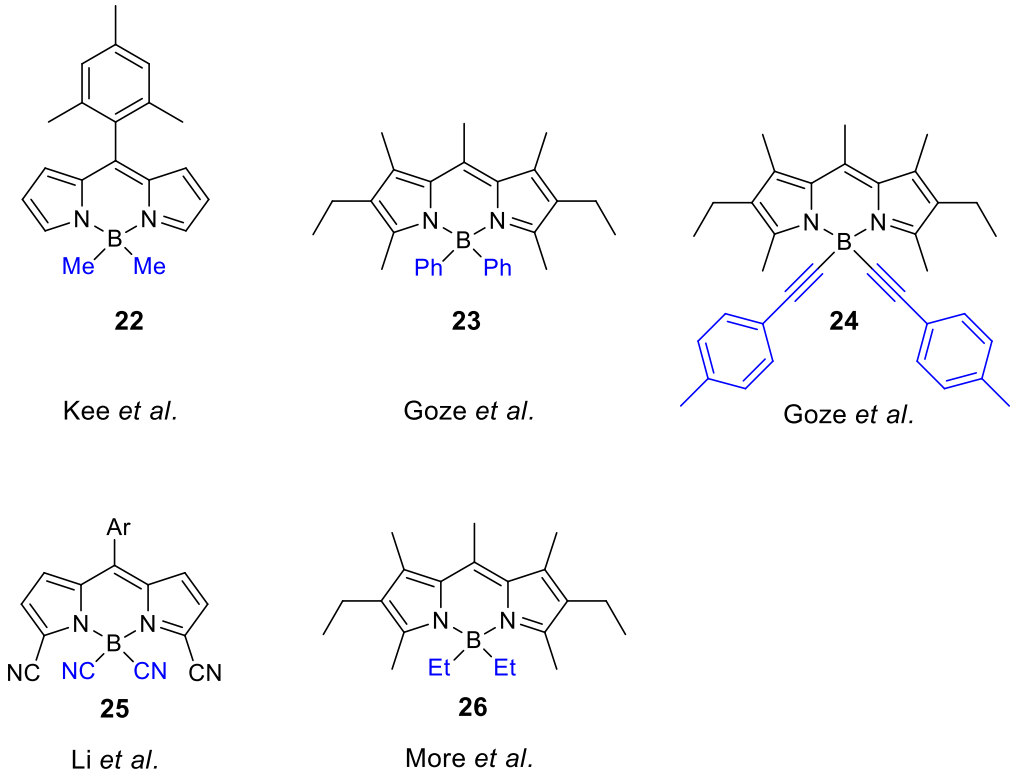

Figure 1.8: Selected examples of 4,4-dialky-, 4,4-diaryl-, and 4,4-diethynyl-BODIPYs: **22**,[105] **23**,[106] **24**,[108] **25**,[15] and **26**.[112]

While carbon-substituted BODIPYs are used for increasing the Stokes shift and stability, oxygen groups on the boron atom increase the BODIPY aqueous solubility. In 1999, Burgess and coworkers demonstrated the first oxygen substitution on the boron center by intramolecular cyclization of 3,5-dihydroxy-ortho phenyl.[113] Since then, a series of 4,4-dialkoxy- and diaryloxy-BODIPYs were synthesized either by refluxing with sodium alkoxide[114] in alcohol or with alcohols mediated by Lewis acid[53] (Figure 1.9, **28** and **29**). On the other hand, Courtis and coworkers[115] focused on the synthesis of mono-alkoxy BODIPYs to be used for bioimaging application.

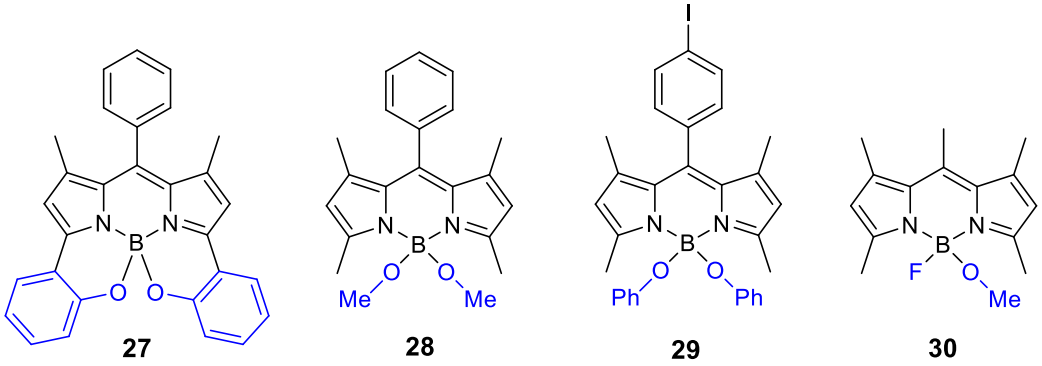

Figure 1.9: Selected examples of 4,4-dialkoxy-BODIPYs: **27**,[113] **28**,[114] **29**,[53] and **30**.[115]

1.3.5 Ring Fusion to the BODIPY core

In the last few decades, the development of compounds emitting in the red and NIR ranges became a focus of research for bioanalytical and optoelectrical imaging applications. Fluorescent organic dyes in the red and near-IR regions are important biomarker tools in DNA sequencing, gel electrophoresis, *in vivo* imaging, and tissue perfusion.[101] In order to reach this longer wavelength (lower energy), extended conjugation via ring fusion became an efficient way to move forward.[116-118] Different approaches were applied for formation of the ring such as aryl-fused pyrroles, 2-acetylphenols,[111] and retro-Diels-Alder (rDA) syntheses of norbornane pyrroles (Figure 1.10).[119-120] Recently, Uppal and coworkers[121] demonstrated aromatization of bicyclohexanyl BODIPY using DDQ as the oxidant agent. Ring fusion provides a red-shifted, sharper fluorescence emission and high fluorescence quantum yields due to the rigidification, which inhibits the rotation of the aromatic groups.

1.4 Applications of BODIPY Dyes

There is a growing demand for new organic fluorophores that are capable of improving the luminescence, electrochemical, and fluorescence properties in all aspects of life sciences. BODIPY dyes have the desired framework and photophysical properties to meet those demands. There are many attractive applications that BODIPYs are involved in, including tunable dyes, environmental

fluorescent indicators, enzyme substrates, fluorescent pH probes, bioimaging, electroluminescent devices, donor-acceptor energy transfer cassettes, fluorescent chemosensors, light-emitting and ion signaling devices, and photosensitizer agents for photodynamic therapy (PDT) of cancer (Figure 1.11).

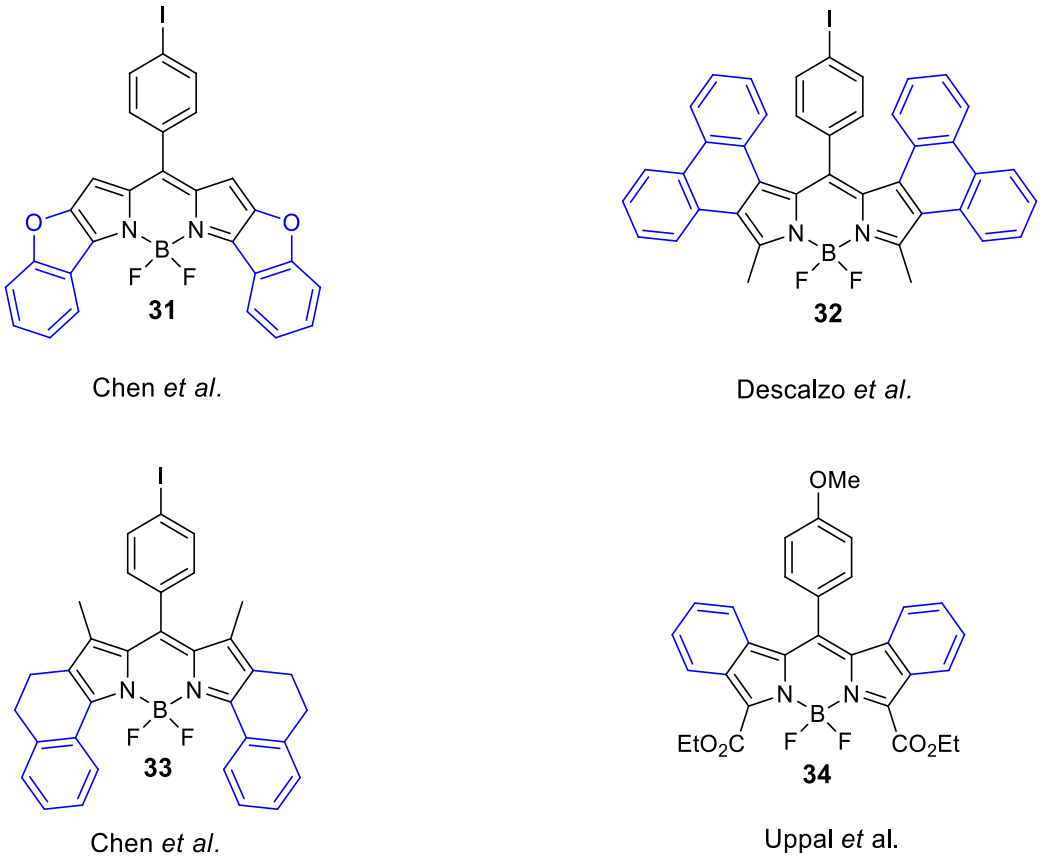

Figure 1.10: Selected examples of 1,3,5,7-BODIPY structures: **32**,[122] **33**,[123] **34**.[122]

1.4.1 Biological Applications

BODIPY compounds, as fluorophores, have become versatile visualization dyes in recent years due to the capability for biological tagging to various desired analytes (proton and metal-bind ions) and to enzymes, polypeptides, proteins, and nucleic acids in DNA. For example, many organic fluorescent dyes have been used for *in vivo* imaging and for binding with a non-radioactive ligand in biological intracellular processes.[101] Due to the recent advancement in bioanalytical and

optoelectrical imaging, rising effort for development of fluorescence dyes in the red and NIR region (600-900 nm) has become more important than ever for application in molecular imaging.

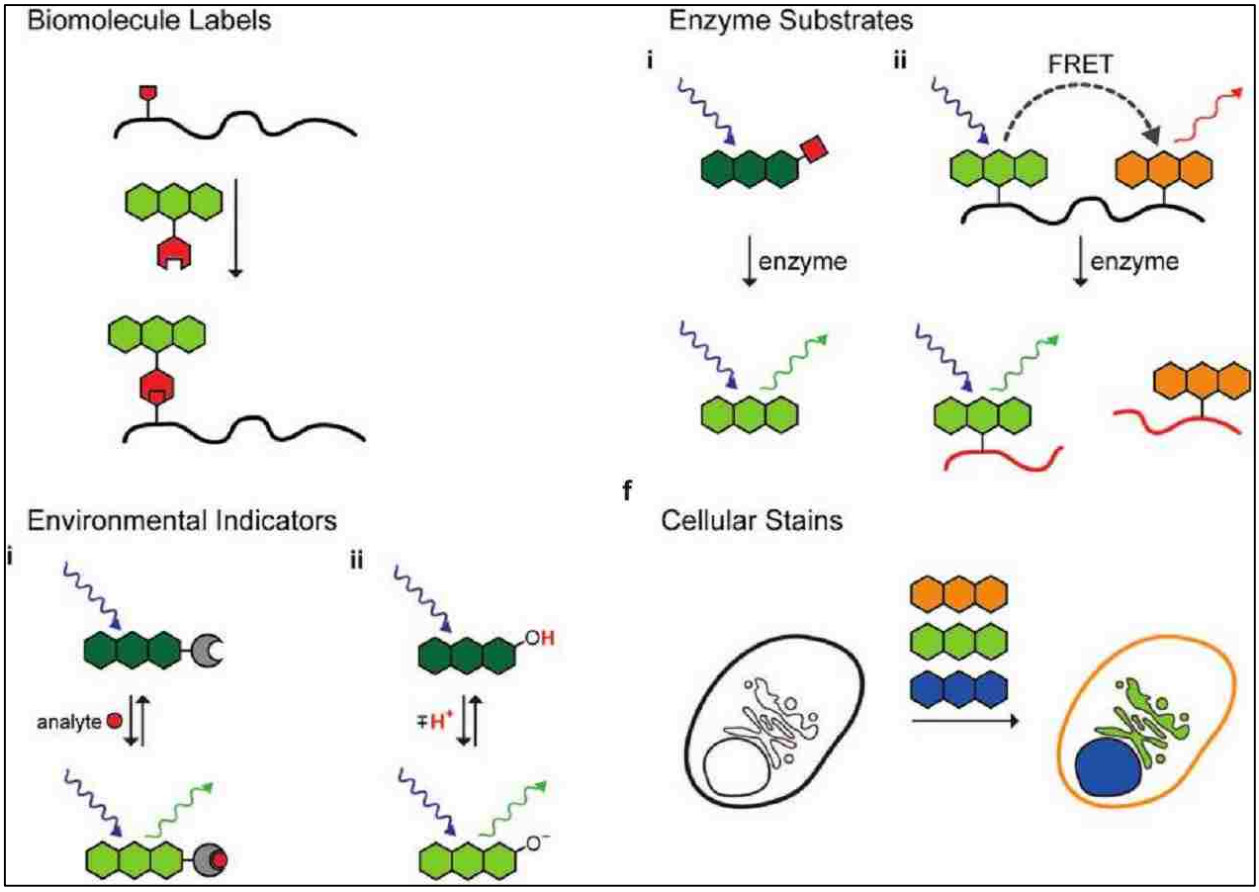

Figure 1.11: Several biological applications of molecular fluorescent probes.[124] Reprint with permission from [124] Copyright (2008) American Chemical Society.

Fluorophores excited and emitting in the red/NIR region of the spectrum provided many advantages. One advantage is that fluorescent dyes in this region can afford significant light penetration and elimination of light scattering, typically caused by endogenous chromophores found in the biological issues. For example, many endogenous chromophores such as nucleic acids, aromatic amino acids, oxy- and deoxy-hemoglobin and chemicals in fluorescene microscopy faced a phenomenon known as tissue autofluorescence. These chromophores usually absorb and emit at short wavelengths, in turn resulting in only minimal penetration depth (Figure 1.12). By introducing fluorophores that can absorb and emit at longer wavelengths, a majority of background

noise can be eliminated, minimizing the autofluorescence which causes problems in the detection and quantification of biological signals.[8,59] Another advantage is the absorption coefficient, which for NIR dyes is drastically lower than other shorter wavelength dyes. As a result, it helps deeper penetration in tissues up to several centimeters.[4]

The low background noise and light scattering in the NIR region are significantly reduced based on the equation describing that the scattering intensity is proportional to the inverse fourth power of the wavelength. This also results in high signal to noise ratio (SNR) thus affording highly sensitivity in detection. In addition, long wavelength light also provides low interference in the Raman scattering and prevents degradation of the sample. There are numerous features for an ideal NIR absorber to be constructed as a fluorescent probe and indicator: photo- and chemo-stability, high molar absorption coefficients, high fluorescence quantum yields, high solubility in aqueous media, and resistance to self-quenching.[1]

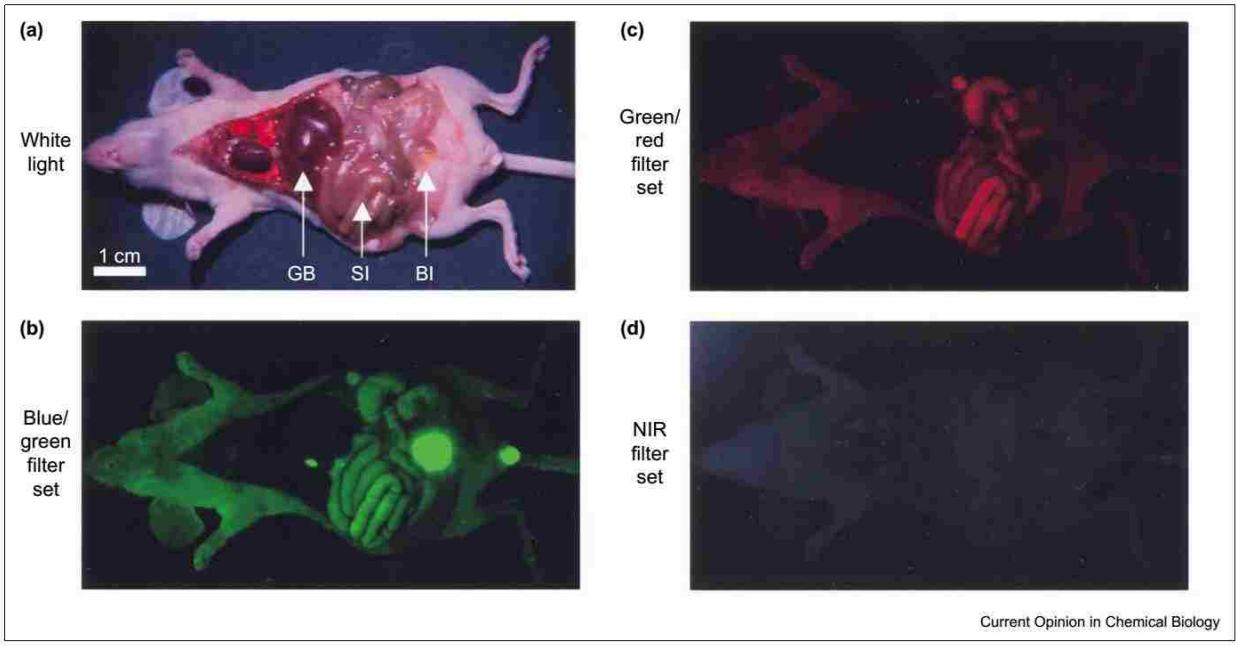

Figure 1.12: Mouse's vital organs and BODIPY fluids autofluorescence with different excitation/emission filters.[125] a) no filter; b) blue/green (460-500nm/505-560nm) filter; c) green/red (525-555nm/590-650 nm) filter; d) NIR (725-775nm/790-830nm) filter. GB = gall bladder, SI = small intestine, BL = bladder. Reprinted with permission from [125] Copyright (2002) Elsevier.

In addition to BODIPYs, other organic dyes such as porphyrin, phthalocyanine, cyanine, fluorescein, and squaraine with high photostability and long wavelength absorption and emission maxima have been extensively investigated and have made great contributions to the science field in the last several decades (Table 1.1). However, these fluorophore dyes have a few limitations, including low fluorescence quantum yields, poor photo- and chemo-stabilities, and also low solubility in aqueous media. To date, only indocyanine green (depited as IDG in Table 1.1) is FDA and EMA-approved as a NIR bioimaging dye to be used for biomedical purposes due to its nontoxic and minimal side effects, as an angiographic contrast agent. However, this dye has a low quantum yield, similar to its parent cyanine dye, and lacks functionalization for additional conjugation to biomolecules.[126] On the other hand, one emerging promising NIR-fluorescent imaging dye is IR Dye®800CW (Table 1.1). This dye has an activated CO_2H group that has the ability to react with biomolecules.[127] This dye is currently in pre-clinical trials.

While many other organic fluorophore dyes have shortcomings, BODIPY dyes process a number of interesting characteristics that make them suitable for applications as indicators, probe sensors, biolabels and stains. Thus, distinct features such as sharp, narrow absorption and emission spectra (for multicolor imaging), not prone to solvent polarity, high molar absorption coefficients, tunability, solubility, and stability make BODIPY the potential fluorophore.

Table 1.1: Commercially available NIR compounds for biomolecular conjugation with absorption and emission wavelength in the NIR region.

Dye name (Manufacturer)	Chemical Structure	Absorption Max (nm)	Emission Max (nm)
ICG (Sigma Aldrich)	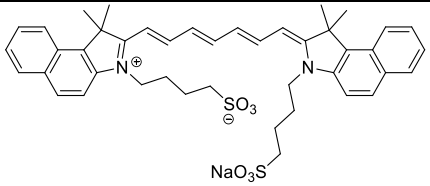	800	810

(Table 1.1 continued)

Dye name (Manufacturer)	Chemical Structure	Absorption Max (nm)	Emission Max (nm)
IRDye 800CW NHS Ester (LI-COR Biosciences)	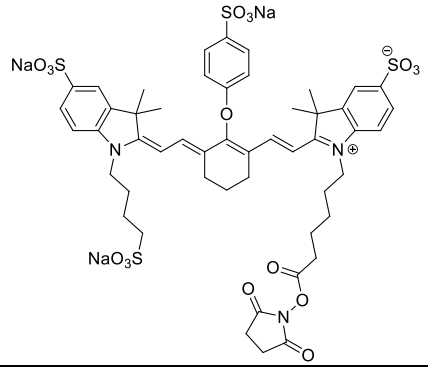	778	794
Dye 783 NHS Ester (Dyomics GmbH.)	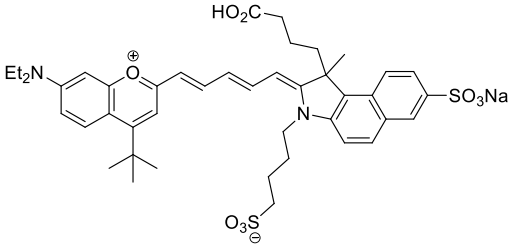	783	800
La Jolla Blue (Hyperion, Inc.)	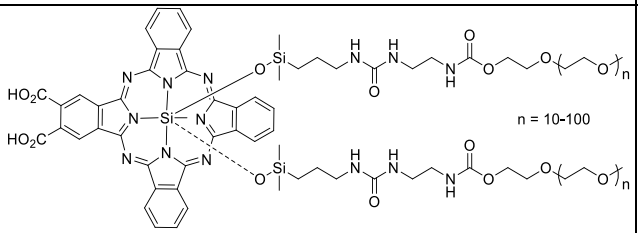	680	700
BODIPY 630/650-X Succinimidyl Ester (Life Technologies Inc.)	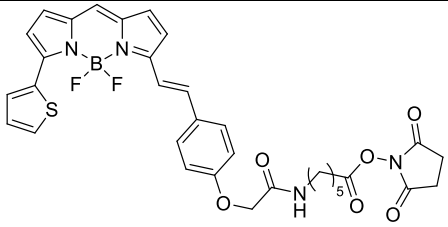	625	640
BODIPY 650/665-X Succinimidyl Ester (Life Technologies, Inc.)	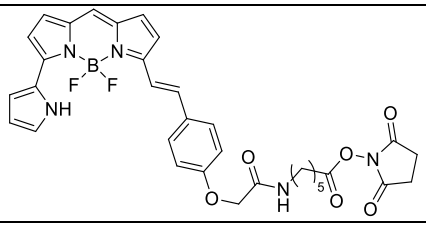	646	660

1.4.2 Cellular Stains

In the microbial world, cellular visualization is an important tool that can provide significant information in studying the physiological and pathological processes of organelles.

Cells that are inked with specific stains have the ability to permeate through cell membranes and allow visibility under the lens of a high powered microscope. Numerous BODIPYs conjugated to various biomolecules have been used for *in vivo* and *in vitro* visualization of intracellular processes. These are commercially available BODIPYs from Life Technologies, Inc, being used for imaging of the endoplasmic reticulum and Golgi apparatus (Table 1.1).

1.4.3 Environmental Indicators

In the last few years, there has been a wide range of development fluorescent chemosensors to use as probes for intracellular pH and metal ions probes (Figure 1.13). The design factors for selective and sensitive sensors are: i) fluorophore-spacer-chelator or ii) intrinsic fluorescent chelators. The two processes that contribute to the fluorophore-spacer-chelator are photoinduced electron transfer (PET) and photoinduced intramolecular charge transfer (ICT). The fluorescent probes are designed based on the idea that the fluorophore and chelator are separated by a short aliphatic spacer in order to diminish the electronic interaction between the fluorophore and the chelator. For example, a chelator on the *meso*-aryl substituent does not interact with the fluorophore due to its perpendicular orientation geometry. PET is the process where the electron-transfer from the electron-donor chelator in the HOMO to the lower HOMO level of the electron-acceptor fluorophore. ICT is the process of internal charge transfer (upon photo-excitation) between an electron-withdrawing group that is conjugated to an electron-donating group of the fluorophore.

1.4.4 Enzyme Substrates

There are strategies for investigating enzymatic activity in live cells. Numerous systems and conjugates have been developed consisting of a BODIPY fluorescent dye conjugated to fatty acids, phospholipids, receptor ligands, and cholesterol for investigating enzymatic activities in

fluorometric assays. The BODIPY fluorophore has been investigated in fluorometric assays to study proteases using a useful tool, fluorescence resonance energy transfer (FRET). When the fluorescent dye binds to protease, it results in a no fluorescence due to the "self-quenching" effect. In the presence of the protease enzyme, it hydrolyzes the conjugated fragments and the fluorescence is restored due to the disruption from intramolecular FRET quenching. The enzymatic cleavage is correlated to the simple on/off fluorescent phenomenon, which in turn results in providing the simple and continuum assays for various proteases.

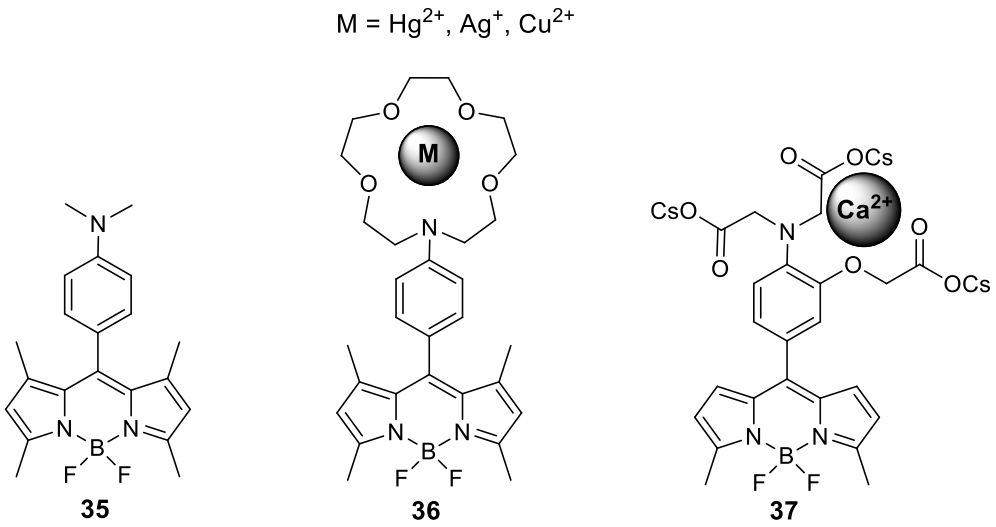

Figure 1.13: Selected examples of *meso*-functionalized BODIPYs as pH and metal ions probes.

Jones and coworkers[128] in 1997 reported two BODIPYs conjugated with casein to study protease enzymatic activity. Recently in 2009, Saba and coworkers[129] demonstrated that BODIPY conjugated to a sphingosine-1-phosphate lyase (SPL) substrate is able to replace the standard radioactive SPL assays (Figure 1.14, **38** and **39**). The BODIPY-labeled SPL provided an efficient way to measure SPL activity in cell tissues.

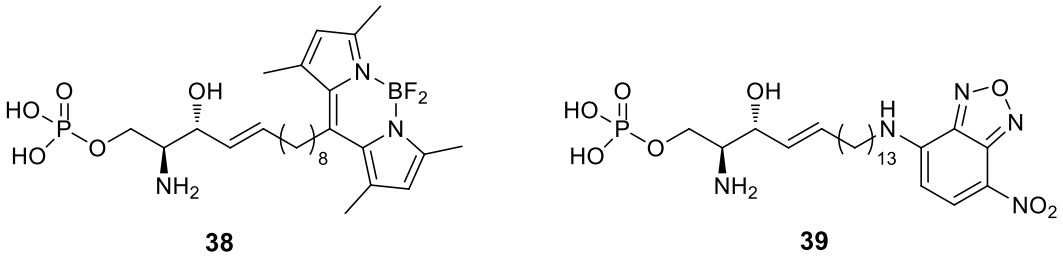

Figure 1.14: BODIPY-S1P **38** and NBD-S1P **39** containing sphingosine.[129]

1.4.5 Biological Labels

Biological labeling has become one of the most common methods used for bioanalytical techniques, particularly in using fluorescent compounds with excellent electronic properties in the UV to the NIR regions. The search for new fluorescent dyes that are capable of easing the way to visualize the function of enzymes, proteins, DNA, and other biomolecules in intracellular processes is undergoing rapid development. BODIPY dyes are a promising target for fluorescent probes and labels due to their remarkable photophysical properties and low cellular toxicities.[59] The small framework size and low molecular weight of BODIPY makes it a good candidate to increase cell permeability for intracellular studies without drastic changes in their biological functions. There are many reports indicating that BODIPYs are used as fluorescent labels to conjugate to specific biological components, such as polylipids, various amino acids, DNA and RNA, dextran, polystyrene micropheres, and proteins.[130-134] In order to attach to a particular biomolecule, the BODIPY dyes must contain a reactive functionalized group: terminal carboxylic acid and sulfonic acids (Figure 1.15).[5] One of the most useful applications of BODIPY dyes is in gel electrophoresis and DNA sequencing, in which BODIPY is conjugated to oligonucleotides and it displays a minimal effect on the DNA fragment mobility.[135] BODIPY-based fluorescent compounds have found uses in HPLC and capillary electrophoresis, especially when it is bound to cysteine residues in proteins.

1.5 Research Outlook

There are numerous efforts on the synthesis and development of functionalized BODIPYs for various applications, as biological probes in the NIR region (>700 nm), and as radioactive agents for positron emission tomography (PET) or SPECT. Thus, there is still much work needed to be done on improving the electronic properties of BODIPY dyes. In addition, there are still new demands for versatile fluorophores with enhanced water solubility and high quantum yields for cellular studies.

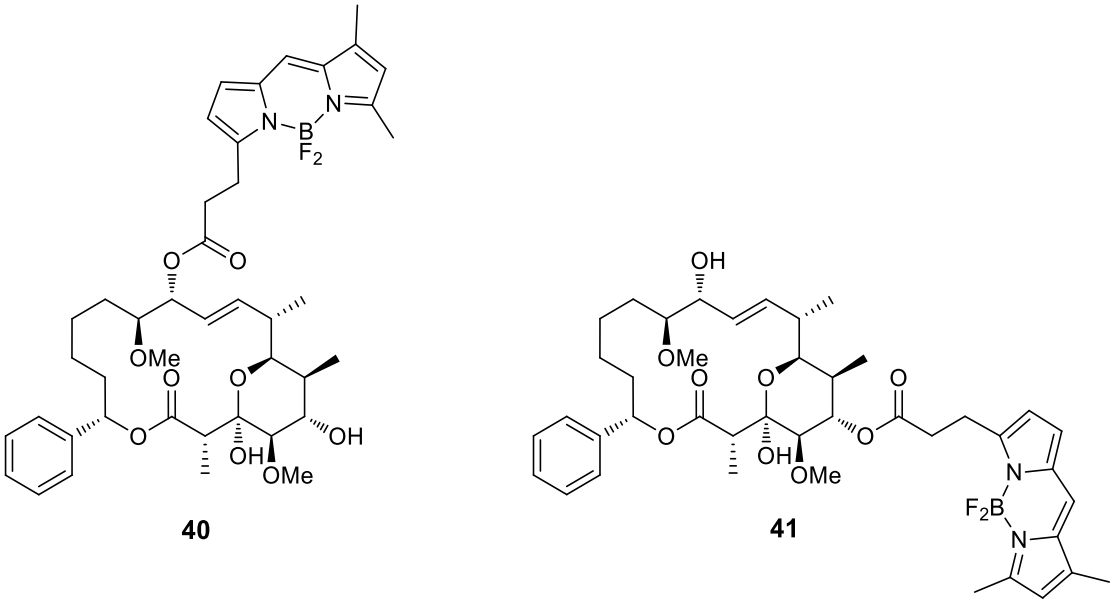

Figure 1.15: Soraphen A derivatives **40** and **41** conjugated to BODIPY.[78]

1.6 References

1. Boens, N.; Leen, V.; Dehaen, W., Fluorescent indicators based on BODIPY. *Chem. Soc. Rev.* **2012**, *41*, 1130-1172.

2. Escobedo, J. O.; Rusin, O.; Lim, S.; Strongin, R. M., NIR Dyes for Bioimaging Applications. *Curr. Opin. Chem. Biol.* **2010**, *14*, 64-70.

3. Ntziachristos, V.; Bremer, C.; Weissleder, R., Fluorescence Imaging with Near-Infrared Light: New Technological Advances that Enable In Vivo Molecular Imaging. *Eur. Radiol.* **2003**, *13*, 195-208.

4. Amiot, C. L.; Xu, S.; Liang, S.; Pan, L.; Zhao, J. X., Near-Infrared Fluorescent Materials for Sensing of Biological Targets. *Sensors* **2008**, *8*, 3082-3105.

5. Niu, S. L.; Massif, C.; Ulrich, G.; Ziessel, R.; Renard, P. Y.; Romieu, A., Water-Solubilisation and Bio-Conjugation of a Red-Emitting BODIPY Marker. *Org. Biomol. Chem.* **2011**, *9*, 66-69.

6. Ulrich, G.; Ziessel, R.; Harriman, A., The Chemistry of Fluorescent BODIPY Dyes: Versatility Unsurpassed. *Angew. Chem. Int. Ed.* **2008**, *47*, 1184-1201.

7. Wang, Y. W.; Descalzo, A. B.; Shen, Z.; You, X. Z.; Rurack, K., Dihydronaphthalene-Fused Boron-Dipyrromethene (BODIPY) Dyes: Insight into the Electronic and Conformational Tuning Modes of BODIPY Fluorophores. *Chem. Eur. J.* **2010**, *16*, 2887-2903.

8. Descalzo, A. B.; Xu, H. J.; Shen, Z.; Rurack, K., Red/Near-Infrared Boron-Dipyrromethene Dyes as Strongly Emitting Fluorophores. *Ann. N.Y. Acad. Sci.* **2008**, *1130*, 164-171.

9. Harreus, A. L., Pyrrole. In *Ullmann's Encyclopedia of Industrial Chemistry*, Wiley-VCH Verlag GmbH & Co. KGaA: 2000.

10. Tram, K.; Yan, H.; Jenkins, H. A.; Vassiliev, S.; Bruce, D., The Synthesis and Crystal Structure of Unsubstituted 4,4-Difluoro-4-bora-3a,4a-diaza-*s*-indacene (BODIPY). *Dyes Pigm.* **2009**, *82*, 392-395.

11. Zheng, Q.; Xu, G.; Prasad, P. N., Conformationally Restricted Dipyrromethene Boron Difluoride (BODIPY) Dyes: Highly Fluorescent, Multicolored Probes for Cellular Imaging. *Chem. Eur. J.* **2008**, *14*, 5812-5819.

12. Qin, W.; Baruah, M.; De Borggraeve, W. M.; Boens, N., Photophysical Properties of an On/Off Fluorescent pH Indicator Excitable with Visible Light Based on a Borondipyrromethene-Linked Phenol. *J. Photochem. Photobiol. A* **2006**, *183*, 190-197.

13. Arroyo, I. J.; Hu, R.; Merino, G.; Tang, B. Z.; Pena-Cabrera, E., The Smallest and One of the Brightest. Efficient Preparation and Optical Description of the Parent Borondipyrromethene System. *J. Org. Chem.* **2009**, *74*, 5719-5722.

14. Schmitt, A.; Hinkeldey, B.; Wild, M.; Jung, G., Synthesis of the Core Compound of the BODIPY Dye Class: 4,4'-Difluoro-4-bora-(3a,4a)-diaza-*s*-indacene. *J. Fluoresc.* **2009**, *19*, 755-758.

15. Li, L.; Nguyen, B.; Burgess, K., Functionalization of the 4,4-Difluoro-4-bora-3a,4a-diaza-*s*-indacene (BODIPY) Core. *Bioorg. Med. Chem. Lett.* **2008**, *18*, 3112-3116.

16. Loudet, A.; Burgess, K., BODIPY Dyes and Their Derivatives: Syntheses and Spectroscopic Properties. *Chem. Rev.* **2007**, *107*, 4891-4932.

17. Thivierge, C.; Bandichhor, R.; Burgess, K., Spectral Dispersion and Water Solubilization of BODIPY Dyes via Palladium-Catalyzed C−H Functionalization. *Org. Lett.* **2007**, *9*, 2135-2138.

18. Meng, G.; Velayudham, S.; Smith, A.; Luck, R.; Liu, H. Y., Color Tuning of Polyfluorene Emission with BODIPY Monomers. *Macromolecules* **2009**, *42*, 1995-2001.

19. Benniston, A. C.; Copley, G., Lighting the Way Ahead with Boron Dipyrromethene (BODIPY) dyes. *Phys. Chem. Chem. Phys.* **2009**, *11*, 4124-4131.

20. Hu, R. R.; Lager, E.; Aguilar-Aguilar, A.; Liu, J. Z.; Lam, J. W. Y.; Sung, H. H. Y.; Williams, I. D.; Zhong, Y. C.; Wong, K. S.; Pena-Cabrera, E.; Tang, B. Z., Twisted Intramolecular Charge Transfer and Aggregation-Induced Emission of BODIPY Derivatives. *J. Phys. Chem. C* **2009**, *113*, 15845-15853.

21. Treibs, A.; Kreuzer, F.-H., Difluorboryl-Komplexe von Di- und Tripyrrylmethenen. *Justus Liebigs Annalen der Chemie* **1968**, *718*, 208-223.

22. Wories, H. J.; Koek, J. H.; Lodder, G.; Lugtenburg, J.; Fokkens, R.; Driessen, O.; Mohn, G. R., A Novel Water-Soluble Fluorescent-Probe: Synthesis, Luminescence and Biological Properties of the Sodium-Salt of the 4-Sulfonato-3,3',5,5'-Tetramethyl-2,2'-Pyrromethen-1,1'-BF_2 Complex. *Recueil Des Travaux Chimiques Des Pays-Bas-Journal of the Royal Netherlands Chemical Society* **1985**, *104*, 288-291.

23. Li, Z.; Mintzer, E.; Bittman, R., First Synthesis of Free Cholesterol-BODIPY Conjugates. *J. Org. Chem.* **2006**, *71*, 1718-1721.

24. Meng, Q.; Kim, D. H.; Bai, X.; Bi, L.; Turro, N. J.; Ju, J., Design and Synthesis of a Photocleavable Fluorescent Nucleotide 3'-*O*-Allyl-dGTP-PC-BODIPY-FL-510 as a Reversible Terminator for DNA Sequencing by Synthesis. *J. Org. Chem.* **2006**, *71*, 3248-3252.

25. Merino, E. J.; Weeks, K. M., Facile Conversion of Aptamers into Sensors Using a 2'-Ribose-Linked Fluorophore. *J. Am. Chem. Soc.* **2005**, *127*, 12766-12767.

26. Peters, C.; Billich, A.; Ghobrial, M.; Hogenauer, K.; Ullrich, T.; Nussbaumer, P., Synthesis of Borondipyrromethene (BODIPY)-Labeled Sphingosine Derivatives by Cross-metathesis Reaction. *J. Org. Chem.* **2007**, *72*, 1842-1845.

27. Bura, T.; Retailleau, P.; Ulrich, G.; Ziessel, R., Highly Substituted BODIPY Dyes with Spectroscopic Features Sensitive to the Environment. *J. Org. Chem.* **2011**, *76*, 1109-1117.

28. Erbas, S.; Gorgulu, A.; Kocakusakogullari, M.; Akkaya, E. U., Non-Covalent Functionalized Swnts as Delivery Agents for Novel BODIPY-Based Potential PDT Sensitizers. *Chem. Commun.* **2009**, 4956-4958.

29. He, H.; Lo, P. C.; Yeung, S. L.; Fong, W. P.; Ng, D. K., Synthesis and in Vitro Photodynamic Activities of Pegylated Distyryl Boron Dipyrromethene Derivatives. *J. Med. Chem.* **2011**, *54*, 3097-3102.

30. Yogo, T.; Urano, Y.; Ishitsuka, Y.; Maniwa, F.; Nagano, T., Highly Efficient and Photostable Photosensitizer Based on BODIPY Chromophore. *J. Am. Chem. Soc.* **2005**, *127*, 12162-12163.

31. Li, F.; Yang, S. I.; Ciringh, Y.; Seth, J.; Martin, C. H.; Singh, D. L.; Kim, D.; Birge, R. R.; Bocian, D. F.; Holten, D.; Lindsey, J. S., Design, Synthesis, and Photodynamics of Light-Harvesting Arrays Comprised of a Porphyrin and One, Two, or Eight Boron-Dipyrrin Accessory Pigments. *J. Am. Chem. Soc.* **1998**, *120*, 10001-10017.

32. Loudet, A.; Bandichhor, R.; Wu, L.; Burgess, K., Functionalized BF_2 Chelated Azadipyrromethene Dyes. *Tetrahedron* **2008**, *64*, 3642-3654.

33. Tan, K.; Jaquinod, L.; Paolesse, R.; Nardis, S.; Di Natale, C.; Di Carlo, A.; Prodi, L.; Montalti, M.; Zaccheroni, N.; Smith, K. M., Synthesis and Characterization of β-Fused Porphyrin-BODIPY® Dyads. *Tetrahedron* **2004**, *60*, 1099-1106.

34. Ulrich, G.; Goze, C.; Guardigli, M.; Roda, A.; Ziessel, R., Pyrromethene Dialkynyl Borane Complexes for "Cascatelle" Energy Transfer and Protein Labeling. *Angew. Chem. Int. Ed.* **2005**, *44*, 3694-3698.

35. Coskun, A.; Akkaya, E. U., Ion Sensing Coupled to Resonance Energy Transfer: A Highly Selective and Sensitive Ratiometric Fluorescent Chemosensor for Ag(I) by a Modular Approach. *J. Am. Chem. Soc.* **2005**, *127*, 10464-10465.

36. Krumova, K.; Oleynik, P.; Karam, P.; Cosa, G., Phenol-Based Lipophilic Fluorescent Antioxidant Indicators: A Rational Approach. *J. Org. Chem.* **2009**, *74*, 3641-3651.

37. Peng, X.; Du, J.; Fan, J.; Wang, J.; Wu, Y.; Zhao, J.; Sun, S.; Xu, T., A Selective Fluorescent Sensor for Imaging Cd^{2+} in Living Cells. *J. Am. Chem. Soc.* **2007**, *129*, 1500-1501.

38. Wang, J.; Qian, X., A Series of Polyamide Receptor Based PET Fluorescent Sensor Molecules: Positively Cooperative Hg^{2+} Ion Binding with High Sensitivity. *Org. Lett.* **2006**, *8*, 3721-3724.

39. Yuan, M.; Zhou, W.; Liu, X.; Zhu, M.; Li, J.; Yin, X.; Zheng, H.; Zuo, Z.; Ouyang, C.; Liu, H.; Li, Y.; Zhu, D., A Multianalyte Chemosensor on a Single Molecule: Promising Structure for an Integrated Logic Gate. *J. Org. Chem.* **2008**, *73*, 5008-5014.

40. Zeng, L.; Miller, E. W.; Pralle, A.; Isacoff, E. Y.; Chang, C. J., A Selective Turn-On Fluorescent Sensor for Imaging Copper in Living Cells. *J. Am. Chem. Soc.* **2006**, *128*, 10-11.

41. Chen, T.; Boyer, J. H.; Trudell, M. L., Synthesis of 2,6-Diethyl-3-methacroyloxymethyl-1,5,7,8-tetramethylpyrromethene-BF_2 for the Preparation of New Solid-State Laser Dyes. *Heteroat. Chem.* **1997**, *8*, 51-54.

42. Mula, S.; Ray, A. K.; Banerjee, M.; Chaudhuri, T.; Dasgupta, K.; Chattopadhyay, S., Design and Development of a New Pyrromethene Dye with Improved Photostability and Lasing

Efficiency: Theoretical Rationalization of Photophysical and Photochemical Properties. *J. Org. Chem.* **2008**, *73*, 2146-2154.

43. Sathyamoorthi, G.; Wolford, L. T.; Haag, A. M.; Boyer, J. H., Selective Side-Chain Oxidation of Peralkylated Pyrromethene-BF_2 Complexes. *Heteroat. Chem.* **1994**, *5*, 245-249.

44. Ziessel, R.; Ulrich, G.; Harriman, A., The chemistry of BODIPY: A New El Dorado for Fluorescence Tools. *New J. Chem.* **2007**, *31*, 496-501.

45. Kamkaew, N.; Norman Scholfield, C.; Ingkaninan, K.; Taepavarapruk, N.; Chootip, K., Bacopa Monnieri Increases Cerebral Blood Flow in Rat Independent of Blood Pressure. *Phytother. Res.* **2013**, *27*, 135-138.

46. Turan, I. S.; Cakmak, F. P.; Yildirim, D. C.; Cetin-Atalay, R.; Akkaya, E. U., Near-IR Absorbing BODIPY Derivatives as Glutathione-Activated Photosensitizers for Selective Photodynamic Action. *Chem. Eur. J.* **2014**, *20*, 16088-16092.

47. Wagner, R. W.; Lindsey, J. S., Boron-Dipyrromethene Dyes for Incorporation in Synthetic Multi-Pigment Light-Harvesting Arrays. *Pure Appl. Chem.* **1996**, *68*, 1373-1380.

48. Jiao, L. J.; Li, J. L.; Zhang, S. Z.; Wei, C.; Hao, E. H.; Vicente, M. G. H., A Selective Fluorescent Sensor for Imaging Cu^{2+} in Living Cells. *New J. Chem.* **2009**, *33*, 1888-1893.

49. Li, L.; Han, J.; Nguyen, B.; Burgess, K., Syntheses and Spectral Properties of Functionalized, Water-Soluble BODIPY Derivatives. *J. Org. Chem.* **2008**, *73*, 1963-1970.

50. Jackson, A. H.; Pandey, R. K.; Rao, K. R. N.; Roberts, E., Reactions on Solid Supports Part II: A Convenient Method for Synthesis of Pyrromethanes Using a Montmorillonite Clay As Catalyst. *Tetrahedron Lett.* **1985**, *26*, 793-796.

51. Bari, S. E.; Iturraspe, J.; Frydman, B., Synthesis of Biliverdins with Stable Extended Conformations. Part II. *Tetrahedron* **1995**, *51*, 2255-2266.

52. Wang, H. J.; Vicente, M. G. H.; Fronczek, F. R.; Smith, K. M., Synthesis and Transformations of 5-Chloro-2,2'-Dipyrrins and Their Boron Complexes, 8-Chloro-BODIPYs. *Chem. Eur. J.* **2014**, *20*, 5064-5074.

53. Tahtaoui, C.; Thomas, C.; Rohmer, F.; Klotz, P.; Duportail, G.; Mely, Y.; Bonnet, D.; Hibert, M., Convenient Method to Access New 4,4-Dialkoxy- and 4,4-Diaryloxy-diaza-*s*-indacene Dyes: Synthesis and Spectroscopic Evaluation. *J. Org. Chem.* **2007**, *72*, 269-272.

54. Sobenina, L. N.; Vasil'tsov, A. M.; Petrova, O. V.; Petrushenko, K. B.; Ushakov, I. A.; Clavier, G.; Meallet-Renault, R.; Mikhaleva, A. I.; Trofimov, B. A., General Route to Symmetric and Asymmetric *meso*-CF_3-3,5-Aryl(hetaryl)- and 3,5-Diaryl(dihetaryl)-BODIPY Dyes. *Org. Lett.* **2011**, *13*, 2524-2527.

55. Nicolaou, K. C.; Claremon, D. A.; Papahatjis, D. P., A Mild Method for the Synthesis of 2-Ketopyrroles from Carboxylic Acids. *Tetrahedron Lett.* **1981**, *22*, 4647-4650.

56. Wallace, D. M.; Leung, S. H.; Senge, M. O.; Smith, K. M., Rational Tetraarylporphyrin Syntheses: Tetraarylporphyrins from the MacDonald Route. *J. Org. Chem.* **1993**, *58*, 7245-7257.

57. Zhao, N.; Vicente, M. G. H.; Fronczek, F. R.; Smith, K. M., Synthesis of 3,8-Dichloro-6-ethyl-1,2,5,7-tetramethyl-BODIPY from an Asymmetric Dipyrroketone and Reactivity Studies at the 3,5,8-Positions. *Chem. Eur. J.* **2015**, *21*, 6181-6192.

58. Uppal, T.; Hu, X.; Fronczek, F. R.; Maschek, S.; Bobadova-Parvanova, P.; Vicente, M. G., Synthesis, Computational Modeling, and Properties of Benzo-Appended BODIPYs. *Chem. Eur. J.* **2012**, *18*, 3893-3905.

59. Jiao, L.; Yu, C.; Uppal, T.; Liu, M.; Li, Y.; Zhou, Y.; Hao, E.; Hu, X.; Vicente, M. G., Long Wavelength Red Fluorescent Dyes from 3,5-Diiodo-BODIPYs. *Org. Biomol. Chem.* **2010**, *8*, 2517-2519.

60. Loudet, A.; Ueno, Y.; Wu, L.; Jose, J.; Barhoumi, R.; Burghardt, R.; Burgess, K., Organelle-Selective Energy Transfer: A Fluorescent Indicator of Intracellular Environment. *Bioorg. Med. Chem. Lett.* **2011**, *21*, 1849-1851.

61. Baruah, M.; Qin, W.; Flors, C.; Hofkens, J.; Vallee, R. A.; Beljonne, D.; Van der Auweraer, M.; De Borggraeve, W. M.; Boens, N., Solvent and pH Dependent Fluorescent Properties of a Dimethylaminostyryl Borondipyrromethene Dye in Solution. *J. Phys. Chem. A* **2006**, *110*, 5998-6009.

62. Atilgan, S.; Ekmekci, Z.; Dogan, A. L.; Guc, D.; Akkaya, E. U., Water Soluble Distyryl-Boradiazaindacenes as Efficient Photosensitizers for Photodynamic Therapy. *Chem. Commun.* **2006**, 4398-4400.

63. Murtagh, J.; Frimannsson, D. O.; O'Shea, D. F., Azide Conjugatable and pH Responsive Near-Infrared Fluorescent Imaging Probes. *Org. Lett.* **2009**, *11*, 5386-5389.

64. Rurack, K.; Kollmannsberger, M.; Daub, J., Molecular Switching in the Near Infrared (NIR) with a Functionalized Boron-Dipyrromethene Dye. *Angew. Chem. Int. Ed.* **2001**, *40*, 385-387.

65. Zhao, W.; Carreira, E. M., Conformationally Restricted Aza-BODIPY: A Highly Fluorescent, Stable, Near-Infrared-Absorbing Dye. *Angew. Chem. Int. Ed.* **2005**, *44*, 1677-1679.

66. Leen, V.; Braeken, E.; Luckermans, K.; Jackers, C.; Van der Auweraer, M.; Boens, N.; Dehaen, W., A Versatile, Modular Synthesis of Monofunctionalized BODIPY Dyes. *Chem. Commun.* **2009**, 4515-4517.

67. Ortiz, M. J.; Garcia-Moreno, I.; Agarrabeitia, A. R.; Duran-Sampedro, G.; Costela, A.; Sastre, R.; Lopez Arbeloa, F.; Banuelos Prieto, J.; Lopez Arbeloa, I., Red-Edge-Wavelength Finely-Tunable Laser Action from New BODIPY Dyes. *Phys. Chem. Chem. Phys.* **2010**, *12*, 7804-7811.

68. Rihn, S.; Retailleau, P.; Bugsaliewicz, N.; Nicola, A. D.; Ziessel, R., Versatile Synthetic Methods for the Engineering of Thiophene-Substituted BODIPY Dyes. *Tetrahedron Lett.* **2009**, *50*, 7008-7013.

69. Rao, M. R.; Mobin, S. M.; Ravikanth, M., Boron-Dipyrromethene Based Specific Chemodosimeter for Fluoride Ion. *Tetrahedron* **2010**, *66*, 1728-1734.

70. Rihn, S.; Retailleau, P.; De Nicola, A.; Ulrich, G.; Ziessel, R., Synthetic Routes to Fluorescent Dyes Exhibiting Large Stokes Shifts. *J. Org. Chem.* **2012**, *77*, 8851-8863.

71. Rohand, T.; Qin, W. W.; Boens, N.; Dehaen, W., Palladium-Catalyzed Coupling Reactions for the Functionalization of BODIPY Dyes with Fluorescence Spanning the Visible Spectrum. *Eur. J. Org. Chem.* **2006**, 4658-4663.

72. Gresser, R.; Hartmann, H.; Wrackmeyer, M.; Leo, K.; Riede, M., Synthesis of Thiophene-Substituted Aza-BODIPYs and Their Optical and Electrochemical Properties. *Tetrahedron* **2011**, *67*, 7148-7155.

73. Jiao, L.; Yu, C.; Li, J.; Wang, Z.; Wu, M.; Hao, E., *β*-Formyl-BODIPYs from the Vilsmeier-Haack Reaction. *J. Org. Chem.* **2009**, *74*, 7525-7528.

74. Ulrich, G.; Ziessel, R., Convenient and Efficient Synthesis of Functionalized Oligopyridine Ligands Bearing Accessory Pyrromethene-BF_2 Fluorophores. *J. Org. Chem.* **2004**, *69*, 2070-2083.

75. Zrig, S.; Remy, P.; Andrioletti, B.; Rose, E.; Asselberghs, I.; Clays, K., Engineering Tuneable Light-Harvesting Systems with Oligothiophene Donors and Mono- or Bis-BODIPY Acceptors. *J. Org. Chem.* **2008**, *73*, 1563-1566.

76. Ziessel, R.; Bonardi, L.; Ulrich, G., Boron Dipyrromethene Dyes: A Rational Avenue for Sensing and Light Emitting Devices. *Dalton Trans.* **2006**, 2913-2918.

77. Wu, L.; Loudet, A.; Barhoumi, R.; Burghardt, R. C.; Burgess, K., Fluorescent Cassettes for Monitoring Three-Component Interactions *in Vitro* and in Living Cells. *J. Am. Chem. Soc.* **2009**, *131*, 9156-9157.

78. Raymer, B.; Kavana, M.; Price, A.; Wang, B.; Corcoran, L.; Kulathila, R.; Groarke, J.; Mann, T., Synthesis and Characterization of a BODIPY-Labeled Derivative of Soraphen A that Binds to Acetyl-Coa Carboxylase. *Bioorg. Med. Chem. Lett.* **2009**, *19*, 2804-2807.

79. Yamada, K.; Toyota, T.; Takakura, K.; Ishimaru, M.; Sugawara, T., Preparation of BODIPY Probes for Multicolor Fluorescence Imaging Studies of Membrane Dynamics. *New J. Chem.* **2001**, *25*, 667-669.

80. Baruah, M.; Qin, W.; Basaric, N.; Borggraeve, W. M. D.; Boens, N., BODIPY-Based Hydroxyaryl Derivatives as Fluorescent pH Probes. *J. Org. Chem.* **2005**, *70*, 4152-4157.

81. Rogers, M. A. T., 2 : 4-Diarylpyrroles. Part I. Synthesis of 2 : 4-Diarylpyrroles and 2 : 2' : 4 : 4'-Tetra-arylazadipyrromethines. *J. Chem. Soc.* **1943**, 590-596.

82. Davies, W. H.; Rogers, M. A. T., 2 : 4-Diarylpyrroles. Part IV. The Formation of Acylated 5-Amino-2 : 4-di-phenylpyrroles from *β*-Benzoyl-*α*-phenylpropionitrile and Some Notes on the Leuckart Reaction. *J. Chem. Soc.* **1944**, 126-131.

83. Knott, E. B., *β*-Cycloylpropionitriles. Part II. Conversion into Bis-2-(5-cyclylpyrrole)azamethin Salts. *J. Chem. Soc.* **1947**, 1196-1201.

84. Allik, T. H.; Hermes, R. E.; Sathyamoorthi, G.; Boyer, J. H., Spectroscopy and Laser Performance of New BF_2-Complex Dyes in Solution. *Proc. SPIE-Int. Soc. Opt. Eng.* **1994**, 240-248.

85. McDonnell, S. O.; O'Shea, D. F., Near-Infrared Sensing Properties of Dimethlyamino-Substituted BF_2-Azadipyrromethenes. *Org. Lett.* **2006**, *8*, 3493-3496.

86. Adarsh, N.; Avirah, R. R.; Ramaiah, D., Tuning Photosensitized Singlet Oxygen Generation Efficiency of Novel Aza-BODIPY Dyes. *Org. Lett.* **2010**, *12*, 5720-5723.

87. Li, Y.; Dolphin, D.; Patrick, B. O., Synthesis of a BF_2 Complex of Indol-2-Yl-isoindol-1-ylidene-amine: A Fully Conjugated Azadipyrromethene. *Tetrahedron Lett.* **2010**, *51*, 811-814.

88. Palma, A.; Tasior, M.; Frimannsson, D. O.; Vu, T. T.; Meallet-Renault, R.; O'Shea, D. F., New On-Bead Near-Infrared Fluorophores and Fluorescent Sensor Constructs. *Org. Lett.* **2009**, *11*, 3638-3641.

89. Yoshii, R.; Nagai, A.; Chujo, Y., Highly Near-Infrared Photoluminescence from Aza-Borondipyrromethene-Based Conjugated Polymers. *J. Polym. Sci. Part A: Polym. Chem.* **2010**, *48*, 5348-5356.

90. Ueno, T.; Urano, Y.; Kojima, H.; Nagano, T., Mechanism-Based Molecular Design of Highly Selective Fluorescence Probes for Nitrative Stress. *J. Am. Chem. Soc.* **2006**, *128*, 10640-10641.

91. Killoran, J.; O'Shea, D. F., Impact of a Conformationally Restricted Receptor on the BF_2 Chelated Azadipyrromethene Fluorosensing Platform. *Chem. Commun.* **2006**, 1503-1505.

92. Goud, T. V.; Tutar, A.; Biellmann, J. F., Synthesis of 8-Heteroatom-substituted 4,4-Difluoro-4-bora-3a,4a-diaza-*s*-indacene Dyes (BODIPY). *Tetrahedron* **2006**, *62*, 5084-5091.

93. Wan, C. W.; Burghart, A.; Chen, J.; Bergstrom, F.; Johansson, L. B.; Wolford, M. F.; Kim, T. G.; Topp, M. R.; Hochstrasser, R. M.; Burgess, K., Anthracene-BODIPY Cassettes: Syntheses and Energy Transfer. *Chem. Eur. J.* **2003**, *9*, 4430-4441.

94. Deniz, E.; Isbasar, G. C.; Bozdemir, O. A.; Yildirim, L. T.; Siemiarczuk, A.; Akkaya, E. U., Bidirectional Switching of Near IR Emitting Boradiazaindacene Fluorophores. *Org. Lett.* **2008**, *10*, 3401-3403.

95. Buyukcakir, O.; Bozdemir, O. A.; Kolemen, S.; Erbas, S.; Akkaya, E. U., Tetrastyryl-BODIPY Dyes: Convenient Synthesis and Characterization of Elusive Near IR Fluorophores. *Org. Lett.* **2009**, *11*, 4644-4647.

96. Rohand, T.; Qin, W. W.; Boens, N.; Dehaen, W., Palladium-Catalyzed Coupling Reactions for the Functionalization of BODIPY Dyes with Fluorescence Spanning the Visible Spectrum. *Eur. J. Org. Chem.* **2006**, 4658-4663.

97. Rohand, T.; Baruah, M.; Qin, W.; Boens, N.; Dehaen, W., Functionalisation of Fluorescent BODIPY Dyes by Nucleophilic Substitution. *Chem. Commun.* **2006**, 266-268.

98. Gibbs, J. H.; Robins, L. T.; Zhou, Z. H.; Bobadova-Parvanova, P.; Cottam, M.; McCandless, G. T.; Fronczek, F. R.; Vicente, M. G. H., Spectroscopic, Computational Modeling and Cytotoxicity of a Series of *meso*-Phenyl and *meso*-Thienyl-BODIPYs. *Bioorg. Med. Chem.* **2013**, *21*, 5770-5781.

99. Pavlopoulos, T. G.; Boyer, J. H.; Shah, M.; Thangaraj, K.; Soong, M. L., Laser Action from 2,6,8-Position Trisubstituted 1,3,5,7-Tetramethylpyrromethene-BF_2 Complexes: Part 1. *Appl. Opt.* **1990**, *29*, 3885-3886.

100. Pavlopoulos, T. G.; Boyer, J. H.; Sathyamoorthi, G., Laser Action from a 2,6,8-Position Trisubstituted 1,3,5,7-Tetramethylpyrromethene-BF_2 Complex: Part 3. *Appl. Opt.* **1998**, *37*, 7797-7800.

101. Niu, S. L.; Ulrich, G.; Ziessel, R.; Kiss, A.; Renard, P. Y.; Romieu, A., Water-Soluble BODIPY Derivatives. *Org. Lett.* **2009**, *11*, 2049-2052.

102. Zhai, J. Y.; Pan, T.; Zhu, J. W.; Xu, Y. M.; Chen, J.; Xie, Y. J.; Qin, Y., Boronic Acid Functionalized Boron Dipyrromethene Fluorescent Probes: Preparation, Characterization, and Saccharides Sensing Applications. *Anal. Chem.* **2012**, *84*, 10214-10220.

103. Goeb, S.; Ziessel, R., Synthesis of Novel Tetrachromophoric Cascade-Type BODIPY Dyes. *Tetrahedron Lett.* **2008**, *49*, 2569-2574.

104. Chen, J. P.; Mizumura, M.; Shinokubo, H.; Osuka, A., Functionalization of Boron Dipyrrin (BODIPY) Dyes through Iridium and Rhodium Catalysis: A Complementary Approach to α- and β-Substituted BODIPYs. *Chem. Eur. J.* **2009**, *15*, 5942-5949.

105. Kee, H. L.; Kirmaier, C.; Yu, L.; Thamyongkit, P.; Youngblood, W. J.; Calder, M. E.; Ramos, L.; Noll, B. C.; Bocian, D. F.; Scheidt, W. R.; Birge, R. R.; Lindsey, J. S.; Holten, D., Structural Control of the Photodynamics of Boron-Dipyrrin Complexes. *J. Phys. Chem. B* **2005**, *109*, 20433-20443.

106. Goze, C.; Ulrich, G.; Mallon, L. J.; Allen, B. D.; Harriman, A.; Ziessel, R., Synthesis and Photophysical Properties of Borondipyrromethene Dyes Bearing Aryl Substituents at the Boron Center. *J. Am. Chem. Soc.* **2006**, *128*, 10231-10239.

107. Goze, C.; Ulrich, G.; Ziessel, R., Unusual Fluorescent Monomeric and Dimeric Dialkynyl Dipyrromethene-Borane Complexes. *Org. Lett.* **2006**, *8*, 4445-4448.

108. Goze, C.; Ulrich, G.; Ziessel, R., Tetrahedral Boron Chemistry for the Preparation of Highly Efficient "Cascatelle" Devices. *J. Org. Chem.* **2007**, *72*, 313-322.

109. Goeb, S.; Ziessel, R., Convenient Synthesis of Green Diisoindolodithienylpyrromethene-Dialkynyl Borane Dyes. *Org. Lett.* **2007**, *9*, 737-740.

110. Bonardi, L.; Ulrich, G.; Ziessel, R., Tailoring the Properties of Boron-Dipyrromethene Dyes with Acetylenic functions at the 2,6,8 and 4-B Substitution Positions. *Org. Lett.* **2008**, *10*, 2183-2186.

111. Ulrich, G.; Goeb, S.; De Nicola, A.; Retailleau, P.; Ziessel, R., Chemistry at Boron: Synthesis and Properties of Red to Near-IR Fluorescent Dyes Based on Boron-Substituted Diisoindolomethene Frameworks. *J. Org. Chem.* **2011**, *76*, 4489-4505.

112. More, A. B.; Mula, S.; Thakare, S.; Sekar, N.; Ray, A. K.; Chattopadhyay, S., Masking and Demasking Strategies for the BF_2-BODIPYs as a Tool for BODIPY Fluorophores. *J. Org. Chem.* **2014**, *79*, 10981-10987.

113. Kim, H.; Burghart, A.; Welch, M. B.; Reibenspies, J.; Burgess, K., Synthesis and Spectroscopic Properties of a New 4-Bora-3a,4a-diaza-s-indacene (BODIPY®) Dye. *Chem. Commun.* **1999**, 1889-1890.

114. Gabe, Y.; Ueno, T.; Urano, Y.; Kojima, H.; Nagano, T., Tunable Design Strategy for Fluorescence Probes Based on 4-Substituted BODIPY Chromophore: Improvement of Highly Sensitive Fluorescence Probe for Nitric Oxide. *Anal. Bioanal. Chem.* **2006**, *386*, 621-626.

115. Courtis, A. M.; Santos, S. A.; Guan, Y.; Hendricks, J. A.; Ghosh, B.; Szantai-Kis, D. M.; Reis, S. A.; Shah, J. V.; Mazitschek, R., Monoalkoxy BODIPYs-A Fluorophore Class for Bioimaging. *Bioconjugate Chem.* **2014**, *25*, 1043-1051.

116. Nagai, A.; Chujo, Y., Aromatic Ring-Fused BODIPY-Based Conjugated Polymers Exhibiting Narrow Near-Infrared Emission Bands. *Macromolecules* **2010**, *43*, 193-200.

117. Nakamura, M.; Tahara, H.; Takahashi, K.; Nagata, T.; Uoyama, H.; Kuzuhara, D.; Mori, S.; Okujima, T.; Yamada, H.; Uno, H., π-Fused bis-BODIPY as a Candidate for NIR Dyes. *Org. Biomol. Chem.* **2012**, *10*, 6840-6849.

118. Okujima, T.; Tomimori, Y.; Nakamura, J.; Yamada, H.; Uno, H.; Ono, N., Synthesis of π-Expanded BODIPYs and Their Fluorescent Properties in the Visible-Near-Infrared Region. *Tetrahedron* **2010**, *66*, 6895-6900.

119. Shen, Z.; Rohr, H.; Rurack, K.; Uno, H.; Spieles, M.; Schulz, B.; Reck, G.; Ono, N., Boron-Diindomethene (BDI) Dyes and Their Tetrahydrobicyclo Precursors-en Route to a New Class of Highly Emissive Fluorophores for the Red Spectral Range. *Chem. Eur. J.* **2004**, *10*, 4853-4871.

120. Wada, M.; Ito, S.; Uno, H.; Murashima, T.; Ono, N.; Urano, T.; Urano, Y., Synthesis and Optical Properties of a New Class of Pyrromethene-BF_2 Complexes Fused with Rigid Bicyclo Rings and Benzo Derivatives. *Tetrahedron Lett.* **2001**, *42*, 6711-6713.

121. Uppal, T.; Hu, X. K.; Fronczek, F. R.; Maschek, S.; Bobadova-Parvanova, P.; Vicente, M. G. H., Synthesis, Computational Modeling, and Properties of Benzo-Appended BODIPYs. *Chem. Eur. J.* **2012**, *18*, 3893-3905.

122. Chen, J.; Burghart, A.; Derecskei-Kovacs, A.; Burgess, K., 4,4-Difluoro-4-bora-3a,4a-diaza-*s*-indacene (BODIPY) Dyes Modified for Extended Conjugation and Restricted Bond Rotations. *J. Org. Chem.* **2000**, *65*, 2900-2906.

123. Descalzo, A. B.; Xu, H. J.; Xue, Z. L.; Hoffmann, K.; Shen, Z.; Weller, M. G.; You, X. Z.; Rurack, K., Phenanthrene-Fused Boron-Dipyrromethenes as Bright Long-Wavelength Fluorophores. *Org. Lett.* **2008**, *10*, 1581-1584.

124. Lavis, L. D.; Raines, R. T., Bright Ideas for Chemical Biology. *ACS Chem. Biol.* **2008**, *3*, 142-155.

125. Frangioni, J. V., *In vivo* Near-Infrared Fluorescence Imaging. *Curr. Opin. Chem. Biol.* **2003**, *7*, 626-634.

126. Marshall, M. V.; Draney, D.; Sevick-Muraca, E. M.; Olive, D. M., Single-Dose Intravenous Toxicity Study of IRDye 800CW in Sprague-Dawley Rats. *Mol. Imaging Biol.* **2010**, *12*, 583-594.

127. Cohen, R.; Vugts, D. J.; Stigter-van Walsum, M.; Visser, G. W. M.; van Dongen, G. A. M. S., Inert Coupling of Irdye800cw and Zirconium-89 to Monoclonal Antibodies for Single- or Dual-Mode Fluorescence and PET Imaging. *Nat. Protoc.* **2013**, *8*, 1010-1018.

128. Jones, L. J.; Upson, R. H.; Haugland, R. P.; PanchukVoloshina, N.; Zhou, M. J.; Haugland, R. P., Quenched BODIPY Dye-Labeled Casein Substrates for the Assay of Protease Activity by Direct Fluorescence Measurement. *Anal. Biochem.* **1997**, *251*, 144-152.

129. Bandhuvula, P.; Li, Z. G.; Bittman, R.; Saba, J. D., Sphingosine 1-Phosphate Lyase Enzyme Assay Using a BODIPY-Labeled Substrate. *Biochem. Biophys. Res. Commun.* **2009**, *380*, 366-370.

130. Kalai, T.; Hideg, K., Synthesis of new, BODIPY-Based Sensors and Labels. *Tetrahedron* **2006**, *62*, 10352-10360.

131. Karolin, J.; Johansson, L. B. A.; Strandberg, L.; Ny, T., Fluorescence and Absorption Spectroscopic Properties of Dipyrrometheneboron Difluoride (BODIPY) Derivatives in Liquids, Lipid-Membranes, and Proteins. *J. Am. Chem. Soc.* **1994**, *116*, 7801-7806.

132. Ehrenschwender, T.; Wagenknechet, H. A., 4,4-Difluoro-4-bora-3a,4a-diaza-*s*-indacene as a Bright Fluorescent Label for DNA. *J. Org. Chem.* **2011**, *76*, 2301-2304.

133. Giessler, K.; Griesser, H.; Gohringer, D.; Sabirov, T.; Richert, C., Synthesis of 3'-BODIPY-Labeled Active Esters of Nucleotides and a Chemical Primer Extension Assay on Beads. *Eur. J. Org. Chem.* **2010**, 3611-3620.

134. Namkung, W.; Padmawar, P.; Mills, A. D.; Verkman, A. S., Cell-Based Fluorescence Screen for K^+ Channels and Transporters Using an extracellular Triazacryptand-based K^+ Sensor. *J. Am. Chem. Soc.* **2008**, *130*, 7794-7795.

135. Goncalves, M. S., Fluorescent Labeling of Biomolecules with Organic Probes. *Chem. Rev.* **2009**, *109*, 190-212.

CHAPTER 2: SYNTHESIS, SPECTROSCOPIC STUDIES, AND COMPUTATIONAL MODELING OF 4,4-DIALKOXY-BODIPYS[a]

2.1 Introduction

Boron-substituted BODIPYs have been explored in the last decade due to their ease of synthetic post-modification, increased aqueous hydrophilic solubility, decreased oxidation/reduction potentials, use as biological probes for bioimaging, and development as cassette devices with donor-acceptor systems.[1-2] Even though replacements of the fluoride atoms with carbon or oxygen nucleophiles have shown no substantial changes on the absorption or emission properties, there are potential enhancements on the Stokes shift and fluorescence quantum yields. Development in boron functionalization has been slow compared to carbon modification of the dipyrromethene core. Nevertheless, nucleophilic substitution at the boron atom remains a tremendous synthetic challenge for further functionalization with various groups.

There are several methods for BODIPY boron-functionalization with oxygen nucleophiles: i) post-modification of *F*-BODIPYs and ii) complexation of dipyrromethenes with reactive boron compounds.[3-4] Derivatization of B-F can be done in a variety of ways: elevated temperature[5-6] with alkoxide or Lewis acid mediated[7-16] with alcohols. For example, Nagano and coworkers[5] demonstrated that refluxing a mixture of 8-phenyl-BODIPY with sodium methoxide in methanol for 14 hours can afford the mono- and di-methoxyl BODIPYs (up to 52% yield). Alternatively, BODIPYs can be heated in a microwave-assisted reactor with alkoxide.[6] However, a milder method[7] was developed via activating of B-F bonds with Lewis acid (aluminum trichloride) followed by addition of various alcohols. The Lewis acid was an essential part for cleavage of fluoride atoms, which led to nucleophilic attack of weak oxygen nucleophiles. Various alcohols

[a] Part of this chapter originally published as Nguyen, A. L.; Bobadova-Parvanova, P.; Hopfinger, M.; Fronczek, F. R.; Smith, K. M.; Vicente, M. G. H., Synthesis and Reactivity of 4,4-Dialkoxy-BODIPYs: An Experimental and Computational Study. *Inorg. Chem.* **2015**, *54*, 3228-3236. Reprinted with permission from [1] Copyright (2015) ACS Publications.

have been demonstrated to directly replace the fluorine atoms, including methanol, ethanol, benzyl alcohol, polyethylene glycol, and phenol. However, the yields for the corresponding 4,4-dialkoxy- and diaryloxy-BODIPYs are often low (ranging from 20% to quantitative) due to difficulty in removal of large excesses of alcohols. Using latter methodologies, antenna-containing BODIPY with donor-acceptor-acceptor triad components and BODIPY-oxazine dyads were developed.[9-11] Furthermore, these mild conditions are being used extensively and found to be compatible with amine, ester, and aldehyde groups.[12] In the last few years, several *O*-BODIPYs have been used in circularly polarized luminescence spectroscopy using the latter methodology.[13-14]

Recently, Thompson and coworkers[17] developed a milder strategy which involves a two step one-pot reaction using boron trichloride with *F*-BODIPYs to afford a reactive intermediate 4,4-dichloro-BODIPY, which readily undergoes reaction with alkoxides or alkyls to give the corresponding 4,4-dialkoxy- and dialkyl-BODIPYs in relatively high yields. Another mild method was reported for the synthesis of 4-monoalkoxy-BODIPYs in moderate yields (38-70%), which involves activation of the BODIPY using trimethylsilyltrifluoromethanesulfonate (TMSOTf) followed by addition of an alcohols.[18] Similar methodology was used previously for boron functionalization in subphthalocyanines via a triflate-subphthalocyanine intermediate.[19] There are several ways for complexation of dipyrromethenes with halogenated boron compounds.[3-4,20] The usefulness of dipyrromethenes as a platform is that many 4,4-functionalized BODIPYs can be synthesized via a one-step reaction.

2.1.1 Radioactive 18-Fluoride Imaging

The use of radioactively labeled atoms (^{123}I, ^{18}F, etc.) for nuclear imaging has become a promising tool for physicians to diagnose many diseased patients. The ability to produce images of particular parts in the body using a trace amount of radioactive nuclei is tremendously

advantageous in the biomedical field. Positron emission tomography (PET) and single photon emission computed tomography (SPECT) have been utilized in many bioimaging applications. The practical uses of PET include creating a three dimensional image upon radiation using the radioactive fluoride to allow mapping of uptake *in vivo*. For imaging of endogenous antibodies and polypeptides, SPECT is preferred over PET due to the slow kinetic measurements and relatively long isotope half-life. Many FDA-approved radiotracers have been used exclusively for clinical theranostic treatments. Moreover, iodinated compounds have emerged as potential radiotherapy candidates in PET and SPECT imaging for bioimaging applications.[21-22] However, the use of [^{18}F]-radiolabelling of BODIPYs as PET/fluorescence dual imaging probes has been extensively studied recently.[23-28] Incorporation of 4-mono-radioactive fluorine onto the boron center of BODIPY can provide PET and fluorescence components for a faster and effective diagnosis in organic and aqueous environments.

2.1.2 Research Prospective

Although several boron functionalization methods have been developed, alternative functionalization strategies must be explored due to low yields and difficult purifications. This chapter aims to report further investigation of these boron-functionalization methodologies and extend them to the synthesis of 4,4-dialkoxy-BODIPYs. In addition, we also explored using Cu(I)-catalyzed alkyne-azide click conditions using 4,4-dipropargyloxy-BODIPY in order to produce the first boron-*bis*(1,2,3)triazole-functionalized BODIPY. In our study, the structural, spectroscopic and fluorescence properties of all the synthesized BODIPYs were investigated and are compared using computational and experimental methods.

2.2 Results and Discussion

2.2.1 Syntheses

Three 8-aryl-1,3,5,7-tetramethyl-BODIPYs **1-3** were synthesized through a classical BODIPY synthetic routes (Scheme 2.1). The route was a 3-step-1-pot synthesis, which began with acid-catalyzed condensation[29-30] of the commercially available 2,4-dimethylpyrrole with the corresponding aryl aldehydes in dichloromethane. An acid catalyst, boron trifluoride etherate ($BF_3 \cdot OEt_2$), was used in order make the carbonyl more electrophilic toward nucleophilic attack. After stirring the reaction mixture under inert argon at room temperature for 48 hours, 2,3-dichloro-5,6-dicyano-1,4-benzoquinone (DDQ) was used as the oxidant to oxidize the dipyrromethanes to dipyrromethenes. The dipyrromethenes were deprotonated under basic conditions with triethylamine (Et_3N), followed by complexation with boron trifluoride etherate ($BF_3 \bullet OEt_2$) to give BODIPYs **1-3** in yields ranging from 6-26%. Electron-donating groups (3,4-dimethoxy BODIPY **2**) and electron-withdrawing groups (4-methoxycarbonyl BODIPY **3**) were introduced at the *meso*-phenyl positions to study the effect on the boron-substitution reaction.

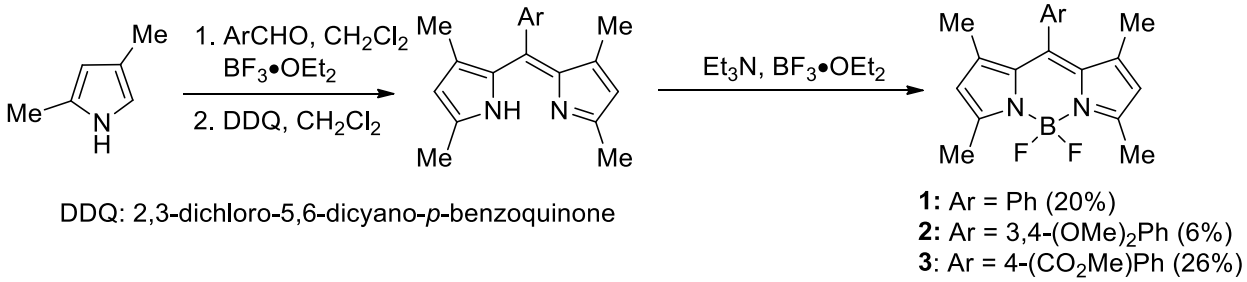

Scheme 2.1: Synthesis of BODIPY **1-3** from acid-catalyzed condensation between 2,4-dimethylpyrrole with aryl aldehydes.

We first began our methodology investigation by employing conditions as previously described by Nagano and coworkers[5] to synthesize 4,4-dimethoxy-BODIPY **1a**. Method A is a one-step reaction between BODIPY **1** with 6 equiv. of sodium methoxide in methanol and the reaction mixture was refluxed for 12 hours to afford the corresponding 4,4-dimethoxy-BODIPY

1a in 66% yield (Scheme 2.2). In addition, TLC also indicated the 4-monoalkoxy-BODIPY intermediate under these conditions. Next, we investigated BODIPYs with electron-donating and electron-withdrawing groups on the 8-phenyl. When BODIPY **2**, containing two electron-donating methoxy groups (positions 3 and 4 of the 8-phenyl group), was exposed to the above reaction conditions, the corresponding 4,4-dimethoxy-BODIPY **2a** was afforded in a yield of 50%. On the other hand, BODIPY **3**, containing an electron-withdrawing (4-methoxycarbonyl), produced the corresponding 4,4-dimethoxy-BODIPY **3a** in poor yield of 4% although 53% of the starting material was recovered.

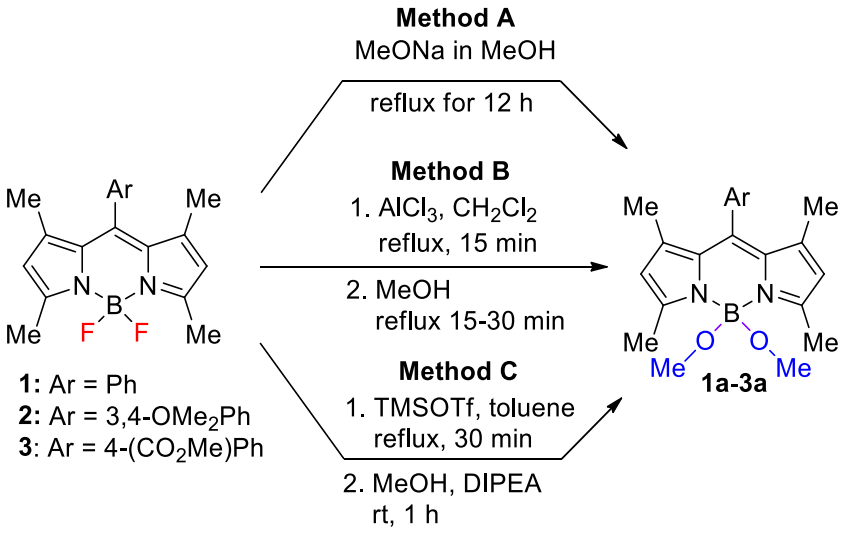

Scheme 2.2: Synthesis of BODIPYs **1a-3a** from Method A-C.

DFT calculations at the B3LYP/6-31+G(d,p) level for evaluation of the atomic charges on BODIPYs **1-3** indicate that there are no significance differences between the charges on the 12-atom BODIPY core. This shows that the electron donating or withdrawing nature of the 8-aryl group does not greatly affect the dipyrromethene core. This could be explained by the loss of electronic communication between the *meso*-aryl and 1,7-dimethyl substituent on the BODIPY core (Figure 2.1) due to the large dihedral angles. With the aim to increase the yields of the substitution reaction in the presence of electron-withdrawing groups, such as in BODIPY **3**, since

the methoxycarbonyl group can be used as a precursor to carboxyl-substituted BODIPYs for further derivatization, we decided to explore alternative methodologies using milder reaction conditions (at lower temperature and with milder nucleophiles).

Table 2.1: Methods A, B, and C for synthesis of 4,4-dimethoxy-BODIPYs 1a, 2a, and 3a with isolated yields.

BODIPY	Method A	Method B	Method C
1a	66%	52%	98%
2a	50%	11%	8%
3a	4%	58%	70%

Our approach was to optimize the conditions as reported by Tahtaoui and coworkers[7] in order to synthesize 4,4-dimethoxy-BODIPY **1a**. Our preliminary investigation began with the absence of and changing Lewis acids as shown on Table 2.2. In the absence of a Lewis acid, the reaction did not proceed and resulted in re-isolation of the starting material BODIPY **1**, which was in agreement with Tahtaoui and coworkers. This indicates that BODIPY **1** requires chelation of a Lewis acid in order to make the B-F bonds more labile toward nucleophilic substitution. Lewis acids such as $Zn(OAc)_2$, $TiCl_4$, $SnCl_2$, $SnCl_4$, and BCl_3 did not produce the desired 4,4-dimethoxy-BODIPY **1a**. Also, the reaction with $TiCl_4$ led to decomposition of the starting material. Indeed, $AlCl_3$ as Lewis acid gave BODIPY **1a** in an isolated 52% yield at reflux temperature after 15 min with excess amount of methanol (278 equiv), which is in agreement with previous reports[7] (entry 6). However, the excess of alcohol were difficult to remove and the product was hard to purify.

At room temperature and with longer reaction time (12 h), the desired BODIPY **1a** was obtained in 44% yield (entry 7). When reducing the amount of methanol equivalent from 278 to 5, BODIPY **1a** was afforded in a lower yield of 19% (entry 8). These preliminary data show that

$AlCl_3$ and an excess of alcohol were necessary for the synthesis of 4,4-dimethoxy-BODIPY **1a** in good yield.[7]

Table 2.2: Preliminary studies for synthesis of 4,4-Dimethoxy-BODIPY 1a using methanol as nucleophile.

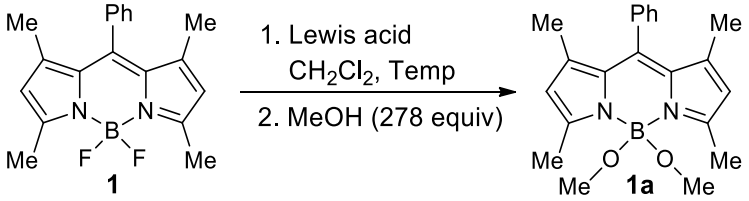

Entry	Lewis Acid	Temp	Product, Yield
1	---	25 °C	1
2	$Zn(OAc)_2$	40 °C	1
3	$TiCl_4$	25 °C	decomp
4	$SnCl_4$	40 °C	1
5	$SnCl_4$	40 °C	1
6	$AlCl_3$	40 °C	1a, 52%
7	$AlCl_3$	25 °C	1a, 44%
8[a]	$AlCl_3$	40 °C	1a, 19%
9	BCl_3	25 °C	1

a: 5.0 equiv of MeOH was used

To further explore the scope of our reaction, we also investigated variation of the solvents at room temperature (Table 2.3). Using acetonitrile, compound **1a** was obtained in 16% yield, which is due to the possible competition reaction between the nitrile and methanol as nucleophiles toward the boron center. With tetrahydrofuran, the oxygen could possible poison the aluminum catalyst to give the starting material **1** before the addition of methanol. Similar to when using methanol, dipyrromethene was the only product due to the possible competing reaction between

methanol and the Lewis acid. These results demonstrated that dichloromethane is the best solvent to use for method B.

Table 2.3: Synthesis of BODIPY 1a in various solvents using Method B at reflux temperature.

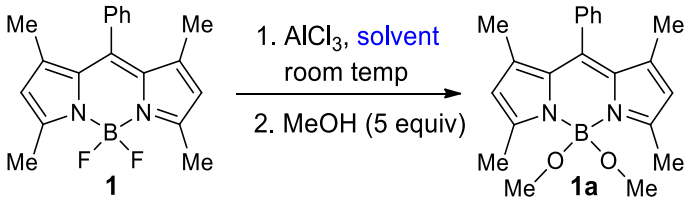

Entry	solvent	Product, Yield
1	dichloromethane	1a, 44%
2	acetonitrile	1a, 16%
3	methanol	dipyrromethene
4	tetrahydrofuran	1

The next step was replacing methanol with a stronger nucleophile, sodium methoxide. As shown on Table 2.4, aluminum chloride as the Lewis acid gave the desired product **1a** in 46% yield. However, these conditions were not reproducible (Table 2.4, entry 1). Similar to Table 2.1, varying the Lewis acids resulted in the recovery of starting material, except for boron trichloride.

Under these conditions (2 equiv. of $AlCl_3$, 278 equiv. of alcohol, reflux in dichloromethane for 15 min), BODIPYs **1a** (52%), **2a** (11%) and **3a** (58%) were afforded in moderate yields (Method B, Scheme 2.2). Notably, BODIPY **3a** was obtained in 58% yield, a remarkable increase in the yield obtained using method A. While method B gave the desired 4,4-dimethoxy-BODIPY in moderate yield, we further investigated the optimization of the conditions and developed new method C. This novel method consists of activating the BODIPY with TMSOTf at elevated temperature, followed by addition of alcohols (5.0 equiv.) and a non-nucleophilic base (DIPEA) at room temperature.

Table 2.4: Preliminary studies for synthesis of 4,4-Dimethoxy-BODIPY 1a using sodium methoxide as nucleophile.

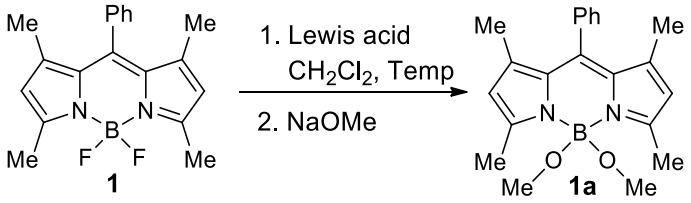

Entry	Lewis Acid	Temp	Product, Yield
1	$AlCl_3$	50 °C	1a, 46%
2	$ZnCl_2$	50 °C	1
3	$MgCl_2$	50 °C	1
4	$SnCl_4$	50 °C	1
5	$InCl_3$	50 °C	1
6	$FeCl_3$	50 °C	1
7	BCl_3	25 °C	1a, 19%

Similar to method B, we also screened various solvents (toluene, dichloromethane, tetrahydrofuran, and chloroform) at room temperature to afford BODIPY **1a** (Table 2.5). The desired BODIPY **1a** yields were obtained at room temperature with toluene (50%), dichloromethane (25%), chloroform (29%), and tetrahydrofuran (0% and 100% of starting material was recovered). The conditions with dichloromethane also gave the starting material **1** (20%) and the mono-substituted (17%) product. Notably, toluene and dichloromethane gave the yields within 2 hours while chloroform required overnight. In addition, silver triflate (AgOTf) was used in place of TMSOTf and resulted in isolation of the starting material. These results indicated that the reaction yields were dependent on the solvent used and reaction temperature.

With Method C using toluene at elevated temperature, compound **1a** was remarkably synthesized in high yield (98%). As expected, compound **3a** was also isolated in high yield (70%) compared to method B (58%). However, compound **2a** with an electron donating group at the *meso*-phenyl afforded a low yield (8%) with uncomplexed dipyrromethene as a by-product. The three methodologies were used for synthesis of 4,4-dimethoxy-BODIPYs **1a**-**3a** as summarized in Table 2.1 with yields ranging from 4% to 98%. Therefore, BODIPYs **1a** and **3a** were accessed in high yield using the newly developed method C, providing an efficient and convenient synthetic route for boron functionalization.

Table 2.5: Synthesis of 4,4-dimethoxy-BODIPY 1a in various solvents using Method C at room temperature.

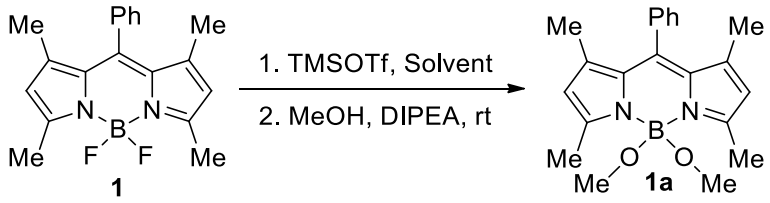

Entry	Solvent	Product, Yield
1	dichloromethane	1a, 25%
2	toluene	1a, 50%
3	chloroform	1a, 29%
4	tetrahydrofuran	1

Since there is wide range of yields obtained for BODIPYs **1a**-**3a** under the three methods, we suspected that the intermediates formed upon fluoride dissociation from boron under these reaction conditions can be investigated using computational modeling. All these reactions likely undergo the same boronium cation intermediate **INT1** formation (Scheme 2.3) and ^{19}F-NMR and X-ray crystallography have confirmed the existent of these cations.[31] DFT modeling showed the

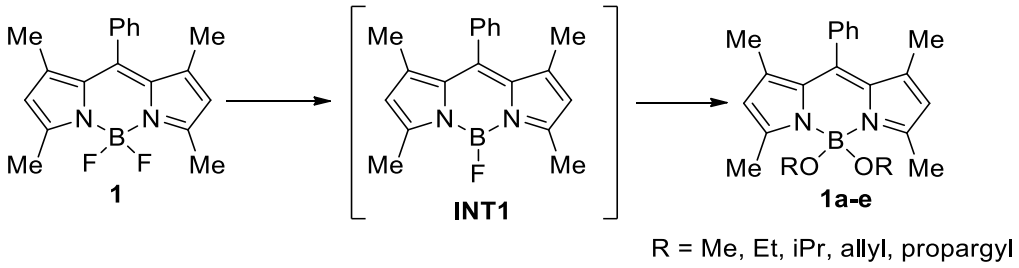

Scheme 2.3: Synthesis of BODIPYs **1a-e** using Methods B and C via Boronium Intermediate **INT1**.

calculated Gibbs free energies for the formation of **INT1** from BODIPY **1** (Table 2.6). The intermediates were computationally modeled for method A (in methanol), method B (in dichloromethane), and method C (in toluene). Indeed, fluoride dissociation from BODIPY **1** in method A requires the least amount of energy (37 kcal/mol) in methanol, followed by 56 kcal/mol in dichloromethane, and the largest amount of energy (92 kcal/mol) in toluene. This tendency can be explained by the three solvents' relative dielectric permittivities: methanol (ε = 32.6), dichloromethane (ε = 8.93), and toluene (ε = 2.37). From these values, the direct dissociation of fluoride ion from BODIPY **1** is likely to occur in method A, since the reaction barrier for the formation of **INT1** can be overcome by refluxing the mixture in methanol at 70-75 ^{o}C. This is unlikely to happen in method B since a larger amount of energy (56 kcal/mol) is required to overcome this barrier. However, computational calculations show that the addition of Lewis acid $AlCl_3$, followed by fluoride dissociation to form the counter ion $AlCl_3F^-$ significantly stabilizes the boronium cation **INT1**. Indeed, this is in agreement with the milder conditions required for method B. Furthermore, the calculations also suggest that the milder reaction can occur at a lower temperature. While performing the reaction entirely at room temperature, BODIPY **1a** was afforded in lower yield (44 vs. 52%) after 12 hours.

For method C, the potential energy barrier of 25 kcal/mol for the fluoride abstraction with triflate anion to give trimethylsilyl fluoride can be easily overcome by refluxing in toluene at 110

°C. Indeed, NMR spectroscopy and X-ray crystallography have shown that such a boronium species bearing a triflate ligand exists.[32] Moreover, our calculations for method A also show similar Gibbs free energies and stabilities for **INT1** from all starting BODIPYs **1**-**3**: for BODIPY **1** (ΔG = 37.4 kcal/mol), for BODIPY **2** (ΔG = 37.5 kcal/mol), and for BODIPY **3** (ΔG = 38.7 kcal/mol).

Table 2.6: Calculated ΔG energies for formation of INT1 through methods A, B, and C.

Method	modeled solvent	Anion	Δ G (kcal/mol)
A	CH_3OH	F-	37
B	CH_2Cl_2	F-	56
B	CH_2Cl_2	$AlCl_3F$-	-22
C	$PhCH_3$	F-	92
C	$PhCH_3$	OTf-	25

Various alcohols were investigated for the synthesis of new 4,4-dialkoxy-BODIPYs **1a**-**e** using the milder methods B and C, as shown in Scheme 2.3 with the isolated yields given in Table 2.7. In method B, all desired BODIPYs were obtained in moderate yields (21-64%) while method C was highly sensitive to the sterics of the alcohol. This is likely due to the close distance of the triflate anion to the boron center.[33] Indeed, no product was obtained for method C when isopropanol was used. It has shown previously that the use of *tert*-butanol/*tert*-butoxide has resulted in BODIPY deboronation.[6] When a larger excess of ethanol was used for BODIPY **1b** using method C, the yield could be increased to 37% and the mono-4-ethoxy-BODIPY was also

afforded in 20% yield. In addition, we also investigated the addition sequence of DIPEA. When we added the DIPEA before addition of alcohols, a 35% yield of BODIPY **1b** resulted. Therefore, in order to obtain the highest yield of the desired 4,4-dialkoxy-BODIPYs, the starting BODIPY and various alcohol nucleophile with selected methods must be considered.

Table 2.7: Synthesis of BODIPYs 1a-e with isolated yields using Method B and C.

BODIPY	R	Method B (%)	Method C (%)
1a	Me	52	98
1b	Et	64	18
1c	^{i}Pr	26	0
1d	allyl	57	30
1e	propargyl	52	40

We also investigated the tolerance of 4,4-dipropargyloxy-BODIPY **1e** toward further functionalization by using the Cu(I)-catalyzed Huisgen cycloaddition conditions as previously reported for the click reaction of alkyne-functionalized BODIPYs with azide containing carbohydrate[34] and folate[35] moieties (Scheme 2.4). As a result, the 4,4-bis(*N*-benzyl-1,2,3-triazole)-BODIPY **4** was obtained in 78% yield from BODIPY **1e**. The click conditions consist of using *in situ* generated copper(I) catalyst from copper(0) and copper (II) sulfate, in the presence of sodium ascorbate and benzyl azide in an aqueous water/THF mixture. To the best of our knowledge this is the first report demonstrated that post-modification of a BODIPY boron functionalized bearing an alkyne group can occur with the click cycloaddition reaction.

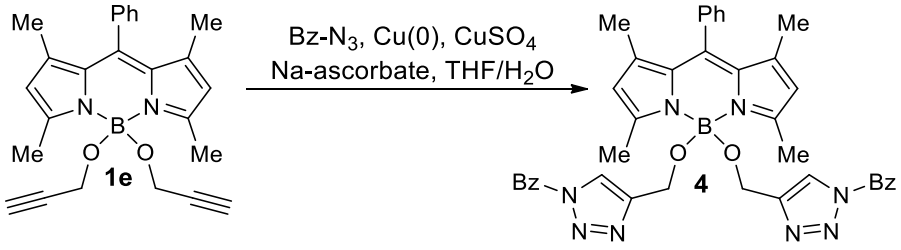

Scheme 2.4: Click reaction of BODIPY **1e**.

2.2.2 Structural Characterization

All BODIPYs were characterized by ^{1}H-, ^{13}C-, and ^{11}B-NMR, HRMS, UV-Vis, fluorescence, and in the case of **1a-c**, **1e**, **3a** and **4** also by X-ray crystallography. The disappearance of the triplet for the BF_2 (at ca. 0.6 ppm) and the appearance of the singlet attributed to $B(OR)_2$ (at ca. 2 ppm) in the ^{11}B-NMR spectra clearly showed the formation of the targeted 4,4-dialkoxy-BODIPY. The ^{1}H-NMR spectrum clearly indicated the formation of the 1,2,3-triazoles of BODIPY **4** with two singlets at 7.50 ppm (triazole) and 5.43 ppm (benzyl CH_2) protons, respectively.

Full structural confirmation of all compounds was obtained from the X-ray crystal structures. Crystals suitable for X-ray analysis were grown from slow evaporation of hexane diffused in dichloromethane (for **1a-c**), and acetone (for **1e** and **3a**). As expected, the *meso*-aryl groups are oriented perpendicular to the dipyrromethene core to avoid steric congestion caused by the 1,7-dimethyl groups. In addition, the alkoxy groups on the boron center adopt a nearly tetrahedral geometry. BODIPYs **1a-c**, **e**, and **3a** structures as shown in Figure 2.1, have at least approximate two-fold symmetry. BODIPY **1b** has crystallographic C_2 symmetry, and BODIPY **1a** has one molecule on a two-fold axis and another in a general position. The central six-membered C_3N_2B rings of all five compounds deviate little from planarity, with mean and maximum deviations of 0.021 and 0.057 Å respectively for **1a**, 0.024 and 0.037 Å for **1b**, 0.003 and 0.005 Å

for **1c**, 0.008 and 0.021 Å for **1e**, 0.035 and 0.075 Å for **3a**, and 0.014 and 0.032 Å for **4**. In all cases, the phenyl plane forms a large dihedral angle with the best plane of the C_9N_2B BODIPY core; these dihedral angles are 84.2 and 83.8˚ (2 independent molecules) for **1a**, 86.5˚ for **1b**, 84.7˚ for **1c**, 79.8 and 82.1˚ (2 independent molecules) for **1e**, 84.0 and 84.6˚ (2 independent molecules) for **3a**, and 78.9 and 79.1˚ (two independent molecules) for **4**. The geometry of the boron atoms is tetrahedral, and 18 B-O bond distances over the six compounds have lengths in the range 1.420(4) – 1.444(5) Å, with an average value of 1.432 Å. These distances are in good agreement with those in the *p*-iodo-aryl analogue of BODIPY **1a**, 1.420(4) and 1.437(3) Å.[7] As in that compound, the conformations of the B-OR groups in all six compounds have the alpha C atoms of both alkyl groups folded symmetrically toward the BODIPY core.

In addition, the geometries of BODIPYs **1a-e** and **4** were also investigated and confirmed computationally. The computational results show that the boron atom adopted a nearly tetrahedral geometry and the 8-aryl groups were oriented nearly perpendicular to the BODIPY plane, which is in agreement with the X-ray data. Surprisingly, there exist two conformers for all BODIPYs, as revealed by the computational optimization of the structures. As shown in Figure 2.2, the most stable conformer **1a** is symmetric (the two B-OR groups symmetrically oriented on both sides of the BODIPY plane, see Figure 2.2a) and in the other conformer **1a'** the $B(OR)_2$ groups positioned sideways, as shown in Figure 2.2b.

The data given in Table 2.8 suggest that there are deviations from planarity (ranging between 15 and 17°) for the non-symmetric conformers of the BODIPYs and there no significant differences in the relative Gibbs free energies between the two conformers. At room temperature,

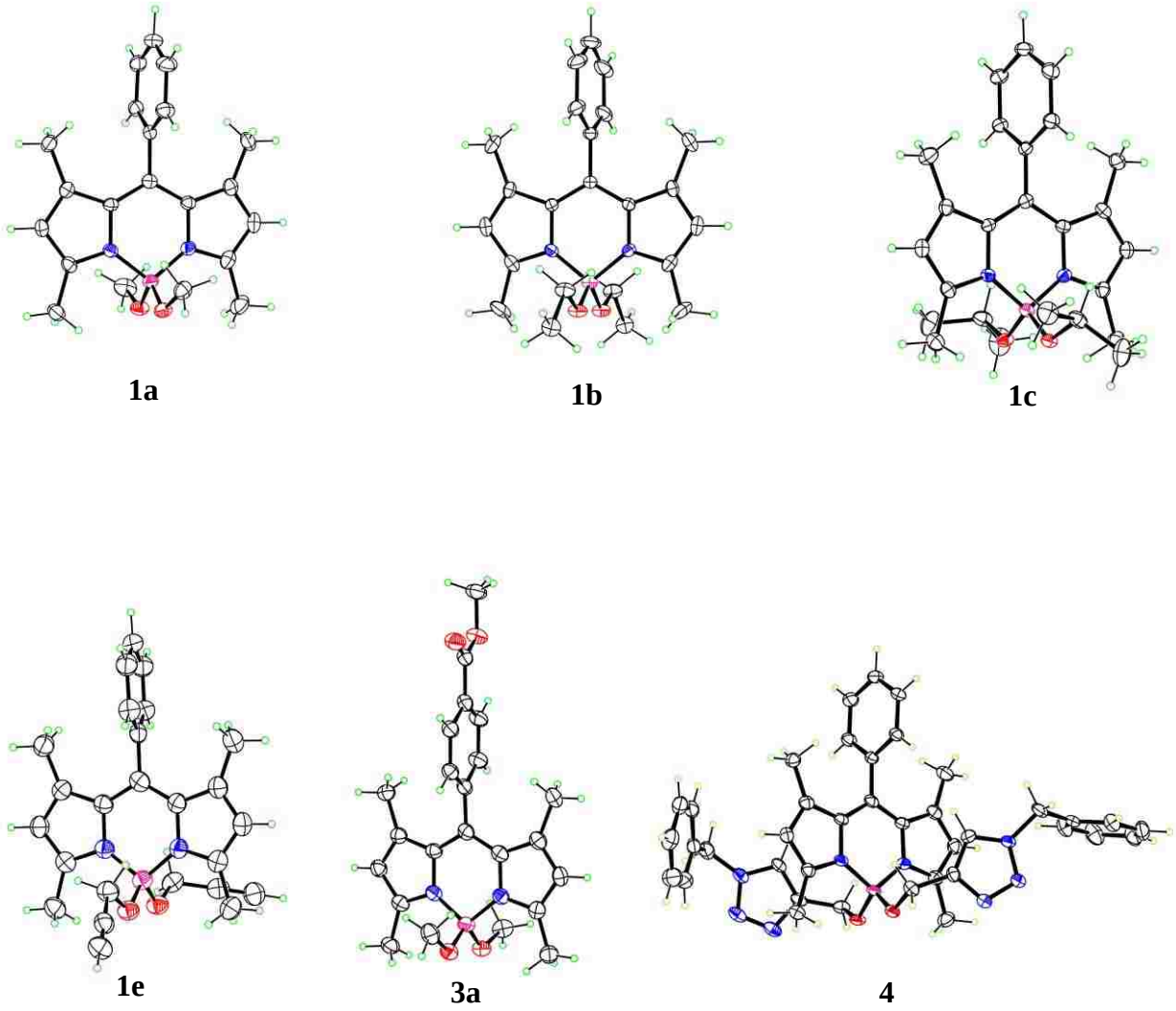

Figure 2.1: Molecular structures of BODIPYs **1a-c**,**e**, **3a**, and **4** from X-ray crystal analysis, with 50% probability ellipsoids. Only one of the independent molecules is shown for those structures with Z' > 1.

the two conformers interconvert rapidly in THF solution since the Gibbs energy differences are very small. However, only the symmetric conformer is depicted in the crystal structures shown in Figure 2.1 while the unsymmetric BODIPY conformer with the boron lying out of the C_3N_2 plane for related BF_2 systems has previously been observed.[36]

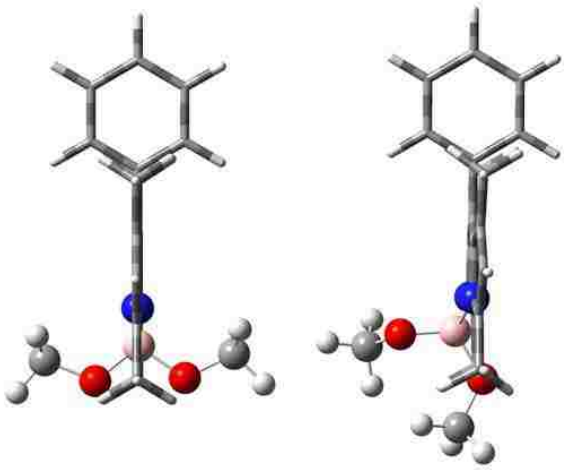

(a) (b)

Figure 2.2: Molecular structures of (a) the symmetric conformer **1a** and (b) the unsymmetric conformer **1a'** from B3LYP/6-31+G(d,p) optimization.

Table 2.8: Calculated relative Gibbs free energies, HOMO and LUMO energies, and HOMO-LUMO gap in THF for the symmetric (1a-e, 4) and unsymmetric (1a'-e', 4') BODIPY conformers.

BODIPY	HOMO (a.u.)	LUMO (a.u.)	Gap (eV)	Δ G (kcal/mol)
1a	-0.20599	-0.09520	3.01	0
1a′	-0.2044	-0.09280	3.04	6.76
1b	-0.20542	-0.09440	3.02	0
1b′	-0.20393	-0.09245	3.03	8.39
1c	-0.20548	-0.09436	3.02	0
1c′	-0.20315	-0.09117	3.05	9.92
1d	-0.20694	-0.09608	3.02	0
1d′	-0.20143	-0.09077	3.01	7.82
1e	-0.21009	-0.09941	3.01	0
1e′	-0.20776	-0.09635	3.03	7.45
4	-0.20686	-0.09602	3.02	0
4′	-0.20778	-0.09638	3.03	6.55

2.2.3 Spectroscopic Study

The spectroscopic properties of BODIPYs **1-1e**, **2-2a**, **3-3a**, and **4** were investigated in tetrahydrofuran and toluene and the results are shown in Table 2.9. All BODIPYs showed absorption bands between 501 and 506 nm and emission bands between 505 and 517 nm in THF and toluene with strong absorption bands (log ε = 4.4-5.7). Indeed, previous studies have showed that replacement of fluorides of BODIPY dyes with alkoxy groups afford only small changes in the absorption and emission wavelengths, which is in agreement with these results.[7-8,12] Moreover, the bis(1,2,3-triazole)-BODIPY **4** in THF and toluene indicated a slight blue-shifted absorption (λ_{max} ca. 495 nm) and thus the largest Stokes shift. The observed experimental data are in agreement with the computational modeling data (Table 2.8), showing similar HOMO-LUMO gaps for BODIPYs **1a**-**e** and **4**. Interestingly, it is impossible to distinguish spectroscopically between the two conformers since the HOMO-LUMO gaps are very similar as shown in Figure 2.2.

In both solvents, the 4,4-dimethoxy-BODIPY derivatives **1a**, **2a** and **3a** bearing flexible methoxy groups show decreased fluorescence quantum yields due to the increased rotational energy lost in non-radiative decay to the ground state. BODIPY derivative **1b** (in THF) and all 4,4-alkoxy-BODIPYs (in toluene) demonstrated this trend in decreased fluorescence quantum yields. Interestingly, BODIPYs **1c** and **1e** bearing the isopropoxy and progargyloxy groups showed significant enhancements in fluorescence quantum yield in THF. This result is in agreement with previous reports showing BODIPY derivatives bearing isopropoxy and benzyloxy groups also have increased fluorescence quantum yields compared to its *F*-BODIPY precursor.[7] In addition, the bis(1,2,3-triazole)-BODIPY **4** also showed enhancement of the fluorescence quantum yield in THF, but not in toluene. Furthermore, bis(1,2,3-triazole)-BODIPY **4** has a larger Stokes shift in

both solvents. These results conclude that substitution at the boron center with alkoxy groups is likely to decrease the quantum yields in toluene, but in a more polar solvent such as THF, certain BODIPYs have shown enhancement of the quantum yields.

Table 2.9: Absorption and emission spectal properties of BODIPYs 1-1e, 2-2a, 3-3a, and 4 in THF and PhMe (in parentheses) at room temperature.

BODIPY	Absorption λ_{max}/nm	Emission λ_{max}/nm	log ε ($M^{-1}.cm^{-1}$)	Φ_f	Stokes' shift (nm)
1	501 (504)	505 (511)	4.96 (5.33)	0.56 (0.96)	4 (7)
1a	502 (504)	507 (512)	4.86 (5.38)	0.44 (0.73)	5 (8)
1b	502 (504)	507 (512)	4.54 (5.24)	0.46 (0.70)	5 (8)
1c	501 (504)	505 (509)	4.70 (5.48)	0.63 (0.70)	4 (5)
1d	503 (505)	507 (511)	4.66 (5.47)	0.56 (0.57)	4 (6)
1e	504 (506)	508 (513)	4.74 (5.04)	0.62 (0.82)	4 (7)
2	501 (505)	505 (509)	5.00 (5.66)	0.93 (0.87)	4 (4)
2a	503 (505)	507 (512)	4.38 (5.06)	0.42 (0.57)	4 (7)
3	503 (506)	508 (515)	4.42 (5.62)	0.43 (0.51)	5 (9)
3a	504 (506)	510 (517)	4.73 (5.48)	0.31 (0.34)	6 (11)
4	494 (496)	511 (512)	4.80 (4.94)	0.72 (0.56)	17 (16)

ε = extinction coefficient; Φ_f = fluorescence quantum yield

2.3 Conclusions

In summary, we have investigated three different methods for the synthesis of 4,4-dimethoxy-BODIPYs containing electron-withdrawing and electron-donating *meso*-aryl groups. Method A consists of heating NaOMe in refluxing methanol at 80 ºC for 12 hours, and gave

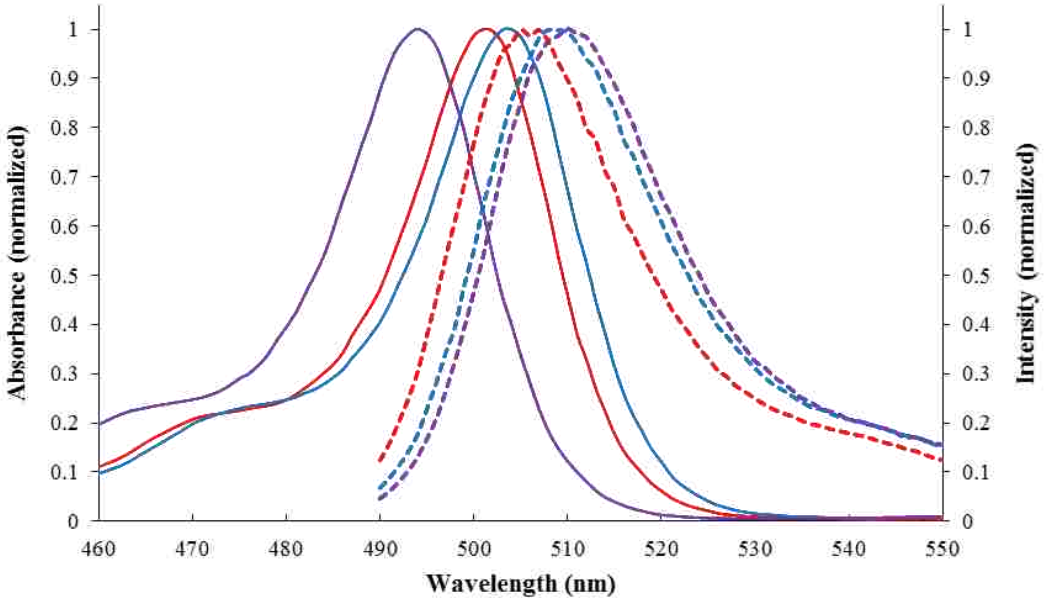

Figure 2.3: Normalized absorption (full lines) and emission (dashed lines) spectra of BODIPYs **1c** (red), **1e** (blue), and **4** (purple) in THF at room temperature.

BODIPY **2a** (8-(3,4-dimethoxyphenyl)) with the highest yield of 50%. Method B involves treating BODIPYs with $AlCl_3$ in refluxing dichloromethane, followed by large excess of alcohol, and afforded the desired 4,4-dialkoxy-BODIPYs **1a-f** in moderate yields ranging from 26% to 64%. On the other hand, method C was the most effective way to synthesize BODIPYs **1a** and **3a** in 98 and 70% yields, respectively. Method C employs TMSOTf in refluxing toluene, followed by addition of 5 equiv. of methanol and DIPEA. However, methanol was best used in method C since all other alcohols as nucleophiles gave lower yields of the targeted 4,4-disubstituted BODIPYs. The 4,4-progargyloxy-BODIPY **1e** was subjected under the Cu(I)-catalyzed Huisgen cycloaddition reaction conditions and produced to the corresponding bis-(1,2,3-triazole)-BODIPY **4**.

These 4,4-dialkoxy-BODIPYs showed minor changes in absorption and emission spectra in THF and toluene. However, BODIPY **4** with two large *N*-benzyl-(1,2,3-triazole) groups on the boron center resulted blue-shifted absorption maxima in both solvents (THF and toluene). All 4,4-

dialkoxy-BODIPYs **1a-e** have shown a decrease in fluorescence quantum yields compared to BODIPY **1** likely due to the higher rotational freedom of the alkoxy groups, therefore increasing the amount of energy lost to non-radiative decay to the ground state. In contrast, BODIPYs **1c**,**e** and **4** showed enhancements in the fluorescence quantum yields in THF. Furthermore, BODIPY **4** displayed the largest Stokes shifts in both solvents.

2.4 Experimental

2.4.1 General Information

All the reagents and solvents were purchased from Sigma-Aldrich and were used without further purification. All reactions were carried out with oven-dried glassware under a dry argon atmosphere. All the reactions were monitored using Sorbent Technologies 0.2 mm silica gel TLC plates with UV-254 nm indicator. Flash column chromatography was performed using Sorbent Technologies 60 Å silica gel (230-400 mesh). Prep-TLC 60 Å silica gel 20 x 20 cm (210-270 µm) was used. All ^{1}H-, ^{13}C-, ^{11}B-NMR spectra were collected on a Bruker AV-400 spectrometer in deuterated chloroform. The $CDCl_3$ chemical shifts (δ) are reported in ppm using as reference 7.27 for proton and 77.16 for carbon and BF_3•OEt_2 was used as reference (0.00 δ) for boron NMR. Coupling constants are reported in Hertz (Hz). All the mass spectra were collected using a Agilent 6210 ESI-TOF mass spectrometer. All melting points were recorded using a MEL-TEMP electrothermal instrument.

2.4.2 Syntheses

General procedure for synthesis of BODIPYs **1-3**.[29-30,37-38] Aryl aldehyde (9.81 mmol) was suspended in anhydrous CH_2Cl_2 (300 mL). 2,4-Dimethylpyrrole (2.12 mL, 20.6 mmol) was added, followed by 6 drops of BF_3•OEt_2 to the reaction mixture. After stirring for 48 h, TLC indicated no more aryl aldehyde in the reaction mixture, and DDQ (1.113 g, 4.91 mmol) in CH_2Cl_2 was then

added. After 1.5 h stirring at room temperature, NEt_3 (10.3 mL, 73.58 mmol) was added and after another 1 h BF_3•OEt_2 (12.1 mL, 98.1 mmol) was added. The final mixture was stirred at room temperature for 6 h and then poured into water (50 mL). The organic layer was washed with water (2 x 50 mL). The combined organic layers were dried over anhydrous Na_2SO_4 and concentrated under reduced pressure. The product was purified by silica gel flash column chromatography using mixtures of petroleum ether and dichloromethane for elution.

4,4-Difluoro-8-phenyl-1,3,5,7-tetramethyl-BODIPY (**1**). Obtained as a green/orange solid (20% yield, 650 mg), mp: 168-169 °C; ^{1}H NMR ($CDCl_3$, 400 MHz) δ 7.47-7.26 (m, 5H), 5.98 (s, 2H), 2.56 (s, 6H), 1.38 (s, 6H); ^{13}C NMR ($CDCl_3$, 100 MHz) δ 155.57, 143.29, 141.87, 135.14, 131.57, 129.26, 129.26, 128.08, 121.34, 14.71, 14.46; ^{11}B NMR ($CDCl_3$, 128 MHz) δ 0.65 (t, J = 33.4 Hz); HRMS (ESI-TOF) *m/z* 324.1718 $[M + H]^+$ calculated for $C_{19}H_{20}BF_2N_2$: 324.1728. These data are in agreement with those previously reported.[29-30]

4,4-Difluoro-8-(3,4-dimethoxyphenyl)-1,3,5,7-tetramethyl-BODIPY (**2**). Obtained as a red solid (6% yield, 229 mg), mp: 182-183 °C; ^{1}H NMR ($CDCl_3$, 400 MHz) δ 6.97 (d, J = 8.1 Hz, 1H), 6.84 (d, J = 8.1 Hz, 1H), 6.78 (s, 1H), 5.60 (s, 2H), 3.96 (s, 3H), 3.86 (s, 3H), 2.56 (s, 6H), 1.49 (s, 6H); ^{13}C NMR ($CDCl_3$, 100 MHz) δ 155.35, 149.80, 149.53, 143.14, 141.59, 131.71, 127.09, 121.12, 120.44, 111.57, 111.10, 56.10, 55.88, 14.53, 14.42; ^{11}B NMR ($CDCl_3$, 128 MHz) δ 0.62 (t, J = 33.0 Hz); HRMS (ESI-TOF) *m/z* 384.1930 $[M + H]^+$ calculated for $C_{21}H_{24}BF_2N_2O_2$: 384.1939. These data are in agreement with those previously reported.[29,37]

4,4-Difluoro-8-(4-methoxycarbonylphenyl)-1,3,5,7-tetramethyl-BODIPY (**3**). Obtained as a bright red solid (26% yield, 483 mg) mp: 181-183 °C; ^{1}H NMR ($CDCl_3$, 400 MHz) δ 8.19 (d, *J* = 8.5 Hz, 2H), δ 7.42 (d, *J* = 8.1 Hz, 2H), 5.99 (s, 2H), 3.98 (s, 3H), 2.57 (s, 6H), 1.37 (s, 6H); ^{13}C NMR ($CDCl_3$, 100 MHz) δ 166.58, 156.10, 143.01, 140.35, 139.94, 131.04, 130.94, 130.48, 128.50, 121.62, 52.50, 14.71, 14.61; ^{11}B NMR ($CDCl_3$, 128 MHz) δ 0.61 (t, *J* = 32.8 Hz); HRMS (ESI-TOF) *m/z* 382.1773 $[M + H]^+$ calculated for $C_{21}H_{22}BF_2N_2O_2$: 382.1752. These data are in agreement with those previously reported.[29,38]

General procedure for synthesis of *O*-BODIPYs using method A. In an oven-dried flask, BODIPY (20.0 mg, 0.062 mmol) and NaOMe (21.0 mg, 0.389 mmol) were dissolved in anhydrous methanol (2 mL). The mixture was refluxed for 12 h and then cooled down to room temperature. The reaction mixture was poured into ice water (5.0 mL), extracted with CH_2Cl_2 (3 x 5.0 mL), washed with brine (1 x 5.0 mL), and dried over anhydrous Na_2SO_4. The crude product was concentrated under reduced pressure and the resulting residue was purified by TLC, using ethyl acetate for elution.

General procedure for synthesis of *O*-BODIPYs using method B. In an oven-dried flask, BODIPY (20.0 mg, 0.062 mmol) and $AlCl_3$ (16.4 mg, 0.123 mmol) were dissolved in anhydrous CH_2Cl_2 (5 mL). The mixture was refluxed for 15 min before alcohol (17.15 mmol, 278.0 equiv) was added. The final reaction mixture was refluxed for 15 min. The mixture was allowed to cool down to room temperature and then concentrated under reduced pressure. The resulting residue was purified by TLC, using the eluents indicated below.

General procedure for syntheis of *O*-BODIPYs using method C. In an oven-dried flask, BODIPY (20 mg, 0.06 mmol) and TMSOTf (28.0 µL, 0.154 mmol) were dissolved in anhydrous toluene (5 mL) and the mixture was refluxed for 30 min. The solution was allowed to cool down to room temperature and alcohol (0.308 mmol, 5.0 equiv) was added, followed by DIPEA (27.0 µL, 0.154 mmol, 2.5 equiv.). After 1 h stirring at room temperature, the crude product was concentrated under reduced pressure and purified by TLC, using the eluents indicated below.

4,4-Dimethoxy-8-phenyl-1,3,5,7-tetramethyl-BODIPY (**1a**). This BODIPY was produced in 66% yield by method A, 58% by method B and 98% by method C. The crude product was purified by TLC (eluent EtOAc) to give an orange solid that was recrystallized from 1:1 hexane/dichloromethane. Mp: 125-130 ^{o}C; ^{1}H NMR ($CDCl_3$, 400 MHz) δ 7.50-7.30 (m, 5H), 5.97 (s, 2H), 2.97 (s, 6H), 2.54 (s, 6H), 1.39 (s, 6H); ^{13}C NMR ($CDCl_3$, 100 MHz) δ 155.77, 141.71, 141.38, 135.81, 133.01, 129.10, 128.82, 128.35, 121.05, 49.24, 14.70, 14.58; ^{11}B NMR ($CDCl_3$, 128 MHz) δ 2.52 (s); HRMS (ESI-TOF) *m/z* 370.1938 $[M + Na]^+$ calculated for $C_{21}H_{25}BN_2NaO_2$: 370.1923. These data are in agreement with literature.[5]

4,4-Dimethoxy-8-(3,4-dimethoxyphenyl)-1,3,5,7-tetramethyl-BODIPY (**2a**). This BODIPY was produced in 50% yield by method A, 11% by method B and 8% by method C. The crude product was purified by TLC (eluent 50:50 hexane/EtOAc) to afford a dark orange/red solid, that was recrystallized from acetone. Mp: 100-105 ^{o}C (decomposes); ^{1}H NMR ($CDCl_3$, 400 MHz) δ 6.97 (d, *J* = 8.1 Hz, 1H), 6.84 (d, *J* = 8.1 Hz, 1H), 6.78 (s, 1H), 5.98 (s, 2H), 3.96 (s, 3H), 3.89 (s, 3H), 2.97 (d, *J* = 12.5 Hz, 6H), 2.54 (s, 6H), 1.49 (s, 6H); ^{13}C NMR ($CDCl_3$, 100 MHz) δ 155.79, 149.85, 149.53, 141.54, 141.37, 133.30, 128.02, 120.96, 120.86, 111.58, 111.53, 56.31,

56.06, 49.33, 49.26, 14.72; ^{11}B NMR ($CDCl_3$, 128 MHz) δ 2.52 (s); HRMS (ESI-TOF) *m/z* 430.2149 $[M + Na]^+$ calculated for $C_{23}H_{29}BN_2NaO_4$: 430.2136.

4,4-Dimethoxy-8-(4-methoxycarbonylphenyl)-1,3,5,7-tetramethyl-BODIPY (**3a**). This BODIPY was produced in 4% yield by method A, 58% by method B and 70% by method C. The crude product was purified by TLC (eluent EtOAc) to afford an orange solid that was recrystallized from acetone. Mp: 100-105 °C (decomposed);. ^{1}H NMR ($CDCl_3$, 400 MHz) δ 8.19 (d, *J* = 8.5 Hz, 2H), δ 7.42 (d, *J* = 8.1 Hz, 2H), 5.99 (s, 2H), 3.98 (s, 3H), 2.97 (s, 6H), 2.57 (s, 6H), 1.37 (s, 6H); ^{13}C NMR ($CDCl_3$, 100 MHz) δ 166.70, 156.34, 141.17, 140.70, 140.21, 132.48, 130.72, 130.37, 128.79, 121.40, 52.50, 49.24, 14.76, 14.73; ^{11}B NMR ($CDCl_3$, 128 MHz) δ 2.51 (s); HRMS (ESI-TOF) *m/z* 428.1992 $[M + Na]^+$ calculated for $C_{23}H_{27}BN_2NaO_4$: 428.1981.

4,4-Diethoxy-8-phenyl-1,3,5,7-tetramethyl-BODIPY (**1b**). This BODIPY was produced in 64% yield by method B and 37% by method C. The crude product was purified via TLC (eluent 80:20 hexane/EtOAc) to give an orange solid, that was recrystallized from 1:1 hexane/dichloromethane. Mp: 140-145 °C; ^{1}H NMR ($CDCl_3$, 400 MHz) δ 7.48-7.29 (m, 5H), 5.95 (s, 2H), 3.07 (q, *J* = 7.0 Hz, 4H), 2.58 (s, 6H), 1.38 (s, 6H), 1.07 (t, *J* = 7.0 Hz, 6H); ^{13}C NMR ($CDCl_3$, 100 MHz) δ 155.87, 141.61, 141.25, 135.85, 132.84, 129.09, 128.80, 128.37, 121.00, 56.64, 17.83, 14.94, 14.59; ^{11}B NMR ($CDCl_3$, 128 MHz) δ 1.82 (s); HRMS (ESI-TOF) *m/z* 398.2251 $[M + Na]^+$ calculated for $C_{23}H_{29}BN_2NaO_2$: 398.2264.

4,4-Diisopropyloxy-8-phenyl-1,3,5,7-tetramethyl-BODIPY (**1c**). This BODIPY was produced in 26% yield by method B and could not be obtained by method C. The crude product

was purified via TLC (eluent 80:20 hexane/EtOAc) to give an orange solid, that was recrystallized from 1:1 hexane/dichloromethane. Mp: 140-145 °C; ^{1}H NMR ($CDCl_3$, 400 MHz) δ 7.49-7.30 (m, 5H), 5.96 (s, 2H), 3.40-3.34 (septuplet, *J* = 6.24 Hz, 2H), 2.61 (s, 6H), 1.39 (s, 6H), 0.89 (d, *J* = 6.08 Hz, 12H); ^{13}C NMR ($CDCl_3$, 100 MHz) δ 156.26, 141.50, 141.42, 135.96, 132.28, 129.06, 128.78, 128.46, 121.16, 63.01, 24.93, 15.76, 14.65; ^{11}B NMR ($CDCl_3$, 128 MHz) δ 1.30 (s); HRMS (ESI-TOF) *m/z* 426.2564 $[M + Na]^+$ calculated for $C_{25}H_{33}BN_2NaO_2$: 426.2575.

4,4-Diallyloxy-8-phenyl-1,3,5,7-tetramethyl-BODIPY (**1d**). This BODIPY was produced in 57% yield by method B and 30% by method C. The crude product was purified by TLC (eluent 80:20 hexane/EtOAc) to give an orange solid that was recrystallized from 1:1 hexane/dichloromethane. Mp: 70-73 °C; ^{1}H NMR ($CDCl_3$, 400 MHz) δ 7.52-7.29 (m, 5H), 5.95 (s, 2H), 5.92-5.82 (m, 2H), 5.15 (d, *J* = 1.84 Hz, 1H), 5.11 (d, *J* = 1.88 Hz, 1H), 4.92 (d, 1H), 4.89 (d, 1H), 3.63 (d, *J* = 5.24 Hz, 4H), 2.56 (s, 6H), 1.38 (s, 6H); ^{13}C NMR ($CDCl_3$, 100 MHz) δ 156.06, 141.53, 138.70, 135.77, 132.78, 129.13, 128.85, 128.34, 128.23, 121.18, 113.42, 63.41, 15.03, 14.59; ^{11}B NMR ($CDCl_3$, 128 MHz) δ 2.01 (s); HRMS (ESI-TOF) *m/z* 422.2251 $[M + Na]^+$ calculated for $C_{25}H_{29}BN_2NaO_2$: 422.2254.

4,4-(Diprop-2-yn-1-yloxy)-8-phenyl-1,3,5,7-tetramethyl-BODIPY (**1e**). This BODIPY was produced in 52% yield by method B and 40% by method C. The crude product was purified via TLC (eluent 80:20 hexane/EtOAc) to give an orange solid, that was recrystallized from 1:1 hexane/dichloromethane. Mp: 70-73 °C; ^{1}H NMR ($CDCl_3$, 400 MHz) δ 7.49-7.27 (m, 5H), 5.97 (s, 2H), 3.86 (s, 4H), 2.61 (s, 6H), 1.52 (s, 2H), 1.40 (s, 6H); ^{13}C NMR ($CDCl_3$, 100 MHz) δ 156.62, 142.22, 141.42, 135.58, 132.79, 129.16, 128.92, 128.26, 121.52, 83.16, 70.83, 49.96,

15.19, 14.58; ^{11}B NMR ($CDCl_3$, 128 MHz) δ 1.78 (s); HRMS (ESI-TOF) *m/z* 418.1938 $[M + Na]^+$ calculated for $C_{25}H_{25}BN_2NaO_2$: 418.1934.

4,4'-(Di-N-Benzyl,-1,2,3,triazoloxy)-8-phenyl-1,3,5,7-tetramethyl-BODIPY (**4**). 4,4-Dipropargyloxy-BODIPY **1e** (15.7 mg, 0.040 mmol, 1.0 equiv.) and Cu(0) (10.1 mg, 0.158 mmol, 4.0 equiv.) were dissolved in a mixture of THF/water (8 mL, 3:1) under inert gas atmosphere. Benzyl azide (0.074 mL, 0.594 mmol, 5.0 equiv.) was added dropwise to the reaction mixture. A solution of $CuSO_4 \cdot 5H_2O$ (7.4 mg, 0.030 mmol, 0.75 equiv.) and sodium ascorbate (15.7 mg, 0.079 mmol, 2.0 equiv.) in THF/water (8 mL, 3:1) was added (after sonication for 30 min) and the reaction mixture was heated for 1.5 h at 70 °C. Once TLC indicated reaction completion the mixture was cooled to room temperature and partitioned between ethyl acetate (30 mL) and water (30 mL). The combined organic layers were dried over Na_2SO_4 and then concentrated under reduced pressure. The crude product was purified via prep-TLC eluted with 20:80 hexane/EtOAc and recrystallized from 3:1 hexane/dichloromethane to afford the bis(1,2,3-triazole)-BODIPY **4** as a dark orange solid (20.4 mg, 78% yield). ^{1}H NMR ($CDCl_3$, 400 MHz) δ 7.50 (s, 2H), 7.36-7.27 (m, 15H), 5.84 (s, 2H), 5.43 (s, 4H), 4.28 (s, 4H), 2.40 (s, 6H), 1.36 (s, 6H); ^{13}C NMR ($CDCl_3$, 100 MHz) δ 155.63, 149.42, 142.17, 135.48, 134.93, 129.21, 129.15, 128.75, 128.35, 128.30, 121.68, 121.48, 56.80, 54.15, 31.06, 29.84, 29.41, 14.96, 14.57; ^{11}B NMR ($CDCl_3$, 128 MHz) δ 2.06 (s); HRMS (ESI-TOF) *m/z* 684.3218 $[M + Na]^+$ calculated for $C_{39}H_{39}BN_8NaO_2$: 684.3229.

2.4.3 X-ray Determined Molecular Structures

Crystal structures were determined using low-temperature data from a Bruker Kappa APEX-II DUO diffractometer with either MoKα or CuKα radiation. For all structures, H atoms

were located from difference maps but constrained in calculated positions during refinement. For **1a**, Z' = 3/2, for **1b**, Z' = 1/2, and for **1e**, **3a** and **4**, Z' = 2. **3a** was the hemihydrate and a nonmerohedral twin, and **4** was also a nonmerohedral twin.

Crystal data **1a**: $C_{21}H_{25}BN_2O_2$, M = 348.24, monoclinic, a = 20.2592(14), b = 11.2886(8), c = 12.7820(8) Å, β = 93.968(3)°, U = 2916.2(3) Å^3, T = 100 K, space group P2/c, Z = 6, D_c = 1.190 g cm^{-3}, μ(Cu Kα) = 0.597 mm^{-1}, 24457 reflections measured, θ_{max} = 68.8˚, 5251 unique (R_{int} = 0.032). The final R = 0.040 (4321 *I>2σ(I)* data), *wR(F2)* = 0.105 (all data), CCDC 1035578.

Crystal data **1b**: $C_{23}H_{29}BN_2O_2$, M = 376.29, monoclinic, a = 9.1588(4), b = 11.4850(7), c = 10.1066(4) Å, β = 96.860(2)°, U = 1055.49(9) Å^3, T = 100 K, space group P2/n, Z = 2, D_c = 1.184 g cm^{-3}, μ(Mo Kα) = 0.075 mm^{-1}, 33635 reflections measured, θ_{max} = 29.4˚ 3096 unique (R_{int} = 0.045). The final R = 0.043 (2411 *I>2σ(I)* data), *wR(F2)* = 0.119 (all data), CCDC 1035579.

Crystal data **1c**: $C_{25}H_{33}BN_2O_2$, M = 404.34, monoclinic, a = 9.0299(11), b = 16.252(2), c = 16.2554(19) Å, β = 102.241(7)°, U = 2331.3(5) Å^3, T = 100 K, space group P2$_1$/c, Z = 4, D_c = 1.152 g cm^{-3}, μ(Mo Kα) = 0.072 mm^{-1}, 12118 reflections measured, θ_{max} = 25.9˚, 4417 unique (R_{int} = 0.091). The final R = 0.058 (2457 *I>2σ(I)* data), *wR(F2)* = 0.134 (all data), CCDC 1035580.

Crystal data **1e**: $C_{25}H_{25}BN_2O_2$, M = 396.28, monoclinic, a = 7.9474(8), b = 11.8269(10), c = 45.453(4) Å, β = 92.521(6)°, U = 4268.2(7) Å^3, T = 100 K, space group P2$_1$/n, Z = 8, D_c = 1.233 g cm^{-3}, μ(Cu Kα) = 0.611 mm^{-1}, 18058 reflections measured, θ_{max} = 67.4˚, 7057 unique (R_{int} = 0.045). The final R = 0.080 (5633 *I>2σ(I)* data), *wR(F2)* = 0.180 (all data), CCDC 1035581.

Crystal data **3a**: $C_{23}H_{27}BN_2O_4$•0.5(H_2O), M = 415.28, triclinic, a = 7.6310(6), b = 15.4871(12), c = 19.4805(16) Å, α = 72.585(4), β = 84.215(4), γ = 89.809(4)˚, U = 2184.7(3) Å^3, T = 100 K, space group P-1, Z = 4, D_c = 1.263 g cm^{-3}, μ(Cu Kα) = 0.703 mm^{-1}, 15119 reflections measured, θ_{max} = 66.9˚, 7555 unique (R_{int} = 0.108). The final R = 0.067 (5951 $I>2\sigma(I)$ data), $wR(F2)$ = 0.196 (all data), CCDC 1035582.

Crystal data **4**: $C_{39}H_{39}BN_8O_2$, M = 662.59, triclinic, a = 11.1659(8), b = 16.0899(12), c = 19.5309(13) Å, α = 90.127(5), β = 92.245(5), γ = 96.332(5)˚, U = 3484.7(4) Å^3, T = 90 K, space group P-1, Z = 4, D_c = 1.263 g cm^{-3}, μ(Cu Kα) = 0.639 mm^{-1}, 33229 reflections measured, θ_{max} = 67.7˚, 11371 unique (R_{int} = 0.062). The final R = 0.049 (8767 $I>2\sigma(I)$ data), $wR(F2)$ = 0.123 (all data), CCDC 1051095.

2.4.4 Steady-state Absorption and Fluorescence Spectroscopy

The photophysical properties of compounds **1**, **1a-e**, **2**, **2a**, **3**, **3a** and **4** were determined by preparing a stock solution with a concentration of 5 × 10^{-5} M and diluting it to appropriate concentrations for absorbance and emission spectra measurements. All the absorption spectra were obtained using a Varian Cary 50 UV/visible spectrophotometer. The optical density, ε, were taken by preparing solution concentrations between 7.5 × 10^{-6} and 2.5 × 10^{-5} M in order to get λ_{max} between 0.5 and 1.0. Emission spectra were measured on a PTI QuantaMaster4/2006SE spectrofluorometer with the slit width set at 3 nm. All absorbance and emission spectra were acquired within 3 h of fresh solution preparation, at room temperature. BODIPYs **1**, **2**, and **3** were used as a standard in THF for calculating the fluorescence quantum yields with an excitation at 480 nm (BODIPY **1** Φ_f = 0.56,[30] BODIPY **2** Φ_f = 0.93,[29] BODIPY **3** Φ_f = 0.43),[29] as previously

reported. Rhodamine 6G (Φ_f = 0.95 in EtOH) was used as the reference for compounds **1**, **1a-e**, **2**, **2a**, **3**, **3a**, and **4** in toluene. A spectrophotometric cell with a path length of 10 mm was used.

2.4.5 Computational Modeling

The reaction mechanism was studied by electronic structure calculations at the B3LYP/6-31+G(d,p) level. The hybrid Becke's Three Parameter DFT Functional was used.[39-40] The solvent effects were taken into account using the Polarized Continuum Model (PCM).[41-42] Atomic charges were calculated following the NPA method.[43-44] The geometries of all structures were optimized without symmetry constraints. The stationary points on the potential energy surface were confirmed with frequency calculations. All calculations were performed using the Gaussian 09 program package.

2.5 References

1. Nguyen, A. L.; Bobadova-Parvanova, P.; Hopfinger, M.; Fronczek, F. R.; Smith, K. M.; Vicente, M. G., Synthesis and Reactivity of 4,4-Dialkoxy-BODIPYs: An Experimental and Computational Study. *Inorg. Chem.* **2015**, *54*, 3228-3236.

2. Loudet, A.; Burgess, K., BODIPY Dyes and Their Derivatives: Syntheses and Spectroscopic Properties. *Chem. Rev.* **2007**, *107*, 4891-4932.

3. Ikeda, C.; Maruyama, T.; Nabeshima, T., Convenient and Highly Efficient Synthesis of Boron-Dipyrrins Bearing an Arylboronate Center. *Tetrahedron Lett.* **2009**, *50*, 3349-3351.

4. Richards, V. J.; Gower, A. L.; Smith, J. E. H. B.; Davies, E. S.; Lahaye, D.; Slater, A. G.; Lewis, W.; Blake, A. J.; Champness, N. R.; Kays, D. L., Synthesis and Characterisation of BODIPY Radical Anions. *Chem. Commun.* **2012**, *48*, 1751-1753.

5. Gabe, Y.; Ueno, T.; Urano, Y.; Kojima, H.; Nagano, T., Tunable Design Strategy for Fluorescence Probes Based on 4-Substituted BODIPY Chromophore: Improvement of Highly Sensitive Fluorescence Probe for Nitric Oxide. *Anal. Bioanal. Chem.* **2006**, *386*, 621-626.

6. Smithen, D. A.; Baker, A. E.; Offman, M.; Crawford, S. M.; Cameron, T. S.; Thompson, A., Use of *F*-BODIPYs as a Protection Strategy for Dipyrrins: Optimization of BF_2 Removal. *J. Org. Chem.* **2012**, *77*, 3439-3453.

7. Tahtaoui, C.; Thomas, C.; Rohmer, F.; Klotz, P.; Duportail, G.; Mely, Y.; Bonnet, D.; Hibert, M., Convenient Method to Access New 4,4-Dialkoxy- and 4,4-Diaryloxy-diaza-*s*-indacene Dyes: Synthesis and Spectroscopic Evaluation. *J. Org. Chem.* **2007**, *72*, 269-272.

8. Tokoro, Y.; Nagai, A.; Chujo, Y., Nanoparticles via H-aggregation of Amphiphilic BODIPY Dyes. *Tetrahedron Lett.* **2010**, *51*, 3451-3454.

9. Wijesinghe, C. A.; El-Khouly, M. E.; Subbaiyan, N. K.; Supur, M.; Zandler, M. E.; Ohkubo, K.; Fukuzumi, S.; D'Souza, F., Photochemical Charge Separation in Closely Positioned Donor-Boron Dipyrrin-Fullerene Triads. *Chem. Eur. J.* **2011**, *17*, 3147-3156.

10. Brizet, B.; Eggenspiller, A.; Gros, C. P.; Barbe, J. M.; Goze, C.; Denat, F.; Harvey, P. D., B,B-Diporphyrinbenzyloxy-BODIPY Dyes: Synthesis and Antenna Effect. *J. Org. Chem.* **2012**, *77*, 3646-3650.

11. Deniz, E.; Battal, M.; Cusido, J.; Sortino, S.; Raymo, F. M., Insights into the Isomerization of Photochromic Oxazines from the Excitation Dynamics of BODIPY-Oxazine Dyads. *Phys. Chem. Chem. Phys.* **2012**, *14*, 10300-10307.

12. Brizet, B.; Bernhard, C.; Volkova, Y.; Rousselin, Y.; Harvey, P. D.; Goze, C.; Denat, F., Boron Functionalization of BODIPY by Various Alcohols and Phenols. *Org. Biomol. Chem.* **2013**, *11*, 7729-7737.

13. Sanchez-Carnerero, E. M.; Gartzia-Rivero, L.; Moreno, F.; Maroto, B. L.; Agarrabeitia, A. R.; Ortiz, M. J.; Banuelos, J.; Lopez-Arbeloa, I.; de la Moya, S., Spiranic BODIPYs: A Ground-Breaking Design to Improve the Energy Transfer in Molecular Cassettes. *Chem. Commun.* **2014**, *50*, 12765-12767.

14. Sanchez-Carnerero, E. M.; Moreno, F.; Maroto, B. L.; Agarrabeitia, A. R.; Ortiz, M. J.; Vo, B. G.; Muller, G.; de la Moya, S., Circularly Polarized Luminescence by Visible-Light Absorption in a Chiral *O*-BODIPY Dye: Unprecedented Design of CPL Organic Molecules from Achiral Chromophores. *J. Am. Chem. Soc.* **2014**, *136*, 3346-3349.

15. Zhang, S.; Wang, Y.; Meng, F.; Dai, C.; Cheng, Y.; Zhu, C., Circularly Polarized Luminescence of AIE-Active Chiral *O*-BODIPYs Induced via Intramolecular Energy Transfer. *Chem. Commun.* **2015**, *51*, 9014-9017.

16. Esnal, I.; Duran-Sampedro, G.; Agarrabeitia, A. R.; Banuelos, J.; Garcia-Moreno, I.; Macias, M. A.; Pena-Cabrera, E.; Lopez-Arbeloa, I.; de la Moya, S.; Ortiz, M. J., Coumarin-BODIPY Hybrids by Heteroatom Linkage: Versatile, Tunable and Photostable Dye Lasers for UV Irradiation. *Phys. Chem. Chem. Phys.* **2015**, *17*, 8239-8247.

17. Lundrigan, T.; Thompson, A., Conversion of *F*-BODIPYs to *Cl*-BODIPYs: Enhancing the Reactivity of *F*-BODIPYs. *J. Org. Chem.* **2013**, *78*, 757-761.

18. Courtis, A. M.; Santos, S. A.; Guan, Y.; Hendricks, J. A.; Ghosh, B.; Szantai-Kis, D. M.; Reis, S. A.; Shah, J. V.; Mazitschek, R., Monoalkoxy BODIPYs-A Fluorophore Class for Bioimaging. *Bioconjugate Chem.* **2014**, *25*, 1043-1051.

19. Guilleme, J.; Gonzalez-Rodriguez, D.; Torres, T., Triflate-Subphthalocyanines: Versatile, Reactive Intermediates for Axial Functionalization at the Boron Atom. *Angew. Chem. Int. Ed.* **2011**, *50*, 3506-3509.

20. Lundrigan, T.; Crawford, S. M.; Cameron, T. S.; Thompson, A., *Cl*-BODIPYs: A BODIPY Class Enabling Facile B-Substitution. *Chem. Commun.* **2012**, *48*, 1003-1005.

21. Darwish, A.; Blacker, M.; Janzen, N.; Rathmann, S. M.; Czorny, S.; Hillier, S. M.; Joyal, J. L.; Babich, J. W.; Valliant, J. F., Triazole Appending Agent (TAAG): A New Synthon for Preparing Iodine-Based Molecular Imaging and Radiotherapy Agents. *ACS Med. Chem. Lett.* **2012**, *3*, 313-316.

22. Pandey, S. K.; Pan, S.; Kant, R.; Kuruvilla, S. A.; Pan, M. L.; Mukherjee, J., Synthesis and Evaluation of 3-^{123}I-iodo-5-[2-(*S*)-3-pyrrolinylmethoxy]-pyridine (niodene) as a Potential Nicotinic $\alpha 4\beta 2$ Receptor Imaging Agent. *Bioorg. Med. Chem. Lett.* **2012**, *22*, 7610-7614.

23. Hendricks, J. A.; Keliher, E. J.; Wan, D.; Hilderbrand, S. A.; Weissleder, R.; Mazitschek, R., Synthesis of $^{[18F]}$BODIPY: Bifunctional Reporter for Hybrid Optical/Positron Emission Tomography Imaging. *Angew. Chem. Int. Ed.* **2012**, *51*, 4603-4606.

24. Li, Z. B.; Lin, T. P.; Liu, S. L.; Huang, C. W.; Hudnall, T. W.; Gabbai, F. P.; Conti, P. S., Rapid Aqueous [^{18}F]-Labeling of a BODIPY Dye for Positron Emission Tomography/Fluorescence Dual Modality Imaging. *Chem. Commun.* **2011**, *47*, 9324-9326.

25. Liu, S.; Lin, T. P.; Li, D.; Leamer, L.; Shan, H.; Li, Z.; Gabbai, F. P.; Conti, P. S., Lewis Acid-Assisted Isotopic ^{18}F-^{19}F Exchange in BODIPY Dyes: Facile Generation of Positron Emission Tomography/Fluorescence Dual Modality Agents for Tumor Imaging. *Theranostics* **2013**, *3*, 181-189.

26. Liu, S. L.; Li, D.; Shan, H.; Gabbai, F. P.; Li, Z. B.; Conti, P. S., Evaluation of ^{18}F-Labeled BODIPY Dye as Potential PET Agents for Myocardial Perfusion Imaging. *Nucl. Med. Biol.* **2014**, *41*, 120-126.

27. Shie, J. J.; Liu, Y. C.; Lee, Y. M.; Lim, C.; Fang, J. M.; Wong, C. H., An Azido-BODIPY Probe for Glycosylation: Initiation of Strong Fluorescence upon Triazole Formation. *J. Am. Chem. Soc.* **2014**, *136*, 9953-9961.

28. Paulus, A.; Desai, P.; Carney, B.; Carlucci, G.; Reiner, T.; Brand, C.; Weber, W. A., Development of a Clickable Bimodal Fluorescent/PET Probe for in Vivo Imaging. *EJNMMI Res* **2015**, *5*, 120.

29. Gibbs, J. H.; Robins, L. T.; Zhou, Z.; Bobadova-Parvanova, P.; Cottam, M.; McCandless, G. T.; Fronczek, F. R.; Vicente, M. G., Spectroscopic, Computational Modeling and Cytotoxicity of a Series of *meso*-Phenyl and *meso*-Thienyl-BODIPYs. *Bioorg. Med. Chem.* **2013**, *21*, 5770-5781.

30. Kollmannsberger, M.; Rurack, K.; Resch-Genger, U.; Daub, J., Ultrafast Charge Transfer in Amino-Substituted Boron Dipyrromethene Dyes and Its Inhibition by Cation Complexation: A New Design Concept for Highly Sensitive Fluorescent Probes. *J. Phys. Chem. A* **1998**, *102*, 10211-10220.

31. Bonnier, C.; Piers, W. E.; Parvez, M.; Sorensen, T. S., Borenium Cations Derived from BODIPY Dyes. *Chem. Commun.* **2008**, 4593-4595.

32. Hudnall, T. W.; Gabbai, F. P., A BODIPY Boronium Cation for the Sensing of Fluoride Ions. *Chem. Commun.* **2008**, 4596-4597.

33. Hopfinger, M. C.; Nguyen, A. L.; Bobadova-Parvanova, P.; Vicente, M. G. H., Computational Insights into the Reaction Mechanism of the Synthesis of Dimethoxy-substituted BODIPY. *Abstr. Pap. Am. Chem. Soc.* **2014**, *247*.

34. Uppal, T.; Bhupathiraju, N. V. S. D. K.; Vicente, M. G. H., Synthesis and Cellular Properties of Near-IR BODIPY–PEG and Carbohydrate Conjugates. *Tetrahedron* **2013**, *69*, 4687-4693.

35. Ke, M. R.; Yeung, S. L.; Ng, D. K.; Fong, W. P.; Lo, P. C., Preparation and in Vitro Photodynamic Activities of Folate-Conjugated Distyryl Boron Dipyrromethene Based Photosensitizers. *J. Med. Chem.* **2013**, *56*, 8475-8483.

36. Wang, H. J.; Vicente, M. G. H.; Fronczek, F. R.; Smith, K. M., Synthesis and Transformations of 5-Chloro-2,2'-Dipyrrins and Their Boron Complexes, 8-Chloro-BODIPYs. *Chem. Eur. J.* **2014**, *20*, 5064-5074.

37. Wang, J. G.; Hou, Y. J.; Li, C.; Zhang, B. W.; Wang, X. S., Selectivity Tune of Fluoride Ion Sensing for Phenolic OH-Containing BODIPY Dyes. *Sensor Actuat B-Chem* **2011**, *157*, 586-593.

38. Qin, W.; Baruah, M.; De Borggraeve, W. M.; Boens, N., Photophysical Properties of an On/Off Fluorescent pH Indicator Excitable with Visible Light Based on a Borondipyrromethene-Linked Phenol. *J. Photochem. Photobiol. A* **2006**, *183*, 190-197.

39. Becke, A. D., Density-Functional Thermochemistry . III. The Role of Exact Exchange. *J. Chem. Phys.* **1993**, *98*, 5648-5652.

40. Lee, C. T.; Yang, W. T.; Parr, R. G., Development of the Colle-Salvetti Correlation-Energy Formula into a Functional of the Electron-Density. *Phys Rev B* **1988**, *37*, 785-789.

41. Miertus, S.; Scrocco, E.; Tomasi, J., Electrostatic Interaction of a Solute with a Continuum - a Direct Utilization of Abinitio Molecular Potentials for the Prevision of Solvent Effects. *Chem. Phys.* **1981**, *55*, 117-129.

42. Tomasi, J.; Mennucci, B.; Cammi, R., Quantum Mechanical Continuum Solvation Models. *Chem. Rev.* **2005**, *105*, 2999-3093.

43. Foster, J. P.; Weinhold, F., Natural Hybrid Orbitals. *J. Am. Chem. Soc.* **1980**, *102*, 7211-7218.

44. Reed, A. E.; Curtiss, L. A.; Weinhold, F., Intermolecular Interactions from a Natural Bond Orbital, Donor-Acceptor Viewpoint. *Chem. Rev.* **1988**, *88*, 899-926.

CHAPTER 3: SYNTHESIS AND CHARACTERIZATION OF 4,4-DICYANO- AND 4,4-FUNCTIONALIZED BODIPYS[a]

3.1 Introduction

Recent growth in fluorescence labeling for bioanalytical purposes has provided new developments in cellular biology, bioimaging, medicine, and pharmacy fields. One of the most promising fluorophores to be used for these applications is boron dipyrromethene (also known as BODIPY). The distinct characteristics of BODIPY are high photochemical and thermal stabilities, large molar extinction coefficients, high fluorescence quantum yields, and ease of modification.

Postmodification of the BODIPY core has been an appealing topic in the past years.[1-3] Functionalization at various positions of the BODIPY core provides new robust organic dyes with fascinating optical properties such as with fluorescence quantum yield, moderate Stokes shifts, and large molar extinction coefficients. However, one of the limitation is the moderate Stokes shift (~20 mm) generally displayed by many known BODIPY dyes. One particular position on the BODIPY framework that is being investigated is the boron center for its potential enhancement of the Stokes shifts and fluorescence quantum yields of BODIPYs.

There are a few boron functionalization approaches toward synthesis of *C*- and *E*-BODIPYs. *C*-BODIPYs have an aryl or alkyl group chelated to the boron center while *E*-BODIPYs have ethynyl groups. The first approach consists of reaction between dipyrromethenes with haloborane compounds.[4-12] Holten and coworkers[4] reported the first 4,4-dialkyl-BODIPYs via dipyrromethene complexation with dialkyboron analogues such as bromodimethylborane, dibutylboron triflate, or 9-BBN triflate. Using the latter methodology, BODIPYs bearing 4-mono- and 4,4'-substituents have been reported.[5] Several groups have reported the use of halogenated

[a] Part of this chapter originally published as Nguyen, A. L.; Fronczek, F. R.; Smith, K. M.; Vicente, M. G. H., Synthesis of 4,4'-functionalized BODIPYs from dipyrrins. *Tetrahedron Lett.* **2015**, *56*, 6348-6351. Reprinted with permission from [1] Copyright (2015) Elsevier Publications.

boranes to introduce oxygen substituents on boron in one step.[6-8] On the other hand, more constrained BODIPYs were synthesized through cyclization of 3,5-diaryl-substituted groups with boron-containing compounds.[9-12]

Another approach is the direct substitution of the fluoride atoms at the boron center with carbon nucleophiles. Using Grignard or organolithium reagents, several *C*- and *E*-BODIPYs were synthesized in one or two steps with dialkyl, diaryl, and dialkynyl groups.[13-21] These *E*-BODIPYs have been shown to induce large Stokes shifts and found to be relatively stable under strong basic and acidic conditions. Using the latter method, dimeric dialkynyl-BODIPYs were reported.[17] A similar strategy was previously employed for the synthesis of a 4,4'-dicyano-BODIPY using trimethylsilylcyanide in the presence of BF_3•OEt_2 or $SnCl_4$ as catalyst.[18] Carbon nucleophiles chelating to the boron center provides a more stable BODIPY compared to its BF_2 precursor.[22]

In order to broaden the scope of boron functionalization, development of milder carbon nucleophiles and unsymmetric substitution on the boron center must be studied. In this chapter, we investigated the reactivity of Lewis acid mediated boron functionalizations and extend this methodology to the synthesis of new 4,4-dicyano-BODIPYs. In addition, we also explored and prepared a series of novel functionalized BODIPYs bearing phenyl and various substituents at the boron center. These compounds **7a-g** and **8a-g** were synthesized in a three step one-pot reaction between dipyrromethenes and dichlorophenylborane, followed by replacement of chloride atom with fluoride and various carbon- and oxygen-centered nucleophiles. These BODIPYs' structural, spectroscopic, and fluorescence properties are reported and discussed in this chapter.

3.2 Results and Discussion

3.2.1 Syntheses

Five BODIPYs **1-5** were synthesized according to previous reports.[23-24] We begin by following a previously reported procedure from Burgess and coworkers[18] for the synthesis of 4,4-dicyano-BODIPYs. Our preliminary investigation began with various Lewis acids (Table 3.1). Using tin tetrachloride ($SnCl_4$) and shorter amount of time (10 min) at ambient temperature, BODIPY **1a** can be synthesized and isolated with 79% yield while boron trifluoride etherate (BF_3•OEt_2) and longer time (2 hours) gave 84% yield. Indeed, the product yield decreased to 39% yield when a milder Lewis acid ($AlCl_3$) was used. However, the isolated yield increased up to 49% at reflux temperature. This is in agreement with our previous studies of reaction conditions at room temperature reflux conditions.[25]

Table 3.1: Preliminary studies for synthesis of Lewis acid mediated 4,4'-dicyano-BODIPY.

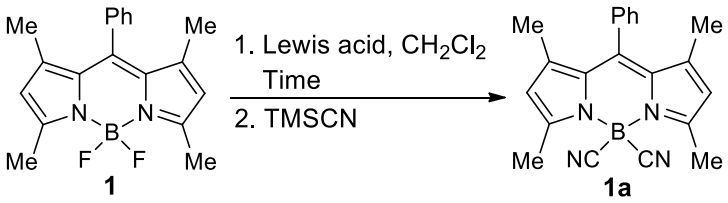

Entry	Lewis acid	Temp	Time	Yield (%)
1	$SnCl_4$	25 °C	10 min	79
2	$BF_3 \cdot OEt_2$	25 °C	2 h	84
3	$AlCl_3$	40 °C	2 h	49
4	$AlCl_3$	25 °C	1 h	39

To further investigate and optimize the scope of our reaction, we subjected BODIPYs **1-5** to Lewis acid mediated substitutions using TMSCN as nucleophile to study their reactivity toward boron functionalization (Table 3.2). When BODIPY **2** containing two electron-donating groups on

the 8-aryl substituent was subjected to above conditions, the corresponding 4,4'-dicyano-BODIPY **2a** was obtained in 37% yield. On the other hand, BODIPY **3** with an electron-withdrawing methoxycarbonyl group on the 8-aryl produced BODIPY **3a** in 65% yield. BODIPYs **4a** and **5a** with *meso*-free and *meso*-phenyl substituent, respectively were obtained in 51% and 81% yields.

Table 3.2: Synthesis of 4,4'-dicyano-BODIPYs 1a-5a with isolated yields.

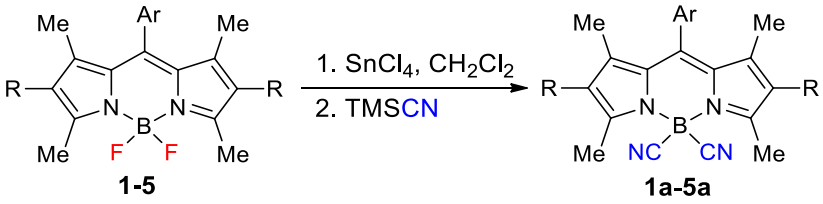

BODIPY	R	Ar	Yield (%)
1a	H	Ph	79
2a	H	3,4-$(OMe)_2$Ph	37
3a	H	4-CO_2MePh	65
4a	Et	Ph	81
5a	Et	H	51

In the presence of a Lewis acid ($AlCl_3$, BF_3•OEt_2, BCl_3 and $SnCl_4$), these methods can afford either the 4-mono- or 4,4'-disubstituted BODIPYs depending on the reaction conditions. In order to prepare 4,4'-difunctionalized BODIPYs containing two different substituents on the boron center, additional synthetic steps are required. The aim of our work is to synthesize 4,4'-difunctionalized BODIPYs in one pot. Our initial synthetic approach was to treat BODIPY **4** with triethylamine and dichlorophenylborane to produce BODIPY **7b**, as previously reported.[8,26] Unfortunately, thin layer chromatography (TLC) indicated presence of the starting material. It has

been recently reported that BODIPYs can react with boron trichloride followed by a Grignard reagent or alkoxide to afford the corresponding difunctionalized BODIPYs.[26]

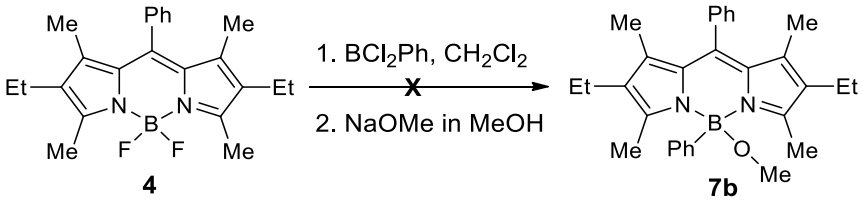

Scheme 3.1: Attempted reaction for synthesis of 4,4-difunctionalized-BODIPY **7b**.

Alternatively, we also attempted to use the commercially available 2,4-dimethyl pyrrole in a three-step one-pot reaction BODIPY synthesis with dichlorophenylborane, followed by sodium methoxide to give BODIPY **6** with phenyl and methoxy substituents with an overall yield of 4%. Due to the low overall percent yield, we investigated the use of dipyrromethenes as our starting material for further functionalization with various nucleophiles.

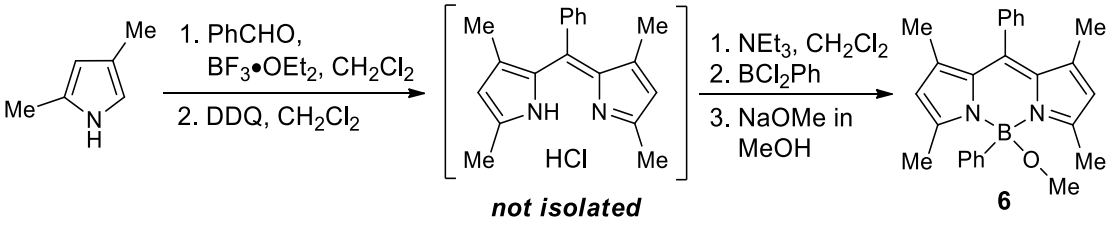

Scheme 3.2: Synthesis of 4,4-difunctionalized-BODIPY **6** from 2,4-dimethyl pyrrole.

The starting dipyrrin hydrochloride salts **7** and **8** were synthesized from ketopyrrole and the corresponding pyrroles as previously reported.[27] The three-step one-pot reaction consists of treating dipyrrins **7** or **8** in anhydrous dichloromethane with 5 equiv of triethylamine (TEA). After 30 min, phenylboron dichloride (5 equiv) was added dropwise to the mixture, followed by 10 equiv of a nucleophile, and the reaction was stirred at room temperature for an additional 1-2 hours to afford the corresponding 4,4-difunctionalized BODIPYs **7a-g** and **8a-g**.

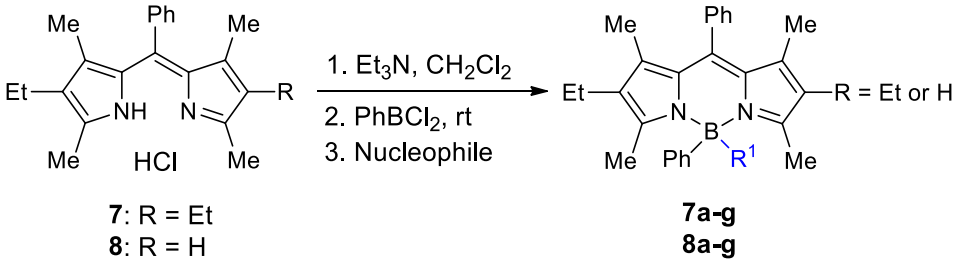

7: R = Et
8: R = H

7a-g
8a-g

Scheme 3.3: One-pot synthesis of BODIPYs from dipyrrins.

For comparison purposes between various substituents on the boron center, dipyrrins **7** and **8** were also reacted with triethylamine and complexation with BF_3•OEt_2 to give *F*-BODIPYs **4** and **9** in 68 and 41% yields, respectively.[28] The isolated yields (14-63%) obtained for the target 4,4'-difunctionalized BODIPYs **7a-g** and **8a-g** are given in Table 3.3. Some nucleophiles resulted in lower yields due to the competing reaction with water to give the hydroxide derivatives as by-products, which have been previously isolated and characterized.[6,29] Using tetrabutylammonium fluoride (TBAF) as the fluoride source, 4-phenyl-BODIPYs **7a** and **8a** were obtained in 52% and 41% yields, respectively which are milder conditions than those reported in the literature.[6,29-30] This indicates that the B-Cl bond strength is weaker and more easily displaced than the B-F bond, and thus the reaction does not require elevated temperature or the presence of Lewis acid activators.

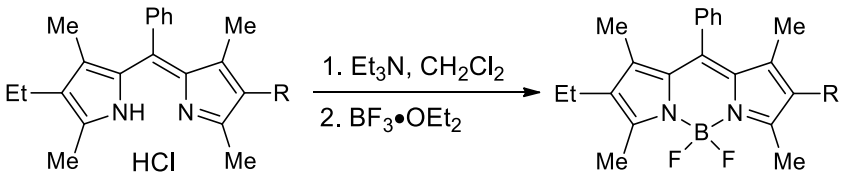

7: R = Et
8: R = H

4: R = Et
9: R = H

Scheme 3.4: Synthesis of *F*-BODIPYs **4** and **9** from dipyrrins.

Hard and soft nucleophiles were screened under our above milder reaction conditions. Soft nucleophile such as trimethylsilyl cyanide (TMSCN) has been used previously for boron

functionalization through Lewis acid mediation (tin tetrachloride or boron trifluoride).[18] However, hard nucleophiles such as alkoxides and acetate also produced the target BODIPYs in moderate yields (Table 3.3). Other nucleophiles containing amine, ester and acetylene functionalities can be employed under our milder conditions, thus allowing for further functionalization or conjugation to the BODIPY through the boron atom.[18,25,31]

Table 3.3: Yields and ^{11}B NMR chemical shifts (128 MHz, $CDCl_3$, all singlets) for BODIPYs 7a-g and 8a-g.

BODIPY	R	R^1	Yield (%)	δ (ppm)
7a	Et	F	52	2.43
7b	Et	OMe	63	2.18
7c	Et	CN	17	-9.42
7d	Et	OAc	25	-0.48
7e	Et	OCH_2CH_2NHBoc	32	1.54
7f	Et	$O(CH_2CH_2O)_3Me$	21	1.63
7g	Et	$OCH_2C{\equiv}CH$	25	1.73
8a	H	F	41	2.23
8b	H	OMe	49	2.10
8c	H	CN	18	-7.43
8d	H	OAc	16	-0.34
8e	H	OCH_2CH_2NHBoc	14	1.10
8f	H	$O(CH_2CH_2O)_3Me$	15	1.21
8g	H	$OCH_2C{\equiv}CH$	31	1.65

The addition of a polyethylene glycol group is used for increasing solubility of BODIPY without changing the absorption and emission wavelengths. We also attempted to deprotect the

Boc group in BODIPY **7e** to give BODIPY **7h**, but the deprotection failed and resulted in BODIPY **7j**. We suspected that the B-O bond is reactive toward TFA conditions as previously reported.[22]

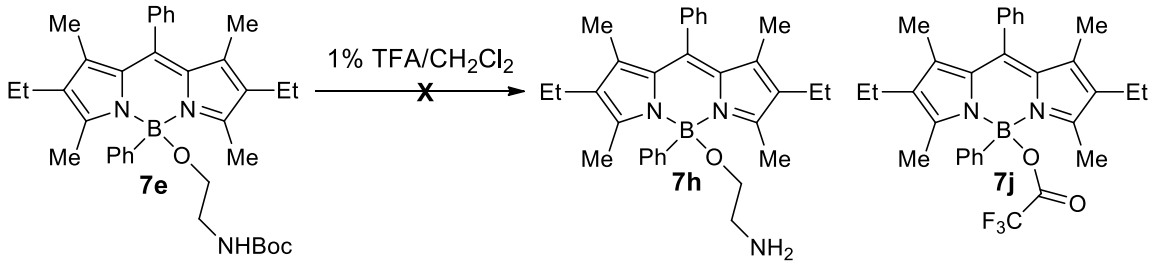

Scheme 3.5: Attempt Boc deprotection reaction of BODIPY **7e**.

3.2.2 Structural Characterization

All BODIPYs were characterized by ^{1}H, ^{13}C, and ^{11}B NMR, HRMS (ESI-TOF), and UV-Vis absorbance and fluorescence spectrophotometry. BODIPYs **1a**, **3a-5a**, **7b**, **7c**, and **8c** were also characterized by X-ray crystallography (see Figure 3.1). Different substituents on the boron center have no substantial effect on the 3,5-dimethyl and 2,6-diethyl chemical shifts. Indeed, the ^{1}H NMR spectra clearly show that the 3,5-methyl groups appear as a singlet around 2.2 ppm and the 1,7-methyl groups at 1.3 ppm for BODIPYs **7a-g**. However, the 1,3,5,7-methyl groups for BODIPYs **8a-g** consist of 4 singlets at 2.2, 2.1, 1.4 and 1.3 ppm. Significant differences were observed in the ^{11}B NMR of the BODIPYs using $BF_3{\bullet}OEt_2$ as reference (δ = 0 ppm), as shown in Table 3.3. The ^{11}B NMR spectra clearly shows the 4,4'-dicyano-BODIPYs **1a-5a** via the singlet peaks attributed to $B(CN)_2$ at ca. -16.9 ppm. Indeed, the ^{11}B NMR spectra showed that the chemical shifts are influenced by the electron density of the substituents bound to boron, which is greater for BODIPYs **1a-5a** and less for the 4-phenyl-BODIPYs **7c** and **8c**, and lowest for the mono-fluorides **7a** and **8a**. BODIPYs **4** and **9** bearing two fluorides, have a triplet peak at 0.7 ppm with ca. $J(^{11}B\text{-}^{19}F)$ = 33 Hz. The ^{11}B NMR spectra clearly shows a singlet for all BODIPYs **7a-g** and **8a-g** with chemical shifts ranging from the mono-fluoride **7a** (2.43 ppm) to the cyano derivative

7c (9.42 ppm). For the case of **7a** and **8a**, the lack of boron-fluorine coupling might be due to quadrupolar broadening, as previously observed.[6,14]

Crystals suitable for X-ray analysis were grown by slow diffusion of hexane in dichloromethane (for BODIPYs **7c** and **8c**) or in ethyl acetate (for BODIPY **7b**) and slow diffusion in dichloromethane for BODIPYs **1a-5a**. Structures are shown in Figure 3.1. The C_3N_2B cores of both of the two independent molecules of **1a** (only one shown in Fig. 1) are nearly planar, with mean deviations 0.012 and 0.017 Å.

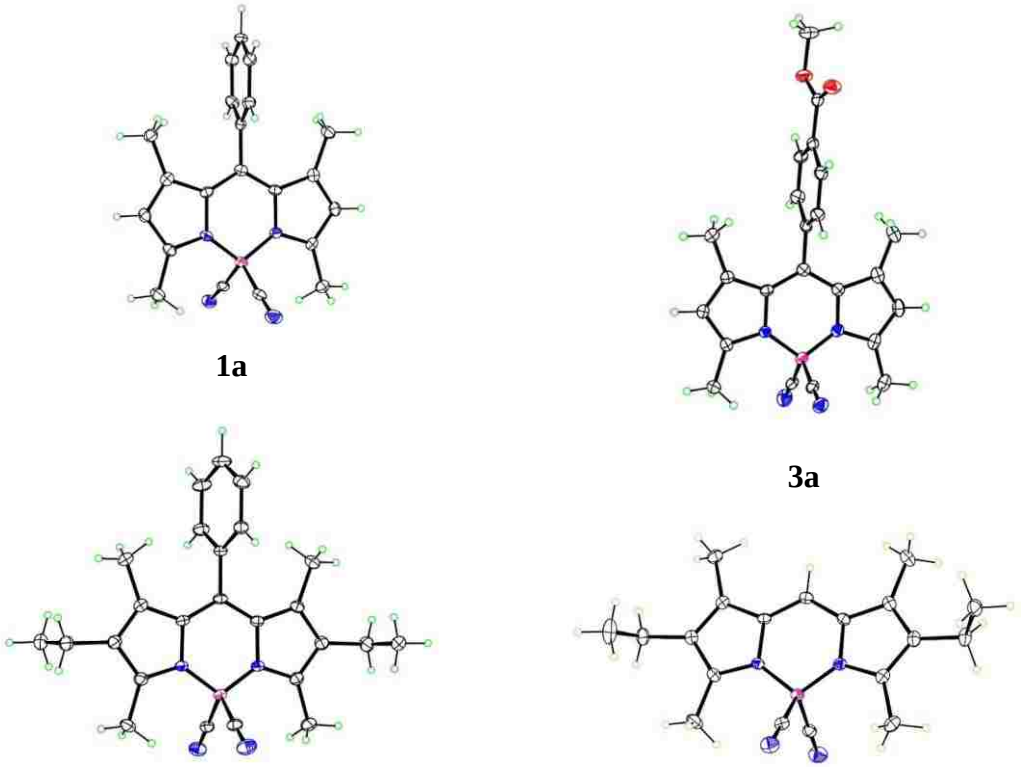

Figure 3.1: Molecular structures of BODIPYs **1a** and **3a-5a** from X-ray crystal analysis, with 50% probability ellipsoids.

The phenyl groups form dihedral angle of 75.8 and 78.8° with those planes. In **3a**, the central ring is nonplanar, with the $B(CN)_2$ substituent tilted such that the B atom is 0.157 Å out of

the plane of the other five atoms. The phenyl group of the *meso* substituent is nearly orthogonal to the central plane, with a dihedral angle of 88.1°. The central ring of **4a** has a similar conformation to that of **3a**, but with a smaller out-of-plane deviation for the B atom, 0.057 Å and a 77.6° dihedral angle for the phenyl ring. In **5a**, the out-of-plane deviation for the B atom is somewhat larger, 0.205 Å. In all cases, the central BN_2C_3 ring is fairly planar, with mean deviation of 0.020 Å for both **7b** and **7c** and 0.056 Å for **8c** (Figure 3.2). The 8-mesophenyl is oriented approximately perpendicular to the BODIPY core plane, to avoid steric hindrance from the 1,7-dimethyl substituents, the dihedral angles being 84.1° for **7b**, 85.3° for **7c**, and 87.6° for **8c**. Likewise, the phenyl group on boron forms dihedral angles with the central ring of 86.1° for **7b**, 85.9° for **7c**, and 83.2° for **8c**.

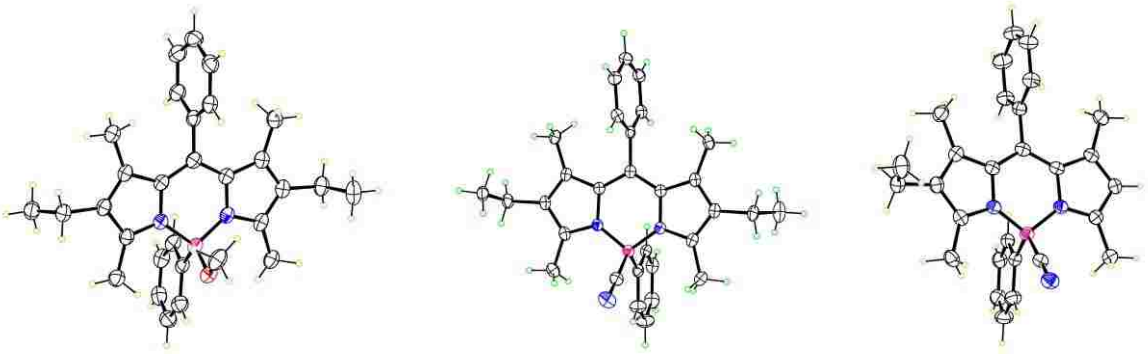

7b **7c** **8c**

Figure 3.2: Molecular structures of BODIPYs **7b-c**, and **8c** from X-ray crystal analysis, with 50% probability ellipsoids.

3.2.3 Spectroscopic Study

The spectroscopic properties of BODIPYs **7a-g**, **8a-g**, **4** and **9** were determined in dichloromethane at room temperature and the results are summarized in Table 3.4. All BODIPYs show absorptions (511-524 nm) in the visible range that correspond to the S_0-S_1 (π-π^*) transition. The symmetric BODIPYs **7a-g** showed strong absorption bonds with high molar absorption

coefficients (log ε = 4.6-4.9) in the range of 521-524 nm and emission bands between 533-537 nm. The asymmetric BODIPYs **8a-g** also showed strong absorption bonds with high molar absorption coefficients (log ε = 4.7-5.0) and blue-shifted absorption bands (511-513 nm) and emission bands (521-523 nm). All BODIPYs showed Stokes shift ranging from 9 to 15 nm.

Table 3.4: Absorption and emission spectroscopic properties of BODIPYs 7a-g, 8a-g, 4, and 9 in CH_2Cl_2 at room temperature.

BODIPYs	Absorption λ_{max} (nm)	Emission λ_{max} (nm)	log ε (M^{-1} cm^{-1})	Φ_f	Stokes' shift (nm)
7a	524	535	4.86	0.53	11
7b	522	537	4.77	0.42	15
7c	521	533	4.63	0.65	12
7d	522	533	4.63	0.64	11
7e	523	533	4.73	0.60	11
7f	523	534	4.82	0.48	11
7g	523	534	4.61	0.51	11
8a	513	523	4.85	0.61	10
8b	512	523	4.92	0.50	11
8c	511	521	4.97	0.78	10
8d	512	522	4.81	0.68	10
8e	513	523	4.76	0.60	10
8f	512	521	4.72	0.51	9
8g	513	523	4.78	0.64	10
4	526	536	4.68	0.74	10
9	514	524	4.49	0.82	10

ε = extinction coefficient; Φ_f = fluorescence quantum yield

BODIPYs bearing flexible groups show decreased fluorescence quantum yields due to increased energy lost to non-radiative decay to the ground state, which is in agreement with

previous observations.[25,32] BODIPYs bearing cyano substituents showed the largest fluorescence quantum yields, 0.65 for **7c** and 0.78 for **8c** when compared to other 4-phenyl-BODIPYs.

3.3 Conclusions

A series of new 4,4'-dicyano-BODIPYs **1a-5a** were investigated and synthesized following a previous procedure. Lewis acid tin tetrachloride provided a convenient and robust methodology for functionalization at the boron center with cyano nucleophile. In addition, a novel route for the preparation of 4,4'-difunctionalized BODIPYs **7a-g** and **8a-g** bearing two different substituents at the boron center was developed. A three step one-pot reaction between dipyrrins with phenylboron dichloride, followed by addition with a nucleophile produced the target BODIPYs in moderate yields ranging from 14% to 63%. BODIPYs **7b** and **8b** containing a methoxide substituent were obtained in the highest yields while lower yields were achieved for milder nucleophiles (alcohols, TMSCN, acetate ion) due to the competing formation of the corresponding 4-hydroxyl-BODIPY derivatives. BODIPYs **7c** and **8c** containing cyano groups on boron exhibit the highest quantum yields compared to other substituents.

3.4 Experimental

3.4.1 General Information

All commercially available reagents were purchased from Sigma-Aldrich and were used without further purification. All anhydrous reactions were carried out with oven-dried glassware under a dry argon atmosphere. All the reactions were monitored by using Sorbent Technologies pre-coated polyester backed TLC (200 µm silica gel with indicator UV-254 nm). Flash column chromatography was performed using Sorbent Technologies 60 Å silica gel (230-400 mesh). Prep-TLC 60 Å silica gel 20 x 20 cm (210-270 µm) was used. All ^{1}H-, ^{13}C-, and ^{11}B-NMR spectral were collected using a Bruker AV-400 spectrometer in deuterated dichloromethane or chloroform as

solvents. The $CDCl_3$ chemical shifts (δ) are reported in ppm with 7.27 for proton and 77.16 for carbon NMR as reference. The CD_2Cl_2 chemical shifts (δ) are reported in ppm with 5.23 for proton and 54.00 for carbon NMR as reference. The BF_3•OEt_2 was used as an external reference (δ 0.00) for boron NMR. Coupling constants are reported in hertz (Hz). All the mass spectra were collected using an Agilent 6210 ESI-TOF mass spectrometer. All melting points were recorded using a MEL-TEMP electrothermal instrument.

3.4.2 Syntheses

General procedure for synthesis of 4,4-dicyano-BODIPYs **1a-5a**.[18] BODIPYs **1-5** were dissolved in anhydrous dichloromethane (3 mL). Tin tetrachloride (1 M in dichloromethane, 0.5 equiv) solution was added dropwise, followed by trimethylsilyl cyanide (7.0 equiv). After 10 min, the reaction was quenched with water and extracted with dichloromethane (2 x 5 mL). The organic layers were washed with sat. $NaHCO_3$ (2 x 5 mL). The combined organic layers were washed with water (2 x 5 mL), dried over Na_2SO_4, and concentrated under reduced pressure.

4,4-Dicyano-8-phenyl-1,3,5,7-tetramethyl-BODIPY (**1a**). The crude product was purified via TLC (eluent 80/20 hexane/ethyl acetate) to give a bright orange solid BODIPY **1a** (16.5 mg, 79%) that was recrystallized from 100% dichloromethane: ^{1}H NMR ($CDCl_3$, 400 MHz) δ 7.49-7.40 (m, 3H), 7.25-7.17 (m, 3H), 6.09 (s, 2H), 2.66 (s, 6H), 1.34 (s, 6H); ^{13}C NMR ($CDCl_3$, 100 MHz) δ 155.91, 144.47, 142.66, 133.97, 129.73, 129.49, 129.45, 127.67, 126.07, 125.33, 122.61, 122.58, 15.43, 14.59; ^{11}B NMR ($CDCl_3$, 128 MHz) δ -16.92 (s); HRMS (ESI-TOF) *m/z* 360.1631 $[M + Na]^+$ calculated for $C_{21}H_{19}BN_4$: 360.1645.

4,4-Dicyano-8-(3,4-dimethoxyphenyl)-1,3,5,7-tetramethyl-BODIPY (**2a**). The crude product was purified via TLC (eluent 50/50 hexane/ethyl acetate) to give a bright orange solid BODIPY **2a** (10.8 mg, 37%) that was recrystallized from 100% acetone: ^{1}H NMR ($CDCl_3$, 400 MHz) δ 7.02 (d, *J* = 8.2 Hz, 1H), 6.84 (dd, *J* = 8.2, 2.0 Hz, 1H), 6.79 (d, *J* = 2.0 Hz, 1H), 6.17 (s, 2H), 3.97 (s, 3H), 3.89 (s, 3H), 2.73 (s, 6H), 1.53 (s, 6H); ^{13}C NMR ($CDCl_3$, 100 MHz) δ 155.83, 150.08, 149.90, 144.46, 142.56, 130.07, 126.05, 122.50, 120.20, 111.71, 110.72, 56.21, 55.97, 15.44, 14.71; ^{11}B NMR ($CDCl_3$, 128 MHz) δ -16.93 (s); HRMS (ESI-TOF) *m/z* 420.1843 $[M + Na]^+$ calculated for $C_{23}H_{23}BN_4O_2$: 420.1828.

4,4-Dicyano-8-(4-methoxycarbonylphenyl)-1,3,5,7-tetramethyl-BODIPY (**3a**). The crude product was purified via TLC (eluent 30/70 hexane/dichloromethane) to give a bright orange solid BODIPY **3a** (18.0 mg, 65%) that was recrystallized from 100% acetone: ^{1}H NMR ($CDCl_3$, 400 MHz) δ 8.23 (d, *J* = 7.9 Hz, 2H), 7.42 (d, *J* = 7.9 Hz, 2H), 6.18 (s, 2H), 3.99 (s, 3H), 2.74 (s, 6H), 1.41 (s, 6H); ^{13}C NMR ($CDCl_3$, 100 MHz) δ 166.22, 156.51, 144.21, 138.65, 131.35, 130.64, 128.13, 122.89, 52.49, 15.48, 14.76; ^{11}B NMR ($CDCl_3$, 128 MHz) δ -16.94 (s); HRMS (ESI-TOF) *m/z* 396.1867 $[M + H]^+$ calculated for $C_{23}H_{21}BN_4O_2$: 396.1869.

4,4-Dicyano-8-phenyl-2,6-diethyl-1,3,5,7-tetramethyl-BODIPY (**4a**). The crude product was purified via TLC (eluent 80/20 hexane/ethyl acetate) to give a bright orange solid BODIPY **4a** (17.5 mg, 81%) that was recrystallized from 1:1 acetone/dichloromethane: ^{1}H NMR ($CDCl_3$, 400 MHz) δ 7.45 (p, *J* = 3.5 Hz, 3H), 7.20 (dd, *J* = 6.8, 3.1 Hz, 3H), 2.62 (s, 6H), 2.28 (q, *J* = 7.6 Hz, 4H), 1.24 (s, 6H), 0.93 (t, *J* = 7.6 Hz, 6H); ^{13}C NMR ($CDCl_3$, 100 MHz) δ 153.97, 141.04, 139.85, 134.78, 134.21, 129.32, 129.27, 127.98, 17.21, 14.51, 13.39, 11.85; ^{11}B NMR ($CDCl_3$,

128 MHz) δ -16.84 (s); HRMS (ESI-TOF) *m/z* 416.2257 $[M + Na]^+$ calculated for $C_{25}H_{27}BN_4$: 416.2264.

4,4-Dicyano-2,6-diethyl-1,3,5,7-tetramethyl-BODIPY (**5a**). The crude product was purified via TLC (eluent 80/20 hexane/ethyl acetate) to give a bright orange solid BODIPY **5a** (12.3 mg, 51%) that was recrystallized from 1:1 acetone/dichloromethane: ^{1}H NMR ($CDCl_3$, 400 MHz) δ 7.07 (s, 1H), 2.66 (s, 6H), 2.45 (q, *J* = 7.5 Hz, 4H), 2.22 (s, 6H), 1.10 (t, *J* = 7.5 Hz, 6H); ^{13}C NMR (101 MHz, Chloroform-*d*) δ 155.15, 138.11, 133.23, 130.74, 119.34, 17.40, 14.48, 13.28, 9.49; ^{11}B NMR ($CDCl_3$, 128 MHz) δ -16.93 (s); HRMS (ESI-TOF) *m/z* 340.1944 $[M + Na]^+$ calculated for $C_{19}H_{23}BN_4$: 340.1949.

General procedure for synthesis of dipyrrins **7** and **8**.[27] 2,4-dimethyl ketopyrrole (1.0 equiv) was dissolved in anhydrous 8:1 pentane/dichloromethane at 0 °C. 2,4-dimethyl pyrrole or 3-ethyl-2,4-dimethyl pyrrole (1.0 equiv) was added dropwise to the stirred mixture and warmed to room temperature. After 24 h, Et_3N (1.0 equiv) was added dropwise to the reaction mixture for an hour and quenched with water (10 mL) and extracted with dichloromethane (10 mL). The combined organic layers were dried over $MgSO_4$ and concentrated under reduced pressure. The crude products were purified by column chromatography (eluent EtOAc to 5% MeOH/EtOAc to 30% MeOH/EtOAc) to afford the corresponding dipyrrins **7** and **8**.

Dipyrrin (**7**). 27% yield: ^{1}H NMR ($CDCl_3$, 400 MHz) δ 7.37 (s, 3H), 7.27-7.21 (m, 2H), 2.28 (s, 6H), 2.24 (q, 4H, *J* = 7.32 Hz) 1.15 (s, 6H), 0.93 (t, 6H, *J* = 7.16 Hz); ^{13}C NMR ($CDCl_3$, 100 MHz) δ 150.25, 138.92, 137.65, 136.08, 134.88, 131.39, 129.73, 128.53, 128.10, 17.69, 15.00,

14.50, 11.85; HRMS (ESI-TOF) *m/z* 333.2325 $[M + H]^+$ calculated for $C_{23}H_{28}N_2$: 333.2335. These data are in agreement with previous reported.[33]

Dipyrrin (**8**). 31% yield: ^{1}H NMR ($CDCl_3$, 400 MHz) δ 7.61 (t, 1H, *J* = 7.36 Hz), 7.51 (t, 2H, *J* = 7.80 Hz), 7.32 (d, 2H, *J* = 7.20 Hz), 6.17 (s, 1H), 2.71 (s, 3H), 2.68 (s, 3H), 2.39 (q, 2H, *J* = 7.52 Hz), 1.41 (s, 3H), 1.34 (s, 3H), 1.04 (t, 3H, *J* = 7.48 Hz); ^{13}C NMR ($CDCl_3$, 100 MHz) δ 139.35, 137.74, 134.40, 130.65, 130.33, 129.88, 129.54, 128.86, 118.19, 50.45, 17.61, 14.67, 14.52, 14.34, 12.29; HRMS (ESI-TOF) *m/z* 305.2012 $[M + H]^+$ calculated for $C_{21}H_{24}N_2$: 305.2024.

General procedure for synthesis of BODIPYs **7a-g** and **8a-g**. Dipyrrins **7** or **8** (1.0 equiv.) were dissolved in anhydrous CH_2Cl_2 (5 mL). Et_3N (5.0 equiv) was added dropwise to the solution at room temperature. Dichlorophenylborane (5.0 equiv) was added dropwise and the mixture was stirred for 1 h. Nucleophile (10.0 equiv) was added dropwise and the final mixture stirred for an additional 1-2 h while followed by TLC. All crude products were concentrated under reduced pressure and purified as described below to afford BODIPYs **7a-g** and **8a-g**.

4-Fluoro-4-phenyl-8-phenyl-2,6-diethyl-1,3,5,7-tetramethyl-BODIPY (**7a**). The crude product was purified via TLC (eluent 50/50 hexane/dichloromethane) to give an orange solid BODIPY **7a** (11.4 mg, 52%) that was recrystallized from 50/50 hexane/EtOAc: mp 210-215 °C; ^{1}H NMR (CD_2Cl_2, 400 MHz) δ 7.57-7.51 (m, 3H), 7.43-7.40 (m, 3H), 7.37-7.35 (m, 1H), 7.20 (t, 2H, *J* = 6.9 Hz), 7.15-7.11 (m, 1H), 2.23 (q, 4H, *J* = 7.6 Hz), 2.17 (s, 6H), 1.32 (s, 6H), 0.91 (t, 3H, *J* = 7.5 Hz); ^{13}C NMR ($CDCl_3$, 100 MHz) δ 153.91, 140.55, 137.07, 136.54, 132.81, 132.10, 132.07, 130.48, 129.11, 129.05, 128.80, 128.73, 128.58, 127.00, 126.09, 17.25, 14.78, 13.20,

13.16, 11.89; ^{11}B NMR ($CDCl_3$, 128 MHz) δ 2.43 (s); HRMS (ESI-TOF) *m/z* 438.2752 $[M + H]^+$ calculated for $C_{29}H_{32}BFN_2$: 438.2740.

4-Methoxy-4-phenyl-8-phenyl-2,6-diethyl-1,3,5,7-tetramethyl-BODIPY (**7b**). The crude product was purified via TLC (eluent 50/50 hexane/dichloromethane) to give an orange solid BODIPY **7b** (29.3 mg, 63%) that was recrystallized from 50/50 hexane/EtOAc: mp 160-165 °C; ^{1}H NMR (CD_2Cl_2, 400 MHz) δ 7.56-7.50 (m, 3H), 7.43-7.36 (m, 4H), 7.15 (t, 2H, *J* = 7.4 Hz), 7.10-7.05 (m, 1H), 3.09 (s, 3H), 2.23 (q, 4H, *J* = 7.6 Hz), 2.16 (s, 6H), 1.32 (s, 6H), 0.90 (t, 3H, *J* = 7.6 Hz); ^{13}C NMR ($CDCl_3$, 100 MHz) δ 153.66, 140.51, 136.91, 136.00, 132.51, 132.36, 131.32, 129.08, 128.89, 128.83, 128.82, 128.58, 126.79, 125.59, 49.20, 17.31, 14.85, 12.86, 11.93; ^{11}B NMR ($CDCl_3$, 128 MHz) δ 2.18 (s); HRMS (ESI-TOF) *m/z* 472.2771 $[M + Na]^+$ calculated for $C_{30}H_{35}BN_2O$: 472.2775.

4-Cyano-4-phenyl-8-phenyl-2,6-diethyl-1,3,5,7-tetramethyl-BODIPY (**7c**). The crude product was purified via TLC (eluent 80/20 hexane/EtOAc) to give an orange solid BODIPY **7c** (8.6 mg, 17%) that was recrystallized from 50/50 hexane/dichloromethane: mp 110-115 °C; ^{1}H NMR (CD_2Cl_2, 400 MHz) δ 7.56-7.54 (m, 3H), 7.49 (d, 2H, *J* = 6.6 Hz), 7.42-7.38 (m, 1H), 7.25 (t, 2H, *J* = 6.9 Hz), 7.21-7.17 (m, 1H), 2.25 (q, 4H, *J* = 7.6 Hz), 2.15 (s, 6H), 1.34 (s, 6H), 0.91 (t, 3H, *J* = 7.6 Hz); ^{13}C NMR ($CDCl_3$, 100 MHz) δ 154.0, 140.43, 136.89, 136.18, 132.76, 132.29, 130.57, 129.11, 128.99, 128.78, 128.73, 128.64, 126.90, 125.70, 17.30, 14.83, 13.55, 11.89; ^{11}B NMR ($CDCl_3$, 128 MHz) δ -9.42 (s); HRMS (ESI-TOF) *m/z* 467.2618 $[M + Na]^+$ calculated for $C_{30}H_{32}BN_3$: 467.2613.

4-Acetoxy-4-phenyl-8-phenyl-2,6-diethyl-1,3,5,7-tetramethyl-BODIPY (**7d**). The crude product was purified via TLC (eluent 80/20 hexane/EtOAc) to give an orange solid BODIPY **7d** (9.5 mg, 25%) that was recrystallized from 50/50 hexane/EtOAc: mp 150-155 °C; ^{1}H NMR (CD_2Cl_2, 400 MHz) δ 7.56-7.48 (m, 3H), 7.44-7.41 (m, 2H), 7.39-7.36 (m, 1H), 7.21 (t, 2H, *J* = 6.8 Hz), 7.17-7.12 (m, 1H), 2.22 (q, 4H, *J* = 7.6 Hz), 2.07 (s, 3H), 2.04 (s, 6H), 1.33 (s, 6H), 0.89 (t, 6H, *J* = 7.6 Hz); ^{13}C NMR ($CDCl_3$, 100 MHz) δ 172.40, 152.41, 140.88, 136.76, 136.71, 132.47, 131.25, 129.10, 129.06, 128.89, 128.60, 126.94, 126.06, 23.19, 17.38, 14.75, 13.12, 12.09; ^{11}B NMR ($CDCl_3$, 128 MHz) δ -0.48 (s); HRMS (ESI-TOF) *m/z* 500.2720 $[M + Na]^+$ calculated for $C_{31}H_{35}BN_2O_2$: 500.2737.

4-(N-Boc-ethanolyl)-4-phenyl-8-phenyl-2,6-diethyl-1,3,5,7-tetramethyl-BODIPY (**7e**). The crude product was purified via TLC (eluent 80/20 Hexane/EtOAc) to give an orange solid BODIPY **7e** (15.5 mg, 32%) that was recrystallized from 50/50 hexane/EtOAc: mp 55-60 °C; ^{1}H NMR (CD_2Cl_2, 400 MHz) δ 7.56-7.51 (m, 3H), 7.45-7.36 (m, 3H), 7.37-7.35 (m, 1H), 7.15 (t, 2H, *J* = 7.4 Hz), 7.10-7.05 (m, 1H), 3.24-3.18 (m, 2H), 3.16-3.15 (m, 2H), 2.21 (q, 4H, *J* = 7.6 Hz), 2.12 (s, 6H), 1.42 (s, 9H), 1.31 (s, 6H), 0.89 (t, 6H, *J* = 7.6 Hz); ^{13}C NMR ($CDCl_3$, 100 MHz) δ 156.34, 153.54, 140.56, 136.81, 136.14, 132.57, 131.21, 129.07, 128.99, 128.83, 128.76, 128.63, 126.71, 125.64, 28.65, 17.30, 14.80, 13.06, 11.93; ^{11}B NMR ($CDCl_3$, 128 MHz) δ 1.54 (s); HRMS (ESI-TOF) *m/z* 601.3561 $[M + Na]^+$ calculated for $C_{36}H_{46}BN_3O_3$: 601.3573.

4-(Triethyleneglycol monomethyl ether)-4-phenyl-8-phenyl-2,6-diethyl-1,3,5,7-tetramethyl-BODIPY (**7f**). The crude product was purified via TLC (eluent 80/20 hexane/EtOAc) to give an orange/red oil BODIPY **7f** (11.4 mg, 21%) that was recrystallized from 50/50

hexane/EtOAc. ^{1}H NMR (CD_2Cl_2, 400 MHz) δ 7.56-7.50 (m, 3H), 7.44-7.40 (m, 3H), 7.38-7.36 (m, 1H), 7.15 (t, 2H, *J* = 8 Hz), 7.10-7.06 (m, 1H), 3.64-3.62 (m, 2H), 3.60-3.57 (m, 6H), 3.51-3.48 (m, 2H), 3.33 (s, 3H), 3.30 (t, 2H, *J* = 5.6 Hz), 2.22 (q, 4H, *J* = 7.6 Hz), 2.15 (s, 6H), 1.31 (s, 6H), 0.89 (t, 6H, *J* = 7.5 Hz); ^{13}C NMR (CD_2Cl_2, 100 MHz) δ 137.26, 136.64, 133.02, 132.64, 131.67, 129.53, 129.41, 129.32, 129.23, 129.00, 127.09, 126.02, 73.21, 72.51, 71.23, 71.14, 70.99, 61.49, 59.18, 17.62, 15.06, 13.21, 12.12; ^{11}B NMR ($CDCl_3$, 128 MHz) δ 1.63 (s); HRMS (ESI-TOF) *m/z* 604.3557 $[M + Na]^+$ calculated for $C_{36}H_{47}BN_2O_4$: 604.3565.

4-(Pro-2-yn-1-yloxy)-4-phenyl-8-phenyl-2,6-diethyl-1,3,5,7-tetramethyl-BODIPY (**7g**). The crude product was purified via TLC (eluent 50/50 hexane/dichloromethane) to give an orange solid BODIPY **7g** (13.9 mg, 25%) that was recrystallized from 50/50 hexane/ethyl acetate: mp 130-135 °C; ^{1}H NMR ($CDCl_3$, 400 MHz) δ 7.56-7.50 (m, 3H), 7.42 (d, 3H, *J* = 6.6 Hz), 7.38-7.34 (m, 1H), 7.17 (t, 2H, *J* = 8.1 Hz), 7.10 (t, 1H, *J* = 7.2 Hz), 3.92 (d, 1H, *J* = 2.4 Hz), 2.22 (q, 4H, *J* = 6.6 Hz), 2.21 (s, 3H), 2.17 (s, 3H), 1.32 (s, 3H), 1.31 (s, 3H), 0.90 (t, 6H, *J* = 7.5 Hz); ^{13}C NMR ($CDCl_3$, 100 MHz) δ 154.19, 140.33, 136.79, 136.34, 132.73, 132.55, 131.20, 129.10, 128.96, 128.81, 128.79, 128.64, 126.73, 125.69, 70.92, 50.09, 17.28, 14.80, 13.22, 11.93; ^{11}B NMR ($CDCl_3$, 128 MHz) δ 1.73 (s); HRMS (ESI-TOF) *m/z* 496.2771 $[M + Na]^+$ calculated for $C_{32}H_{35}BN_2O$: 496.2754.

4-Fluoro-4-phenyl-8-phenyl-6-ethyl-1,3,5,7-tetramethyl-BODIPY (**8a**). The crude product was purified via TLC (eluent 50/50 hexane/dichloromethane) to give an orange solid BODIPY **8a** (11.4 mg, 41%) that was recrystallized from 50/50 hexane/EtOAc: mp 120-125 °C; ^{1}H NMR (CD_2Cl_2, 400 MHz) δ 7.57-7.51 (m, 3H), 7.43-7.40 (m, 3H), 7.37-7.35 (m, 1H), 7.20 (t, 2H, *J* =

6.8 Hz), 7.16-7.12 (m, 1H), 5.88 (s, 1H), 2.24 (q, 2H, *J* = 7.6 Hz), 2.19 (s, 3H), 2.15 (s, 3H), 1.39 (s, 3H), 1.35 (s, 3H), 0.91 (t, 3H, *J* = 7.6 Hz); ^{13}C NMR ($CDCl_3$, 100 MHz) δ 141.27, 140.64, 136.12, 133.58, 132.06, 132.02, 129.17, 129.11, 128.84, 128.62, 128.43, 127.05, 126.19, 120.85, 17.25, 15.35, 14.68, 14.56, 13.32, 11.94; ^{11}B NMR ($CDCl_3$, 128 MHz) δ 2.23 (s); HRMS (ESI-TOF) *m/z* 410.2439 $[M + H]^+$ calculated for $C_{27}H_{28}BFN_2$: 410.2398.

4-Methoxy-4-phenyl-8-phenyl-6-ethyl-1,3,5,7-tetramethyl-BODIPY (**8b**). The crude product was purified via TLC (eluent dichloromethane) to give an orange solid BODIPY **8b** (34.4 mg, 49%) that was recrystallized from 50/50 hexane/EtOAc: mp 120-125 °C; ^{1}H NMR (CD_2Cl_2, 400 MHz) δ 7.57-7.51 (m, 3H), 7.43-7.36 (m, 4H), 7.15 (t, 2H, *J* = 7.3 Hz), 7.10-7.06 (m, 1H), 5.86 (s, 1H), 3.10 (s, 3H), 2.24 (q, 2H, *J* = 7.5 Hz), 2.19 (s, 3H), 2.13 (s, 3H), 1.38 (s, 3H), 1.34 (s, 3H), 0.91 (t, 3H, *J* = 7.6 Hz); ^{13}C NMR ($CDCl_3$, 100 MHz) δ 155.61, 153.68, 141.30, 139.67, 137.10, 136.54, 133.41, 132.38, 131.94, 131.56, 129.21, 129.03, 128.77, 128.73, 126.91, 125.77, 120.71, 60.59, 49.27, 21.24, 17.37, 15.24, 14.82, 14.71, 14.40, 13.04, 12.06; ^{11}B NMR ($CDCl_3$, 128 MHz) δ 2.10 (s); HRMS (ESI-TOF) *m/z* 444.2458 $[M + Na]^+$ calculated for $C_{28}H_{31}BN_2O$: 444.2468.

4-Cyano-4-phenyl-8-phenyl-6-ethyl-1,3,5,7-tetramethyl-BODIPY (**8c**). The crude product was purified via TLC (eluent 80/20 hexane/EtOAc) to give an orange solid BODIPY **8c** (5.1 mg, 18%) that was recrystallized from 50/50 hexane/dichloromethane: mp 90-95 °C; ^{1}H NMR (CD_2Cl_2, 400 MHz) δ 7.57-7.53 (m, 3H), 7.50-7.48 (m, 2H), 7.42-7.38 (m, 2H), 7.25 (t, 2H, *J* = 6.8 Hz), 7.22-7.18 (m, 1H), 5.96 (s, 1H), 2.26 (q, 2H, *J* = 9.3 Hz), 2.17 (s, 3H), 2.13 (s, 3H), 1.40 (s, 3H), 1.37 (s, 3H), 0.92 (t, 3H, *J* = 7.5 Hz); ^{13}C NMR (CD_2Cl_2, 100 MHz) δ 141.53, 133.25,

129.78, 129.71, 129.49, 128.94, 128.80, 128.01, 127.39, 121.82, 112.37, 17.66, 16.00, 14.84, 14.06, 12.28; ^{11}B NMR ($CDCl_3$, 128 MHz) δ -7.43 (s); HRMS (ESI-TOF) *m/z* 439.2305 $[M + Na]^+$ calculated for $C_{28}H_{28}BN_3$: 439.2297.

4-Acetoxy-4-phenyl-8-phenyl-6-ethyl-1,3,5,7-tetramethyl-BODIPY (**8d**). The crude product was purified via TLC (eluent 80/20 hexane/EtOAc) to give an orange solid BODIPY **8d** (3.2 mg, 16%) that was recrystallized from 50/50 hexane/EtOAc: mp 100-105 °C; ^{1}H NMR ($CDCl_3$, 400 MHz) δ 7.55-7.49 (m, 5H), 7.45-7.43 (m, 2H), 7.22 (t, 2H, *J* = 7.1 Hz), 7.19-7.16 (m, 1H), 5.82 (s, 1H), 2.24 (q, 2H, *J* = 7.5 Hz), 2.11 (s, 3H), 2.05 (s, 3H), 2.02 (s, 3H), 1.38 (s, 3H), 1.33 (s, 3H), 0.88 (t, 3H, *J* = 7.3 Hz); ^{13}C NMR ($CDCl_3$, 100 MHz) δ 172.45, 154.27, 152.31, 146.25, 141.63, 140.05, 137.76, 136.32, 133.25, 132.42, 132.21, 131.78, 129.15, 128.95, 128.90, 128.70, 128.43, 127.01, 126.19, 120.86, 29.85, 23.15, 17.35, 15.75, 15.35, 14.69, 14.65, 14.34, 13.66, 13.24, 12.06; ^{11}B NMR ($CDCl_3$, 128 MHz) δ -0.34 (s); HRMS (ESI-TOF) *m/z* 472.2407 $[M + Na]^+$ calculated for $C_{29}H_{31}BN_2O_2$: 472.2397.

4-(N-Boc-ethanolyl)-4-phenyl-8-phenyl-6-ethyl-1,3,5,7-tetramethyl-BODIPY (**8e**). The crude product was purified via TLC (eluent 80/20 hexane/EtOAc) to give an orange solid BODIPY **8e** (5.0 mg, 14%) that was recrystallized from 50/50 hexane/EtOAc: mp 60-65 °C; ^{1}H NMR ($CDCl_3$, 400 MHz) δ 7.56-7.51 (m, 3H), 7.45-7.41 (m, 3H), 7.37-7.36 (m, 1H), 7.17 (t, 2H, *J* = 6.8 Hz), 7.10 (t, 1H, *J* = 7.0 Hz), 5.85 (s, 1H), 3.24 (t, 2H, *J* = 5.0 Hz), 3.18 (t, 2H, *J* = 4.6 Hz), 2.22 (q, 2H, *J* = 7.9 Hz), 2.15 (s, 3H), 2.09 (s, 3H), 1.43 (s, 9H), 1.37 (s, 3H), 1.33 (s, 3H), 0.90 (t, 3H, *J* = 7.5 Hz); ^{13}C NMR (CD_2Cl_2, 100 MHz) δ 132.78, 129.60, 129.50, 129.15, 129.03, 127.15, 126.21, 120.97, 61.04, 28.74, 28.64, 17.61, 15.46, 14.92, 14.78, 13.38, 12.18; ^{11}B NMR ($CDCl_3$,

128 MHz) δ 1.10 (s); HRMS (ESI-TOF) *m/z* 601.3561 $[M + Na]^+$ calculated for $C_{36}H_{46}BN_3O_3$: 601.3573.

4-(Tri(ethyleneglycol monomethyl ether)-4-phenyl-8-phenyl-6-ethyl-1,3,5,7-tetramethyl-BODIPY (**8f**). The crude product was purified via TLC (eluent 80/20 hexane/EtOAc) to give an orange/red oil BODIPY **8f** (6.1 mg, 15%) that was recrystallized from 50/50 hexane/EtOAc. ^{1}H NMR (CD_2Cl_2, 400 MHz) δ 7.56-7.51 (m, 3H), 7.42 (t, 3H, *J* = 6.3 Hz), 7.38-7.34 (m, 1H), 7.16 (t, 2H, *J* = 6.8 Hz), 7.12-7.07 (m, 1H), 5.85 (s, 1H), 3.64-3.61 (m, 2H), 3.60-3.56 (m, 6H), 3.51-3.48 (m, 2H), 3.33 (s, 3H), 3.33-3.28 (m, 2H), 2.23 (q, 2H, *J* = 7.8 Hz), 2.17 (s, 3H), 2.12 (s, 3H), 1.38 (s, 3H), 1.33 (s, 3H), 0.90 (t, 3H, *J* = 7.6 Hz); ^{13}C NMR (CD_2Cl_2, 100 MHz) δ 156.02, 154.00, 141.85, 140.19, 137.69, 136.84, 133.86, 132.81, 132.49, 132.24, 129.58, 129.46, 129.15, 129.10, 127.30, 127.12, 126.21, 126.12, 120.90, 73.22, 73.01, 72.52, 71.23, 71.16, 70.99, 61.54, 59.18, 17.63, 15.43, 14.96, 14.78, 13.34, 12.18; ^{11}B NMR ($CDCl_3$, 128 MHz) δ 1.21 (s); HRMS (ESI-TOF) *m/z* 576.3244 $[M + Na]^+$ calculated for $C_{34}H_{43}BN_2O_4$: 576.3240.

4-(Pro-2-yn-1-yloxy)-4-phenyl-8-phenyl-6-ethyl-1,3,5,7-tetramethyl-BODIPY (**8g**). The crude product was purified via TLC (eluent 50/50 hexane/dichloromethane) to give an orange solid BODIPY **8g** (7.0 mg, 31%) that was recrystallized from 50/50 hexane/EtOAc: mp 120-125 °C; ^{1}H NMR (CD_2Cl_2, 400 MHz) δ 7.57-7.51 (m, 3H), 7.43-7.41 (m, 3H), 7.38-7.36 (m, 1H), 7.17 (t, 2H, *J* = 6.9 Hz), 7.13-7.09 (m, 1H), 5.87 (s, 1H), 3.94 (q, 2H, *J* = 1.7 Hz), 2.27 (t,), 2.19 (s, 3H), 2.14 (s, 3H), 1.38 (s, 3H), 1.34 (s, 3H), 0.90 (t, 3H, *J* = 7.5 Hz); ^{13}C NMR (CD_2Cl_2, 100 MHz) δ 156.38, 154.17, 141.85, 140.58, 138.17, 136.66, 134.12, 132.70, 132.25, 129.63, 129.51, 129.18, 129.06, 129.02, 127.23, 126.30, 121.09, 84.51, 71.40, 50.35, 17.60, 15.56, 14.90, 14.78, 13.55, 12.20; ^{11}B

NMR ($CDCl_3$, 128 MHz) δ 1.65 (s); HRMS (ESI-TOF) *m/z* 468.2458 $[M + Na]^+$ calculated for $C_{30}H_{31}BN_2O$: 468.2449.

General procedure for synthesis of BODIPYs **4** and **9**. Dipyrrins **7** or **8** (1.0 equiv.) were dissolved in anhydrous CH_2Cl_2 (5 mL). Et_3N (7.5 equiv) was added dropwise followed by $BF_3 \cdot OEt_2$ (10.0 equiv). The final mixture was stirred for an additional 1 h. The crude products were concentrated under reduced pressure and purified via TLC (eluent 50/50 hexane/dichloromethane) to afford BODIPYs **4** and **9**.

4,4-Difluoro-8-phenyl-2,6-diethyl-1,3,5,7-tetramethyl-BODIPY (**4**). This BODIPY was isolated as an orange solid (41.2 mg, 68%) that was recrystallized from 50/50 hexane/EtOAc: mp 175-180 °C; ^{1}H NMR ($CDCl_3$, 400 MHz) δ 7.49-7.47 (m, 3H), 7.30-7.28 (m, 2H), 2.55 (s, 6H), 2.31 (q, 4H, *J* = 7.6 Hz), 1.29 (s, 6H), 0.99 (t, 3H, *J* = 7.6 Hz); ^{13}C NMR ($CDCl_3$, 100 MHz) δ 153.80, 140.33, 138.54, 135.94, 132.87, 130.91, 129.14, 128.85, 128.40, 17.20, 14.74, 12.62, 11.74; ^{11}B NMR ($CDCl_3$, 128 MHz) δ 0.69 (t, *J* = 33.5 Hz); HRMS (ESI-TOF) *m/z* 402.2164 $[M + Na]^+$ calculated for $C_{23}H_{27}BF_2N_2$: 402.2143. These data are in agreement with those previously reported.[8]

4,4-Difluoro-8-phenyl-6-ethyl-1,3,5,7-tetramethyl-BODIPY (**9**). This BODIPY was isolated an orange solid (27.2 mg, 41%) that was recrystallized from 50/50 hexane/EtOAc: mp 195-200 °C; ^{1}H NMR ($CDCl_3$, 400 MHz) δ 7.49-7.48 (m, 3H), 7.30-7.27 (m, 2H), 5.95 (s, 1H), 2.56 (s, 6H), 2.32 (q, 2H, *J* = 7.6 Hz), 1.36 (s, 3H), 1.31 (s, 3H), 0.99 (t, 3H, *J* = 7.6 Hz); ^{13}C NMR ($CDCl_3$, 100 MHz) δ 155.56, 153.98, 142.07, 141.03, 139.49, 135.55, 133.63, 131.42, 129.20,

128.96, 128.26, 120.70, 29.84, 17.21, 14.67, 14.61, 14.40, 12.77, 11.82; ^{11}B NMR ($CDCl_3$, 128 MHz) δ 0.67 (t, *J* = 33.3 Hz); HRMS (ESI-TOF) *m/z* 352.2031 $[M + H]^+$ calculated for $C_{21}H_{23}BF_2N_2$: 352.2034.

3.4.3 X-ray Determined Molecular structures

Crystal structures were determined using low-temperature data from a Bruker Kappa APEX-II DUO diffractometer with either Mo Kα or Cu Kα radiation. For all structures, H atoms were located from difference maps but constrained in calculated positions during refinement.

Crystal data **1a**: $C_{21}H_{19}BN_4$, *M* = 338.21, monoclinic, *a* = 23.449(6), *b* = 7.1532(18), *c* = 21.231(5) Å, *U* = 3561.2(15) Å^3, *T* = 100 K, space group $Pca2_1$, *Z* = 8, Dc = 1.262 g cm^{-3}, μ (Cu Kα) = 0.08 mm^{-1}, 9965 reflections measured, θ_{max} = 26.8˚, 3858 unique (R_{int} = 0.043). The final *R* = 0.037 (3858 *I>2σ(I)* data), *wR(F2)* = 0.088 (all data), CCDC 1457137.

Crystal data **3a**: $C_{23}H_{21}BN_4O_2$, *M* = 396.25, monoclinic, *a* = 9.6379(6), *b* = 29.7309(19), *c* = 7.1824(5) Å, *U* = 2009.5(2) Å^3, *T* = 100 K, space group $P2_1/c$, *Z* = 4, Dc = 1.310 g cm^{-3}, μ (Cu Kα) = 0.09 mm^{-1}, 1798 reflections measured, θ_{max} = 26.4˚, 4065 unique (R_{int} = 0.044). The final *R* = 0.046 (2670 *I>2σ(I)* data), *wR(F2)* = 0.110 (all data), CCDC 1457138.

Crystal data **4a**: $C_{25}H_{27}BN_4$, *M* = 394.32, monoclinic, *a* = 20.4760(3), *b* = 11.3191(2), *c* = 11.2060(2) Å, *U* = 2231.02(6) Å^3, *T* = 100 K, space group Cc, *Z* = 4, Dc = 1.174 g cm^{-3}, μ (Cu Kα) = 0.07 mm^{-1}, 9990 reflections measured, θ_{max} = 29.2˚, 3028 unique (R_{int} = 0.034). The final *R* = 0.034 (2878 *I>2σ(I)* data), *wR(F2)* = 0.089 (all data), CCDC 1457139.

Crystal data **5a**: $C_{19}H_{23}BN_4$, *M* = 318.22, monoclinic, *a* = 13.8407(4), *b* = 8.5881(2), *c* = 16.2914(4) Å, *U* = 1778.09(8) $Å^3$, *T* = 100 K, space group $P2_1/c$, *Z* = 4, Dc = 1.189 g cm^{-3}, μ (Cu Kα) = 0.07 mm^{-1}, 9892 reflections measured, θ_{max} = 30.1˚, 5209 unique (R_{int} = 0.043). The final *R* = 0.045 (3990 *I>2σ(I)* data), *wR(F2)* = 0.120 (all data), CCDC 1457139.

Crystal data **7b**: $C_{30}H_{35}BN_2O$, *M* = 450.41, monoclinic, *a* = 11.7029(5), *b* = 13.0834(6), *c* = 17.1865(7) Å, *U* = 2502.11(19) $Å^3$, *T* = 90 K, space group $P2_1/n$, *Z* = 4, Dc = 1.196 g cm^{-3}, μ (Cu Kα) = 0.55 mm^{-1}, 11723 reflections measured, θ_{max} = 63.7˚, 4074 unique (R_{int} = 0.046). The final *R* = 0.041 (3284 *I>2σ(I)* data), *wR(F2)* = 0.115 (all data), CCDC 1415153.

Crystal data **7c**: $C_{30}H_{32}BN_3$, *M* = 445.40, triclinic, *a* = 8.0820(5), *b* = 10.8718(6), *c* = 15.3444(9) Å, *β* = 91.560(4)°, *U* = 1247.30(13) $Å^3$, *T* = 100 K, space group PI, *Z* = 2, Dc = 1.186 g cm^{-3}, μ(CuKα) = 0.53 mm^{-1}, 11402 reflections measured, θ_{max} = 67.7˚, 4208 unique (R_{int} = 0.032). The final *R* = 0.045 (3469 *I>2σ(I)* data), *wR(F2)* = 0.113 (all data), CCDC 1415154.

Crystal data **8c**: $C_{28}H_{28}BN_3$, *M* = 417.34, orthorhombic, *a* = 7.4105(5), *b* = 14.0956(10), *c* = 22.5059(17) Å, *U* = 2350.9(3) $Å^3$, *T* = 90 K, space group $P2_12_12_1$, *Z* = 4, Dc = 1.179 g cm^{-3}, μ(CuKα) = 0.53 mm^{-1}, 10612 reflections measured, θ_{max} = 68.3˚, 4063 unique (R_{int} = 0.051). The final *R* = 0.045 (3417 *I>2σ(I)* data), *wR(F2)* = 0.109 (all data), CCDC 1415155.

3.4.4 Steady-state Absorption and Fluorescence Spectroscopy

The photophysical properties of these compounds **7a-g**, **8a-g**, **4** and **9** in dichloromethane at room temperature were measured by preparing a stock solution with a concentration of 5×10^{-5}

M and diluting it to appropriate concentrations for absorbance and emission spectra measurements. All the absorption spectra were obtained using a Perkin Elmer Lambda 35 UV/VIS Spectrometer. The optical density, ε, were taken by preparing solution concentrations between 7.5×10^{-6} and 2.5×10^{-5} M in order to get λ_{max} between 0.5 and 1.0. Emission spectra were measured on a Perkin Elmer LS 55 Luminescence spectrometer with the slit width set at 3 nm. All absorbance and emission spectra were acquired within 3 h of fresh solution preparation, at room temperature. A spectrophotometric cell with a path length of 10 nm was used.

3.5 References

1. Nguyen, A. L.; Fronczek, F. R.; Smith, K. M.; Vicente, M. G. H., Synthesis of 4,4′-Functionalized BODIPYs from Dipyrrins. *Tetrahedron Lett.* **2015**, *56*, 6348-6351.

2. Loudet, A.; Burgess, K., BODIPY Dyes and Their Derivatives: Syntheses and Spectroscopic Properties. *Chem. Rev.* **2007**, *107*, 4891-4932.

3. Boens, N.; Verbelen, B.; Dehaen, W., Postfunctionalization of the BODIPY Core: Synthesis and Spectroscopy. *Eur. J. Org. Chem.* **2015**, 6577-6595.

4. Kee, H. L.; Kirmaier, C.; Yu, L.; Thamyongkit, P.; Youngblood, W. J.; Calder, M. E.; Ramos, L.; Noll, B. C.; Bocian, D. F.; Scheidt, W. R.; Birge, R. R.; Lindsey, J. S.; Holten, D., Structural Control of the Photodynamics of Boron-Dipyrrin Complexes. *J. Phys. Chem. B* **2005**, *109*, 20433-20443.

5. Bonnier, C.; Piers, W. E.; Ali, A. A. S.; Thompson, A.; Parvez, M., Perfluoroaryl-Substituted Boron Dipyrrinato Complexes. *Organometallics* **2009**, *28*, 4845-4851.

6. Hudnall, T. W.; Lin, T. P.; Gabbai, F. P., Substitution of Hydroxide by Fluoride at the Boron Center of a BODIPY Dye. *J. Fluorine Chem.* **2010**, *131*, 1182-1186.

7. Richards, V. J.; Gower, A. L.; Smith, J. E. H. B.; Davies, E. S.; Lahaye, D.; Slater, A. G.; Lewis, W.; Blake, A. J.; Champness, N. R.; Kays, D. L., Synthesis and Characterisation of BODIPY Radical Anions. *Chem. Commun.* **2012**, *48*, 1751-1753.

8. Lundrigan, T.; Crawford, S. M.; Cameron, T. S.; Thompson, A., *Cl*-BODIPYs: a BODIPY Class Enabling Facile *B*-Substitution. *Chem. Commun.* **2012**, *48*, 1003-1005.

9. Kim, H.; Burghart, A.; Welch, M. B.; Reibenspies, J.; Burgess, K., Synthesis and Spectroscopic Properties of a New 4-Bora-3a,4a-diaza-*s*-indacene (BODIPY) Dye. *Chem. Commun.* **1999**, 1889-1890.

10. Ikeda, C.; Maruyama, T.; Nabeshima, T., Convenient and Highly Efficient Synthesis of Boron-Dipyrrins Bearing an Arylboronate Center. *Tetrahedron Lett.* **2009**, *50*, 3349-3351.

11. Ikeda, C.; Ueda, S.; Nabeshima, T., Aluminium Complexes of N_2O_2-type Dipyrrins: the First Hetero-Multinuclear Complexes of Metallo-Dipyrrins with High Fluorescence Quantum Yields. *Chem. Commun.* **2009**, 2544-2546.

12. Yamamura, M.; Yazaki, S.; Seki, M.; Matsui, Y.; Ikeda, H.; Nabeshima, T., A Facile and High-Yield Formation of Dipyrrin-Boronic Acid Dyads and Triads: a Light-Harvesting System in the Visible Region Based on the Efficient Energy Transfer. *Org. Biomol. Chem.* **2015**, *13*, 2574-2581.

13. Ulrich, G.; Goze, C.; Guardigli, M.; Roda, A.; Ziessel, R., Pyrromethene Dialkynyl Borane Complexes for "Cascatelle" Energy Transfer and Protein Labeling. *Angew. Chem. Int. Ed.* **2005**, *44*, 3694-3698.

14. Goze, C.; Ulrich, G.; Mallon, L. J.; Allen, B. D.; Harriman, A.; Ziessel, R., Synthesis and Photophysical Properties of Borondipyrromethene Dyes Bearing Aryl Substituents at the Boron Center. *J. Am. Chem. Soc.* **2006**, *128*, 10231-10239.

15. Goze, C.; Ulrich, G.; Ziessel, R., Unusual Fluorescent Monomeric and Dimeric Dialkynyl Dipyrromethene-Borane Complexes. *Org. Lett.* **2006**, *8*, 4445-4448.

16. Goze, C.; Ulrich, G.; Ziessel, R., Tetrahedral Boron Chemistry for the Preparation of Highly Efficient "Cascatelle" Devices. *J. Org. Chem.* **2007**, *72*, 313-322.

17. Goeb, S.; Ziessel, R., Convenient Synthesis of Green Diisoindolodithienylpyrromethene-Dialkynyl Borane Dyes. *Org. Lett.* **2007**, *9*, 737-740.

18. Li, L.; Nguyen, B.; Burgess, K., Functionalization of the 4,4-Difluoro-4-bora-3a,4a-diaza-*s*-indacene (BODIPY) Core. *Bioorg. Med. Chem. Lett.* **2008**, *18*, 3112-3116.

19. Bonardi, L.; Ulrich, G.; Ziessel, R., Tailoring the Properties of Boron-Dipyrromethene Dyes with Acetylenic Functions at the 2,6,8 and 4-B Substitution Positions. *Org. Lett.* **2008**, *10*, 2183-2186.

20. Niu, S. L.; Ulrich, G.; Ziessel, R.; Kiss, A.; Renard, P. Y.; Romieu, A., Water-Soluble BODIPY Derivatives. *Org. Lett.* **2009**, *11*, 2049-2052.

21. Ulrich, G.; Goeb, S.; De Nicola, A.; Retailleau, P.; Ziessel, R., Chemistry at Boron: Synthesis and Properties of Red to Near-IR Fluorescent Dyes Based on Boron-Substituted Diisoindolomethene Frameworks. *J. Org. Chem.* **2011**, *76*, 4489-4505.

22. Yang, L. J.; Simionescu, R.; Lough, A.; Yan, H. B., Some Observations Relating to the Stability of the BODIPY Fluorophore under Acidic and Basic Conditions. *Dyes Pigm.* **2011**, *91*, 264-267.

23. Gibbs, J. H.; Robins, L. T.; Zhou, Z.; Bobadova-Parvanova, P.; Cottam, M.; McCandless, G. T.; Fronczek, F. R.; Vicente, M. G., Spectroscopic, Computational Modeling and Cytotoxicity of a Series of *meso*-Phenyl and *meso*-Thienyl-BODIPYs. *Bioorg. Med. Chem.* **2013**, *21*, 5770-5781.

24. Kollmannsberger, M.; Rurack, K.; Resch-Genger, U.; Daub, J., Ultrafast Charge Transfer in Amino-Substituted Boron Dipyrromethene Dyes and Its Inhibition by Cation Complexation: A New Design Concept for Highly Sensitive Fluorescent Probes. *J. Phys. Chem. A* **1998**, *102*, 10211-10220.

25. Nguyen, A. L.; Bobadova-Parvanova, P.; Hopfinger, M.; Fronczek, F. R.; Smith, K. M.; Vicente, M. G., Synthesis and Reactivity of 4,4-Dialkoxy-BODIPYs: an Experimental and Computational Study. *Inorg. Chem.* **2015**, *54*, 3228-3236.

26. Lundrigan, T.; Thompson, A., Conversion of *F*-BODIPYs to *Cl*-BODIPYs: Enhancing the Reactivity of *F*-BODIPYs. *J. Org. Chem.* **2013**, *78*, 757-761.

27. Tahtaoui, C.; Thomas, C.; Rohmer, F.; Klotz, P.; Duportail, G.; Mely, Y.; Bonnet, D.; Hibert, M., Convenient Method to Access New 4,4-Dialkoxy- and 4,4-Diaryloxy-diaza-*s*-indacene Dyes: Synthesis and Spectroscopic Evaluation. *J. Org. Chem.* **2007**, *72*, 269-272.

28. Lundrigan, T.; Baker, A. E.; Longobardi, L. E.; Wood, T. E.; Smithen, D. A.; Crawford, S. M.; Cameron, T. S.; Thompson, A., An Improved Method for the Synthesis of *F*-BODIPYs from Dipyrrins and Bis(dipyrrin)s. *Org. Lett.* **2012**, *14*, 2158-2161.

29. Li, Z. B.; Lin, T. P.; Liu, S. L.; Huang, C. W.; Hudnall, T. W.; Gabbai, F. P.; Conti, P. S., Rapid Aqueous [^{18}F]-Labeling of a BODIPY Dye for Positron Emission Tomography/Fluorescence Dual Modality Imaging. *Chem. Commun.* **2011**, *47*, 9324-9326.

30. Liu, S.; Lin, T. P.; Li, D.; Leamer, L.; Shan, H.; Li, Z.; Gabbai, F. P.; Conti, P. S., Lewis Acid-Assisted Isotopic ^{18}F-^{19}F Exchange in BODIPY Dyes: Facile Generation of Positron Emission Tomography/Fluorescence Dual Modality Agents for Tumor Imaging. *Theranostics* **2013**, *3*, 181-189.

31. Brizet, B.; Eggenspiller, A.; Gros, C. P.; Barbe, J. M.; Goze, C.; Denat, F.; Harvey, P. D., *B*,*B*-Diporphyrinbenzyloxy-BODIPY Dyes: Synthesis and Antenna Effect. *J. Org. Chem.* **2012**, *77*, 3646-3650.

32. Brizet, B.; Bernhard, C.; Volkova, Y.; Rousselin, Y.; Harvey, P. D.; Goze, C.; Denat, F., Boron Functionalization of BODIPY by Various Alcohols and Phenols. *Org. Biomol. Chem.* **2013**, *11*, 7729-7737.

33. Crawford, S. M.; Thompson, A., Conversion of 4,4-Difluoro-4-bora-3a,4a-diaza-*s*-indacenes (*F*-BODIPYs) to Dipyrrins with a Microwave-Promoted Deprotection Strategy. *Org. Lett.* **2010**, *12*, 1424-1427.

CHAPTER 4: SYNTHESIS AND CHARACTERIZATION OF BODIPY-CARBOHYDRATE CONJUGATES AND CHIRAL BODIPYS FOR BIOIMAGING

4.1 Introduction

In the last 10 years, the growth of *in vivo* molecular imaging has progressed rapidly for evaluation of cancer for collaborations among physicians, imaging specialists, chemists, and physicists.[1] There are three types of molecular imaging: metabolic, targeted, and physiologic. One category of molecular imaging is targeted imaging which consists of fluorophore labeling with a specific ligand that bonds to a receptor. On the other hand, metabolic imaging involves the visualization of metabolic processes of glucose uptake by cells.

The three most common modes of *in vivo* oncologic imaging are nuclear medicine imaging, optical imaging, and magnetic resonance imaging (MRI). Nuclear medicine imaging is a noninvasive treatment that uses a small amount of radioactive tracer with temporal/spatial detection to diagnose a variety of diseases. Positron emission tomography (PET) and single photon emission computed tomographic (SPECT) are the two methods used for *in vivo* nuclear imaging. The advantage of PET and SPECT is their ability to detect the radiotracer amount in a matter of minutes. PET and SPECT are used as imaging techniques that barely disturb the biological system. PET produces higher image resolution than SPECT by using coincident rays to determine radionucleotide location. SPECT is a more cost efficient option that produces a broader image range, compared to PET, by using a collimator to select for certain angles of incidence of radionucleotide emissions. SPECT imaging modalities, when using advanced equipment, in small animal systems can produce an image resolution better than PET. Although PET and SPECT are advantageous, they do have certain limitations. SPECT has a limit on isotope combinations; so multiple isotopes have to be targeted many times to produce a single image. Both PET and SPECT are more expensive than other imaging methods and they potentially expose patients to more

radioactivity due the ionizing radiation so it is recommended that these tests are performed at a minimum for the safety of the patient.

In metabolic imaging, one particular glucose analog, fluoro-2-deoxy-D-glucose (FDG), has been used extensively for chemotherapeutic uses in order to study the glucose uptake in the body. However, when FDG was injected at therapeutic drug dose, it was found to cause toxicity to the nervous central system and thus was discarded.[2] The alternative analog, ^{18}F-2-deoxy-D-glucose (^{18}F-FDG), which is sensitive in PET and can be used to approximate the amount of glucose uptake during glycolysis. It enters the cell through glucose transporters (GLUTs) and is then phosphorylated. Dephosphorylation by glucose-6-phosphotase allows for a flow of ^{18}F-FDG in a cell, however the process is extremely slow due to naturally low levels of glucose-6-phosphotase present. It was suggested that ^{18}F-FDG is much more successful in healthy cells undergoing aerobic respiration than in malignant cells that utilize anaerobic respiration. During aerobic respiration in cells, glycolysis begins to slow down in the presence of oxygen as predicted by the Pasteur effect. The Warburg effect demonstrates that malignant cells use a glycolytic anaerobic respiration pathway even in the presence of oxygen. Although it is less efficient than aerobic respiration; this is a possible adaptation to long-term hypoxia experienced in tumors.[3-4] The half-life of radioactive ^{18}F is 110 min, which is long enough to carry out the synthesis and transport it to an imaging laboratory.

4.1.1 Click Chemistry

Nobel Laureate Professor Barry Sharpless first introduced click chemistry in 2001. Since then, it has become a popular method used in many diverse fields. The characteristics of click chemistry are fast reactions and high reaction yields, easy to purify, versatile, and regiospecific.[5] One of the most widely used class of click reaction is copper-catalyzed Huisgen 1,3-dipolar

cycloaddition (HDC) reaction. This reaction does not require high temperature conditions and results in regiospecific 1,4-substituted products. Although "click reactions" was developed in 2001, the utility of click chemistry in BODIPY's core or 8-phenyl were not reported until the last few years. Approaches to conjugate biomolecules via the *meso*-phenyl with folate,[6] polyethylene glycol and carbohydrate,[7] and zinc-TPP[8-9] have been reported. The triazole group can directly insert into the dipyrromethene core at either the 2,6-positions[10] or 3,5-positions.[10-11] On the other hand, the triazole has also provided a linker between fluorophores for intramolecular resonance energy transfer (RET).[12-14] However, having triazole moieties on the boron center for post functionalization of *F*-BODIPY has not been reported until recently.[15]

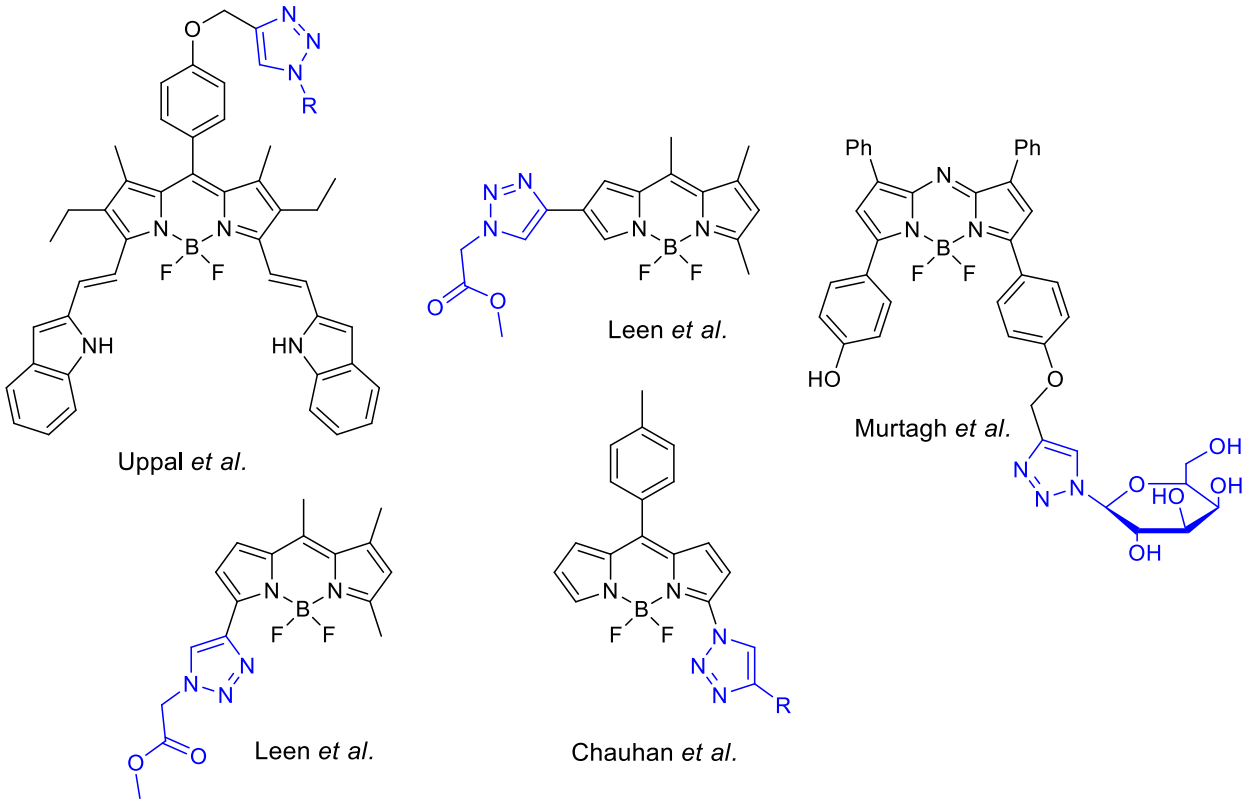

Figure 4.1: Selected examples of (1,2,3-triazole)-BODIPYs.

4.1.2 Chiral fluorophore

Chiral recognition has been growing in the last few decades for determination of enantiomeric purity in many chiral functional groups using organic fluorophores.[16] The study of chiral properties of organic molecules is very important in drug discovery and pharmaceutical chemistry. Fluorophores that are capable of distinguishing one enantiomer from another have an advantage in rapid chiral assays. Some examples of BODIPYs containing a chiral functionality have been reported.[17-20] Ziessel and coworkers reported the synthesis of 4-mono-aryl BODIPY which has hydrogen bonding between the fluoride atom and 3-aldehyde hydrogen. On the other hand, Sanchez-Carnerero *et al.* demonstrated that a chiral *O*-BODIPY can be applied in circularly polarized luminescence (CPL) spectroscopy with a 1,1'-binaphthyl moiety on the boron center.

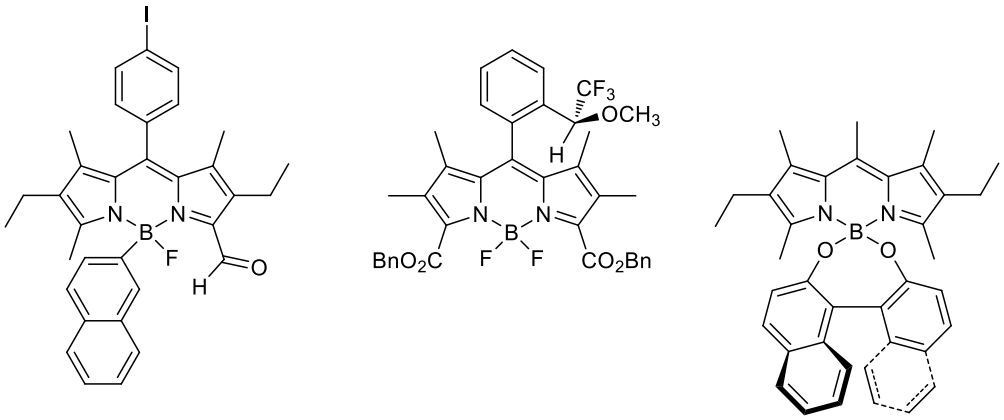

Ziessel *et al.* Stoeckli-Evans *et al.* Sanchez-Carnerero *et al.*

Figure 4.2: Selected examples of chiral BODIPYs.

In order to extend the scope of (1,2,3-triazole)-BODIPYs synthesis, we decided to design and synthesize new fluorophores containing mono-, di-, and tri-(1,2,3-triazole)-BODIPYs bearing a carbohydrate framework in order to study and compare their biological properties. In addition, the synthesis of chiral BODIPY is investigated for chiral recognition applications or stereoselective aldol reactions.

4.2 Results and Discussion

4.2.1 Syntheses of (1,2,3-triazole)-BODIPYs

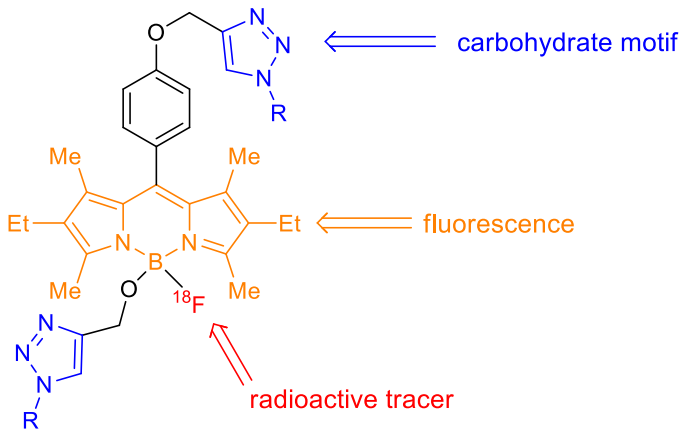

Figure 4.3: Our designed synthetic platform.

The goal for this project was to synthesize a series of fluorescent bioconjugates comprising of a BODIPY fluorophore bearing a triazole group connected to carbohydrate moiety for target-specific cell accumulation. This has been previously investigated for synthesis of porphyrins and related macrocycles with conjugates for use as photosensitizers for PDT.[21-23] In addition, mono radioactive ^{18}F can be installed on the boron center as a dual-modality fluorescent probe.[24]

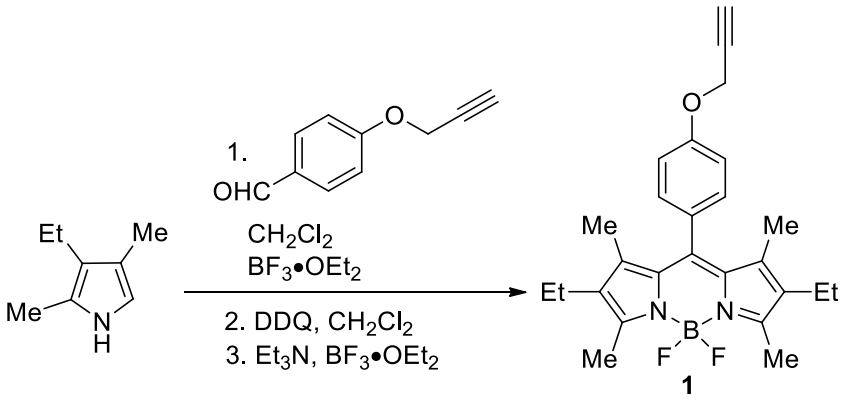

Scheme 4.1: Synthesis of BODIPY **1** from 3-ethyl-,2,4-dimethyl pyrrole.

The starting BODIPY **1** was synthesized, as previously reported,[7,25] by condensation between the commercially available 3-ethyl-2,4-dimethylpyrrole and *p*-propargyloxy-

benzaldehyde using a 3-step-1-pot reaction in high yield, as shown in Scheme 4.1. The progaryloxy benzaldehyde was synthesized as a crude product via Williamson reaction between propargyl bromide and *p*-hydroxyl benzaldehyde, according to the literature procedure.[25]

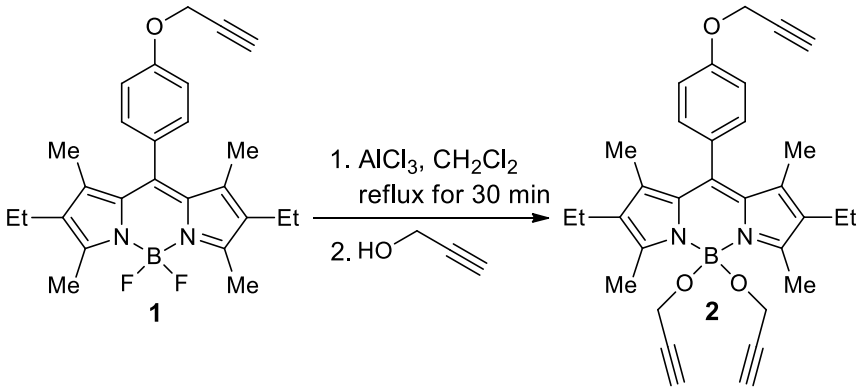

Scheme 4.2: Synthesis of 4,4-dipropargyl-BODIPY **2**.

The propargyloxy groups were introduced at the boron center via activation of BODIPY **1** with aluminum chloride[15,26] followed by excess propargyl alcohol to afford tri-alkyne BODIPY **2** in 69% yield (Scheme 4.2). The goal was to provide three terminal alkyne groups for further functionalization using click chemistry.

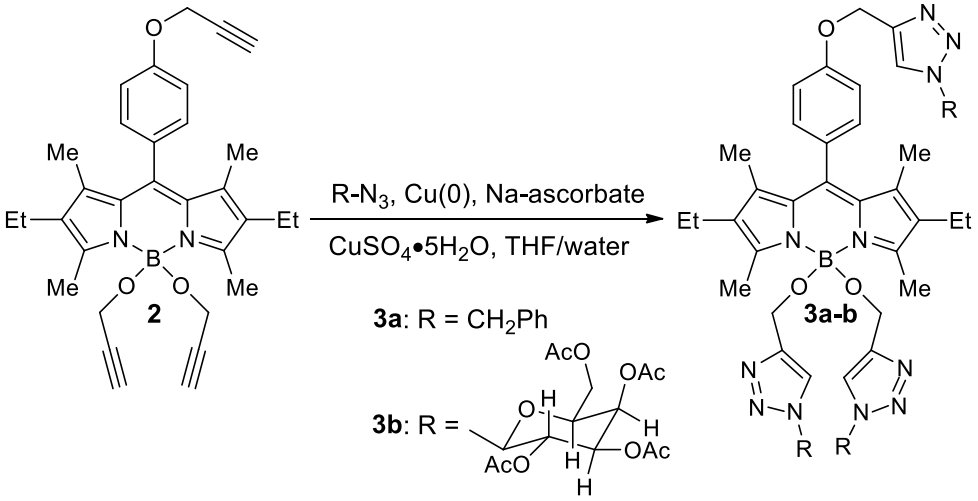

Scheme 4.3: Synthesis of BODIPYs **3a** and **3b**.

BODIPY **2** was subjected to either commercially available benzyl azide or 1-azido-1-deoxy-β-D-glucopyranoside tetraacetate, using solution-phase "click" conditions, which consists of copper(II) sulfate, copper(0) and sodium ascorbate in THF/water (3:1), to give tri-(1,2,3-triazoles)-BODIPYs **3a** and **3b**. Under an inert gas atmosphere, the mixture were refluxed at 70 °C for 6 h for compounds **3a** and **3b**. Upon reaction completion, the mixture was cooled to room temperature and partitioned between ethyl acetate and water to remove the generated copper salt by-product. The combined organic layers were dried over Na_2SO_4 and concentrated under reduced pressure. The crude products were purified using preparative-TLC (thin layer chromatography) to give tri-(1,2,3-triazoles)-BODIPYs **3a** and **3b** in 76% and 64% yields, respectively. Indeed, the click reaction has provided a high yield to conjugate glucose derivate or benzyl to BODIPYs core.

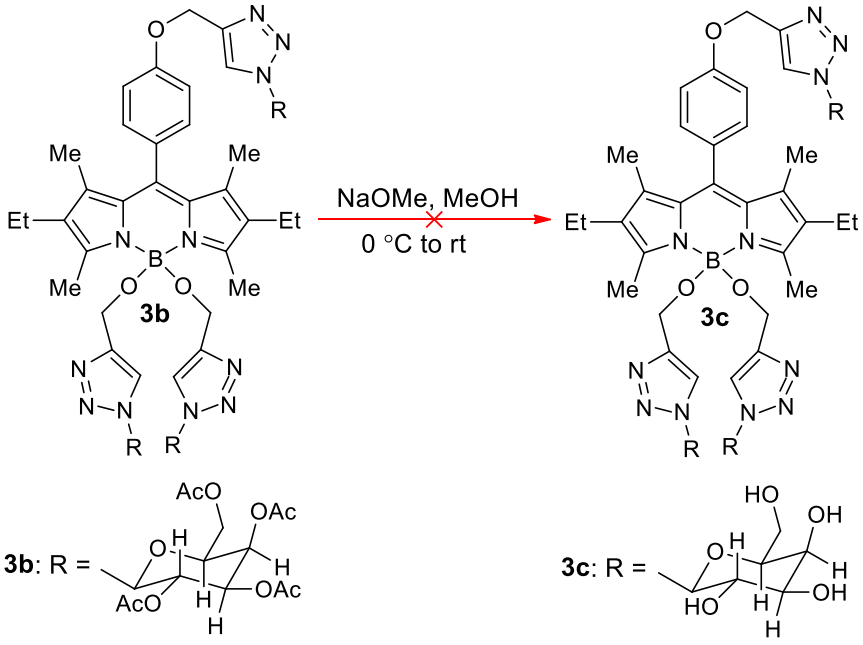

Scheme 4.4: Fail attempted hydrolysis of BODIPY **3b**.

We then attempted to hydrolyze compound **3b** under basic condition (NaOMe in MeOH) at 0 °C to give **3c**, but the reaction failed. We also attempted various hydrolysis conditions such as

BBr_3 or NaOH. The BBr_3 conditions gave the corresponding dipyrromethene while the NaOH conditions replaced the BF_2 with $B(OH)_2$.

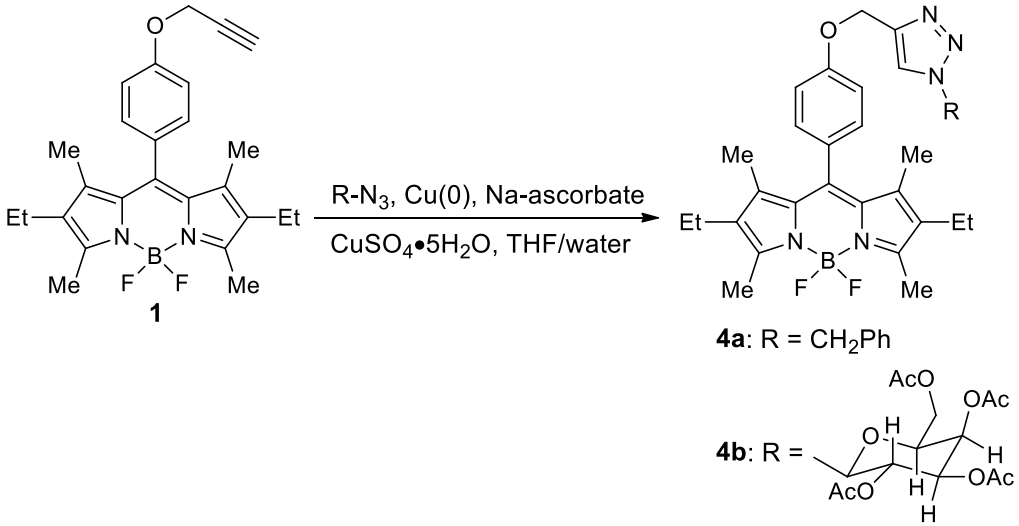

Scheme 4.5: Synthesis of BODIPYs **4a** and **4b**.

Having the optimized conditions for the tri-(1,2,3-triazole)-BODIPYs, we turned our attention to the synthesis of mono- and di-(1,2,3-triazole)-BODIPYs. For the mono-azido synthesis, BODIPY **1** was exposed to Cu(I)-catalyzed azide-alkyne cycloaddition with commercially available benzyl azide or 1-azido-1-deoxy-β-D-glucopyranoside tetraacetate to afford BODIPY **4a** (93%) and the mono-triazole-tetraacetate-sugar BODIPY **4b** (82%) as shown in Scheme 4.5. The mono-triazole-sugar BODIPY **4b** was hydrolyzed under basic conditions to give the desired glucose triazole **4c** in 93% yield. Surprisingly, the B-$(OR)_2$ was still intact under strong nucleophilic reaction conditions such as NaOMe as confirmed by ^{1}H-, ^{13}C- and ^{11}B-NMR spectroscopy and also HRMS. Note, when hydrolysis was attempted at room temperature, the B-$(OR)_2$ moiety was removed to give dipyrromethene.

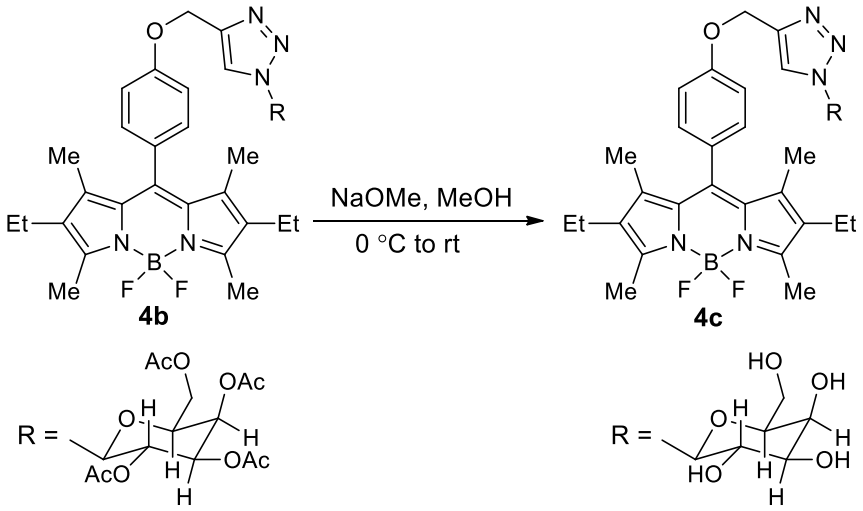

Scheme 4.6: Hydrolysis of BODIPY **4b**.

In order to synthesize the di-triazole-sugar BODIPY, compound **4a** was exposed to aluminum chloride ($AlCl_3$), followed by excess propargyl alcohol to give *meso*-triazolephenyl BODIPY **5a** in 73% yield (Scheme 4.7). The *meso*-triazolephenyl BODIPY **5a** was subjected to Cu(I)-catalyzed azide-alkyne cycloaddition with commercially available 1-azido-1-deoxy-β-D-glucopyranoside tetraacetate to afford compound **6a** in 72% yield. BODIPY **6a** was purified by silica gel column chromatography but the compound was immobile. Then we decided to use neutral alumina column chromatography and were able to isolate the targeted product in good yield. We also attempted to subject BODIPY **6a** to hydrolysis conditions (NaOMe in MeOH at 0 °C) but obtained the 4,4-dihydroxy product. In addition, if we treated BODIPY **5a** with the commercially available unprotected glucose azide under the same click reaction conditions, we recovered the starting material and dipyrromethene as a by-product.

4.2.2 Synthesis of chiral BODIPY

We now turned to the synthesis of BODIPY with a boron atom bearing a chiral motif. We began our investigation by introducing a carboxylate group to the boron center through two different methods. Method B consists of treating BODIPY **7** with $AlCl_3$ and excess addition of

acetic acid to give BODIPY **8b** in moderate yield (42%). The conditions were milder and required a shorter time than those previously reported.[27-28] However, when BODIPY **7** was exposed using method C, a mixture of 4-mono- and 4,4-disubstituted BODIPYs **8a** and **8b** were obtained with 8% and 14% yields, respectively. Even though method B gave a high yield of the di-substituted product, this method typically required an excess amount of the nucleophile (278 equiv.). For that reason, we decided to use method C for our next investigation.

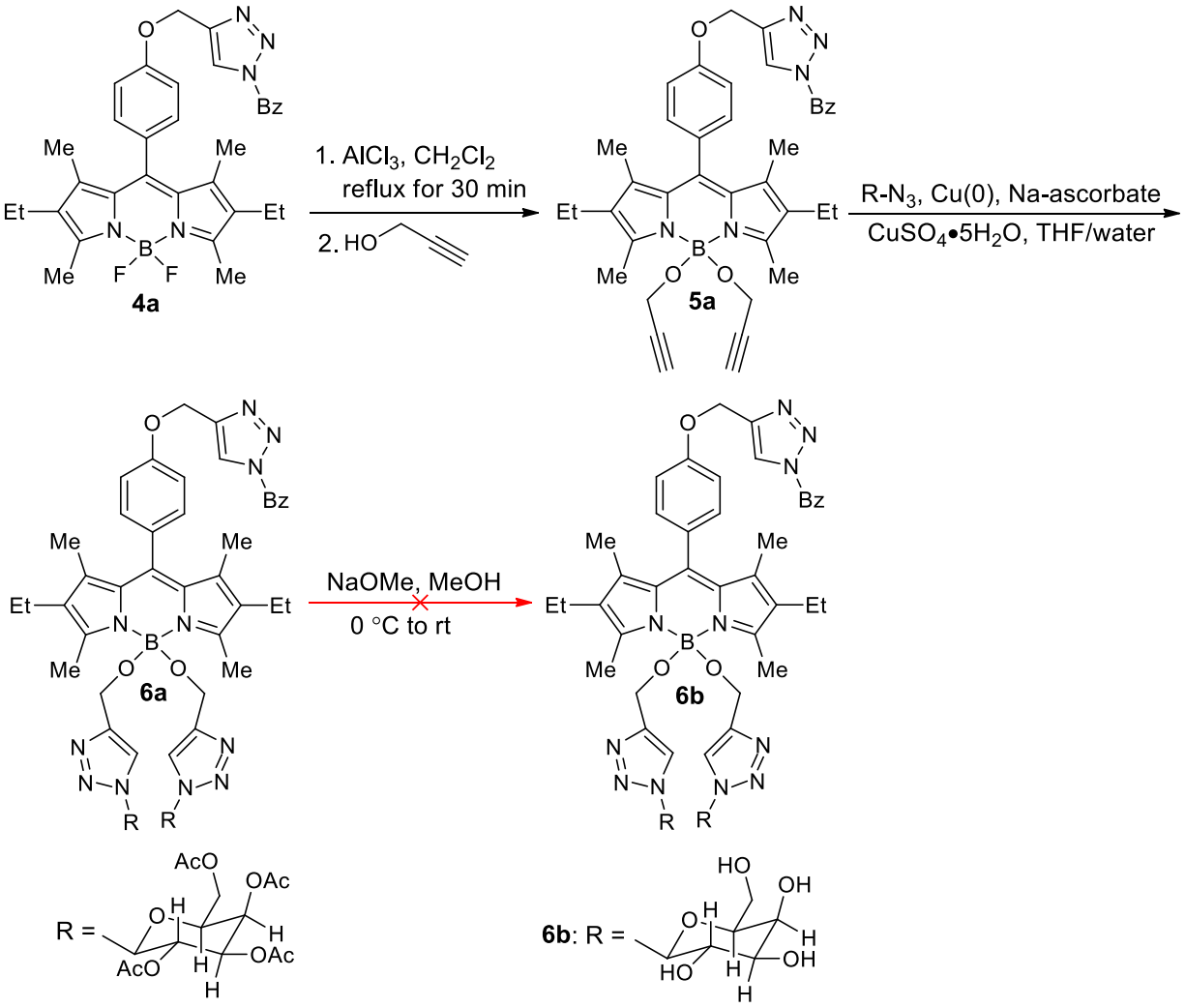

Scheme 4.7: Synthesis of 4,4-tri(1,2,3-triazole)-BODIPY.

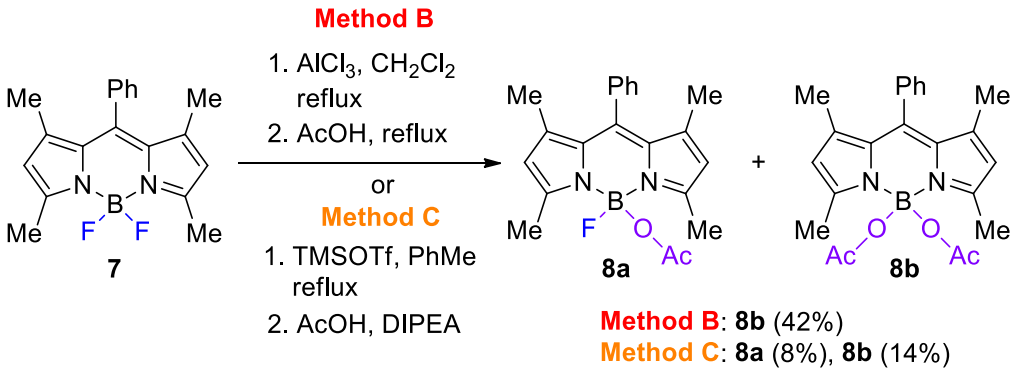

Scheme 4.10: Synthesis of 4-acetyl- and 4,4-diacetyl-BODIPYs.

To further explore the extent of this reaction, we used 4-bromobenzoic acid as the nucleophile using method C and were able to obtain the targeted BODIPY **9** in 5% yield (Scheme 4.11). BODIPY **9** was characterized by ^{1}H- and ^{11}B-NMR spectroscopy and X-ray crystallography.

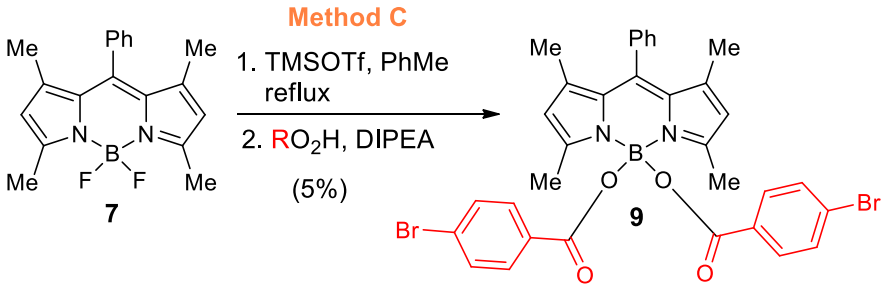

Scheme 4.11: Synthesis of carboxylate BODIPY **9**.

Next, we investigated an amino acid containing carboxylic acid. When we tried tryptophan with Boc-protected amine using method C, we were hoping to isolate the mono- or di-substituted products. Interestingly, the product obtained was the cyclic BODIPY product **10** (Scheme 4.12). To the best of our knowledge, this is the first report of a chiral group and nitrogen atom on the boron center. This compound has a potential for fluorescent chiral recognition. In addition, BODIPY **10** was characterized by ^{1}H- and ^{11}B-NMR spectroscopy and X-ray crystallography.

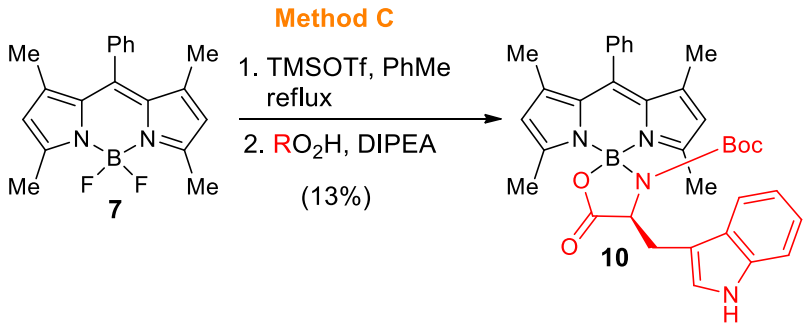

Scheme 4.12: Synthesis of chiral BODIPY **10**.

These results prompted us to further investigate unprotected amino acids. When amino acids without Boc or Fmoc groups were used, the resulting products were dipyrromethenes. It is possible that electron withdrawing Boc protecting group makes the nitrogen atom less basic. We decided to use ethanolamine as the nucleophile with methods B and C. Similar to acetate, the di-substituted product **11b** was obtained in 70% yield with method B while a mixture of mono- and di-products was obtained with method C in 14% and 10% yields, respectively. This indicates that the indole of the tryptophan plays a steric factor and facilitates the cyclization.

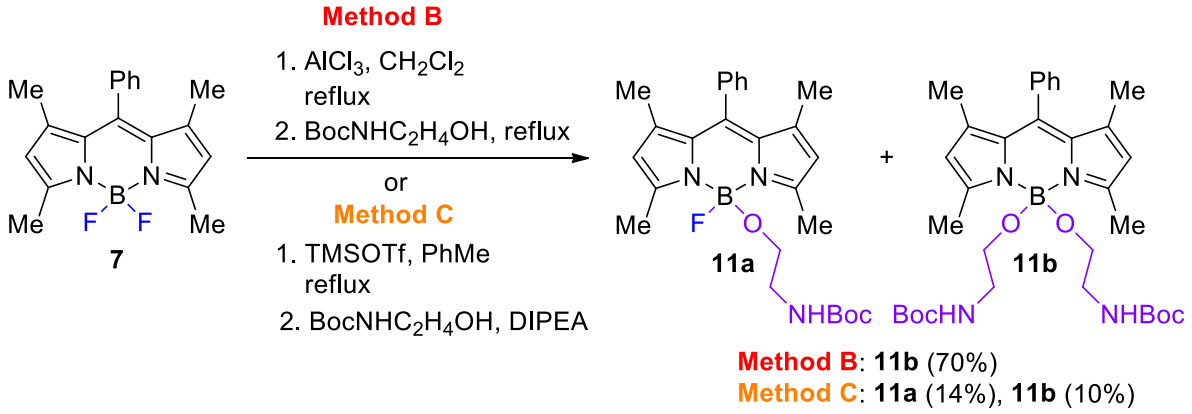

Scheme 4.13: Synthesis of 4-mono- and 4,4-disubstituted BODIPYs.

Finally, we used ethylene glycol as the nucleophile using methods B and C (Scheme 4.14). We were able to obtain the targeted BODIPY **12** in 21% and 37% yields, respectively.

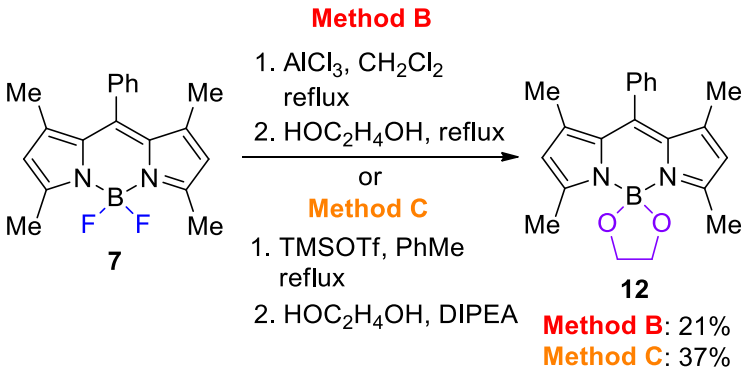

Scheme 4.14: Synthesis of cyclic 4,4-dialkoxy BODIPY **12**.

4.2.3 Structural Characterization

All BODIPYs were characterized by ^{1}H-, ^{13}C-, and ^{11}B-NMR, and HRMS. BODIPYs **4a-b**, **9**, **10**, **11a** and **12** were characterized by X-ray crystallography (see Figures 4.4 and 4.5). The disappearance of the triplet for the BF_2 (at ca. 0.6 ppm) and the appearance of the singlet attributed to $B(OR)_2$ (at ca. 2 ppm) in the ^{11}B-NMR spectra clearly showed the formation of the targeted 4,4-dialkoxy-BODIPY. The ^{1}H-NMR spectrum clearly indicated the formation of the 1,2,3-triazoles of BODIPY **3a-b, 4a-c, and 6a** with singlets ranging from 7.50-8.12 ppm.

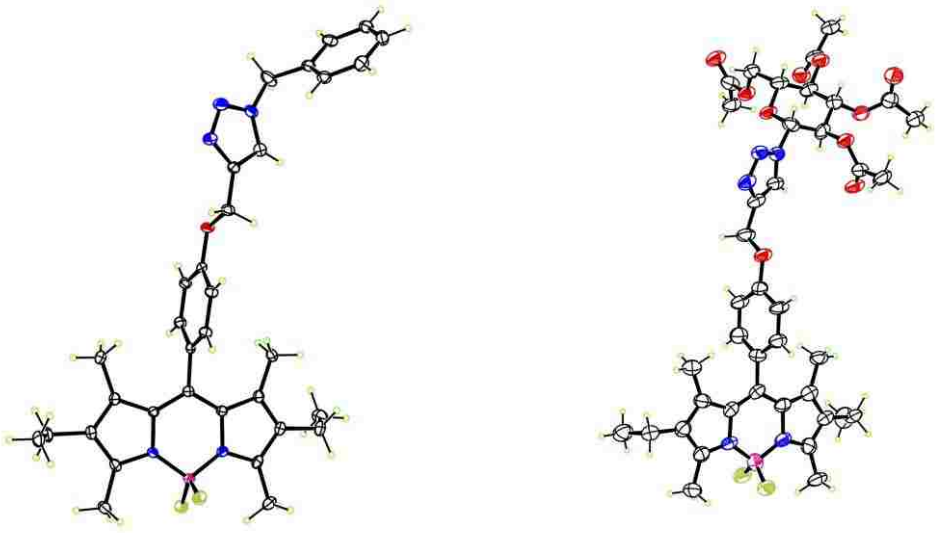

4a **4b**

Figure 4.4: Molecular structures of BODIPYs **4a-b** from X-ray crystal analysis, with 50% probability ellipsoids.

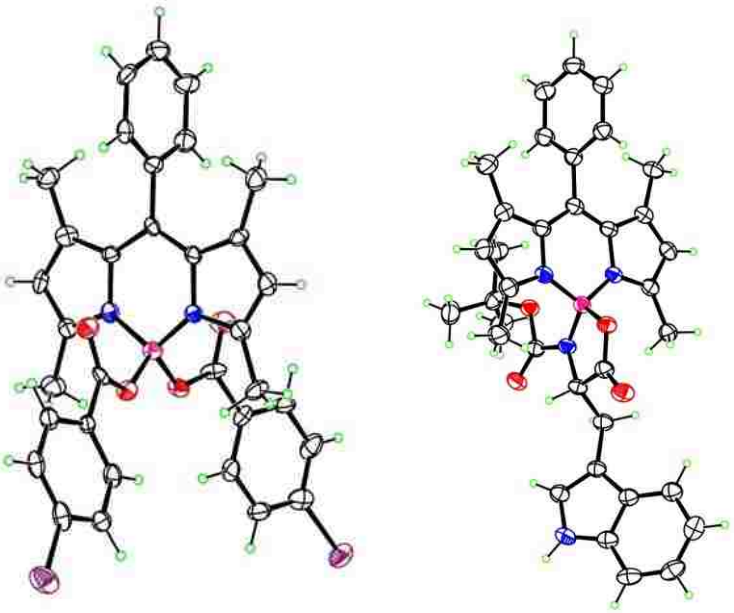

9 **10**

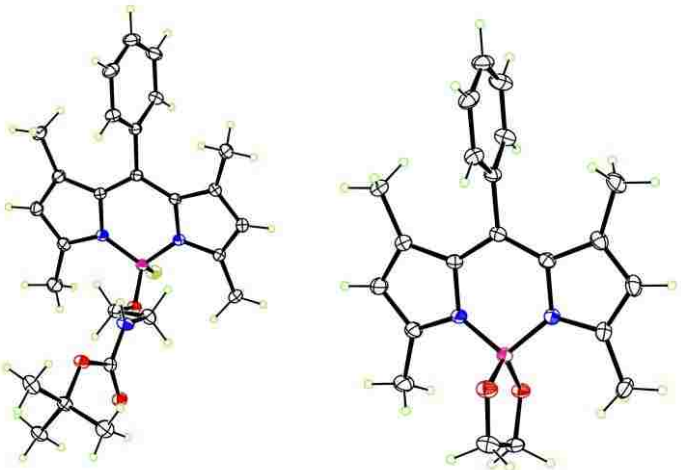

11a **12**

Figure 4.5: Molecular structures of BODIPYs **9**, **10**, **11a** and **12** from X-ray crystal analysis, with 50% probability ellipsoids.

Full structural confirmation of all compounds was obtained from the X-ray crystal structures. Crystals suitable for X-ray analysis were grown by slow evaporation of dichloromethane diffused in acetone (for **4a-b**), hexane in dichloromethane (for **9**, **11a**, and **12**),

and EtOAc in MeOH (for **10**). The alkoxy groups on the boron center adopt a nearly tetrahedral geometry.

4.3 Conclusions

A series of six 1,2,3-triazole-BODIPYs were synthesized in high yields under the Cu(I)-catalyzed Huisgen cycloaddition reaction conditions. A BODIPY bearing one triazole group was shown to undergo hydrolysis while two or three triazole resulted in the 4,4-hydroxyl product. Acetyl and 1,2-Boc-aminoalcohol groups were introduced to the boron center through two different methods. Method B was the most effective way to give the di-substituted BODIPYs **8b** and **11b** in 42% and 70% yields, respectively. Method C gave a mixture of 4-mono-acetyl-BODIPYs **8a** (8%) and 4,4-di-acetyl-BODIPY **8b** (14%) and 4-mono-alkoxy **11a** (14%) and 4,4-dialkoxy **11b** (10%). A novel BODIPY bearing a chiral moiety was synthesized using method C and X-ray crystallography confirmed its identity.

4.4 Experimental

4.4.1 General Considerations

All commercially available reagents were purchased from Sigma-Aldrich and were used without further purification. All anhydrous reactions were carried out with oven-dried glassware under a dry argon atmosphere. All the reactions were monitored by using Sorbent Technologies pre-coated polyester backed TLC (200 µm silica gel with indicator UV-254 nm). Flash column chromatography was performed using Sorbent Technologies 60 Å alumina neutral (230-400 mesh). All preparative-TLC were used with Silica Gel 60 Å silica gel 20 x 20 cm (210-270 µm). All ^{1}H-, ^{13}C-, ^{11}B-NMR spectral were collected using AV-400 spectrometer (operating at 400 MHz for ^{1}H NMR and 100 MHz for ^{13}C NMR) and deuterated acetone or chloroform as solvents. The $CDCl_3$ chemical shifts (δ) are reported ppm with 7.27 for proton and 77.16 for carbon NMR as

reference. The $(CD_3)_2CO$ chemical shift (δ) are reported ppm with 2.05 for proton and 29.84 and 206.26 for carbon NMR as reference. The BF_3•OEt_2 chemical shift (δ) is reported with 0.00 for boron NMR as reference. Coupling constants are reported in Hertz (Hz). All the mass spectra were collected using an Agilent 6210 ESI-TOF mass spectrometer.

4.4.2 Syntheses

BODIPY (**1**). The BODIPY **1** was synthesized according to the literature.[7,25] ^{1}H NMR ($CDCl_3$, 400 MHz) δ 7.20 (d, *J* = 8.0 Hz, 2H), 7.09 (d, *J* = 8.0 Hz, 2H), 4.77 (s, 2H), 2.57 (s, 1H), 2.54 (s, 6H), 2.31 (q, *J* = 7.3 Hz, 4H), 1.33 (s, 6H), 0.99 (t, *J* = 7.4 Hz, 6H); ^{13}C NMR ($CDCl_3$, 100 MHz) δ 158.06, 153.70, 140.04, 138.51, 132.81, 129.60, 128.94, 115.64, 75.97, 56.14, 17.18, 14.75, 12.60, 11.94; ^{11}B NMR ($CDCl_3$, 128 MHz) δ 0.68 (t, *J* = 33.3 Hz).

BODIPY (**2**). In an oven-dried flask, *meso*-alkynylphenyl-BODIPY **1** (100 mg, 0.230 mmol, 1.0 equiv.) and $AlCl_3$ (61 mg, 0.460 mmol, 2.0 equiv.) were dissolved in anhydrous CH_2Cl_2 (20 mL). The mixture was refluxed for 30 min and propargyl alcohol (3.7 mL, 64.007 mmol, 278.0 equiv.) was added for an additional 30 min. After the mixture was cooled to room temperature and stirred for 2 h, the crude product was concentrated under reduced pressure. The crude product was purified via TLC (eluent 80:20 hexane/EtOAc) to afford BODIPY **2** (80.6 mg, 69% yield) as an orange solid, that was recrystallized from 1:1 hexane/dichloromethane. ^{1}H NMR ($CDCl_3$, 400 MHz) δ 7.21 (d, *J* = 8 Hz, 2H), 7.09 (d, *J* = 8 Hz, 2H), 4.78 (s, 2H), 3.81 (s, 4H), 2.57 (s, 6H), 2.31 (q, *J* = 7.3 Hz, 4H), 2.04 (s, 2H), 1.33 (s, 6H), 0.98 (t, *J* = 7.2 Hz, 6H); ^{13}C NMR ($CDCl_3$, 100 MHz) δ 157.86, 154.72, 139.39, 137.15, 132.71, 132.30, 129.69, 129.38, 115.44, 83.27, 78.15, 75.80, 70.44, 56.06, 49.80, 17.11, 14.71, 12.75, 11.89; ^{11}B NMR ($CDCl_3$, 128 MHz) δ 1.76 (s); HRMS (ESI-TOF) *m/z* 528.2669 $[M + Na]^+$ calculated for $C_{32}H_{35}BN_2O_3$: 528.2681.

BODIPY (**3a**). BODIPY **2** (17.5 mg, 0.035 mmol, 1.0 equiv.) and Cu(0) (2.2 mg, 0.035 mmol, 1.0 equiv.) were dissolved in a mixture of THF/water (8 mL, 3:1) under inert gas atmosphere. Benzyl azide (0.043 mL, 0.346 mmol, 10.0 equiv.) was added dropwise to the reaction mixture. A solution of $CuSO_4 \cdot 5H_2O$ (1.7 mg, 0.007 mmol, 0.2 equiv.) and sodium-ascorbate (3.4 mg, 0.017 mmol, 0.5 equiv.) in THF/water (8 mL, 3:1) was added (after sonication for 30 min) and the reaction mixture was heated for 22 h at 70 °C. Once TLC indicated complete consumption of starting material, the mixture was cooled to room temperature and partitioned between ethyl acetate (30 mL) and water (30 mL). The combined organic layers were dried over Na_2SO_4 and then concentrated under reduced pressure. The crude product was purified via TLC (eluted 20:80 hexane/EtOAc) to afford triazoles BODIPY **3a** (23.8 mg, 76% yield) and was recrystallized from 1:3 acetone/hexanes. ^{1}H NMR ($CDCl_3$, 400 MHz) δ 7.59 (s, 1H), 7.38-7.23 (m, 15H), 7.17 (d, *J* = 8.0 Hz, 2H), 7.07 (d, *J* = 8 Hz, 2H), 5.57 (s, 2H), 5.42 (s, 4H), 5.25 (s, 2H), 4.22 (s, 4H), 2.39 (s, 6H), 2.22 (q, *J* = 7.12 Hz, 4H), 1.28 (s, 6H), 0.93 (t, *J* = 6.8 Hz, 6H); ^{13}C NMR ($CDCl_3$, 100 MHz) δ 158.67, 153.79, 149.71, 144.31, 140.18, 137.32, 134.93, 134.51, 132.72, 132.53, 129.85, 129.31, 129.24, 129.11, 129.00, 128.90, 128.69, 128.27, 128.24, 122.78, 121.65, 115.35, 62.21, 56.84, 54.43, 54.10, 21.15, 17.20, 14.81, 14.30, 12.62, 11.99; ^{11}B NMR ($CDCl_3$, 128 MHz) δ 2.10 (s); HRMS (ESI-TOF) *m/z* 927.4589 $[M + Na]^+$ calculated for $C_{53}H_{56}BN_{11}O_3$: 927.4593.

BODIPY (**3b**). Tri-alkynyl-BODIPY **2** (27.2 mg, 0.054 mmol, 1.0 equiv.), Cu(0) (13.7 mg, 0.215 mmol, 4.0 equiv.), and 1-azido-1-deoxy-β-D-glucopyranoside tetraacetate (301 mg, 0.806 mmol, 15.0 equiv.) were dissolved in a mixture of THF/water (8 mL, 3:1) under an inert gas atmosphere. A solution of $CuSO_4 \cdot 5H_2O$ (10.1 mg, 0.040 mmol, 0.75 equiv.) and sodium-ascorbate (21.3 mg, 0.107 mmol, 2.0 equiv.) in THF/water (8 mL, 3:1) was added (after sonication for 30

min) and the reaction mixture was heated for 14 h at 70 °C. Once TLC indicated complete consumption of starting material, the mixture was cooled to room temperature and partitioned between ethyl acetate (30 mL) and water (30 mL). The combined organic layers were dried over Na_2SO_4 and then concentrated under reduced pressure. The crude product was purified via alumina neutral flash chromatography (eluent 100% EtOAc to 95:5 EtOAc/MeOH) to give BODIPY **3b** (56.3 mg, 64% yield) and was recrystallized from EtOAc. ^{1}H NMR ($(CD_3)_2CO$, 400 MHz) δ 8.43 (s, 1H), 8.12 (s, 1H), 7.98 (d, *J* = 8.0 Hz, 2H), 7.37 (d, *J* = 8.0 Hz, 2H), 7.27 (d, *J* = 8.0 Hz, 2H), 6.30 (d, *J* = 8.0 Hz, 1H), 6.22 (d, *J* = 8.1 Hz, 1H), 6.17 (d, *J* = 8.1 Hz, 1H), 5.64 (d, *J* = 8.0 Hz, 2H), 5.62 (s, 6H), 5.54 (d, 2H), 5.29 (d, 2H), 4.36-4.32 (m, 4H), 4.26-4.23 (m, 4H), 4.22-4.19 (m, 4H), 2.54 (s, 6H), 2.35 (q, *J* = 7.52 Hz, 4H), 2.04 (s, 9H), 2.01 (s, 9H), 1.97 (s, 9H), 1.79 (s, 9H), 1.41 (s, 6H), 0.98 (t, *J* = 7.44 Hz, 6H); ^{13}C NMR ($CDCl_3$, 100 MHz) δ 170.79, 170.34, 170.14, 169.30, 154.93, 141.63, 137.82, 133.43, 130.86, 123.73, 121.79, 121.42, 116.44, 86.06, 85.88, 75.42, 75.32, 73.65, 71.53, 71.46, 68.93, 68.86, 62.91, 62.8, 57.10, 55.03, 20.71, 20.68, 20.59, 20.28, 20.23, 17.73, 15.14, 12.98, 12.33; ^{11}B NMR ($CDCl_3$, 128 MHz) δ 2.05 (s); HRMS (ESI-TOF) *m/z* 1647.6033 $[M + Na]^+$ calculated for $C_{74}H_{92}BN_{11}O_{30}$: 1647.6019.

BODIPY (**4a**). BODIPY **1** (30 mg, 0.069 mmol, 1.0 equiv.) and Cu(0) (4.4 mg, 0.069 mmol, 1.0 equiv.) were dissolved in a mixture of THF/water (8 mL, 3:1) under an inert gas atmosphere. Benzyl azide (0.022 mL, 0.180 mmol, 2.6 equiv.) was added dropwise to the reaction mixture. A solution of $CuSO_4 \cdot 5H_2O$ (3.4 mg, 0.014 mmol, 0.2 equiv.) and sodium-ascorbate (6.8 mg, 0.035 mmol, 0.5 equiv.) in THF/water (8 mL, 3:1) was added (after sonication for 30 min) and the reaction mixture was heated for 6 h at 70 °C. Once TLC indicated complete consumption of starting material, the mixture was cooled to room temperature and partitioned between ethyl

acetate (30 mL) and water (30 mL). The combined organic layers were dried over Na_2SO_4 and then concentrated under reduced pressure. The crude product was purified via TLC (eluent 50:50 hexane/EtOAc) to afford BODIPY **4a** (36.4 mg, 93% yield) and was recrystallized from 1:3 dichloromethane/hexane. ^{1}H NMR ($CDCl_3$, 400 MHz) δ 7.60 (s, 1H), 7.39-7.28 (m, 5H), 7.18 (d, *J* = 8.0 Hz, 2H), 7.09 (d, *J* = 8.0 Hz, 2H), 5.58 (s, 2H), 5.25 (s, 2H), 2.54 (s, 6H), 2.30 (q, *J* = 7.4 Hz, 4H), 1.31 (s, 6H), 1.00 (t, *J* = 7.16 Hz, 6H); ^{13}C NMR ($CDCl_3$, 100 MHz) δ 158.75, 153.69, 144.24, 140.11, 138.49, 134.52, 132.81, 131.23, 129.66, 129.30, 129.00, 128.63, 128.26, 122.83, 115.41, 62.18, 54.42, 17.18, 14.74, 12.59, 11.91; ^{11}B NMR ($CDCl_3$, 128 MHz) δ 0.68 (t, *J* = 33.7 Hz); HRMS (ESI-TOF) m/z 589.2910 $[M + Na]^+$ calculated for $C_{33}H_{36}BF_2N_5O$: 589.2895.

BODIPY (**4b**). BODIPY **1** (50 mg, 0.115 mmol, 1.0 equiv.), Cu(0) (14.6 mg, 0.230 mmol, 2.0 equiv.), and 1-azido-1-deoxy-β-D-glucopyranoside tetraacetate (214.9 mg, 0.576 mmol, 5 equiv.) were dissolved in a mixture of THF/water (8 mL, 3:1) under an inert gas atmosphere. A solution of $CuSO_4 \cdot 5H_2O$ (11.5 mg, 0.046 mmol, 0.4 equiv.) and sodium-ascorbate (22.8 mg, 0.115 mmol, 1.0 equiv.) in THF/water (8 mL, 3:1) was added (after sonication for 30 min) and the reaction mixture was heated for 21 h at 70 °C. Once TLC indicated complete consumption of starting material, the mixture was cooled to room temperature and partitioned between ethyl acetate (30 mL) and water (30 mL). The combined organic layers were dried over Na_2SO_4 and then concentrated under reduced pressure. The crude product was purified via TLC (eluent 50:50 hexane/EtOAc) to afford BODIPY **4b** (76.5 mg, 82% yield) and was recrystallized from 1:3 dichloromethane/hexane. ^{1}H NMR ($(CD_3)_2CO$, 400 MHz) δ 8.43 (s, 1H), 7.30-7.25 (m, 4H), 6.30 (d, *J* = 8.1 Hz, 1H), 5.67 (t, *J* = 9.4 Hz, 1H), 5.57 (t, *J* = 9.4 Hz, 1H), 5.31 (s, 2H), 4.40-4.36 (m, 1H), 4.30-4.25 (m, 1H), 4.21-4.18 (m, 1H), 2.49 (s, 6H), 2.35 (q, *J* = 7.5 Hz, 4H), 2.00 (s, 3H),

1.98 (s, 3H), 1.96 (s, 3H), 1.83 (s, 3H), 1.39 (s, 6H), 0.99 (t, J = 7.5 Hz, 6H); ^{13}C NMR ($(CD_3)_2CO$, 100 MHz) δ 170.76, 170.35, 170.17, 169.40, 160.18, 154.24, 144.92, 141.80, 139.29, 133.58, 131.97, 130.56, 129.01, 123.76, 116.55, 86.07, 75.43, 73.52, 71.53, 68.84, 62.78, 62.63, 20.67, 20.58, 20.27, 17.56, 15.04, 12.66, 12.19; ^{11}B NMR ($CDCl_3$, 128 MHz) δ 0.67 (t, J = 33.9 Hz); HRMS (ESI-TOF) *m/z* 829.3391 $[M + Na]^+$ calculated for $C_{40}H_{48}BF_2N_5O_{10}$: 829.3384.

BODIPY (**4c**). BODIPY **4b** (22.5 mg, 0.028 mmol, 1.0 equiv.) and NaOMe (6.3 mg, 0.117 mmol, 4.2 equiv.) were dissolved in MeOH (5 mL) at 0 °C. The mixture was stirred for 30 min and then warmed to room temperature. Once TLC indicated complete consumption of starting material, Dowex 50WX8 H^+ resin was added and stirred until the solution is neutral. The resin was filtered off and crude product was concentrated by reduced pressure. The crude product was purified using alumina column chromatography (eluent 50:50 dichloromethane/acetone) to afford BODIPY **4c** (16.5 mg, 93% yield) and was recrystallized from 1:6 water/dichloromethane. ^{1}H NMR ($(CD_3)_2CO$, 400 MHz) δ 8.31 (s, 1H), 7.29 (s, 4H), 5.70 (d, 1H), 5.30 (s, 2H), 4.71 (d, J = 4.0 Hz, 2H), 4.64 (d, J = 4.0 Hz, 2H), 4.46 (d, J = 4.0 Hz, 2H), 4.04-3.98 (m, 1H), 3.89-3.82 (m, 2H), 3.74-3.63 (m, 3H), 3.60-3.54 (m, 1H), 2.49 (s, 6H), 2.35 (q, J = 7.56 Hz, 4H), 1.39 (s, 6H), 0.99 (t, J = 7.5 Hz, 6H); ^{13}C NMR ($(CD_3)_2CO$, 100 MHz) δ 160.63, 154.58, 139.65, 133.91, 132.32, 130.92, 129.27, 124.43, 116.81, 89.39, 81.17, 78.92, 74.19, 71.41, 62.98, 62.90, 17.91, 15.39, 13.02, 12.55; ^{11}B NMR ($CDCl_3$, 128 MHz) δ 0.60 (t, J = 34.3 Hz); HRMS (ESI-TOF) *m/z* 639.3149 $[M + H]^+$ calculated for $C_{32}H_{40}BF_2N_5O_6$: 639.3109.

BODIPY (**5a**). In an oven-dried flask, BODIPY **4a** (45.2 mg, 0.080 mmol, 1.0 equiv.) with $AlCl_3$ (21 mg, 0.159 mmol, 2.0 equiv.) were dissolved in anhydrous CH_2Cl_2 (10 mL). The mixture

was refluxed for 30 min and propargyl alcohol (1.278 mL, 22.143 mmol, 278.0 equiv.) was added for an additional 30 min. After the reaction cooled to room temperature and stirred for 1 h, the crude product was concentrated under reduced pressure. The crude product was purified via TLC (eluent 50:50 hexane/EtOAc) to afford BODIPY **5a** (37.3 mg, 73% yield) and was recrystallized from 1:1 hexane/EtOAc. ^{1}H NMR ($CDCl_3$, 400 MHz) δ 7.59 (s, 1H), 7.39-7.32 (m, 5H), 7.19 (d, *J* = 8.0 Hz, 2H), 7.08 (d, *J* = 8.0 Hz, 2H), 5.58 (s, 2H), 5.25 (s, 2H), 3.80 (s, 4H), 2.57 (s, 6H), 2.30 (q, *J* = 7.3 Hz, 4H), 2.04 (s, 2H), 1.30 (s, 6H), 0.98 (t, *J* = 6.8 Hz, 6H); ^{13}C NMR ($CDCl_3$, 100 MHz) δ 158.64, 154.75, 144.26, 139.56, 137.21, 134.52, 132.77, 132.40, 129.82, 129.28, 129.11, 128.97, 128.25, 122.80, 115.28, 83.35, 70.55, 62.18, 54.41, 49.88, 17.20, 14.81, 12.83, 11.96; ^{11}B NMR ($CDCl_3$, 128 MHz) δ 1.77 (s); HRMS (ESI-TOF) *m/z* 661.3309 $[M + Na]^+$ calculated for $C_{39}H_{42}BN_5O_3$: 661.3318.

BODIPY (**6a**). BODIPY **5a** (7.8 mg, 0.012 mmol, 1.0 equiv.), Cu(0) (3.1 mg, 0.049 mmol, 4.0 equiv.), and 1-azido-1-deoxy-β-D-glucopyranoside tetraacetate (68.3 mg, 0.183 mmol, 15 equiv.) were dissolved in a mixture of THF/water (4 mL, 3:1) under an inert gas atmosphere. A solution of $CuSO_4 \cdot 5H_2O$ (2.3 mg, 0.009 mmol, 0.75 equiv.) and sodium-ascorbate (4.8 mg, 0.024 mmol, 2.0 equiv.) in THF/water (4 mL, 3:1) was added (after sonication for 30 min) and the reaction mixture was heated for 21 h at 70 °C. Once TLC indicated complete consumption of starting material, the mixture was cooled to room temperature and partitioned between ethyl acetate (30 mL) and water (30 mL). The combined organic layers were dried over Na_2SO_4 and then concentrated under reduced pressure. The crude product was purified via alumina column chromatography (eluent 100% EtOAc to 1:1 EtOAc/acetone) to afford BODIPY **6a** (12.1 mg, 72% yield) and was recrystallized from acetone. ^{1}H NMR ($(CD_3)_2CO$, 400 MHz) δ 8.12 (s, 2H), 7.97

(s, 2H), 7.39-7.36 (m, 5H), 7.35 (d, *J* = 8.1 Hz, 2H), 7.24 (d, *J* = 8.2 Hz, 2H), 6.17 (d, *J* = 8.0 Hz, 2H), 5.68 (s, 2H), 5.64 (t, *J* = 9.48 Hz, 2H), 5.53 (t, *J* = 9.48 Hz, 2H), 5.29 (s, 2H), 4.16 (s, 4H), 2.54 (s, 6H), 2.34 (q, *J* = 7.32 Hz, 4H), 2.04 (s, 6H), 2.01 (s, 6H), 1.97 (s, 6H), 1.79 (s, 6H), 1.41 (s, 6H), 0.98 (t, *J* = 7.48 Hz, 6H); ^{13}C NMR ($(CD_3)_2CO$, 100 MHz) δ 200.13, 199.00, 197.50, 196.91, 189.04, 181.45, 170.60, 169.75, 167.30, 159.01, 155.38, 142.14, 133.87, 130.27, 129.70, 129.47, 121.88, 116.89, 86.36, 75.80, 74.12, 71.94, 69.41, 57.60, 54.81, 50.28, 21.20, 21.07, 20.76, 15.63, 13.45, 12.77; ^{11}B NMR ($(CD_3)_2CO$, 128 MHz) δ 2.16 (s); HRMS (ESI-TOF) *m/z* 1407.5552 $[M + Na]^+$ calculated for $C_{67}H_{80}BN_{11}O_{21}$: 1407.5546.

BODIPY (**7**). Benzaldehyde (1.0 mL, 9.81 mmol) was suspended in anhydrous CH_2Cl_2 (300 mL). 2,4-Dimethylpyrrole (2.12 mL, 20.6 mmol) was added, followed by 6 drops of BF_3•OEt_2 to the reaction mixture. After stirring for 48 h, TLC indicated no more aryl aldehyde in the reaction mixture, and DDQ (1.113 g, 4.91 mmol) in CH_2Cl_2 was then added. After 1.5 h stirring at room temperature, NEt_3 (10.3 mL, 73.58 mmol) was added and after another 1 h BF_3•OEt_2 (12.1 mL, 98.1 mmol) was added. The final mixture was stirred at room temperature for 6 h and then poured into water (50 mL). The organic layer was washed with water (2 x 50 mL). The combined organic layers were dried over anhydrous Na_2SO_4 and concentrated under reduced pressure. The product was purified by silica gel flash column chromatography using mixtures of petroleum ether and dichloromethane to afford BODIPY **7** as a green/orange solid (20% yield, 650 mg). ^{1}H NMR ($CDCl_3$, 400 MHz) δ 7.47-7.26 (m, 5H), 5.98 (s, 2H), 2.56 (s, 6H), 1.38 (s, 6H); ^{13}C NMR ($CDCl_3$, 100 MHz) δ 155.57, 143.29, 141.87, 135.14, 131.57, 129.26, 129.26, 128.08, 121.34, 14.71, 14.46; ^{11}B NMR ($CDCl_3$, 128 MHz) δ 0.65 (t, *J* = 33.4 Hz); HRMS (ESI-TOF) *m/z* 324.1718 $[M + H]^+$

calculated for $C_{19}H_{20}BF_2N_2$: 324.1728. These data are in agreement with those previously reported.[29-30]

Synthesis of BODIPY **8b** using method B. In an oven-dried flask, BODIPY **7** (20.0 mg, 0.062 mmol, 1.0 equiv.) with $AlCl_3$ (16.5 mg, 0.123 mmol, 2.0 equiv.) were dissolved in anhydrous CH_2Cl_2 (5 mL). The mixture was refluxed for 30 min and acetic acid (0.987 mL, 17.236 mmol, 278.0 equiv.) was added for an addition 30 min. After the reaction cooled to room temperature and stirred for 2 h, the crude product was concentrated under reduced pressure. The crude product was purified via TLC (eluent 50:50 hexane/EtOAc) to afford BODIPY **8b** (10.4 mg, 42% yield) as an orange solid, that was recrystallized from 1:1 hexane/dichloromethane. ^{1}H NMR ($CDCl_3$, 400 MHz) δ 7.47 (d, *J* = 5.6 Hz, 3H), 7.39 (d, *J* = 5.7 Hz, 2H), 5.94 (s, 2H), 2.45 (s, 6H), 2.05 (s, 6H), 1.39 (s, 6H); ^{13}C NMR ($CDCl_3$, 100 MHz) δ 171.61, 152.98, 142.99, 135.36, 133.12, 129.09, 128.86, 128.27, 121.44, 23.09, 14.73; ^{11}B NMR ($CDCl_3$, 128 MHz) δ -0.40 (s); HRMS (ESI-TOF) *m/z* 426.1836 $[M + Na]^+$ calculated for $C_{23}H_{25}BN_2O_4$: 426.1851.

Synthesis of BODIPYs **8a** and **8b** using method C. In an oven-dried flask, BODIPY **7** (20 mg, 0.062 mmol, 1.0 equiv.) and TMSOTf (28.0 µL, 0.154 mmol, 2.5 equiv.) were dissolved in anhydrous toluene (5 mL) and the mixture was refluxed for 30 min. The solution was allowed to cool down to room temperature and acetic acid (18 µL, 0.308 mmol, 5.0 equiv.) was added, followed by DIPEA (27.0 µL, 0.154 mmol, 2.5 equiv.). After 1 h stirring at room temperature, the crude product was concentrated under reduced pressure and was purified via TLC (eluent 50:50 hexane/EtOAc) to afford BODIPYs **8a** (1.7 mg, 8% yield) and **8b** (3.4 mg, 14% yield).

BODIPY (**8a**). Recrystallized from 1:1 hexane/dichloromethane. ^{1}H NMR ($CDCl_3$, 400 MHz) δ 7.56-7.36 (m, 3H), 7.31-7.29 (m, 2H), 5.96 (s, 2H), 2.50 (s, 6H), 2.01 (s, 3H), 1.57 (s, 6H); ^{11}B NMR ($CDCl_3$, 128 MHz) δ 0.33 (d, *J* = 26.88 Hz); HRMS (ESI-TOF) *m/z* 386.1687 [M + Na]$^{+}$ calculated for $C_{21}H_{22}BFN_2O_2$: 386.1697.

BODIPY (**8b**). Recrystallized from 1:1 hexane/dichloromethane. ^{1}H NMR ($CDCl_3$, 400 MHz) δ 7.47 (d, *J* = 5.6 Hz, 3H), 7.39 (d, *J* = 5.7 Hz, 2H), 5.94 (s, 2H), 2.45 (s, 6H), 2.05 (s, 6H), 1.39 (s, 6H); ^{13}C NMR ($CDCl_3$, 100 MHz) δ 171.61, 152.98, 142.99, 135.36, 133.12, 129.09, 128.86, 128.27, 121.44, 23.09, 14.73; ^{11}B NMR ($CDCl_3$, 128 MHz) δ -0.40 (s); HRMS (ESI-TOF) *m/z* 426.1836 [M + Na]$^{+}$ calculated for $C_{23}H_{25}BN_2O_4$: 426.1851.

BODIPY (**9**). In an oven-dried flask, BODIPY **7** (20 mg, 0.062 mmol, 1.0 equiv.) and TMSOTf (28.0 µL, 0.154 mmol, 2.5 equiv.) were dissolved in anhydrous toluene (5 mL) and the mixture was refluxed for 30 min. The solution was allowed to cool down to room temperature and 4-bromobenzoic acid (61.9 mg, 0.308 mmol, 5.0 equiv) was added, followed by DIPEA (27.0 µL, 0.154 mmol, 2.5 equiv.). After 1 h stirring at room temperature, the crude product was concentrated under reduced pressure and was purified via TLC (eluent 50:50 hexane/EtOAc) to afford BODIPY **9** (2.1 mg, 5% yield) and was recrystallized from 1:1 hexane/dichloromethane. ^{1}H NMR ($CDCl_3$, 400 MHz) δ 8.05 (d, *J* = 8.1 Hz, 4H), 7.59 (d, *J* = 8.1 Hz, 4H), 7.26 (s, 5H), 5.92 (s, 2H), 2.36 (s, 6H); ^{11}B NMR ($CDCl_3$, 128 MHz) δ 0.48 (s).

BODIPY (**10**). In an oven-dried flask, BODIPY **7** (20 mg, 0.062 mmol, 1.0 equiv.) and TMSOTf (28.0 µL, 0.154 mmol, 2.5 equiv.) were dissolved in anhydrous toluene (5 mL) and the

mixture was refluxed for 30 min. The solution was allowed to cool down to room temperature and Boc-Trp-OH (94.0 mg, 0.308 mmol, 5.0 equiv) was added, followed by DIPEA (54.0 µL, 0.154 mmol, 5.0 equiv.). After 1 h stirring at room temperature, the crude product was concentrated under reduced pressure and was purified via TLC (eluent 50:50 hexane/EtOAc) to afford BODIPY **10** (4.9 mg, 13% yield) and was recrystallized from 1:1 MeOH/EtOAc. ^{1}H NMR ($CDCl_3$, 400 MHz) δ 8.13 (s, 1H), 8.07 (s, 1H), 7.53-7.45 (m, 4H), 7.41-7.32 (m, 3H), 7.26 (s, 4H), 7.17 (dd, *J* = 6.6, 3.3 Hz, 3H), 6.03 (s, 1H), 5.95 (s, 1H), 4.53 (d, *J* = 9.0 Hz, 1H), 3.72 (d, *J* = 13.8 Hz, 1H), 3.37 (dd, *J* = 13.6, 9.0 Hz, 2H), 2.52 (s, 3H), 2.17 (s, 3H), 1.38 (d, *J* = 6.6 Hz, 6H), 1.25 (s, 9H). ^{11}B NMR ($CDCl_3$, 128 MHz) δ 1.66 (s); HRMS (ESI-TOF) *m/z* 589.2986 $[M + H]^+$ calculated for $C_{35}H_{38}BN_4O_4$: 589.3004.

Synthesis of BODIPY **11b** using method B. In an oven-dried flask, BODIPY **7** (20.0 mg, 0.062 mmol, 1.0 equiv.) with $AlCl_3$ (16.5 mg, 0.123 mmol, 2.0 equiv.) were dissolved in anhydrous CH_2Cl_2 (5 mL). The reaction was refluxed for 30 min and N-Boc-ethanolamine (0.143 mL, 0.925 mmol, 15.0 equiv.) was added for an additional 30 min. After the reaction cooled to room temperature and stirred for 2 h, the crude product was concentrated under reduced pressure. The crude product was purified via TLC (eluent 50:50 hexane/EtOAc) to afford BODIPY **8b** (26.2 mg, 70% yield) as an orange solid, that was recrystallized from 1:1 hexane/dichloromethane. ^{1}H NMR ($CDCl_3$, 400 MHz) δ 7.54-7.46 (m, 3H), 7.32-7.28 (m, 2H), 5.96 (s, 2H), 3.22-3.12 (m, 4H), 3.12-3.00 (m, 4H), 2.56 (s, 6H), 1.42 (s, 18H), 1.37 (s, 6H); ^{13}C NMR ($CDCl_3$, 100 MHz) δ 156.95, 156.24, 155.20, 142.12, 135.34, 132.73, 129.18, 128.95, 128.20, 121.44, 79.73, 62.69, 60.99, 43.28, 42.42, 28.55, 28.49, 14.83, 14.56; ^{11}B NMR ($CDCl_3$, 128 MHz) δ 2.05 (s); HRMS (ESI-TOF) *m/z* 628.3517 $[M + Na]^+$ calculated for $C_{33}H_{47}BN_4O_6$: 628.3507.

Synthesis of BODIPYs **11a** and **11b** using method C. In an oven-dried flask, BODIPY **7** (20 mg, 0.062 mmol, 1.0 equiv.) and TMSOTf (28.0 µL, 0.154 mmol, 2.5 equiv.) were dissolved in anhydrous toluene (5 mL) and the mixture was refluxed for 30 min. The solution was allowed to cool down to room temperature and *N*-Boc-ethanolamine (48 µL, 0.308 mmol, 5.0 equiv) was added, followed by DIPEA (27.0 µL, 0.154 mmol, 2.5 equiv.). After 1 h stirring at room temperature, the crude product was concentrated under reduced pressure and was purified via TLC (eluent 50:50 hexane/EtOAc) to afford BODIPYs **11a** (3.9 mg, 14% yield) and **11b** (3.8 mg, 10% yield).

BODIPY (**11a**). Recrystallized from 1:1 hexane/dichloromethane. ^{1}H NMR ($CDCl_3$, 400 MHz) δ 7.53-7.45 (m, 3H), 7.36-7.24 (m, 2H), 5.97 (s, 2H), 3.17 (t, *J* = 5.3 Hz, 2H), 3.09 (t, *J* = 5.0 Hz, 2H), 2.56 (s, 6H), 1.42 (s, 9H), 1.38 (s, 6H); ^{13}C NMR ($CDCl_3$, 100 MHz) δ 142.68, 135.26, 132.15, 129.22, 129.02, 128.17, 128.14, 121.42, 28.57, 28.51, 14.84, 14.54; ^{11}B NMR ($CDCl_3$, 128 MHz) δ 1.47 (d, *J* = 23.04 Hz); HRMS (ESI-TOF) *m/z* 487.2540 $[M + H]^+$ calculated for $C_{31}H_{30}BN_3O_2$: 487.2535.

BODIPY (**11b**). Recrystallized from 1:1 hexane/dichloromethane. ^{1}H NMR ($CDCl_3$, 400 MHz) δ 7.54-7.46 (m, 3H), 7.32-7.28 (m, 2H), 5.96 (s, 2H), 3.22-3.12 (m, 4H), 3.12-3.00 (m, 4H), 2.56 (s, 6H), 1.42 (s, 18H), 1.37 (s, 6H); ^{13}C NMR ($CDCl_3$, 100 MHz) δ 156.95, 156.24, 155.20, 142.12, 135.34, 132.73, 129.18, 128.95, 128.20, 121.44, 79.73, 62.69, 60.99, 43.28, 42.42, 28.55, 28.49, 14.83, 14.56; ^{11}B NMR ($CDCl_3$, 128 MHz) δ 2.05 (s); HRMS (ESI-TOF) *m/z* 628.3517 $[M + Na]^+$ calculated for $C_{33}H_{47}BN_4O_6$: 628.3507.

BODIPY (**12**). In an oven-dried flask, BODIPY **7** (20 mg, 0.062 mmol, 1.0 equiv.) and TMSOTf (28.0 µL, 0.154 mmol, 2.5 equiv.) were dissolved in anhydrous toluene (5 mL) and the mixture was refluxed for 30 min. The solution was allowed to cool down to room temperature and ethylene glycol (17.0 µL, 0.308 mmol, 5.0 equiv) was added, followed by DIPEA (27.0 µL, 0.154 mmol, 2.5 equiv.). After 1 h stirring at room temperature, the crude product was concentrated under reduced pressure and was purified via TLC (eluent 50:50 hexane/EtOAc) to afford BODIPY **12** (8.0 mg, 37% yield), that was recrystallized from 1:1 hexane/dichloromethane. ^{1}H NMR ($CDCl_3$, 400 MHz) δ 7.50 (d, *J* = 5.7 Hz, 3H), 7.31 (d, *J* = 4.2 Hz, 3H), 5.97 (s, 2H), 4.30 (s, 4H), 2.57 (s, 6H), 1.38 (s, 6H); ^{13}C NMR ($CDCl_3$, 100 MHz) δ 133.32, 129.82, 129.09, 128.75, 128.55, 128.28, 65.89, 29.84, 15.26, 14.66; ^{11}B NMR ($CDCl_3$, 128 MHz) δ 5.90 (s); HRMS (ESI-TOF) *m/z* 346.1962 $[M + H]^+$ calculated for $C_{21}H_{23}BN_2O_2$: 346.1959.

4.4.3 X-ray Determined Molecular structures

Crystal structures were determined using low-temperature data from a Bruker Kappa APEX-II DUO diffractometer with either Mo Kα or Cu Kα radiation. For all structures, H atoms were located from difference maps but constrained in calculated positions during refinement.

Crystal data **4a**: $C_{33}H_{36}BF_2N_5O$, *M* = 567.48, triclinic, *a* = 11.1039(3), *b* = 11.3734(3), *c* = 12.9720(4) Å, *U* = 1445.82(7) Å^3, *T* = 90 K, space group P1, *Z* = 2, Dc = 1.304 g cm^{-3}, µ (Cu Kα) = 0.09 mm^{-1}, 5542 reflections measured, θ_{max} = 30.5˚, 8843 unique (R_{int} = 0.040). The final *R* = 0.053 (8843 $I>2\sigma(I)$ data), *wR(F2)* = 0.129 (all data).

Crystal data **4b**: $C_{40}H_{48}BF_2N_5O_{10}$, *M* = 807.64, monoclinic, *a* = 13.3965(15), *b* = 9.2534(10), *c* = 17.1816(19) Å, *U* = 2059.0(4) $Å^3$, *T* = 90 K, space group $P2_1$, *Z* = 2, Dc = 1.303 g cm^{-3}, μ (Cu Kα) = 0.83 mm^{-1}, 1814 reflections measured, θ_{max} = 59.0˚, 4680 unique (R_{int} = 0.060). The final *R* = 0.062 (4680 *I>2σ(I)* data), *wR(F2)* = 0.131 (all data).

Crystal data **9**: $C_{33}H_{27}BBr_3N_2O_4$, *M* = 686.20, Orthorhombic, *a* = 8.537(1), *b* = 10.710(2), *c* = 32.867(5) Å, *U* = 3005.1(8) $Å^3$, *T* = 100 K, space group $P2_12_12_1$, *Z* = 4, Dc = 1.517 g cm^{-3}, μ (Cu Kα) = 2.74 mm^{-1}, 3292 reflections measured, θ_{max} = 25.7˚, 5682 unique (R_{int} = 0.146). The final *R* = 0.068 (5682 *I>2σ(I)* data), *wR(F2)* = 0.104 (all data).

Crystal data **10**: $C_{35}H_{37}BN_4O_4$, *M* = 588.50, monoclinic, *a* = 11.4670(8), *b* = 8.8110(6), *c* = 15.9543(11) Å, *U* = 1581.82(19) $Å^3$, *T* = 90 K, space group $P2_1$, *Z* = 2, Dc = 1.236 g cm^{-3}, μ (Cu Kα) = 0.65 mm^{-1}, 4547 reflections measured, θ_{max} = 60.1˚, 4657 unique (R_{int} = 0.040). The final *R* = 0.028 (4657 *I>2σ(I)* data), *wR(F2)* = 0.071 (all data).

Crystal data **11a**: $C_{26}H_{33}BFN_3O_3$, *M* = 465.36, monoclinic, *a* = 5.9290(2), *b* = 25.0122(14), *c* = 16.4436(8) Å, *U* = 2429.9(2) $Å^3$, *T* = 90 K, space group $P2_1/c$, *Z* = 4, Dc = 1.272 g cm^{-3}, μ (Cu Kα) = 0.09 mm^{-1}, 7361 reflections measured, θ_{max} = 33.2˚, 9239 unique (R_{int} = 0.030). The final *R* = 0.049 (9239 *I>2σ(I)* data), *wR(F2)* = 0.128 (all data).

Crystal data **12**: $C_{21}H_{23}BN_2O_2$, *M* = 346.22, monoclinic, *a* = 11.306(2), *b* = 8.9098(10), *c* = 17.990(3) Å, *U* = 1812.0(5) $Å^3$, *T* = 100 K, space group $P2_1/n$, *Z* = 4, Dc = 1.269 g cm^{-3}, μ (Cu

Kα) = 0.08 mm^{-1}, 4878 reflections measured, θ_{max} = 34.8˚, 7459 unique (R_{int} = 0.051). The final

R = 0.057 (7459 $I>2\sigma(I)$ data), *wR(F2)* = 0.153 (all data).

4.5 References

1. Alford, R.; Ogawa, M.; Choyke, P. L.; Kobayashi, H., Molecular Probes for the *in Vivo* Imaging of Cancer. *Mol. BioSyst.* **2009**, *5*, 1279-1291.

2. Kelloff, G. J.; Hoffman, J. M.; Johnson, B.; Scher, H. I.; Siegel, B. A.; Cheng, E. Y.; Cheson, B. D.; O'Shaughnessy, J.; Guyton, K. Z.; Mankoff, D. A.; Shankar, L.; Larson, S. M.; Sigman, C. C.; Schilsky, R. L.; Sullivan, D. C., Progress and Promise of FDG-PET Imaging for Cancer Patient Management and Oncologic Drug Development. *Clin. Cancer Res.* **2005**, *11*, 2785-2808.

3. Bui, T.; Thompson, C. B., Cancer's Sweet Tooth. *Cancer Cell* **2006**, *9*, 419-420.

4. Kim, J. W.; Dang, C. V., Cancer's Molecular Sweet Tooth and the Warburg Effect. *Cancer Res.* **2006**, *66*, 8927-8930.

5. Hein, C. D.; Liu, X. M.; Wang, D., Click Chemistry, a Powerful Tool for Pharmaceutical Sciences. *Pharm. Res.* **2008**, *25*, 2216-2230.

6. Ke, M. R.; Yeung, S. L.; Ng, D. K.; Fong, W. P.; Lo, P. C., Preparation and *in Vitro* Photodynamic Activities of Folate-Conjugated Distyryl Boron Dipyrromethene Based Photosensitizers. *J. Med. Chem.* **2013**, *56*, 8475-8483.

7. Uppal, T.; Bhupathiraju, N. V. S. D. K.; Vicente, M. G. H., Synthesis and Cellular Properties of Near-IR BODIPY-PEG and Carbohydrate Conjugates. *Tetrahedron* **2013**, *69*, 4687-4693.

8. Eggenspiller, A.; Takai, A.; El-Khouly, M. E.; Ohkubo, K.; Gros, C. P.; Bernhard, C.; Goze, C.; Denat, F.; Barbe, J. M.; Fukuzumi, S., Synthesis and Photodynamics of Fluorescent Blue BODIPY-Porphyrin Tweezers Linked by Triazole Rings. *J. Phys. Chem. A* **2012**, *116*, 3889-3898.

9. Ganapathi, E.; Madhu, S.; Ravikanth, M., Synthesis and Properties of Triazole Bridged BODIPY-Conjugates. *Tetrahedron* **2014**, *70*, 664-671.

10. Wirtz, M.; Gruter, A.; Rebmann, P.; Dier, T.; Volmer, D. A.; Huch, V.; Jung, G., Two-Color Emissive Probes for Click Reactions. *Chem. Commun.* **2014**, *50*, 12694-12697.

11. Leen, V.; Leemans, T.; Boens, N.; Dehaen, W., 2-and 3-Monohalogenated BODIPY Dyes and Their Functionalized Analogues: Synthesis and Spectroscopy. *Eur. J. Org. Chem.* **2011**, 4386-4396.

12. Yilmaz, M. D.; Bozdemir, O. A.; Akkaya, E. U., Light Harvesting and Efficient Energy Transfer in a Boron-Dipyrrin (BODIPY) Functionalized Perylenediimide Derivative. *Org. Lett.* **2006**, *8*, 2871-2873.

13. Zhang, X.; Xiao, Y.; Qian, X., Highly Efficient Energy Transfer in the Light Harvesting System Composed of Three Kinds of Boron-Dipyrromethene Derivatives. *Org. Lett.* **2008**, *10*, 29-32.

14. Zhang, C.; Zhao, J.; Wu, S.; Wang, Z.; Wu, W.; Ma, J.; Guo, S.; Huang, L., Intramolecular RET Enhanced Visible Light-Absorbing BODIPY Organic Triplet Photosensitizers and Application in Photooxidation and Triplet-Triplet Annihilation Upconversion. *J. Am. Chem. Soc.* **2013**, *135*, 10566-10578.

15. Nguyen, A. L.; Bobadova-Parvanova, P.; Hopfinger, M.; Fronczek, F. R.; Smith, K. M.; Vicente, M. G., Synthesis and Reactivity of 4,4-Dialkoxy-BODIPYs: An Experimental and Computational Study. *Inorg. Chem.* **2015**, *54*, 3228-3236.

16. Pu, L., Fluorescence of Organic Molecules in Chiral Recognition. *Chem. Rev.* **2004**, *104*, 1687-1716.

17. Gossauer, A.; Nydegger, F.; Kiss, T.; Sleziak, R.; Stoeckli-Evans, H., Synthesis, Chiroptical Properties, and Solid-State Structure Determination of Two New Chiral Dipyrrin Difluoroboryl Chelates. *J. Am. Chem. Soc.* **2004**, *126*, 1772-1780.

18. Haefele, A.; Zedde, C.; Retailleau, P.; Ulrich, G.; Ziessel, R., Boron Asymmetry in a BODIPY Derivative. *Org. Lett.* **2010**, *12*, 1672-1675.

19. Lerrick, R. I.; Winstanley, T. P.; Haggerty, K.; Wills, C.; Clegg, W.; Harrington, R. W.; Bultinck, P.; Herrebout, W.; Benniston, A. C.; Hall, M. J., Axially Chiral BODIPYs. *Chem. Commun.* **2014**, *50*, 4714-4716.

20. Sanchez-Carnerero, E. M.; Moreno, F.; Maroto, B. L.; Agarrabeitia, A. R.; Ortiz, M. J.; Vo, B. G.; Muller, G.; de la Moya, S., Circularly Polarized Luminescence by Visible-Light Absorption in a Chiral *O*-BODIPY Dye: Unprecedented Design of CPL Organic Molecules from Achiral Chromophores. *J. Am. Chem. Soc.* **2014**, *136*, 3346-3349.

21. Sibrian-Vazquez, M.; Jensen, T. J.; Vicente, M. G., Synthesis and Cellular Studies of PEG-Functionalized *meso*-Tetraphenylporphyrins. *J. Photochem. Photobiol. B* **2007**, *86*, 9-21.

22. Sibrian-Vazquez, M.; Jensen, T. J.; Fronczek, F. R.; Hammer, R. P.; Vicente, M. G., Synthesis and Characterization of Positively Charged Porphyrin-Peptide Conjugates. *Bioconjug. Chem.* **2005**, *16*, 852-863.

23. Sibrian-Vazquez, M.; Jensen, T. J.; Hammer, R. P.; Vicente, M. G., Peptide-Mediated Cell Transport of Water Soluble Porphyrin Conjugates. *J. Med. Chem.* **2006**, *49*, 1364-1372.

24. Paulus, A.; Desai, P.; Carney, B.; Carlucci, G.; Reiner, T.; Brand, C.; Weber, W. A., Development of a Clickable Bimodal Fluorescent/PET Probe for in Vivo Imaging. *EJNMMI Res* **2015**, *5*, 120.

25. Giguère, J.-B.; Thibeault, D.; Cronier, F.; Marois, J.-S.; Auger, M.; Morin, J.-F., Synthesis of [2]- and [3]Rotaxanes through Sonogashira Coupling. *Tetrahedron Lett.* **2009**, *50*, 5497-5500.

26. Tahtaoui, C.; Thomas, C.; Rohmer, F.; Klotz, P.; Duportail, G.; Mely, Y.; Bonnet, D.; Hibert, M., Convenient Method to Access New 4,4-Dialkoxy- and 4,4-Diaryloxy-diaza-*s*-indacene Dyes: Synthesis and Spectroscopic Evaluation. *J. Org. Chem.* **2007**, *72*, 269-272.

27. Jiang, X.-D.; Zhang, J.; Furuyama, T.; Zhao, W., Development of Mono- and Di-AcO Substituted BODIPYs on the Boron Center. *Org. Lett.* **2012**, *14*, 248-251.

28. Durán-Sampedro, G.; Agarrabeitia, A. R.; Cerdán, L.; Pérez-Ojeda, M. E.; Costela, A.; García-Moreno, I.; Esnal, I.; Bañuelos, J.; Arbeloa, I. L.; Ortiz, M. J., Carboxylates versus Fluorines: Boosting the Emission Properties of Commercial BODIPYs in Liquid and Solid Media. *Adv. Funct. Mater.* **2013**, *23*, 4195-4205.

29. Gibbs, J. H.; Robins, L. T.; Zhou, Z.; Bobadova-Parvanova, P.; Cottam, M.; McCandless, G. T.; Fronczek, F. R.; Vicente, M. G., Spectroscopic, Computational Modeling and Cytotoxicity of a Series of *meso*-Phenyl and *meso*-Thienyl-BODIPYs. *Bioorg. Med. Chem.* **2013**, *21*, 5770-5781.

30. Kollmannsberger, M.; Rurack, K.; Resch-Genger, U.; Daub, J., Ultrafast Charge Transfer in Amino-Substituted Boron Dipyrromethene Dyes and Its Inhibition by Cation Complexation: A New Design Concept for Highly Sensitive Fluorescent Probes. *J. Phys. Chem. A* **1998**, *102*, 10211-10220.

CHAPTER 5: CHLORINATION OF ALCOHOLS AND ASYMMETRIC S_N1 REACTION[a]

5.1 Introduction

5.1.1 Chlorination

Alkyl chlorides are useful building blocks in organic chemistry. Transformation of unreactive alcohols into reactive alkyl halides has proven to produce important intermediates in many organic syntheses.[1-3] Chlorination reactions have become widespread in organic chemistry and useful in organic synthesis. The chlorination reaction mechanism typically requires the activation of an unreactive alcohol to give a better leaving group. Then in the presence of an excess of chloride anions, S_N2 attack at the adjacent, electropositive carbon atom to give the corresponding alkyl chloride product.

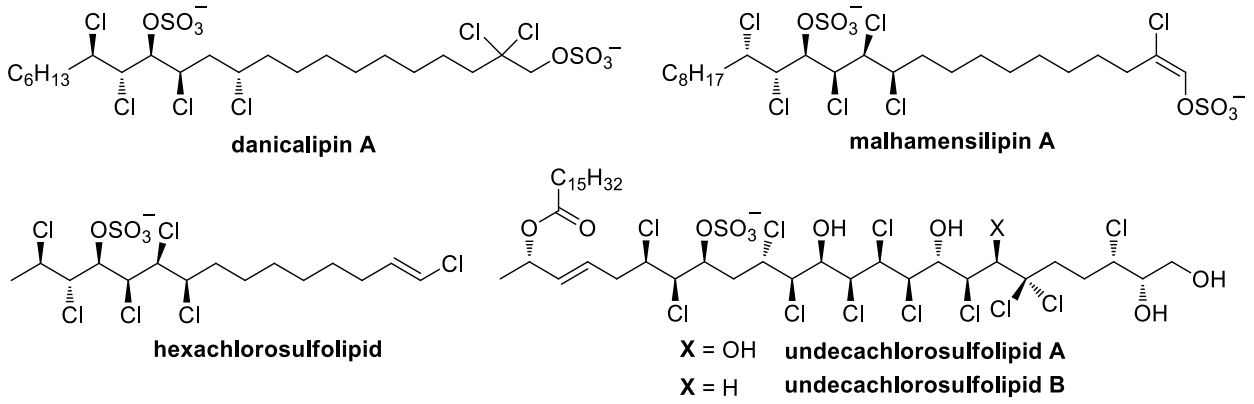

Figure 5.1: Structures of chlorosulfolipid natural products: danicalipin A,[4-6] malhamensilipin A,[4,7-9] hexachlorosulfolipid,[10] undecachlorosulfolipid A and B.[11]

More than 2000 known natural products containing the alkyl chloride motif have displayed enormous antibiotic and cytotoxic activities.[12] The chlorosulfolipids are one class of polychlorinated natural product and some examples include danicalipin A,[4-6] malhamensilipin A,[4,7-9] hexachlorosulfolipid,[10] and undecachlorosulfolipid[11] (Figure 5.1). Malhamensilipin A, a

[a] Part of this chapter originally published as Ayala, C. E.; Villalpando, A.; Nguyen, A. L.; McCandless, G. T.; Kartika, R. Chlorination of Aliphatic Primary Alcohols via Triphosgene-Triethylamine Activation. *Org. Lett.* **2012**, *14*, 3676-3679. Reprinted with permission from [1]

protein tyrosine kinase inhibitor, has antimicrobial activity which can be extracted from *Poterioochromonas malhamensis*.

Classic chlorination methods using chlorinating agents such as thionyl chloride ($SOCl_2$),[13] phosphorus chloride (PCl_5),[14-17] Lucas' reagent,[18-19] and Appel[20] reagents have been reported to convert alcohols to the corresponding alkyl chlorides (Scheme 5.1). The use of toxic halogenating agents is unappealing to organic chemists because these chlorinating agents resulted in inseparable or gaseous byproducts. Chlorination using Appel's reagent typically results in inversion of stereochemistry.

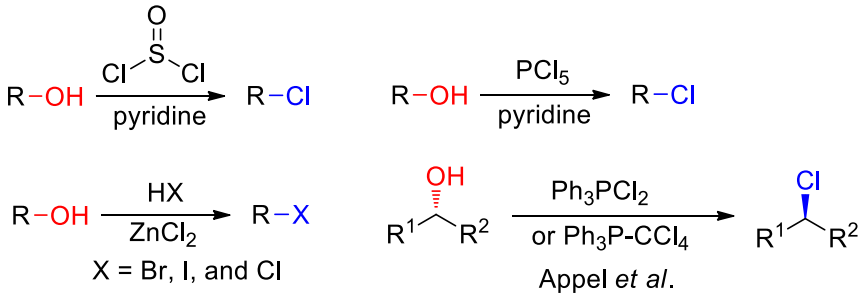

Scheme 5.1: Classical chlorination methods.

Recently, several new methods have been developed for chlorination reactions (Scheme 5.2). Vilsmeier and Haack's salt was reported as a reagent to chlorinate primary alcohols.[21] However, the disadvantage of this method is due to long reaction time, selectivity for only primary alcohols, and low yields (47%-70%). In 2004, Baba and coworkers[22] reported a direct chlorination reaction of alcohols under neutral conditions with $HSiMe_2Cl$ and benzil as an additive. The transformation produces moderate yields of alkyl chlorides at high temperature. However, transformation of a primary alcohol such as 2-phenylethanol did not give the chlorinated product. They also reported highly regioselective chlorination for tertiary alcohols over primary alcohols using the $HSiMe_2Cl$/benzil/cat. $InCl_2$ conditions. Recently in 2010, Denton et *al.*[23] demonstrated rapid chlorination of primary and secondary alcohols under phosphine oxide-catalyzed conditions.

Using $(COCl)_2$ and Ph_3PO conditions have been shown to result in high yield but removal of the phosphine oxides by-products during purification remains a challenge. Jeong and coworkers[24] have shown an alternative method towards chlorination by using strong organic base DBU and sulfonylating agents to afford the alkyl chloride product in moderate yields.

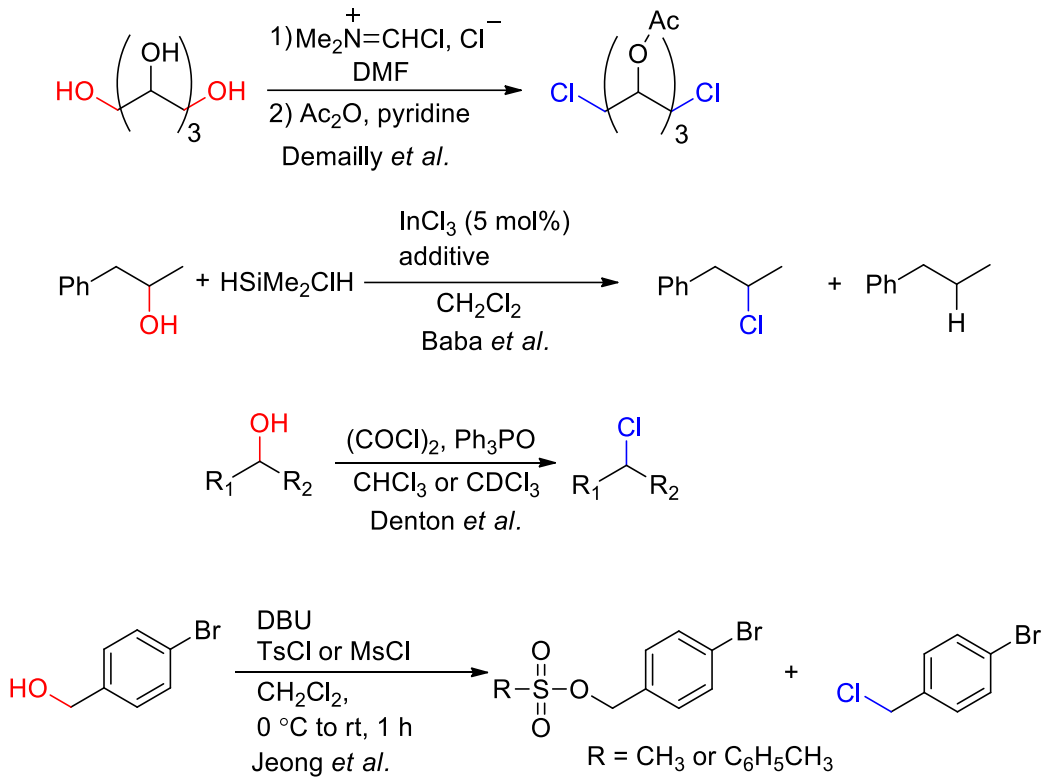

Scheme 5.2: Recent chlorination methods.

5.1.2 A Chiral auxiliary for an Asymmetric S_N1 reaction

Substitution reactions are ubiquitous in many organic chemistry transformations. In organic chemistry, there are many substitution reactions such as nucleophilic, electrophilic, radical, and organometallic reactions. There are two types of nucleophilic substitution reaction: S_N2, and S_N1. The S_N2 reaction gives inversion of stereochemistry while the S_N1 reaction results in a racemic mixture. In order to control enantioselectivity in a S_N1 reaction, the nucleophilic attack must be induced via chirality substrate control such as a chiral auxiliary. Chiral auxiliaries have

become an essential tool for organic chemists to synthesize stereospecific natural products and pharmaceutical drugs. In 1975, Nobel laureate E. J. Corey developed the use of chiral auxiliaries in order to control the stereochemical outcome of a given compound in an organic transformation.[25] There are three steps to induce stereoselective transformation with auxiliary incorporation: i) the chiral auxiliary is coupled to the target substrate; ii) the compound undergoes diastereoselective conversions; and iii) cleavage of the chiral auxiliary to result in an enantioselective product. Evans and coworkers[26-27] introduced the concept of oxazolidinone auxiliaries and it has been widely used in complex natural synthesis. For example, many stereoselective reactions such as aldol reactions,[27] alkylation reactions,[28] and Diels-Alder reactions[29-30] have utilized this methodology. Numerous groups have subsequently extended and improved this chiral auxiliary asymmetric induction.[31-33] For example, Olivo and coworkers[34] particularly focused on indene-based thiazolidinethione as the chiral auxiliary replacement. There are many ways for removal of the oxazolidinone auxiliary and transforming it to other functional groups.

5.2 Results and Discussion

5.2.1 Chlorination Syntheses

To explore mild reaction conditions for chemoselective chlorination of primary alcohols in presence of tertiary alcohols, 3-phenylbutane-1,3-diol (CAS#7133-68-8) was used as a model substrate. There are currently two different pathways to synthesize the 1,3-diol. The first pathway requires acetophenone **1**, which is commerically available, to react with allylmagnesium bromide in a Grignard reaction, which resulted in the desired homoallyl alcohol **2** in 93% yield (Scheme 5.3). The alkene product **2** was subjected to reductive ozonolysis gas (O_3) to give the intermediate

molozonide, which was then reduced by $NaBH_4$ to achieve the 1,3-diol **4** in 77% yield. Although path 1 gave the target compound in good yield, we also investigated an alternative way.

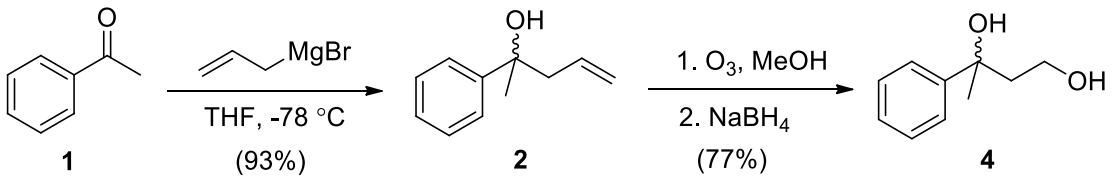

Scheme 5.3: Path 1 towards synthesis of 3-phenylbutane-1,3-diol **4**.

Path 2, the less efficient pathway, began by reacting ethyl acetate and acetophenone through an aldol reaction (Scheme 5.4). Strong base, such as LDA, deprotonates the α proton of ethyl acetate to form the enolate. The anion in the α position of the enolate then attacks the carbonyl of acetophenone **1** to produce ester **3**. The crude materials were taken on to the next step without purification. The ester product **3** was reduced by $LiAlH_4$ in THF to give 1,3-diol **4** in 69% over two steps.

The diol was treated with various chlorinating reagents for preliminary studies, as depicted in Table 5.1. Classical chlorinating agents such as $SOCl_2$ and PCl_5 have resulted in crude complex mixtures.

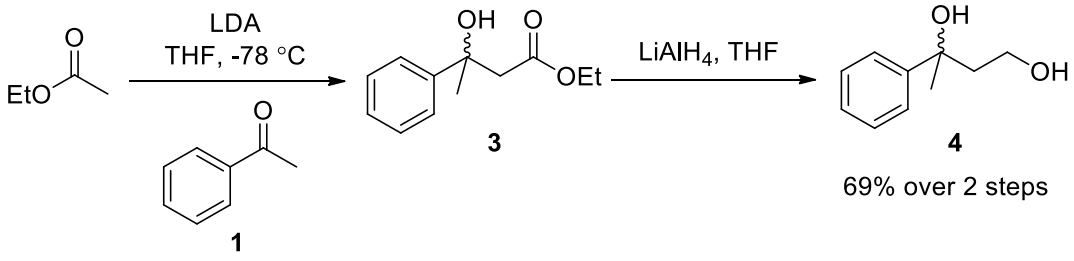

Scheme 5.4: Path 2 towards synthesis of 3-phenylbutane-1,3-diol **4**.

Next, CCl_4-PPh_3 and triphosgene-PPh_3 were investigated (entries 1 and 2) and produced the chlorinated product **4a** in 30% and 78%, respectively. The triphenylphosphine by-products were responsible for these modest yields. In the presence of triphosgene and triethylamine, the

chloro-alcohol product was obtained rapidly in a yield of 98%. Indeed, when phosgene was used in place of triphosgene, the desired product **4a** was still obtained but in a lower yield of 89%. On the other hand, other bases such as pyridine and Hünig's base (DIPEA) were also investigated and these reactions resulted in cyclic carbonate **8**.

Table 5.1: Preliminary studies on chlorination of 1,3-diol 4 with various chlorinate reagents.

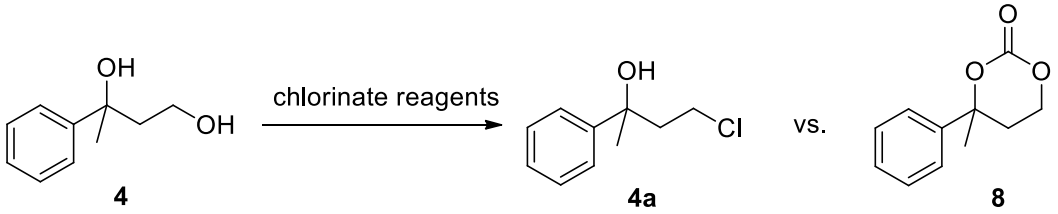

Entry	Chlorinate reagents	4a, yield (%)	8, yield (%)
1	CCl_4, PPh_3	30	---
2	Triphosgene, PPh_3	78	---
3	Triphosgene, TEA	98	---
4	Phosgene, TEA	89	---
5	Triphosgene, Pyridine	---	86
6	Triphosgene, DIPEA	---	45

TEA: triethylamine, CCl_4: carbon tetrachloride, PPh_3: triphenylphosphine

Our typical chlorination protocol includes 0.5 equiv. of triphosgene and 2.5 equiv of triethylamine under anhydrous conditions in dichloromethane. The reaction started at 0 °C and then was warmed to room temperature. Based on TLC, it was shown that the starting material was fully consumed within 5 minutes. However, the reaction was stirred for an additional 3 hours for general purpose for all the diols. The 1,3-diols **4**-**7** containing primary and tertiary alcohols were converted into their corresponding chloroalcohol products **4a**-**7a** in excellent yield ranging from 85-98%. It was initally suspected that chlorination could possibly occur at the primary and tertiary hydroxyl positions.

Table 5.2: Chemoselective chlorination of aliphatic primary alcohol vs. tertiary alcohol

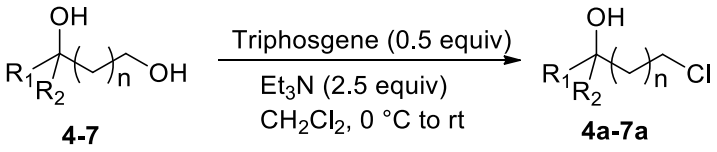

entry	starting material	product	yield
1	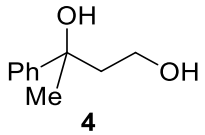 **4**	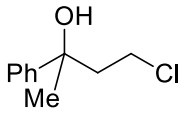 **4a**	98%
2	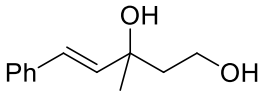 **5**	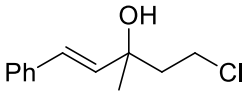 **5a**	85%
3	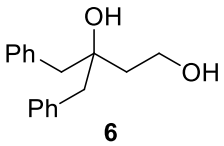 **6**	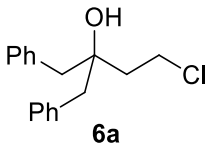 **6a**	97%
4	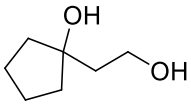 **7**	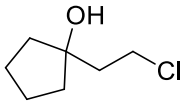 **7a**	96%

However, the chlorination reactions were chemoselective only for primary alcohols in the presence of tertiary alcohols. In addition, non-anhydrous conditions were also performed and effectively resulted in an excellent yield of 98%.

To further our investigation, various groups binding to the tertiary carbon were synthesized and studied. As shown in Table 5.1, highly ionizable tertiary alcohols were unaffected by the activation reagents due to sterically demanding substituents such as phenyl and methyl. In addition, whenever the phenyl and methyl were substituted with larger substituents, primary alcohols were

still converted to its corresponding primary chloride products. My role in the published chlorination paper was to investigate aliphatic alcohols and substitute other bases while other co-authors (Ayala and Villalpando) were to investigate different functional group compatibility, secondary alcohols and α–branched alcohols.

5.2.2 Asymmetric S_N1 Reaction

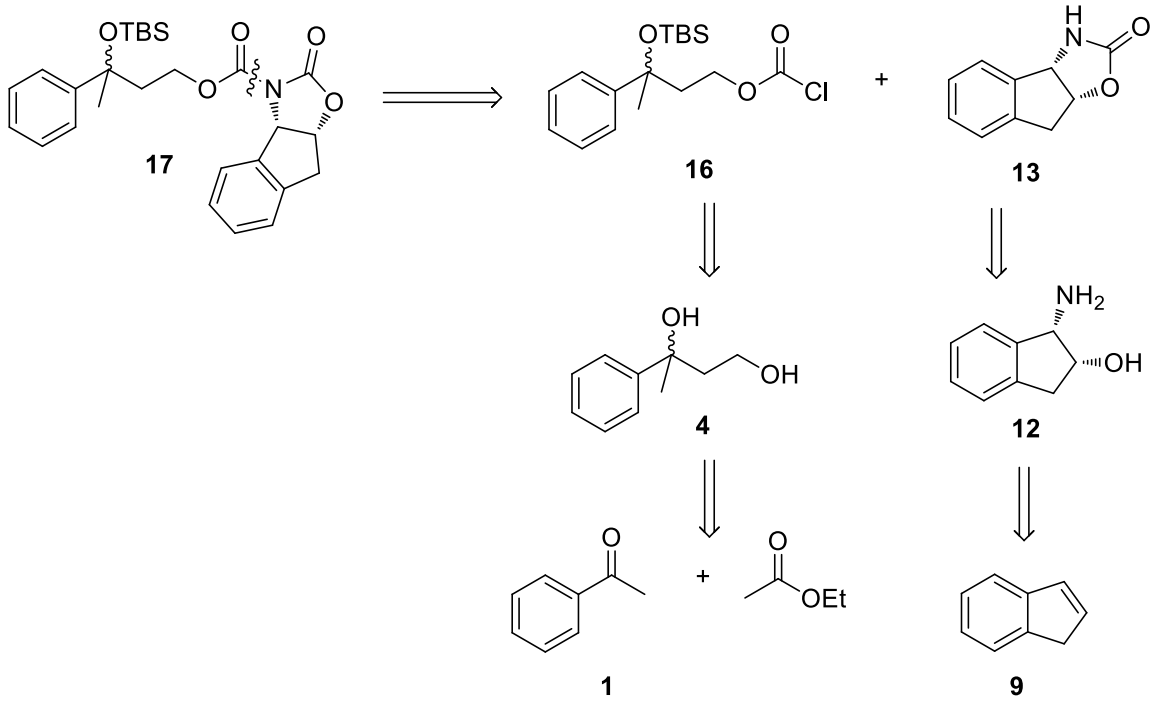

Scheme 5.5: Retrosynthetic analysis of oxazolidinone **17**.

As shown in retrosynthetic Scheme 5.5, the target compound **17** can be derived from acylation between chloroformate **16** and oxazolidone **13**. This fragment **16** comes from 1,3-diol **4** through a series steps of protection and deprotection. The diol will be synthesized through two pathways. The first pathway consists of treating acetophenone with Grignard reagent and ozonolysis. Fragment **13** can be made through cyclization of aminoalcohol **12**. The amino alcohol **12** can be synthesized from the commercially available indene **9**, which was previously reported.[35]

Our first approach was to treat commercially available indene **9** with osmium tetroxide, *N*-methylmorpholine-*N*-oxide (NMO), and water in an Upjohn dihydroxylation reaction to produce racemic diol **10** in 89% yield, as shown in Scheme 5.6. The next step was to treat the diol with acetonitrile and sulfuric acid to form a cyclic imine as an intermediate. By introducing a nucleophile such as water, the heterocycle opened up to give ammonium-alcohol enantiomers **11a** and **11b**.

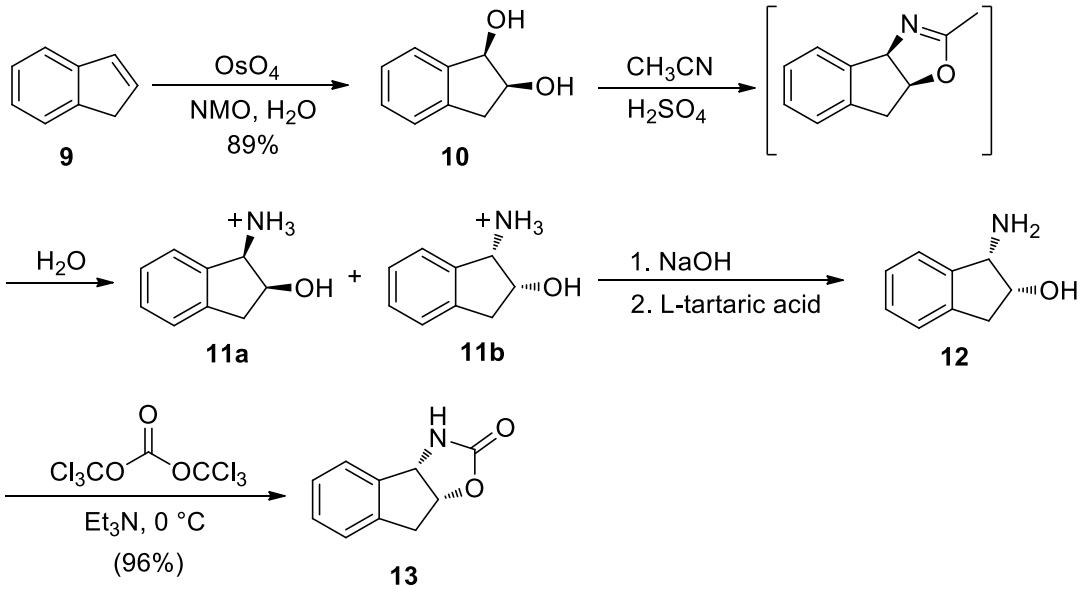

9 **10** **11a** **11b** **12** **13**

Scheme 5.6: Synthesis of oxazolidone **13** from commerically available indene **9**.

The next approach was to perform kinetic resolution on the two enantiomers with L-tartaric acid. In order to distinguish between the two amino alcohol enantiomers, methods such as recrystallization and filtration were applied. The targeted amino alcohol **12** was separated as a recrystallized solid. Unfortunately, when comparing the optical rotation for the amino alcohol to the authentic commercially available amino alcohol from Aldrich, the values were significantly different. The optical rotation for our synthesized amino alcohol was +26.13° and for the authentic amino alcohol was -96.6°. Therefore, the authentic commercial amino alcohol was used for the

next step. The amino alcohol **12** was treated with phosgene and triethylamine and afforded oxazolidinone **13** in 96% yield (Scheme 5.6).

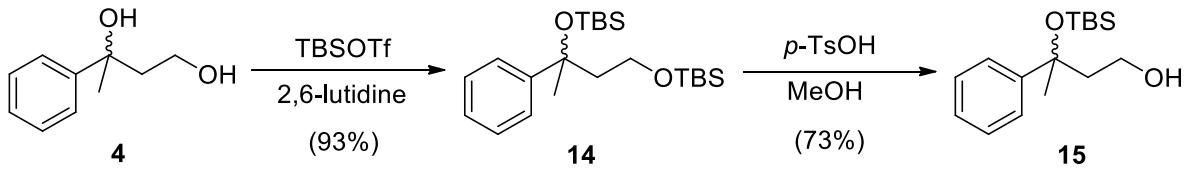

Scheme 5.7: Protection and selective deprotection of 1,3-diol **4**.

With fragment **13** in hand, we next turned our attention to fragment **16**. The hydroxyl groups of 1,3-diol **4** were subjected to mixture of *tert*-butyldimethylsilyl triflate (TBSOTf) and 2,6-lutidine to give 1,3-di-O-TBS compound **14** in an excellent yield of 93% (Scheme 5.7). Then compound **14** was exposed to selective deprotection of the primary TBS ether with *p*-toluenesulfonic acid (*p*-TsOH) in methanol to produce alcohol **15** in 73% yield. The alcohol was then reacted with phosgene to form chloroformate **16** in 75% yield as a crude product (Scheme 5.8). No purification was performed on the chloroformate since it is very unstable on silica gel and to moisture. The chloroformate was carried into the next step of the synthesis.

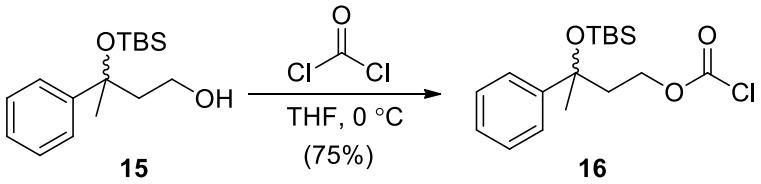

Scheme 5.8: Synthesis of chloroformate **16**.

As shown in Table 5.3, we explored acylation coupling conditions between chloroformate **16** and oxazolidone **13** in order to synthesize the target oxazolidinone **17**. Screening of various bases in THF at different temperature afforded the desired compound **17** with a wide range of yields ranging from no product to 59% yield. When triethylamine was used as the base, the target compound **17** was obtained in 52% yield, while no product was produced when 1,8-

diazabicyclo[5.4.0]undec-7-ene (DBU), pyridine and diisopropylethylamine (DIPEA) were used. When a mixture of TEA and DMAP was used, the yield increased to 59%. Surprisingly, stronger bases such as *n*-BuLi resulted in a yield of 49% while *sec*-BuLi only gave trace amount of the desired product. The reaction with *n*-BuLi proceeded in the fastest time when compared to other bases.

Table 5.3: Optimized acylation reaction conditions for synthesis of oxazolidinone 17.

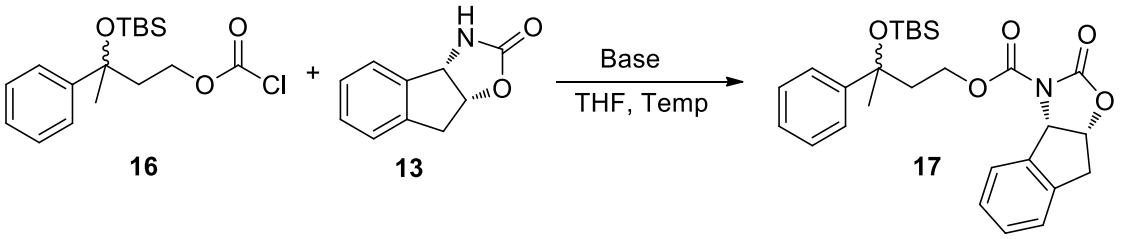

Entry	Base	Temp	17, Yield (%)
1	Triethylamine	0 °C	52
2	DBU	0 °C	0
3	Triethylamine + DMAP	0 °C	59
4	DIPEA	0 °C	0
5	NaH	0 °C	23
6	n-BuLi	-78 °C	49
7	sec-BuLi	-78 °C	trace
8	LDA	-78 °C	22
9	Pyridine	0 °C	0

Next, we explored using n-BuLi at various temperatures and reaction times (Table 5.4). At higher temperature, the yields of compound **17** decreased possibly due to the degradation of THF. The degradation transforms n-butylithium into butane and inhibits the reaction. With longer times (6-8 h), the yields are relatively unchanged and ranged from 37-43%.

Table 5.4: Optimization of coupling conditions between chloroformate 16 and oxazolidone 13.

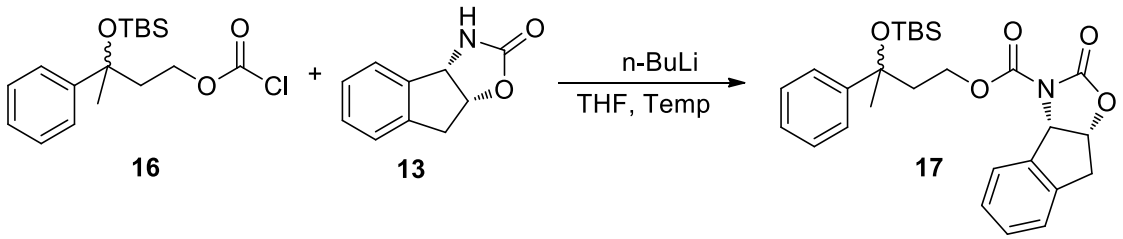

Entry	Time	Temp	17, Yield (%)
1	3 h	-78 °C	49
2	3 h	-40 °C	31
3	3 h	0 °C	9
4	6 h	-78 °C	37
5	8 h	-78 °C	43

With compound **17** in hand, we now turned our attention to perform the asymmetric S_N1 reaction. Oxazolidinone **17** undergoes ionization with $BF_3 \bullet OEt_2$ to form a tertiary carbocation and furan undergoes nucleophilic attack to give oxazolidinone **18** in 96% yield (Scheme 5.9). The optical rotation is [α] = +146.2 for compound **18**. Finally, hydrolytic cleavage of the chiral auxiliary is performed with potassium carbonate and methanol to give the alcohol **19**. The optical rotation is [α] = +2.3, which shows that the alcohol **19** is enantiopure.

5.3 Conclusions

In summary, a series of chloroalcohol compounds **4a**-**7a** were synthesized in high yields (85-98%) via triphosgene-triethylamine activation conditions. The chlorination reaction was chemoselective only for primary alcohols in the presence of tertiary alcohols due to steric hindrance. Other bases such as pyridine and diisopropylethylamine resulted in the cyclic carbonate **8**. Fragment **13** was made through a series of steps from the commerically available indene **9** while fragment **16** was made from the commercially available acetophenone **1**. Oxazolidinone **17** was

synthesized in moderate yield from acylation reaction between chloroformate **16** and oxazolidone **13**. Compound **17** was ionizated with Lewis acid (BF_3•OEt_2) and undergoes nucleophilic attack with furan in an asymmetric S_N1 reaction to give compound **18** in excellent yield of 96%. The oxazolidone was cleaved under hydrolysis conditions to produce alcohol **19** in good yield of 48%.

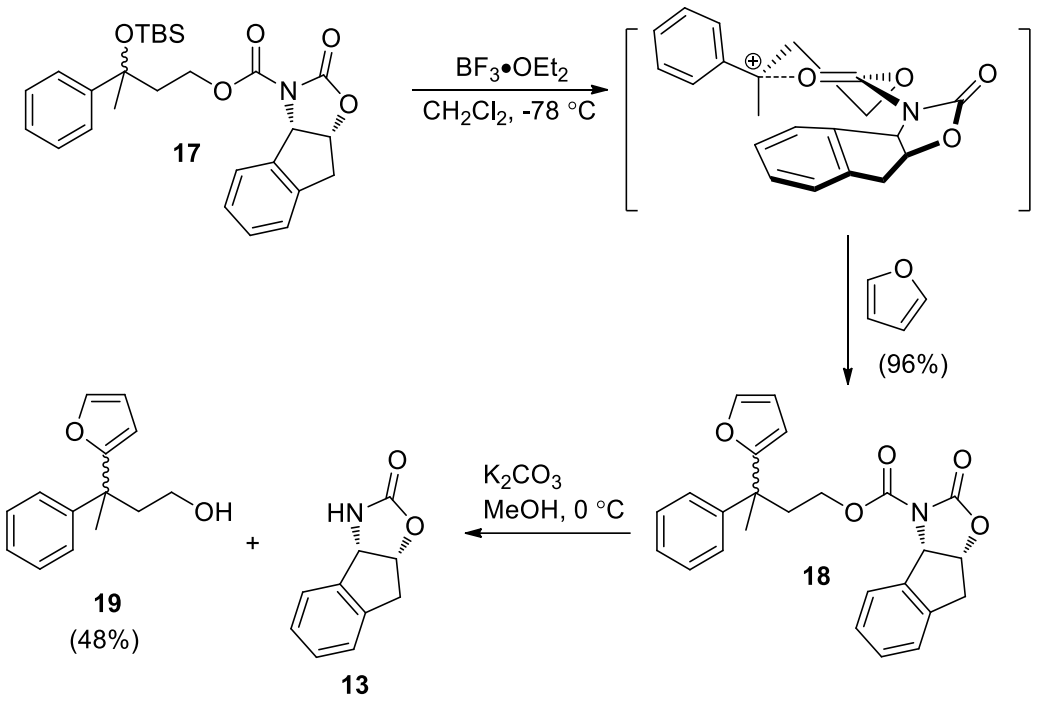

Scheme 5.9: S_N1 reaction and auxiliary cleavage.

5.4 Experimental

5.4.1 General Information

2-Phenyl-4-penten-2-ol (**2**). Acetophenone (0.500 g, 4.16 mmol) was dissolved in THF (42 mL) and cooled to -78 °C. AllyMgBr (4.57 mL, 4.51 mmol) was added dropwise to the reaction mixture. After 45 minutes, the reaction was quenched with half saturated NH_4Cl (20 mL) and extracted with EtOAc (3 x 20 mL). The combined organic layers were dried over $MgSO_4$, filtered,

and concentrated under reduced pressure. The crude product was purified via silica (90/10 Hex/EtOAc) to afford alcohol **2** (93%, 0.630 g).

(±)-3-Phenylbutane-1,3-diol (**4**). Path 1: Alcohol **2** (25.0 mg, 0.154 mmol) was dissolved in MeOH (5 mL) and cooled to 0 °C. O_3 was bubbled into the solution until the solution turned blue. $NaBH_4$ (11.7 mg, 0.308 mmol) was added as solid and warmed to room temperature. The crude product was purified via silica (eluent 60/40 Hex/EtOAc) to afford 1,3-diol **4** (77%, 19.8 mg). ^{1}H NMR ($CDCl_3$, 250 MHz) δ 7.47-7.18 (m, 5H), 3.75 (dq, *J* = 9.5, 4.6 Hz, 1H), 3.62-3.45 (m, 1H), 2.12-2.01 (m, 2H), 1.58 (s, 3H).

(±)-3-Phenylbutane-1,3-diol (**4**). Path 2: DIPEA (3.9 mL, 27.4 mmol) was suspended in anhydrous THF (100 mL) and cooled to -78 °C. n-butyllithium (11.0 mL, 27.4 mmol) was added dropwise, followed by anhydrous EtOAc (2.5 mL, 25.7 mmol) and then acetophenone (2 mL, 17.1 mmol). After 1.5 hours, the reaction mixture was quenched with half saturated NH_4Cl (20 mL) and extracted with EtOAc (3 x 20 mL). The combined organic layers were dried over $MgSO_4$, filtered, and concentrated under reduced pressure to afford crude ester **3**. The crude ester **3** was taken to next step without purification. The $LiAlH_4$ (0.715 g, 18.8 mmol) was dissolved in THF (250 mL) and cooled to 0 °C. The ester was added to the reaction mixture and rinsed three times with THF. After 15 min, the mixture was quenched with water (0.72 mL) and then washed with 15% NaOH (0.72 mL) and then water (2.2 mL). The aqeous layers were extracted with EtOAc (200 mL), dried over small amount of $MgSO_4$, filtered, and concentrated under reduced pressure. The crude product was purified via silica (eluent 60/40 Hex/EtOAc) to afford 1,3 diol **4** (69% over two steps, 1.96 g). ^{1}H NMR ($CDCl_3$, 250 MHz) δ 7.47-7.18 (m, 5H), 3.75 (dq, *J* = 9.5, 4.6 Hz, 1H), 3.62-3.45 (m, 1H), 2.12-2.01 (m, 2H), 1.58 (s, 3H).

General Procedure for Chlorination. In an over-dried flask, diol (2.00 mmol) was dissolved in anhydrous CH_2Cl_2 (15 mL) and cooled to 0 °C. Triethylamine (5.00 mmol) was added dropwise to the reaction mixture, followed by triphosgene (1.00 mmol). The reaction was warmed up to room temperature and stirred for an addition 3 hours. The mixture was quenched with saturated $NaHCO_3$ (30 mL). The aqueous layer was extracted with CH_2Cl_2 (2 x 30 mL). The combined organic layers were dried over $MgSO_4$, filtered, and concentrated under reduced pressure.

(±)-4-Chloro-2-phenylbutan-2-ol (**4a**). Diol **4** (332 mg, 2.00 mmol, CAS #7133-68-8) was utilized along with the requisite amounts of triethylamine and triphosgene. The crude product was purified via silica (eluent 90/10 hexane/EtOAc) to give a colorless oil **4a** (98%, 361 mg). ^{1}H NMR ($CDCl_3$, 250 MHz) δ 7.46-7.24 (m, 5H), 3.56 (ddd, *J* = 10.8, 8.4, 7.8 Hz, 1H), 3.35 (ddd, *J* = 10.7, 8.9, 6.4 Hz, 1H), 2.35-2.29 (m, 2H), 2.04 (s, 1H), 1.62 (s, 3H); ^{13}C NMR ($CDCl_3$, 62.5 MHz) δ 146.30, 128.36, 126.94, 124.48, 74.24, 46.54, 40.42, 30.70; IR (cm^{-1}): f = 3553, 3421, 3028, 2931, 1375, 1099, 699; HRMS (ESI-TOF) *m/z* 167.0622 $[M - OH]^+$ calculated for $C_{10}H_{12}Cl$: 167.0626.

(±)-(E)-5-Chloro-3-phenylpent-1en-3-ol (**5a**). Diol **5** (385 mg, 2.00 mmol) was utilized along with the requisite amounts of triethylamine and triphosgene. The crude product was purified via silica (eluent 90/10 hexane/EtOAc) to give a yellow oil **5a** (85%, 356 mg). ^{1}H NMR ($CDCl_3$, 250 MHz) δ 7.42- 7.23 (m, 5H), 6.64 (d, *J* = 16.1 Hz, 1H), 6.25 (d, *J* = 16.1 Hz, 1H), 3.74-3.56 (m, 2H), 2.25-2.06 (m, 2H), 1.79 (s, 1H), 1.45 (s, 3H). ^{13}C NMR ($CDCl_3$, 62.5 MHz,) δ 136.40, 134.92, 128.55, 127.87, 127.61, 126.40, 72.75, 44.94, 40.33, 28.86; IR (cm^{-1}): f = 3553, 3399, 3026, 2928, 1272, 969, 692; HRMS (ESI-TOF) *m/z* 193.0779 $[M - OH]^+$ calculated for $C_{12}H_{14}Cl$: 193.0787.

2-Benzyl-4-chloro-1-phenylbutan-2-ol (**6a**). Diol **6** (550 mg, 2.00 mmol, CAS #497845-92-8) was utilized along with the requisite amounts of triethylamine and triphosgene. The crude product was purified via silica (eluent 90/10 hexane/EtOAc) to give a colorless oil **6a** (97%, 532 mg). ^{1}H NMR ($CDCl_3$, 250 MHz) δ 7.40-7.22 (m, 10H), 3.72-3.66 (m, 2H), 2.83 (s, 4H), 1.99-1.92 (m, 2H), 1.55 (s, 1H); ^{13}C NMR ($CDCl_3$, 62.5 MHz) δ 136.36, 130.59, 128.41, 126.80, 73.74, 45.81, 41.39, 40.25; IR (cm^{-1}): f = 3561, 3468, 3028, 2923, 1453, 1089, 700; HRMS (ESI-TOF) *m/z* 297.1022 $[M + Na]^+$ calculated for $C_{17}H_{19}ClNaO$: 297.1000.

1-(2-Chloroethyl)cyclopentanol (**7a**). Diol **7** (260 mg, 2.00 mmol, CAS #73089-93-7) was utilized along with the requisite amounts of triethylamine and triphosgene. The crude product was purified via silica (eluent 70/30 pentane/Et_2O) to give a colorless oil **7a** (96%, 285 mg). ^{1}H NMR ($CDCl_3$, 250 MHz); δ 3.72-3.66 (m, 2H), 2.12-2.01 (m, 2H), 1.83-1.55 (m, 8H), 1.41 (s, 1H); ^{13}C NMR ($CDCl_3$, 62.5 MHz) δ 81.47, 44.05, 41.07, 39.70, 23.32; IR (cm^{-1}): f = 3393, 2961, 2874, 1452, 1211, 731; HRMS (ESI-TOF) *m/z* 131.0622 $[M - OH]^+$ calculated for $C_7H_{12}Cl$: 131.0634.

(±)-4-Methyl-4-phenyl-1,3-dioxan-2-one (**8**). Diol **4** (332 mg, 2.00 mmol) was utilized along with the requisite amounts of pyridine (0.40 mL, 5.00 mmol) and triphosgene (297 mg, 0.500 mmol). The crude product was purified via silica (eluent 60/40 hexane/EtOAc) to give a colorless oil **8** (86%, 329 mg). ^{1}H NMR ($CDCl_3$, 250 MHz) δ 7.40-7.25 (m, 5H), 4.31 (ddd, ddd, *J* = 11.2, 4.7, 4.2 Hz, 1H), 4.03 (ddd, *J* = 11.2, 10.0, 4.5 Hz, 1H), 2.46-2.26 (m, 2H), 1.70 (s, 3H); ^{13}C NMR ($CDCl_3$, 62.5 MHz) δ 148.62, 142.24, 128.76, 127.83, 123.80, 84.26, 64.99, 33.16, 29.99; IR (cm^{-1}): f = 2983, 2917, 1733, 1087, 699; HRMS (ESI-TOF) *m/z* 215.0684 $[M + Na]^+$ calculated for $C_{11}H_{12}NaO_3$: 215.0698.

5.4.2 Asymmetric S_N1 Syntheses

Compound (**10**). Indene **9** (2mL, 17.15 mmol) was suspended in THF (28.5 mL). After 30 min, tert-butanol (28.5 mL) was added, followed by water (5.67 mL) and NMO (2.05 g, 18.86 mmol). One crystal solid of OsO_4 was added to the reaction mixture. The reaction was stirred overnight, quenched with $Na_2S_2O_3$ (50 mL), and extracted with ethyl acetate (50 mL). The combined organic layers were dried over $MgSO_4$, filtered, and concentrated under reduced pressure. The crude product was purified via silica (eluent 50/50 Hex/EtOAc) to afford diol **10** (89% yield, 2.2838 g).

Compound (**12**). Diol **10** (3.88 g, 25.8 mmol) was dissolved in dry acetonitrile (25 mL). The reaction was cooled to 0 °C and H_2SO_4 (2.875 mL) was added dropwise. The reaction mixture was warmed to room temperature. After 6 hours, the mixture was quenched with water (15 mL), diluted with water (15 mL), and concentrated by atmosphere pressure. The reaction residue was refluxed at 100 °C overnight and warmed to room temperature. Then isobutanol (15 mL) was added, followed by NaOH (50% solution, 15 mL) and diluted with tert-butanol (15 mL). The aqeuous was extracted with ethyl acetate (5 x 10 mL) and dried over $MgSO_4$. The crude amino alcohols mixture (4.54 g, 30.44 mmol) were dissolved in MeOH (68 mL). L-tartaric acid (5.05 g, 33.48 mmol) dissolved in MeOH (68 mL) were added to the reaction and refluxed for 3 hours. Then the mixture was cooled to room temperature and recrystallized with methanol to afford amino alcohol **12** (210 mg).

Compound (**13**). Commercially available amino alcohol **12** (2.5 g, 16.75 mmol) was suspended in CH_2Cl_2 (180 mL). The reaction was cooled to 0 °C and triethylamine (5.84 mL, 41.89

mmol) was added dropwise. Then triphosgene (1.987 g, 6.70 mmol) dissolved in CH_2Cl_2 (10 mL) were cannula over to the reaction mixture. The reaction was quenched with half saturated NH_4Cl (200 mL) after stirring for 2 hours. The mixture was extracted with CH_2Cl_2 (50 mL). The combined organic layers were dried over $MgSO_4$, filtered, and concentrated under reduced pressure to afford a white yellow solid oxazolidone **13** (96%, 3.048 g).

Compound (**14**). 1,3 diol **4** (0.9371 g, 5.64 mmol) was dissolved in anhydrous CH_2Cl_2 (33.6 mL) and cooled to -78 °C. Then 2,6-lutidine (2.63 mL, 22.5 mmol) was added dropwise, followed by TBSOTf (3.107 mL, 13.53 mmol). After 1 hour, the reaction was warmed to room temperature and continued stirring for additional 1 hour. The mixture was quenched with half saturated $NaHCO_3$ (10 mL) and extracted with CH_2Cl_2 (3 x 10 mL). The combined organic layers were dried over $MgSO_4$, filtered, and concentrated under reduced pressure. The crude product was purified via silica (eluent 100% hexanes to 95/5 Hex/EtOAc) to afford ligh yellow oil TBS ether **14** (93%, 2.0706 g). ^{1}H NMR ($CDCl_3$, 250 MHz) δ 7.61-7.22 (m, 6H), 3.85 (td, *J* = 9.5, 6.1 Hz, 1H), 3.53 (td, *J* = 9.6, 6.1 Hz, 1H), 2.20 (dt, *J* = 16.6, 8.4 Hz, 2H), 1.78 (s, 3H), 1.13 (s, 9H), 1.00 (s, 9H), 0.28 (s, 3H), 0.14 (s, 3H), 0.11 (d, *J* = 3.1 Hz, 6H).

Compound (**15**). 1,3-TBS ether **14** (0.200 g, 0.507 mmol) was dissolved in anhydrous MeOH (25 mL) and cooled to 0 °C. TsOH (0.012g, 0.06 mmol) was added as solid to the reaction mixture. After 1 hour, the mixture was quenched with a drop of triethylamine and concentrated under reduced pressure. The crude product was purified via silica (eluent 90/10 Hex/EtOAc) to afford a colorless oil compound **15** (73%, 0.104 g). ^{1}H NMR ($CDCl_3$, 250 MHz) δ 7.49-7.20 (m, 5H), 3.62 (t, *J* = 6.1 Hz, 2H), 2.03 (tt, *J* = 14.1, 7.1 Hz, 2H), 1.73 (s, 3H), 0.98 (s, 9H), 0.14 (s, 3H), -0.04 (s, 3H).

Compound (**16**). Alcohol **15** (100 mg, 0.357 mmol) was dissolved in THF (6 mL) and cooled to 0 °C. Phosgene (0.256 mL, 15% in toluene, 0.392 mmol) solution was added and the reaction was warmed to room temperature. After 15 minutes, the reaction was quenched with cold saturated $NaHCO_3$ (5 mL) and extracted with cold pentane (5 mL). The organic layer was dried over $MgSO_4$, filtered, and concentrated under reduced pressure to afford the crude chloroformate **16** (75%, 92.3 mg). ^{1}H NMR ($CDCl_3$, 250 MHz) δ 7.59-7.14 (m, 11H), 4.45-4.26 (m, 2H), 4.09 (ddd, *J* = 10.6, 9.2, 6.2 Hz, 1H), 2.23 (ddd, *J* = 16.8, 12.8, 6.8 Hz, 2H), 1.68 (s, 3H), 0.98 (s, 11H), 0.16 (s, 3H), 0.02 (s, 3H).

Compound (**17**). Oxazolidone **13** (64.6 mg, 0.188 mmol) was dissolved in THF (1 mL) and cooled to -78 °C. n-BuLi (0.088 mL, 2.135 M in hexane, 0.188 mmol) was added dropwise to the reaction. Chloroformate **16** (30.0 mg, 0.171 mmol) dissolved in THF (1 mL) was cannula over the reaction mixture. After 3 hours, the reaction was quenched with half saturated NH_4Cl (5 mL) and extracted with EtOAc (3 x 5 mL). The combined organic layers were dried over $MgSO_4$, filtered, and concentrated under reduced pressure. The crude product was purified via silica (eluent 80/20 Hex/EtOAc) to afford compound **17** (49%, 40 mg). ^{1}H NMR ($CDCl_3$, 250 MHz) δ 7.59-7.40 (m, 3H), 7.40-7.14 (m, 7H), 5.49 (dd, *J* = 15.4, 7.0 Hz, 1H), 5.20 (dq, *J* = 8.3, 4.0 Hz, 1H), 4.56-4.36 (m, 1H), 4.27-4.11 (m, 1H), 3.34 (s, 2H), 2.49-2.18 (m, 2H), 1.70 (d, *J* = 3.6 Hz, 3H), 1.00 (s, 9H), 0.18 (s, 3H), 0.03 (d, *J* = 1.4 Hz, 3H).

Compound (**18**). Compound **17** (78.0 mg, 0.162 mmol) was dissolved in anhydrous CH_2Cl_2 (8 mL) and cooled to -78 °C. Furan (0.083 mL, 1.134 mmol) was added, followed by BF_3•OEt_2 (0.080 mL, 0.648 mmol) to the reaction and warmed to room temperature. After 1 hour, the

reaction mixture was quenched with saturated $NaHCO_3$ (10 mL) and extracted with CH_2Cl_2 (3 x 10 mL). The combined organic layers were dried over $MgSO_4$, filtered, and concentrated under reduced pressure. The crude product was purified via silica (eluent 80/20 Hex/EtOAc) to afford compound **18** (96%, 64.7 mg). ^{1}H NMR ($CDCl_3$, 250 MHz) δ 7.61 (d, *J* = 7.4 Hz, 1H), 7.42-7.12 (m, 11H), 6.38-6.31 (m, 1H), 6.23 (d, *J* = 2.9 Hz, 1H), 5.64 (t, *J* = 6.5 Hz, 1H), 5.32-5.15 (m, 1H), 4.45-4.21 (m, 2H), 3.37 (d, *J* = 3.3 Hz, 2H), 2.76-2.46 (m, 2H), 1.74 (s, 3H); ^{13}C NMR ($CDCl_3$, 62.5 MHz) δ 159.90, 151.35, 151.02, 145.84, 141.54, 139.57, 138.40, 129.93, 128.29, 127.97, 126.55, 126.40, 126.38, 126.12, 125.27, 109.84, 105.99, 64.78, 63.53, 42.38, 38.61, 37.83, 29.62, 25.92.

Compound (**19**). Compound **18** (12.3 mg, 0.029 mmol) was dissolved in MeOH (2 mL) and cooled to 0 °C. Potassium carbonate (8.1 mg, 0.059 mmol) was added as solid to the reaction and warmed to room temperature. After 1.5 hours, the reaction was quenched with half saturated NH_4Cl (2 mL) and extracted with EtOAc (3 x 2 mL). The combined organic layers were dried over $MgSO_4$, filtered, and concentrated under reduced pressure. The crude product was purified via silica (eluent 80/20 Hex/EtOAc) to afford alcohol **19** (48%, 3.0 mg). ^{1}H NMR ($CDCl_3$, 250 MHz) δ 7.37-7.11 (m, 7H), 6.34 (dd, *J* = 3.2, 1.9 Hz, 1H), 6.22-6.14 (m, 1H), 3.69-3.48 (m, 2H), 2.53-2.23 (m, 2H), 1.67 (s, 3H).

5.5 References

1. Ayala, C. E.; Villalpando, A.; Nguyen, A. L.; McCandless, G. T.; Kartika, R., Chlorination of Aliphatic Primary Alcohols via Triphosgene-Triethylamine Activation. *Org. Lett.* **2012**, *14*, 3676-3679.

2. Krief, A.; Laval, A.-M., Coupling of Organic Halides with Carbonyl Compounds Promoted by SmI_2, the Kagan Reagent. *Chem. Rev.* **1999**, *99*, 745-777.

3. Jana, R.; Pathak, T. P.; Sigman, M. S., Advances in Transition Metal (Pd, Ni, Fe)-Catalyzed Cross-Coupling Reactions Using Akyl-Organometallics as Reaction Partners. *Chem. Rev.* **2011**, *111*, 1417-1492.

4. Chung, W. J.; Carlson, J. S.; Vanderwal, C. D., General Approach to the Synthesis of the Chlorosulfolipids Danicalipin A, Mytilipin A, and Malhamensilipin A in Enantioenriched Form. *J. Org. Chem.* **2014**, *79*, 2226-2241.

5. Umezawa, T.; Shibata, M.; Kaneko, K.; Okino, T.; Matsuda, F., Asymmetric Total Synthesis of Danicalipin A and Evaluation of Biological Activity. *Org. Lett.* **2011**, *13*, 904-907.

6. Yoshimitsu, T.; Nakatani, R.; Kobayashi, A.; Tanaka, T., Asymmetric Total Synthesis of (+)-Danicalipin A. *Org. Lett.* **2011**, *13*, 908-911.

7. Bedke, D. K.; Shibuya, G. M.; Pereira, A. R.; Gerwick, W. H.; Vanderwal, C. D., A Concise Enantioselective Synthesis of the Chlorosulfolipid Malhamensilipin A. *J. Am. Chem. Soc.* **2010**, *132*, 2542-2543.

8. Chen, J. L.; Proteau, P. J.; Roberts, M. A.; Gerwick, W. H.; Slate, D. L.; Lee, R. H., Structure of Malhamensilipin A, an Inhibitor of Protein Tyrosine Kinase, from the Cultured Chrysophyte *Poterioochromonas Malhamensis*. *J. Nat. Prod.* **1994**, *57*, 524-527.

9. Pereira, A. R.; Byrum, T.; Shibuya, G. M.; Vanderwal, C. D.; Gerwick, W. H., Structure Revision and Absolute Configuration of Malhamensilipin A from the Freshwater Chrysophyte *Poterioochromonas malhamensis*. *J. Nat. Prod.* **2010**, *73*, 279-283.

10. Yoshimitsu, T.; Fukumoto, N.; Nakatani, R.; Kojima, N.; Tanaka, T., Asymmetric Total Synthesis of (+)-Hexachlorosulfolipid, a Cytotoxin Isolated from Adriatic Mussels. *J. Org. Chem.* **2010**, *75*, 5425-5437.

11. Nilewski, C.; Deprez, N. R.; Fessard, T. C.; Li, D. B.; Geisser, R. W.; Carreira, E. M., Synthesis of Undecachlorosulfolipid A: Re-evaluation of the Nominal Structure. *Angew. Chem. Int. Ed.* **2011**, *50*, 7940-7943.

12. Shibata, M.; Kanady, J. S.; Vanderwal, C. D., Stereoselective Dichlorination of Allylic Alcohol Derivatives to Access Key Stereochemical Arrays of the Chlorosulfolipids. *J. Am. Chem. Soc.* **2008**, *130*, 12514-12518.

13. Gilman, H.; Kirby, J. E., Some Rearrangement Reactions of Alpha-naphthylmethylmagnesium Chloride. *J. Am. Chem. Soc.* **1929**, *51*, 3475-3478.

14. Miller, S. P.; Gurley, F. C., A Convenient Apparatus for Chlorination with Phosphorus Penta-Chloride. *J. Am. Chem. Soc.* **1915**, *37*, 1361-1361.

15. Olah, G. A.; Schillin.P; Renner, R.; Kerekes, I., Radical Reactions . I. Phosphorus Chloride Catalyzed Chlorination of Alkanes, Cycloalkanes, and Arylalkanes. *J. Org. Chem.* **1974**, *39*, 3472-3478.

16. Uemura, S.; Okazaki, H.; Onoe, A.; Okano, M., Chlorination of Norbornene and Cyclooctadienes with Sulfuryl Chloride and Phosphorus(V) Chloride - Ionic vs Radical Chlorination with Each Reagent. *Bull. Chem. Soc. Jpn.* **1978**, *51*, 3568-3570.

17. Yamada, M.; Nakamura, Y.; Hasegawa, T.; Itoh, A.; Kuroda, S.; Shimao, I., Oxidative Chlorination of 1,10-Phenanthroline and Its Derivatives by Phosphorus-Pentachloride in Phosphoryl Chloride. *Bull. Chem. Soc. Jpn.* **1992**, *65*, 2007-2009.

18. Lucas, H. J., A new test for distinguishing the primary, secondary and tertiary saturated alcohols. *J. Am. Chem. Soc.* **1930**, *52*, 802-804.

19. Kjonaas, R. A.; Riedford, B. A., A Study of the Lucas Test. *J. Chem. Ed.* **1991**, *68*, 704-706.

20. Appel, R., Tertiary Phosphane-Tetrachloromethane, a Versatile Reagent for Chlorination, Dehydration, and P-N Linkage. *Angew. Chem. Int. Ed.* **1975**, *14*, 801-811.

21. Benazza, M.; Uzan, R.; Beaupère, D.; Demailly, G., Direct Regioselective Chlorination of Unprotected Hexitols and Pentitols by Vilsmeier and Haack's salt. *Tetrahedron Lett.* **1992**, *33*, 4901-4904.

22. Yasuda, M.; Yamasaki, S.; Onishi, Y.; Baba, A., Indium-Catalyzed Direct Chlorination of Alcohols using Chlorodimethylsilane-Benzil as a Selective and Mild System. *J. Am. Chem. Soc.* **2004**, *126*, 7186-7187.

23. Denton, R. M.; An, J.; Adeniran, B., Phosphine Oxide-Catalysed Chlorination Reactions of Alcohols under Appel Conditions. *Chem. Commun.* **2010**, *46*, 3025-3027.

24. Kim, H. W.; Lee, Y. S.; Shetty, D.; Lee, H. J.; Lee, D. S.; Chung, J. K.; Lee, M. C.; Chung, K. H.; Jeong, J. M., Facile Chlorination of Benzyl Alcohols Using 1,8-Diazabicyclo[5.4.0]undec-7-ene (DBU) and Sulfonyl Chlorides. *Bull. Korean Chem. Soc.* **2010**, *31*, 3434-3436.

25. Corey, E. J.; Ensley, H. E., Preparation of an Optically-Active Prostaglandin Intermediate Via Asymmetric Induction. *J. Am. Chem. Soc.* **1975**, *97*, 6908-6909.

26. Gossauer, A.; Nydegger, F.; Kiss, T.; Sleziak, R.; Stoeckli-Evans, H., Synthesis, Chiroptical Properties, and Solid-State Structure Determination of Two New Chiral Dipyrrin Difluoroboryl Chelates. *J. Am. Chem. Soc.* **2004**, *126*, 1772-1780.

27. Evan, D. A.; Bartroli, J.; Shih, T. L., Enantioselective Aldol Condensations. 2. Erythro-Selective Chiral Aldol Condensationsvia Boron Enolates. *J. Am. Chem. Soc.* **1981**, *103*, 2127-2129.

28. Evans, D. A.; Ennis, M. D.; Mathre, D. J., Asymmetric Alkylation Reactions of Chiral Imide Enolates - a Practical Approach to the Enantioselective Synthesis of α-Substituted Carboxylic Acid Derivatives. *J. Am. Chem. Soc.* **1982**, *104*, 1737-1739.

29. Evans, D. A.; Chapman, K. T.; Hung, D. T.; Kawaguchi, A. T., Transition-State π-Solvation by Aromatic Rings: An Electronic Contribution to Diels-Alder Reaction Diastereoselectivity. *Angew Chem Int Edit* **1987**, *26*, 1184-1186.

30. Evans, D. A.; Chapman, K. T.; Bisaha, J., New Asymmetric Diels-Alder Cycloaddition Reactions. Chiral *α,β*-Unsaturated Carboximides as Practical Chiral Acrylate and Crotonate Dienophile Synthons. *J. Am. Chem. Soc.* **1984**, *106*, 4261-4263.

31. Guz, N. R.; Phillips, A. J., Practical and Highly Selective Oxazolidinethione-Based Asymmetric Acetate Aldol Reactions with Aliphatic Aldehydes. *Org. Lett.* **2002**, *4*, 2253-2256.

32. Zhang, Y.; Sammakia, T., Synthesis of a New *N*-Acetyl Thiazolidinethione Reagent and Its Application to a Highly Selective Asymmetric Acetate Aldol Reaction. *Org. Lett.* **2004**, *6*, 3139-3141.

33. Crimmins, M. T.; Shamszad, M., Highly Selective Acetate Aldol Additions Using Mesityl-Substituted Chiral Auxiliaries. *Org. Lett.* **2007**, *9*, 149-152.

34. Osorio-Lozada, A.; Olivo, H. F., Indene-Based Thiazolidinethione Chiral Auxiliary for Propionate and Acetate Aldol Additions. *Org. Lett.* **2008**, *10*, 617-620.

35. Larrow, J. F.; Roberts, E.; Verhoeven, T. R.; Ryan, K. M.; Senanayake, C. H.; Reider, P. J.; Jacobsen, E. N., (1*S*,2*R*)-1-aminoindan-2-ol. *Organic Syntheses, Vol 76 - 1999* **1999**, *76*, 46-56.

APPENDIX A: NMR Characterization of Compounds Found in Chapter 2

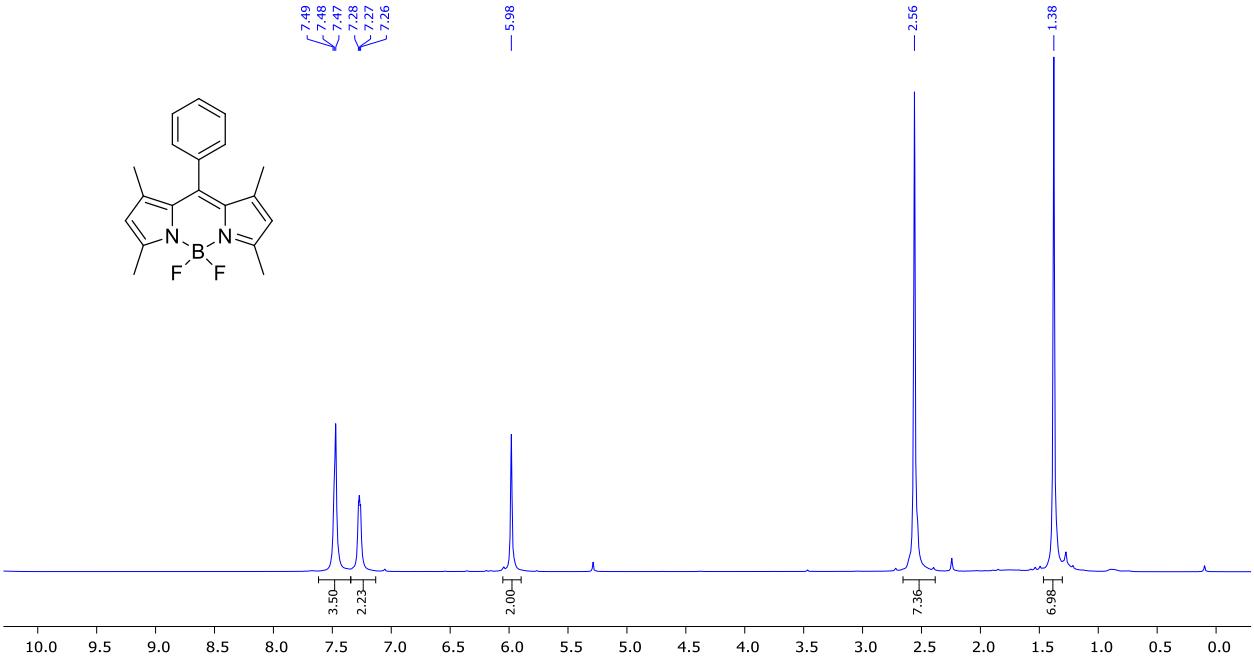

Figure A.1: ^{1}H NMR of BODIPY **1** in $CDCl_3$ (400 MHz)

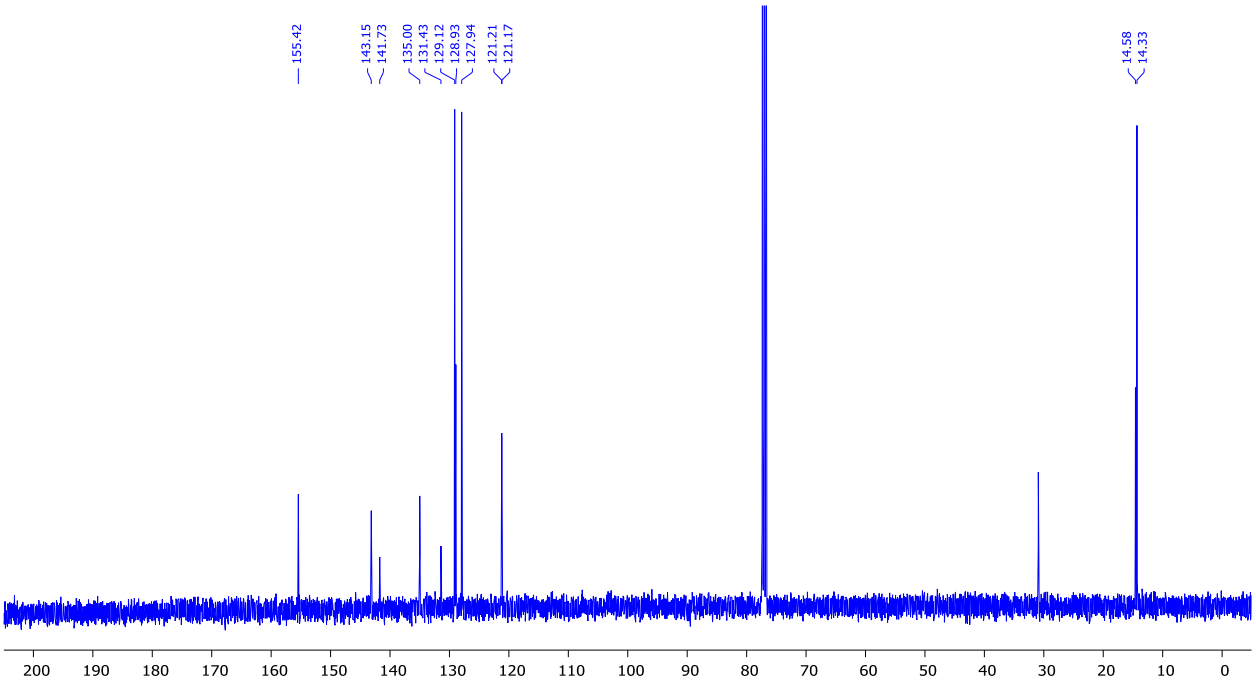

Figure A.2: ^{13}C NMR of BODIPY **1** in $CDCl_3$ (100 MHz)

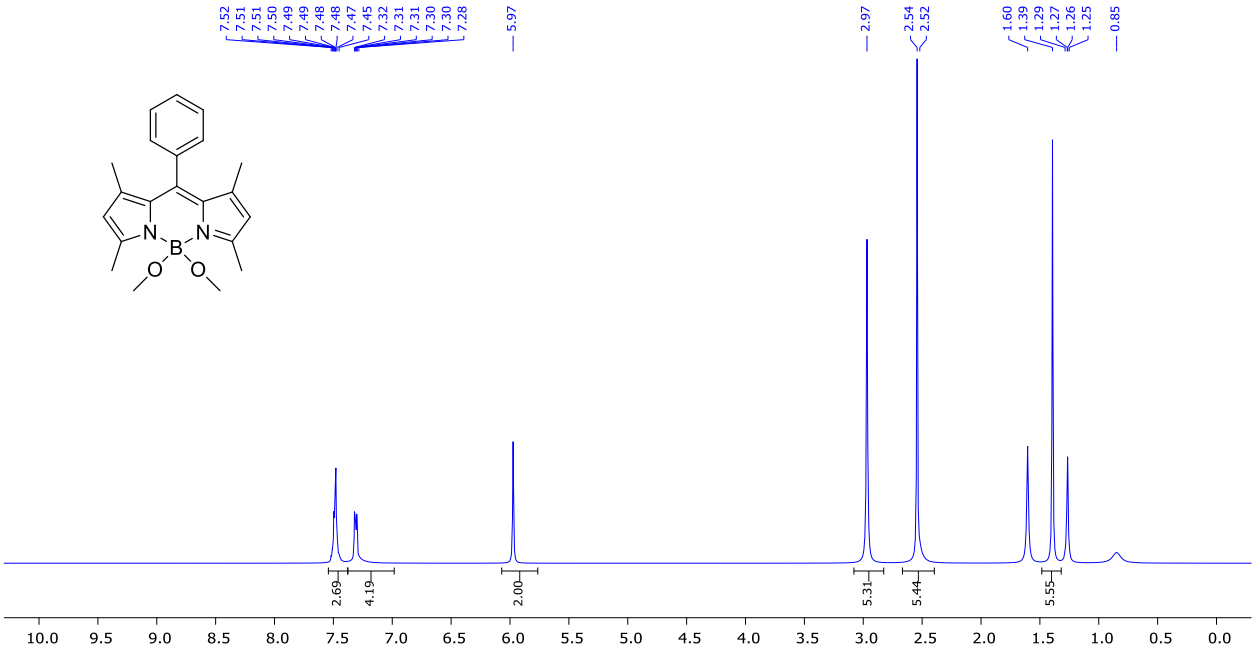

Figure A.3: ^{1}H NMR of BODIPY **1a** in $CDCl_3$ (400 MHz)

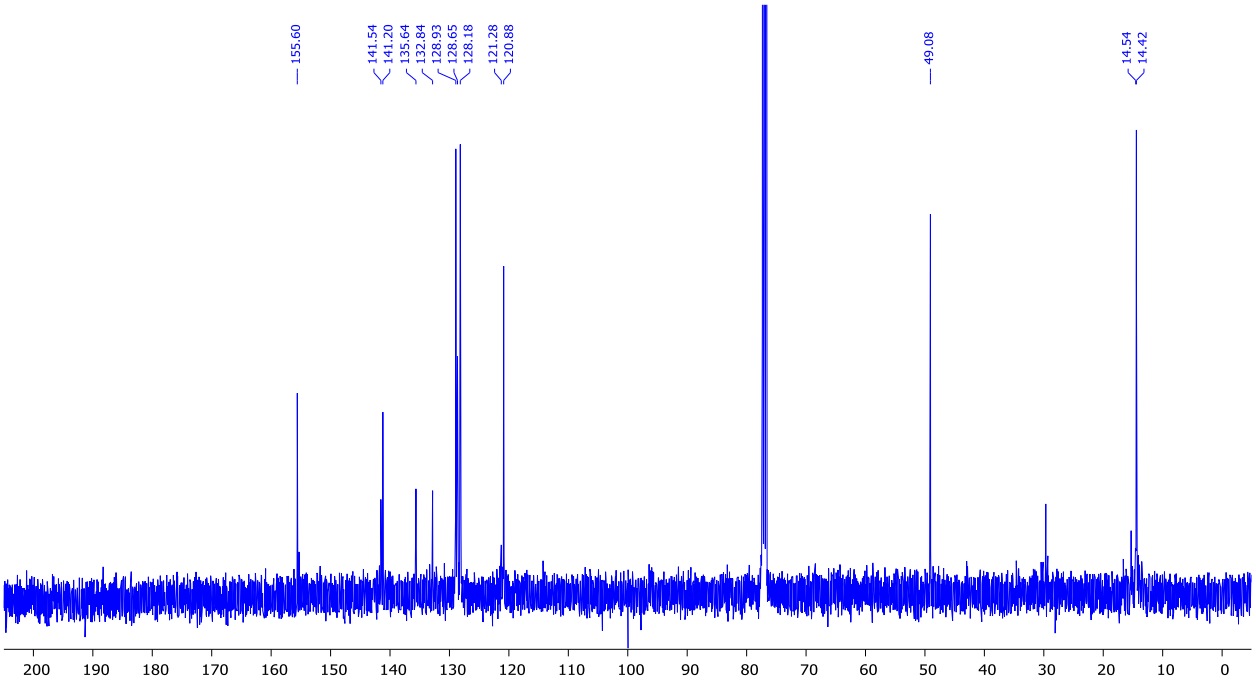

Figure A.4: ^{13}C NMR of BODIPY **1a** in $CDCl_3$ (100 MHz)

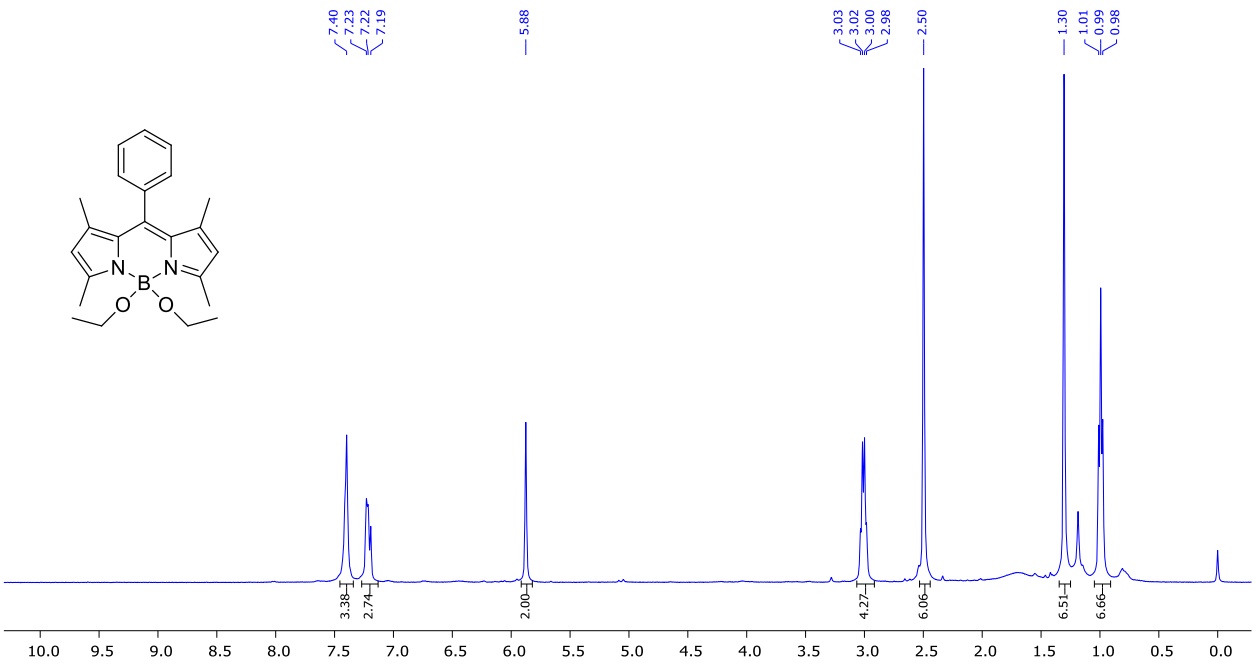

Figure A.5: ^{1}H NMR of BODIPY **1b** in $CDCl_3$ (400 MHz)

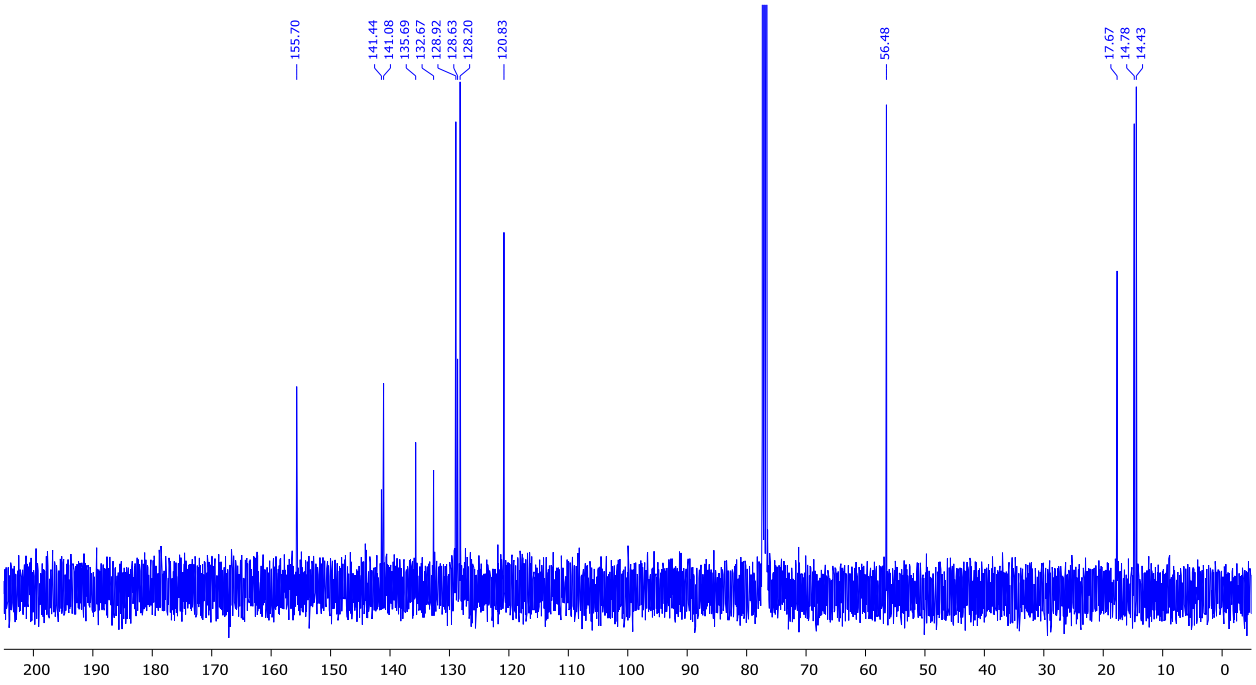

Figure A.6: ^{13}C NMR of BODIPY **1b** in $CDCl_3$ (100 MHz)

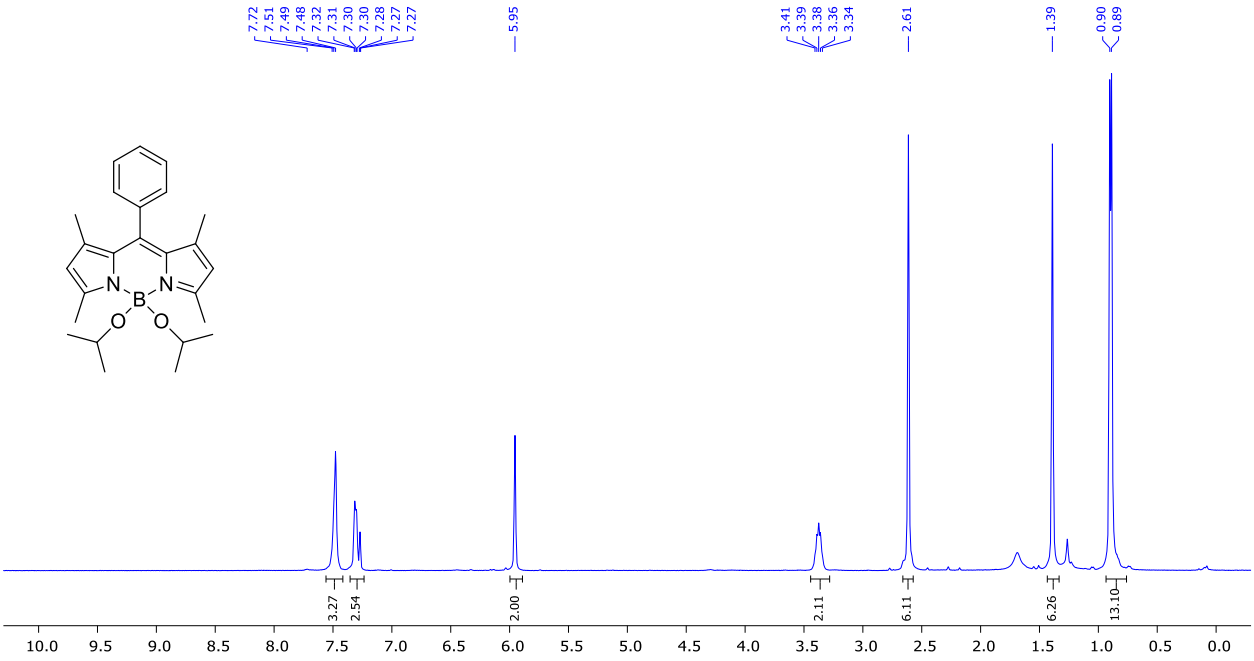

Figure A.7: ^{1}H NMR of BODIPY **1c** in $CDCl_3$ (400 MHz)

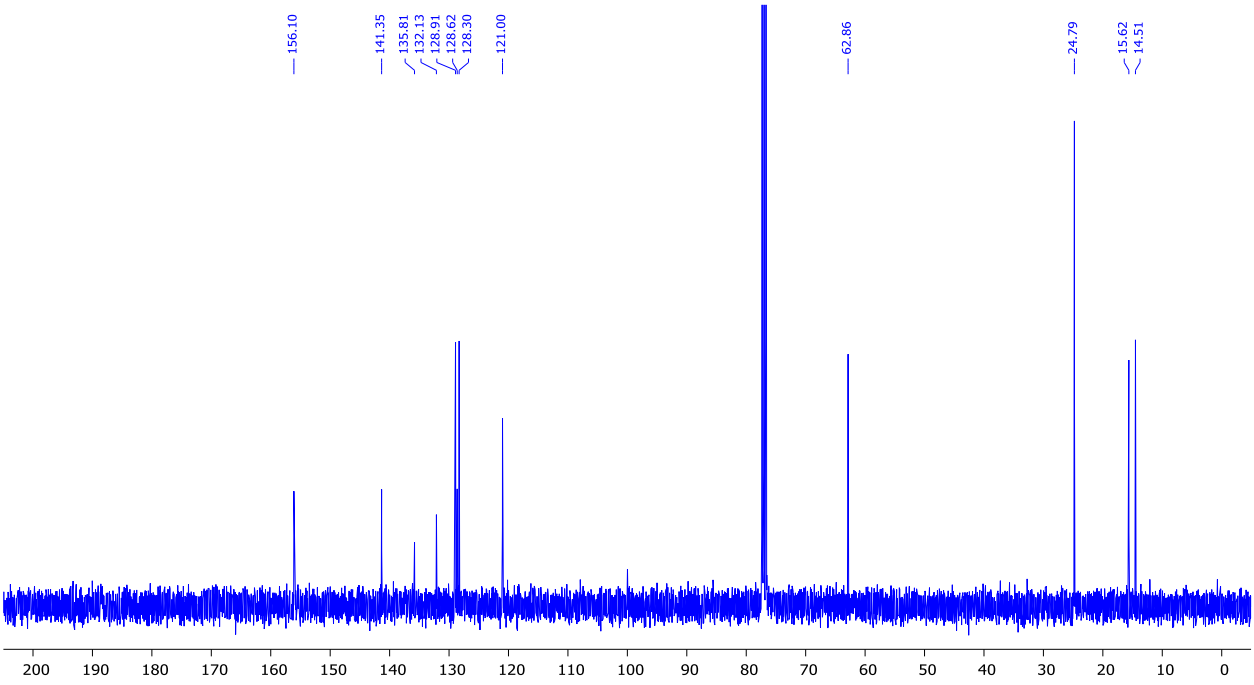

Figure A.8: ^{13}C NMR of BODIPY **1c** in $CDCl_3$ (100 MHz)

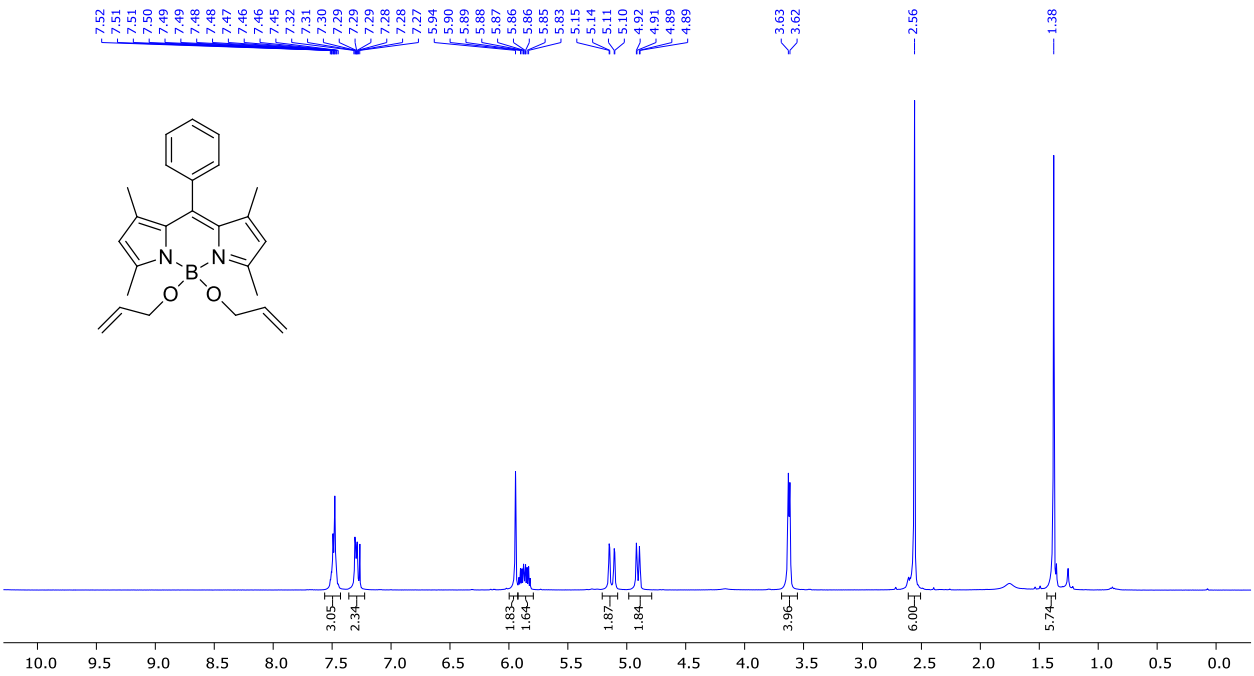

Figure A.9: ^{1}H NMR of BODIPY **1d** in $CDCl_3$ (400 MHz)

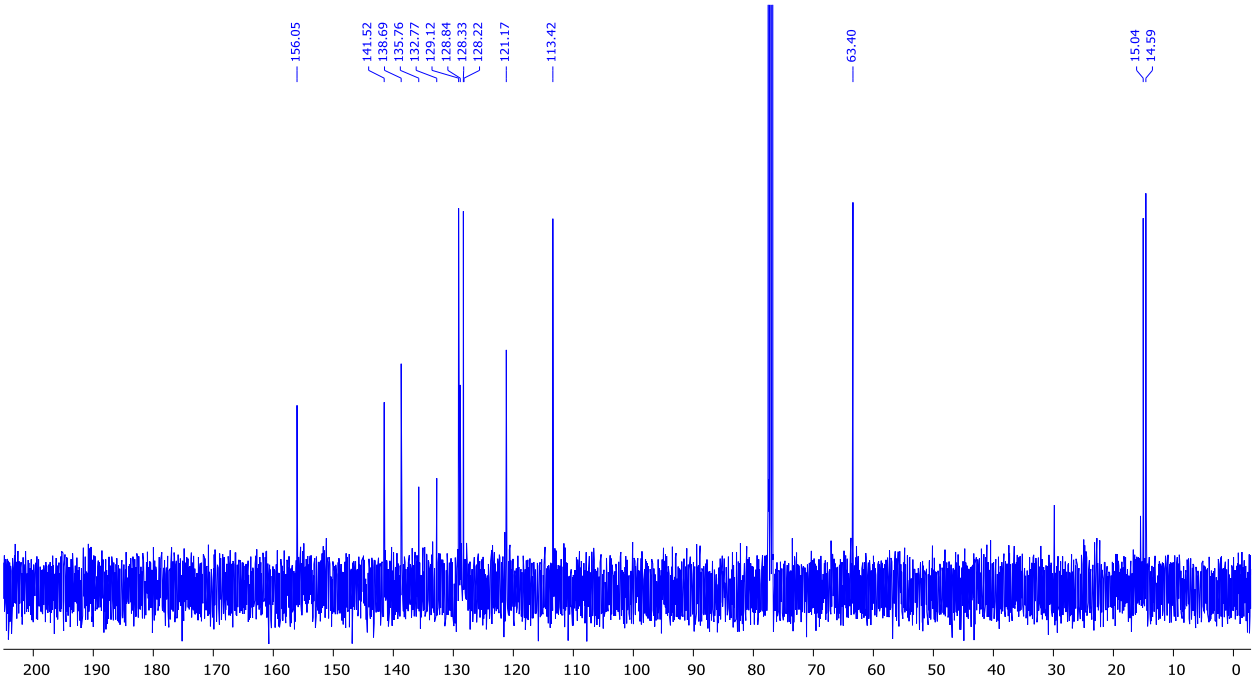

Figure A.10: ^{13}C NMR of BODIPY **1d** in $CDCl_3$ (100 MHz)

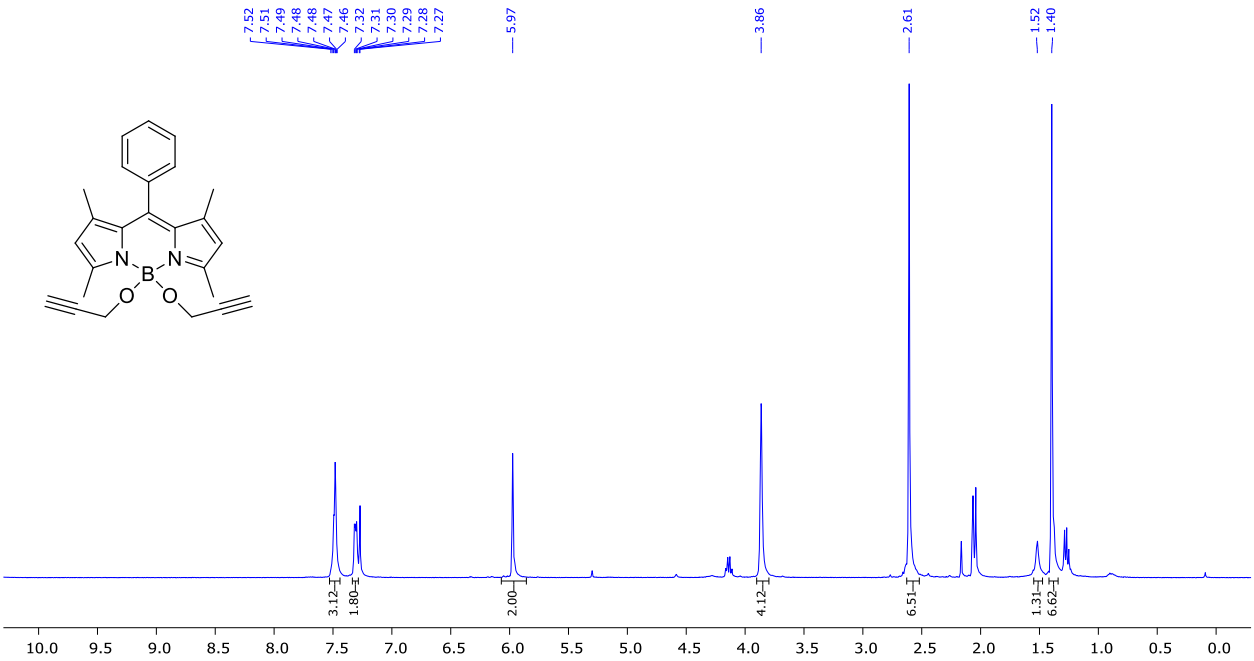

Figure A.11: ^{1}H NMR of BODIPY **1e** in $CDCl_3$ (400 MHz)

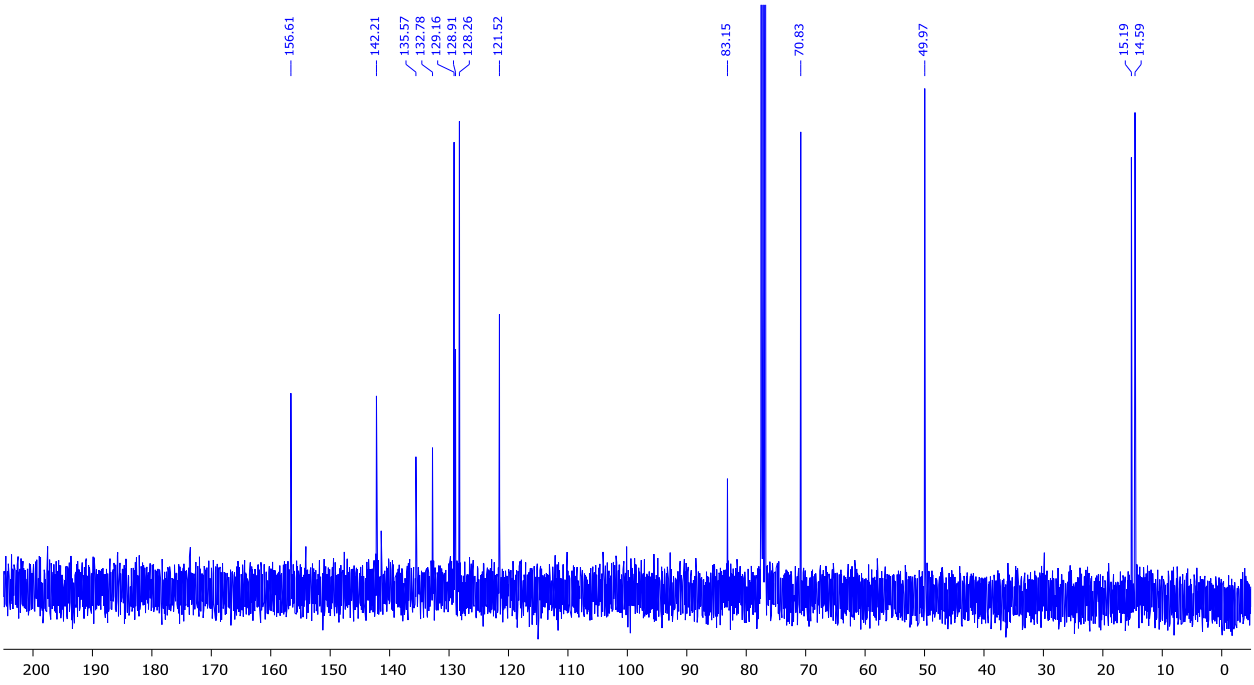

Figure A.12: ^{13}C NMR of BODIPY **1e** in $CDCl_3$ (100 MHz)

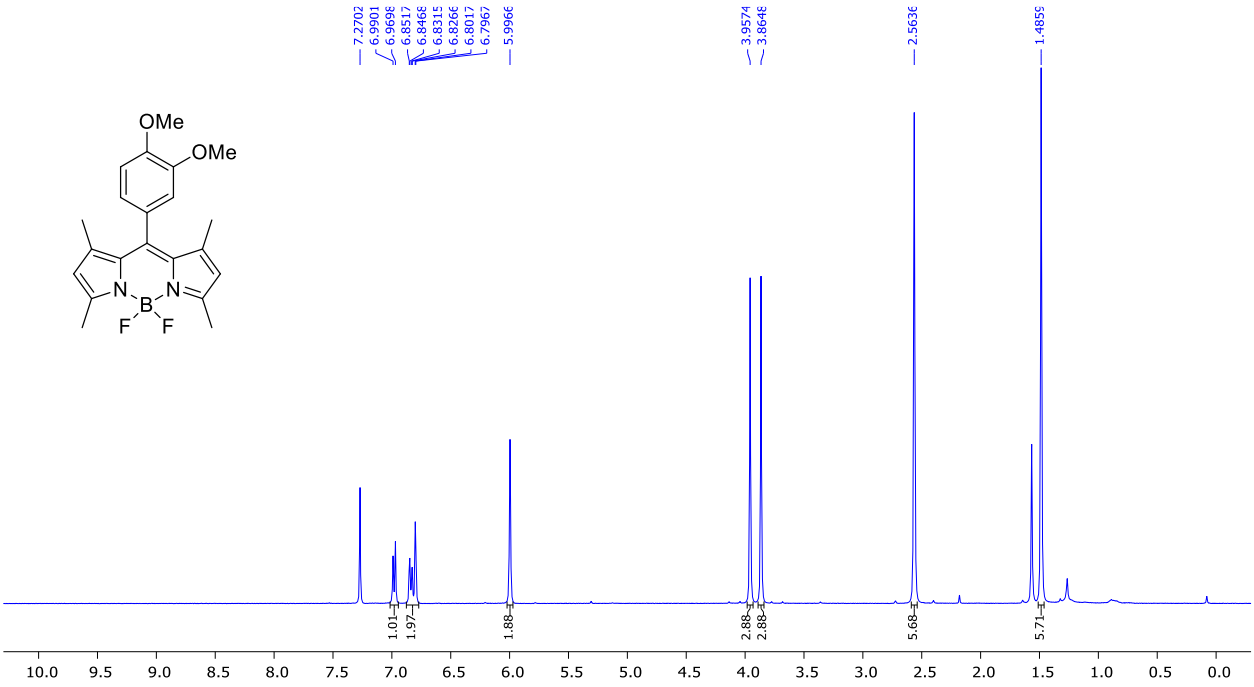

Figure A.13: ^{1}H NMR of BODIPY **2** in $CDCl_3$ (400 MHz)

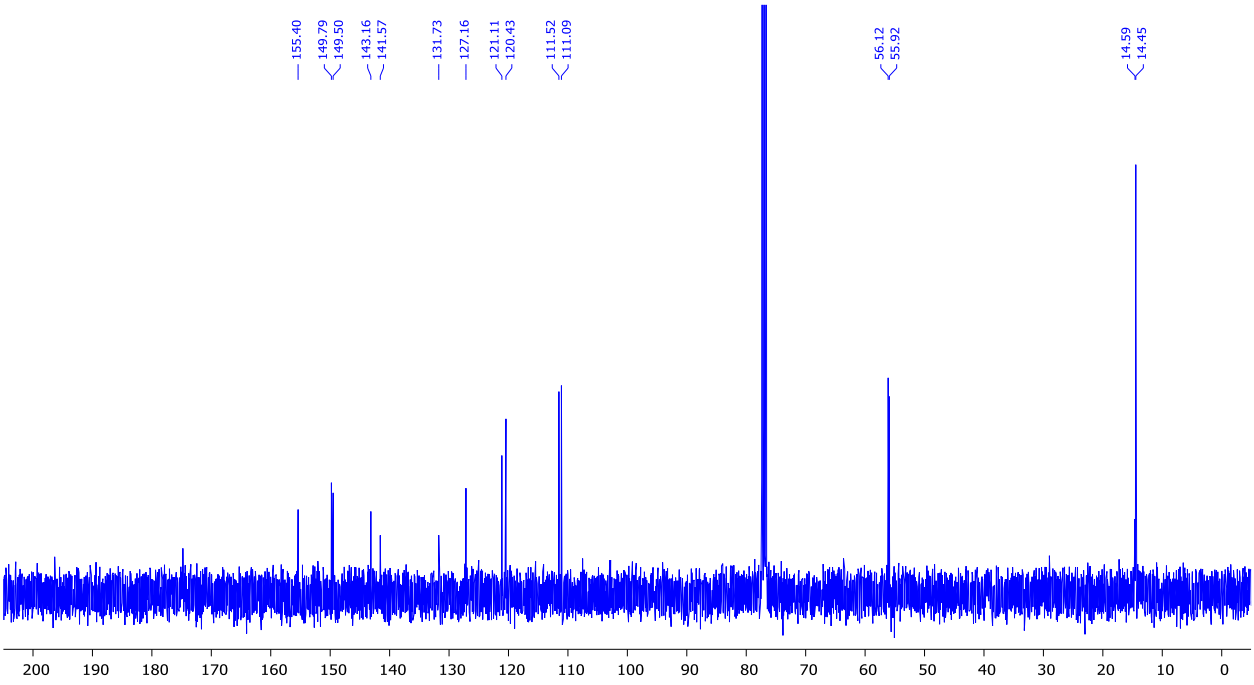

Figure A.14: ^{13}C NMR of BODIPY **2** in $CDCl_3$ (100 MHz)

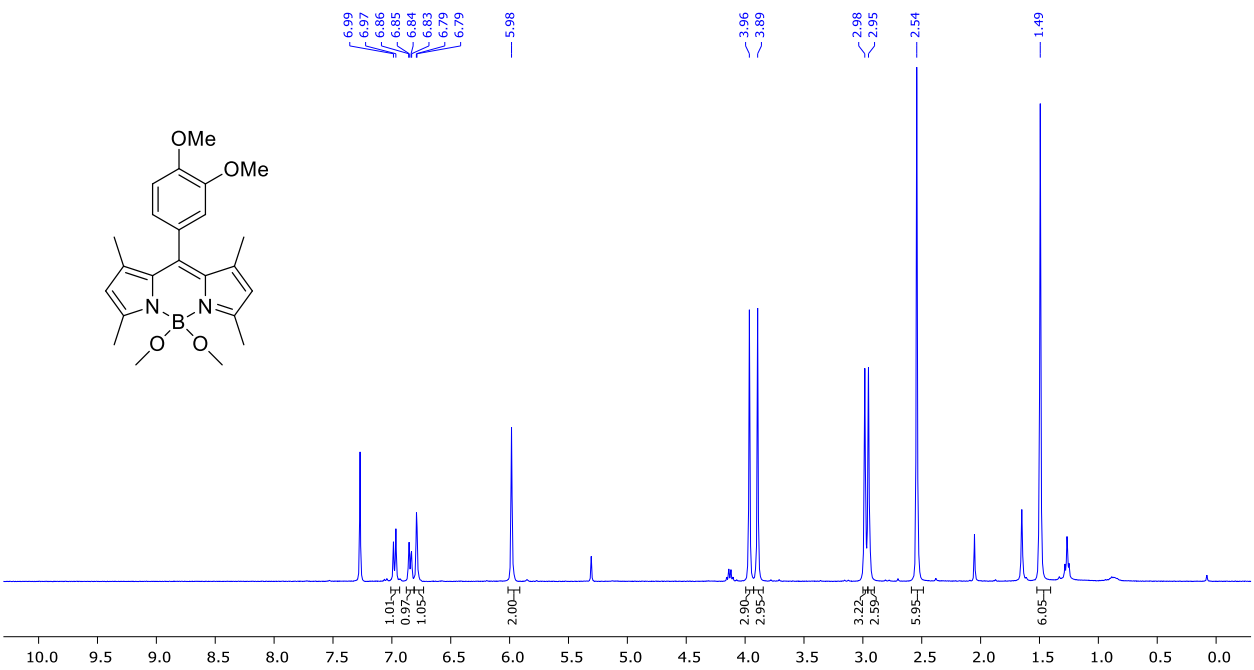

Figure A.15: ^{1}H NMR of BODIPY **2a** in $CDCl_3$ (400 MHz)

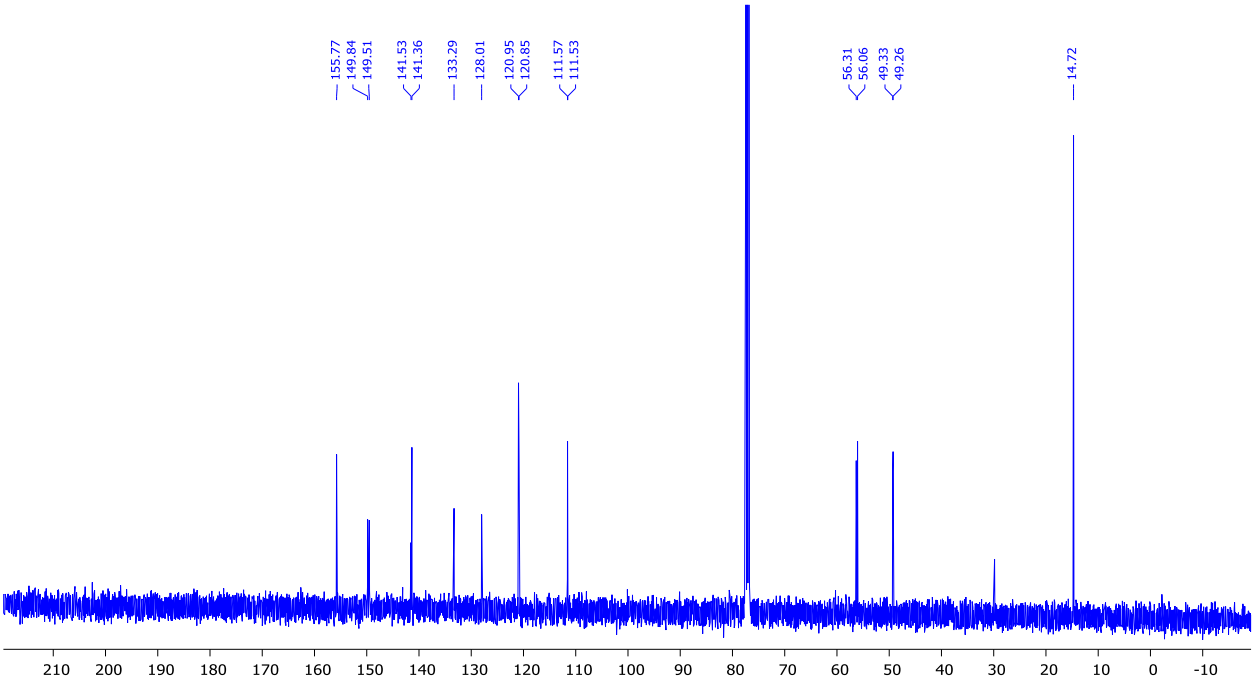

Figure A.16: ^{13}C NMR of BODIPY **2a** in $CDCl_3$ (100 MHz)

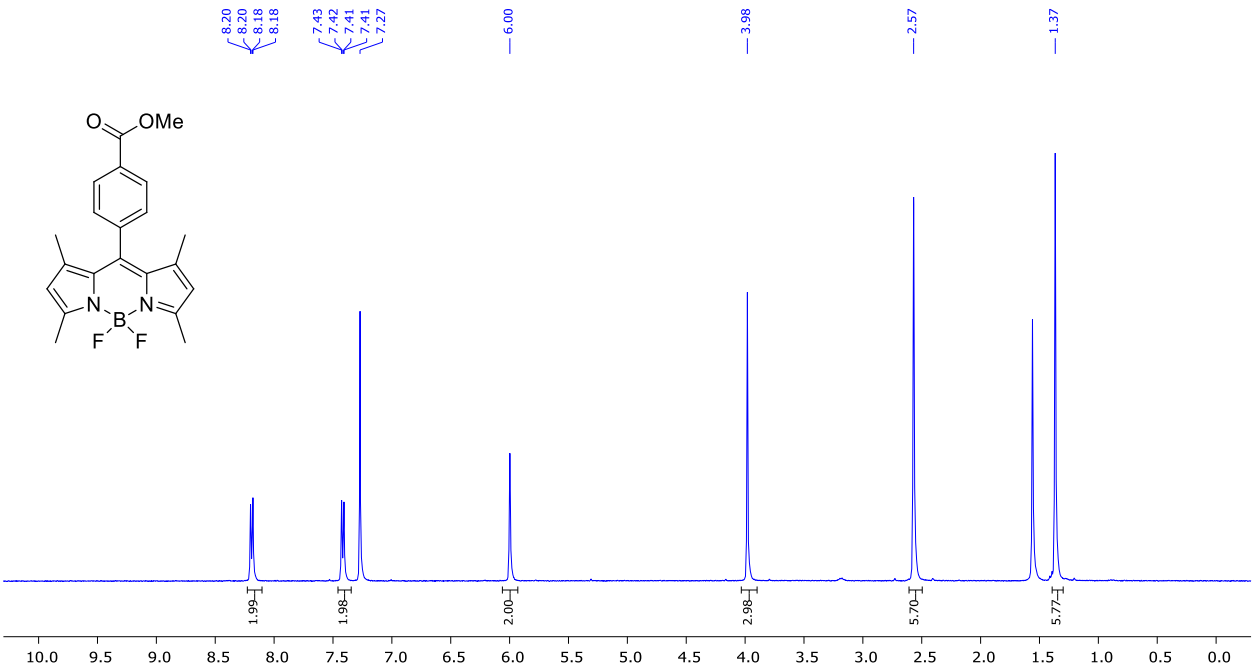

Figure A.17: ^{1}H NMR of BODIPY **3** in $CDCl_3$ (400 MHz)

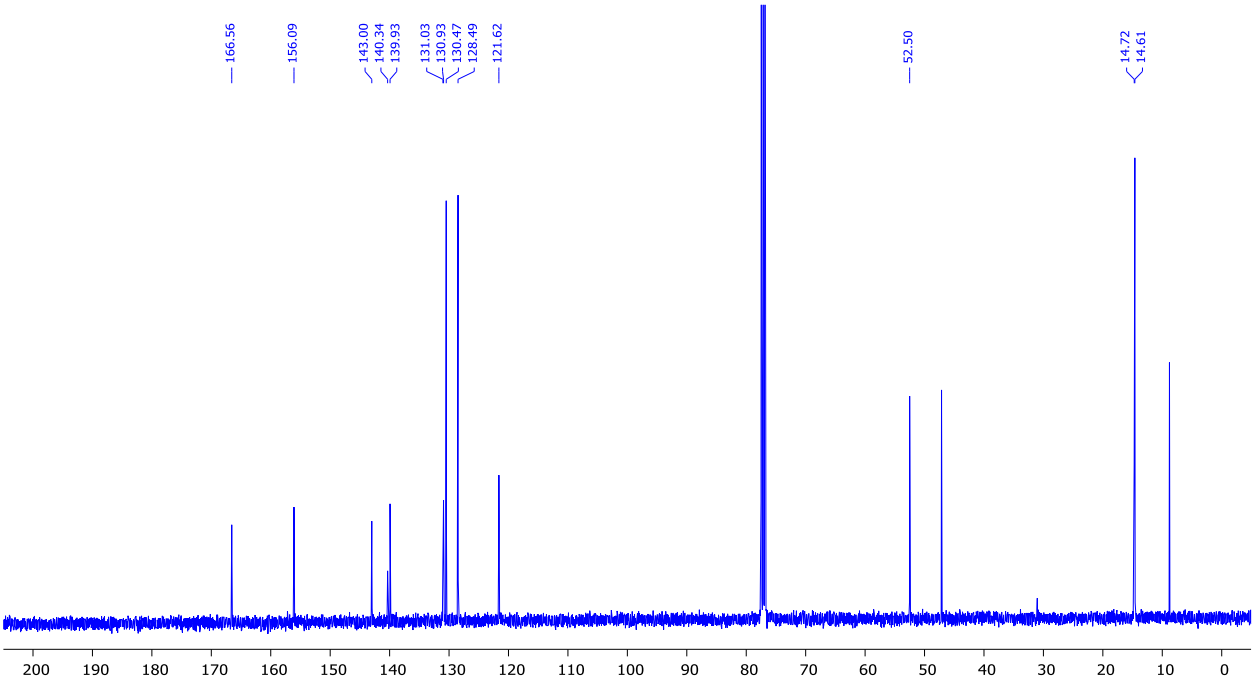

Figure A.18: ^{13}C NMR of BODIPY **3** in $CDCl_3$ (100 MHz)

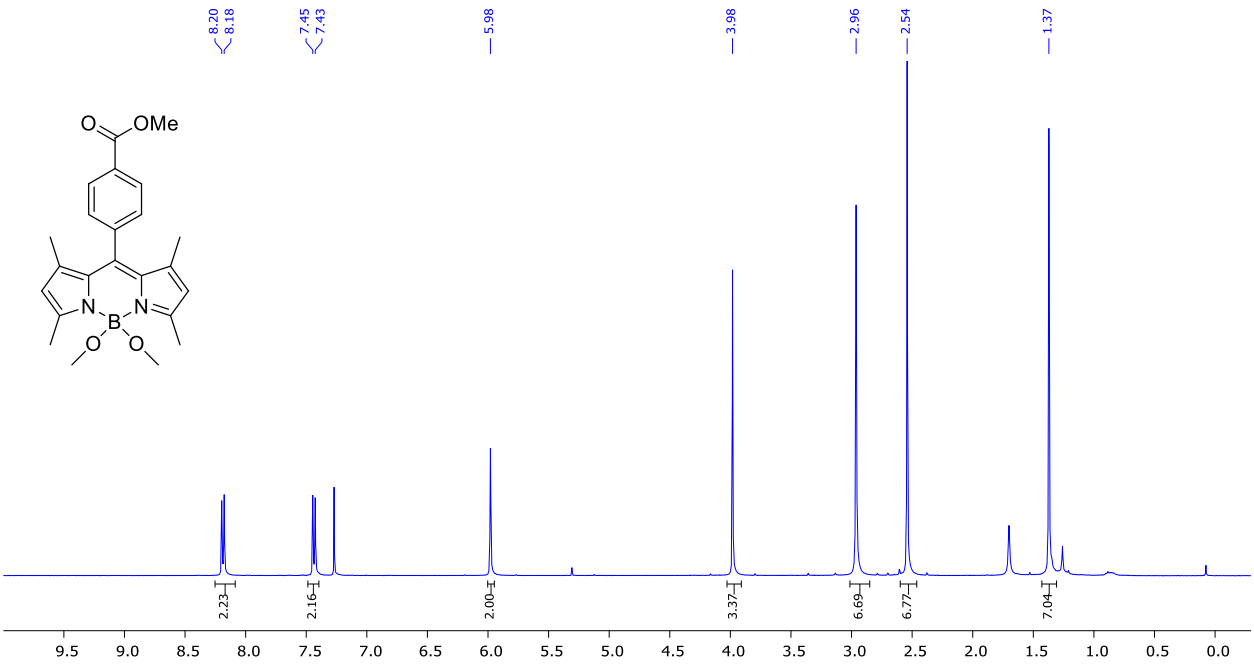

Figure A.19: ^{1}H NMR of BODIPY **3a** in $CDCl_3$ (400 MHz)

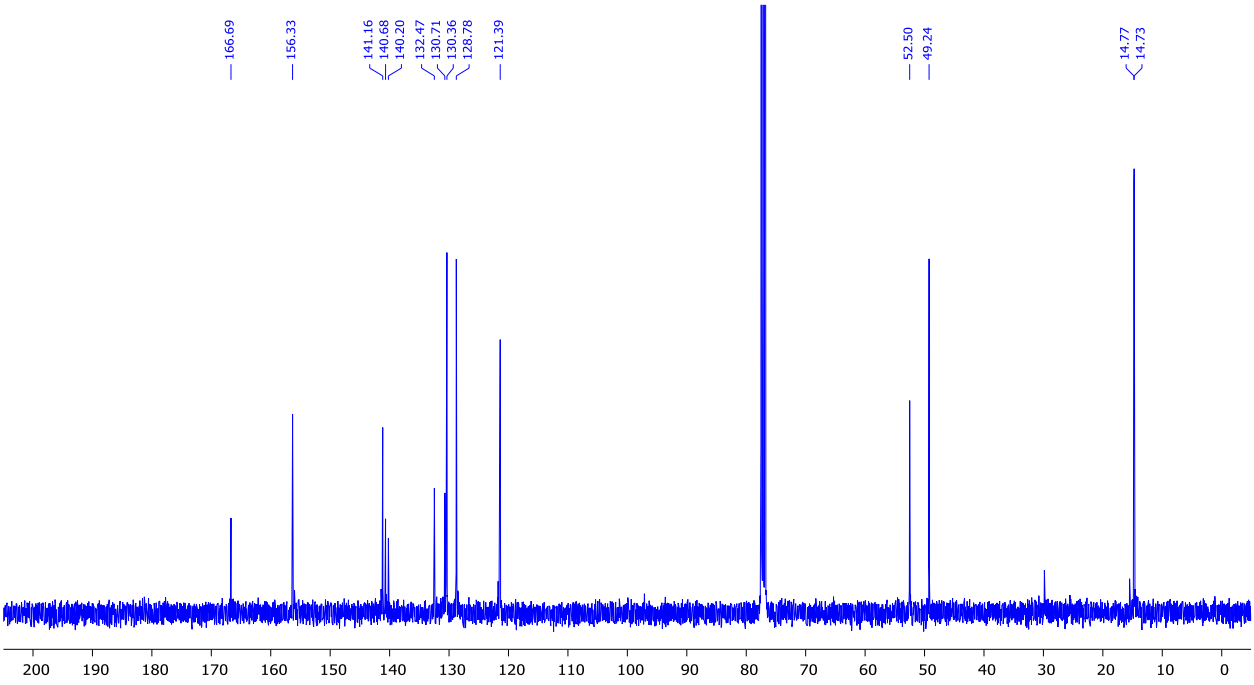

Figure A.20: ^{13}C NMR of BODIPY **3a** in $CDCl_3$ (100 MHz)

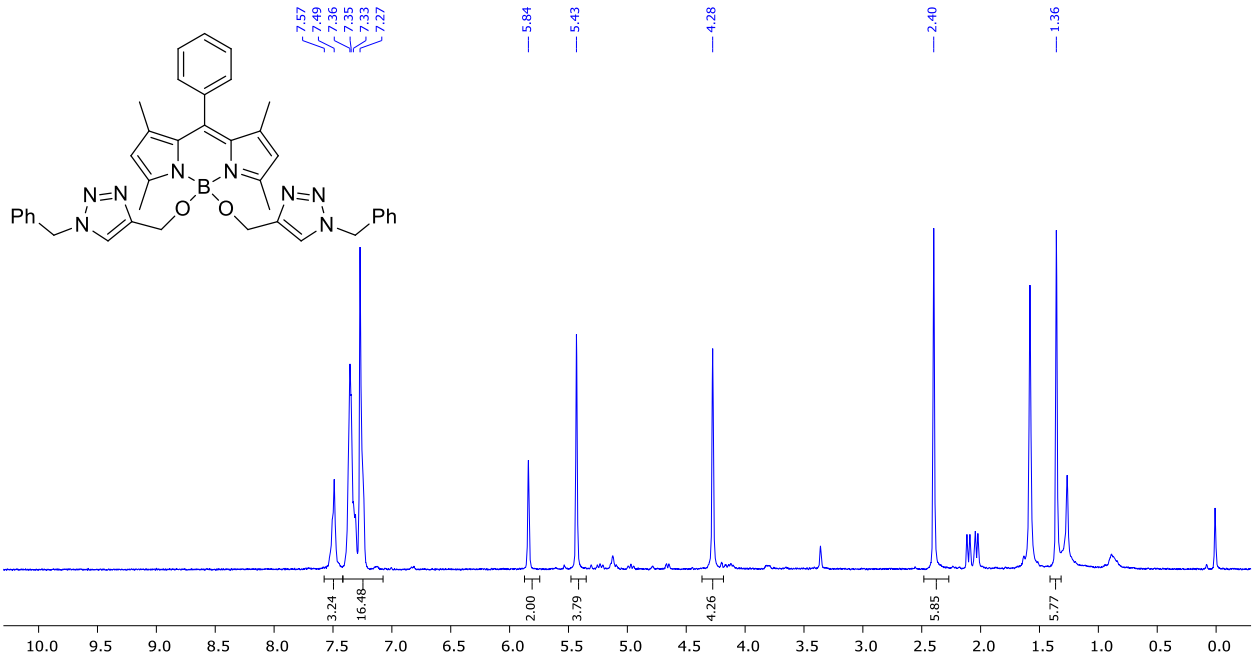

Figure A.21: ^{1}H NMR of BODIPY **4** in $CDCl_3$ (400 MHz)

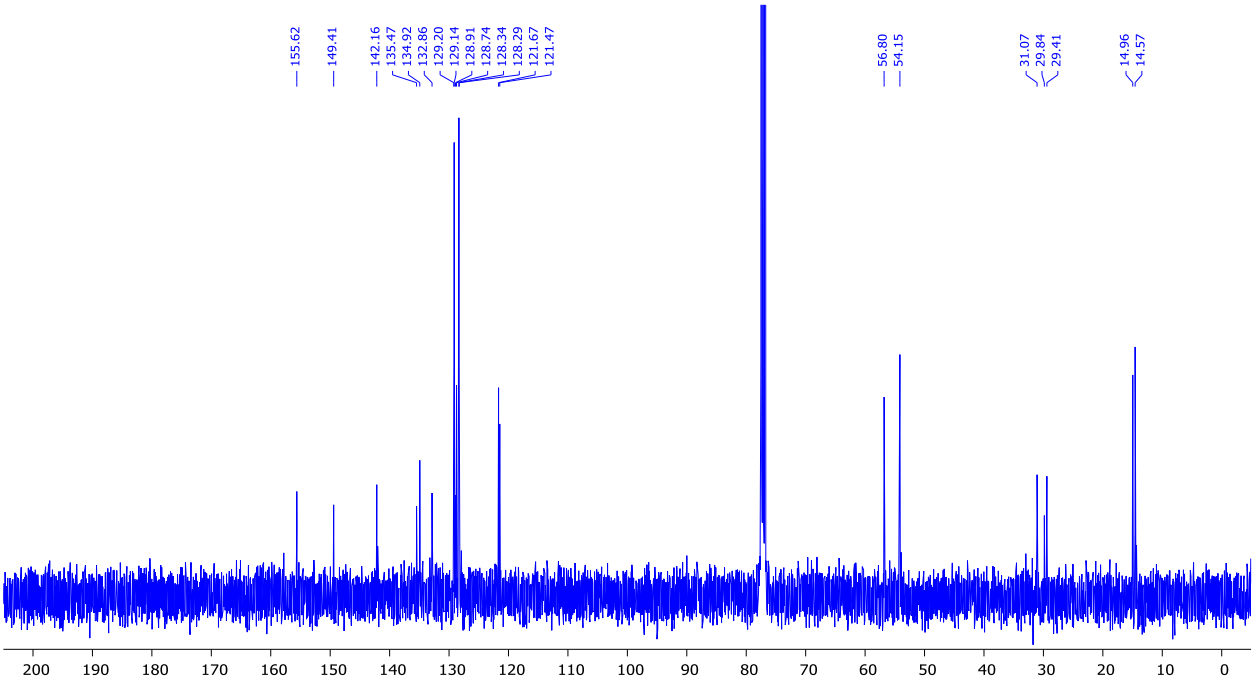

Figure A.22: ^{13}C NMR of BODIPY **4** in $CDCl_3$ (100 MHz)

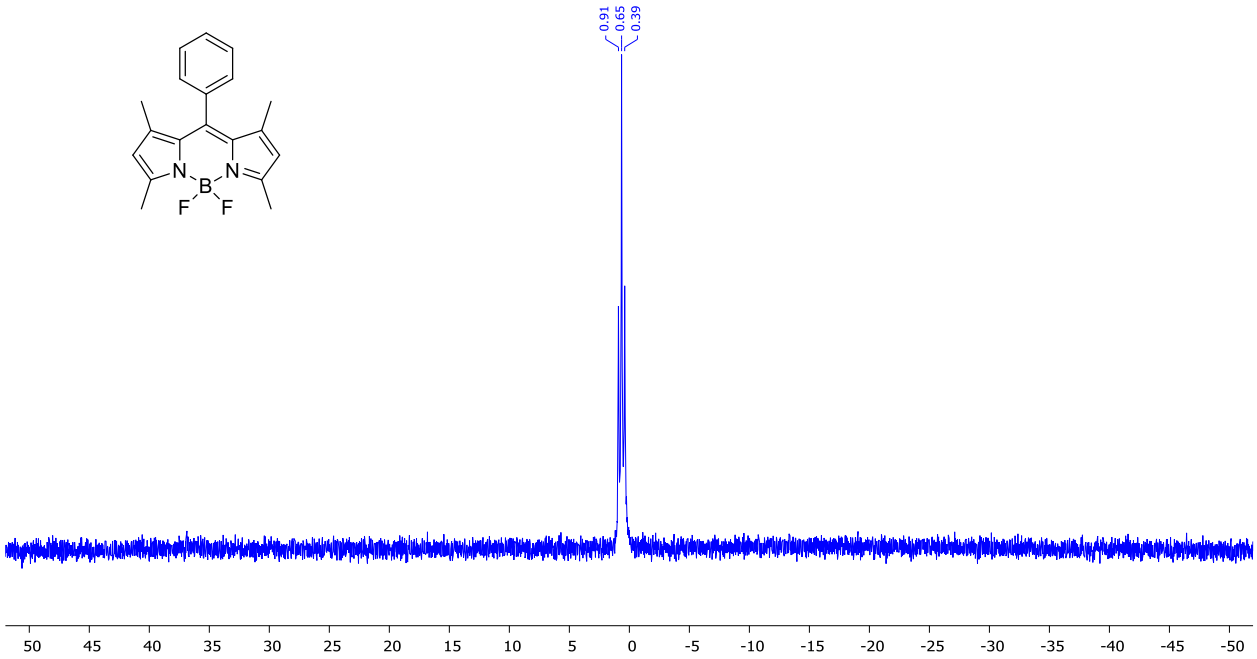

Figure A.23: ^{11}B NMR of BODIPY **1** in $CDCl_3$ (128 MHz)

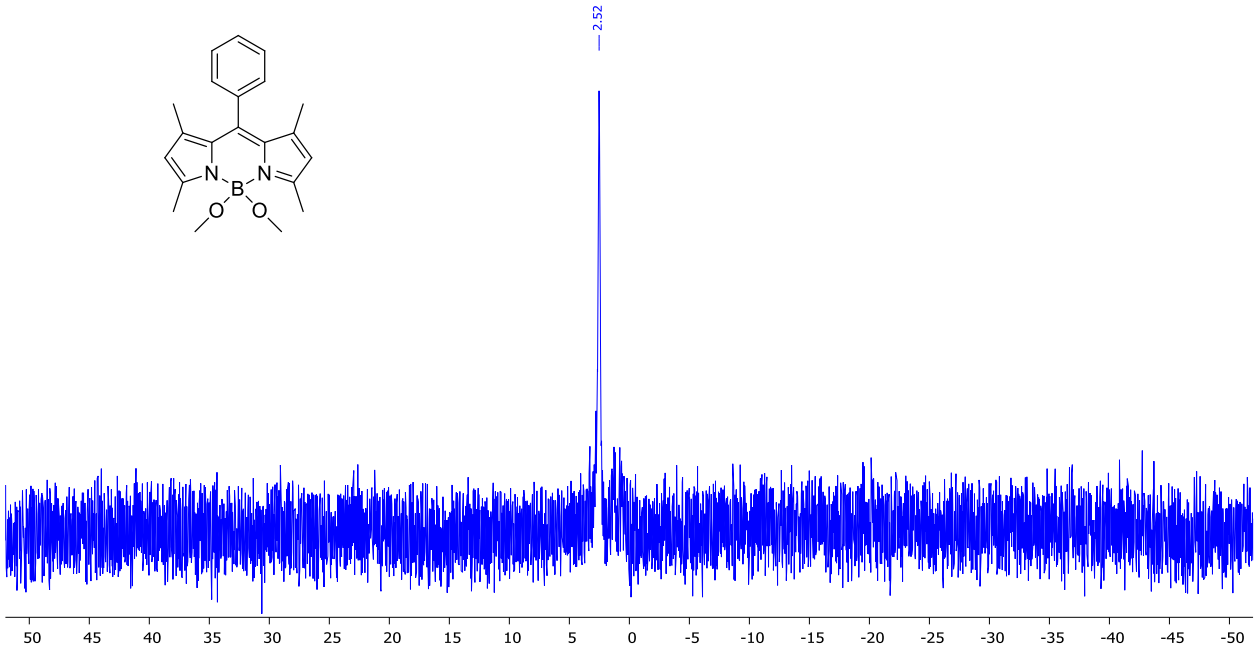

Figure A.24: ^{11}B NMR of BODIPY **1a** in $CDCl_3$ (128 MHz)

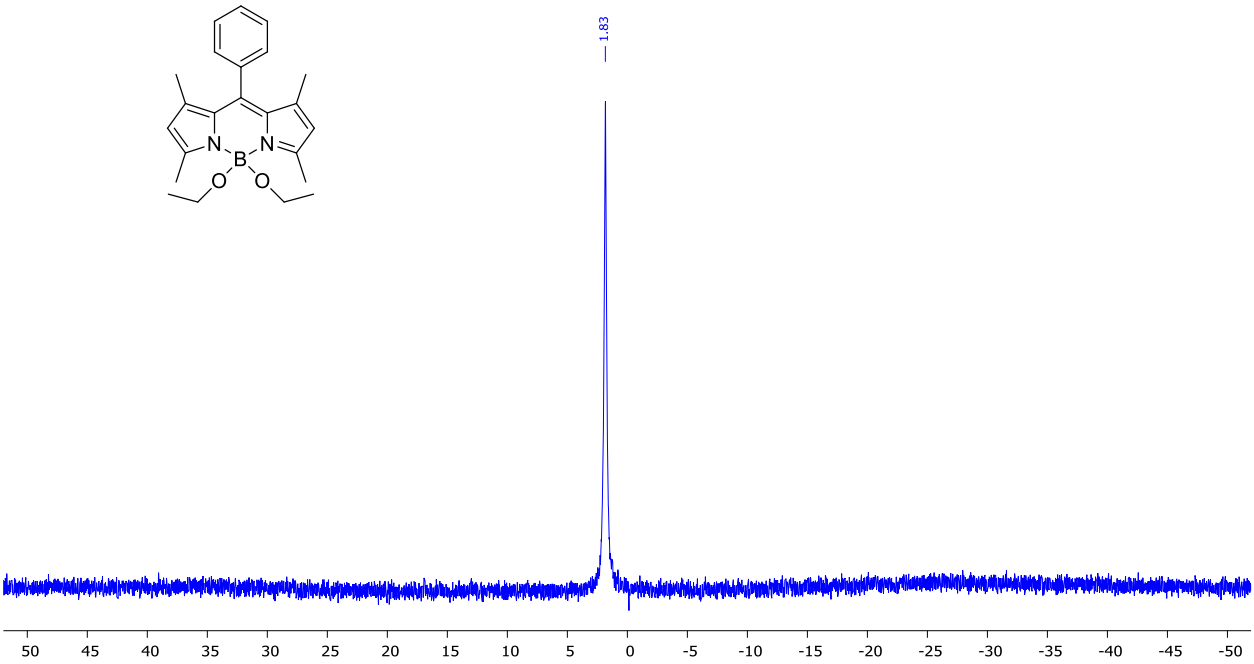

Figure A.25: ^{11}B NMR of BODIPY **1b** in $CDCl_3$ (128 MHz)

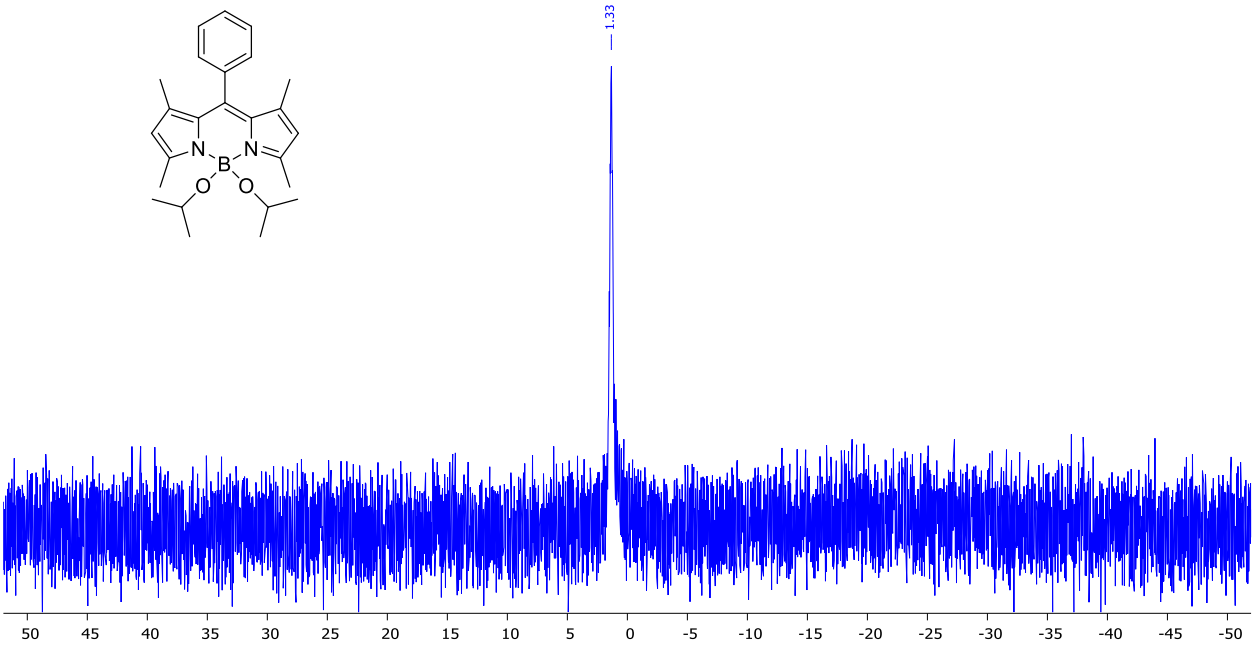

Figure A.26: ^{11}B NMR of BODIPY **1c** in $CDCl_3$ (128 MHz)

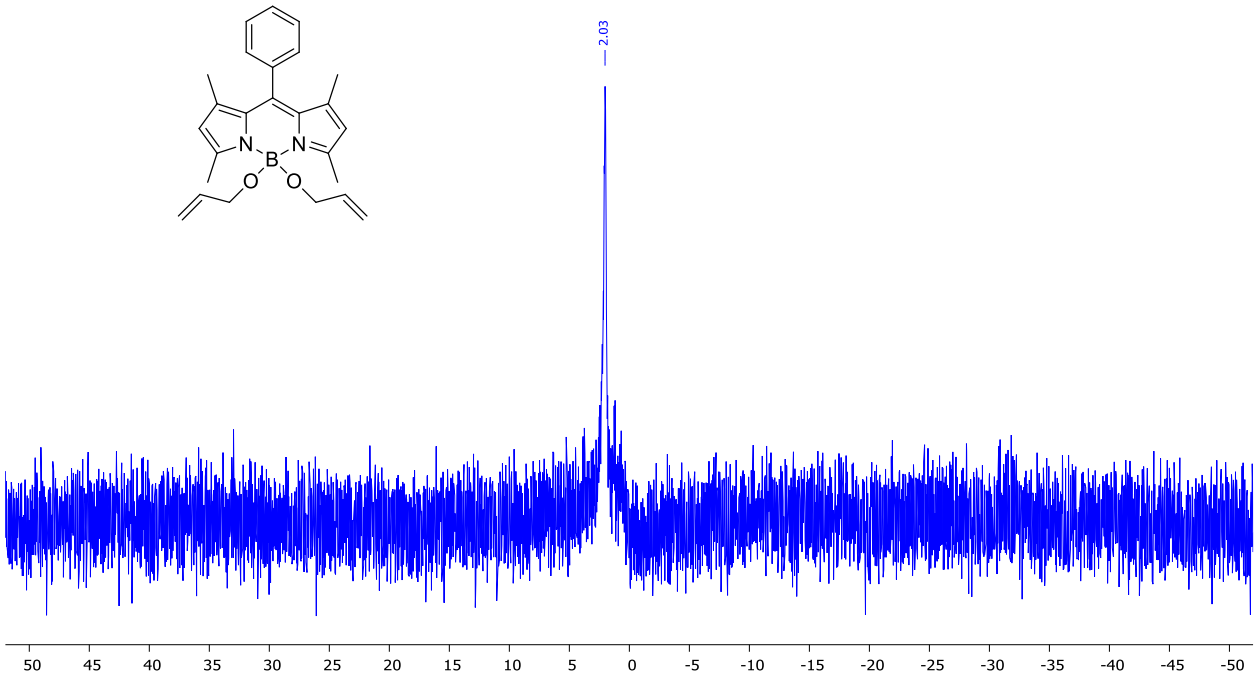

Figure A.27: ^{11}B NMR of BODIPY **1d** in $CDCl_3$ (128 MHz)

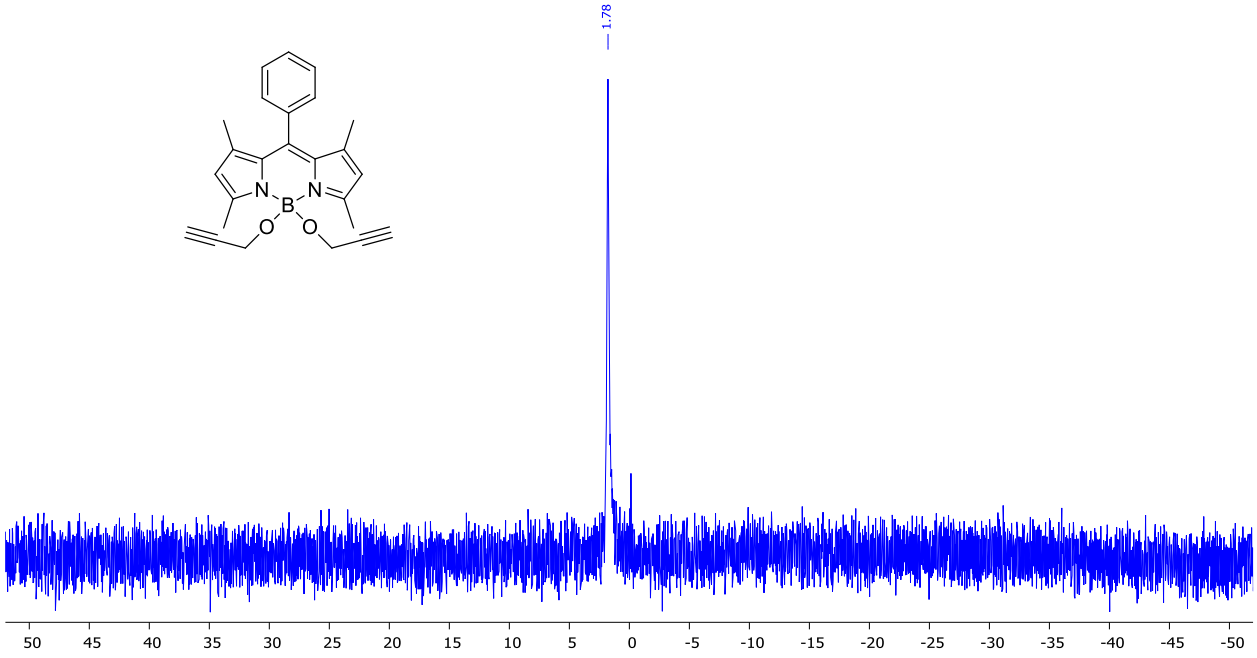

Figure A.28: ^{11}B NMR of BODIPY **1e** in $CDCl_3$ (128 MHz)

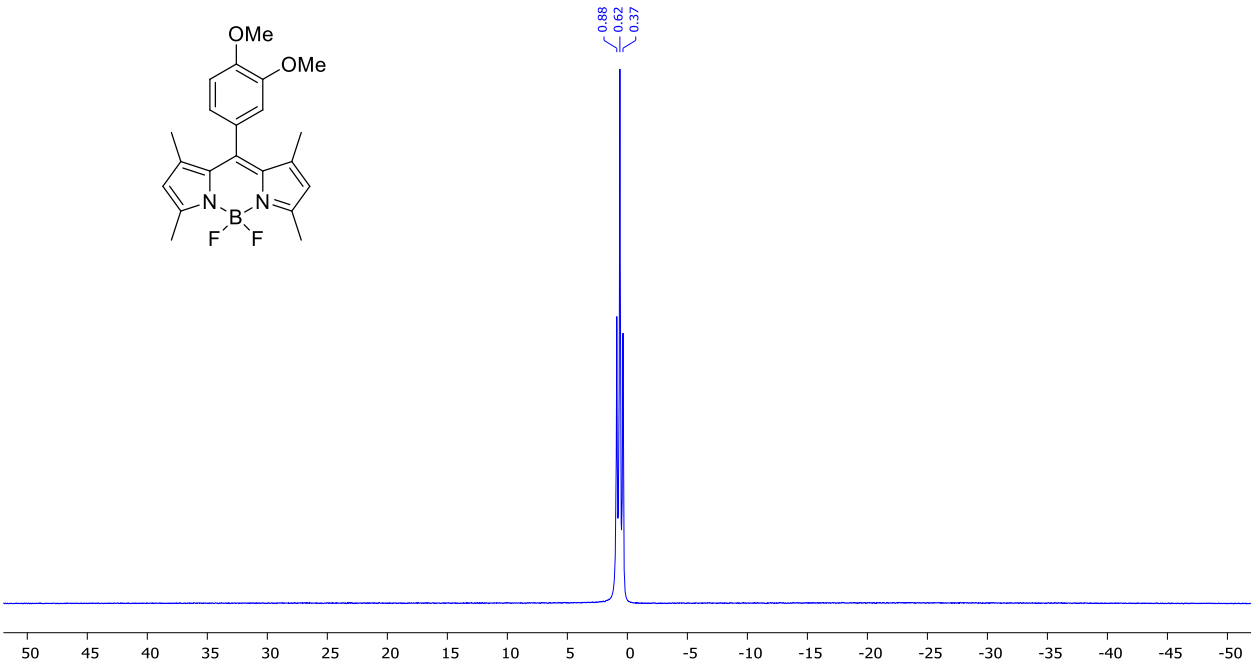

Figure A.29: ^{11}B NMR of BODIPY **2** in $CDCl_3$ (128 MHz)

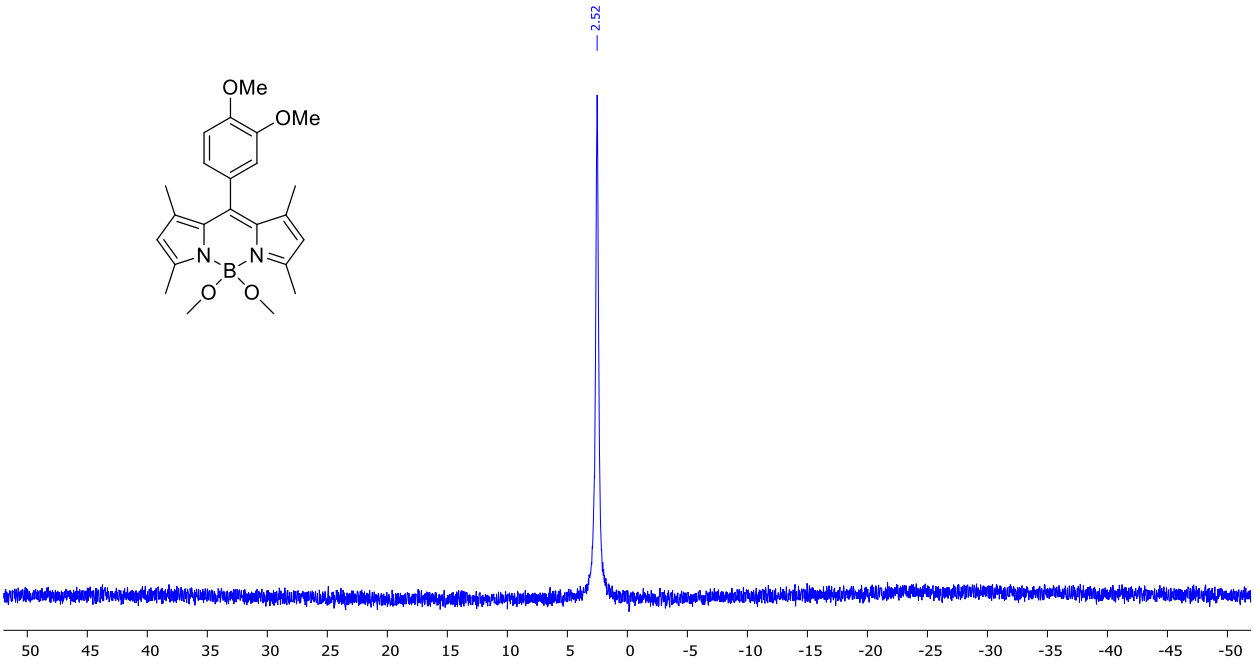

Figure A.30: ^{11}B NMR of BODIPY **2a** in $CDCl_3$ (128 MHz)

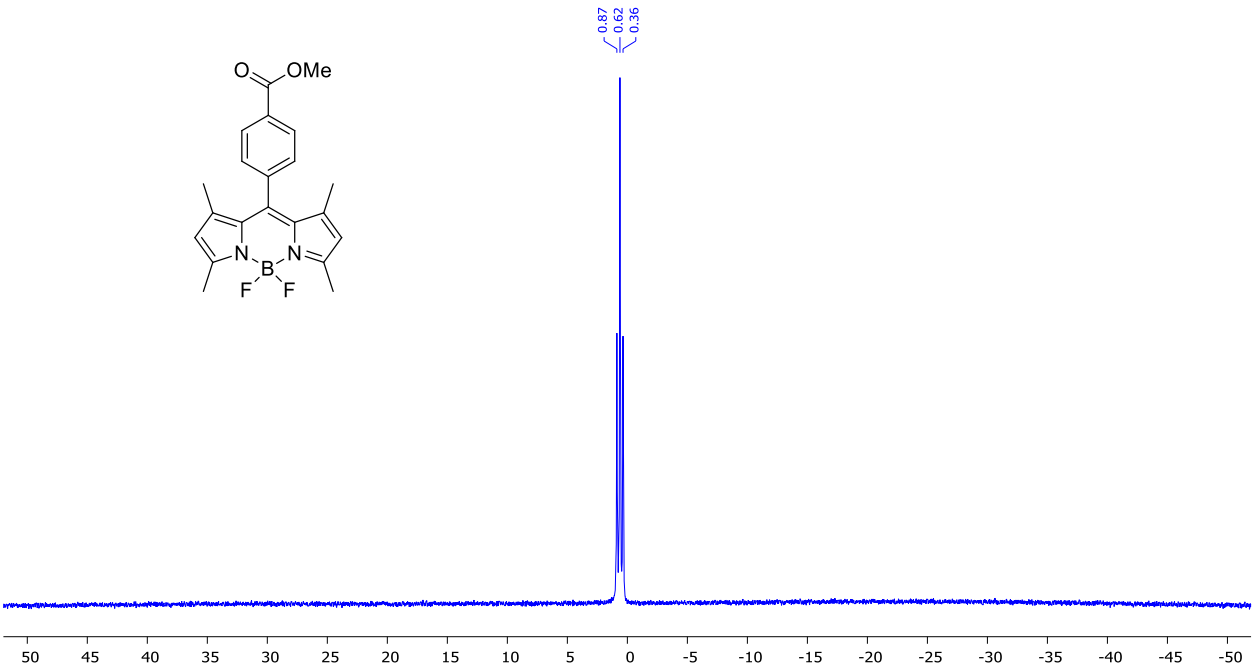

Figure A.31: ^{11}B NMR of BODIPY **3** in $CDCl_3$ (128 MHz)

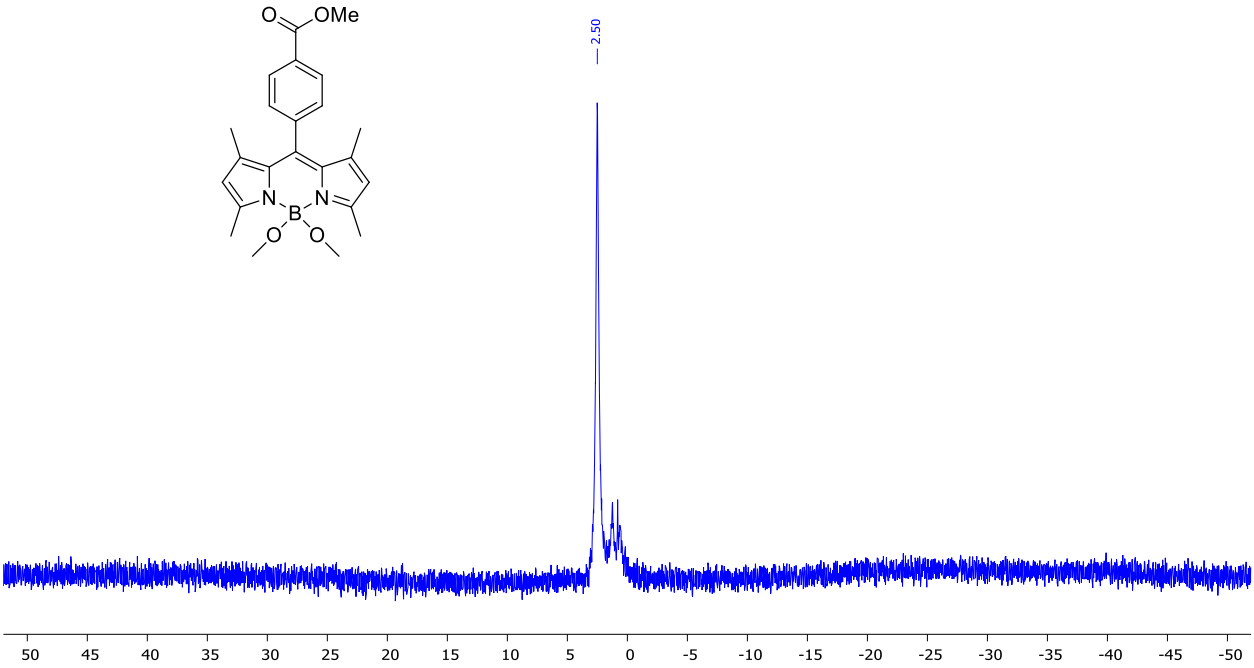

Figure A.32: ^{11}B NMR of BODIPY **3a** in $CDCl_3$ (128 MHz)

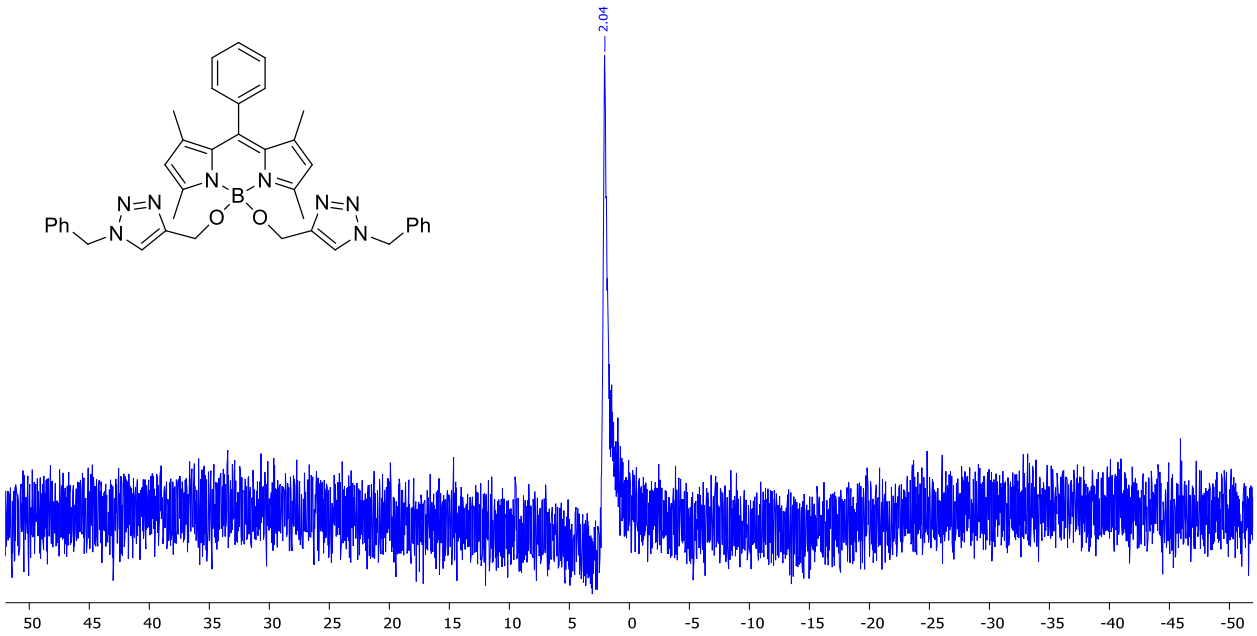

Figure A.33: ^{11}B NMR of BODIPY **4** in $CDCl_3$ (128 MHz)

APPENDIX B: NMR Characterization of Compounds Found in Chapter 3

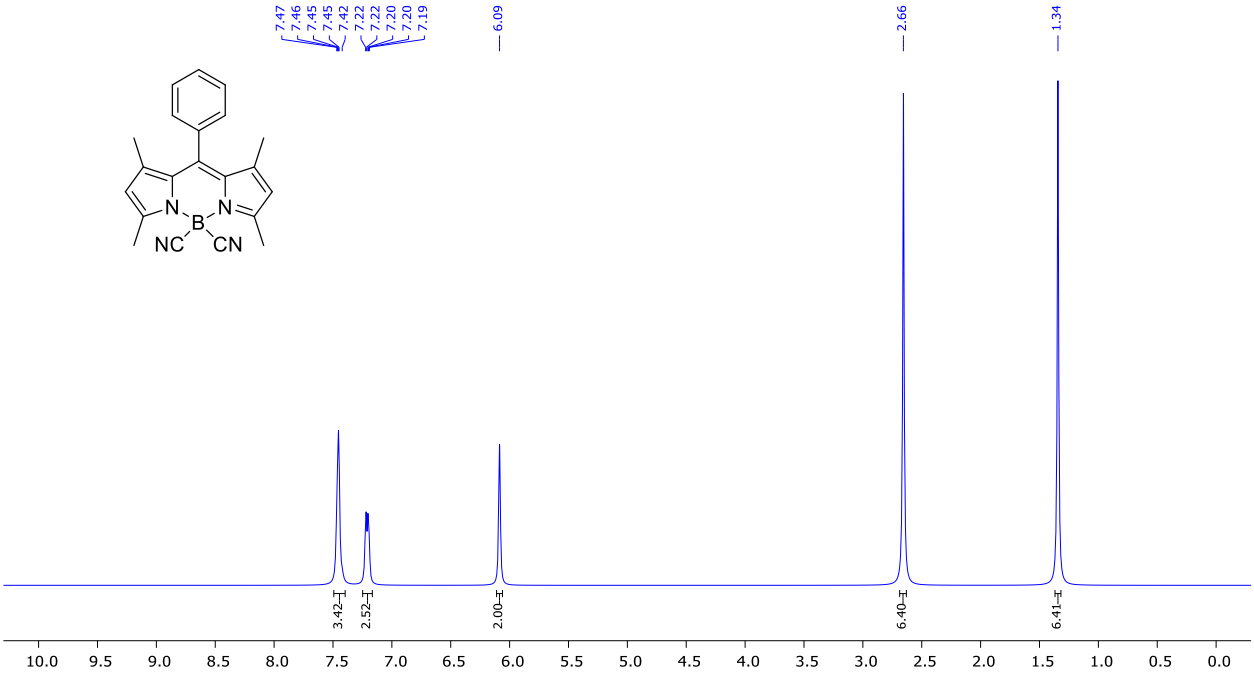

Figure B.1: ^{1}H NMR of BODIPY **1a** in $CDCl_3$ (400 MHz)

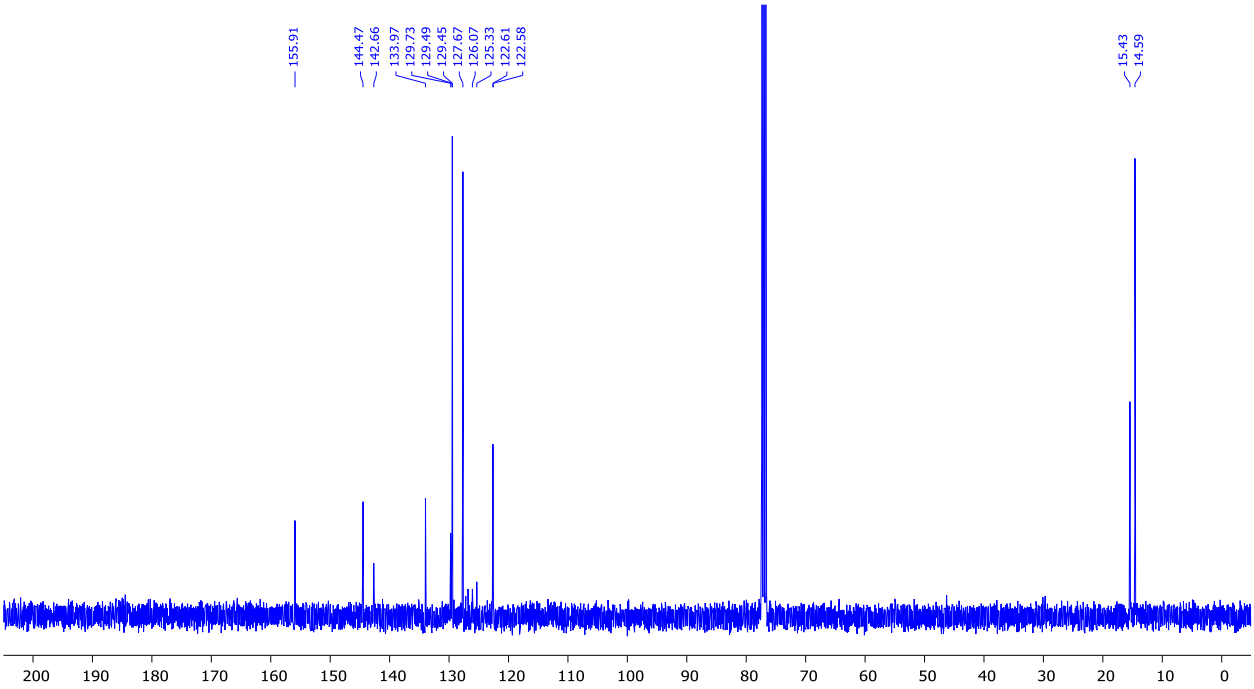

Figure B.2: ^{13}C NMR of BODIPY **1a** in $CDCl_3$ (100 MHz)

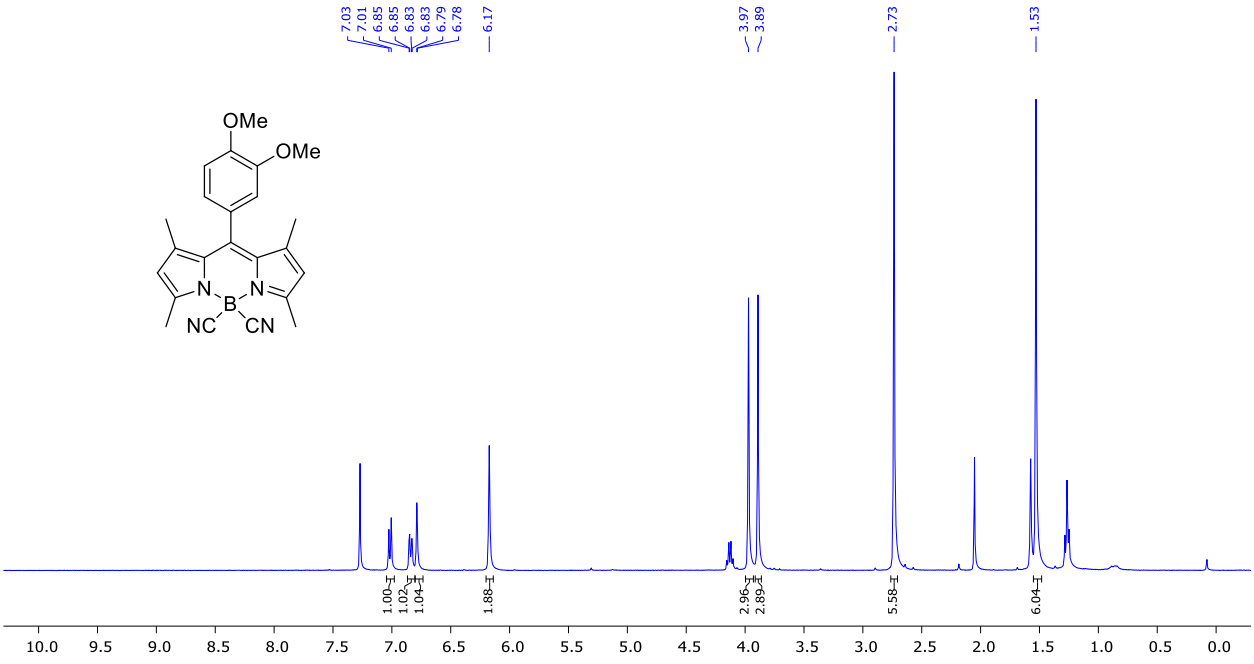

Figure B.3: ^{1}H NMR of BODIPY **2a** in $CDCl_3$ (400 MHz)

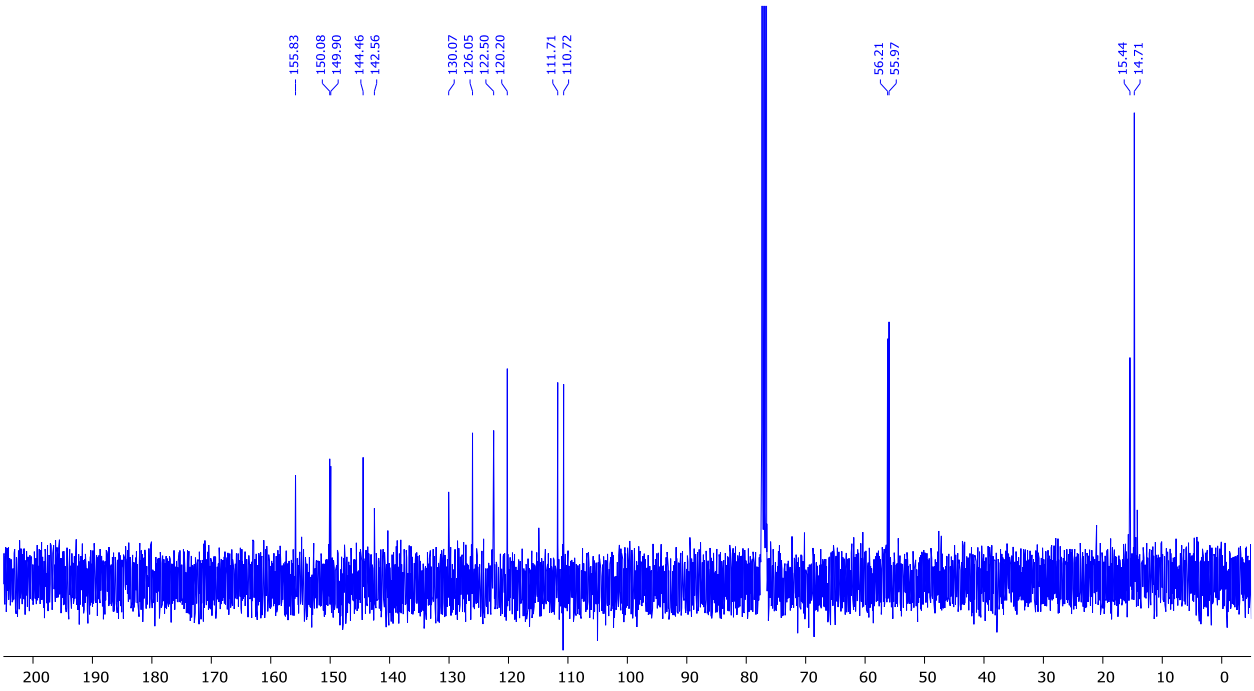

Figure B.4: ^{13}C NMR of BODIPY **2a** in $CDCl_3$ (100 MHz)

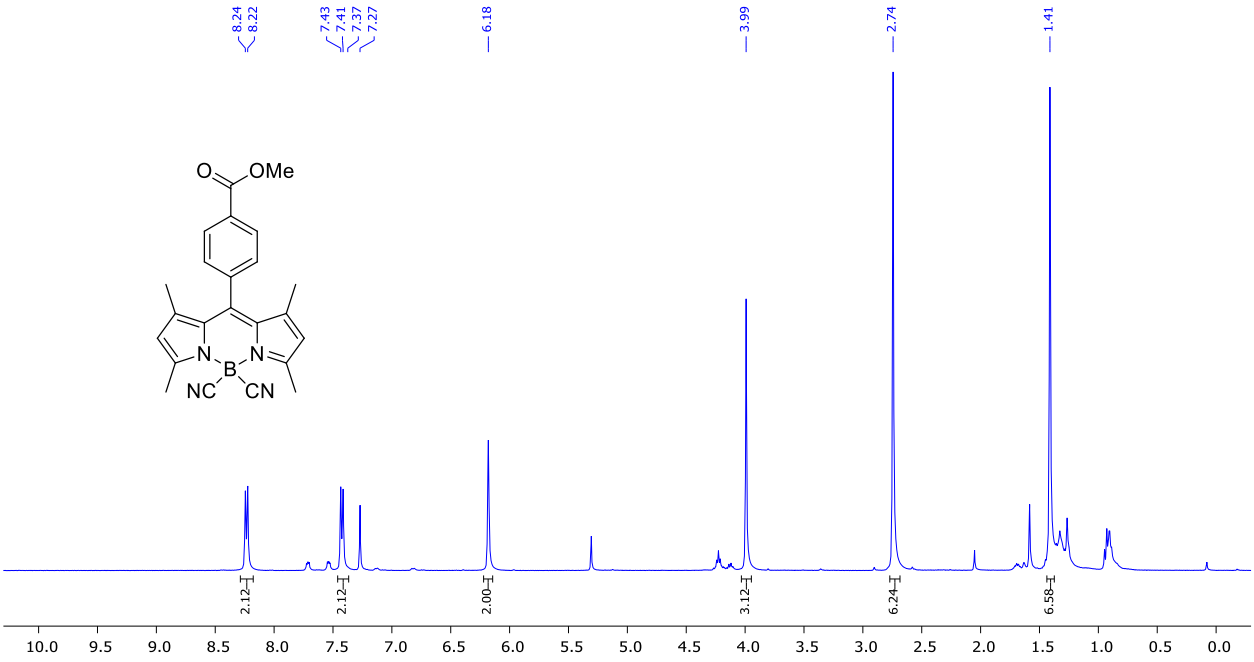

Figure B.5: ^{1}H NMR of BODIPY **3a** in $CDCl_3$ (400 MHz)

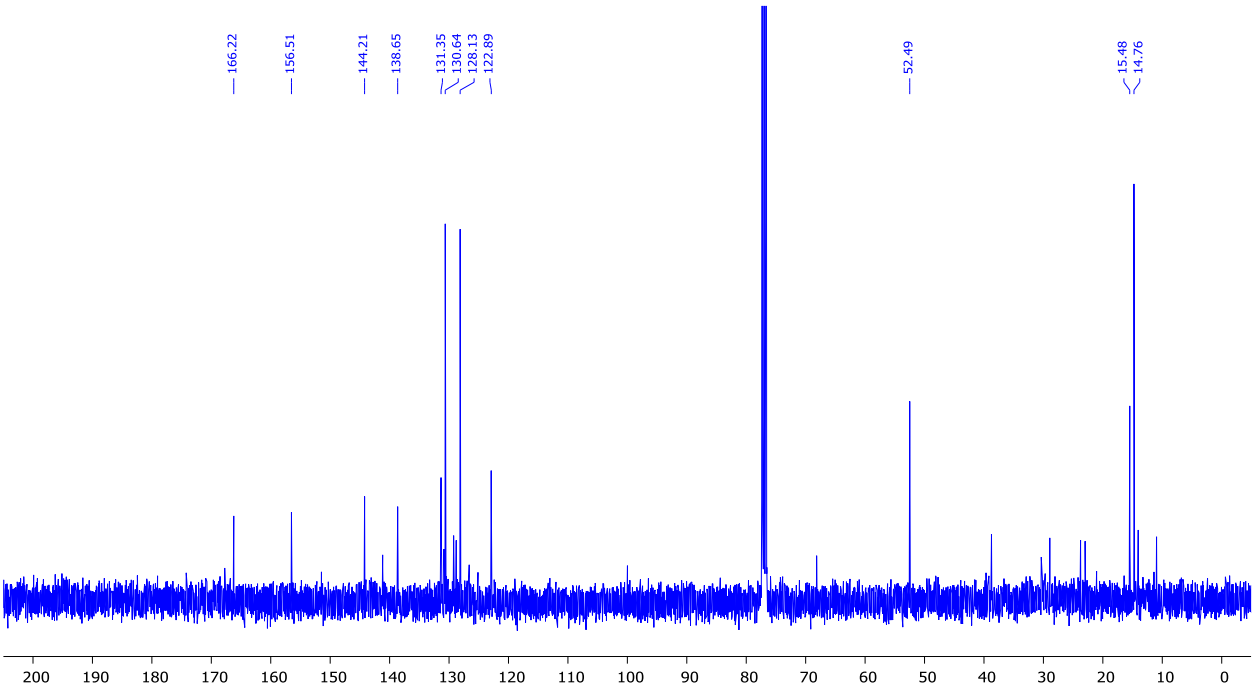

Figure B.6: ^{13}C NMR of BODIPY **3a** in $CDCl_3$ (100 MHz)

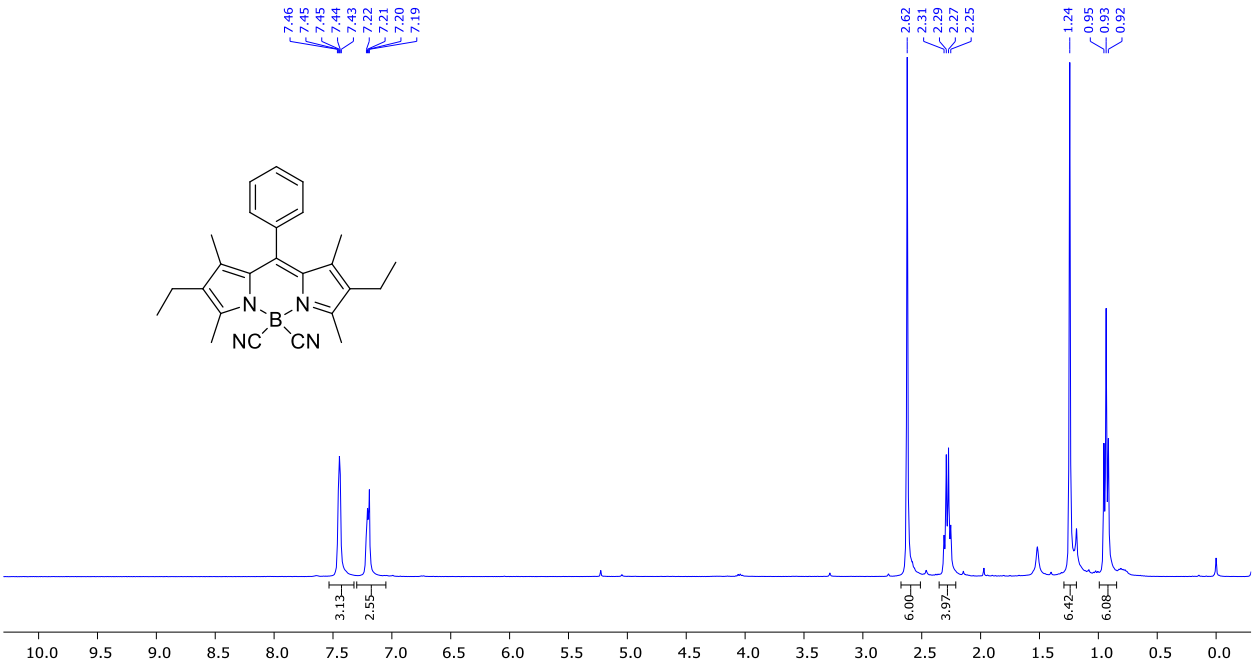

Figure B.7: ^{1}H NMR of BODIPY **4a** in $CDCl_3$ (400 MHz)

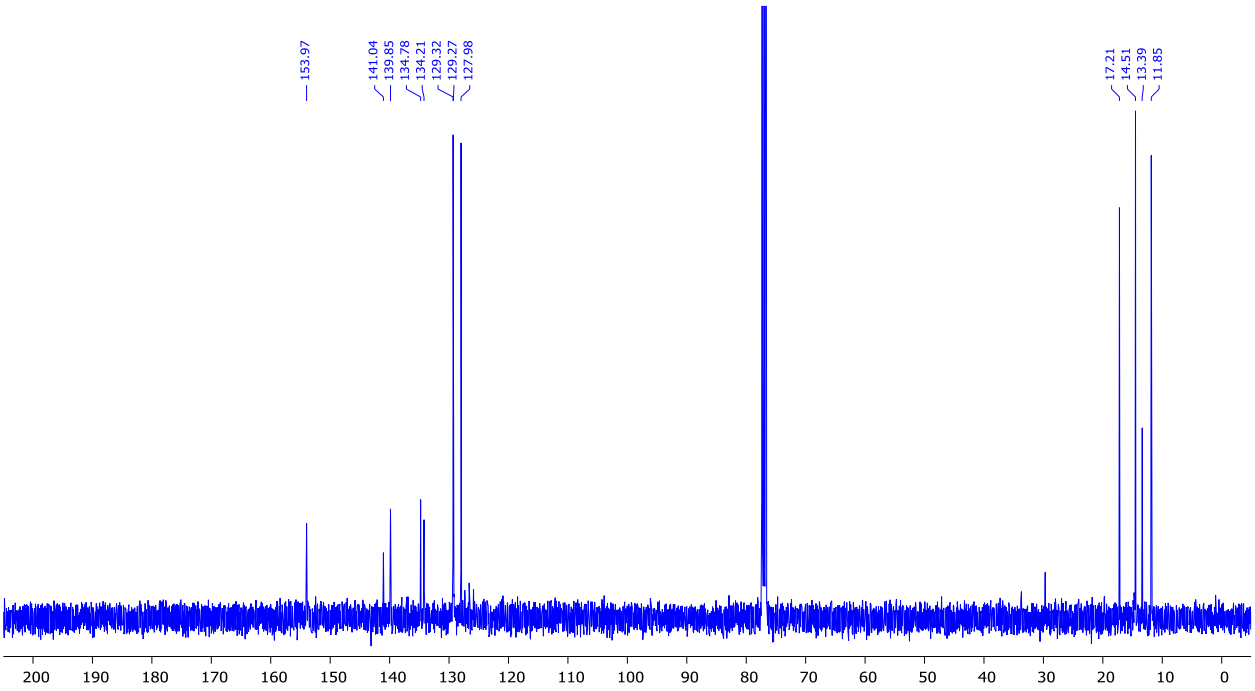

Figure B.8: ^{13}C NMR of BODIPY **4a** in $CDCl_3$ (100 MHz)

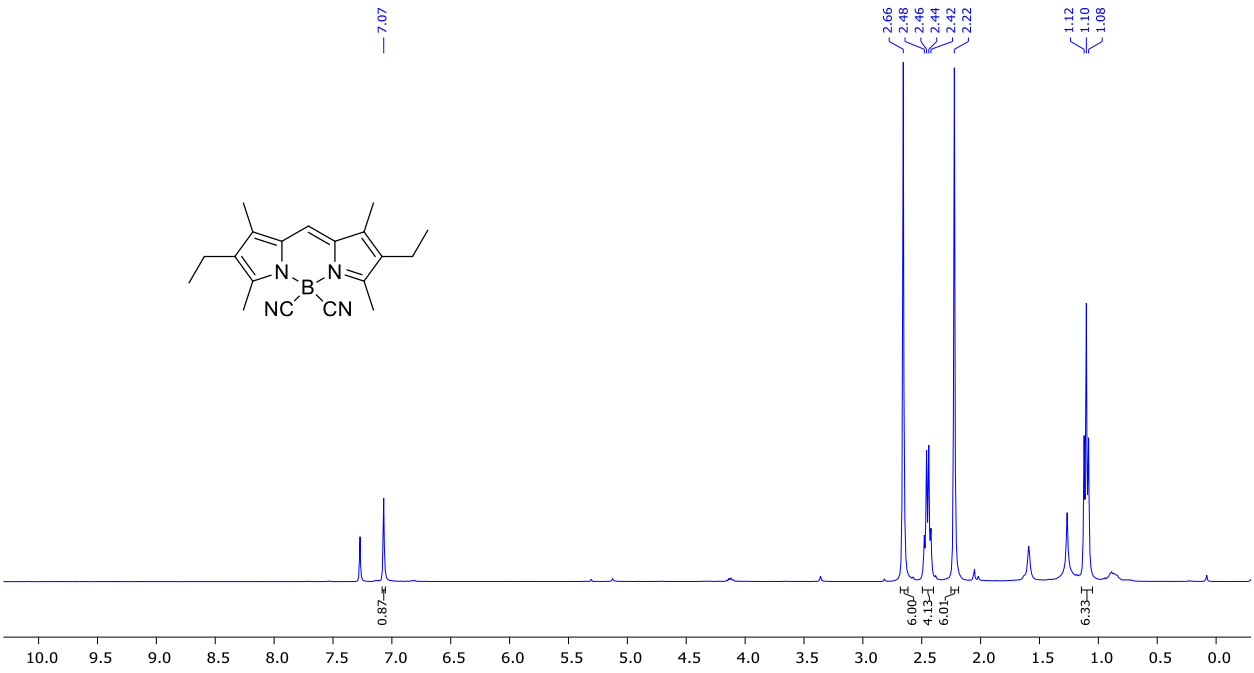

Figure B.9: ^{1}H NMR of BODIPY **5a** in $CDCl_3$ (400 MHz)

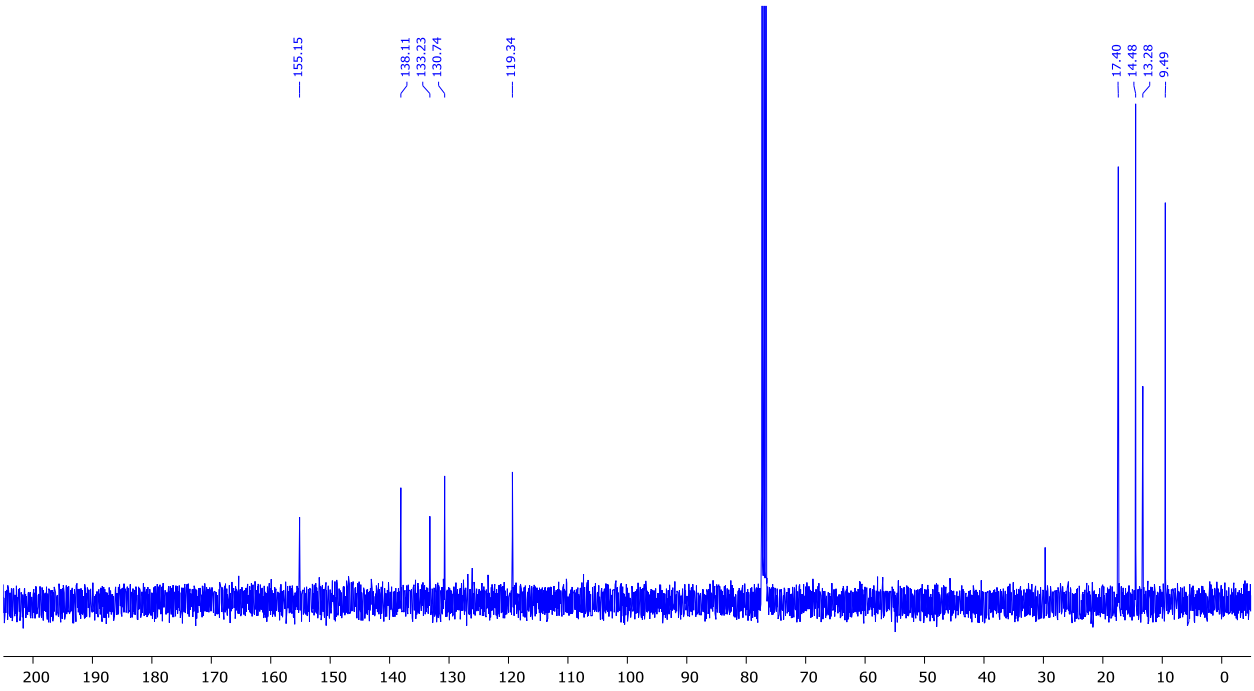

Figure B.10: ^{13}C NMR of BODIPY **5a** in $CDCl_3$ (100 MHz)

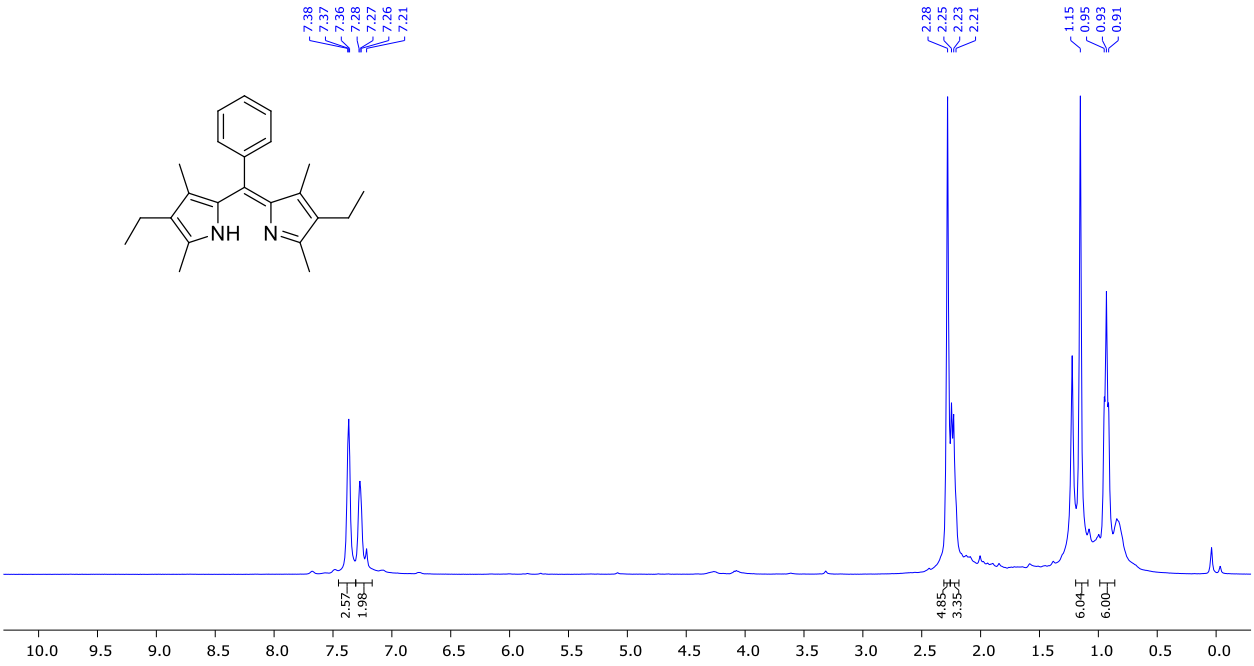

Figure B.11: ^{1}H NMR of Dipyrrin **7** in $CDCl_3$ (400 MHz)

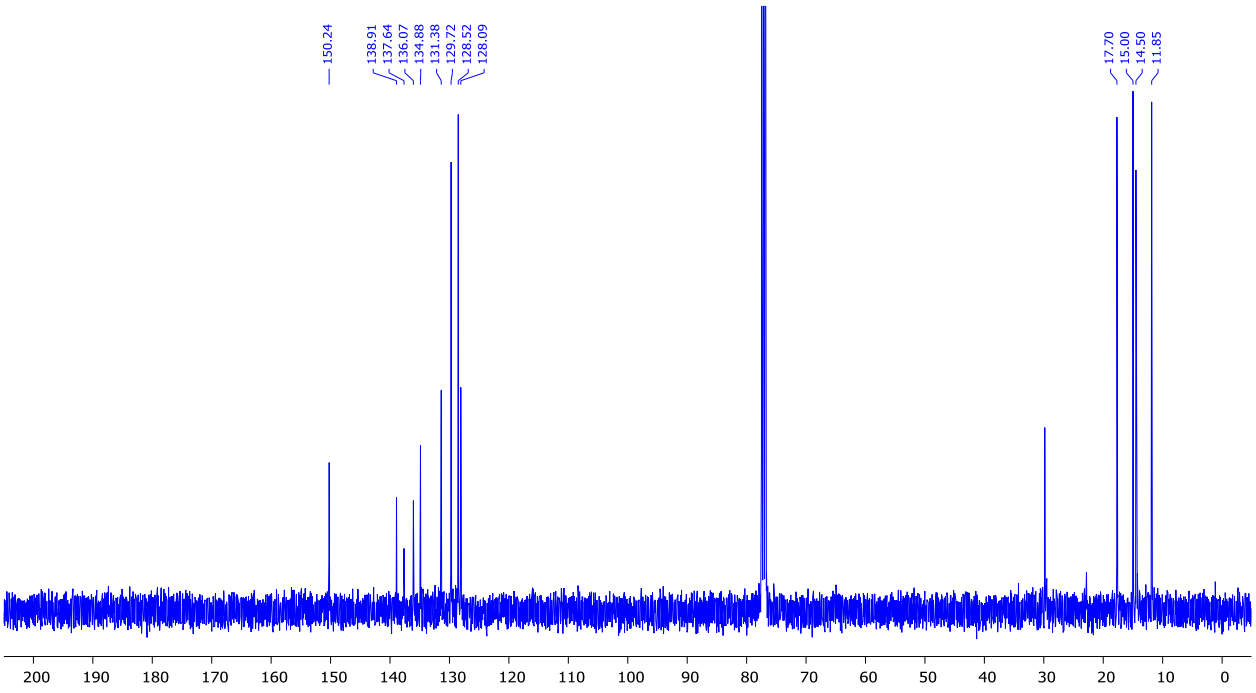

Figure B.12: ^{13}C NMR of Dipyrrin **7** in $CDCl_3$ (100 MHz)

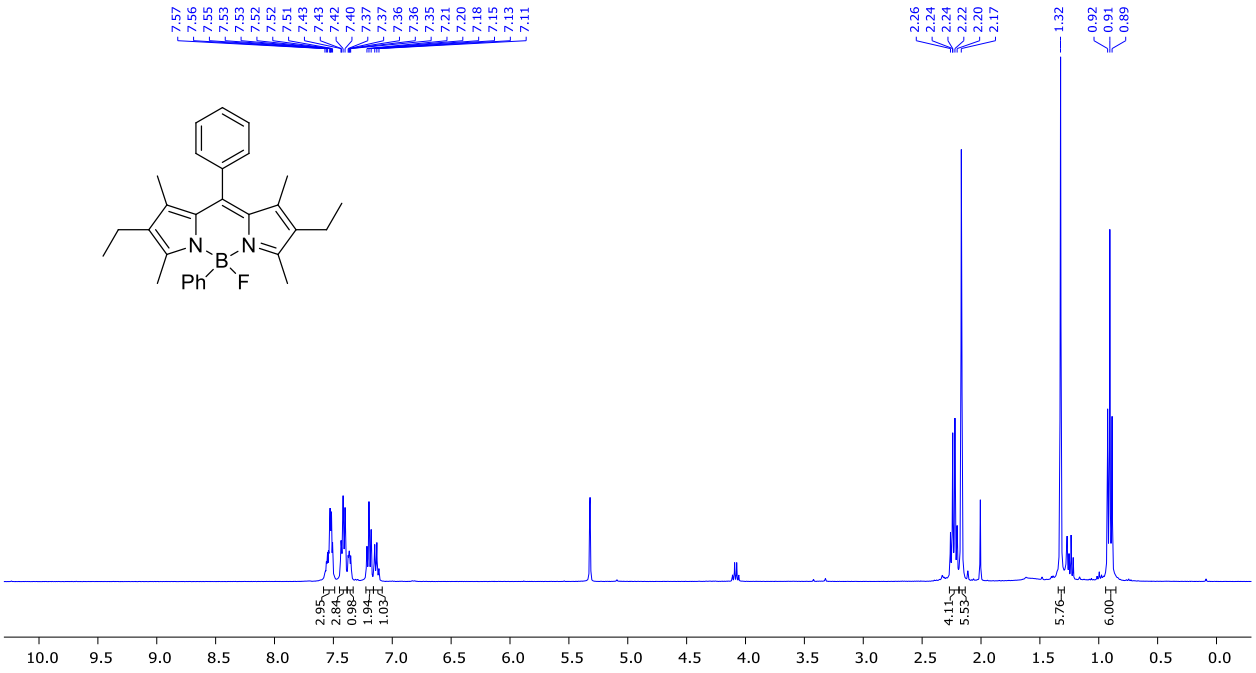

Figure B.13: ^{1}H NMR of BODIPY **7a** in CD_2Cl_2 (400 MHz)

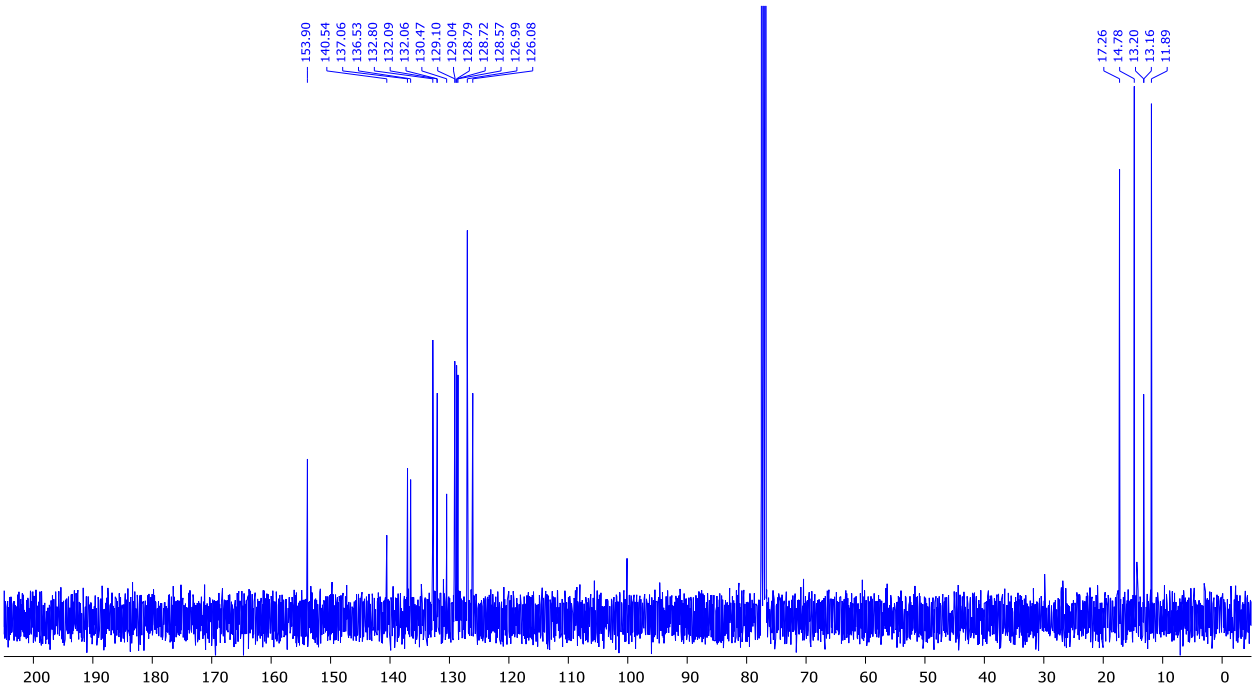

Figure B.14: ^{13}C NMR of BODIPY **7a** in $CDCl_3$ (100 MHz)

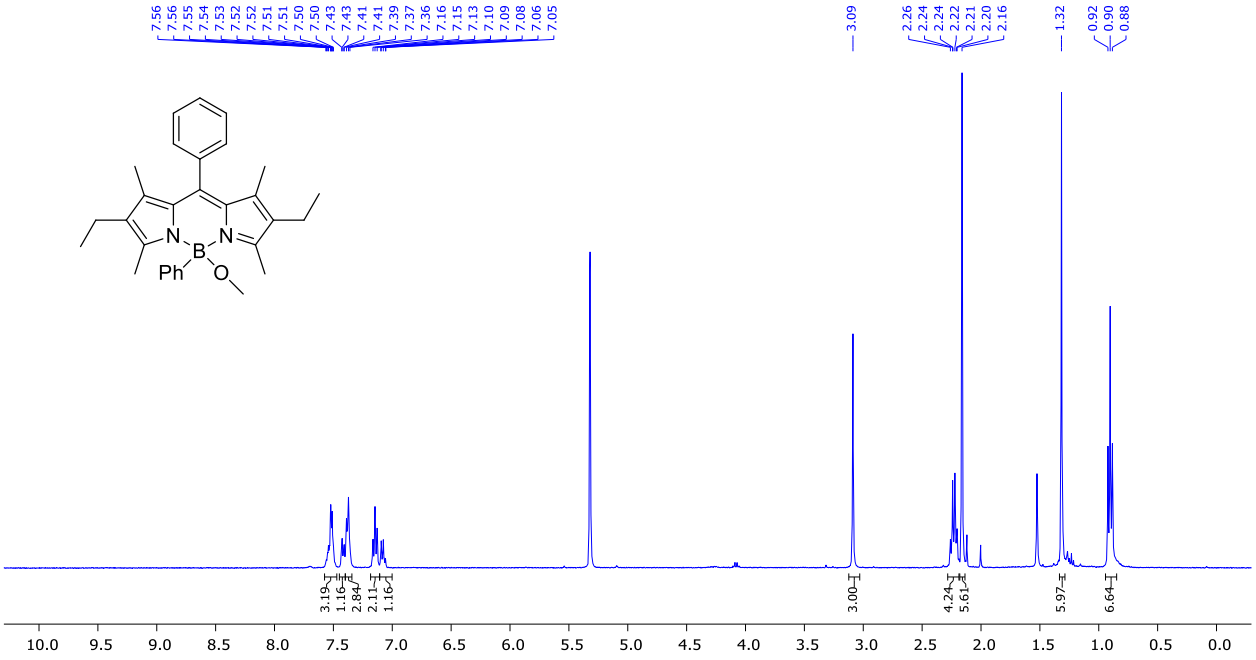

Figure B.15: ^{1}H NMR of BODIPY **7b** in CD_2Cl_2 (400 MHz)

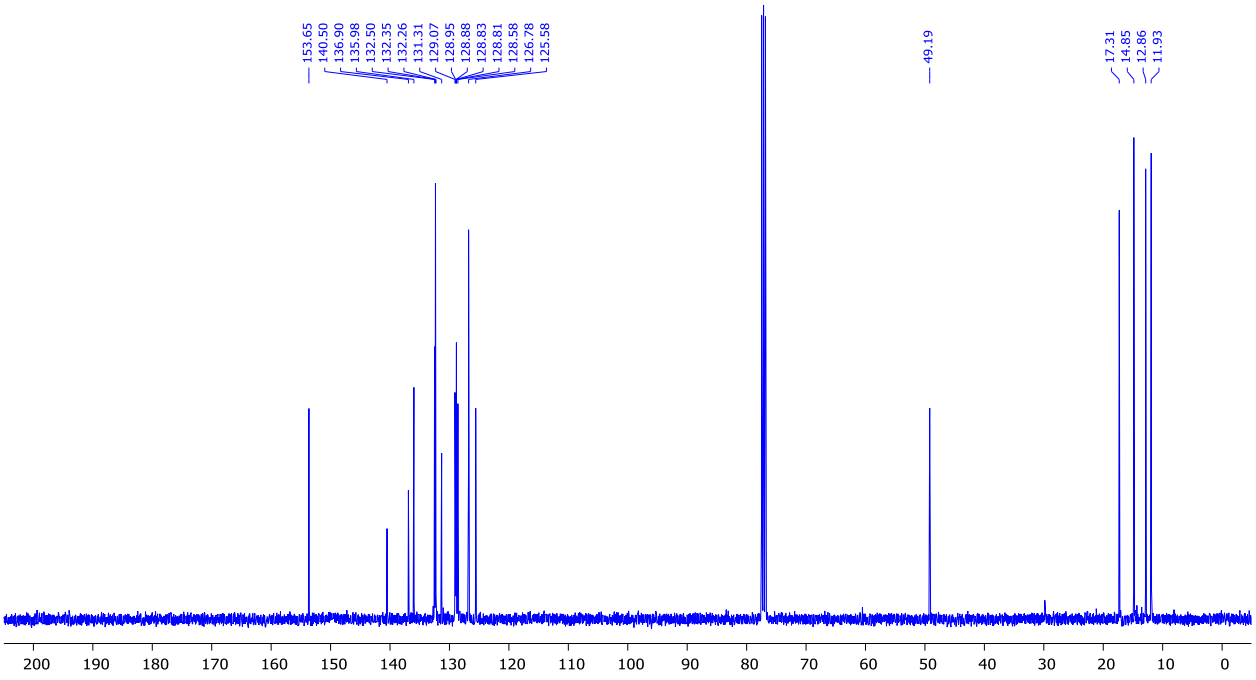

Figure B.16: ^{13}C NMR of BODIPY **7b** in $CDCl_3$ (100 MHz)

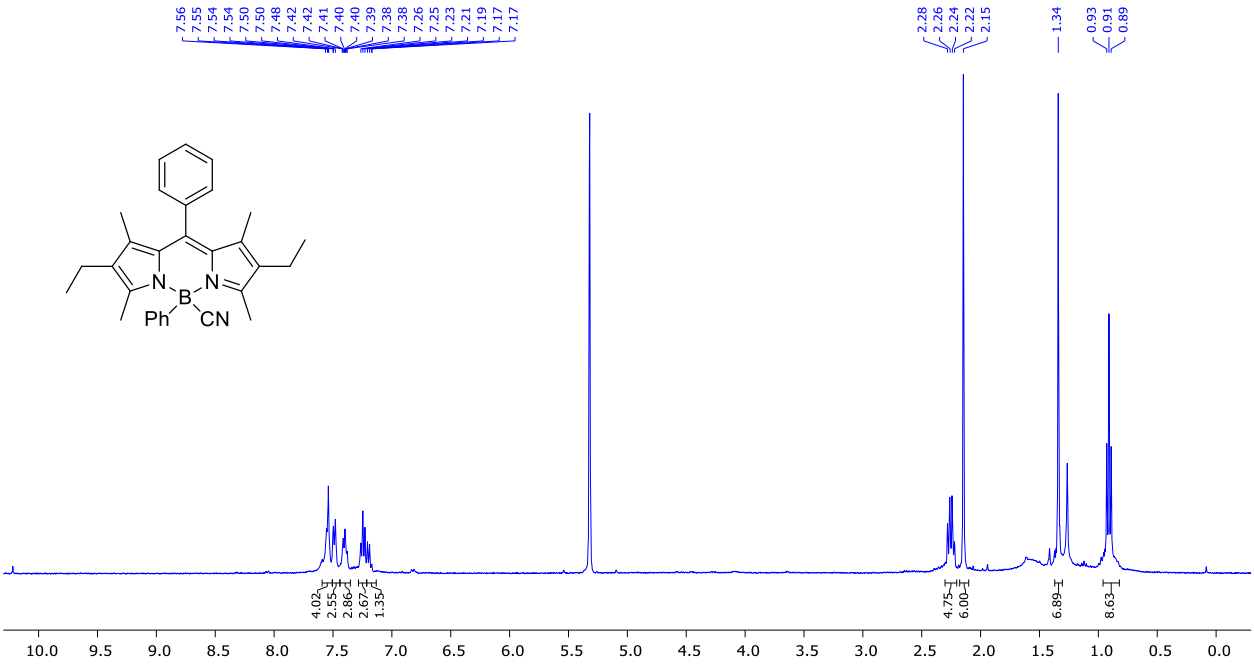

Figure B.17: ^{1}H NMR of BODIPY **7c** in CD_2Cl_2 (400 MHz)

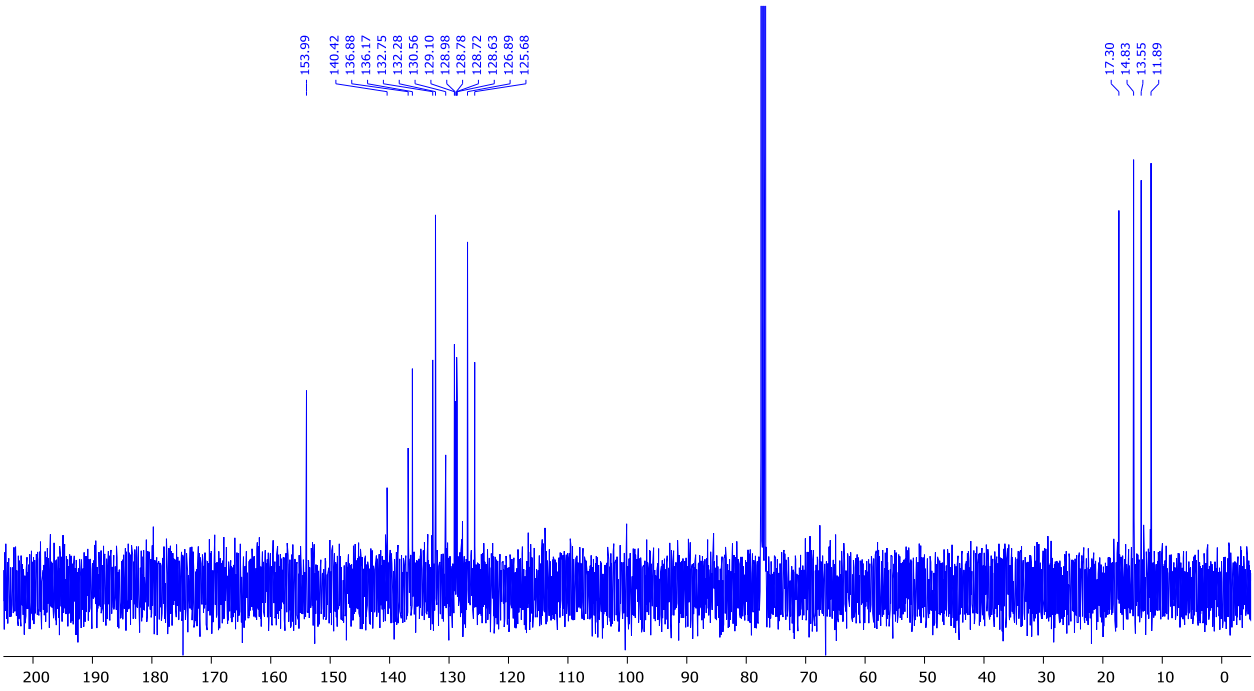

Figure B.18: ^{13}C NMR of BODIPY **7c** in $CDCl_3$ (100 MHz)

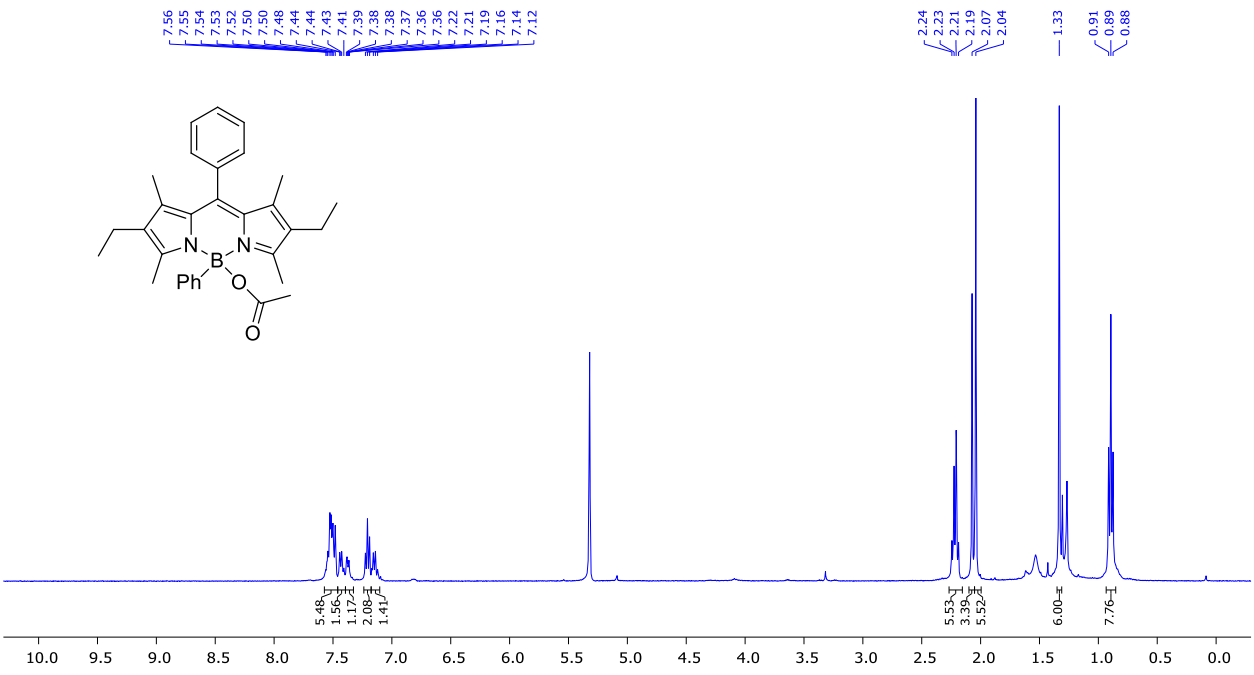

Figure B.19: ^{1}H NMR of BODIPY **7d** in CD_2Cl_2 (400 MHz)

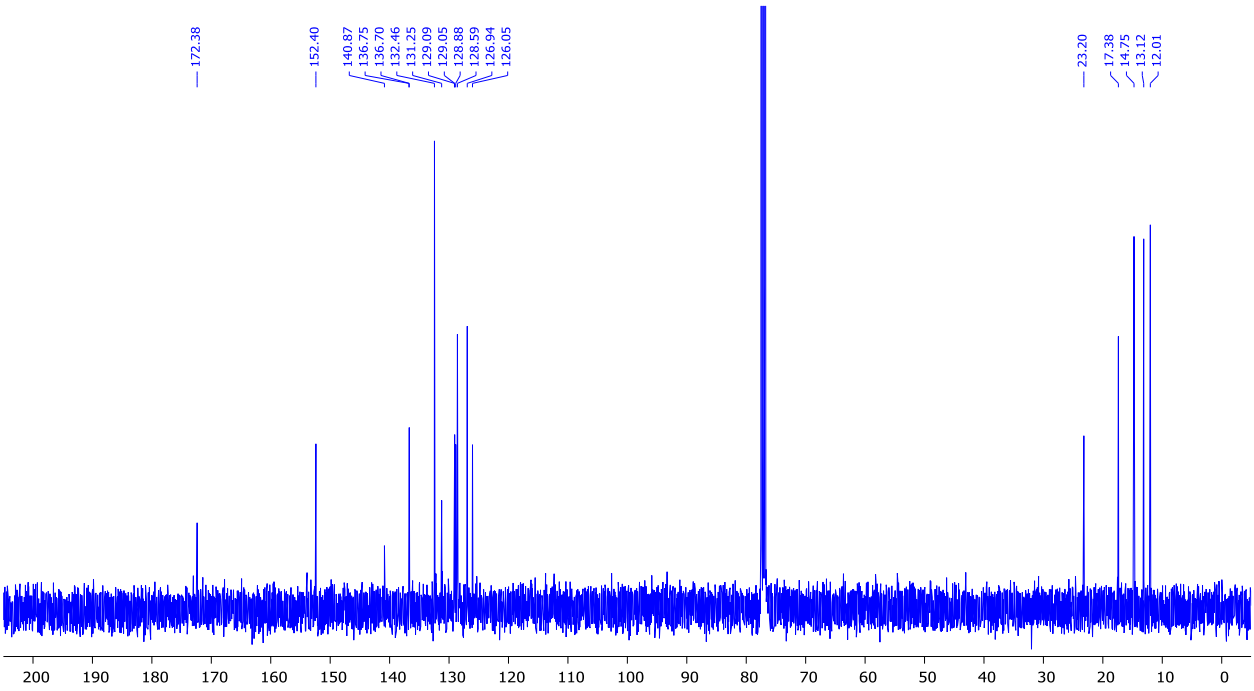

Figure B.20: ^{13}C NMR of BODIPY **7d** in $CDCl_3$ (100 MHz)

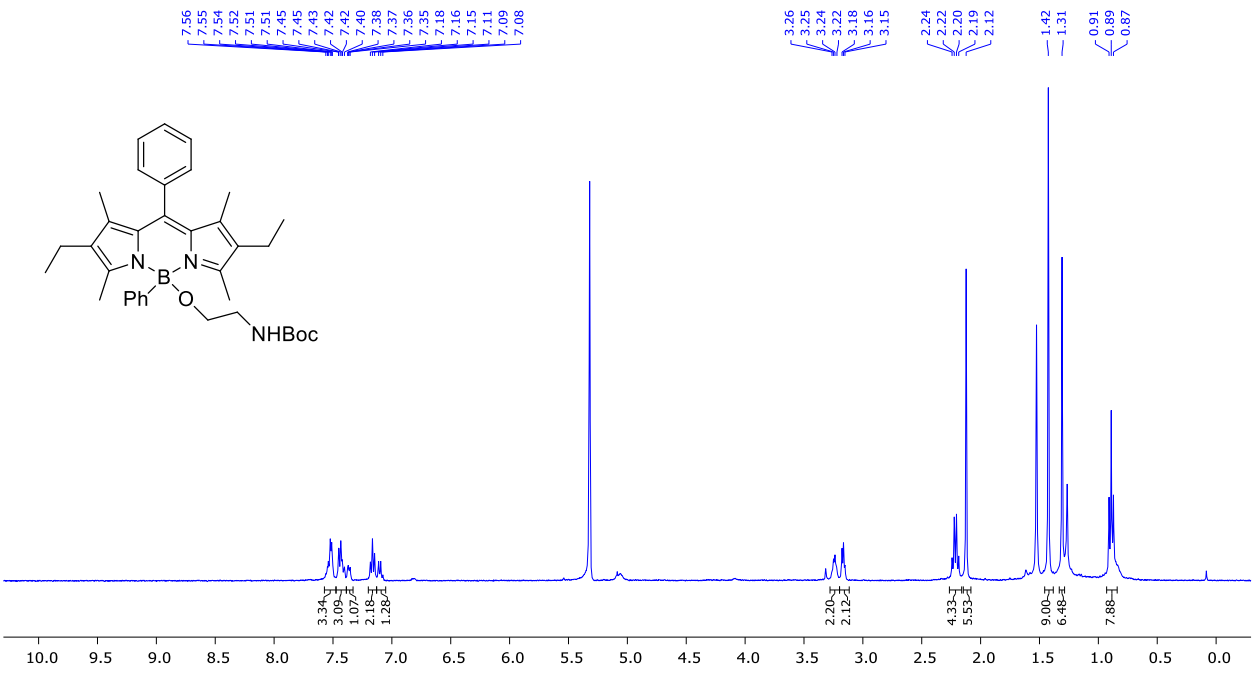

Figure B.21: ^{1}H NMR of BODIPY **7e** in CD_2Cl_2 (400 MHz)

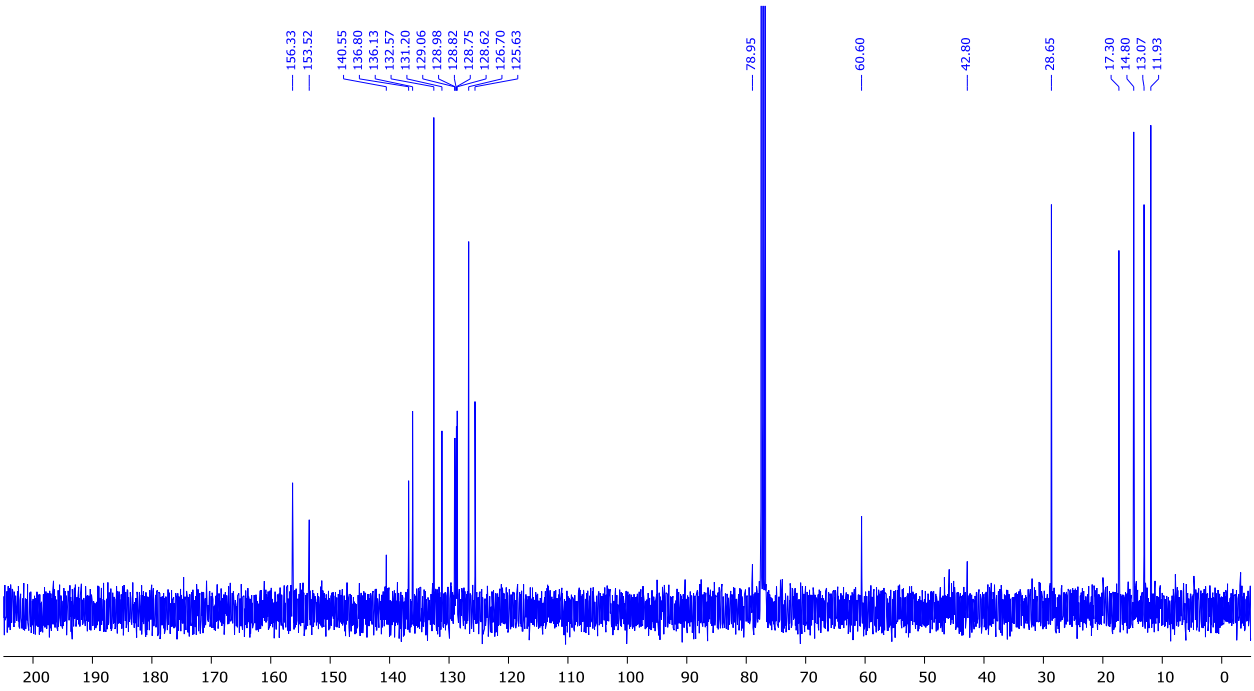

Figure B.22: ^{13}C NMR of BODIPY **7e** in $CDCl_3$ (100 MHz)

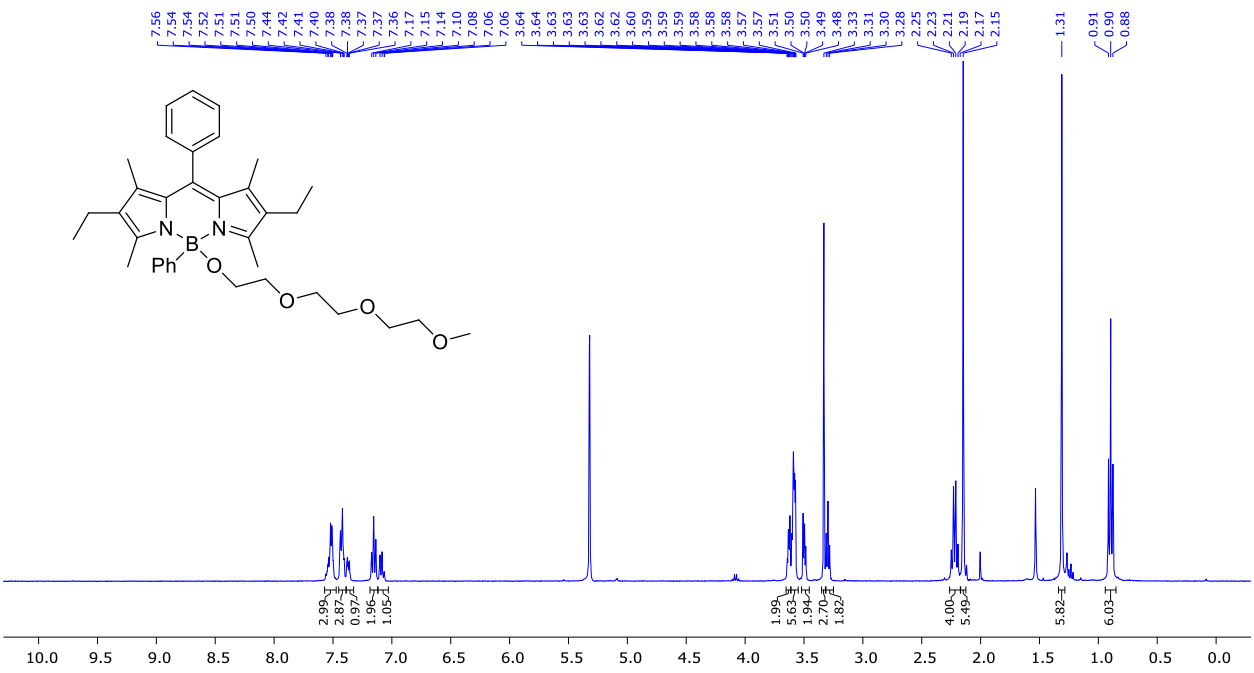

Figure B.23: ^{1}H NMR of BODIPY **7f** in CD_2Cl_2 (400 MHz)

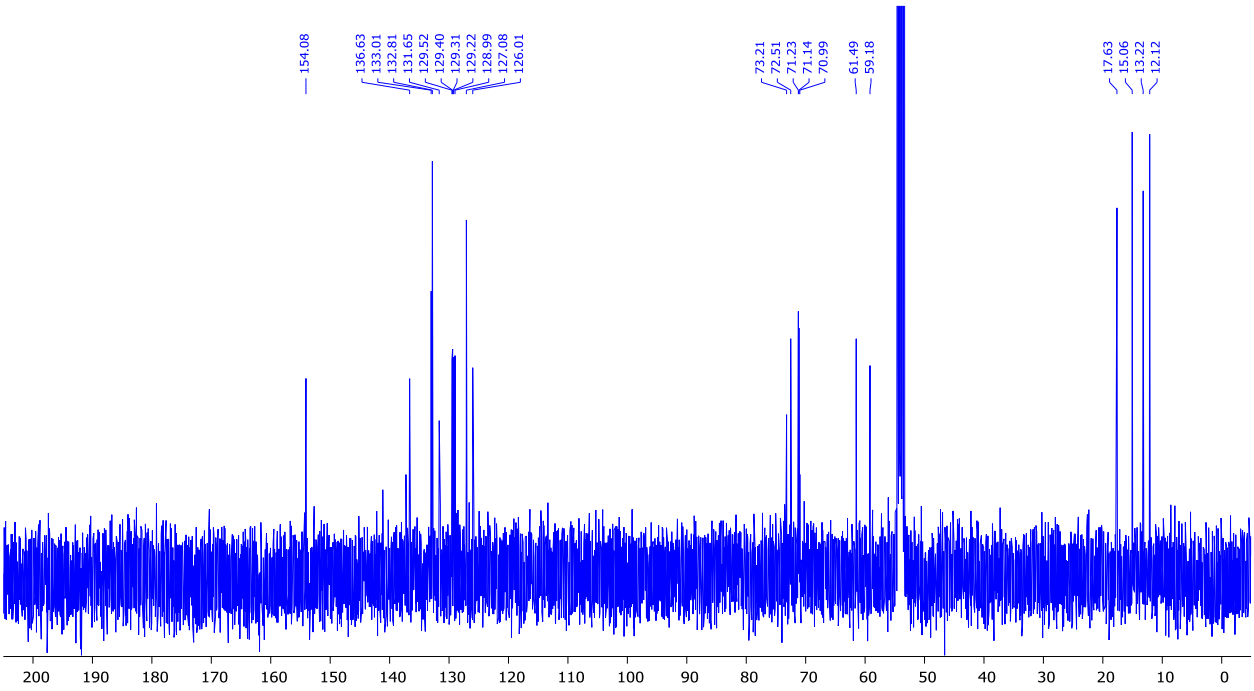

Figure B.24: ^{13}C NMR of BODIPY **7f** in CD_2Cl_2 (100 MHz)

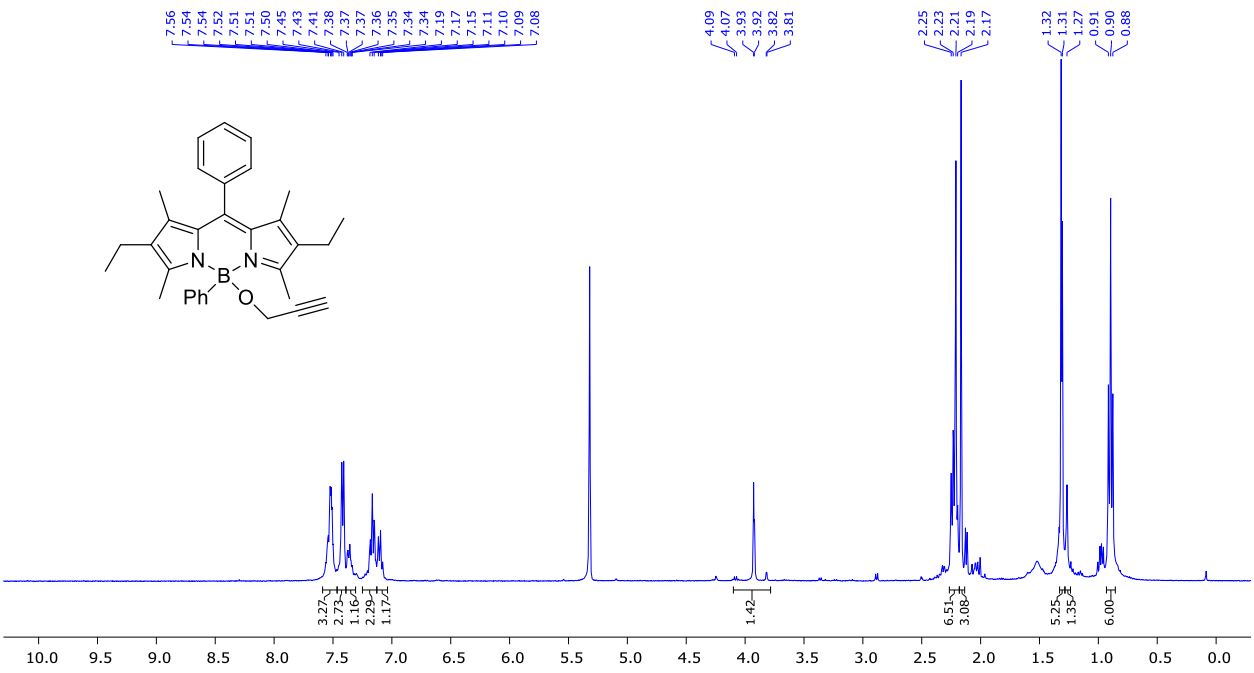

Figure B.25: ^{1}H NMR of BODIPY **7g** in CD_2Cl_2 (400 MHz)

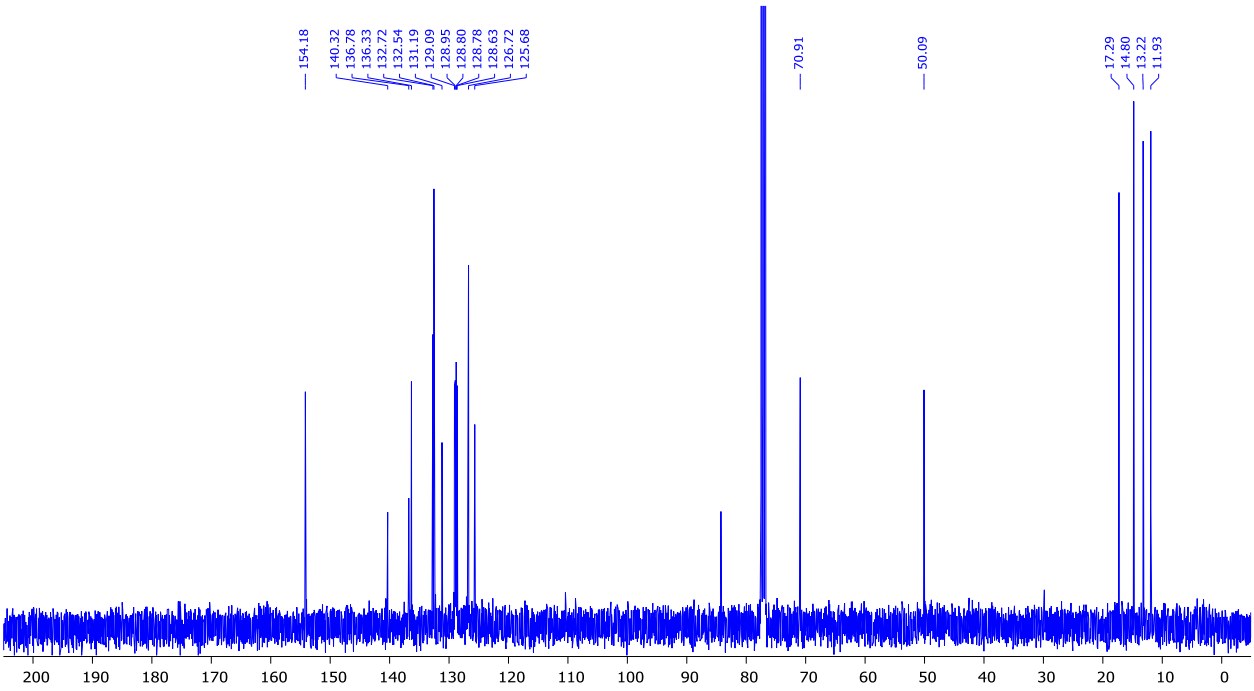

Figure B.26: ^{13}C NMR of BODIPY **7g** in $CDCl_3$ (100 MHz)

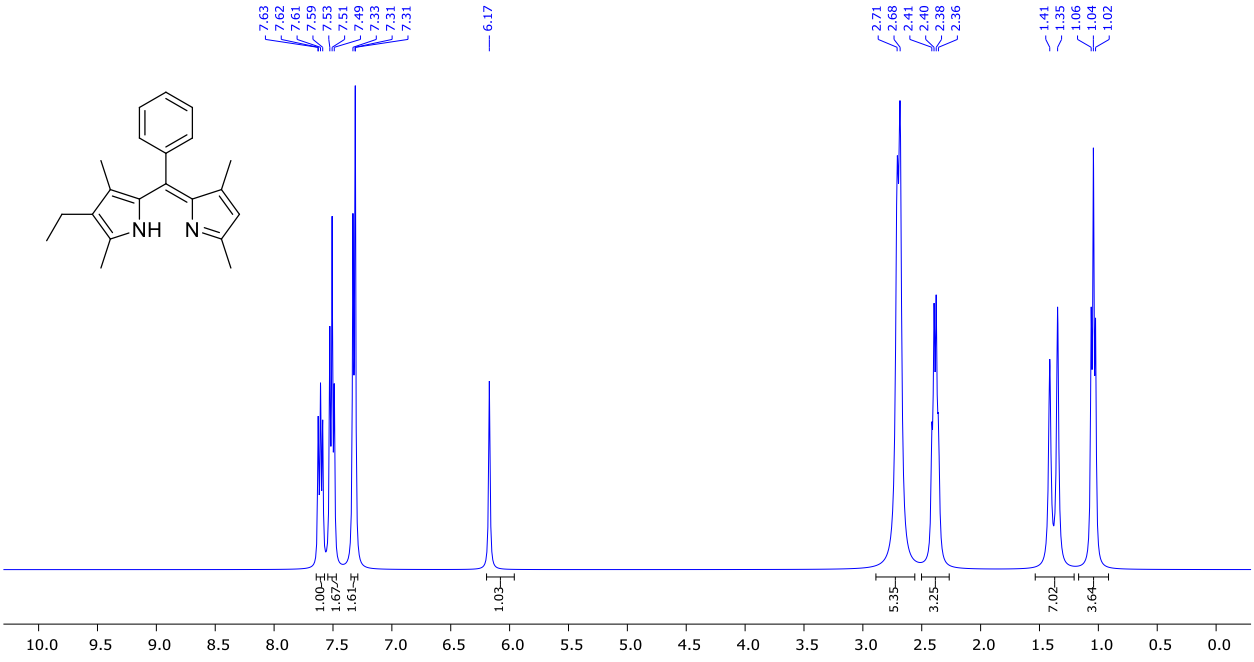

Figure B.27: ^{1}H NMR of Dipyrrin **8** in $CDCl_3$ (400 MHz)

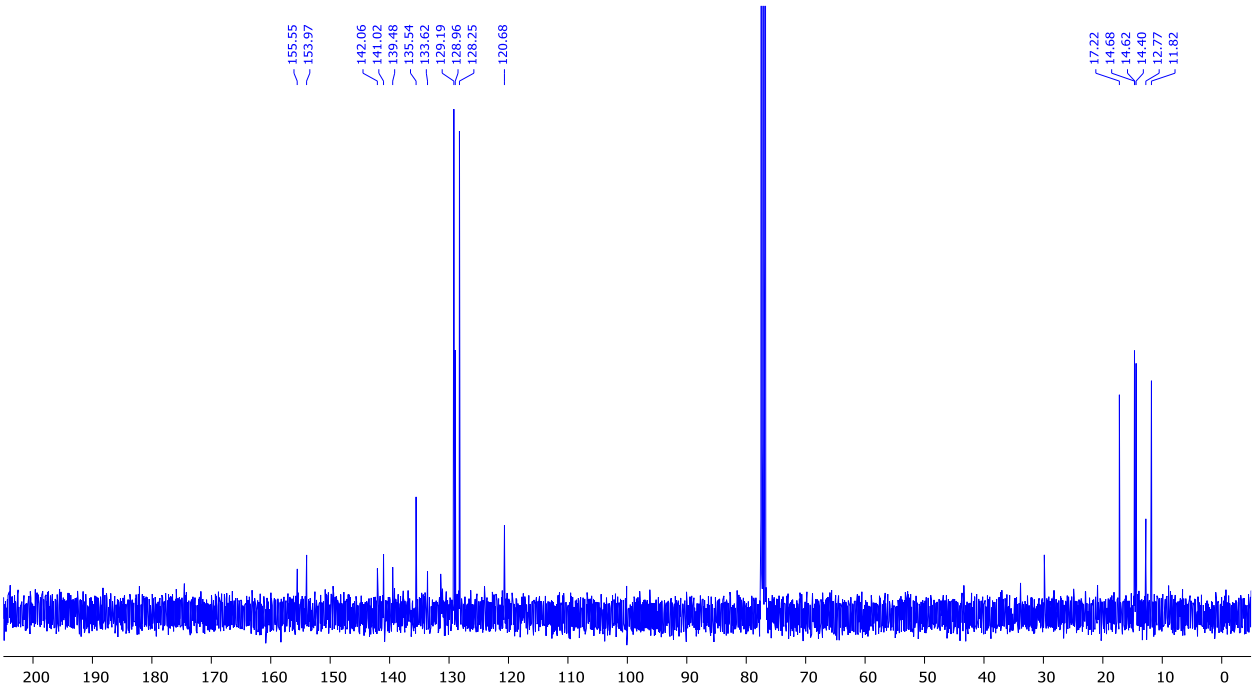

Figure B.28: ^{13}C NMR of Dipyrrin **8** in $CDCl_3$ (100 MHz)

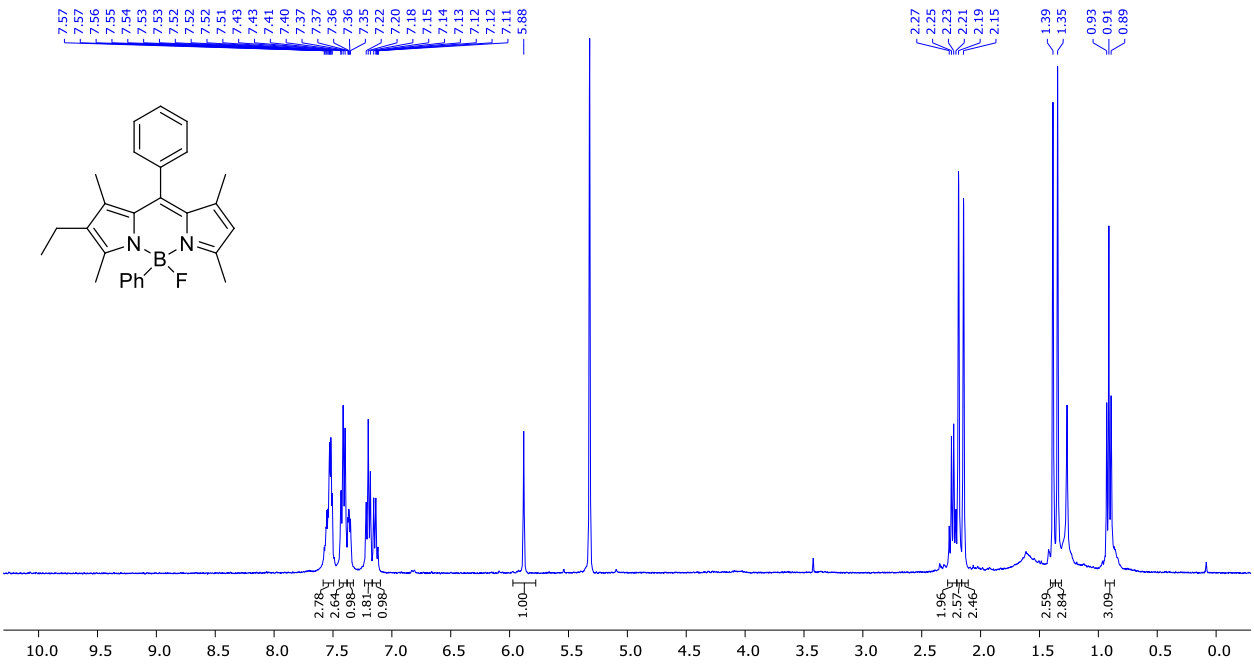

Figure B.29: ^{1}H NMR of BODIPY **8a** in CD_2Cl_2 (400 MHz)

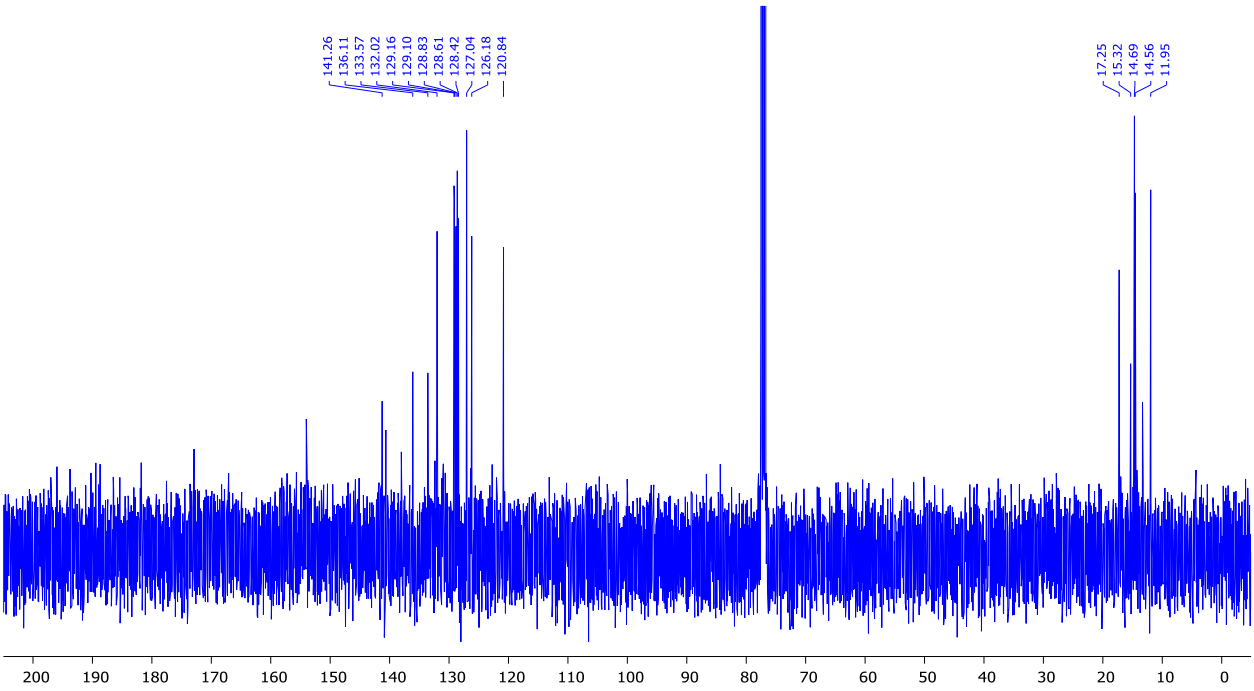

Figure B.30: ^{13}C NMR of BODIPY **8a** in $CDCl_3$ (100 MHz)

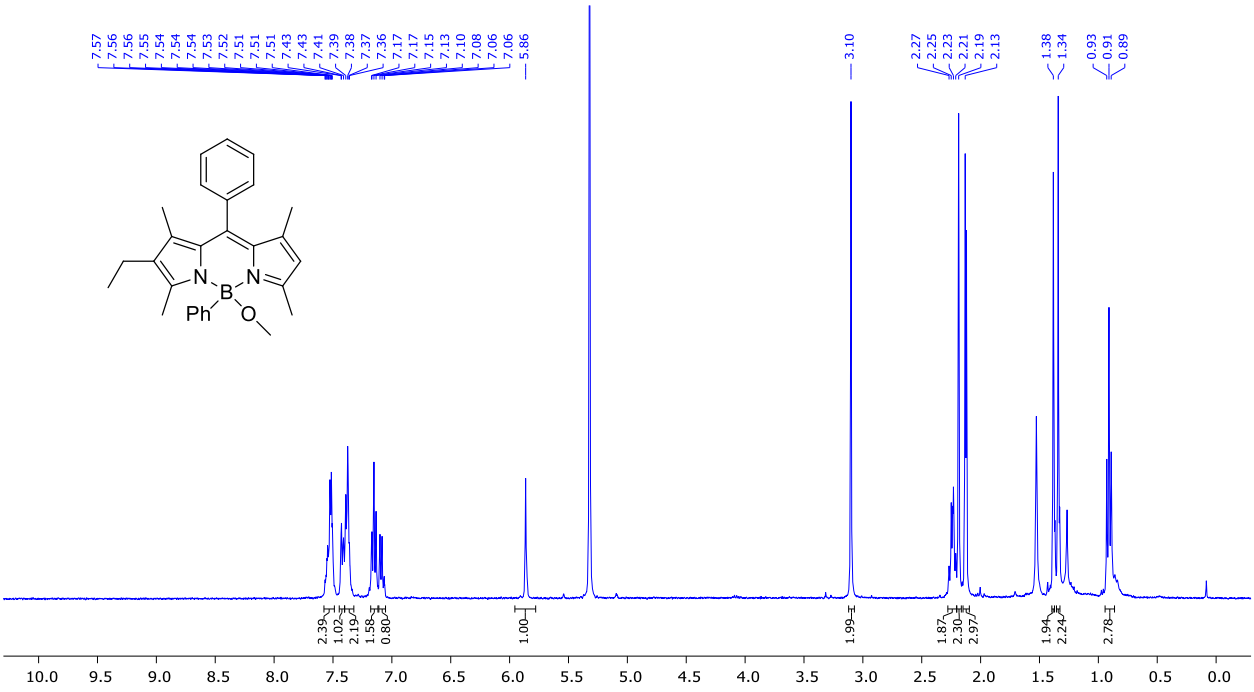

Figure B.31: ^{1}H NMR of BODIPY **8b** in CD_2Cl_2 (400 MHz)

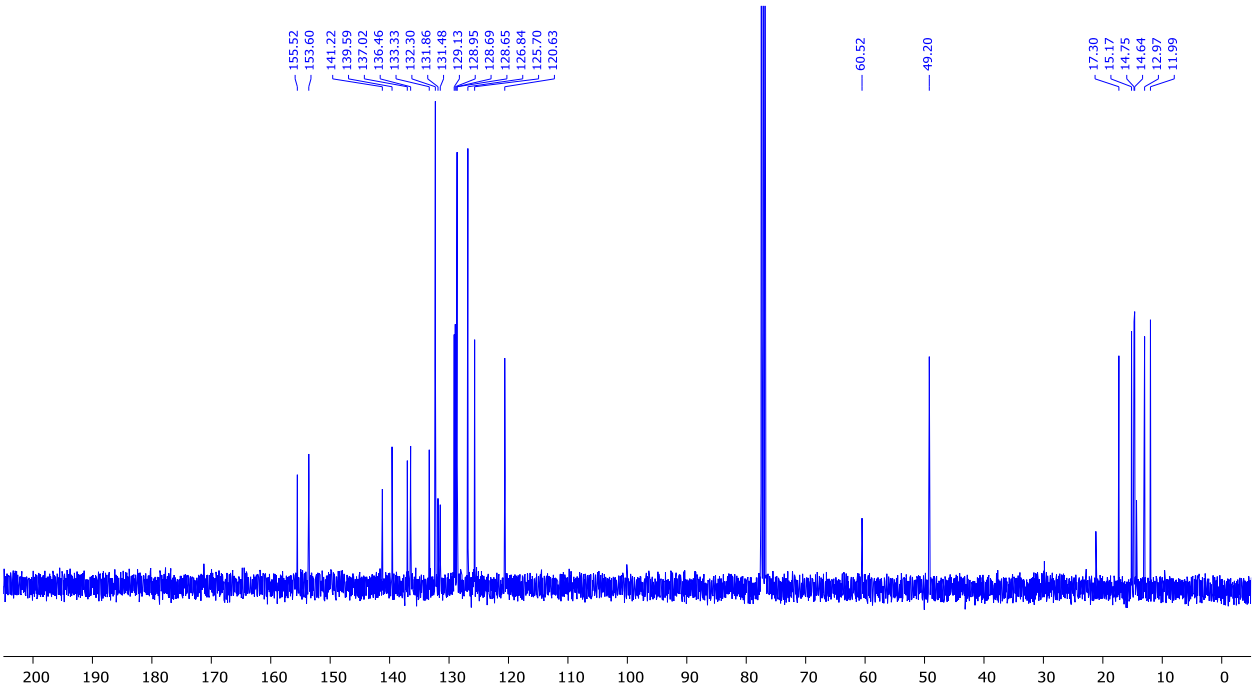

Figure B.32: ^{13}C NMR of BODIPY **8b** in $CDCl_3$ (100 MHz)

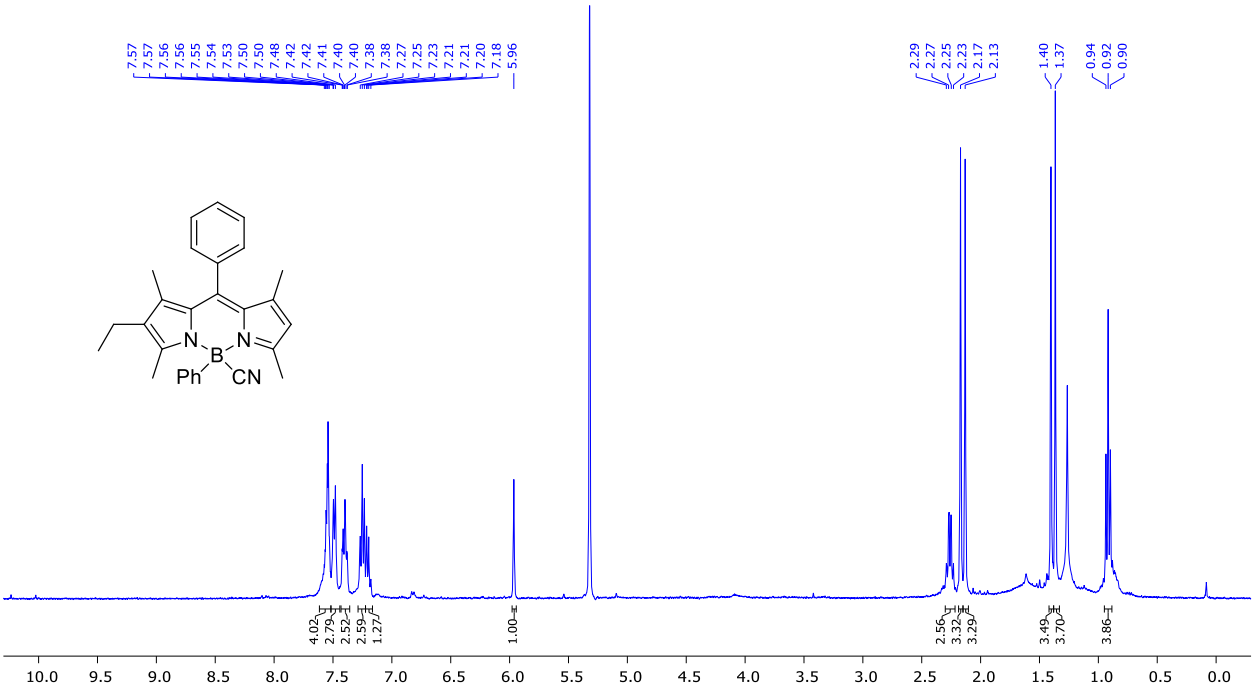

Figure B.33: ^{1}H NMR of BODIPY **8c** in CD_2Cl_2 (400 MHz)

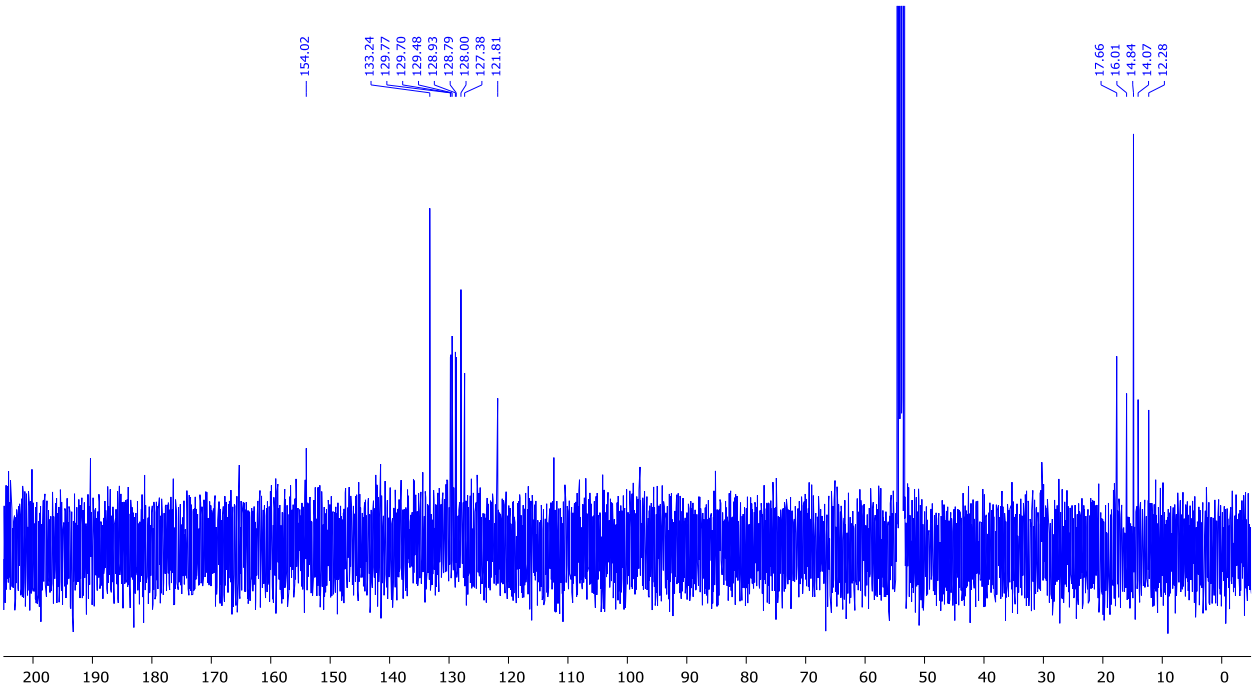

Figure B.34: ^{13}C NMR of BODIPY **8c** in CD_2Cl_2 (100 MHz)

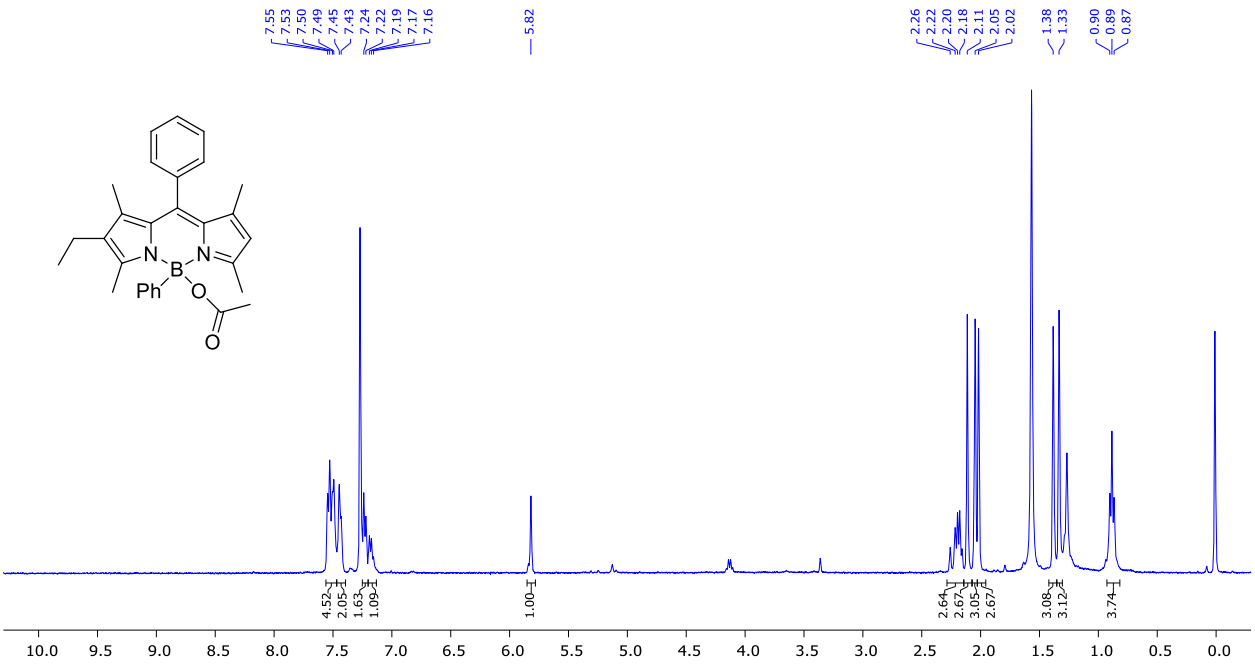

Figure B.35: ^{1}H NMR of BODIPY **8d** in $CDCl_3$ (400 MHz)

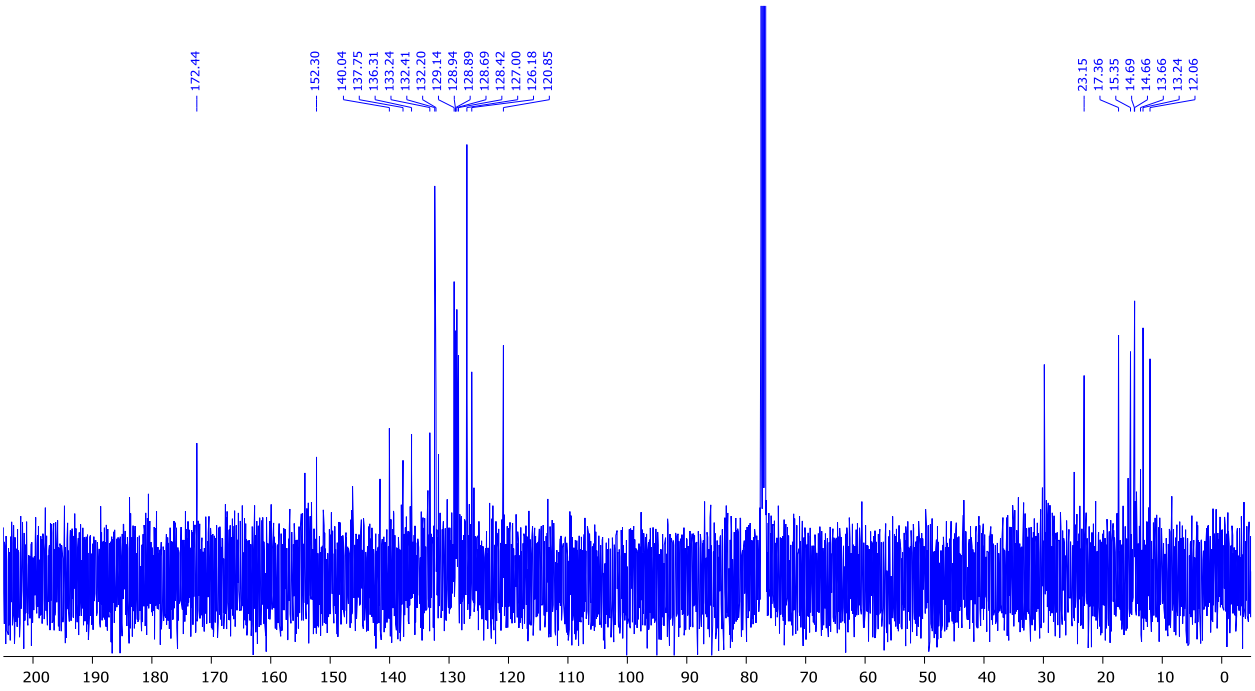

Figure B.36: ^{13}C NMR of BODIPY **8d** in $CDCl_3$ (100 MHz)

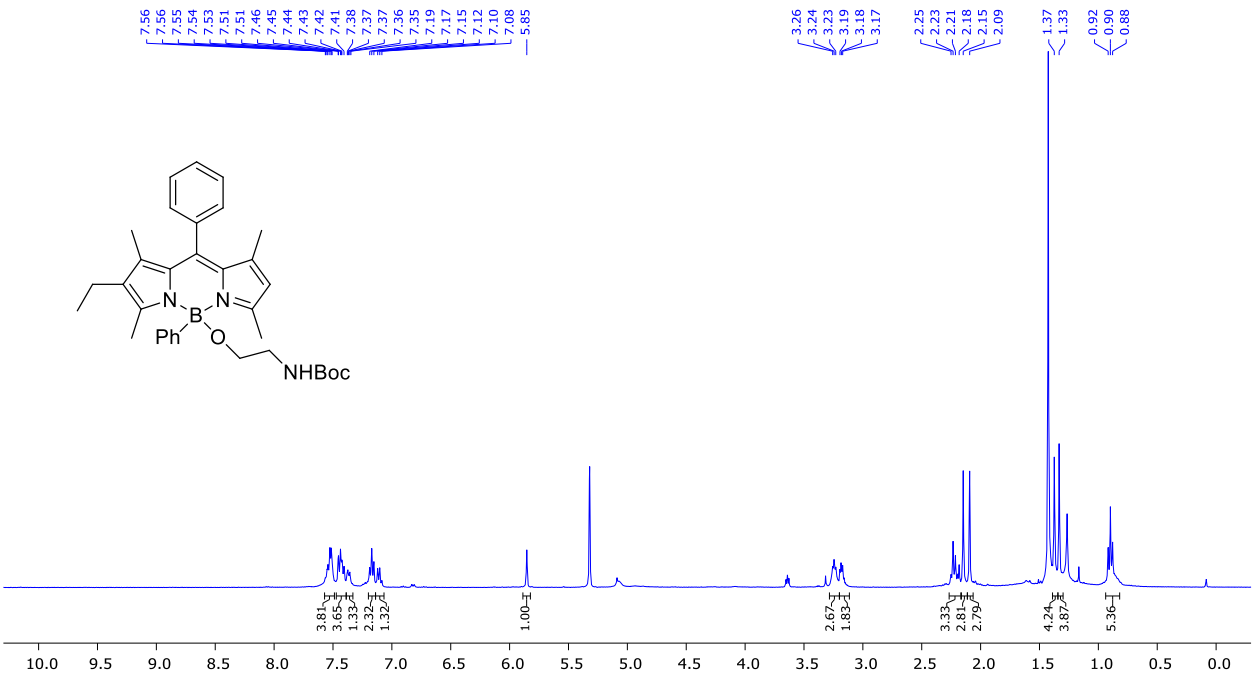

Figure B.37: ^{1}H NMR of BODIPY **8e** in CD_2Cl_2 (400 MHz)

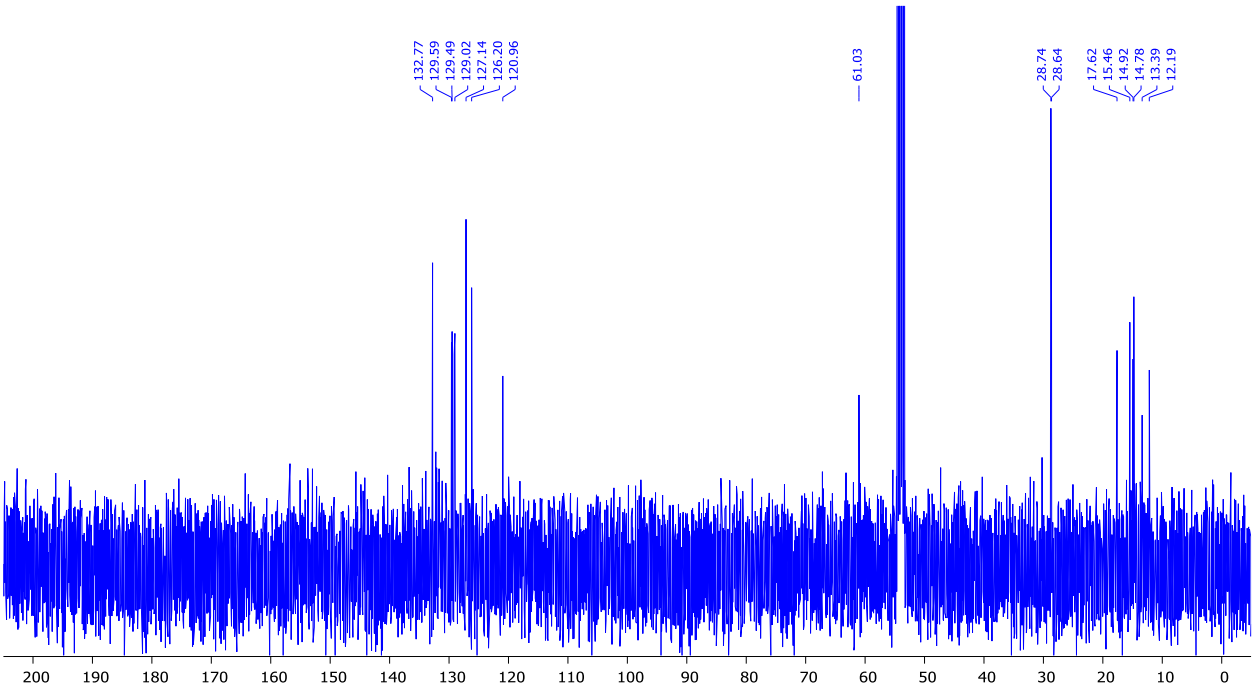

Figure B.38: ^{13}C NMR of BODIPY **8e** in CD_2Cl_2 (100 MHz)

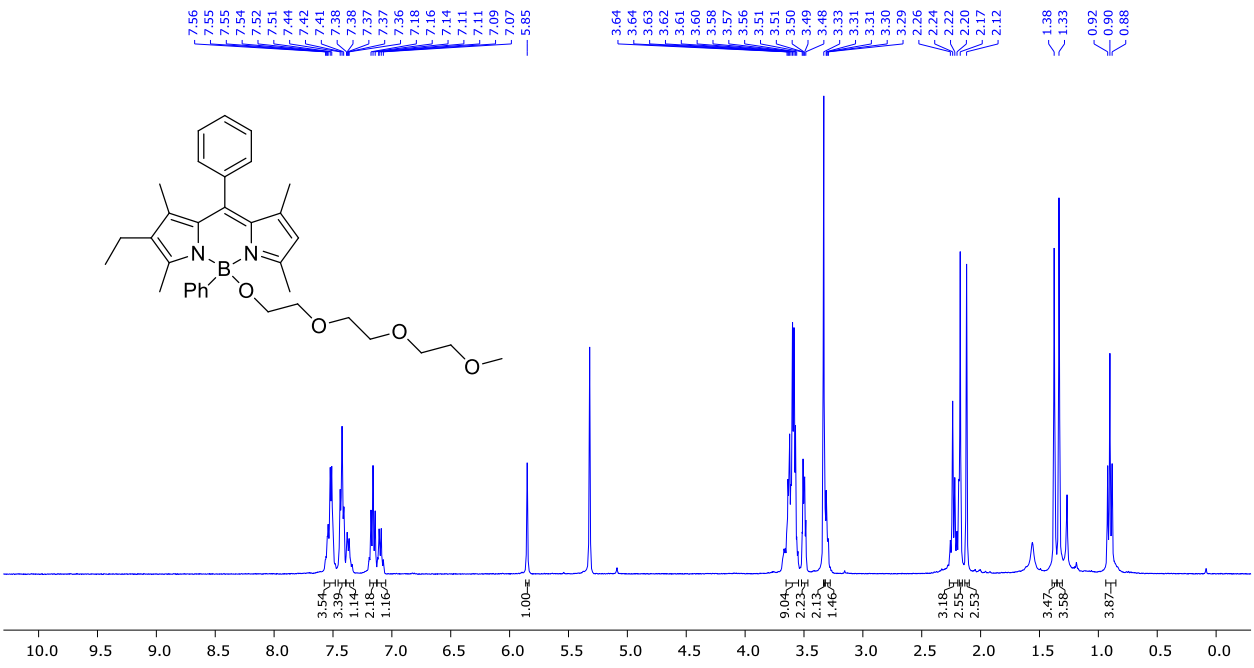

Figure B.39: ^{1}H NMR of BODIPY **8f** in CD_2Cl_2 (400 MHz)

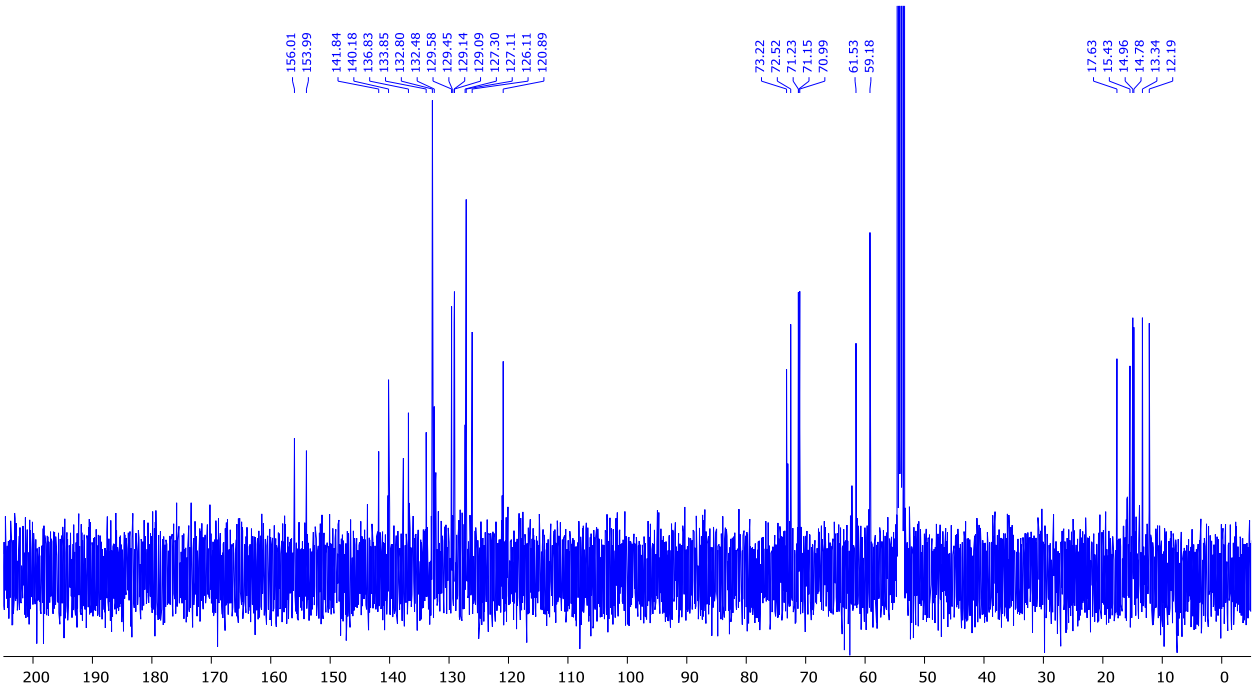

Figure B.40: ^{13}C NMR of BODIPY **8f** in CD_2Cl_2 (100 MHz)

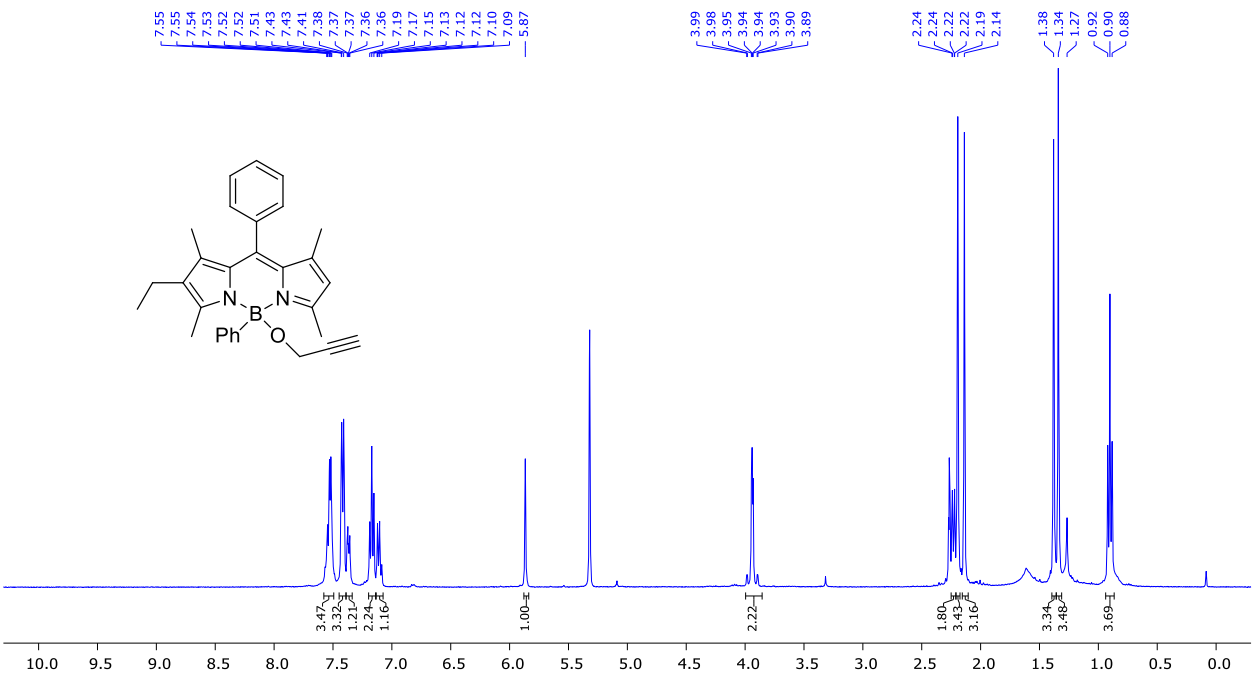

Figure B.41: ^{1}H NMR of BODIPY **8g** in CD_2Cl_2 (400 MHz)

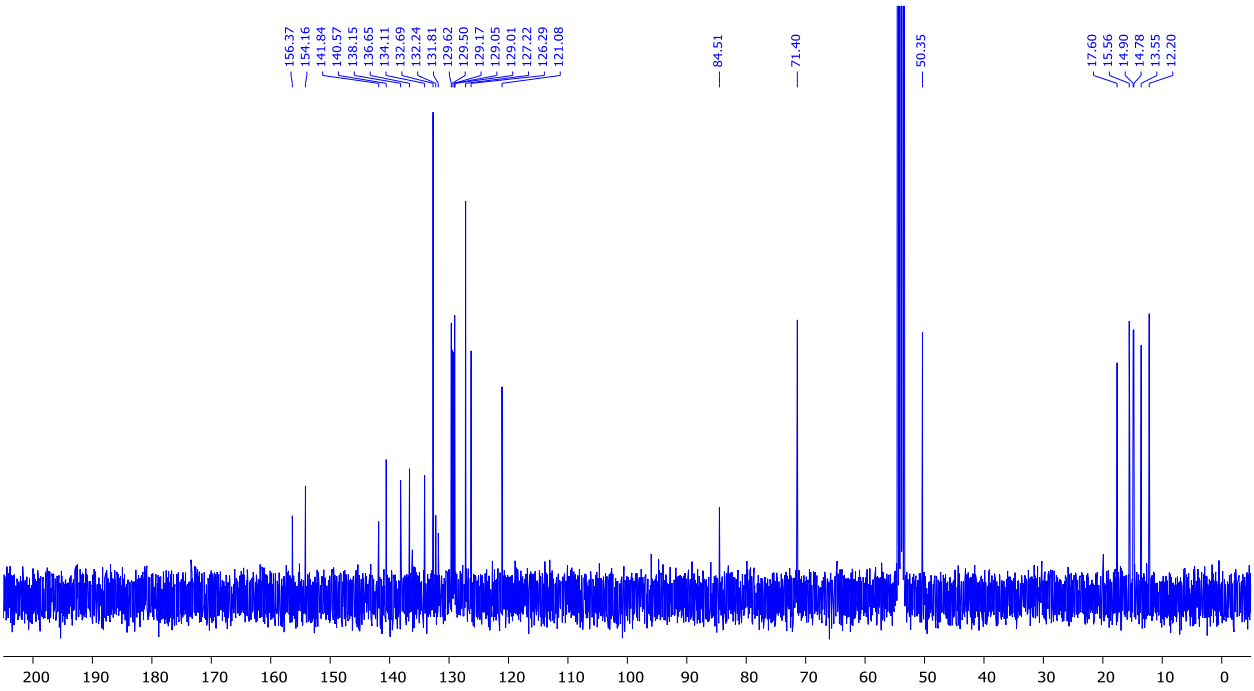

Figure B.42: ^{13}C NMR of BODIPY **8g** in CD_2Cl_2 (100 MHz)

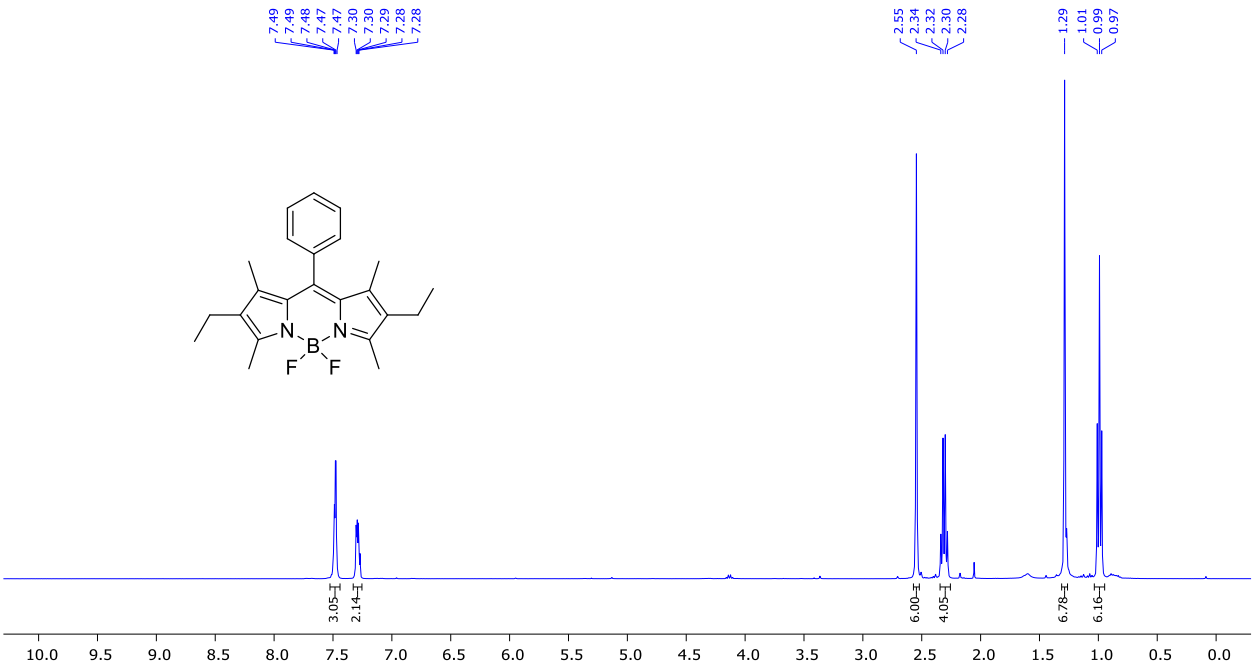

Figure B.43: ^{1}H NMR of BODIPY **4** in $CDCl_3$ (400 MHz)

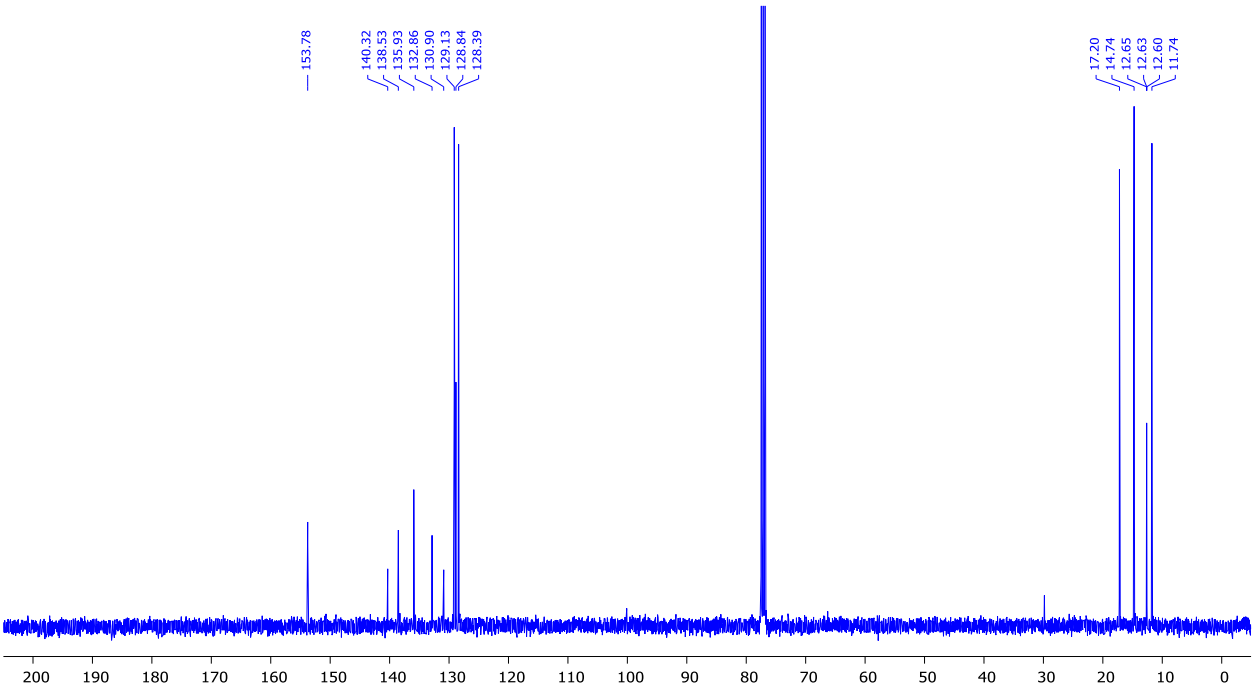

Figure B.44: ^{13}C NMR of BODIPY **4** in $CDCl_3$ (100 MHz)

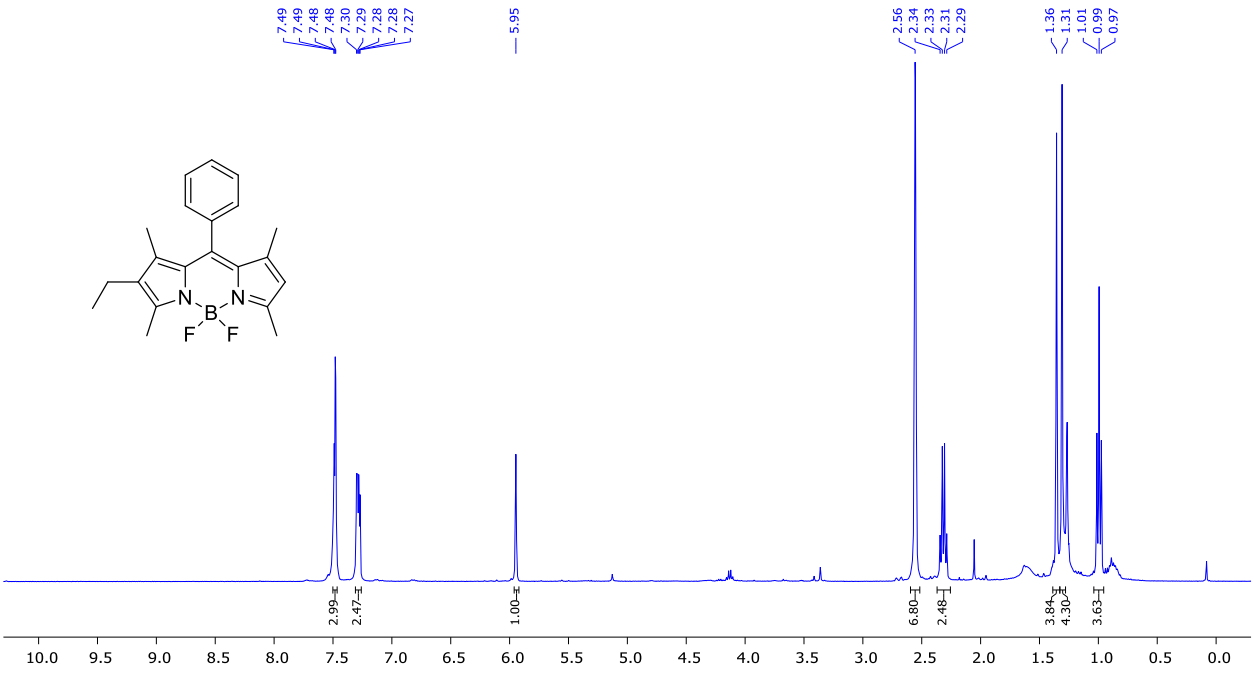

Figure B.45: ^{1}H NMR of BODIPY **9** in $CDCl_3$ (400 MHz)

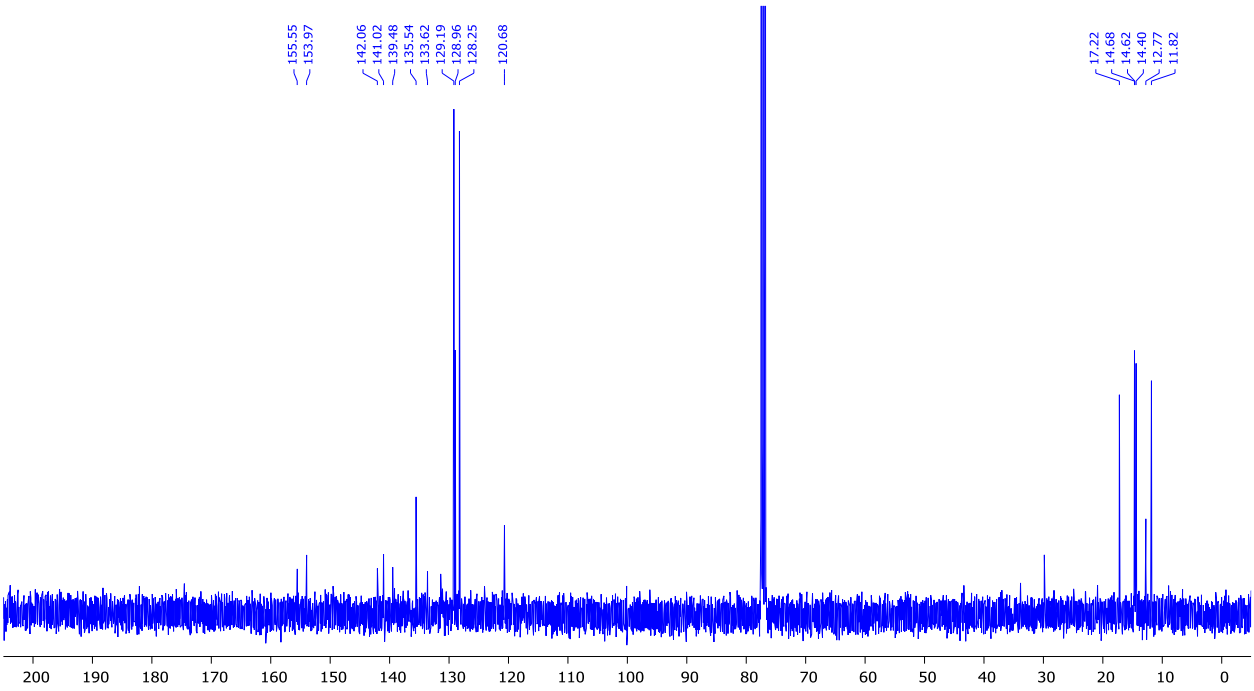

Figure B.46: ^{13}C NMR of BODIPY **9** in $CDCl_3$ (100 MHz)

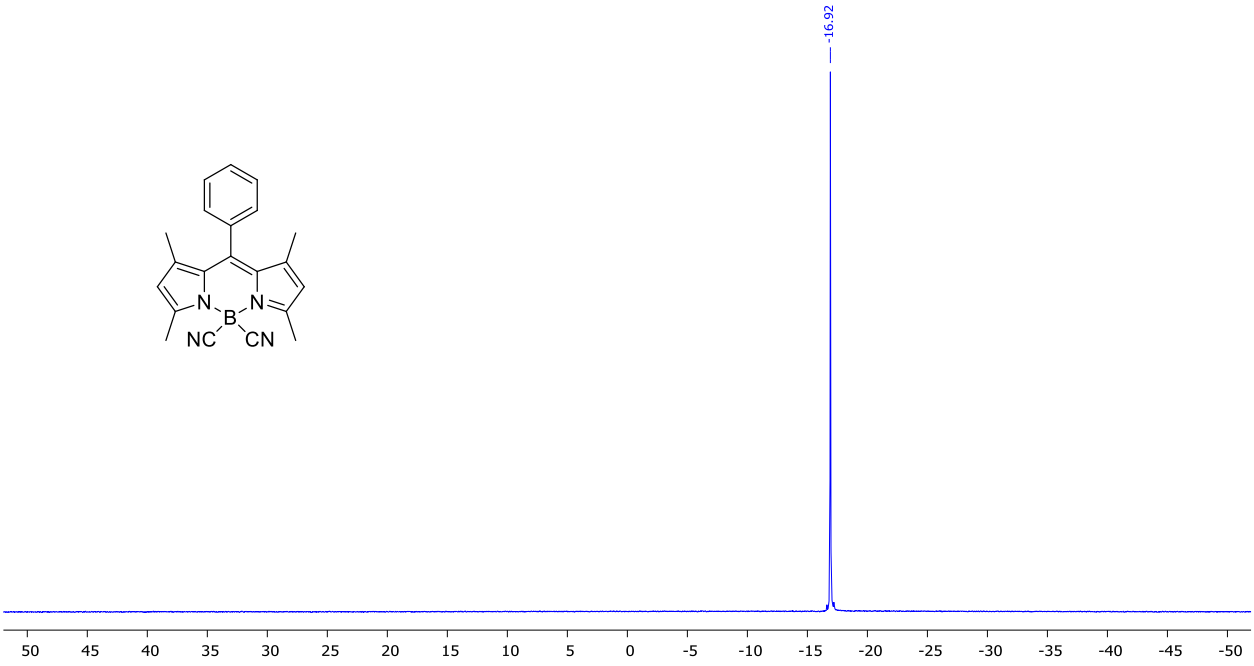

Figure B.47: ^{11}B NMR of BODIPY **1a** in $CDCl_3$ (128 MHz)

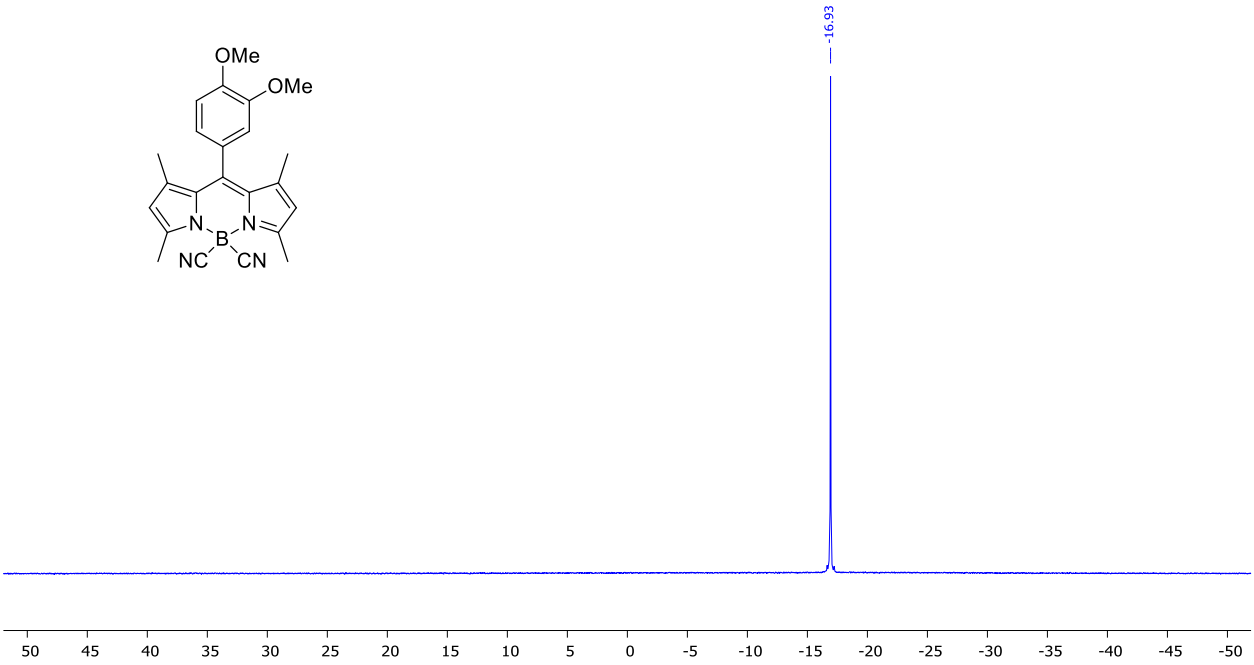

Figure B.48: ^{11}B NMR of BODIPY **2a** in $CDCl_3$ (128 MHz)

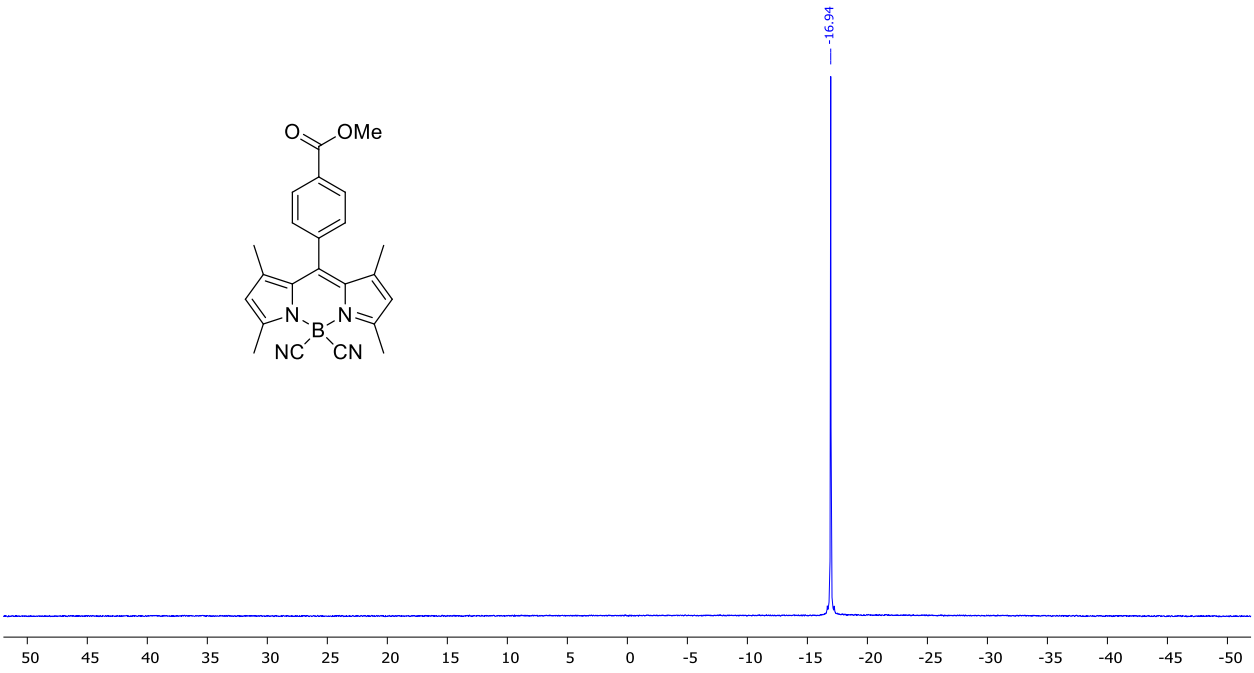

Figure B.49: ^{11}B NMR of BODIPY **3a** in $CDCl_3$ (128 MHz)

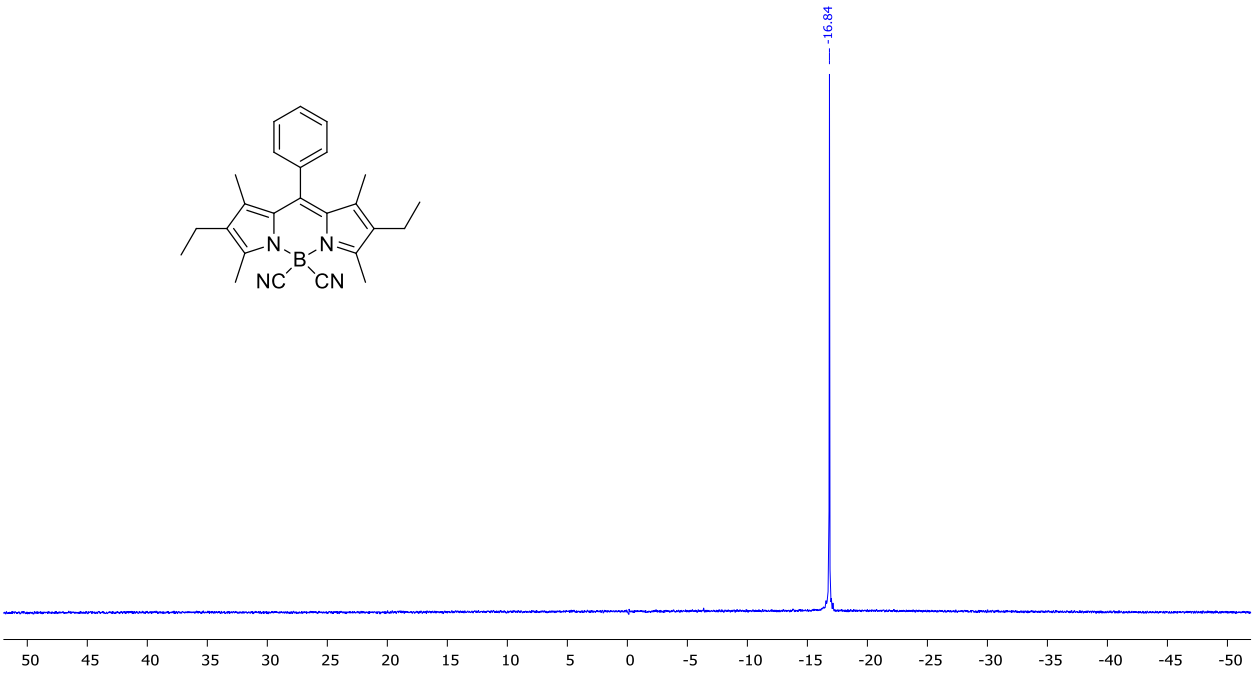

Figure B.50: ^{11}B NMR of BODIPY **4a** in $CDCl_3$ (128 MHz)

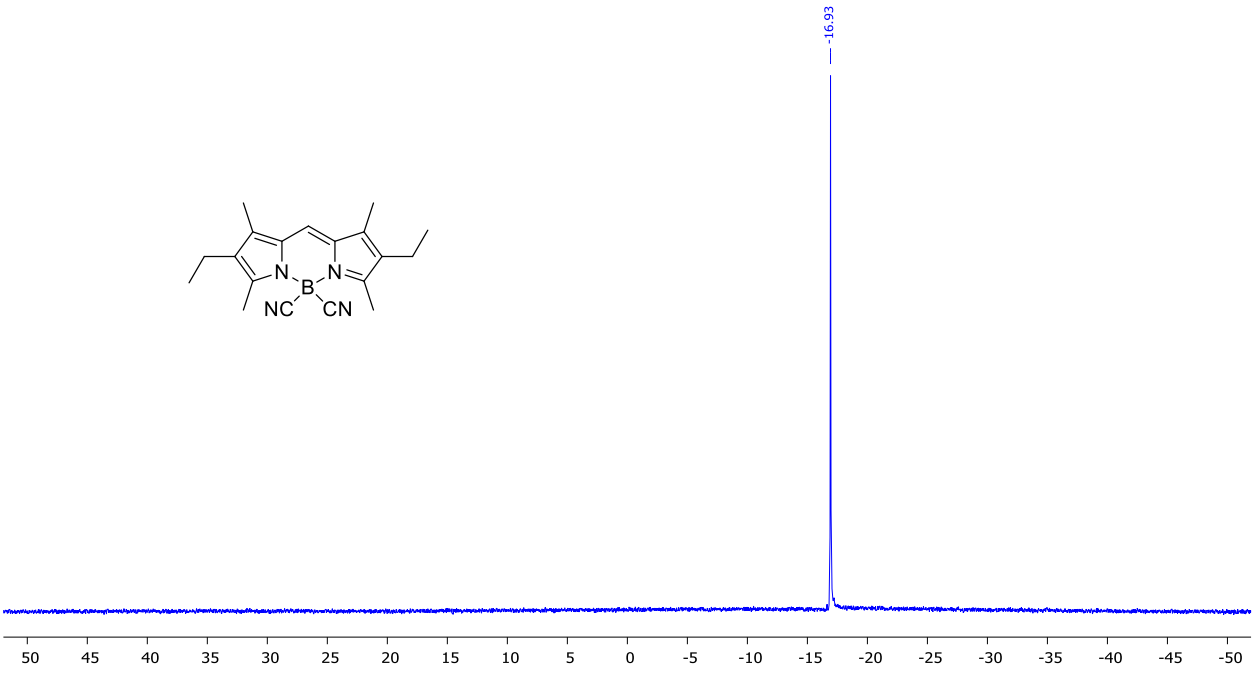

Figure B.51: ^{11}B NMR of BODIPY **5a** in $CDCl_3$ (128 MHz)

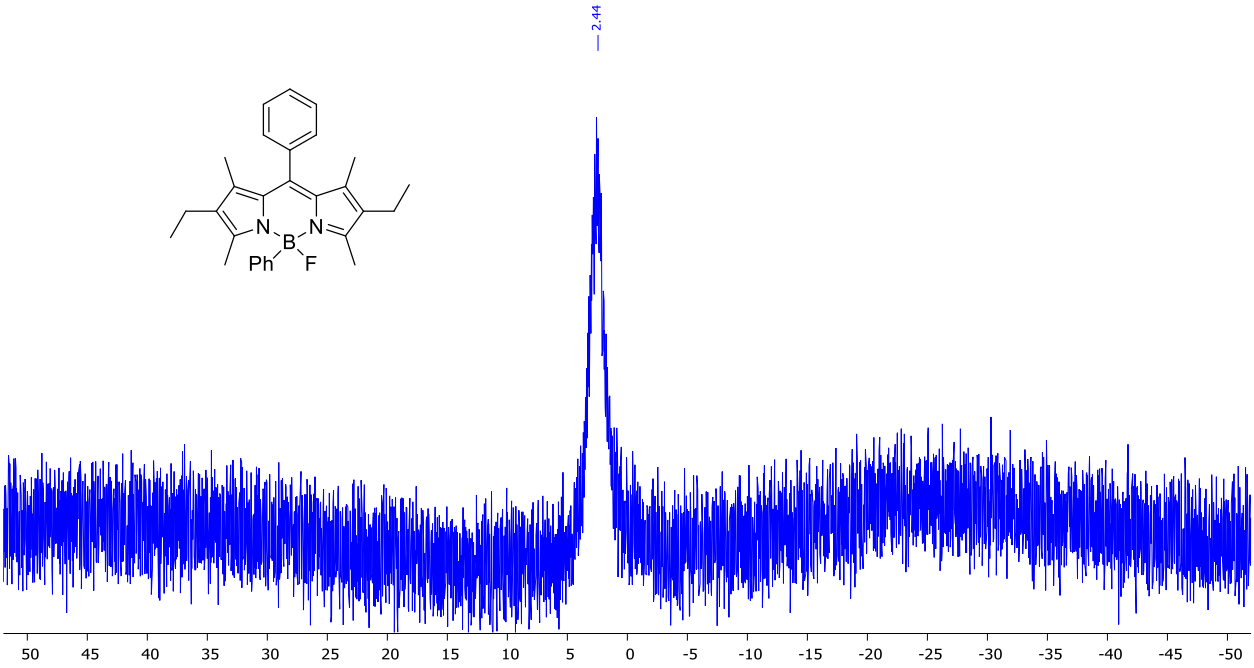

Figure B.52: ^{11}B NMR of BODIPY **7a** in $CDCl_3$ (128 MHz)

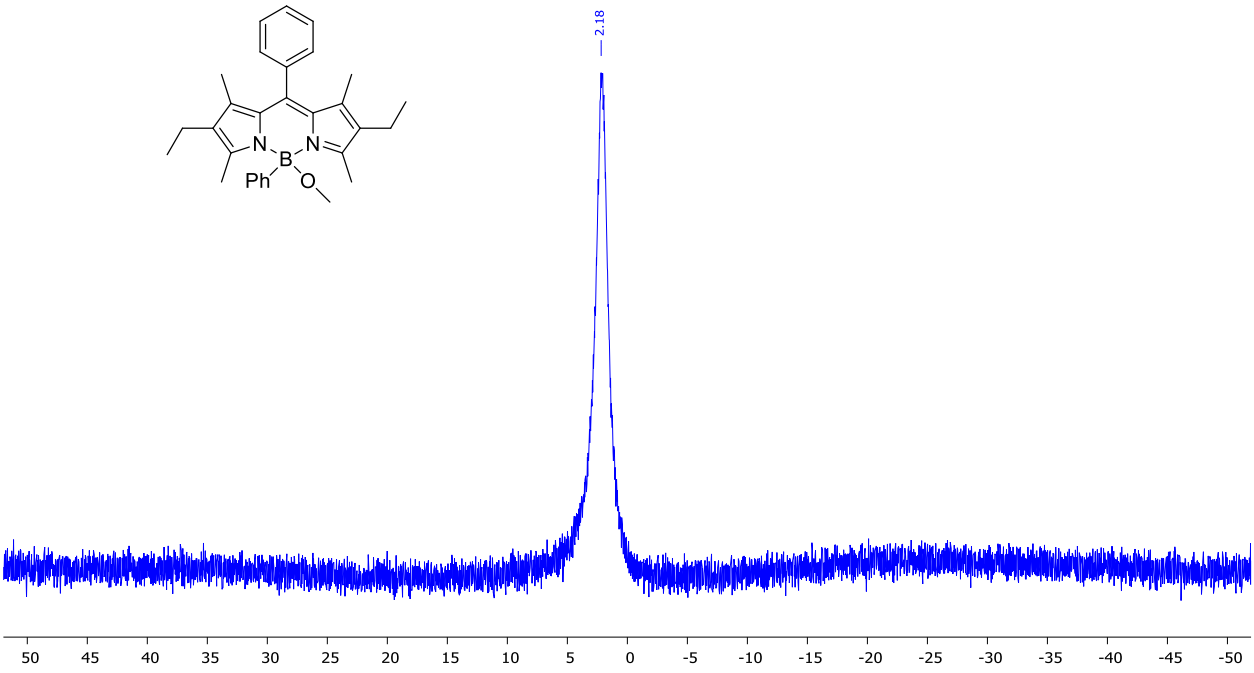

Figure B.53: ^{11}B NMR of BODIPY **7b** in $CDCl_3$ (128 MHz)

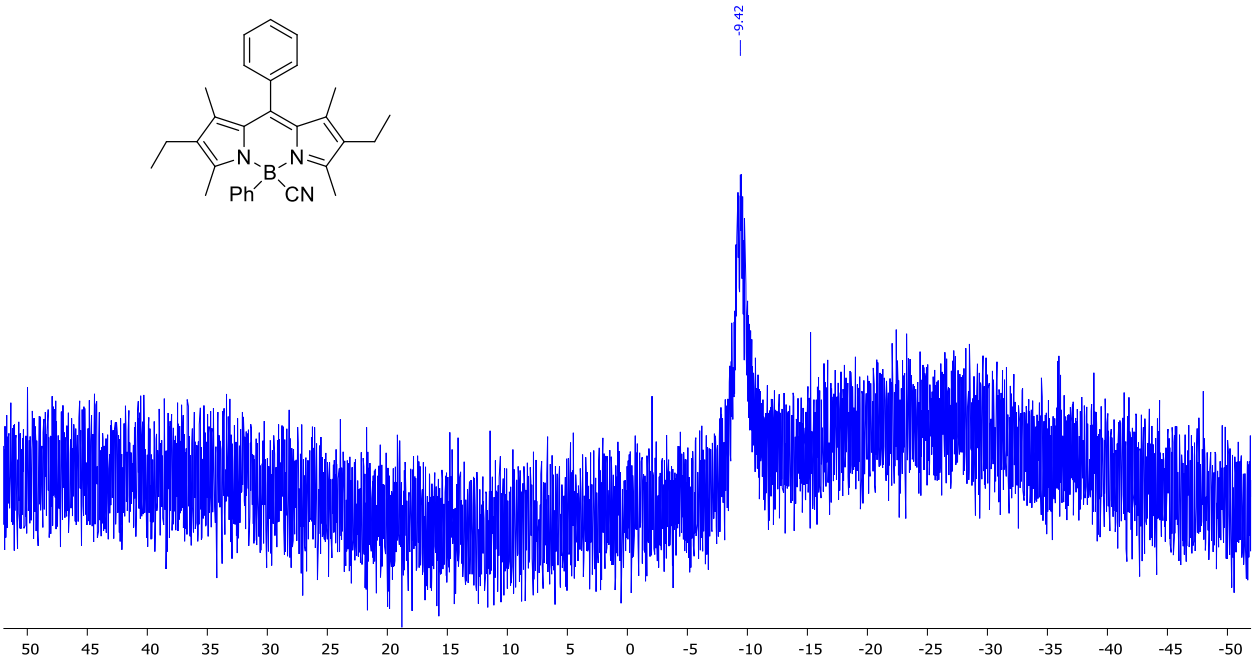

Figure B.54: ^{11}B NMR of BODIPY **7c** in $CDCl_3$ (128 MHz)

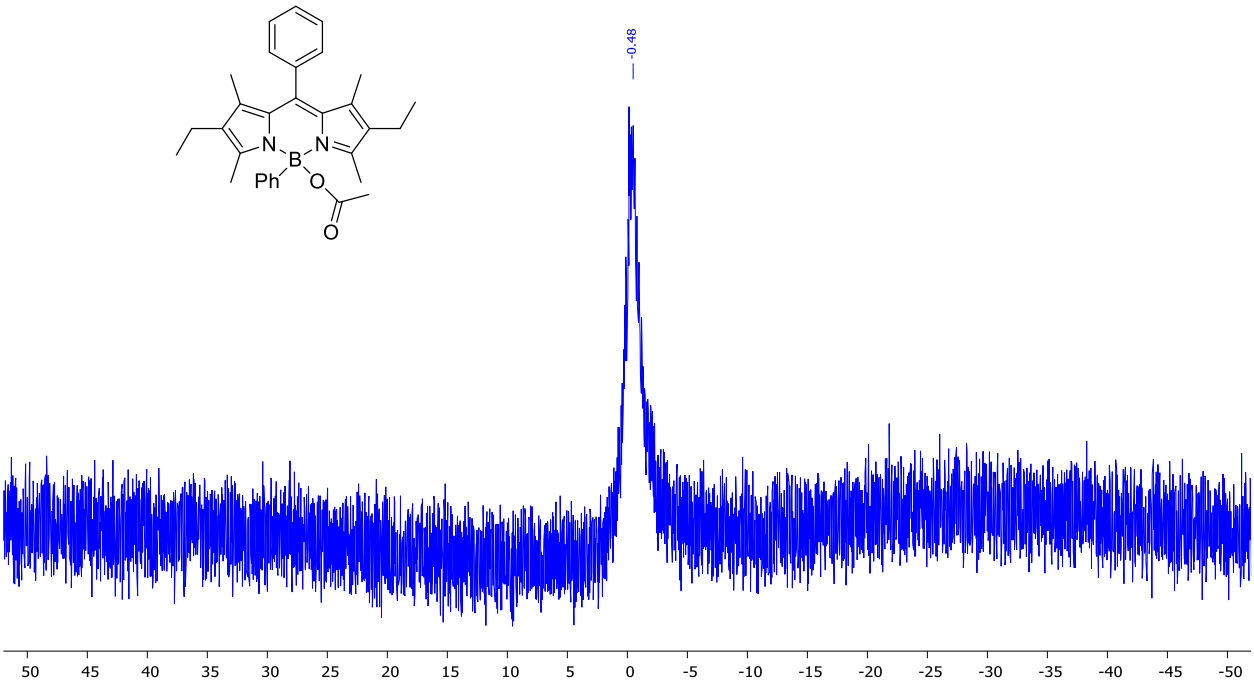

Figure B.55: ^{11}B NMR of BODIPY **7d** in $CDCl_3$ (128 MHz)

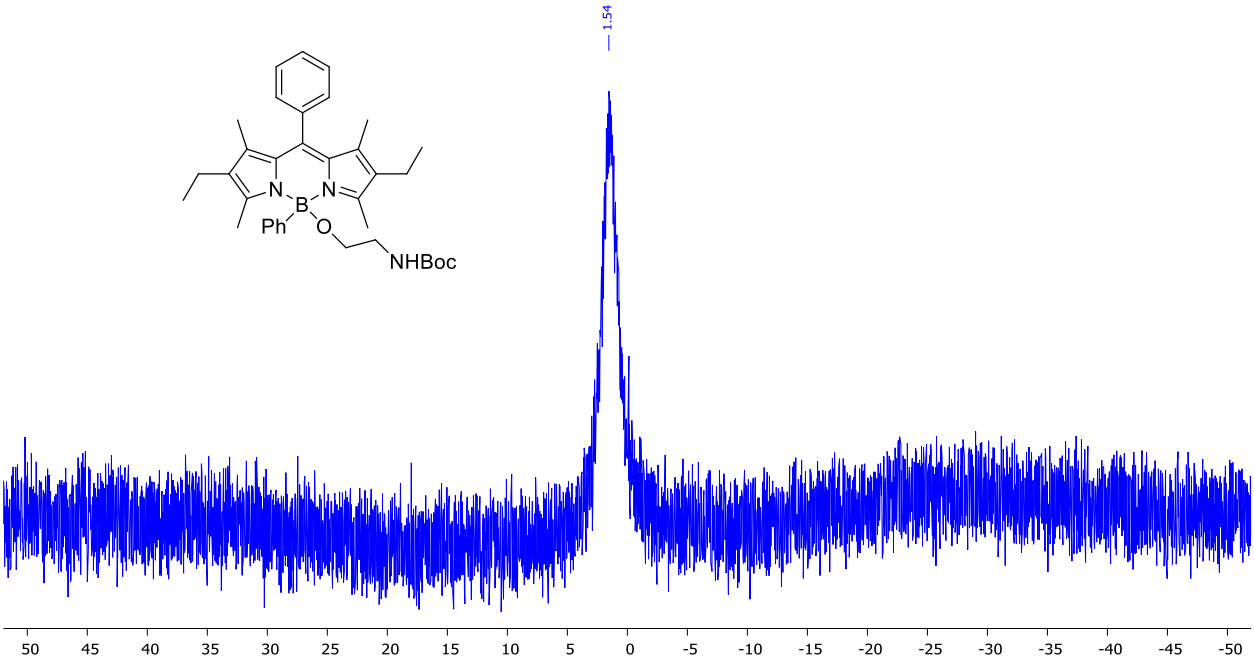

Figure B.56: ^{11}B NMR of BODIPY **7e** in $CDCl_3$ (128 MHz)

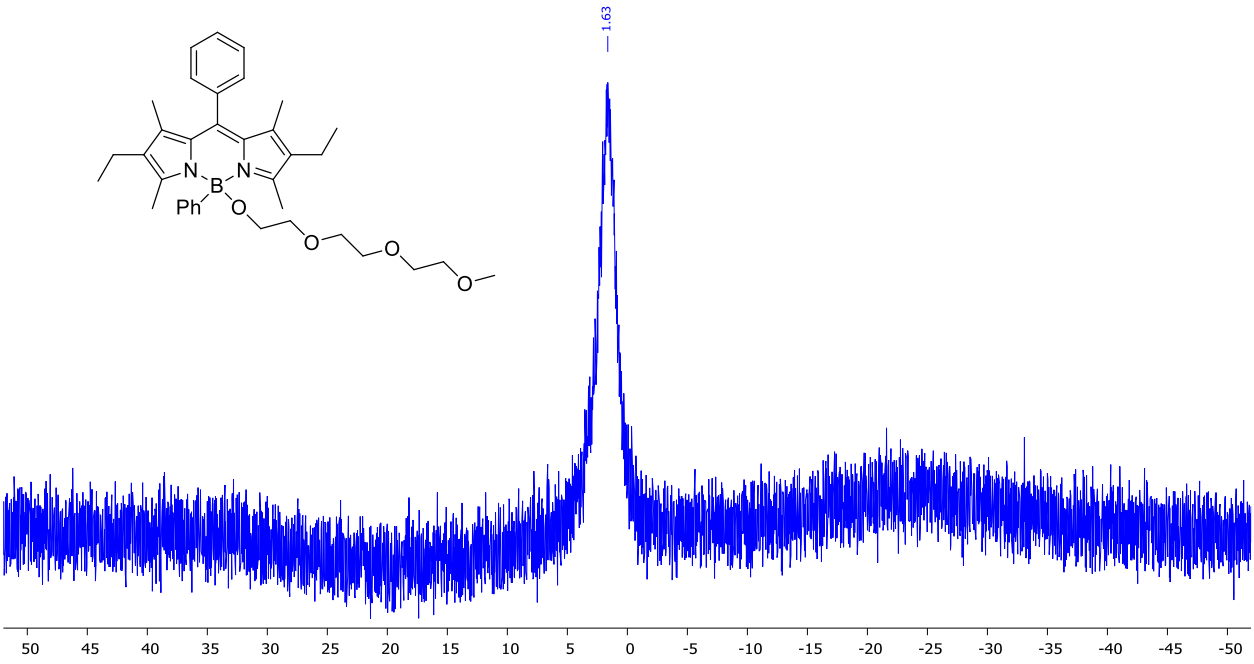

Figure B.57: ^{11}B NMR of BODIPY **7f** in $CDCl_3$ (128 MHz)

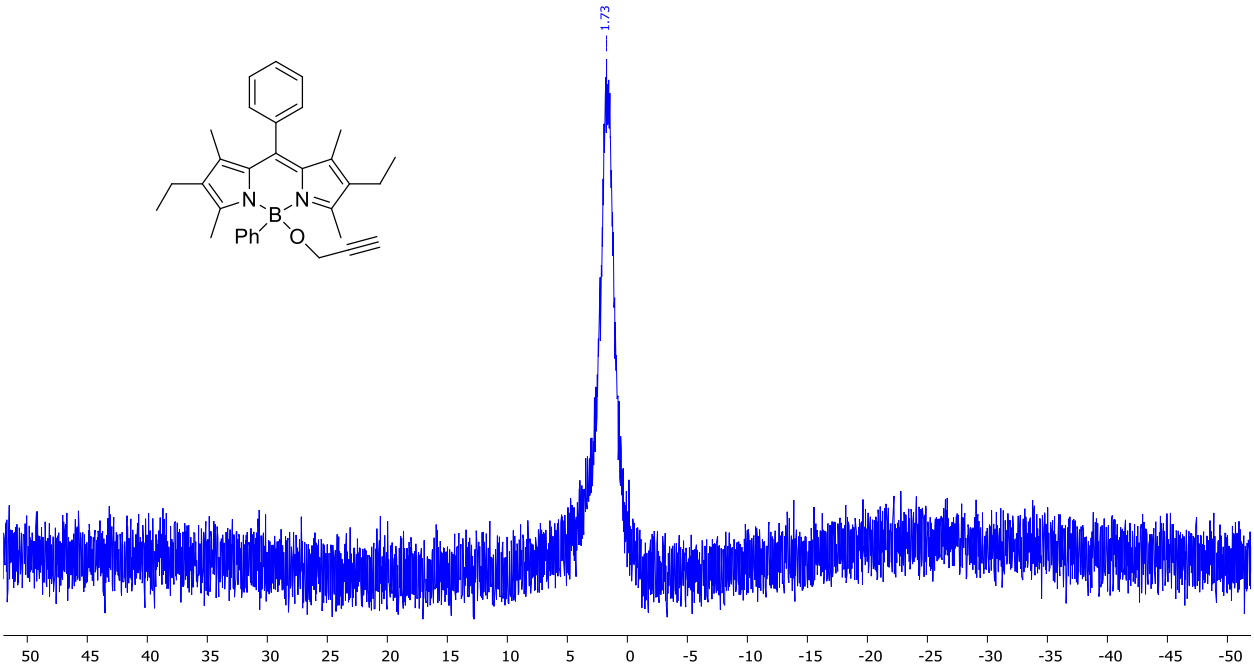

Figure B.58: ^{11}B NMR of BODIPY **7g** in $CDCl_3$ (128 MHz)

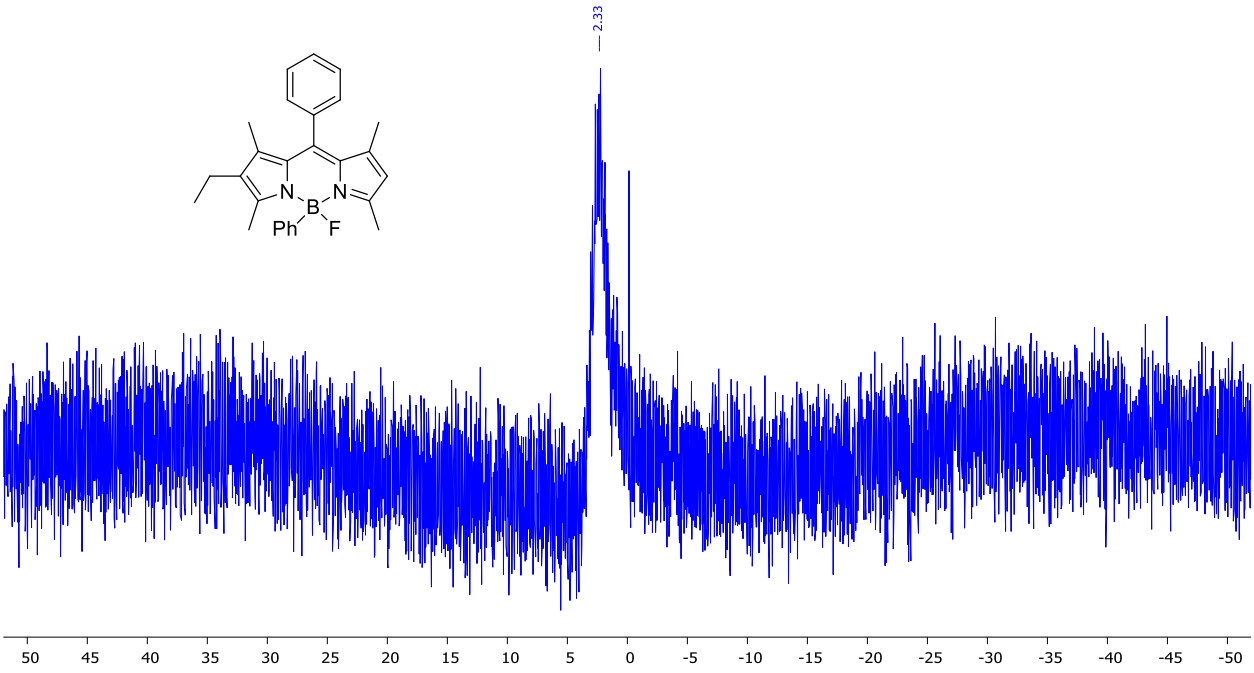

Figure B.59: ^{11}B NMR of BODIPY **8a** in $CDCl_3$ (128 MHz)

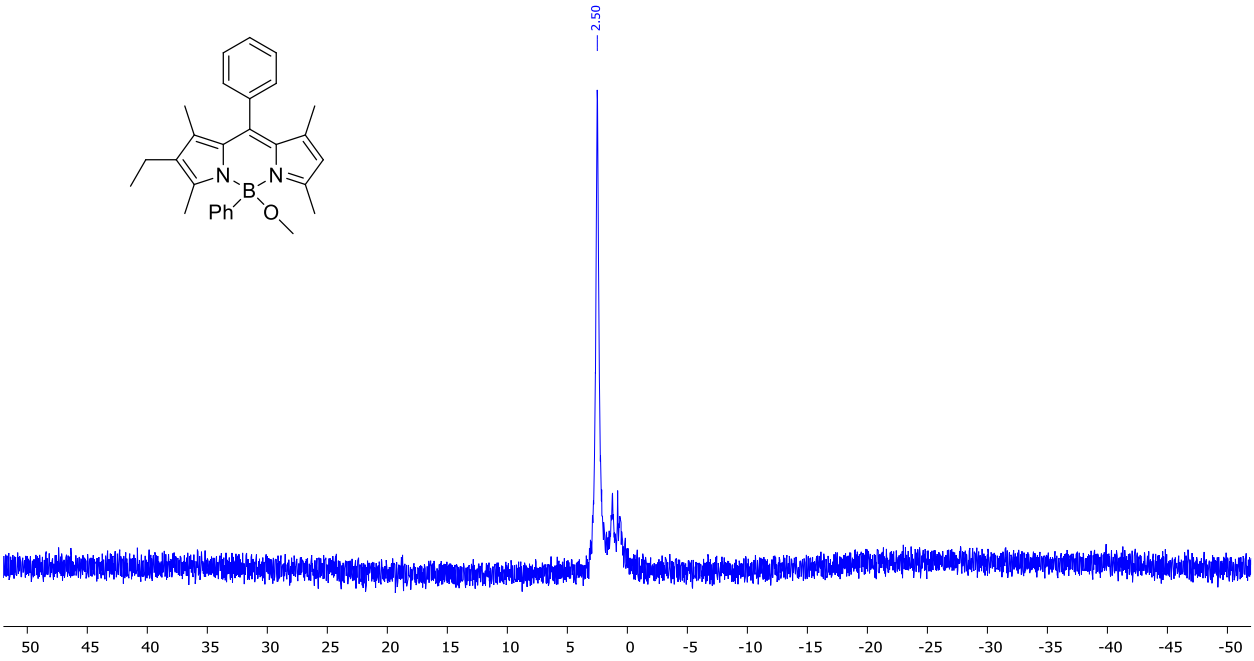

Figure B.60: ^{11}B NMR of BODIPY **8b** in $CDCl_3$ (128 MHz)

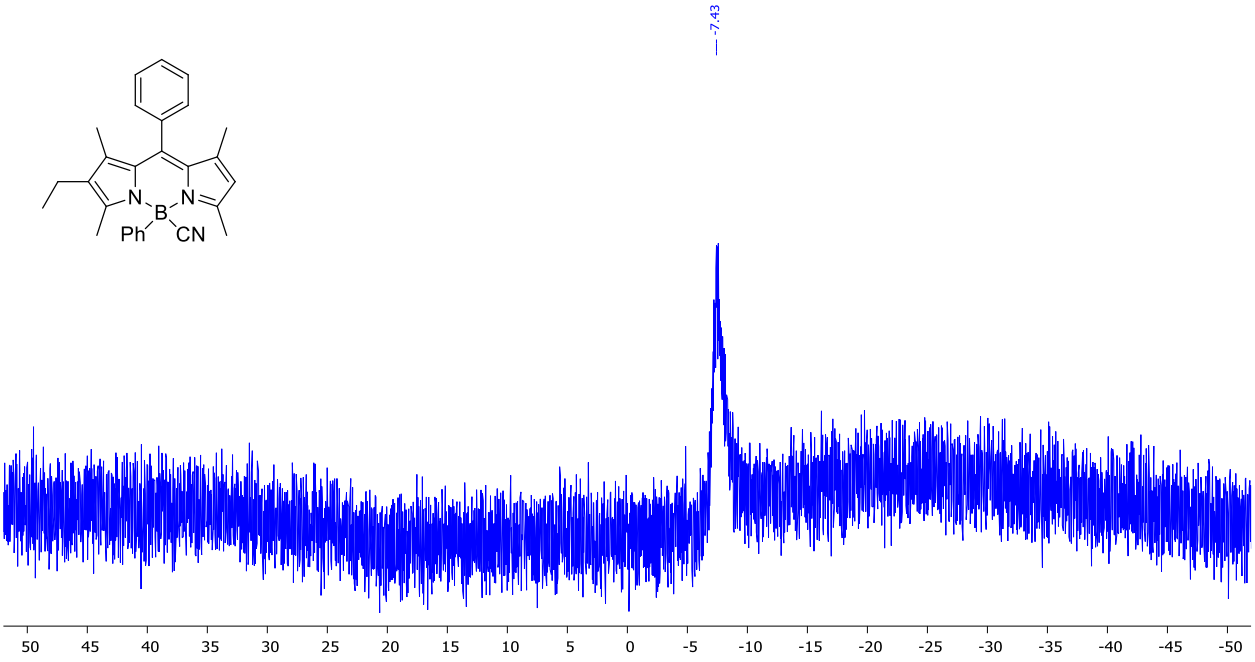

Figure B.61: ^{11}B NMR of BODIPY **8c** in $CDCl_3$ (128 MHz)

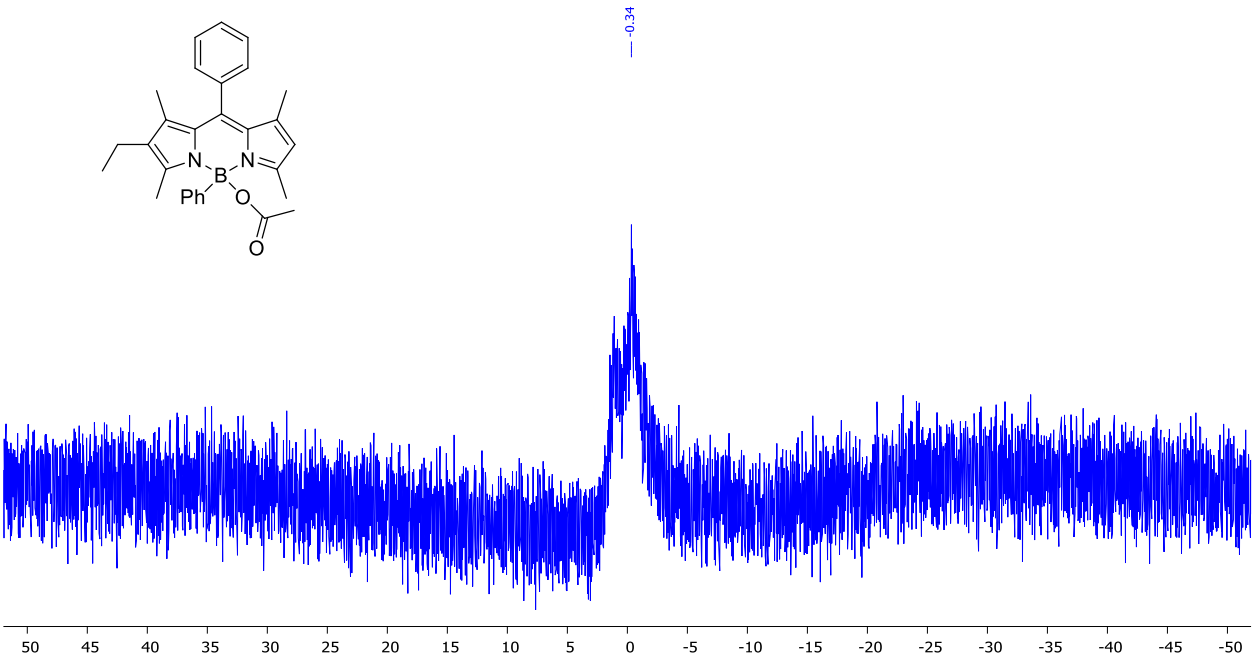

Figure B.62: ^{11}B NMR of BODIPY **8d** in $CDCl_3$ (128 MHz)

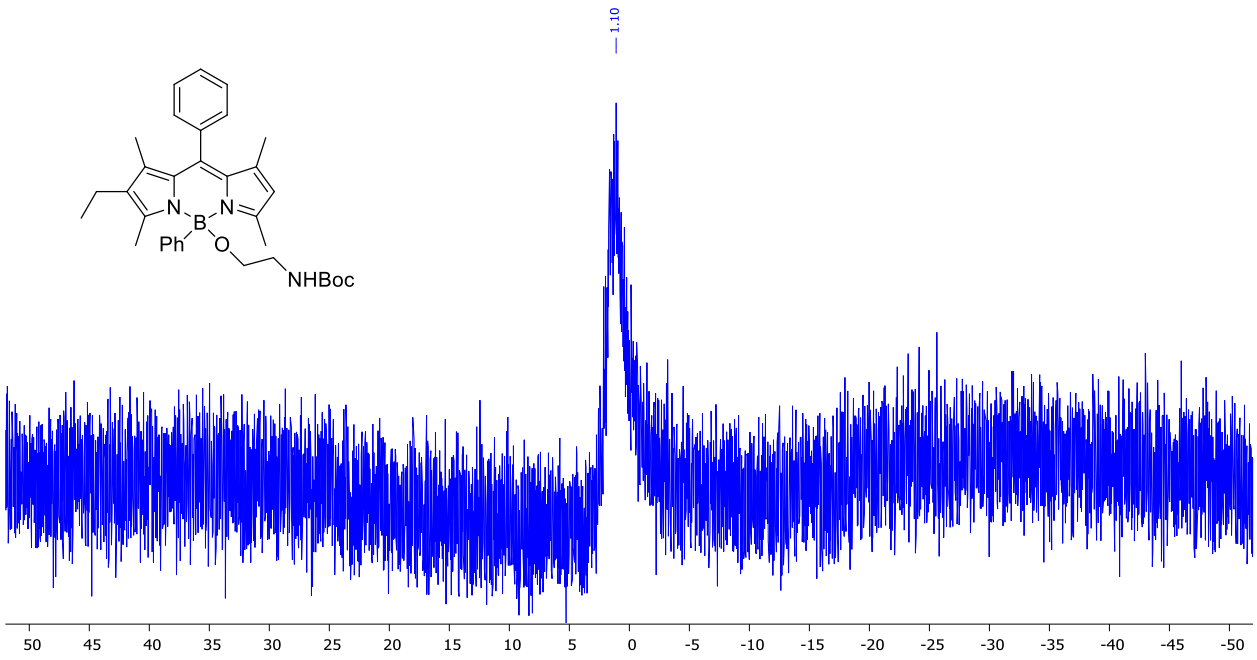

Figure B.63: ^{11}B NMR of BODIPY **8e** in $CDCl_3$ (128 MHz)

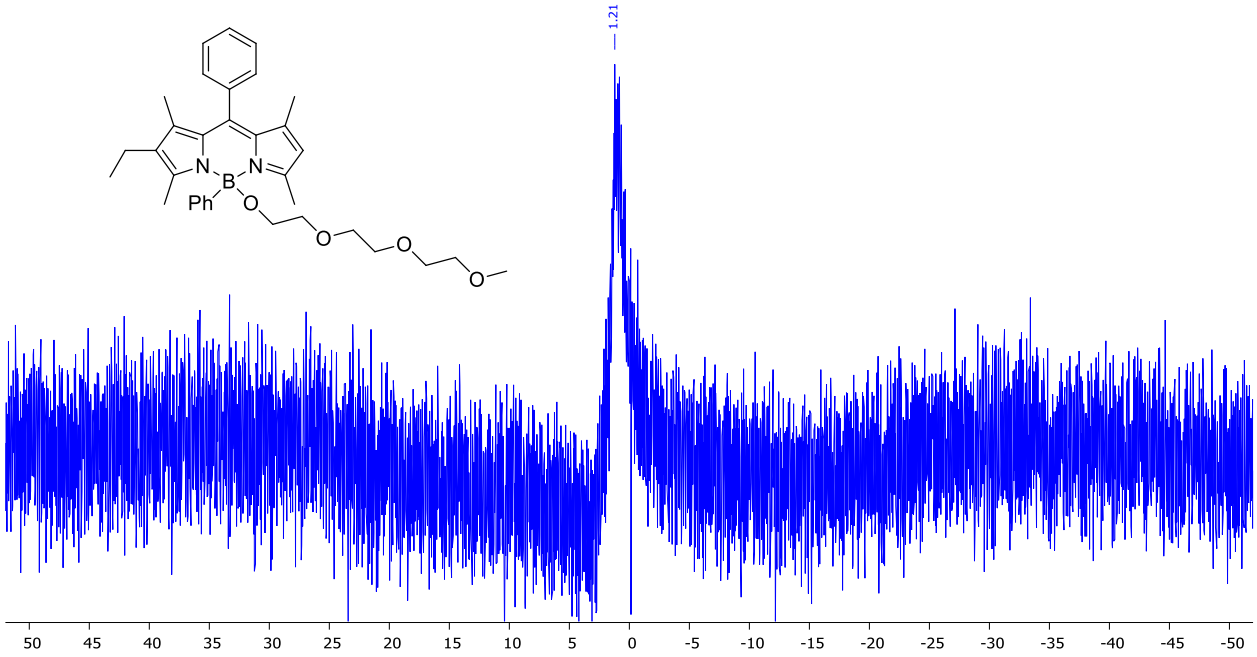

Figure B.64: ^{11}B NMR of BODIPY **8f** in $CDCl_3$ (128 MHz)

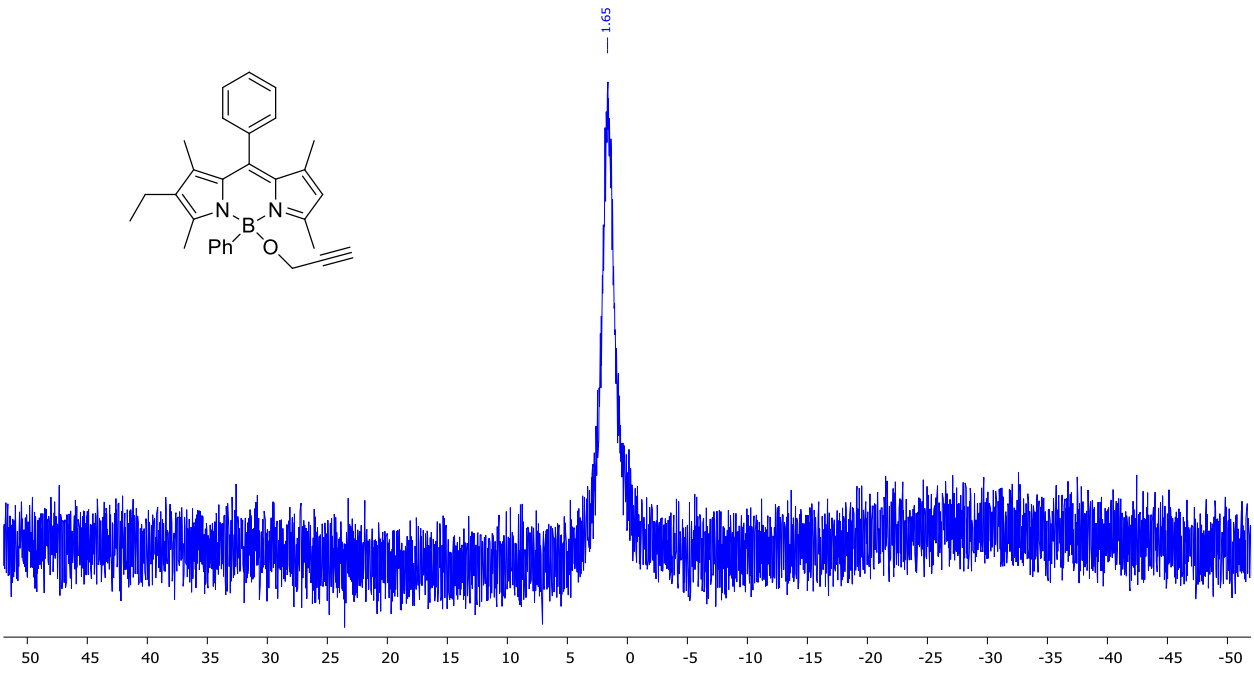

Figure B.65: ^{11}B NMR of BODIPY **8g** in $CDCl_3$ (128 MHz)

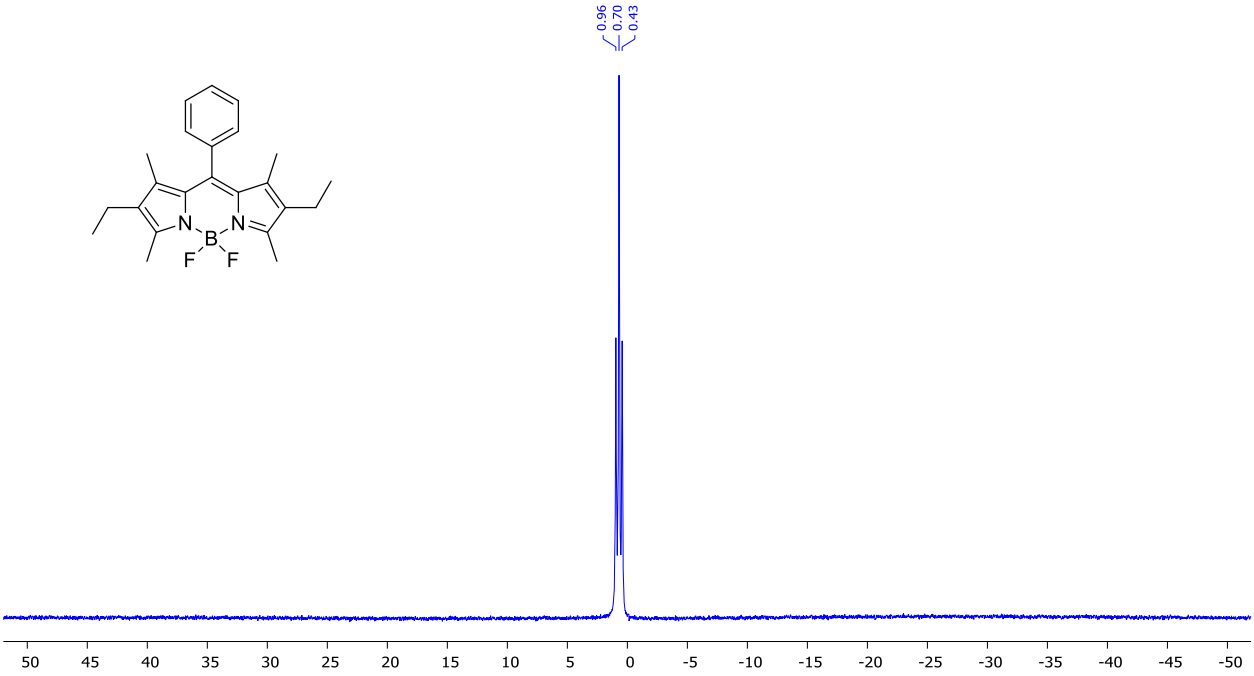

Figure B.66: ^{11}B NMR of BODIPY **4** in $CDCl_3$ (128 MHz)

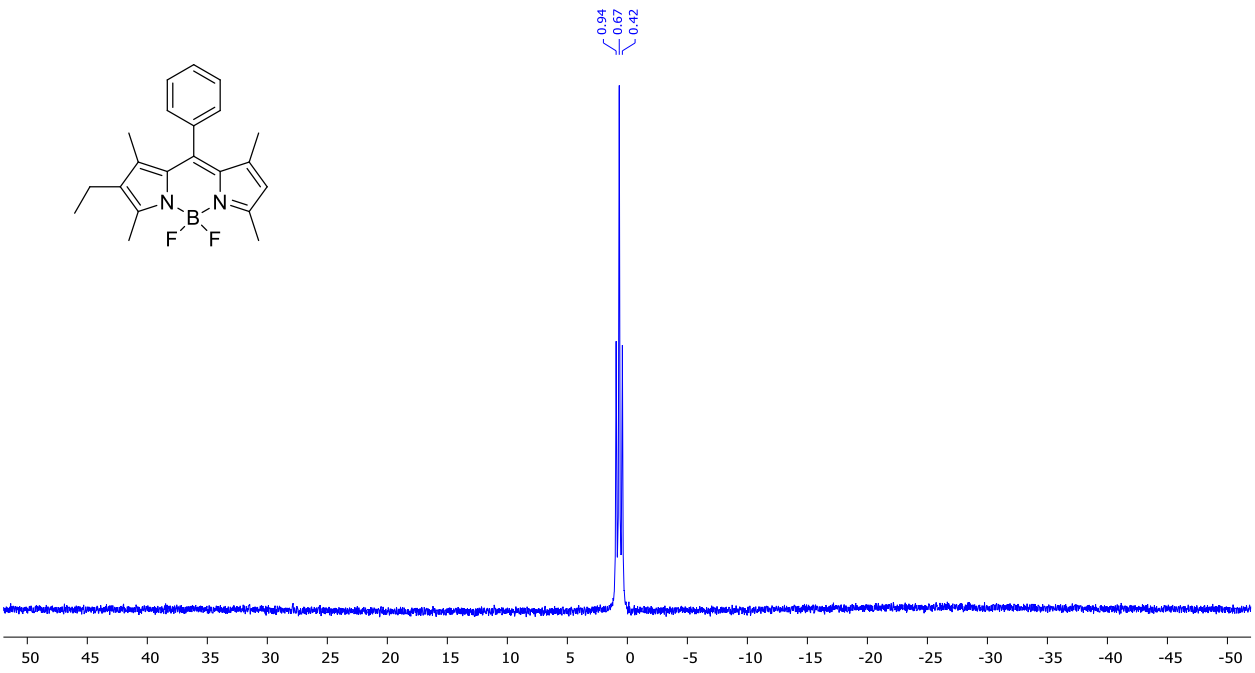

Figure B.67: ^{11}B NMR of BODIPY **9** in $CDCl_3$ (128 MHz)

APPENDIX C: NMR Characterization of Compounds Found in Chapter 4

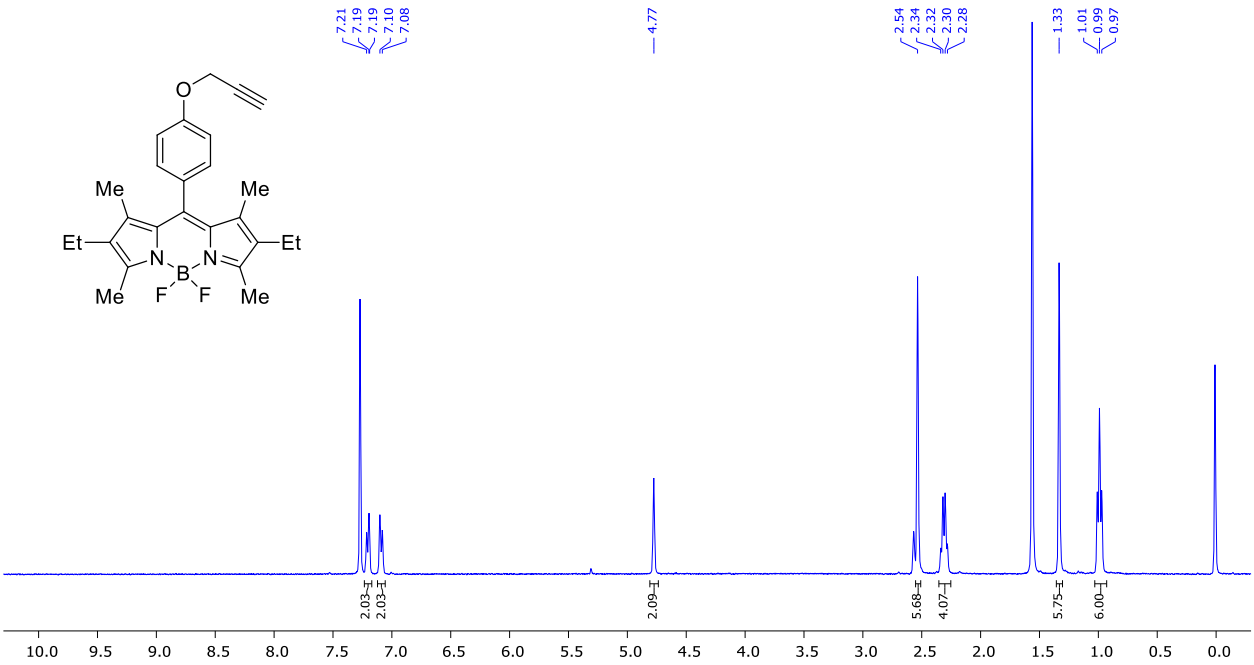

Figure C.1: ^{1}H NMR of BODIPY **1** in $CDCl_3$ (400 MHz)

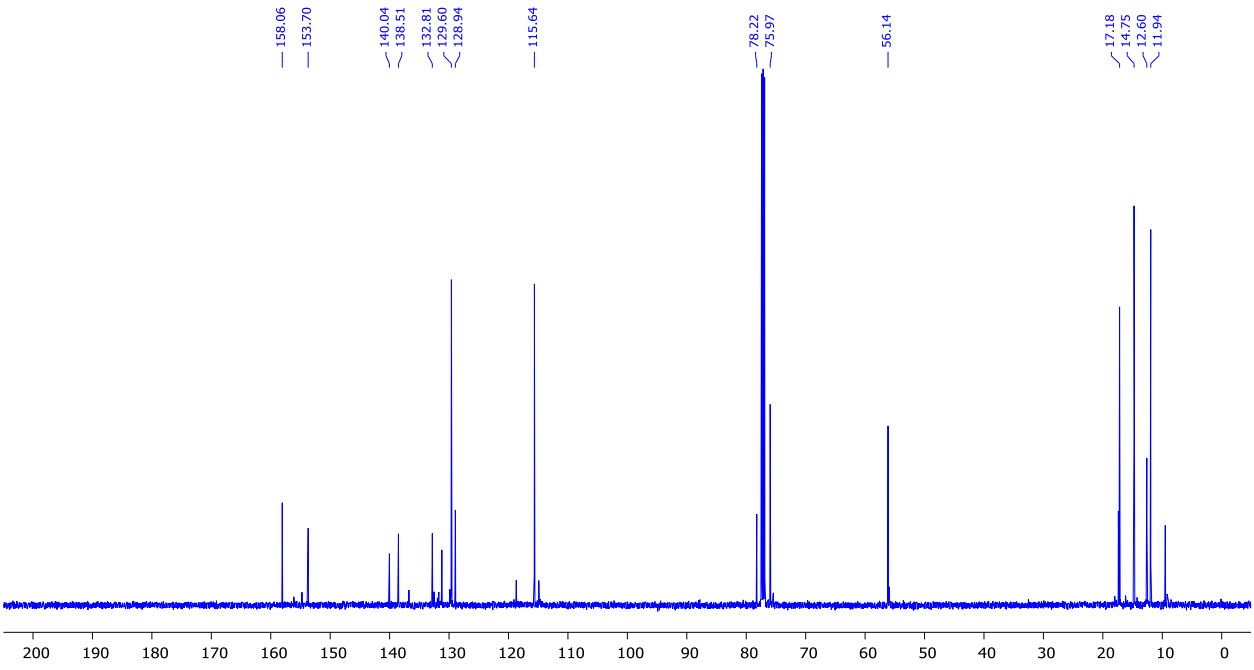

Figure C.2: ^{13}C NMR of BODIPY **1** in $CDCl_3$ (100 MHz)

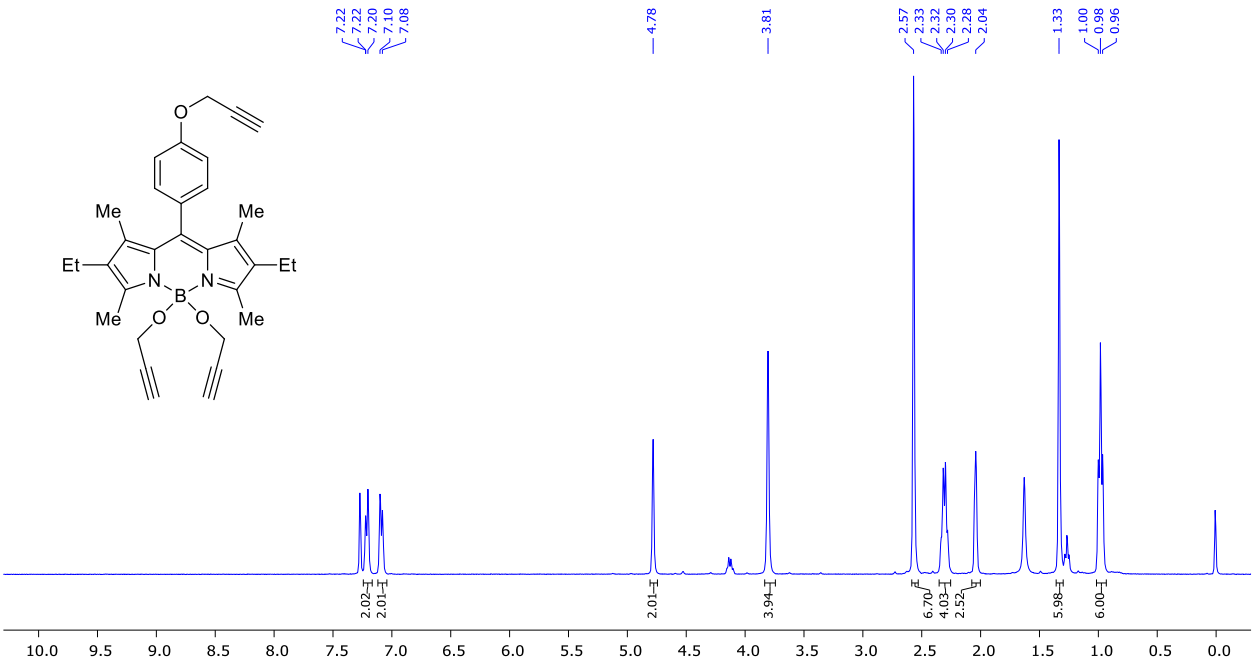

Figure C.3: ^{1}H NMR of BODIPY **2** in $CDCl_3$ (400 MHz)

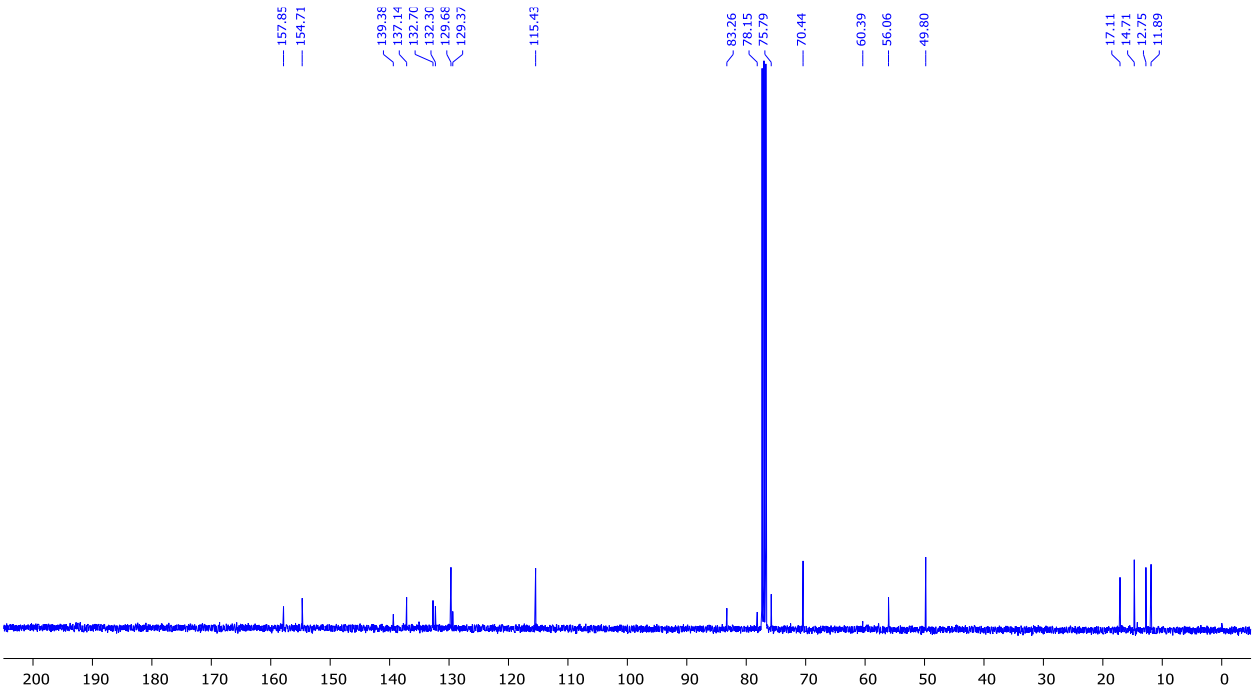

Figure C.4: ^{13}C NMR of BODIPY **2** in $CDCl_3$ (100 MHz)

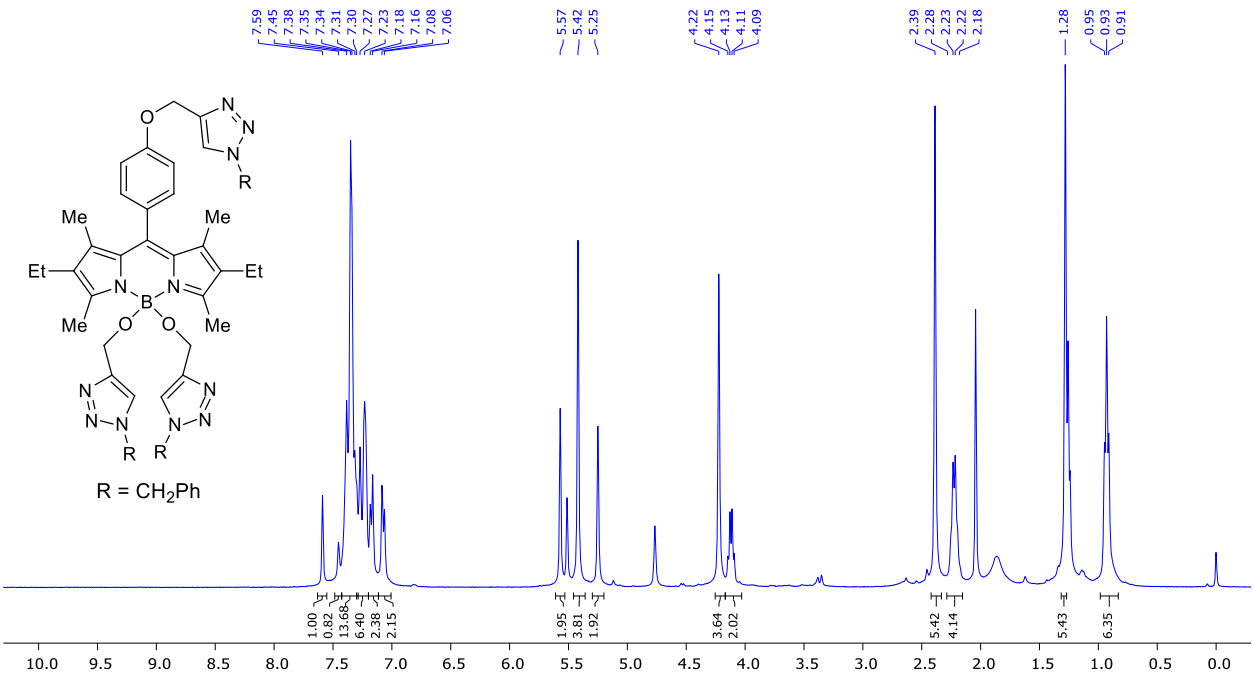

Figure C.5: ^{1}H NMR of BODIPY **3a** in $CDCl_3$ (400 MHz)

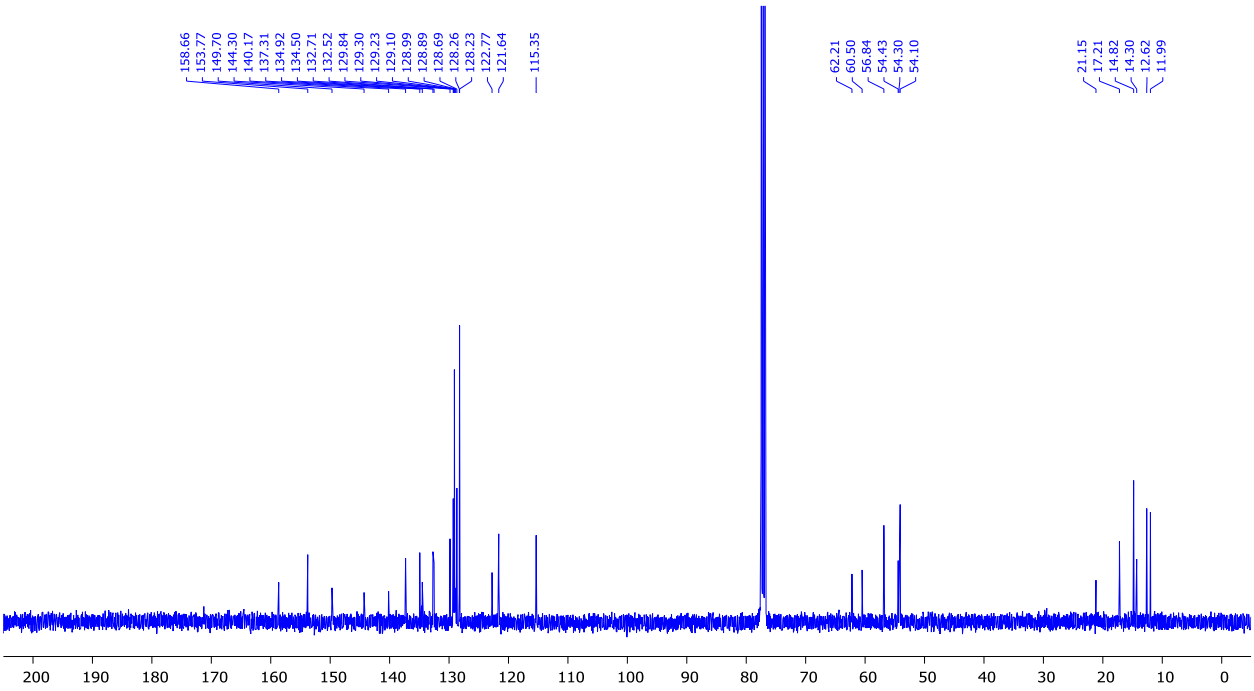

Figure C.6: ^{13}C NMR of BODIPY **3a** in $CDCl_3$ (100 MHz)

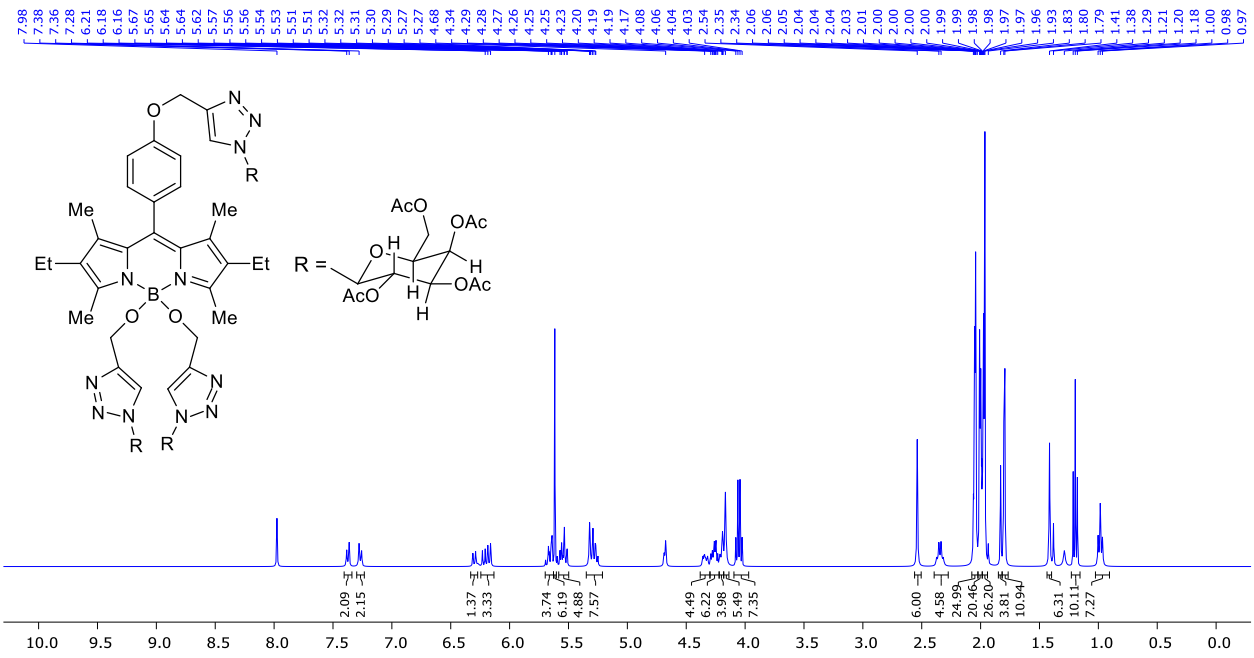

Figure C.7: ^{1}H NMR of BODIPY **3b** in acetone (400 MHz)

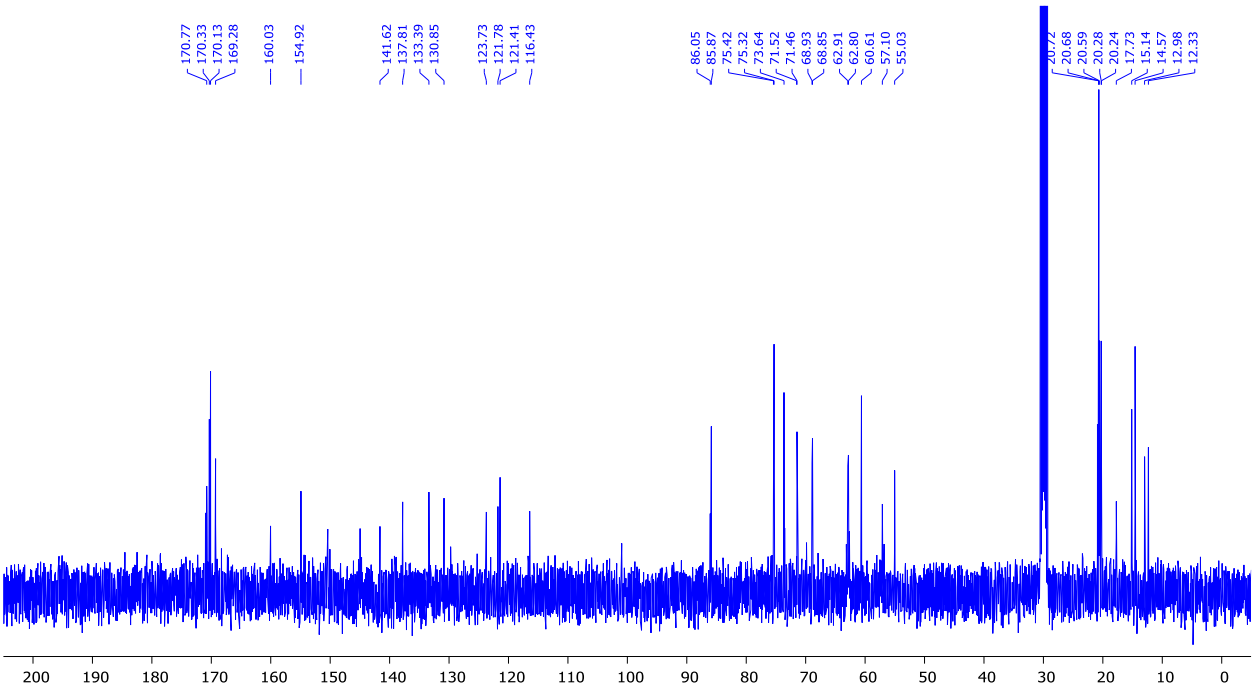

Figure C.8: ^{13}C NMR of BODIPY **3b** in acetone (100 MHz)

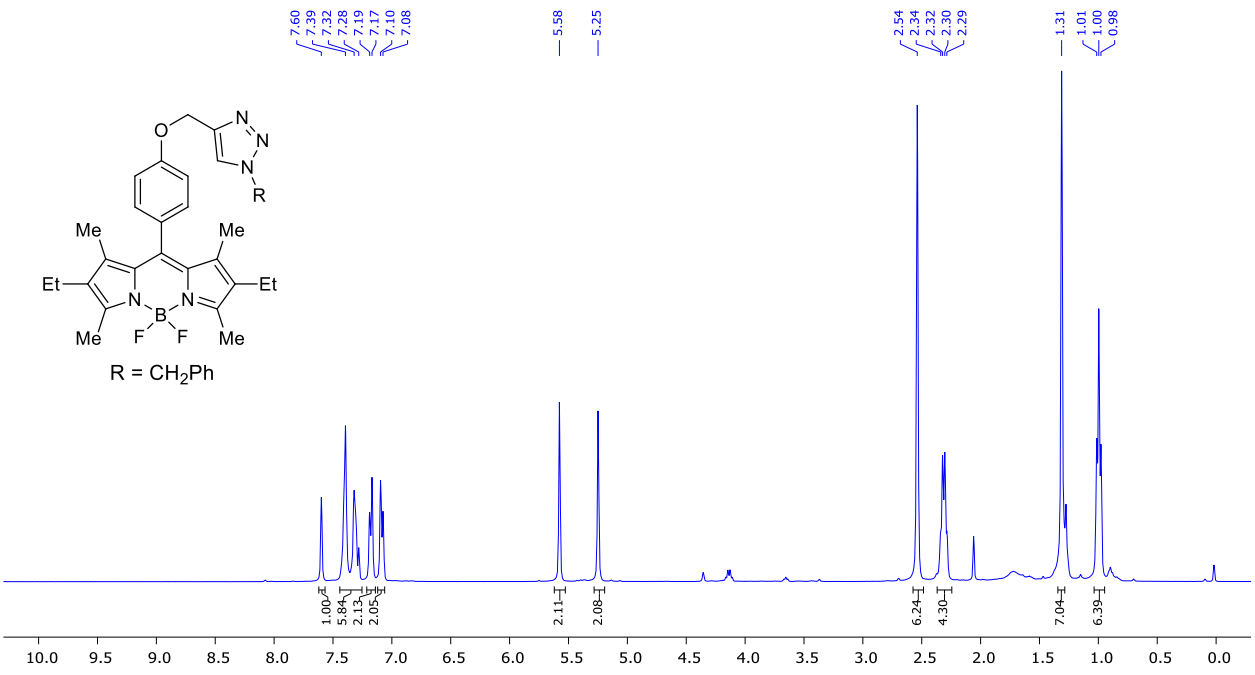

Figure C.9: ^{1}H NMR of BODIPY **4a** in CDCl3 (400 MHz)

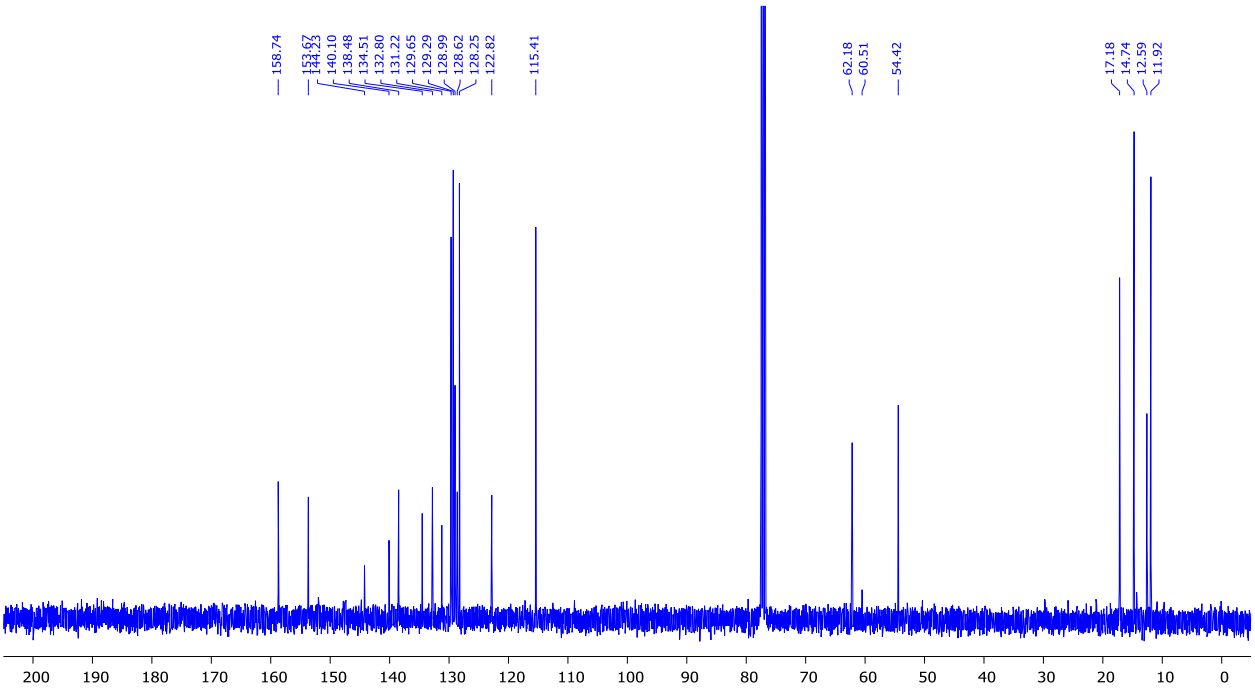

Figure C.10: ^{13}C NMR of BODIPY **4a** in $CDCl_3$ (100 MHz)

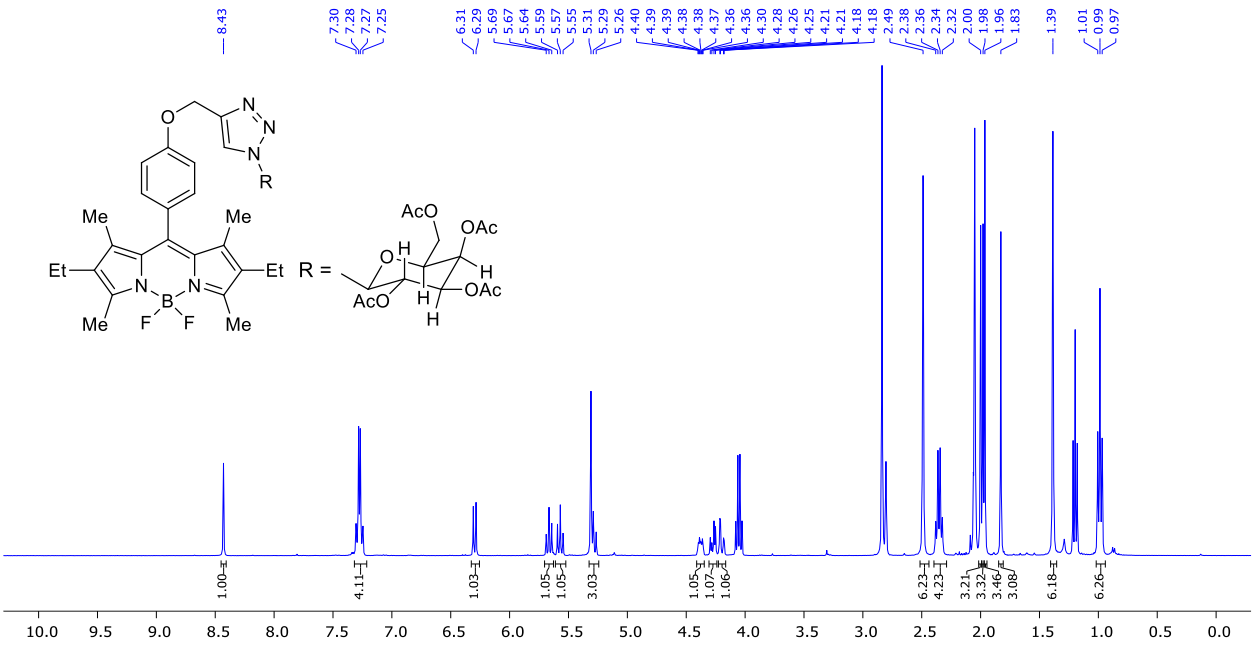

Figure C.11: ^{1}H NMR of BODIPY **4b** in acetone (400 MHz)

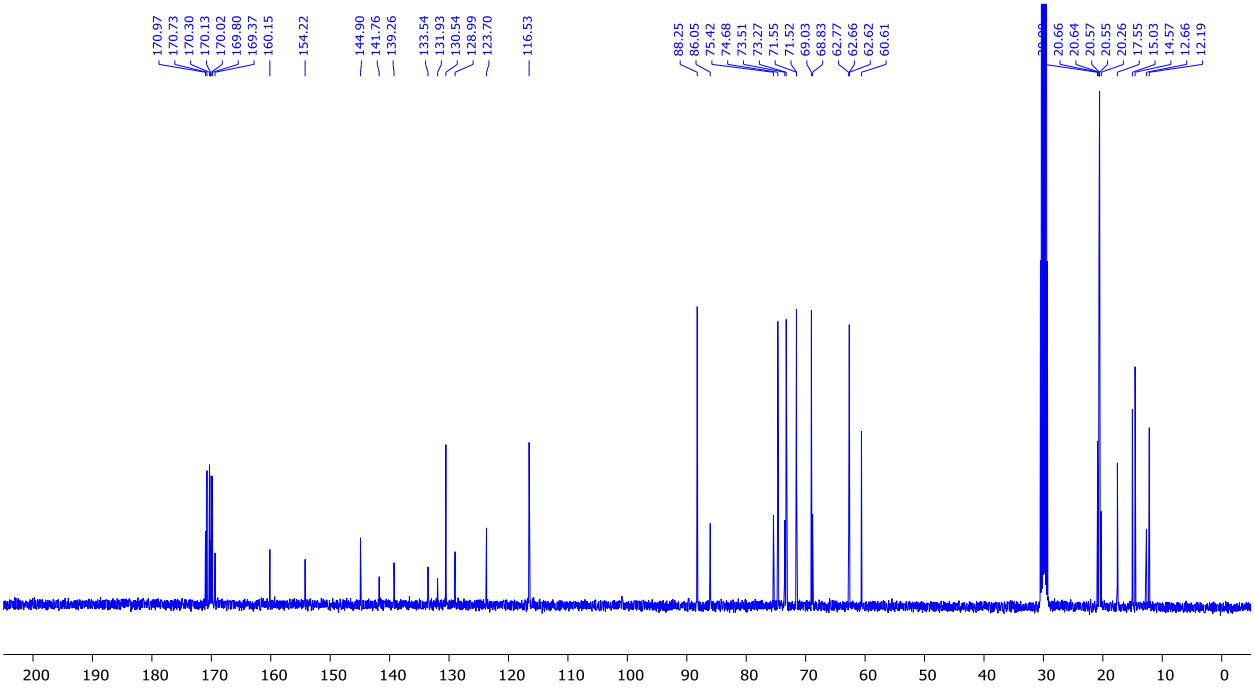

Figure C.12: ^{13}C NMR of BODIPY **4b** in acetone (100 MHz)

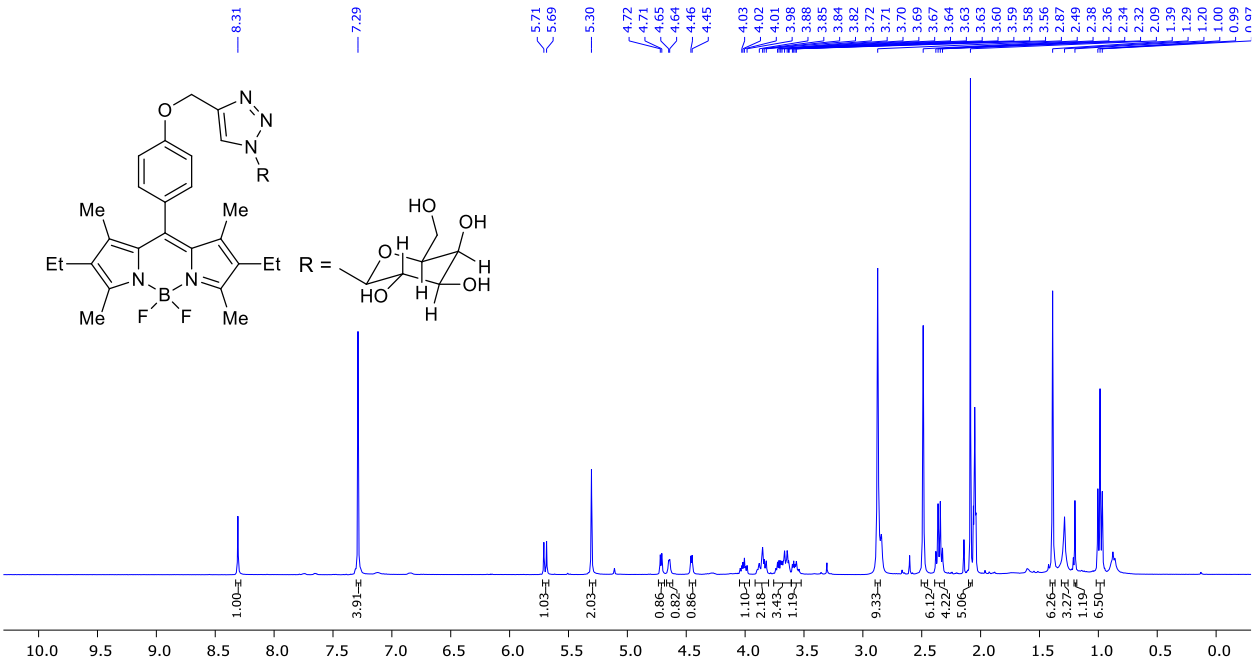

Figure C.13: ^{1}H NMR of BODIPY **4c** in acetone (400 MHz)

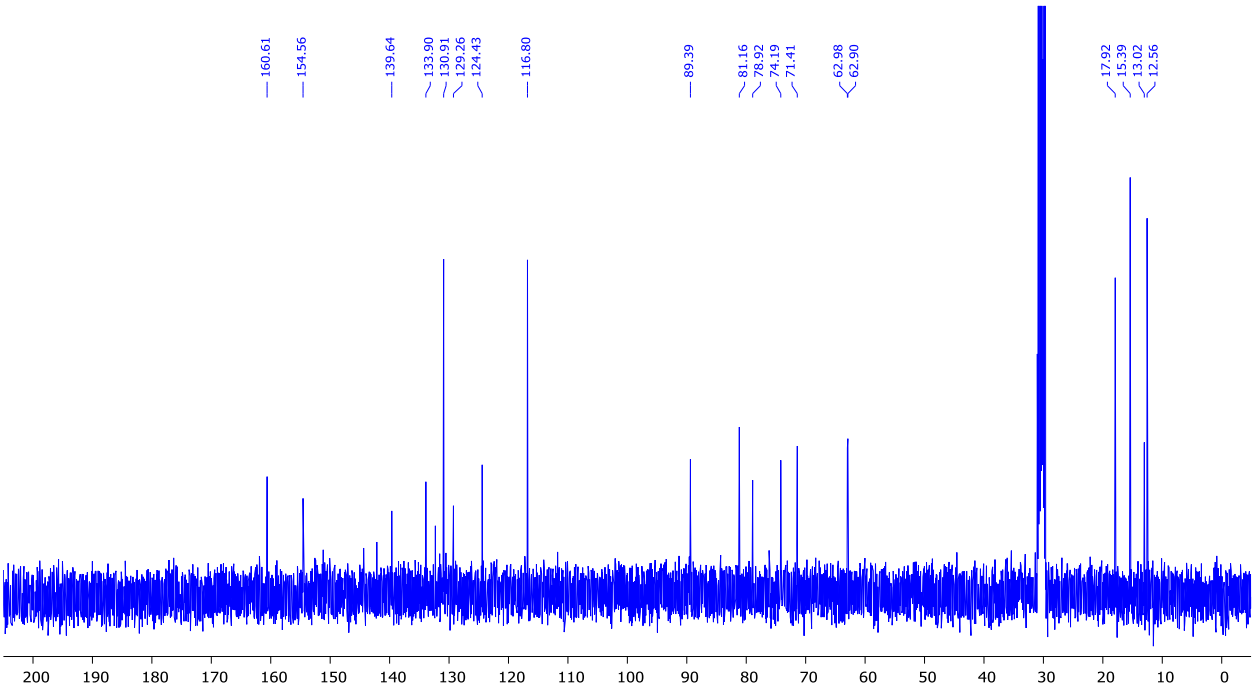

Figure C.14: ^{13}C NMR of BODIPY **4c** in $CDCl_3$ (100 MHz)

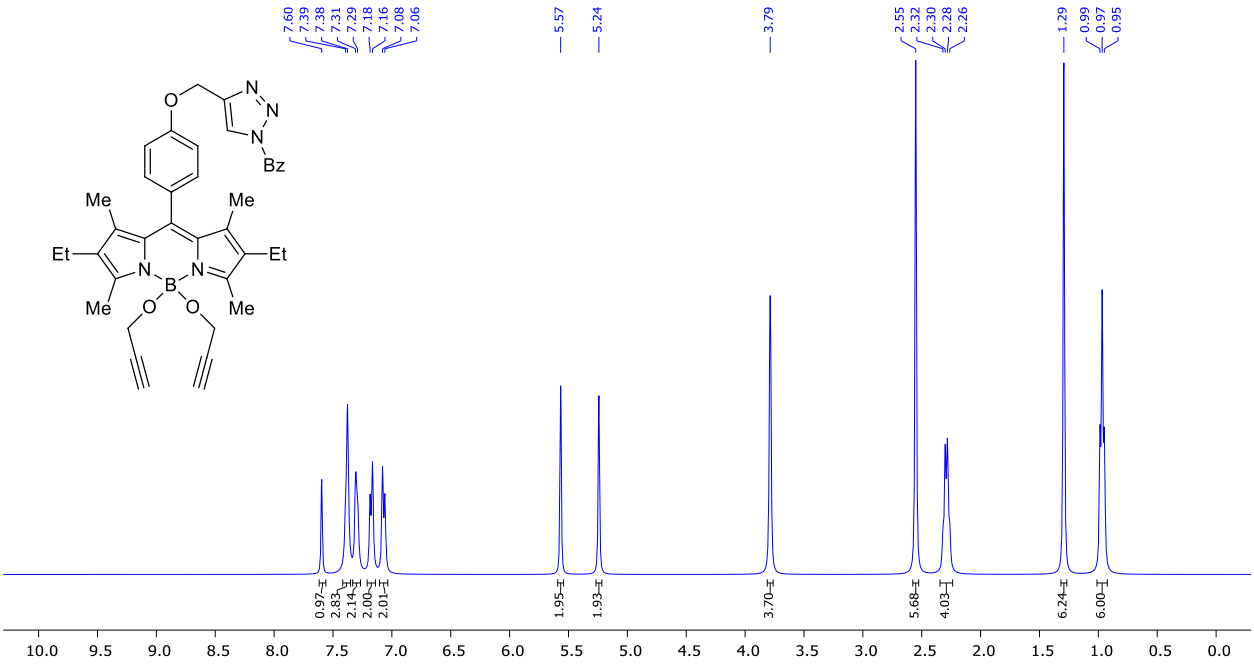

Figure C.15: ^{1}H NMR of BODIPY **5a** in $CDCl_3$ (400 MHz)

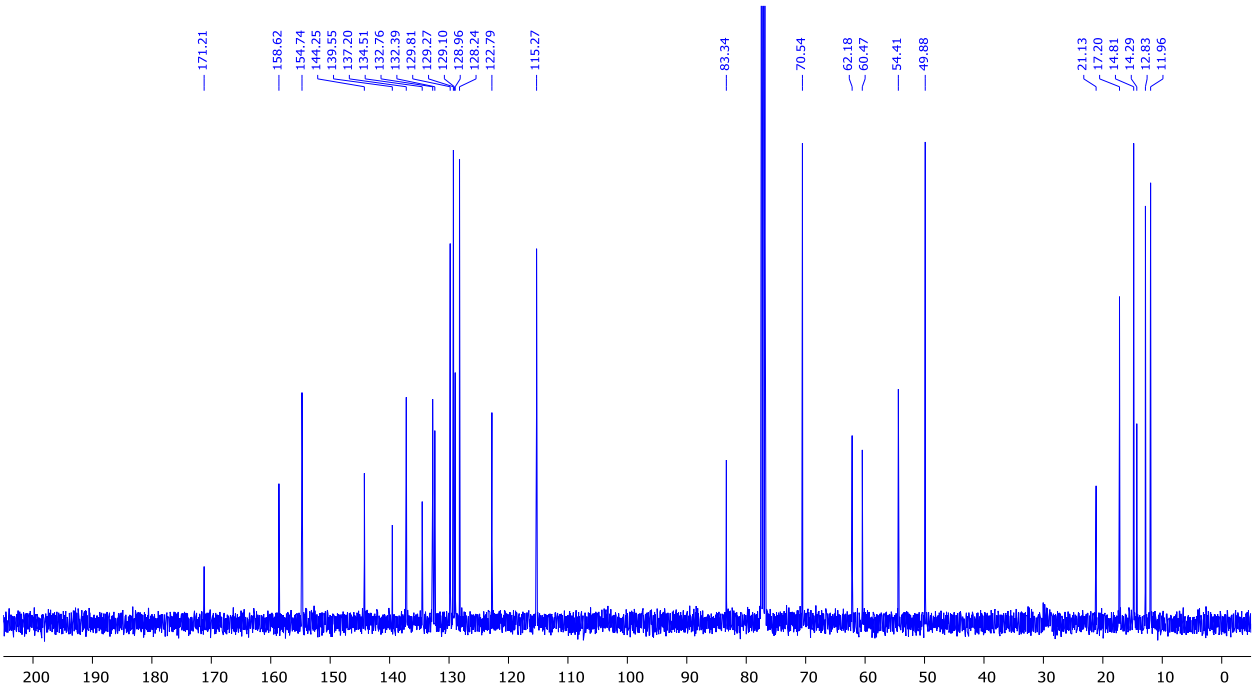

Figure C.16: ^{13}C NMR of BODIPY **5a** in $CDCl_3$ (100 MHz)

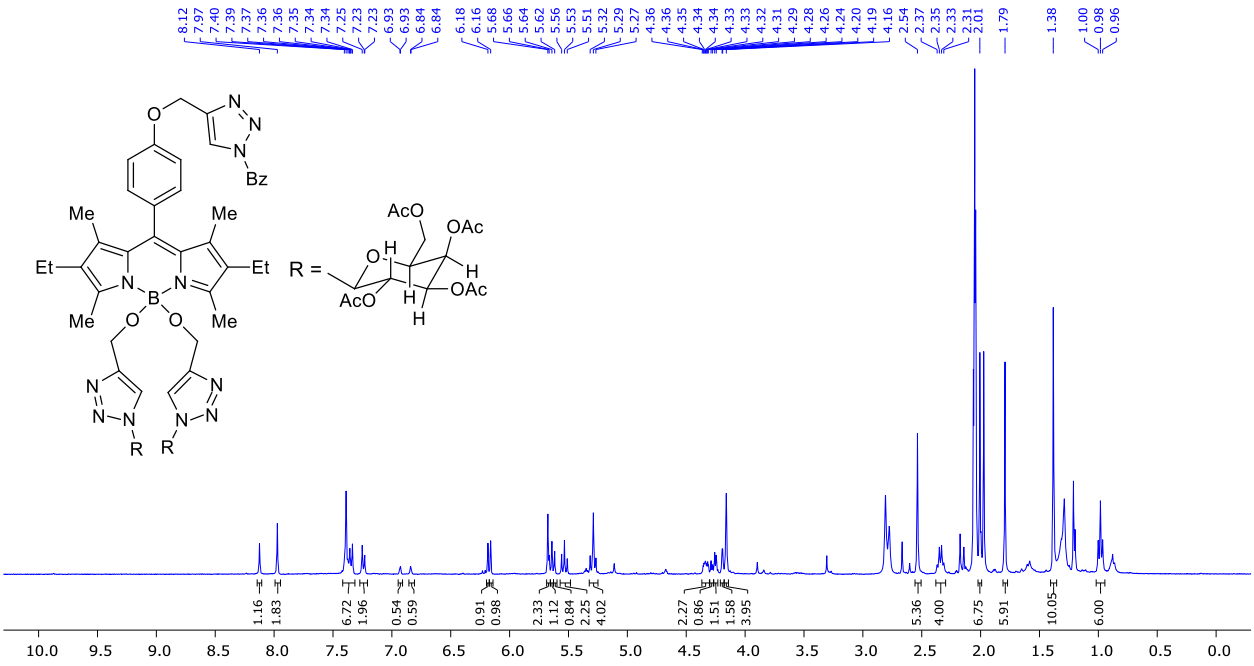

Figure C.17: ^{1}H NMR of BODIPY **6a** in acetone (400 MHz)

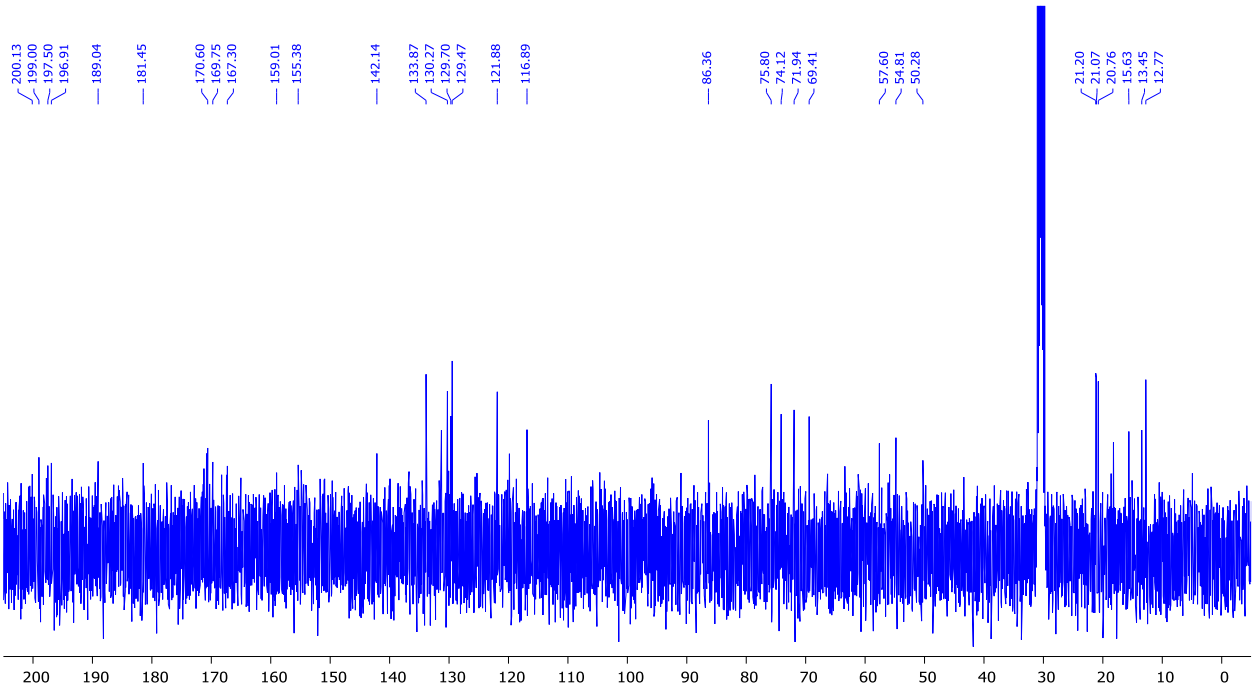

Figure C.18: ^{13}C NMR of BODIPY **6a** in acetone (100 MHz)

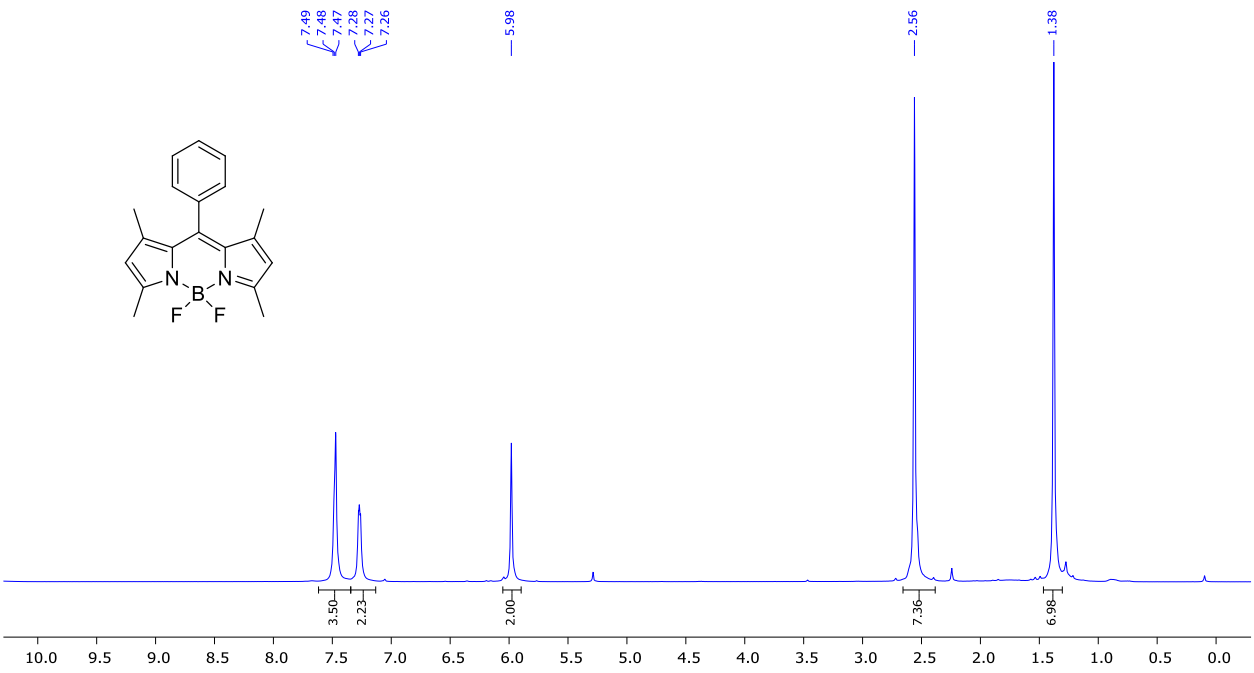

Figure C.19: ^{1}H NMR of BODIPY **7** in acetone (400 MHz)

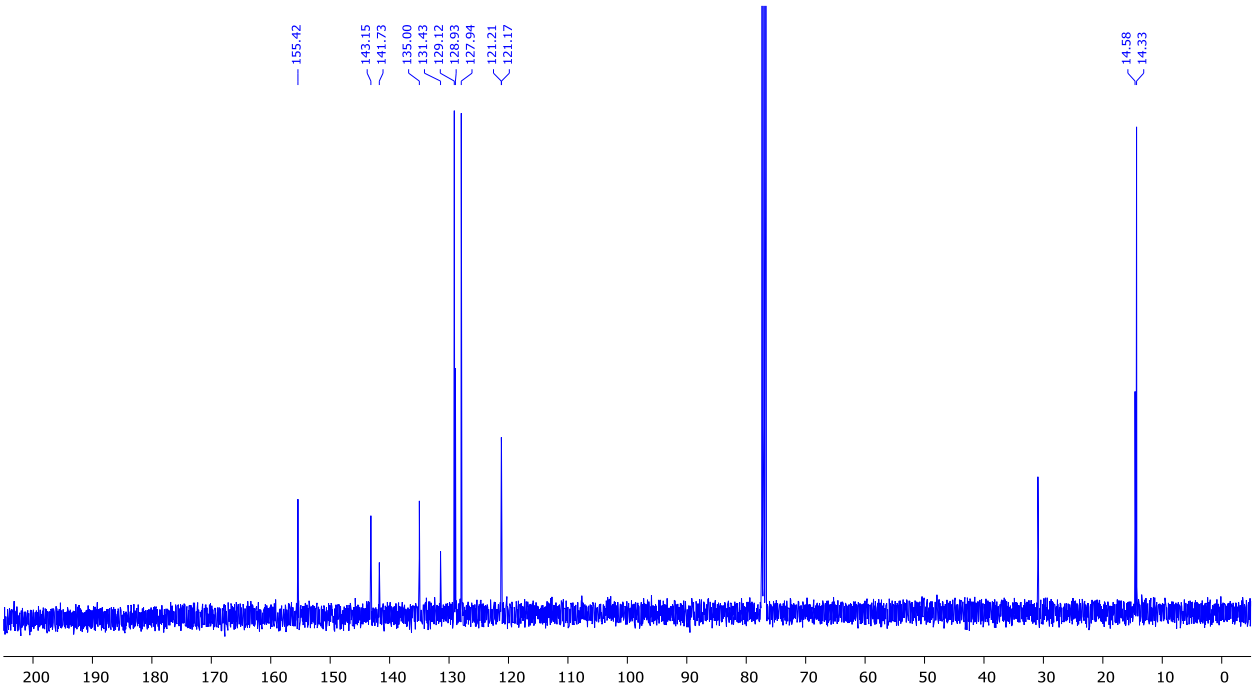

Figure C.20: ^{13}C NMR of BODIPY **7** in $CDCl_3$ (100 MHz)

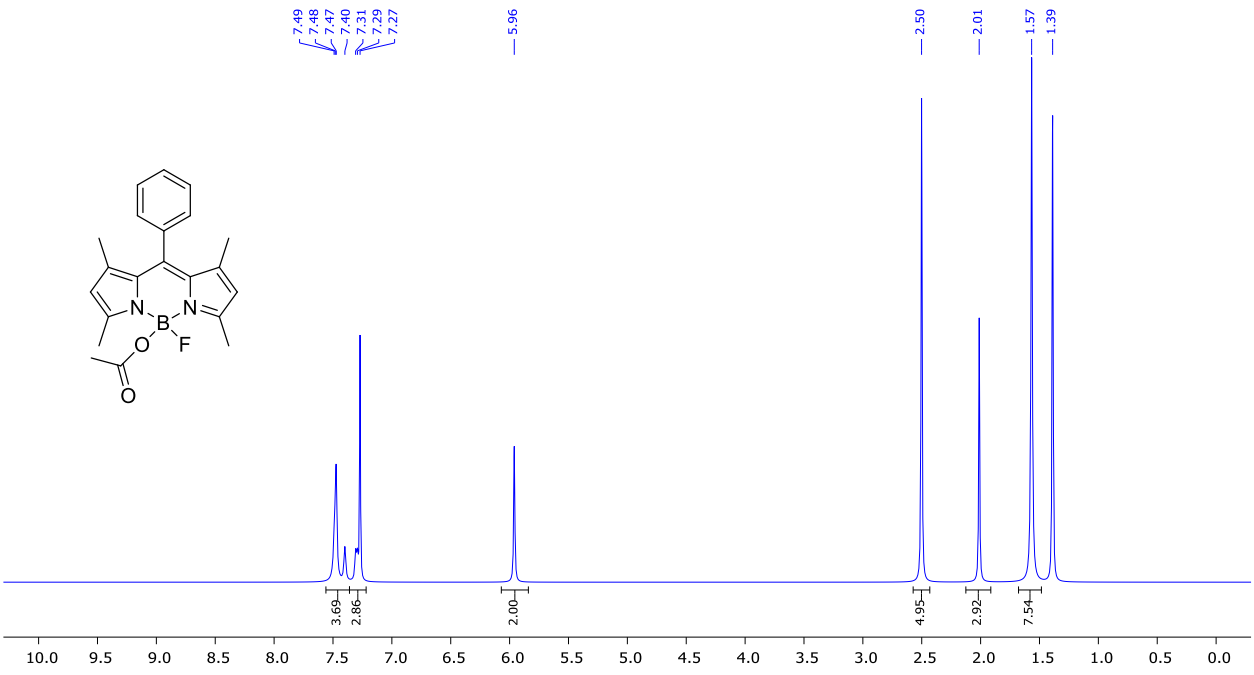

Figure C.21: ^{1}H NMR of BODIPY **8a** in $CDCl_3$ (400 MHz)

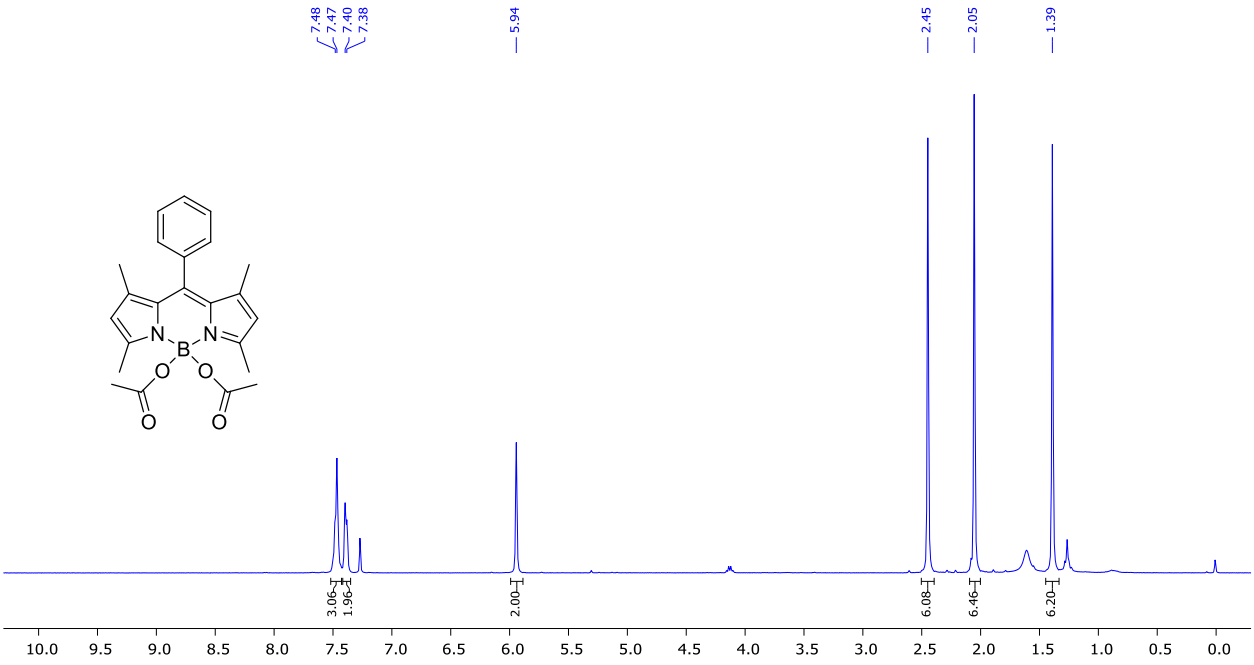

Figure C.22: ^{1}H NMR of BODIPY **8b** in $CDCl_3$ (400 MHz)

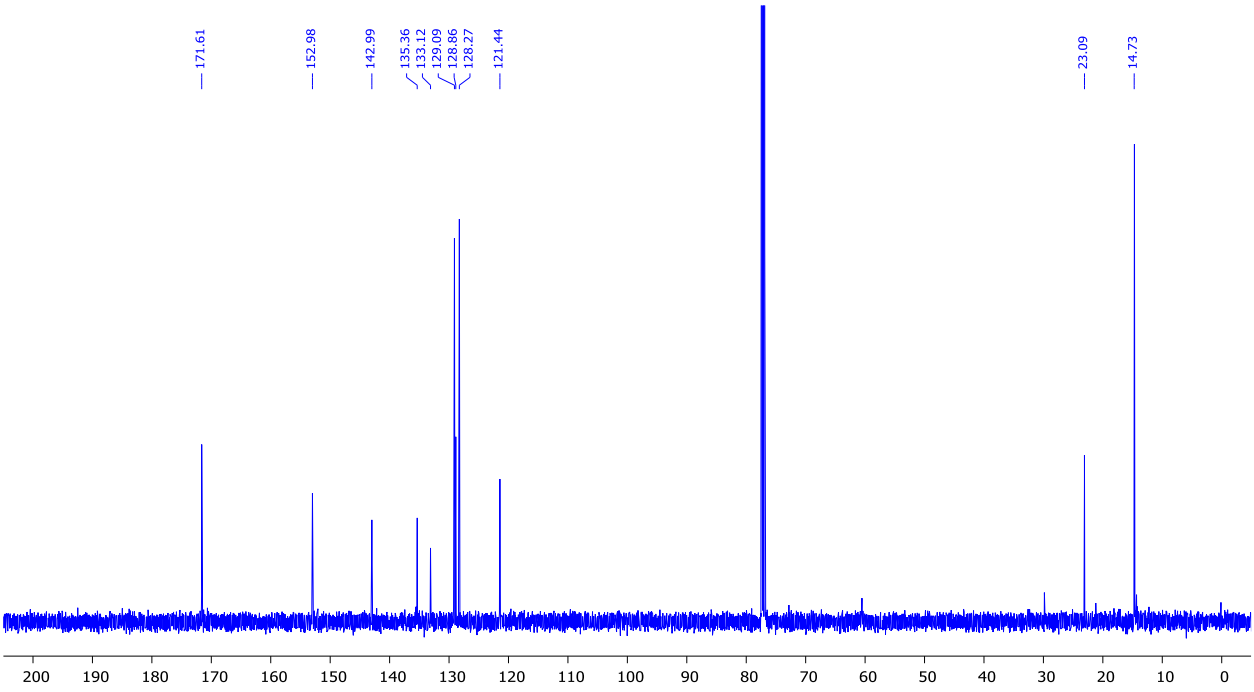

Figure C.23: ^{13}C NMR of BODIPY **8b** in $CDCl_3$ (100 MHz)

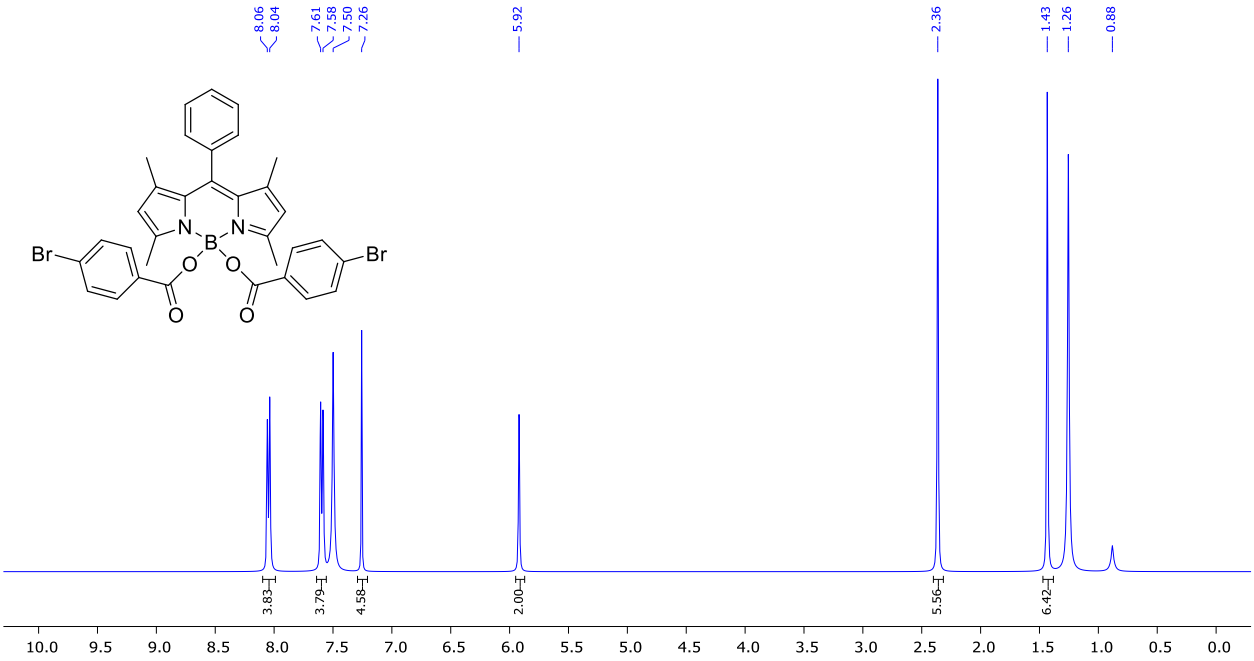

Figure C.24: ^{1}H NMR of BODIPY **9** in $CDCl_3$ (400 MHz)

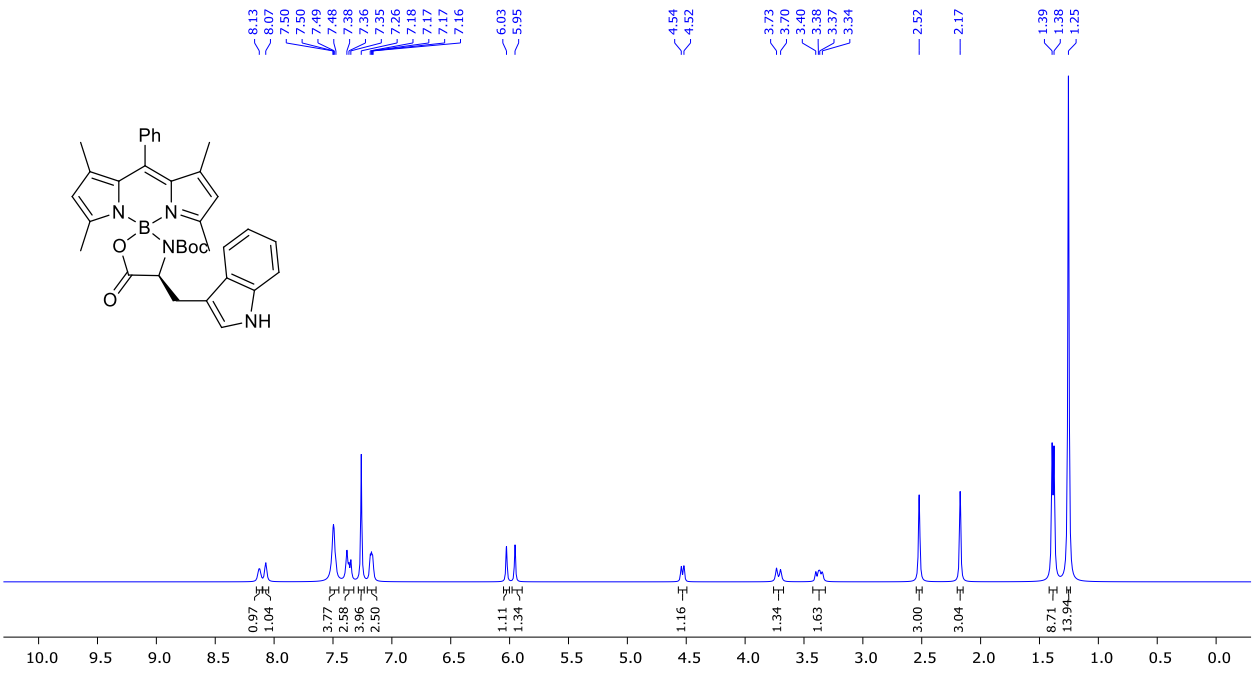

Figure C.25: ^{1}H NMR of BODIPY **10** in $CDCl_3$ (400 MHz)

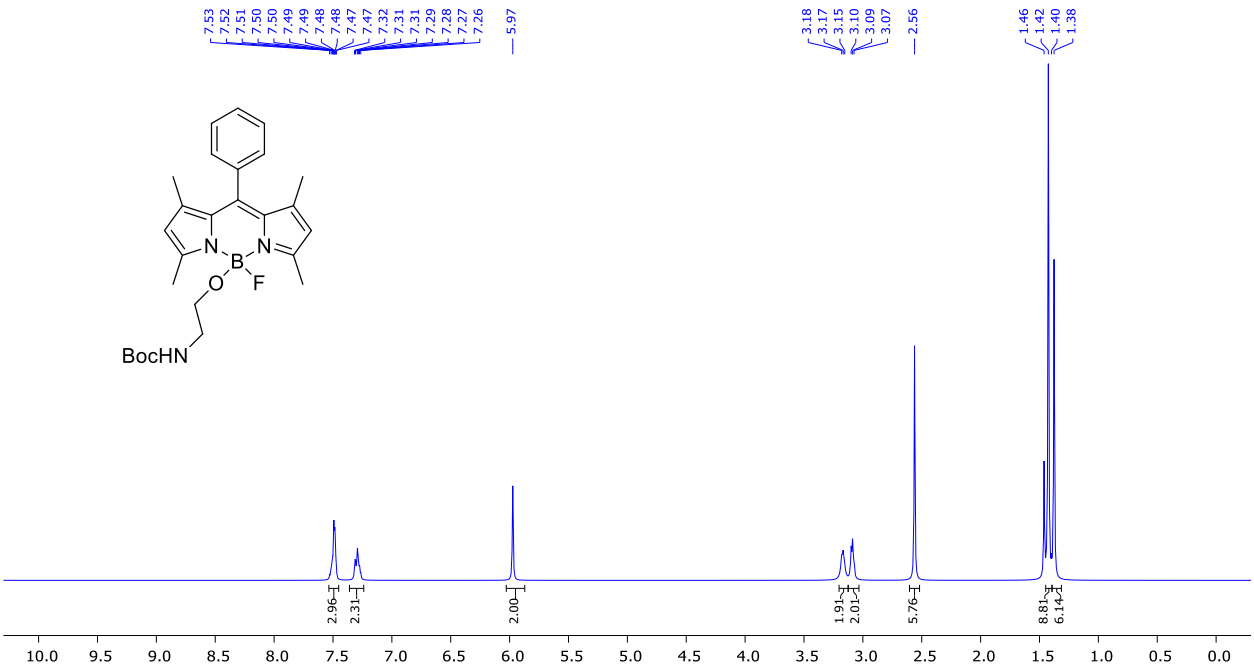

Figure C.26: ^{1}H NMR of BODIPY **11a** in $CDCl_3$ (400 MHz)

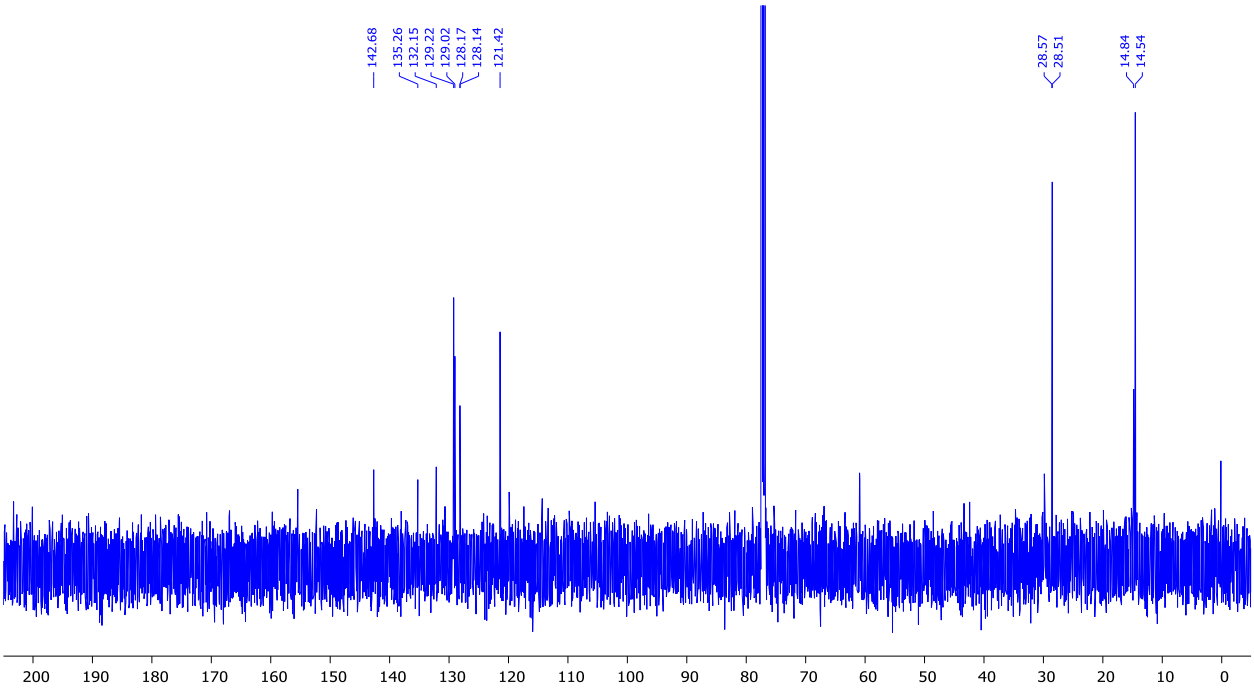

Figure C.27: ^{13}C NMR of BODIPY **11a** in $CDCl_3$ (100 MHz)

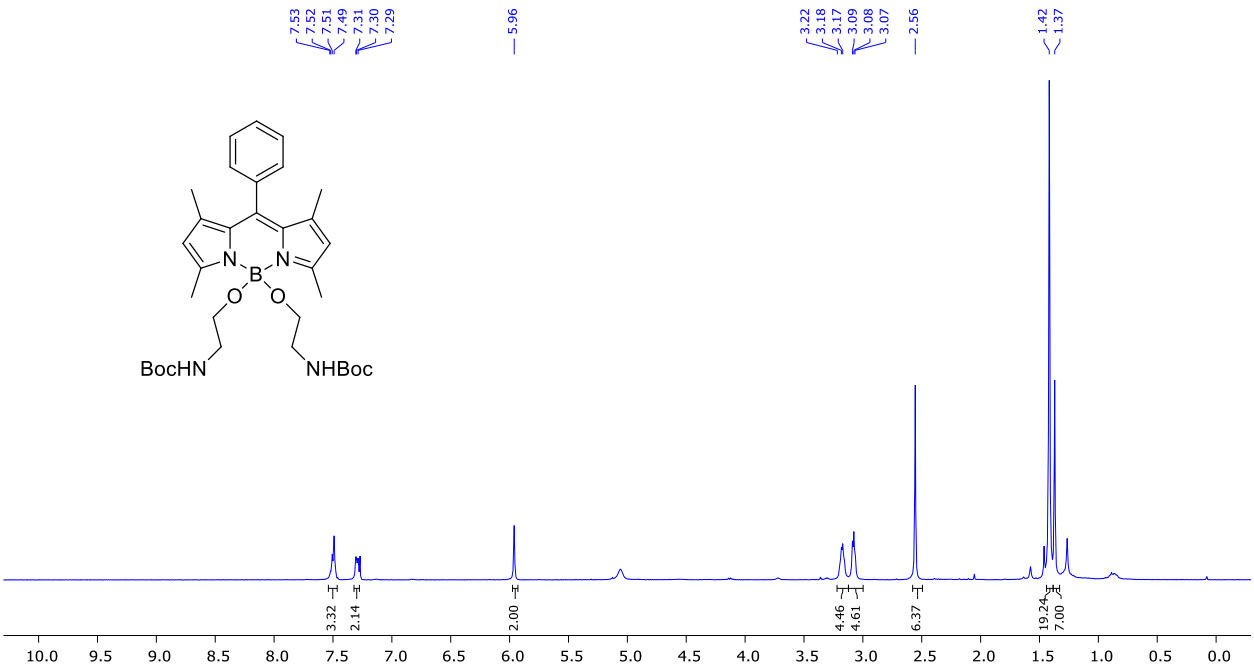

Figure C.28: ^{1}H NMR of BODIPY **11b** in $CDCl_3$ (400 MHz)

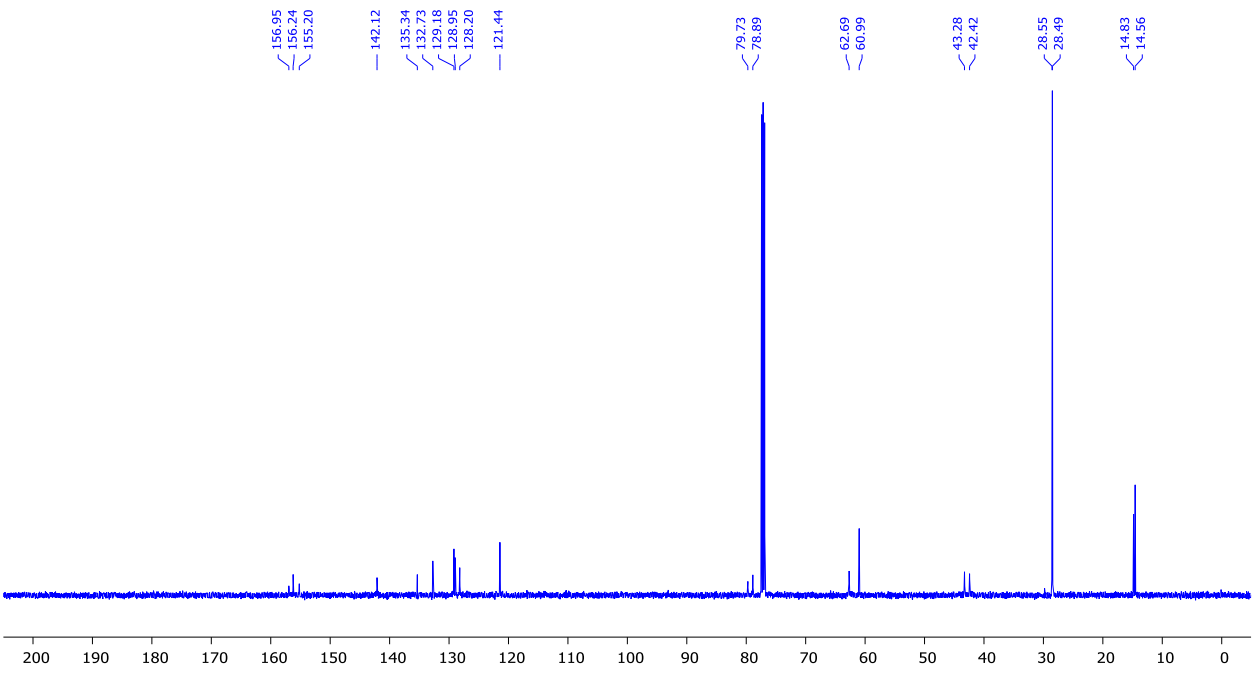

Figure C.29: ^{13}C NMR of BODIPY **11b** in $CDCl_3$ (100 MHz)

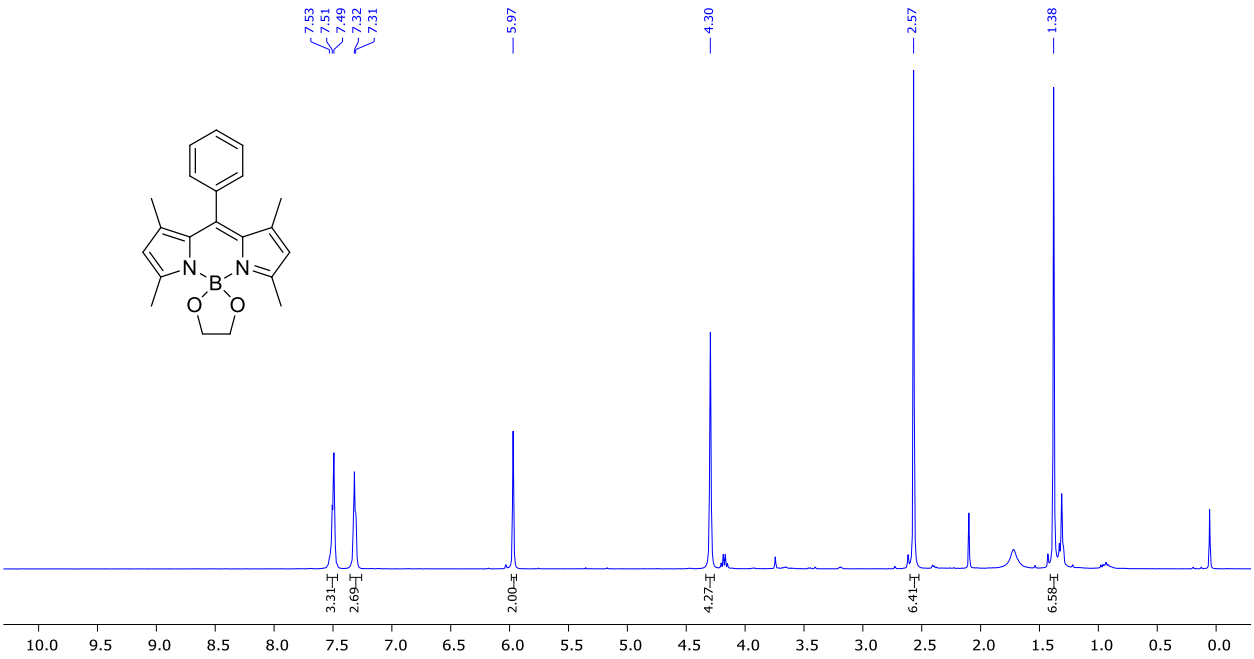

Figure C.30: ^{1}H NMR of BODIPY **12** in $CDCl_3$ (400 MHz)

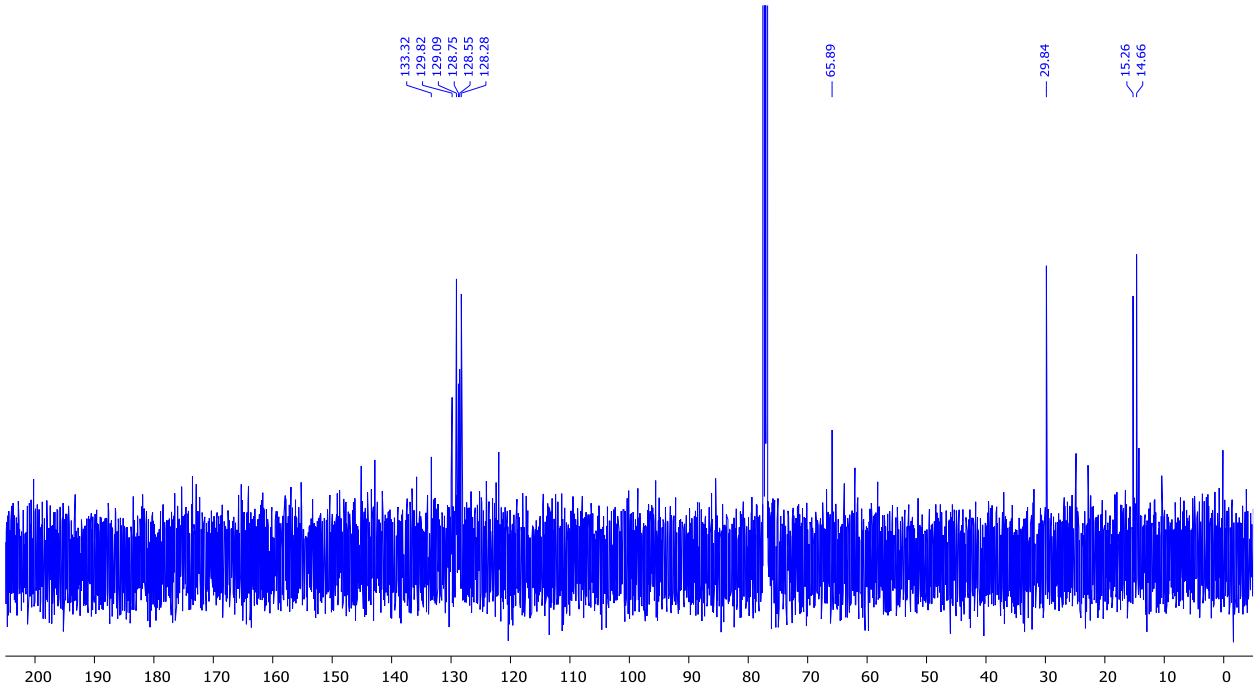

Figure C.31: ^{13}C NMR of BODIPY **12** in $CDCl_3$ (100 MHz)

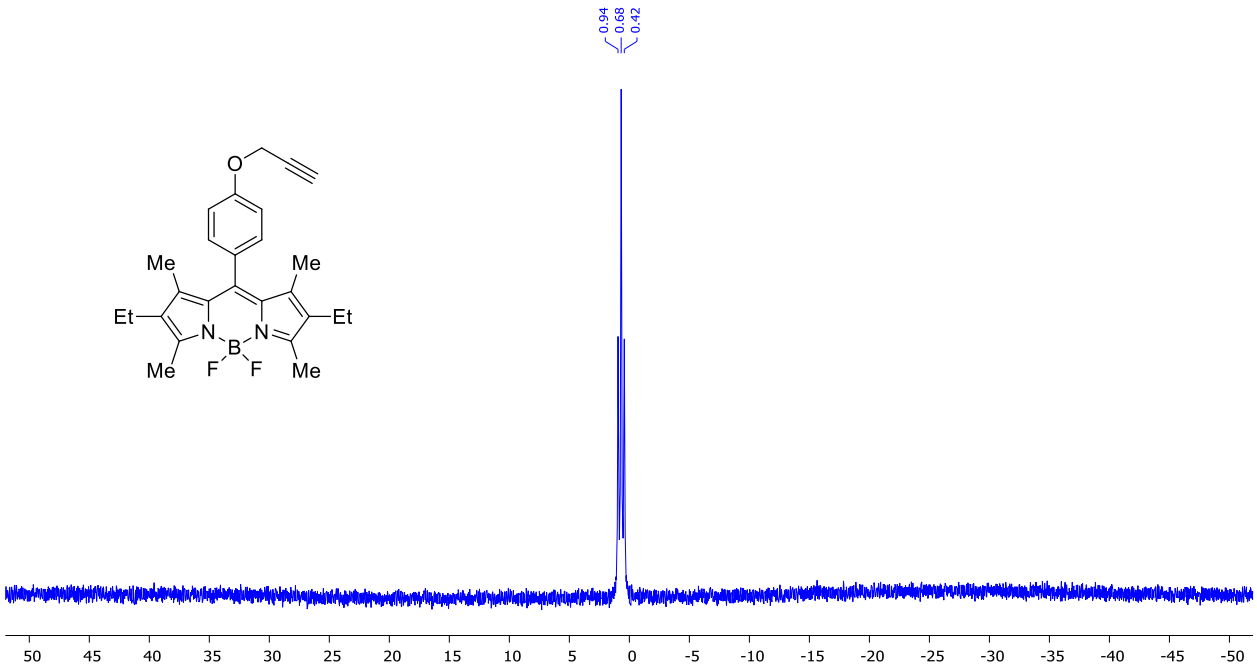

Figure C.32: ^{11}B NMR of BODIPY **1** in $CDCl_3$ (128 MHz)

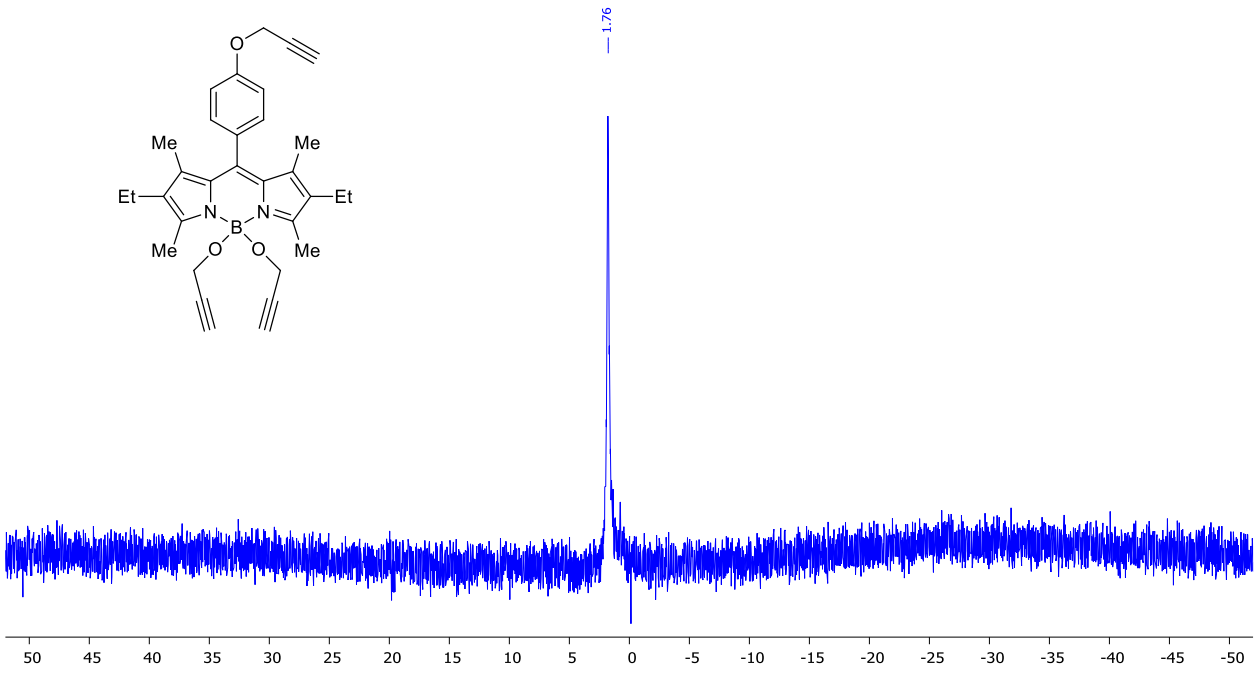

Figure C.33: ^{11}B NMR of BODIPY **2** in $CDCl_3$ (128 MHz)

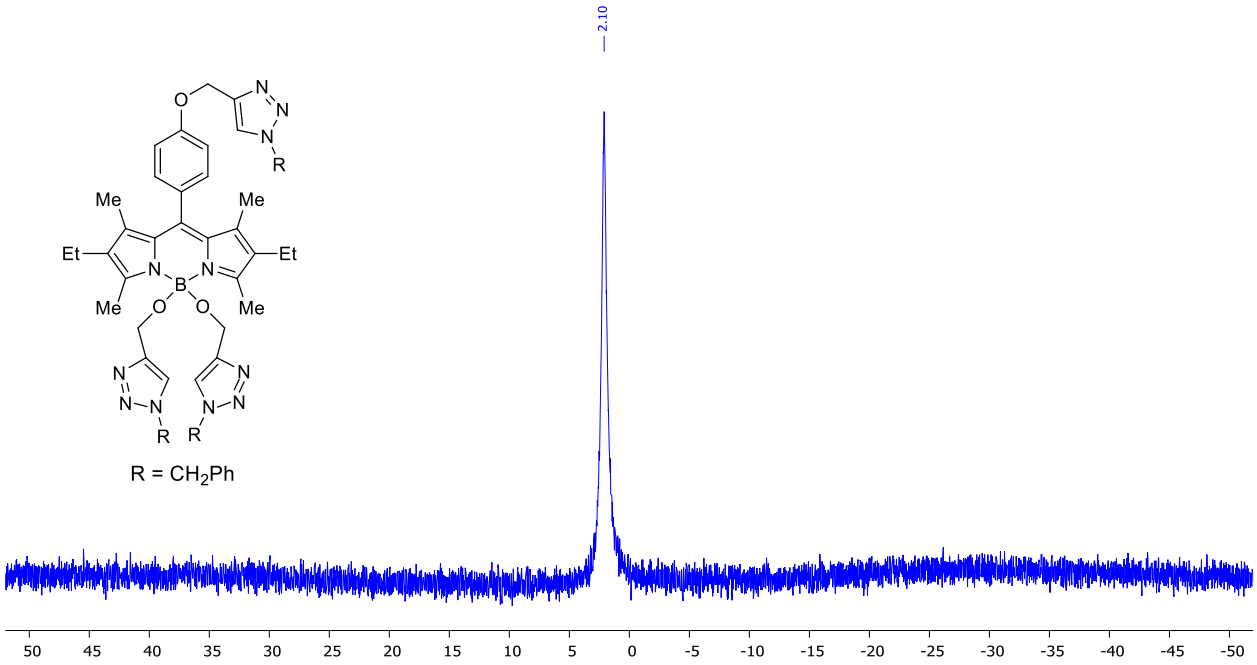

Figure C.34: ^{11}B NMR of BODIPY **3a** in $CDCl_3$ (128 MHz)

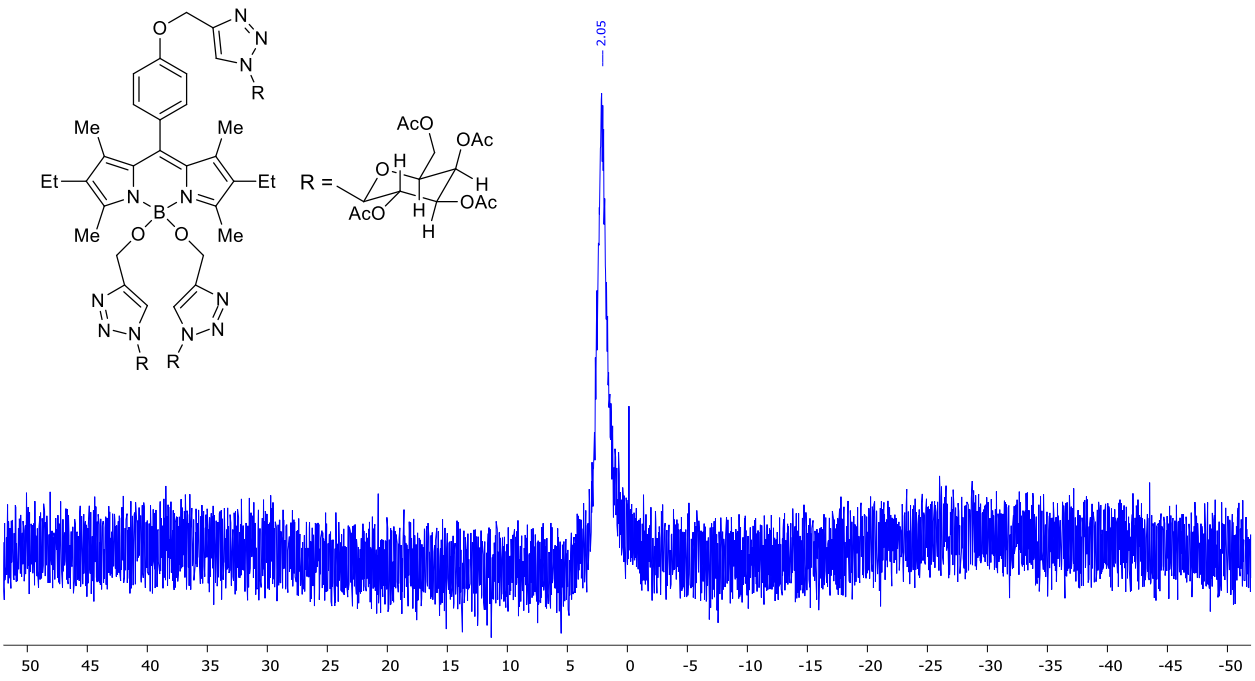

Figure C.35: ^{11}B NMR of BODIPY **3b** in $CDCl_3$ (128 MHz)

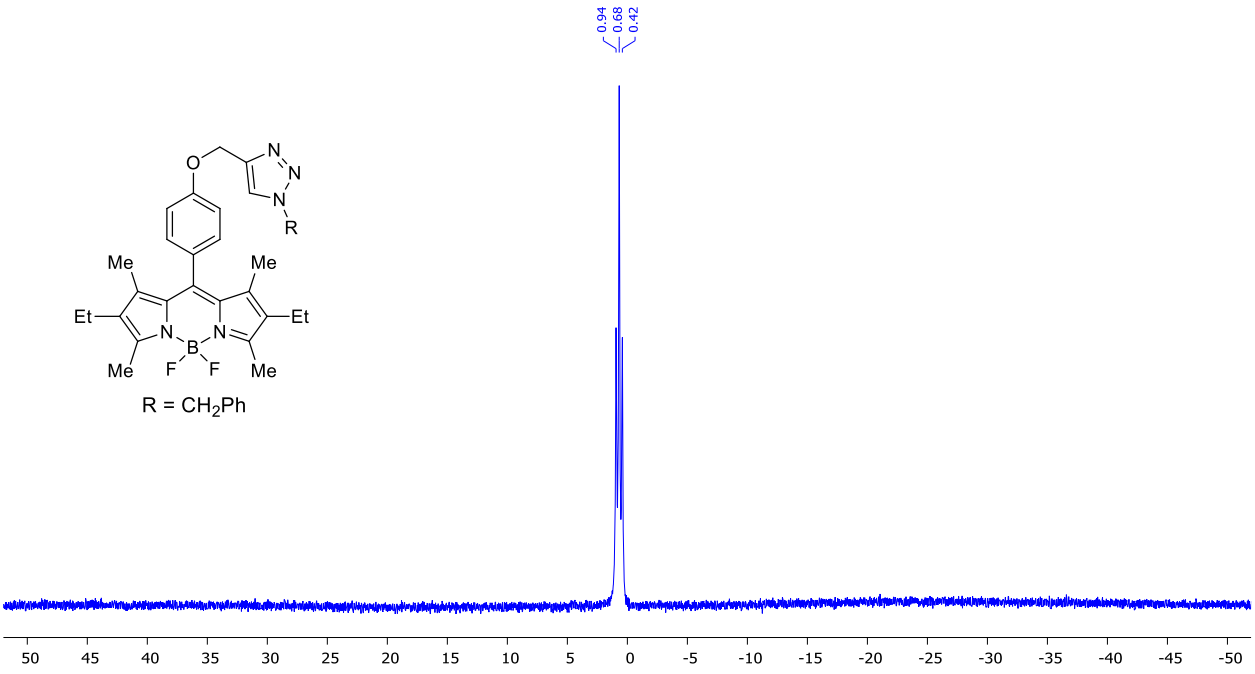

Figure C.36: ^{11}B NMR of BODIPY **4a** in $CDCl_3$ (128 MHz)

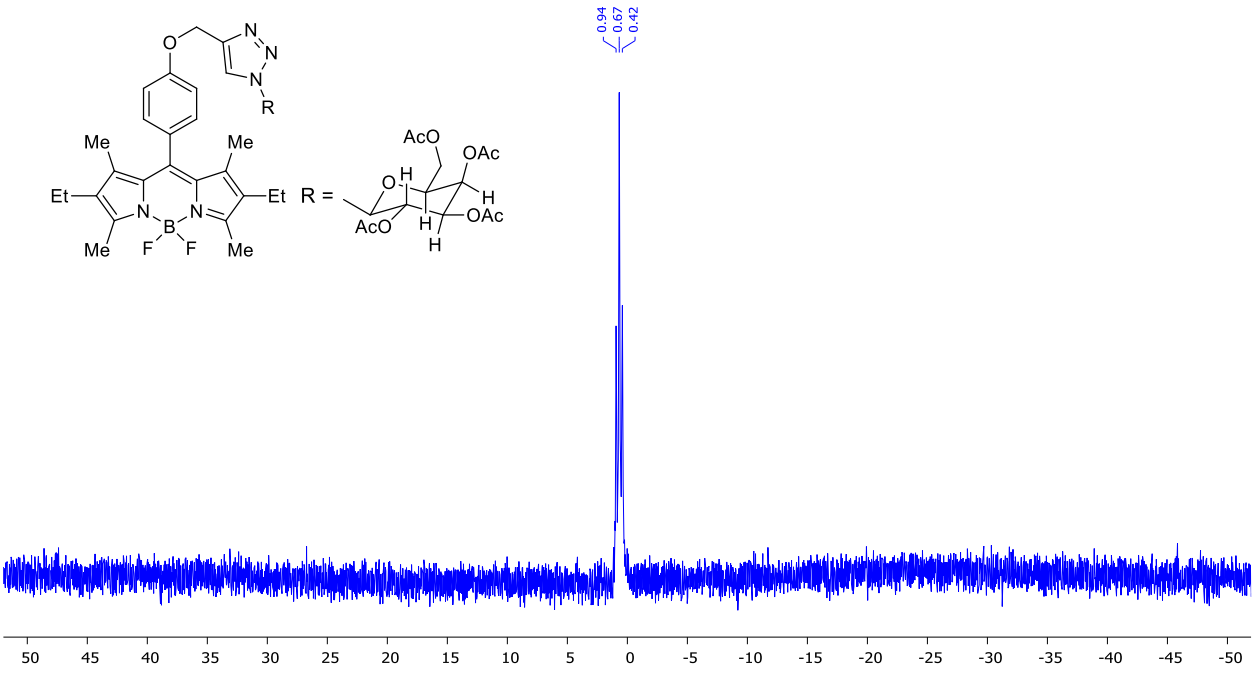

Figure C.37: ^{11}B NMR of BODIPY **4b** in $CDCl_3$ (128 MHz)

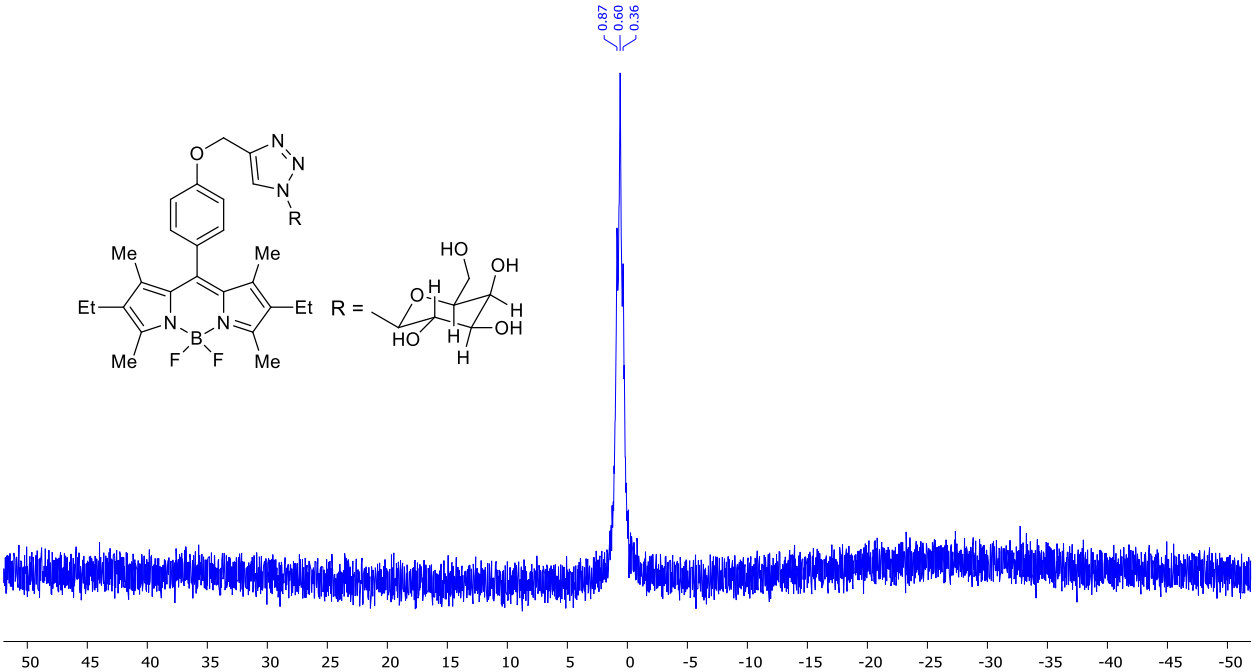

Figure C.38: ^{11}B NMR of BODIPY **4c** in $CDCl_3$ (128 MHz)

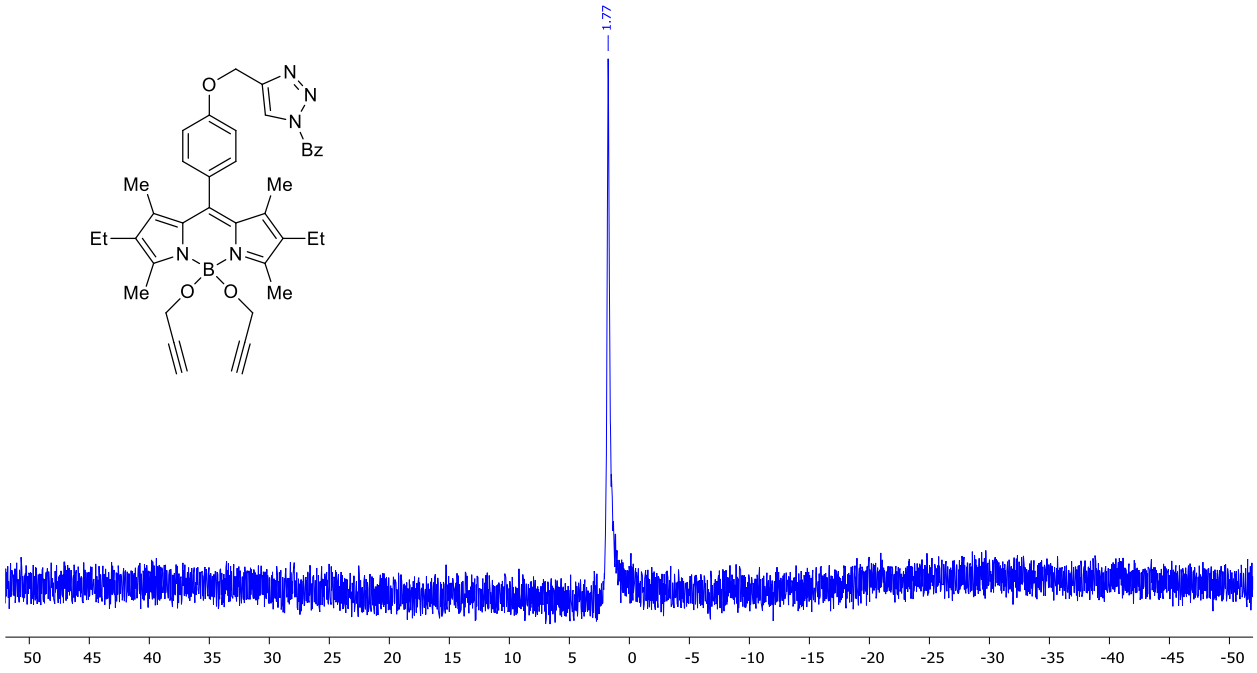

Figure C.39: ^{11}B NMR of BODIPY **5a** in $CDCl_3$ (128 MHz)

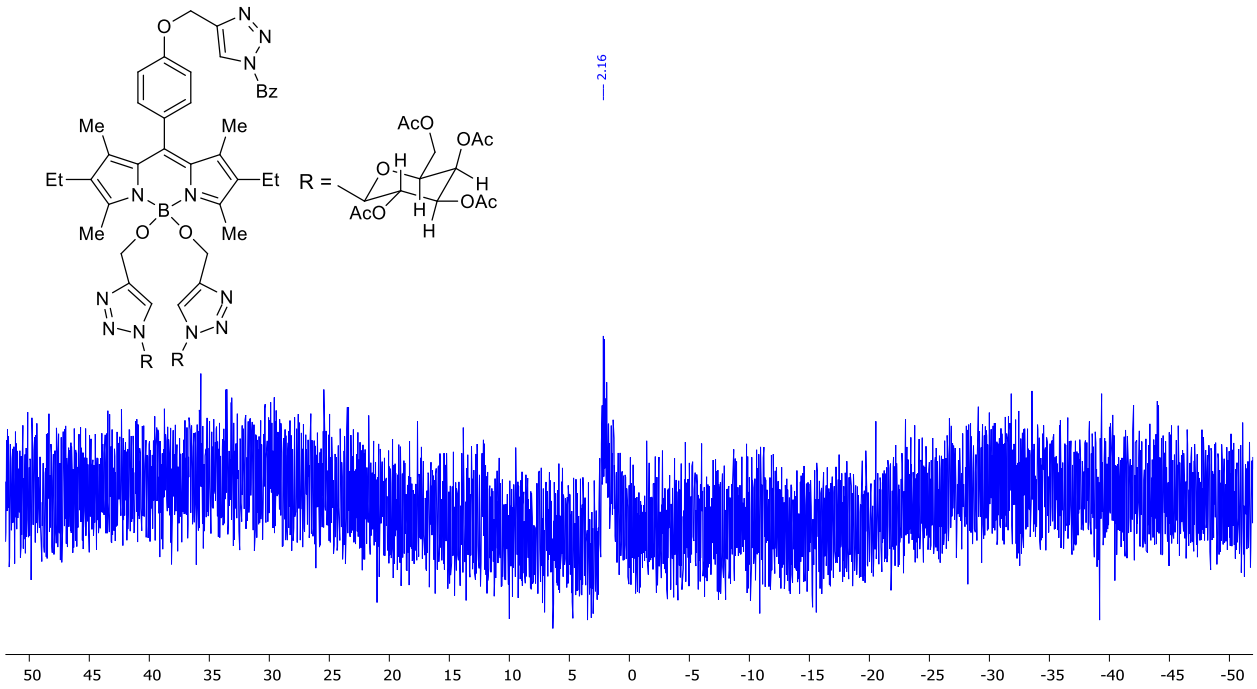

Figure C.40: ^{11}B NMR of BODIPY **6a** in $((CD_3)_2CO$ (128 MHz)

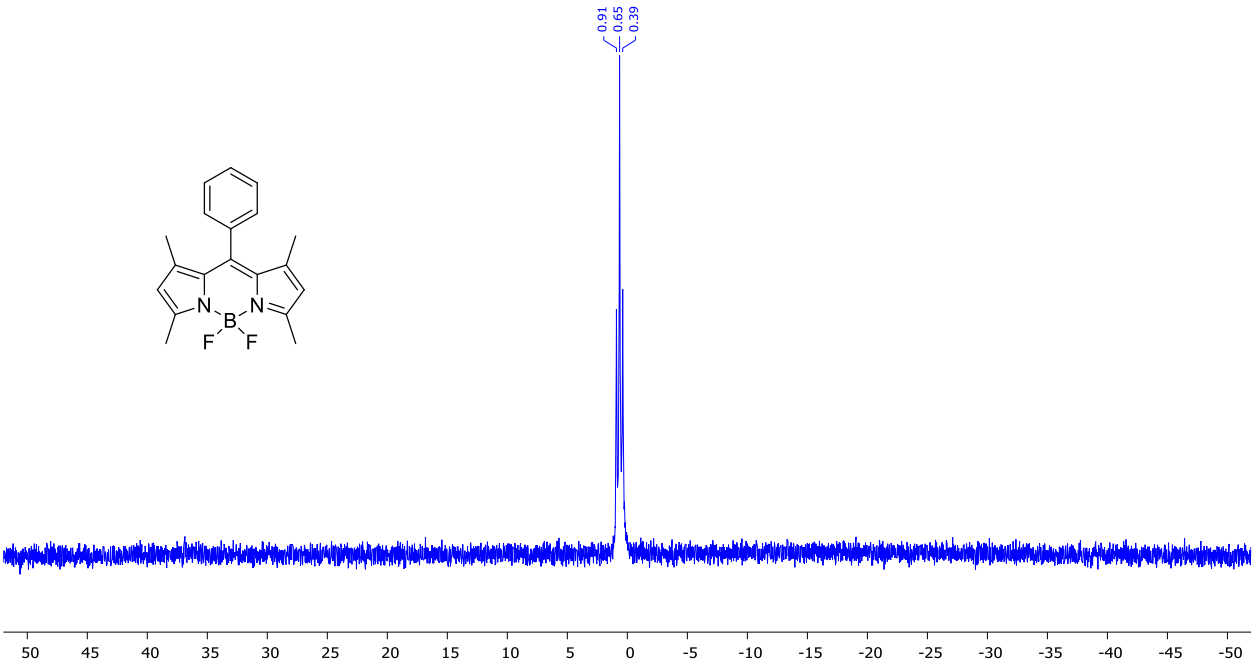

Figure C.41: ^{11}B NMR of BODIPY **7** in $CDCl_3$ (128 MHz)

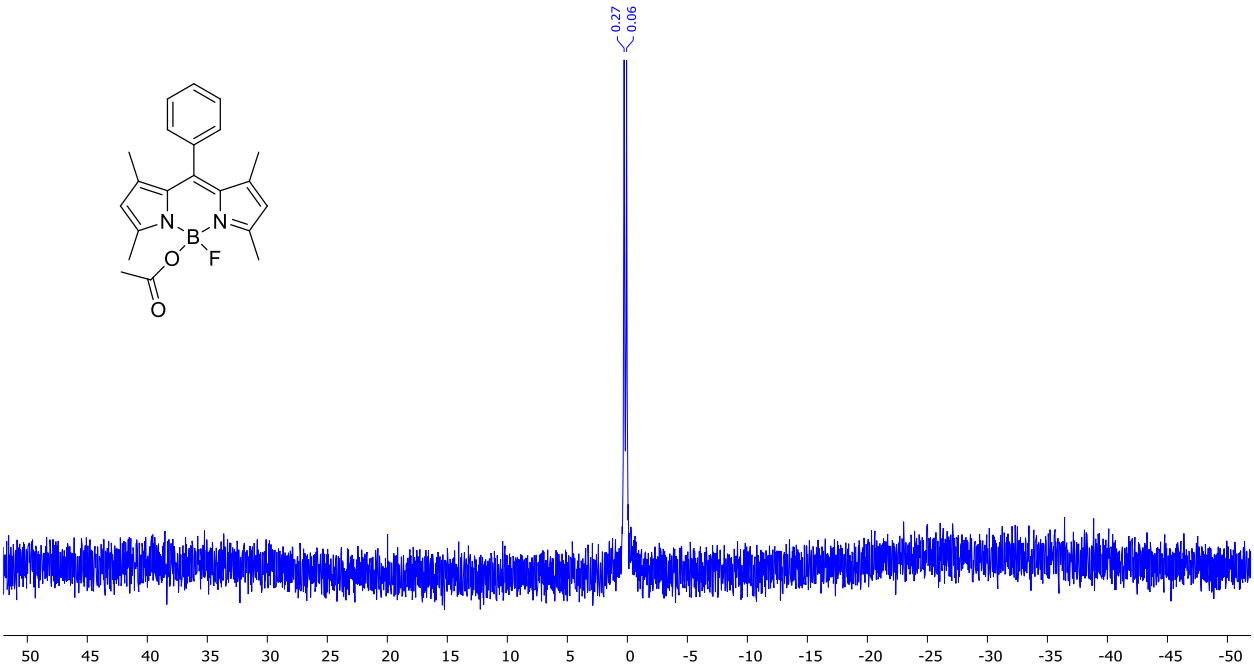

Figure C.42: ^{11}B NMR of BODIPY **8a** in $CDCl_3$ (128 MHz)

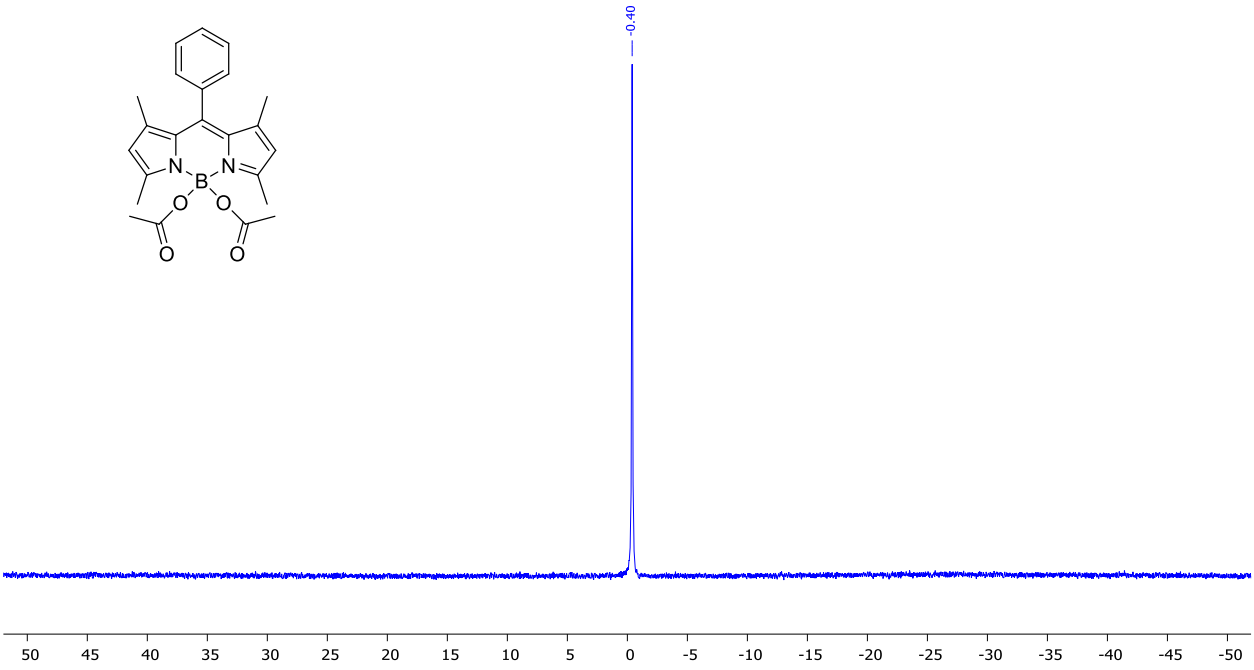

Figure C.43: ^{11}B NMR of BODIPY **8b** in $CDCl_3$ (128 MHz)

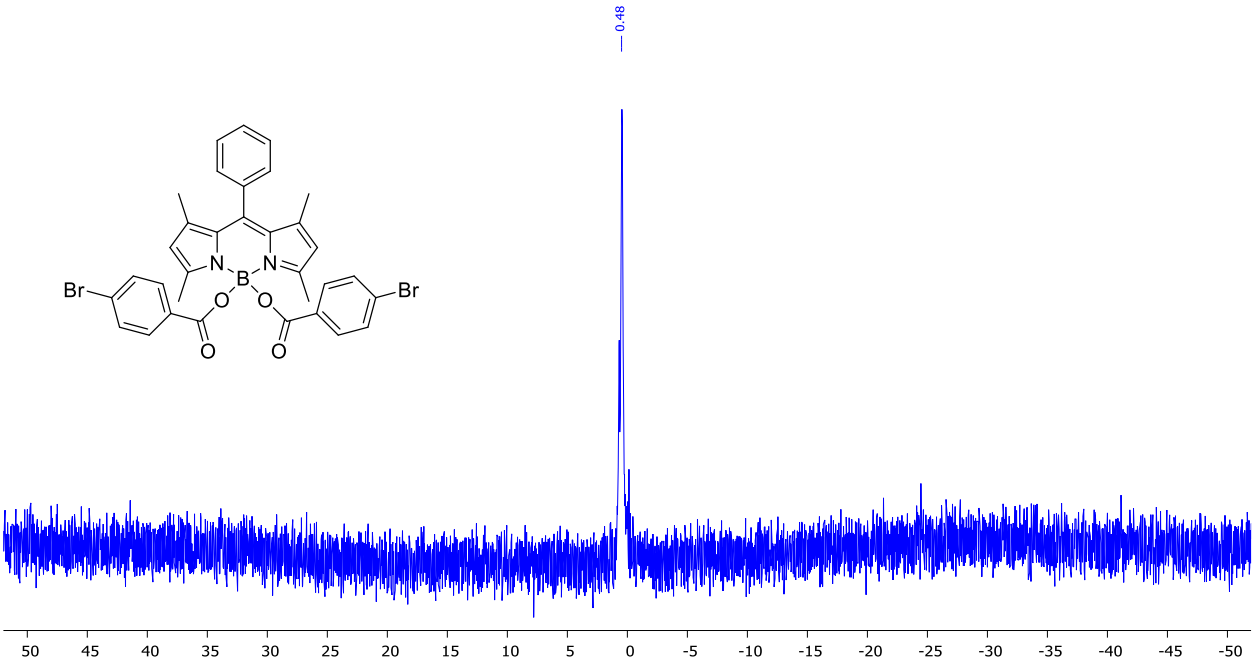

Figure C.44: ^{11}B NMR of BODIPY **9** in $CDCl_3$ (128 MHz)

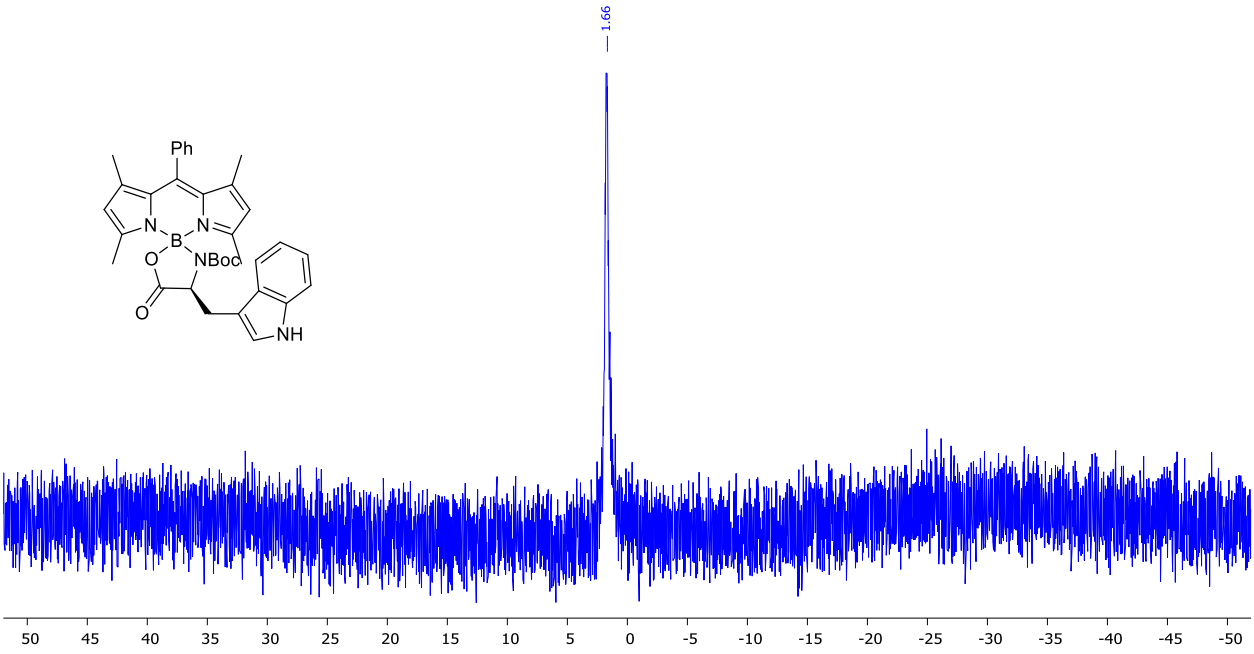

Figure C.45: ^{11}B NMR of BODIPY **10** in $CDCl_3$ (128 MHz)

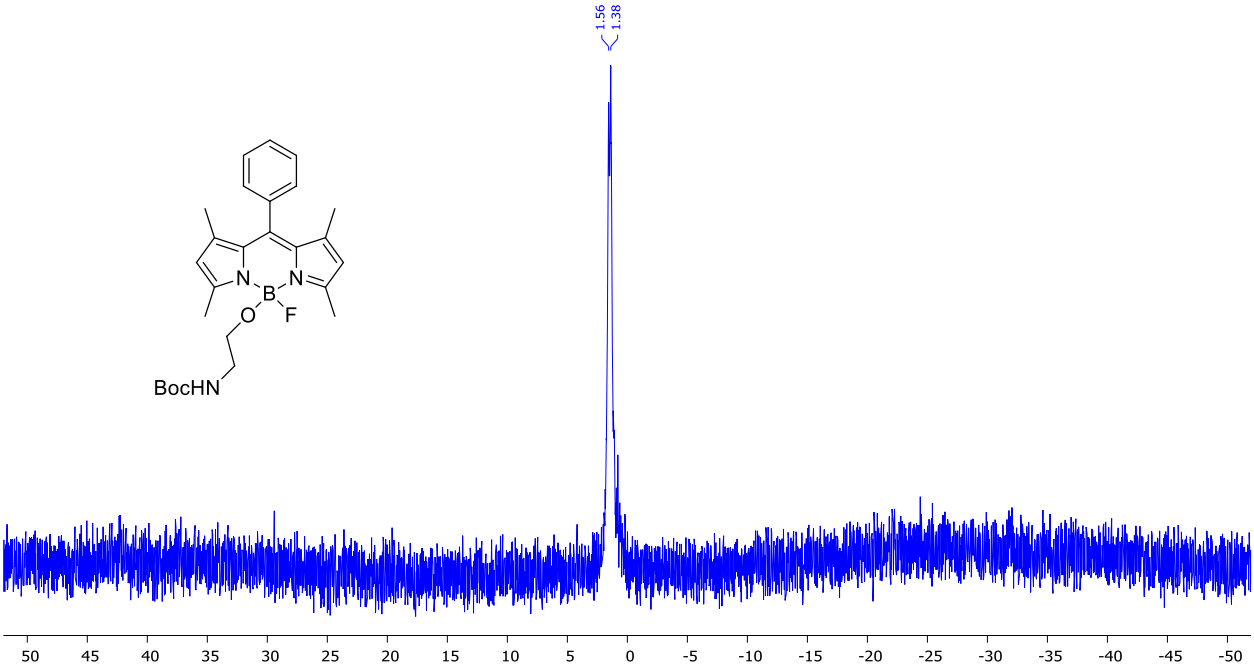

Figure C.46: ^{11}B NMR of BODIPY **11a** in $CDCl_3$ (128 MHz)

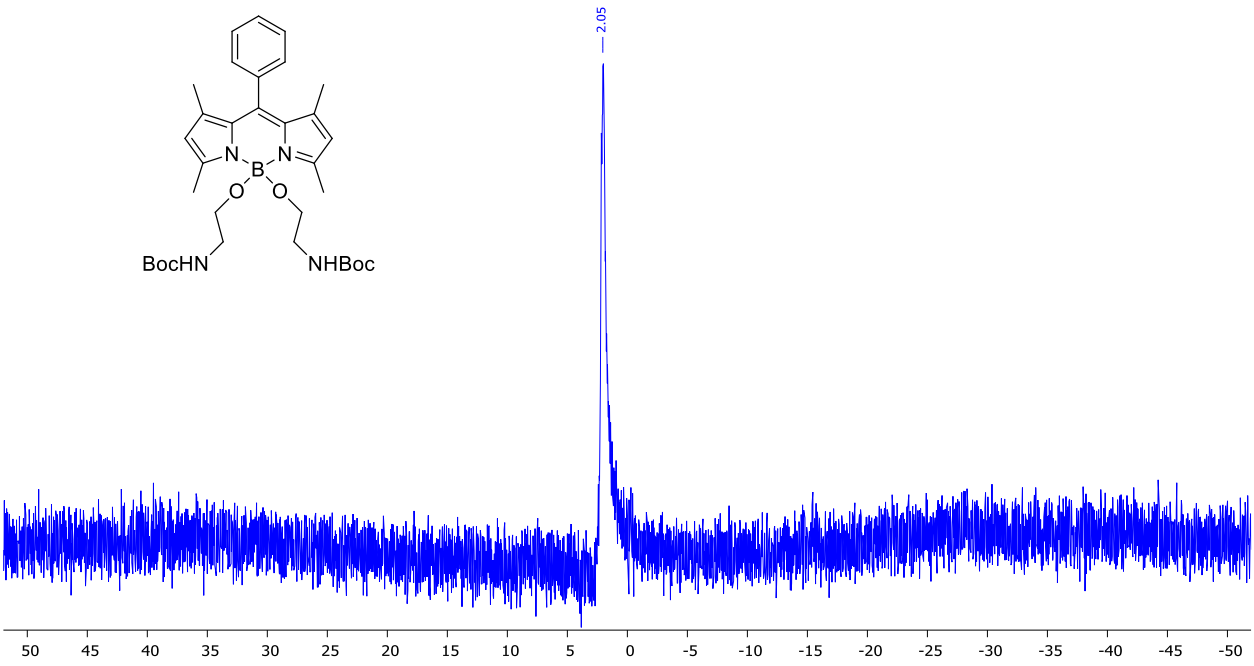

Figure C.47: ^{11}B NMR of BODIPY **11b** in $CDCl_3$ (128 MHz)

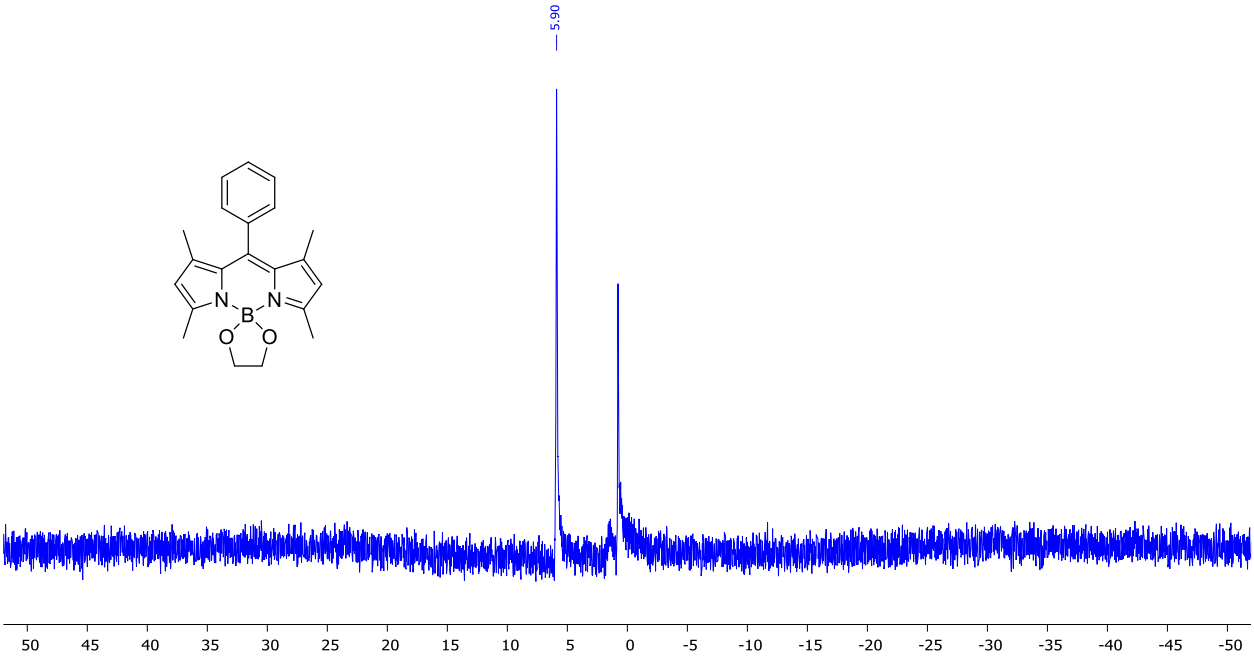

Figure C.48: ^{11}B NMR of BODIPY **12** in $CDCl_3$ (128 MHz)

APPENDIX D: NMR Characterization of Compounds Found in Chapter 5

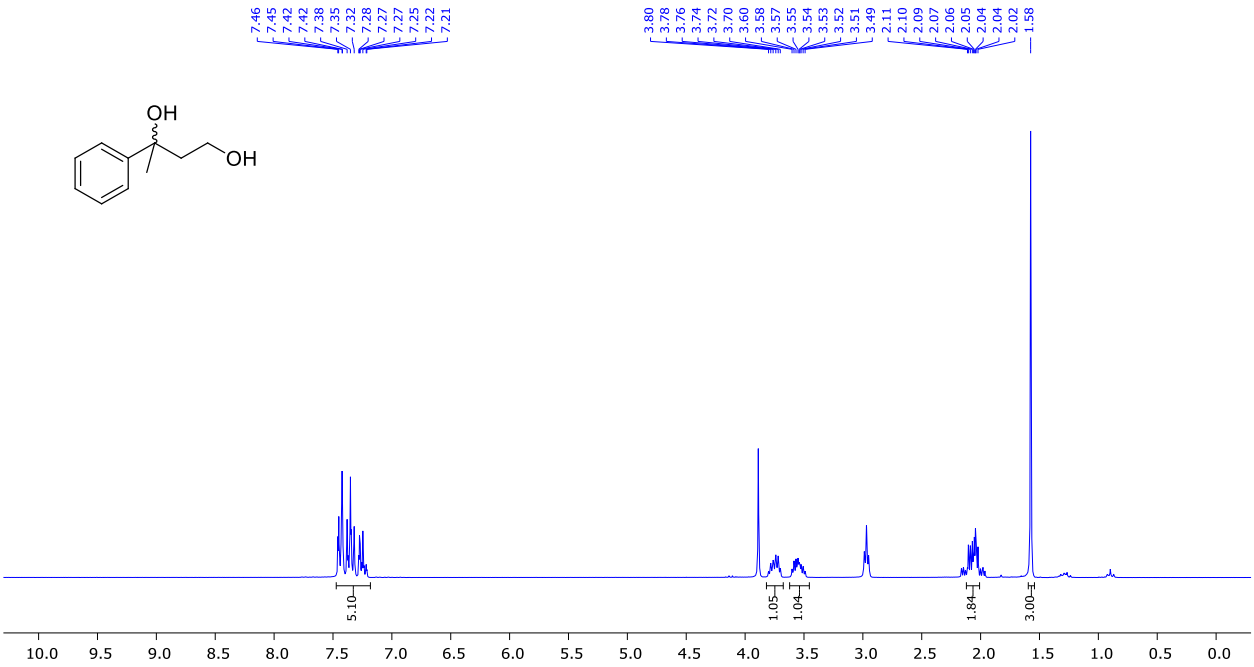

Figure D.1: ^{1}H NMR of compound **4** in $CDCl_3$ (250 MHz)

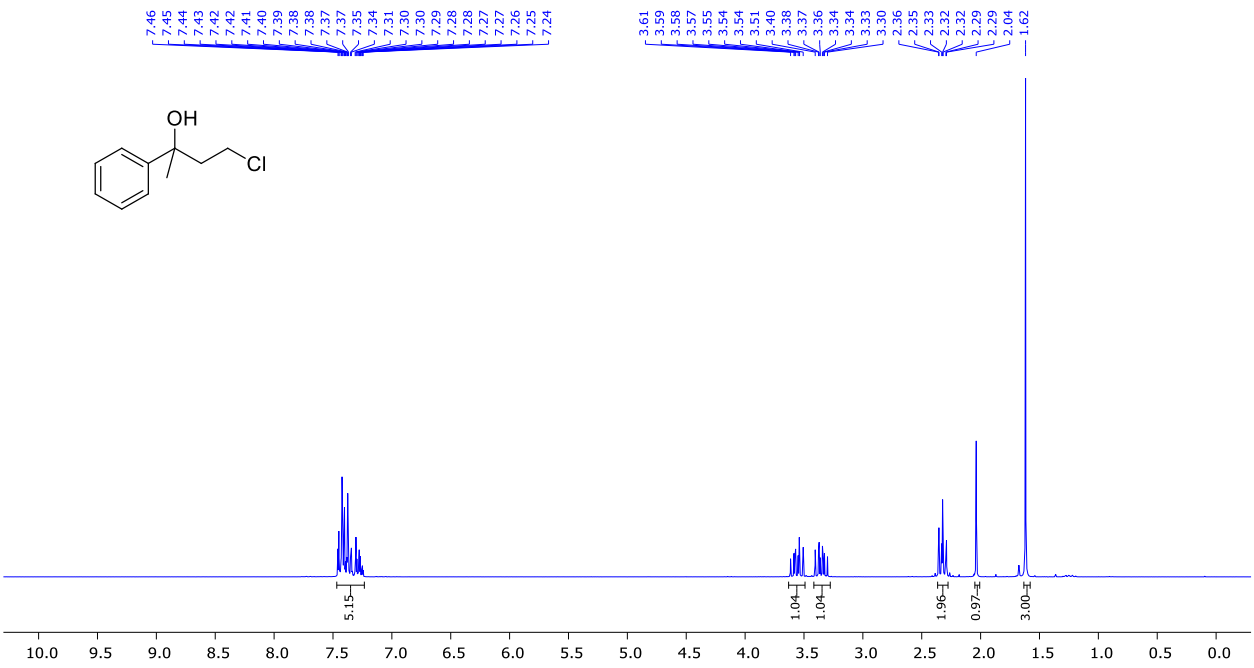

Figure D.2: ^{1}H NMR of compound **4a** in $CDCl_3$ (250 MHz)

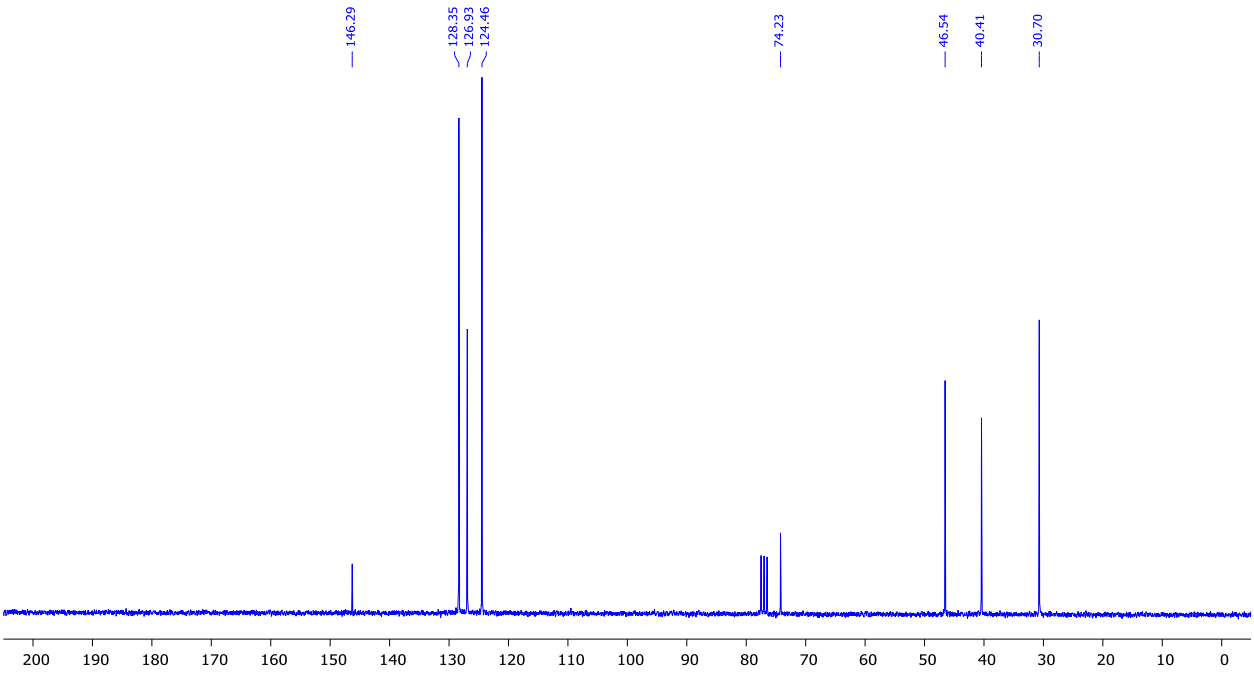

Figure D.3: ^{13}C NMR of compound **4a** in $CDCl_3$ (62.5 MHz)

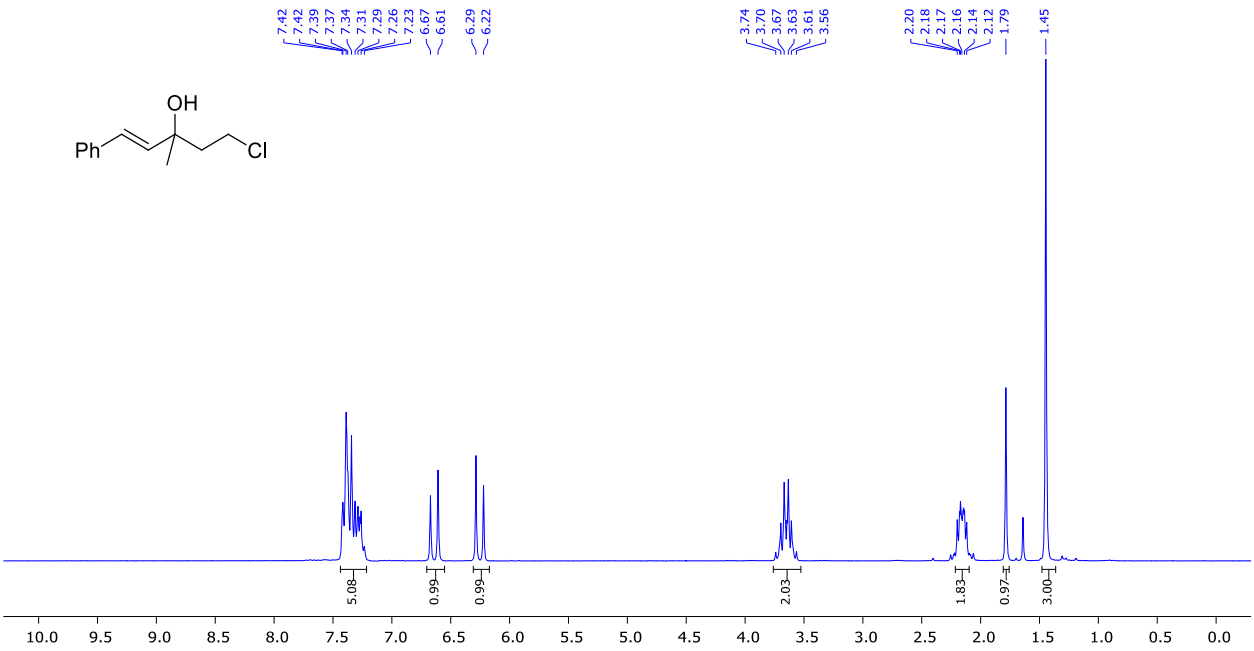

Figure D.4: ^{1}H NMR of compound **5a** in $CDCl_3$ (250 MHz)

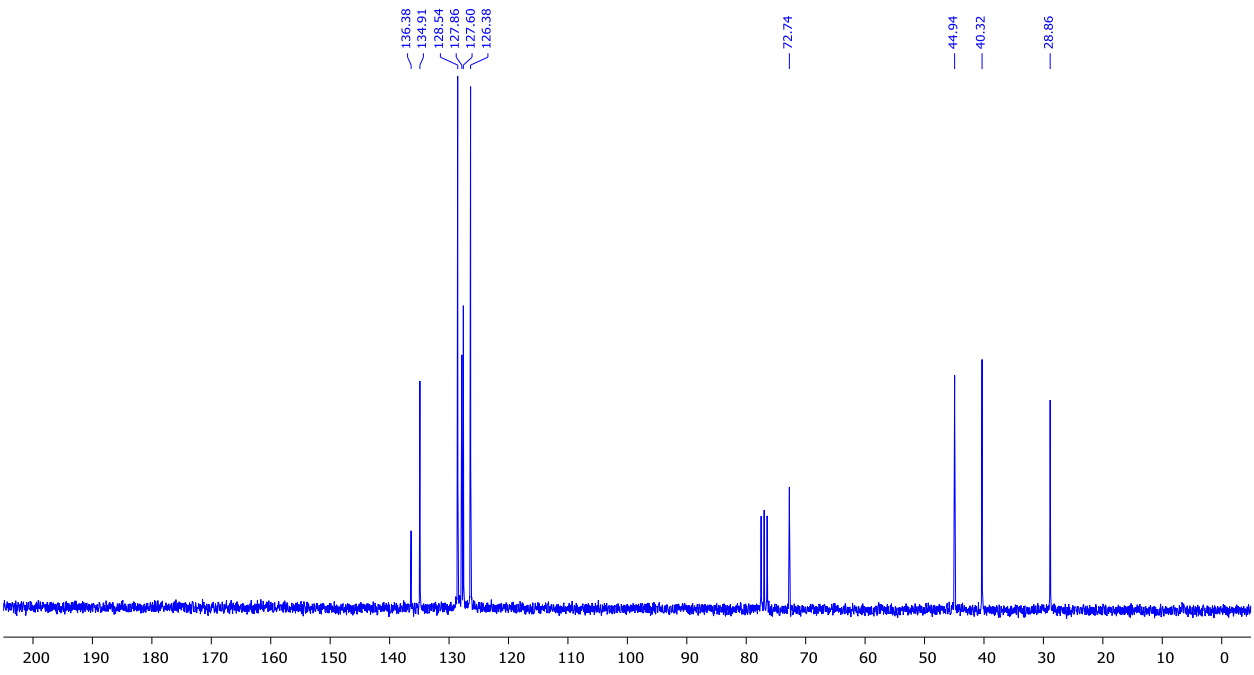

Figure D.5: ^{13}C NMR of compound **5a** in $CDCl_3$ (62.5 MHz)

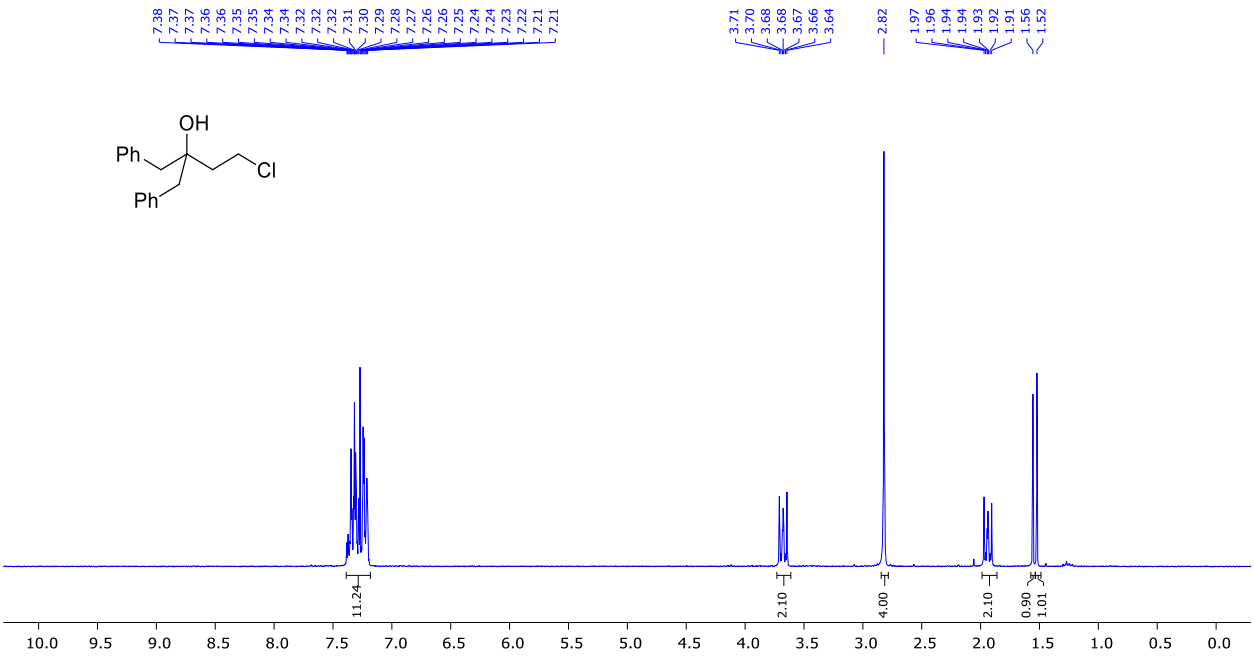

Figure D.6: ^{1}H NMR of compound **6a** in $CDCl_3$ (250 MHz)

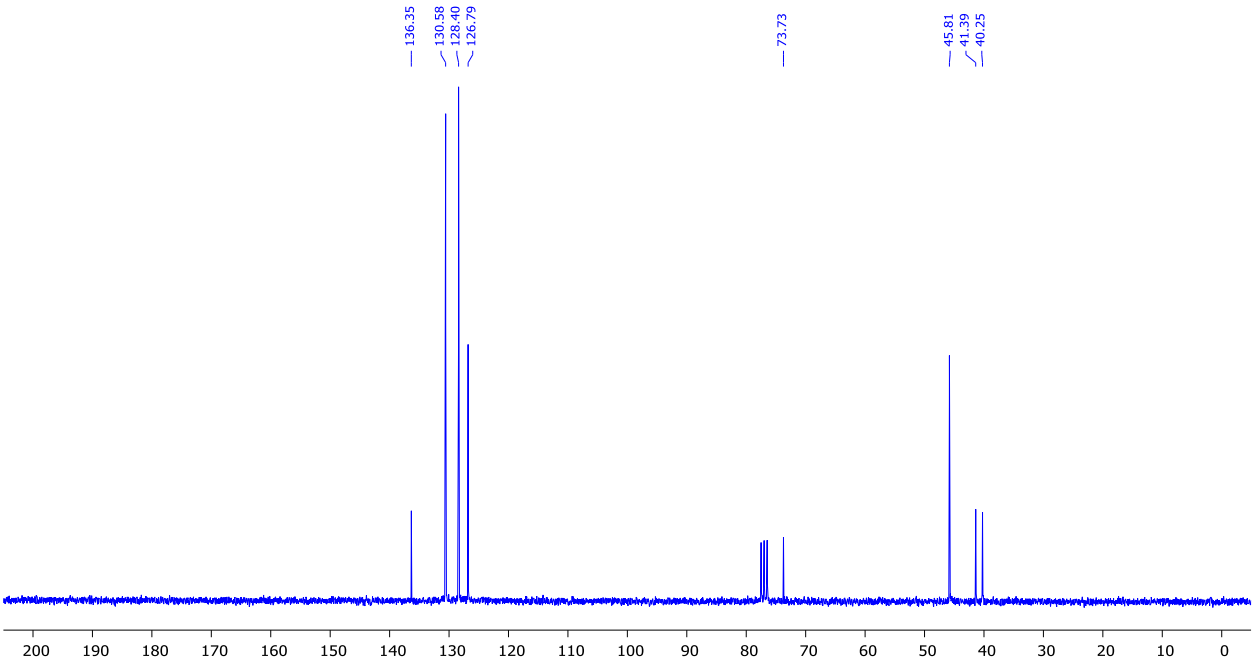

Figure D.7: ^{13}C NMR of compound **6a** in $CDCl_3$ (62.5 MHz)

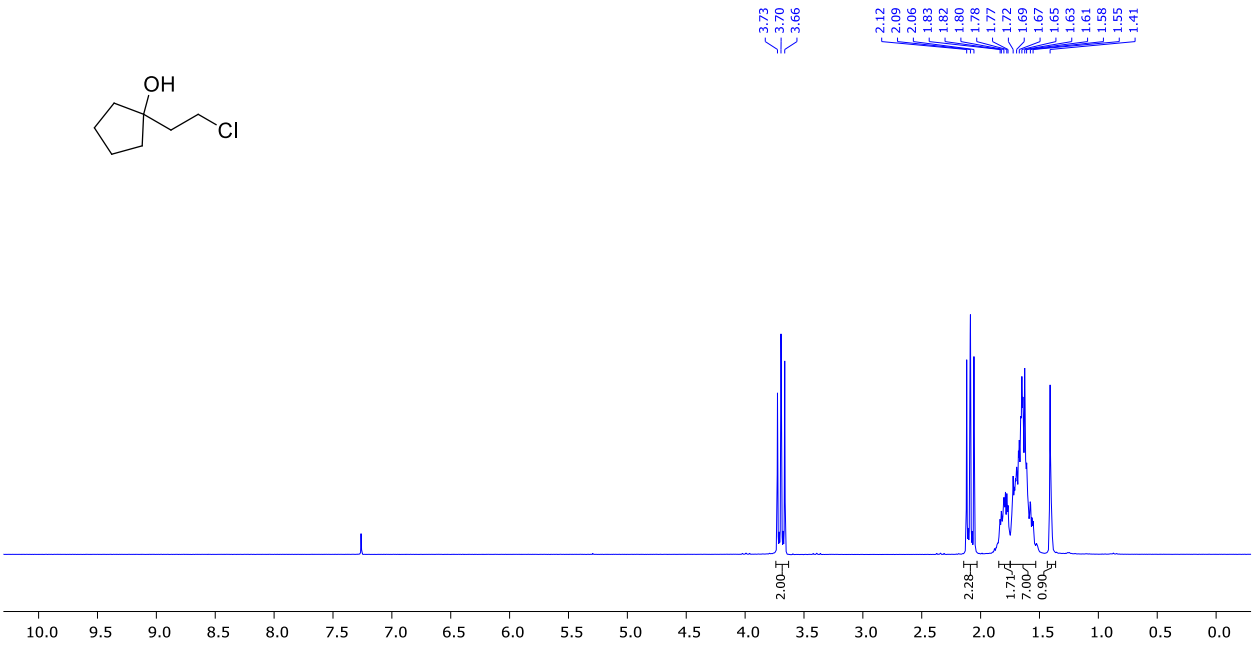

Figure D.8: ^{1}H NMR of compound **7a** in $CDCl_3$ (250 MHz)

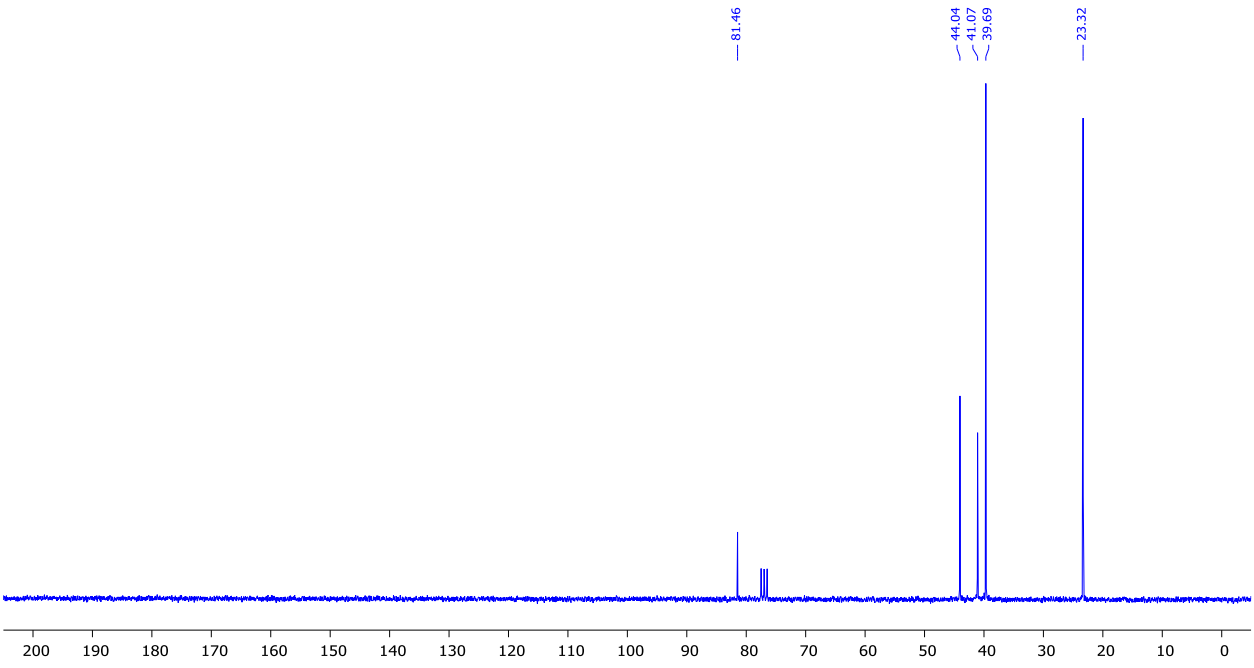

Figure D.9: ^{13}C NMR of compound **7a** in $CDCl_3$ (62.5 MHz)

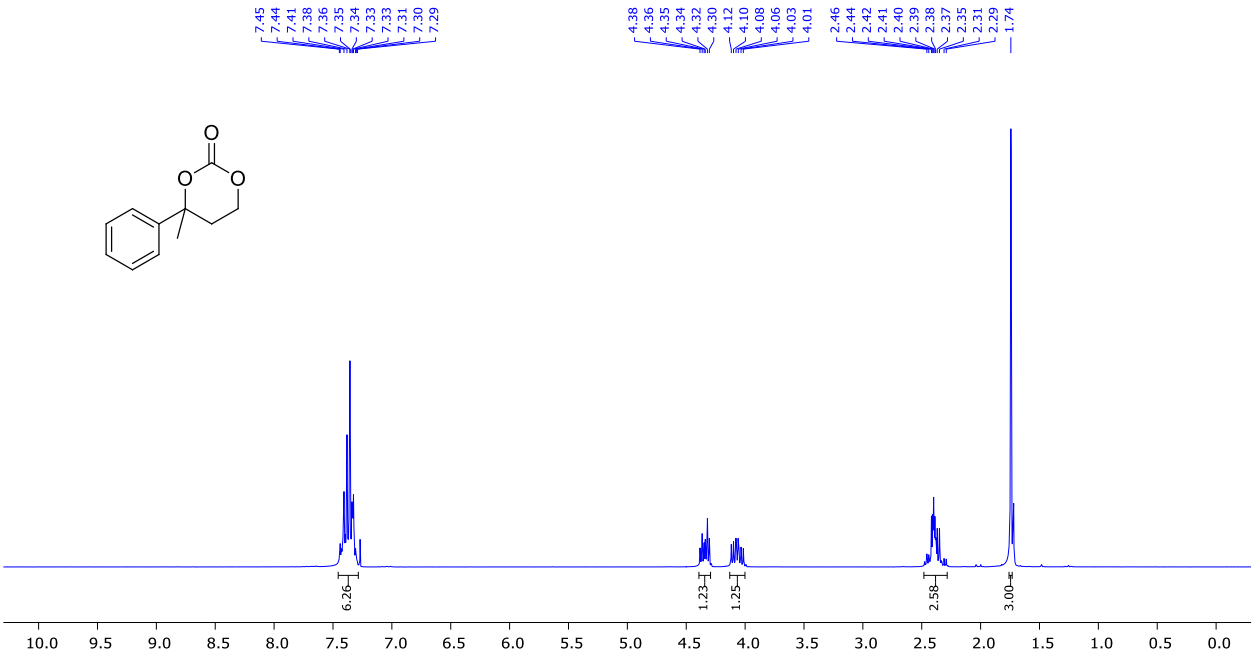

Figure D.10: ^{1}H NMR of compound **8** in $CDCl_3$ (250 MHz)

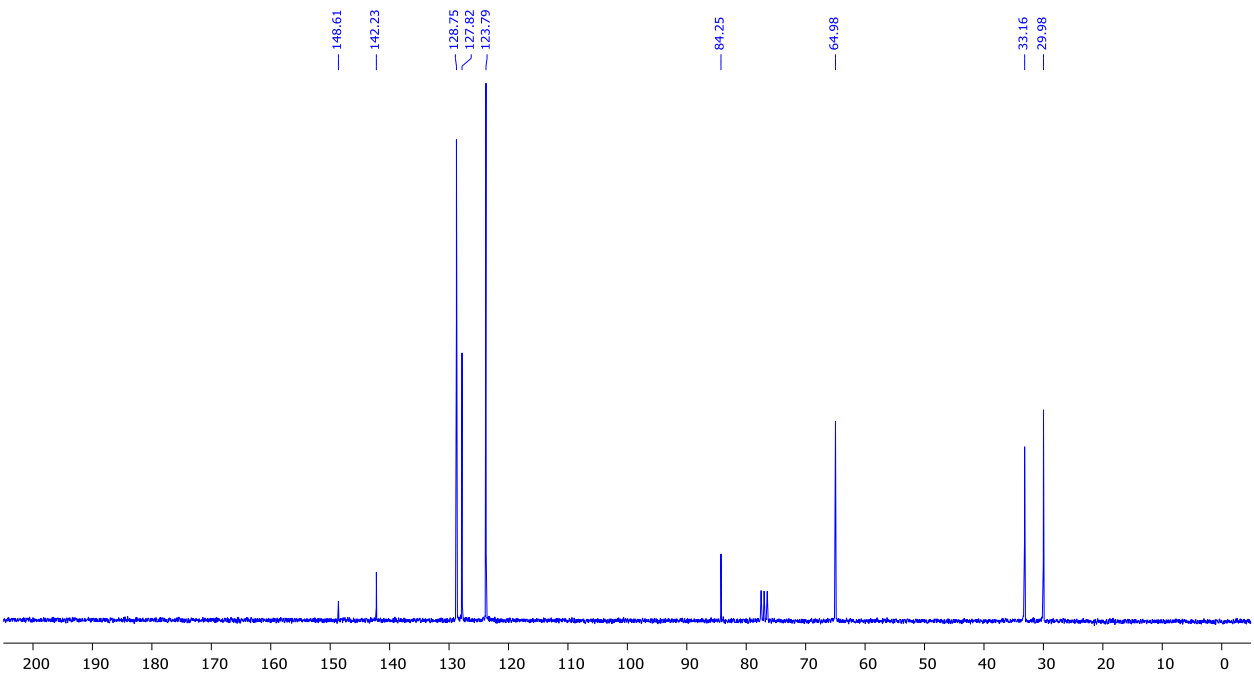

Figure D.11: ^{13}C NMR of compound **8** in $CDCl_3$ (62.5 MHz)

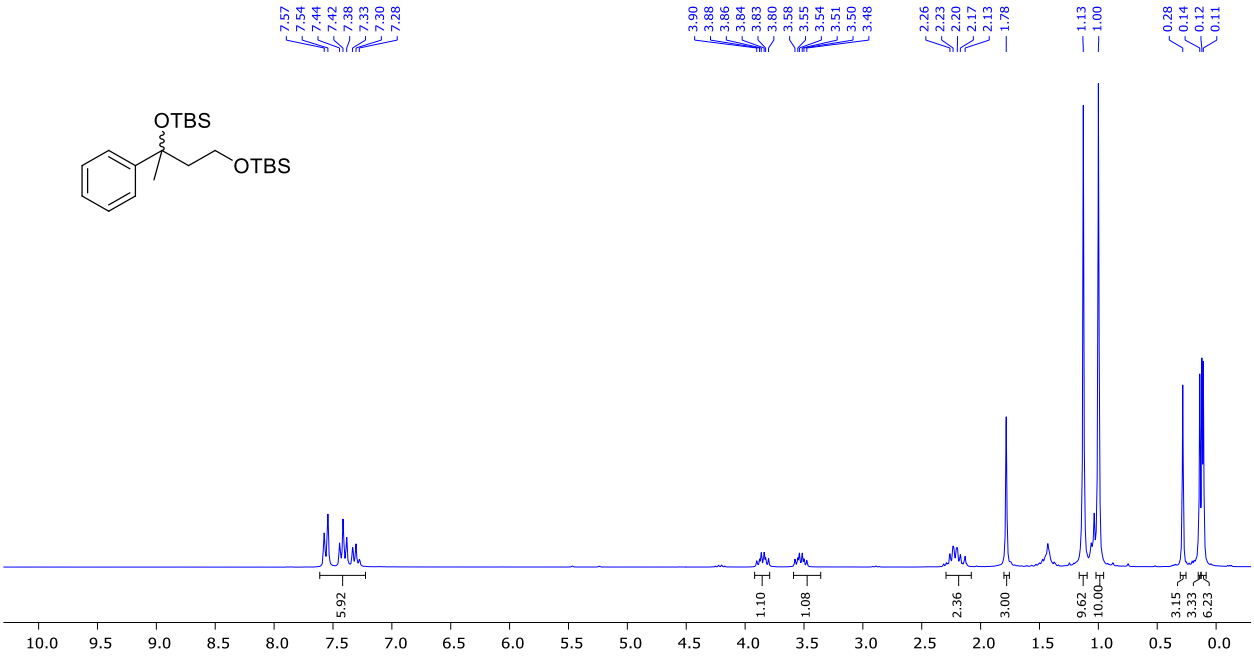

Figure D.12: ^{1}H NMR of compound **14** in $CDCl_3$ (250 MHz)

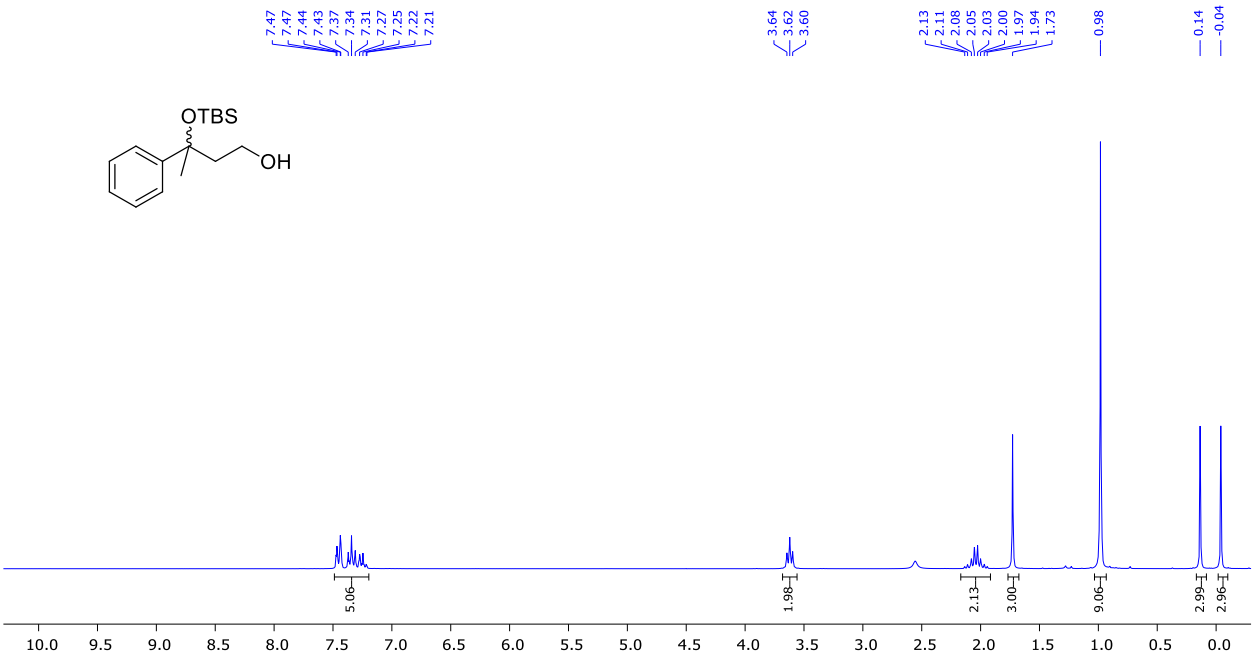

Figure D.13: ^{1}H NMR of compound **15** in $CDCl_3$ (250 MHz)

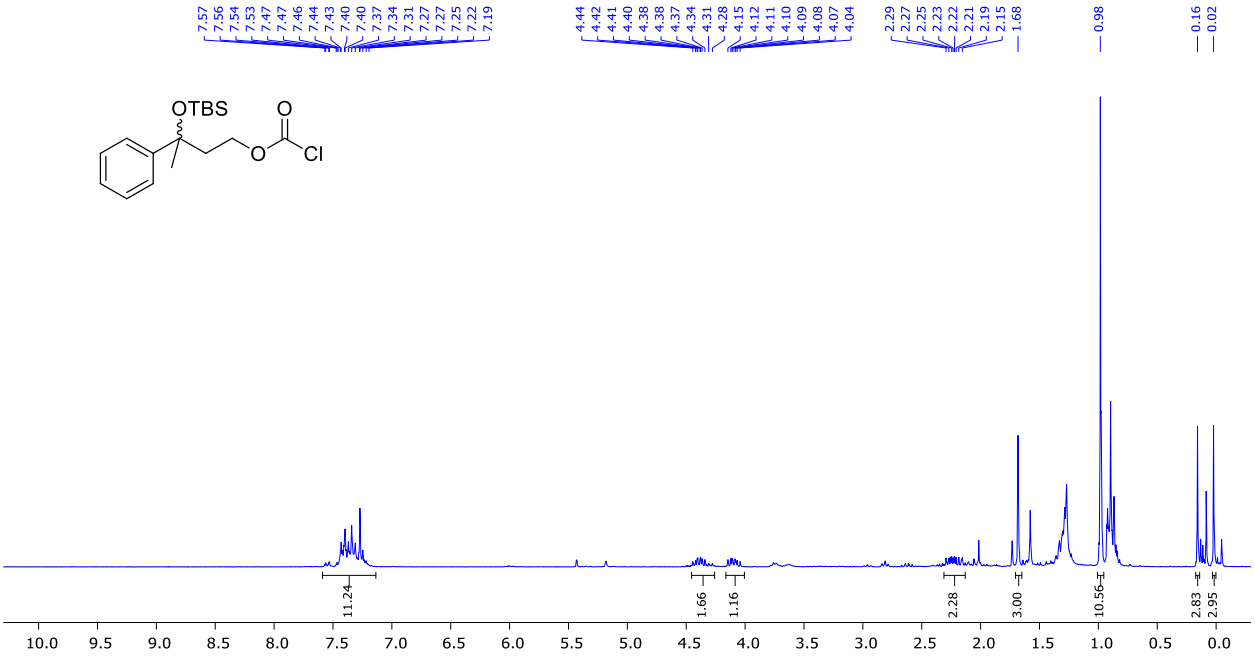

Figure D.14: ^{1}H NMR of compound **16** in $CDCl_3$ (250 MHz)

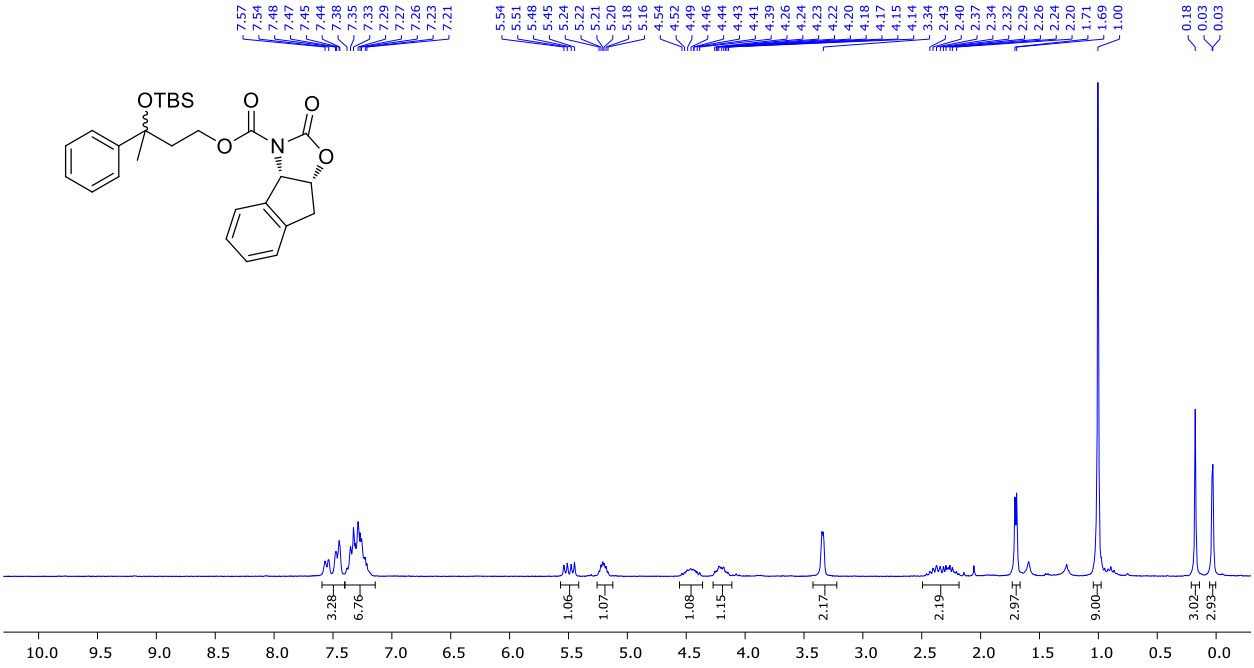

Figure D.15: ^{1}H NMR of compound **17** in $CDCl_3$ (250 MHz)

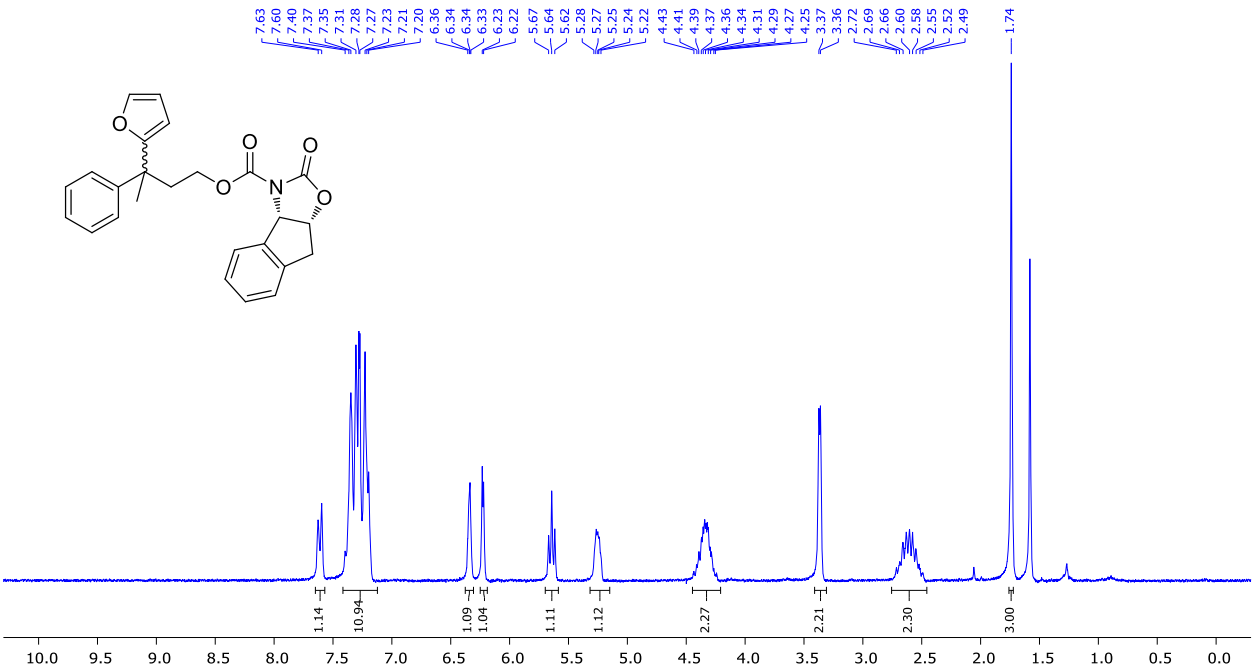

Figure D.16: ^{1}H NMR of compound **18** in $CDCl_3$ (250 MHz)

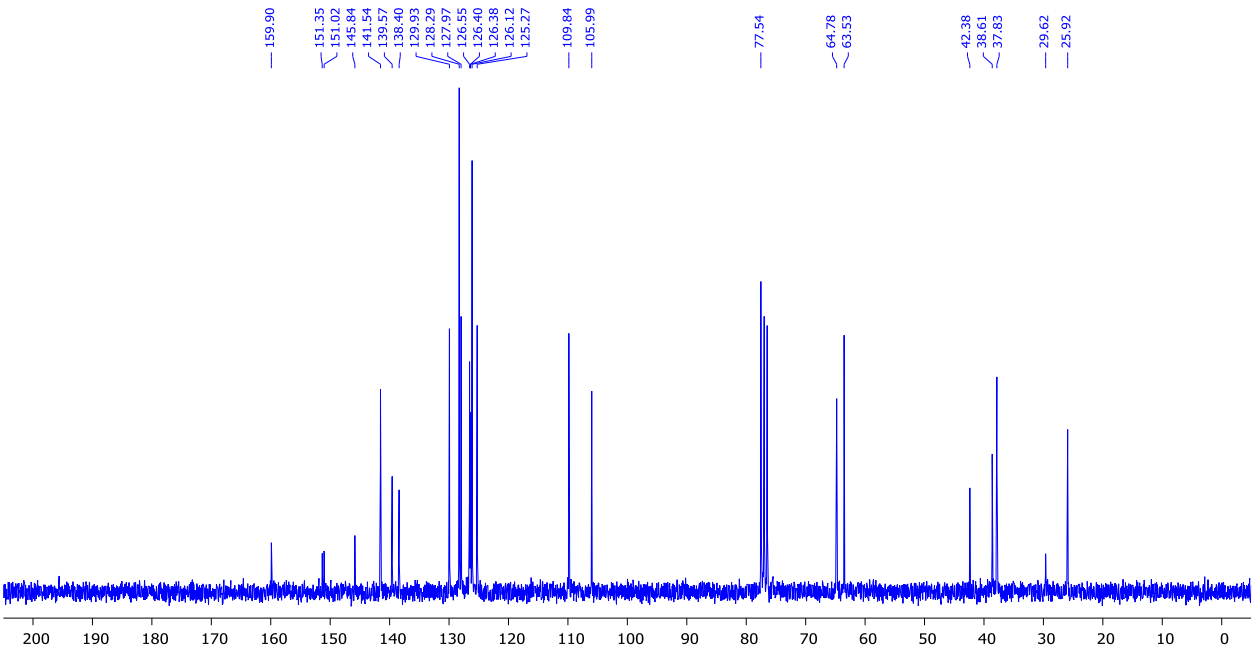

Figure D.17: ^{13}C NMR of compound **18** in $CDCl_3$ (62.5 MHz)

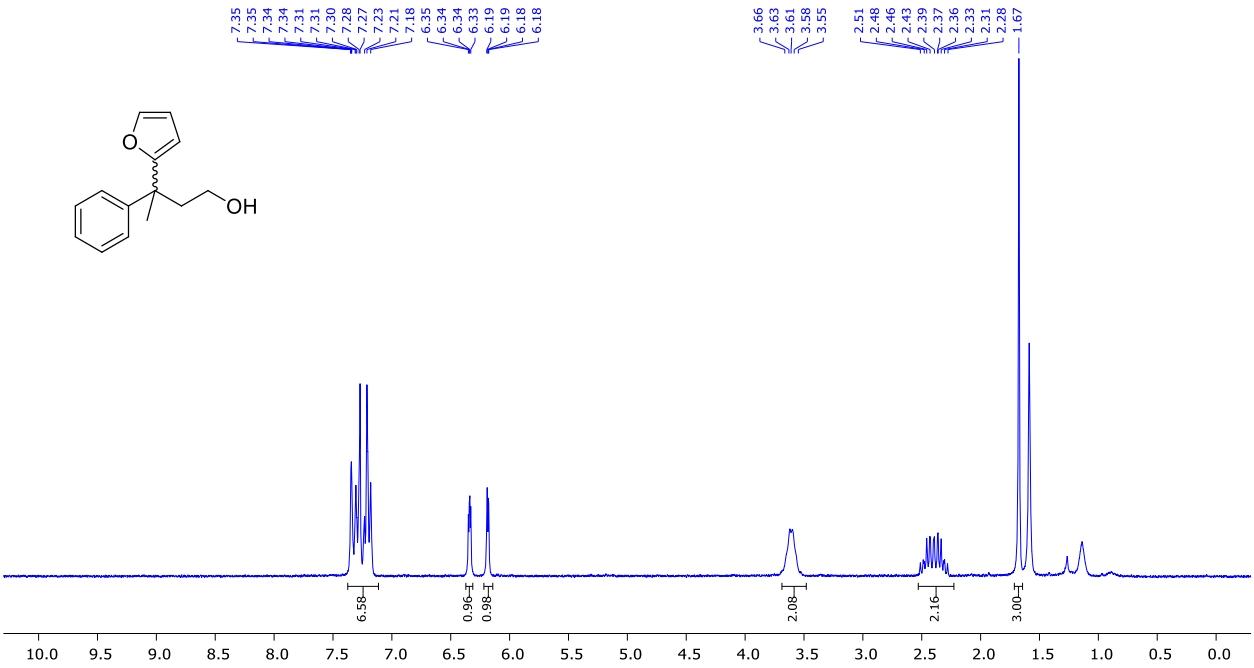

Figure D.18: ^{1}H NMR of compound **19** in $CDCl_3$ (250 MHz)

Title:	Synthesis and Reactivity of 4,4-Dialkoxy-BODIPYs: An Experimental and Computational Study
Author:	Alex L. Nguyen, Petia Bobadova-Parvanova, Melissa Hopfinger, et al
Publication:	Inorganic Chemistry
Publisher:	American Chemical Society
Date:	Apr 1, 2015

PERMISSION/LICENSE IS GRANTED FOR YOUR ORDER AT NO CHARGE

This type of permission/license, instead of the standard Terms & Conditions, is sent to you because no fee is being charged for your order. Please note the following:

- Permission is granted for your request in both print and electronic formats, and translations.
- If figures and/or tables were requested, they may be adapted or used in part.
- Please print this page for your records and send a copy of it to your publisher/graduate school.
- Appropriate credit for the requested material should be given as follows: "Reprinted (adapted) with permission from (COMPLETE REFERENCE CITATION). Copyright (YEAR) American Chemical Society." Insert appropriate information in place of the capitalized words.
- One-time permission is granted only for the use specified in your request. No additional uses are granted (such as derivative works or other editions). For any other uses, please submit a new request.

ELSEVIER LICENSE
TERMS AND CONDITIONS

Nov 17, 2015

This is a License Agreement between Alex Nguyen ("You") and Elsevier ("Elsevier") provided by Copyright Clearance Center ("CCC"). The license consists of your order details, the terms and conditions provided by Elsevier, and the payment terms and conditions.

All payments must be made in full to CCC. For payment instructions, please see information listed at the bottom of this form.

Supplier	Elsevier Limited The Boulevard,Langford Lane Kidlington,Oxford,OX5 1GB,UK
Registered Company Number	1982084
Customer name	Alex Nguyen
Customer address	15888 Antietam avenue BATON ROUGE, LA 70817
License number	3751481185698
License date	Nov 17, 2015
Licensed content publisher	Elsevier
Licensed content publication	Tetrahedron Letters
Licensed content title	Synthesis of 4,4′-functionalized BODIPYs from dipyrrins
Licensed content author	Alex L. Nguyen,Frank R. Fronczek,Kevin M. Smith,M. Graça H. Vicente
Licensed content date	18 November 2015
Licensed content volume number	56
Licensed content issue number	46
Number of pages	4
Start Page	6348
End Page	6351
Type of Use	reuse in a thesis/dissertation
Portion	full article
Format	electronic
Are you the author of this Elsevier article?	Yes
Will you be translating?	No

Title of your thesis/dissertation	BORON FUNCTIONALIZATION OF BODIPY DYES, AND THEIR EVALUATION AS BIOIMAGING AGENTS
Expected completion date	May 2016
Estimated size (number of pages)	250
Elsevier VAT number	GB 494 6272 12
Permissions price	0.00 USD
VAT/Local Sales Tax	0.00 USD / 0.00 GBP
Total	0.00 USD
Terms and Conditions	

Title: Chlorination of Aliphatic Primary Alcohols via Triphosgene–Triethylamine Activation

Author: Caitlan E. Ayala, Andres Villalpando, Alex L. Nguyen, et al

Publication: Organic Letters

Publisher: American Chemical Society

Date: Jul 1, 2012

PERMISSION/LICENSE IS GRANTED FOR YOUR ORDER AT NO CHARGE

This type of permission/license, instead of the standard Terms & Conditions, is sent to you because no fee is being charged for your order. Please note the following:

- Permission is granted for your request in both print and electronic formats, and translations.
- If figures and/or tables were requested, they may be adapted or used in part.
- Please print this page for your records and send a copy of it to your publisher/graduate school.
- Appropriate credit for the requested material should be given as follows: "Reprinted (adapted) with permission from (COMPLETE REFERENCE CITATION). Copyright (YEAR) American Chemical Society." Insert appropriate information in place of the capitalized words.
- One-time permission is granted only for the use specified in your request. No additional uses are granted (such as derivative works or other editions). For any other uses, please submit a new request.

VITA

Alex L. Nguyen was born in Saigon, Vietnam and is engaged to Trang T. H. Nguyen. His family immigrated to the US in 1997 and has resided in Baton Rouge, Louisiana since. After he took Intermediate Organic Chemistry with Dr. Carol Taylor as the instructor, he was fascinated with unique transformations in organic chemistry and joined Taylor's group the following semester to begin his undergraduate research. He earned a Bachelor of Science degree from Louisiana State University (LSU) in May of 2011. With his continued interests in organic chemistry, he entered the chemistry doctoral program in the Chemistry Department at LSU, Baton Rouge, Louisiana in August 2011. He joined the laboratory of Dr. M. Graça H. Vicente and Dr. Kevin M. Smith shortly afterward. He is currently a candidate for the degree of Doctor of Philosophy at the May 2016 commencement.